

# 2013 Remote Sensing

[www.spie.org/rs](http://www.spie.org/rs)

# 2013 Security+ Defence

[www.spie.org/sd](http://www.spie.org/sd)

## Technical Summaries

**Conference:** 23–26 September 2013

**Exhibition:** 24–25 September 2013

**Location**

Internationales Congress Center  
Dresden, Germany



**SPIE**<sup>®</sup>



# SPIE Remote Sensing



**Charles R. Bostater**  
 Marine-Environmental Optics Lab &  
 Remote Sensing Center,  
 Florida Institute of Technology  
 (United States)  
*2013 Symposium Chair*



**Ulrich Michel**  
 University of Education Heidelberg,  
 Germany  
*2013 Symposium Co-Chair*

# SPIE Security+Defence



**David H. Titterton**  
 Defence Science and Technology Lab.,  
 United Kingdom  
*2013 Symposium Chair*

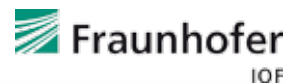


**Reinhard Ebert**  
 Fraunhofer IOSB, Institute of  
 Optronics, System Technologies  
 and Image Exploitation, Germany  
*2013 Symposium Co-Chair*

Cooperating Organisations



Cooperating Organisations



SPIE would like to express its deepest appreciation to the symposium chairs, conference chairs, Programme committees, and session chairs who have so generously given of their time and advice to make this symposium possible. The symposium, like our other conferences and activities, would not be possible without the dedicated contribution of our participants and members.

This Programme is based on commitments received up to the time of publication and is subject to change without notice.

# Contents

## SPIE Remote Sensing

8887: Remote Sensing for Agriculture, Ecosystems, and Hydrology XV . . . . .	4
8888: Remote Sensing of the Ocean, Sea Ice, Coastal Waters, and Large Water Regions 2013 . . . . .	30
8889: Sensors, Systems, and Next-Generation Satellites XVII . . . . .	39
8890A: Remote Sensing of Clouds and the Atmosphere XVIII. . . . .	62
8890B: Optics in Atmospheric Propagation and Adaptive Systems XVI . . . . .	74
8891: SAR Image Analysis, Modeling, and Techniques XIII . . . . .	78
8892: Image and Signal Processing for Remote Sensing XIX . . . . .	87
8893: Earth Resources and Environmental Remote Sensing/ GIS Applications IV. . . . .	112
8894: Lidar Technologies, Techniques, and Measurements for Atmospheric Remote Sensing IX . . . . .	133
8895: High-Performance Computing in Remote Sensing III . . . . .	145

## SPIE Security+Defence

8896: Electro-Optical and Infrared Systems: Technology and Applications X . .	151
8897A: Electro-Optical Remote Sensing VII . .	163
8897B: Military Applications in Hyperspectral Imaging and High Spatial Resolution Sensing . . . . .	171
8898A: Technologies for Optical Countermeasures X . . . . .	173
8898B: High-Power Lasers 2013: Technology and Systems . . . . .	178
8899A: Emerging Technologies. . . . .	183
8899B: Quantum-Physics-Based Information Security II . . . . .	187
8899C: Unmanned/Unattended Sensors and Sensor Networks X . . . . .	192
8900: Millimetre Wave and Terahertz Sensors and Technology VI . . . . .	198
8901A: Optics and Photonics for Counterterrorism, Crime Fighting and Defence IX . . . . .	207
8901B: Optical Materials and Biomaterials in Security and Defence Systems Technology X . . . . .	214
Plenaries . . . . .	218

# Conference 8887: Remote Sensing for Agriculture, Ecosystems, and Hydrology XV

Tuesday - Thursday 24–26 September 2013

Part of Proceedings of SPIE Vol. 8887 Remote Sensing for Agriculture, Ecosystems, and Hydrology XV

8887-1, Session 1

## Assessing the potential of hyperspectral imagery to map bark beetle-induced forest damages

Fabian Fassnacht, Albert-Ludwigs-Univ. Freiburg (Germany);  
Hooman Latifi, Julius-Maximilians-Univ. Würzburg (Germany);  
Aniruddha Ghosh, Pawan Kumar Joshi, TERI Univ. (India);  
Barbara Koch, Albert-Ludwigs-Univ. Freiburg (Germany)

Biotic damages were found to make up for the largest fraction of all damage sources within European forests. Therefore natural hazards connected to insect outbreaks e.g. those induced by the European bark beetle (*Ips typographus* L.) are amongst the most important phenomena affecting forest health in various regions of Europe. Accurate and up-to-date maps illustrating the spatial distribution of bark beetle -damaged trees is of great value for forest practitioners for the effective planning of sanitary measurements and to draw future predictions on bark beetle infestation dynamics. In the present study, three scenarios of bark beetle damage mapping from hyperspectral remote sensing data were examined. Airborne hyperspectral data (HyMAP) was combined with a genetic algorithm (GA) for feature selection and a supervised Support Vector Machines classification to produce forest damage maps. In addition to the original reflectance from the hyperspectral HyMap data, two derivatives of the original information (1st order Savitzky-Golay derivation (SAGO) and continuum removed spectra (CONTREM)) were used as input to the classification workflow. Main differences between scenarios lay in the definition of the damage classes (being used to extract the spectral signatures). The trained classifier was additionally applied to a second independent hyperspectral image in two of the scenarios. This was done to evaluate the stability of the spectral signatures derived from the training samples and to get an idea of whether an automatic classification based on spectral libraries could be a useful classification tool for practitioners. The classes derived from scenarios eventually served as input to the feature selection by means of GA. In addition, in each classification approach the number of input bands was altered to assess the performance of the classifier with differing amounts of spectral information.

Results of the study indicate that accurate mapping of several damage classes was not possible with acceptable accuracies with the applied methodology. Especially the defined green attack stage was heavily over-classified and although the overall accuracies (OAs) were acceptable (80 %) when considering all defined classes, the qualitative analysis of the produced maps demonstrated that results were not beneficial for forest practitioners. On the other hand, the separation of trees with visible damages from undamaged trees was possible with very high OAs (up to 96%). These results could also be transferred to the second independent hyperspectral image, in which the sole separation between healthy and damaged trees was possible with OAs of 94%-97%. Lower but still reasonable OAs (76% - 85%) were found when all defined classes were considered. Main error sources were confusions between damaged trees and sparsely vegetated soil.

Considering the wavelengths of GA selected bands it was found that many bands in the visual part of the spectrum, close to the green peak as well as around the chlorophyll absorption feature and the red edge rise got selected. In some of the tested cases further bands in the SWIR and one in the NIR at 1076 nm showed high stabilities in the GA selection procedure.

8887-2, Session 1

## Spatial and temporal uncertainty source analysis for Lidar driven individual tree growth projections

George Z. Gertner, Univ. of Illinois at Urbana-Champaign (United States)

The United States Forest Service Forest Vegetation Simulator (FVS) is a very widely used growth model developed for projecting

individual trees and forest development through time. FVS is now being used to evaluate a variety of global change scenarios as it relates to forest health, carbon life cycle analysis, sustainability, wildlife habitat, wildland fires, etc. In this paper, an uncertainty budget is developed for FVS projections, where initial models inputs are spatially explicit single-tree stem maps developed with small-footprint airborne lidar. An uncertainty budget shows the overall precision of estimates/predictions made with a system, partitioned according to different types of uncertainty sources within and outside of the system. In a comprehensive fashion, sources of uncertainties due to measurements, classification, sampling, parameter estimates, are accounted for in the lidar derived stem maps and within the FVS system. Spatially identifying the sources of uncertainties in time, modeling their accumulation and propagation, and finally, quantifying them locally on a tree basis and globally on a forest level are presented. Uncertainties in future forest responses due to uncertainties in projected global climatic change predictions that will also drive this type of forest model will also be discussed.

There are benefits to having an uncertainty budget for users of these types of models. The primary benefit is the acknowledgment that uncertainties exist; and it is reported. When using the model, the user will know that there is uncertainty and will use the model with full knowledge of the uncertainty and the risk of making the correct predictions (or incorrect predictions). The second most important benefit is that in a systematic fashion the decision-maker will understand the sources of uncertainties in the predictions.

8887-3, Session 1

## Mapping tropical rainforest canopies using multi-temporal spaceborne imaging spectroscopy

Ben Somers, VITO NV (Belgium); Gregory P. Asner, Carnegie Institution for Science (United States)

A thorough understanding of tropical rainforest dynamics is required to improve biodiversity conservation and forest management. To date, the full potential of optical remote sensing of rainforests has not been met in the context of monitoring of vegetation in these systems. The most critical bottleneck for the detailed monitoring of these ecosystems using traditional remote sensing technology is that image interpretation is complicated by the high spectral similarity between co-existing plant species. From this perspective, recent developments in hyperspectral remote sensing offer potential advantages. The high spectral detail provided by these new generation sensors allows for better discrimination of subtle physiological changes among plant species, whereas the systematic revisits of currently available and upcoming space-borne sensors allow for a continuous monitoring of ecosystem changes. Here we evaluated an alternative spectral unmixing strategy combining (i) a time series of EO-1 Hyperion images and (ii) an automated feature selection strategy in Multiple Endmember Spectral Mixture Analysis (MESMA). Our strategy for floristic mapping of forest canopies starts by compiling a time series of EO-1 Hyperion images into a single data cube and quantifying for each image in the time series the spectral separability of the different species mixtures (using the Separability Index). This spectral separability analysis, which is based on species-specific spectral libraries, subsequently allows us to define for each of the species combinations the temporal spectral subset that optimizes spectral separability among the different species in the mixture. So, for each species mixture a potentially different temporal spectral subset is selected. Second, the image time series is ingested into a modified Multiple Endmember Spectral Mixture Analysis, referred to as Waveband Adaptive Spectral Mixture Analysis (WASMA). Based on the same iterative mixture analysis cycle principles as used in MESMA, WASMA evaluates for each pixel the different endmember combination models. However, as opposed to MESMA, our new approach does not use a rigid spectral set of wavebands but adapts the subset according to the specific endmember combination as identified in the spectral separability phase. The model with the lowest residual error between the observed mixed spectrum and the modeled spectrum is assigned to the pixel. Thereby, WASMA allows the spectral subsets used in the unmixing algorithm to change on a per pixel basis as such

improving tree species specific mapping. The potential of the new approach for floristic mapping of tree species in Hawaiian rainforests was quantitatively demonstrated using both simulated and actual hyperspectral image time-series (i.e. EO-1 Hyperion). The dominant overstory tree species are the native *Metrosideros polymorpha* and *Acacia koa* and invasive *Psidium cattleianum* and *Morella faya*. With a Cohen's Kappa coefficient of 0.65, our approach provided a more accurate tree species map compared to MESMA (Kappa = 0.54). In addition, by the selection of spectral subsets our approach was about 90% faster than MESMA. The flexible or adaptive use of band sets in spectral unmixing as such provides an interesting avenue to address spectral similarities in complex vegetation canopies.

## 8887-4, Session 1

### Optimization of spectral bands for hyperspectral remote sensing of forest vegetation

Yegor V. Dmitriev, Institute of Numerical Mathematics (Russian Federation); Vladimir V. Kozoderov, Lomonosov Moscow State Univ. (Russian Federation)

Remotely sensed images in visible and near infrared region (VNIR) are frequently used for mapping and studying changes in the forest vegetation cover. Data from hyperspectral sensors having tens and hundreds VNIR spectral bands are frequently used for detailed classification, in particular, for retrieval of species and ages of forest stands. However the high spectral resolution commonly leads to instability of training classifiers and thus the optimal selection of spectral bands used is needed.

During the last several years we are engaged in applications of hyperspectral airborne remote sensing for classification and retrieval of parameters of vegetation on regional scales. The imaging spectrometers developed by the Russian Science and Production Enterprise "Lepton" (Moscow, Zelenograd) is employed for collecting hyperspectral airborne imagery during the flight campaigns for the selected test areas of Tver region of Russia, for which we have had available ground-based forest inventory data.

The supervised classifier used for the recognition of the land surface objects is based on the Bayesian classification principle. Prior probabilities of classes are driven by the results of texture classification of the scenes under processing. The corresponding probability density functions (PDF) are estimated in the feature space formed by the normalized spectral radiances. Bayesian based classifiers suffer from the "curse of dimensionality" problem. Increasing the feature space dimensionality, we need to use considerably more independent training samples for the PDF estimation.

For regularization of classifiers used we have to optimally reduce the feature space by selecting the most informative spectral bands. The standard forward selection (or step-up) method includes bands providing a maximum decrease of the total probability of error in the classifier until the decrease becomes insignificant. The optimal set of bands obtained using this method is commonly very sensitive to small changes of the training set. We proposed the method which allows us to overcome this problem.

In the first step we select the spectral bands ensuring the exact classification of some groups of objects such as water, soils and vegetation using the training set. To find estimates of the classification error we applied the known holdout cross-validation method with the parameter 0.5. The bands obtained are used as the starting ones for the further classification procedure. In the second step we obtain the optimal sets of bands for the groups of objects which can't be exactly distinguished – subclasses of water and soils, species of meadow and forest vegetation, ages of trees for areas of the uniform composition. Combining the forward selection and the stochastic resampling for each of these groups, we obtain the set of optimal subsequences of the bands, from which we form further the stable sequences using the maximum likelihood approach that is optimal for the groups mentioned above. These sequences of the selected spectral bands were used for processing hyper-spectral images of Tver forestry. The comparison with the ground-based information shows the validity of the method proposed.

The work was supported by Ministry of Education and Science of the Russian Federation and by Russian Foundation for Basic Research.

## 8887-5, Session 2

### Ingesting MODIS land surface classification into AOD retrievals

Barry M. Gross, Adam Atia, The City College of New York (United States); Nabin Malakar, The City College of New York (CCNY) (United States); Ana J. Picon, U.S. Patent and Trademark Office (United States); Fred Moshary, The City College of New York (United States)

As urbanization continues to grow, retrieval of aerosols in higher urbanized areas becomes more important and successful unbiased retrievals in urban areas will become more important both for air quality and in climate applications. However, retrieval of AOD by satellite remote sensing measurements over land is complicated by the fact that the Top of Atmosphere (TOA) reflectance is a combination of the desired atmospheric path reflectance as well as the ground reflectance. To avoid this problem, AOD retrieval with the MODIS instrument attempts to isolate "dark" pixels such as dense dark vegetation.

To account for land surface reflection properties, the latest MODIS retrieval algorithm over land tries to improve on surface albedo modeling using collocated MODIS and AERONET sky radiometer data to improve the VIS – SWIR ratios. However, the matchup data taken on a global scale still was heavily concentrated over vegetated areas since there are very few urban AERONET sites and the resulting surface models are incapable of describing the urban surface reflection ratios properly.

On the other hand, MODIS land classification data may be able to provide more information that will allow us to use urban based surface models to improve on retrievals. The purpose of this presentation is to demonstrate that the C005 surface models trained on a global scale and used by the MODIS algorithm to estimate the ground reflectance is not appropriate for urban areas and that the use of Urban based surface models together with a land classification flag can remove biases and improve retrieval.

In this presentation, we illustrate the use of this approach in processing operational 10km level 2 MODIS retrievals. In figure 1a, the urban classification of the North East US is displayed while the VIS/SWIR ration as a function of the modified vegetation (MVI) index is given in figure 1b. We note that for high MVI, the C005 model is reasonable but for low MVI, the C005 model behaves differently at low MVI.

It should be pointed out that the very different behavior in the VIS/SWIR ratio is due to the spectral difference between soil/vegetation mixtures and urban surface/vegetation mixtures. Statistical Modeling using the ASTER spectral library which stores the spectral response of different materials is in reasonable quantitative agreement with the observations.

Therefore, we can use a "Boolean" approach where the C005 retrievals are adjusted only if the pixels are determined to be urban dominated. Then, we use the urban model for the VIS/SWIR ratio which has a very different quantitative and quantitative behavior difference. When applied to areas such as the NYC area where heavy urbanized behavior is observed, large biases in the AOD retrieval are removed.

In addition, we explore the robustness of this approach over different urbanized regions and assess other factors which may come into play. Finally, we explore the approach for high resolution data (3km) as part of the operational collect 6.

## 8887-6, Session 2

### Using high resolution CIR imagery in the classification of non-cropped areas in agricultural landscapes in the UK

Jerome O'Connell, Ute Bradter, Tim Benton, Univ. of Leeds (United Kingdom)

Food security is increasingly being recognized as one of the most pressing global issues. It remains a significant challenge to deliver high levels of food production in a way that does not damage the environment and compromise other ecosystem services. International research suggests considerable potential in improving the provision

of ecosystem services such as carbon sequestration, water quality, flood alleviation, pollination and pest control through targeted management at landscape rather than farm scale. This requires policy to be implemented in a spatially explicit context, so that features located where they will have greater benefit for ecosystem services are valued more highly than those in locations where they will have less impact. With data on yields, on landscape-level biodiversity and an understanding of the spatial land use of key ecosystem service providers (e.g. pollinators), mathematical models can advise on the optimal management of individual farms and fields. The constraint is that data on landscape-level biodiversity are only sparsely available due to the costs of collecting a range of biodiversity measures on the ground over large areas.

This study, which is part of a wider project on modelling of biodiversity and ecosystem services, aims to help fill this information gap by using high spatial resolution remote sensing data to classify non-cropped areas in agricultural landscapes. The accuracy of various edge detection filters (i.e. Sobel, Canny, Lee Sigma, Laplacian) to detect boundary pixels indicative of transitions between cropped and non-cropped areas will be tested in a 55,000 ha area of east England (52.38° lat, 0.81° long) using the UK's Landmap Colour Infra Red (CIR) aerial photography dataset. Accuracy assessment will be done based on existing vector data on hedgerow and margin locations within the study area. A multiple ring buffer will be created and a distance function used to examine the spatial correlation between the edge pixels and the vector data. The intensity of the edge pixels will then be used in a regional growth algorithm to create a 40 m buffer around all boundary areas. Statistical (e.g. variance, coefficient of variance), textural (e.g. grey level coherence matrix) and spectral (e.g. vegetation thresholds) variables will then be used in an object orientated hierarchical classification scheme to classify hedgerows, herbaceous ground vegetation and trees (i.e. typical non-cropped habitats) within these boundary areas. Once validated in the test area the system will be calibrated to suit imagery taken in multiple landscapes of varying composition scale and temporal resolution using localized variables instead of fixed parameters. Large scale mapping of non-cropped areas in agricultural landscapes will provide a valuable dataset for ecological modelling of biodiversity and ecosystem services and therefore aid policy makers and landowners in the targeted creation and maintenance of habitats to enhance the sustainability of intensively managed landscapes.

### 8887-7, Session 2

#### **Alternating least-squares unmixing for the extraction of sub-pixel information from agricultural areas**

Laurent Tits, Katholieke Univ. Leuven (Belgium); Ben Somers, VITO NV (Belgium); Wouter Saeys, Pol Coppin, Katholieke Univ. Leuven (Belgium)

Multivariate Curve Resolution with Alternating Least Squares (ALS) is a blind source separation method commonly used in Chemometrics to simultaneously estimate the absorption spectrum and concentration of the different components in a chemical sample.

In this study, the transferability of ALS from Chemometrics to agricultural Remote Sensing is evaluated. In hyperspectral agricultural image scenes, mixed pixels prevail due to the discontinuous open canopies typical for most (perennial) cropping systems. Due to this subpixel contribution of background soils and shadows, a direct interpretation of hyperspectral imagery and the extraction of biophysical parameters from the measured hyperspectral signature is hampered. Spectral unmixing (or sub-pixel feature extraction) has become an indispensable processing step for proper hyperspectral image interpretation in agricultural areas. Yet, traditional unmixing techniques only allow to estimate the sub-pixel cover distribution of the different components but fail to provide an estimate of the pure spectral signature of the crop component from a mixed hyperspectral signal. This info is crucial however, as this pure crop signature can be used to monitor the health status of the trees, without the background contamination of the soil component hampering the correct interpretation of the image. Here we anticipate that ALS can provide a solution. ALS estimates both the concentration and the absorption spectra of the different components in a chemical sample and this can easily be translated into estimating both the subpixel cover fraction and spectral signature of the different components (endmembers) in a mixed image pixel. This extraction of the pure vegetation spectrum

can on its turn lead to an improved estimation of biophysical crop parameters. The ALS model was tested on simulated hyperspectral images of Citrus orchards in which ray-tracing software was used to realistically incorporate spectral variability, multiple scattering and shadowing effects. Both the accuracy of the extracted cover fractions and the pure spectral signatures of the crop were assessed, as well as the accuracy with which the biophysical parameters of the trees (i.e. chlorophyll content, leaf water content and Leaf Area Index) could be derived from the extracted crop signature. Two different stress distributions were induced, i.e. stress at block-level, and randomly distributed stress. ALS indeed allowed to simultaneously estimate the subpixel cover distribution (RMSE < 0.10), as well as the pure spectral signatures of the different endmembers per pixel (Relative RMSE < 0.12). This extracted tree signature enabled a considerable improvement of the extraction of the biophysical parameters (R<sup>2</sup> up to 0.43). In addition, large patches of stressed trees could be better detected than isolated stressed trees. ALS thus provides a promising new image analysis tool for agricultural remote sensing. Current research focuses on the validation of the proposed methodology on a real 2 m resolution hyperspectral image of a citrus orchard.

### 8887-8, Session 2

#### **Integrated analysis of ASTER and Landsat data to map land cover change using vegetation indices**

Wafa T. Nori, Univ. of Kordofan (Sudan); Elmar Csaplovics, Technische Univ. Dresden (Germany)

This paper reviews change detection by different vegetation indices primarily in forest ecosystems. A variety of digital change detection techniques has been developed in the past three decades. Spectral vegetation indices are among the most broadly used satellite data products providing key measurements for climate, hydrologic, land cover change detection, natural resource management and sustainable development.

The objective of this study was to evaluate the potential for monitoring forest change in El Rawashda forest, Sudan, using Landsat ETM data and Aster data for two periods (2000 - 2003 and 2003 - 2006). This was accomplished by performing three widely used vegetation indices: Normalized Difference Vegetation Index (NDVI), Soil Adjusted Vegetation Index (SAVI), and Transformed Difference Vegetation Index (TDVI). These indices were applied to a case study in El Rawashda forest reserve, Gedaref State, Sudan, and their results and accuracy were discussed.

Landsat 7 Enhanced Thematic Mapper (ETM+) data acquired on March 29 of the year 2000, ETM+ data acquired on March 22, 2003 and Aster data acquired on February 26, 2006 were used for analyzing an area covering approximately 27290 hectares as area of interest.

El Rawashda forest reserve, Gedaref State is situated at approximately latitude 140 15 N and longitude 350 45 E. Climatologically El Rawashda lies in the semiarid zone. The forest is located near the transition between two main vegetation types of low-rainfall woodland savanna on clay: *Acacia mellifera* thorn land and *Acacia seyal*-*Balanites aegyptiaca* woodland. The length of the rainy season fluctuates around the four months between June and September reaching its peak in August. Most of the rains fall from June/July to October/November.

Vegetation index and difference images were constructed for all three vegetation indices (NDVI, SAVI and TDVI). Changes in vegetation cover have been highlighted by subtracting 2000 vegetation index values from 2003 values and 2003 vegetation index values from 2006 values. Accuracy assessment based on change/no-change pixels was performed. The result of the reference map for change/no change was subtracted from the result of change/no change map of each vegetation indices change detection technique Results showed that the vegetation index maps obtained by NDVI and SAVI transformations within each computational group were similar in terms of spatial distribution pattern and statistical characteristics. As far as the degree of greenness of vegetation was concerned, the TDVI appeared to be the most sensitive. For the first period, the highest accuracy was obtained by SAVI (62.5%); however, the poorest accuracy was achieved by TDVI (59.5%). For the second period, NDVI revealed the highest accuracy (60.1%), whereas both NDVI and SAVI counted accuracy of 59.2%. Generally, the study proved that all vegetation indices produced reasonable approaches to map land cover changes over time and help to pinpoint deforestation and regrowth in the study area.

## 8887-9, Session 2

### Analysis of urban heat island and NDVI changes in Nanning City based on Landsat TM and HJ data

Zhenghua Chen, Guangxi Univ. (China)

Small satellites of HJ are mainly used for environment and disaster monitoring which were launched by China in 2008. Both of HJ-1A and HJ-1B have a CCD camera of 30 meter resolution and with a swath of 700km. In addition, the HJ-1A has a hyperspectral sensor with the spatial resolution of 100m and swath of 50km, while the HJ-1B has a thermal infrared sensor with the spatial resolution of 150-300m and swath of 700km. The two satellites network form a 2-day revisit cycle.

Nanning is located in south of China, about 150 kilometers away from boundary. It is the permanent city of China – ASEAN (Association of Southeast Asian Nations) Expo held. Its economy developed largely in recent two decades, and urban heat island problem came apparent that realized even by common citizens. At the same time urban area expanded the scale which caused obvious NDVI decrease.

In this paper, Landsat/TM data in 2000 and HJ data in 2010 will be used. The data need preprocessed such as geometric projection and radiometric correction before surface temperature and NDVI are calculated. During sunny days surface temperature retrieving process is established by mono-window algorithm with modifying the parameter calculating formulas. And then several aspects will be analyzed and discussed as follows:

- 1) The city heat and NDVI distribution in 2000 and 2010 respectively, also some statistical results of them, such as the maximum, minimum and mean values.
- 2) The relationship between average temperature and the degree of the vegetation covered in the sampling area. And then calculate regression function of the NDVI and surface temperature.
- 3) Some suggestions about vegetation plantation plan will be provided because the city government is making Nanning the “City of Green”.

## 8887-10, Session 3

### Estimation of turbidity along the Guadalquivir estuary using Landsat TM and ETM+ images

Miriam M. Carpintero, Eva Contreras, Univ. de Córdoba (Spain); Agustín Millares, Univ. de Granada (Spain); María José Polo-Gómez, Grupo de Dinámica Fluvial e Hidrología (Spain)

Estuarine water in Mediterranean basins have high suspended sediment concentrations due to both the fine textured nature of the materials reaching the final stretch of the fluvial network, and agricultural predominance of soil uses upstream. To study the temporal and spatial distribution of turbidity, it is necessary to have a monitoring network of water quality along the study area with enough temporal and spatial resolution, which is not always available. In this way, in the last decades the use of satellite images for estimation of water quality parameters as the turbidity has been an alternative that allows mapping turbidity surface distributions, and to obtain time series for this parameter at high spatial resolution.

The Guadalquivir River estuary (Southwestern Spain) expands along 105 km between Alcalá del Río dam, upstream, and its mouth in Sanlúcar de Barrameda. It is an Atlantic mesotidal estuary (Diez-Minguito et al., 2010) with a mainly longitudinal salinity gradient. The sediments in the estuary are very fine textured due to the high length of the river and, mainly, the extreme trapping efficiency of the dense reservoir network upstream along 57500 km<sup>2</sup> of the contributing area. With an average value of 0.5-45 g L<sup>-1</sup> for the suspended sediment range along the estuary, extreme values up to 160 g L<sup>-1</sup> can be found associated to persistent turbidity events forced by different combination of conditions.

This work shows the turbidity evolution using algorithms previously developed in areas with similar characteristics to our study area. The aptitude of their application in our study area and the need to make local calibrations that collect specific conditions for their subsequent development and validation was analyzed. These algorithms allow us to obtain turbidity values from reflectance of satellite images from different spectral bands. In order to do this, Landsat TM y ETM+

images collected from August 2008 to 2010 were used, which were preventively radiometric and atmospherically preprocessed. The turbidity values obtained were contrasted with in situ measurements provided by the automatic monitoring network that transmits in real-time turbidity data with frequency intervals of 15 minutes since October 2004 along the estuary.

The results show that in the most of points there is an overestimation of the estimated values, using a common algorithm for the entire period of study, respect in situ measurements, especially in spring and summer, with estimated values of 304 NTU and measured values of 60 NTU for 10 May 2009 in the mouth of the estuary. However, this trend is not so much marked for the rest of the year, reached at the subestimation on 11 February 2009 with estimated values of 1826 NTU and measured values of 3978 NTU. This reveals how the particular meteorological conditions and own characteristics of our estuary make the reflectance values always not to follow the same behavior pattern. Resulting to a single algorithm for entire period of study without reproducing the reliability of the real situation and justify the need for local calibration.

## 8887-11, Session 3

### Comparison of approaches for water surface area segmentation using high resolution TerraSAR-X data for reservoir monitoring in a large semi-arid catchment in northeastern Brazil

Iris Kleine, Christian Rogass, Helmholtz-Zentrum Potsdam Deutsches GeoForschungsZentrum GFZ (Germany); Pedro H. Medeiros, IFCE (Brazil); Nora Meyer zu Erpen, EADS Astrium GmbH (Germany); Saskia Förster, Helmholtz-Zentrum Potsdam Deutsches GeoForschungsZentrum GFZ (Germany)

The semi-arid Northeast of Brazil is characterized by distinct rainy and dry seasons. The water supply of the local population is based on reservoirs in which precipitation is collected. There are over 150 reservoirs in the 933 km<sup>2</sup> Benguê catchment, but little is known about the dynamic of the reservoirs. In this study, we use TerraSAR-X imagery for a year-long monitoring of reservoir surface areas and their seasonal changes. The precise extraction of the reservoir surface areas forms the basis of the monitoring. Therefore, we tested a pixel-based threshold classification, a feature-based segmentation (mean shift) and a manual digitization. The results of the manual digitization and threshold classification were similar as both tended to underestimate the water surface area in comparison to GPS in situ data. The mean shift segmentation, however, tended to spread over the shorelines into the surrounding areas. The distinction of small reservoirs and similar looking dark areas proved to be a challenge for the threshold classification and mean shift segmentation. We used the threshold classification for the analysis of 47 TerraSAR-X images, complemented by several approaches for the removal of misclassification in the reservoir data set. The viewing direction of the TerraSAR-X sensor was also important for the distinction of the entire area of the reservoirs. Geometric effects at the shorelines shaded parts of the water surface area. For the monitoring of the reservoir area with only one viewing direction we derived an empirical geometry correction factor.

## 8887-12, Session 3

### Correlation between the habitats productivity and species richness

#### (amphibians and reptiles) in Portugal, through remote sensed data

Ana Cláudia M. Teodoro, Univ. de Porto (Portugal); Neftali P. Sillero, Susana Alves, Lia Duarte, Univ. of Porto (Portugal)

Many reptile and amphibians species are threatened by habitat loss, modification, and fragmentation. However, the way in which changes in landscape patterns influence intraspecific ecological processes is not completely understood [1]. Remotely sensed data are powerful for characterizing habitat at broad extents, for example to describe

landscape configuration, habitats characteristics and for assessing biodiversity.

The Portuguese Atlas of Amphibians and Reptiles was published in 2008 [2]. The project database, with more than 82 000 of records, was used to produce species distribution maps. The field work (carried out between January of 2003 and November of 2005) for amphibians were performed using dip-netting, egg search on water vegetation and margins, refuge search, night search for calls and raining-night search by car for migrating individuals on roads [3] Reptiles were searched using visual encounter surveys and refuge search [3]. All the observations were recorded with GPS devices (Garmin @12 and Garmin @ e-Trex Venture). The maximum error of GPS points never exceeded 12 m. During this project two types of maps were produced in a GIS environment: i) species distribution, and ii) "species richness" (number of species per grid) [3].

Several biogeographic theories propose that the species richness depends on the structure and ecosystems diversity. The habitats productivity can be evaluated through satellite imagery, namely using vegetation indices (e.g., NDVI). Therefore, using the data presented in the Portuguese Atlas of Amphibians and Reptiles [2] the correlation between species richness and remote sensing products was analysed into different spatial resolutions: 1 km (Vegetation data), 250 m (MODIS NDVI products) and 30 m (Landsat images).

Three different study areas were chosen to perform this research. The studies areas selected corresponded to the Landsat scenes path 203 and rows 31, 32 and 33. The three areas selected corresponded to areas with different climatic and habitat characteristics, located in the north, center and south of Portugal. The NDVI indices and all the images were calculated/processed in an open source software. Several plugins were developed in order to automatize several procedures. The correlation analysis allowed to conclude that habitats with high productivity (high NDVI) presented high values of species richness (high R2). Moreover, the satellite data with more spatial resolution (Landsat) is most suitable for this type of studies.

[1] Cardozo, G., Margarita Chiaraviglio, M., 2008. Landscape changes influence the reproductive behaviour of a key 'capital breeder' snake (*Boa constrictor occidentalis*) in the Gran Chaco region, Argentina. *Biological Conservation*, 141, 3050-3058.

[2] Loureiro, A., Ferrand de Almeida, N., Carretero, M.A. & Paulo, O.S. (eds.) (2008): *Atlas dos Anfíbios e Répteis de Portugal*. Instituto da Conservação da Natureza e da Biodiversidade, Lisboa. 257 pp.

[3] Sillero, N., Celaya, L., & Martín-Alfageme, S. (2005). Using GIS to Make An Atlas: A Proposal to Collect, Store, Map and Analyse Chorological Data for Herpetofauna. *Revista Española de Herpetología*, 19, 87-101

### 8887-13, Session 3

## Water surface temperature profiles for the Rhine River derived from Landsat ETM+ data

Katharina Fricke, Björn Baschek, Bundesanstalt für Gewässerkunde (Germany)

Water temperature influences physical and chemical parameters of rivers and streams and is an important parameter for water quality. It is a crucial factor for the existence and the growth of animal and plant species in the river ecosystem. The aim of the research project "Remote sensing of water surface temperature" at the Federal Institute of Hydrology (BfG), Germany, is to supplement point measurements of water temperature with remote sensing methodology. The research area investigated here is the Upper and Middle Rhine River, where continuous measurements of water temperature are already available for several water quality monitoring stations. Satellite imagery is used to complement these point measurements and to generate longitudinal temperature profiles for a better systematic understanding of the changes in river temperature along its course.

Several products for sea surface temperature derived from radiances in the thermal infrared are available, but for water temperature from rivers less research has been carried out. Problems arise from the characteristics of the river valley and morphology and the proximity to the riverbank. Depending on the river width, a certain spatial resolution of the satellite images is necessary to allow for an accurate identification of the river surface temperature and several problems. The bands from ASTER, Landsat TM and ETM+ sensors in the thermal infrared region offer a possibility to extract the water temperature of

a sufficiently wide river such as the Rhine. Mixing of the upper water layers simplifies the comparison of temperatures from satellite and in situ measurements. The extracted radiance temperatures can be used to interpolate between in situ measurements available only for a limited number of points along the river course and to create longitudinal temperature profiles for rivers at multiple points in time.

For this purpose, several temperature data sets derived from Landsat and ASTER radiances and ASTER temperature products and in situ measurements were compared. The observed radiance temperatures are strongly influenced by the atmosphere. Thus, a correction of atmospheric influences on radiances measured at the top of the atmosphere was necessary and two different methods for atmospheric correction (ATCOR 2 and single atmospheric profiles calculated with MODTRAN) were applied. The correction results showed that for both methods, the correct choice of atmospheric profiles is very important. Additionally, problems such as cloud cover, shadowing effects, georeferencing errors, different emissivity of water and land, adjacency and mixed pixel effects had to be accounted for and their effects on the radiance temperatures will be discussed.

From the corrected radiances and the ASTER temperature product, example profiles of the surface water temperature in the Upper and Middle Rhine could be calculated for different seasons. On the basis of these profiles, temperature gradients are identified and the possibility to detect heat or cooling discharge from tributaries and other sources is evaluated.

### 8887-14, Session 3

## Fluorescence LIDAR remote sensing of oils: merging spectral and time-decay measurements

Lorenzo Palombi, David Lognoli, Valentina Raimondi, Istituto di Fisica Applicata Nello Carrara (Italy)

The fluorescence lidar is considered an effective and reliable tool for the detection and classification of oil spills, since it is able to detect oils in several scenarios that are highly unfavourable to other techniques. The fluorescence lidar technique is in fact able to detect oil also in water-oil emulsions, on weeds or ice banks and in sediments under the water surface.

Fluorescence-based classification of oils typically relies on the detection of the spectral signature of the oil. Another method of classification is based on fluorescence time-decay measurements of oils, which have fluorescence lifetimes ranging from 1 ns to 20 ns. This type of technique as well is suitable for remote sensing applications and is based on measurement of the average fluorescence lifetime at a limited number of different emission wavelengths.

In this paper we present a method that merges both fluorescence spectral and time decay signatures of oils for enhancing the potential, in terms of oil classification, of the technique. The hyperspectral fluorescence matrixes, which are resolved both in the spectral and temporal domains, are obtained by using a fluorescence lidar system. The lidar uses a tripled-frequency Nd:YAG laser emitting at 355 nm as excitation source. The collecting optics is a Newtonian telescope (1 m focal length, f/4). The collected light is spectrally dispersed by a spectrometer and detected by an intensified 512x512-pixel CCD camera. The dispersion-detection system performs a nominal spectral resolution from 0.02 nm/ch to 0.5 nm/ch depending on the used grating. The intensified camera is gateable with a minimum gating time down to 5 ns. The nanosecond nominal temporal resolution is achieved by sequentially delaying the time between the laser shot and the camera gating time that is fixed at its minimum. The acquired time-wavelength matrix can be processed to take into account the convolution effects of the laser pulse temporal shape and gating time to obtain time evolution parameters for each measured spectral channel with sub nanosecond precision. The technique is also suitable for monitoring the degradation process of an oil slick by tracking simultaneously the variations in the spectral shape and in the decay time of the different components of the fluorescence signal. The lidar system is also equipped with a computer-controlled motorized steering mirror for acquiring images of the investigated scenarios by using a whiskbroom acquisition mode.



8887-15, Session 3

**Assessing distribution patterns, extent and current condition of Mangrove in Iranian coast of Persian Gulf**

Alireza Salehipour Milani, Razyeh Lak, Geological Survey of Iran (Iran, Islamic Republic of)

Iranian mangrove forests occur between 25°11'N to 27°52'N. These forests exist in the north part of the Persian Gulf and Oman Sea, along three Maritime Provinces in the south of Iran. These provinces respectively from southwest to southeast of Iran, include Bushehr, Hormozgan and Sistan & Balouchestan. The Mangroves play important roles mainly in aquaculture and finishing. And beside that they are great nursery for aquatic animals like fishes and place of reproduction for birds. As well as protection of shorelines against massive waves and tsunamis. Approximately 35% of world mangrove area was lost during the last several decades of the twentieth century (in countries for which sufficient data exist), which encompass about half of the area of mangroves. Likewise, the 2010 update of the World Mangrove Atlas (WMA) indicated a fifth of the world's mangrove ecosystems have been lost since 1980. Now, scientists have used satellite images to compile the most comprehensive map of mangroves worldwide, which should help in future efforts in monitoring and conservation. We determined the spatial extent of the mangrove forest in the Persian Gulf using remotely sensed satellite data and estimated changes in the spatial extent of the forest from the 1973 through 2008 using Landsat satellite images from Multispectral Scanner Landsat (MSS) (1976), Thematic Mapper (TM) (1989), Enhanced Thematic Mapper plus (ETM+) (2000, 2006) and IRS LISS III (2008) sensors. In this research we used normalized differential vegetation index (NDVI). Change detection was applied and mangrove in the study area was found to have increased by about 65% from 1974 to 2008.

8887-16, Session 4

**A case study of a precision fertilizer application task generation for wheat based on classified hyperspectral data from UAV combined with farm history data**

Jere Kaivosoja, Liisa Pesonen, MTT Agrifood Research Finland (Finland); Jouko Kleemola, Tmi Jouko Kleemola (Finland); Ilkka Pölönen, Heikki A. Salo, Univ. of Jyväskylä (Finland); Eija Honkavaara, Finnish Geodetic Institute (Finland); Heikki Saari, Jussi H. Mäkynen, VTT Photonic Devices and Measurement Solutions (Finland); Ari Rajala, MTT Agrifood Research Finland (Finland)

Different remote sensing methods for detecting variations in agricultural fields have been studied long time. Typically the aim is to gain better yields and optimize inputs while reducing the environmental loads by employing precision farming techniques. There are already existing systems for planning and applying e.g. nitrogen fertilizers to the cereals. However, several reasons such as high costs, adaptability, reliability and resolution aspects together with a final products dissemination have activated researchers to seek alternative and more flexible methods by applying new technologies to the remote sensing. With unmanned aerial vehicle (UAV) based airborne methods, data collection can be performed cost-efficiently especially with desired spatial and temporal resolutions and also below clouds and under diverse weather conditions. Also, a new Fabry-Perot interferometer based hyperspectral imaging technology implemented in an UAV has been introduced to determine for instance infield variations in crop productivity. On top of this, there has been lack of adapting determined variations into the farming practices. In this research, we studied advanced possibilities of exploiting classified raster maps originating from the hyperspectral data cube to produce an application task for a precision fertilizer application aiming for a higher yield.

The UAV flight campaign with the hyperspectral imaging system in a wheat test field was performed in Finland at the 60 degrees of latitude in the summer 2012. Based on the campaign and as a starting point of this study, we had a classified raster maps estimating the biomass and nitrogen contents at stem elongation phase (accumulated temperature sum 320 °C), representing approximately stage 34

in the Zadoks scale. By applying agricultural and technological knowledge, we combined the classified maps together with relative yield maps from three previous years and with the spring fertilization map weighting each input separately. We used the previous yield maps to estimate a spatial yield potential and the smoothed nitrogen input map to avoid an overload. Then we generalized the combined results and transformed it to a vectorized zonal task map suitable for farm machinery. As results, we present the selected weights for each dataset in the processing chain and the resultant variable rate application (VRA) task. A plant nitrogen content of 3 % and about 1700 kg/ha of dry biomass were selected as the main dividing levels for the nitrogen application rates deriving lower rates when exceeded. The extra fertilization was shown to be beneficial. However, our study is indicating that even with absolute value estimations produced by remote sensing, there are still checking, fitting and estimations required. The effects and logics of different datasets are discussed in detail in the paper outlining the requirements for the accuracy of image classification. The presented case study showed a promising way how to produce precision application tasks for nitrogen fertilization from classified high resolution image mosaics.

8887-17, Session 4

**Assessing pasture quality and degradation status using hyperspectral imaging: a case study from western Tibet**

Lukas W. Lehnert, Philipps-Univ. Marburg (Germany); Hanna Meyer, Faculty of Geography, Philipps-University of Marburg (Germany); Nele Meßer, Department of Geography, University of Bonn (Germany); Christoph Reudenbach, Jörg Bendix, Faculty of Geography, Philipps-University of Marburg (Germany)

Alpine grasslands on the Tibetan Plateau (TP) are suffering from pasture degradation induced by over-grazing, climate change and improper livestock management. Meanwhile, the status of pastures is largely unknown especially in poor accessible western parts on the TP. The aim of this case study was to assess the suitability of hyperspectral imaging to predict quality and amount of forage on the western TP. Therefore, 18 ground-based hyperspectral images taken with a Specim eNIR camera along two transects on a winter pasture were used to estimate leaf chlorophyll content, green plant cover (PV) and proportion of grasses. For calibration and validation purposes, chlorophyll content of 20 grass plants was measured in situ with a chlorophyll meter. From the images reference spectra of grass and non-grass species were collected. PV was assessed from similarity of images to mean vegetation spectra using spectral angle mapper and simple threshold classifications. A set of 48 previously published hyperspectral vegetation indices (VI) was used as predictors to estimate chlorophyll content and to discriminate grass and non-grass pixels. Separation into grass and non-grass species was performed using partial least squares (PLS) discriminant analysis and chlorophyll content was estimated with PLS regression. The accuracy of the models was assessed with leave-one-out cross validation and normalised root mean square errors (nRMSE) for chlorophyll and contingency matrices for grass classification and total PV separation. Highest error rates were observed for discrimination between vegetated and non-vegetated parts, whilst accuracies of grass and non grass separation (Overall accuracy = 0.98) and chlorophyll estimation were higher (nRMSE = 10.7). PV, grass percentage and chlorophyll content were combined to estimate forage amount and quality along both transects.

8887-18, Session 4

**Hyperspectral imaging based biomass and nitrogen content estimations from lightweight UAV**

Ilkka Pölönen, Univ. of Jyväskylä (Finland); Heikki Saari, VTT Technical Research Ctr. of Finland (Finland); Jere Kaivosoja, MTT Agrifood Research Finland (Finland); Eija Honkavaara, Finnish Geodetic Institute (Finland); Liisa Pesonen, MTT Agrifood Research Finland (Finland)

In this paper we introduce results from the UASI (Unmanned airplane system innovations) -project. Project was multidisciplinary research project between VTT, MTT, Metla and University of Jyväskylä. In this project we developed novel miniature size hyperspectral imager. Key-innovation here is the Fabry-Perot interferometer (FPI), which tunes imaged wavebands. This hyperspectral imager takes whole plane at once, which enables stereoscopic and spectrometric measurements from light-weight imaging platforms such as UAV's. Imager works between 450 to 900 nm and it takes images size 2048x2048 pixels. With 2x binning image size is 1024x648 pixels. The amount of spectral bands and their place can be flexibly select because of FPI. In this research we used 30 bands from 500 nm to 870 nm.

During summers 2011 and 2012 we collected hyperspectral data from Finnish wheat and barley fields. Both year also field samples (1m x 1m) were collected. Samples properties were measured in the laboratory conditions. The measurements included dry biomass, wetness, nitrogen content etc... Hyperspectral images were tailored to one image mosaic. Also some radiometric corrections was made. From data cube we extracted features based on unmixing. KNN-based estimator was trained based on field sample measurements. As a final result estimator gives us biomass and nitrogen content estimation maps with high spatial resolution (one pixel is 10 cm x 10cm). Results are promising and those show that whole concept of small hyperspectral imager, UAV and data analysis is ready to operational use. Based on biomass and nitrogen content estimations it is possible make more accurate fertilization maps.

#### 8887-19, Session 4

### Remote estimation of nitrogen contents of summer corn leaf by hyperspectral reflectance using spectral vegetation indices

Muhammad Naveed Tahir, Pir Mehr Ali Shah Arid Agriculture Univ. Rawalpindi (Pakistan) and Northwest A&F Univ. (China); Jun Li, Fuqi Yao, Northwest A&F Univ. (China)

Accuracy and precision of nitrogen estimation can be improved by hyperspectral remote sensing that leads effective management of nitrogen application in precision agriculture. The objectives of this experiment were to identify N sensitive spectral wavelengths, their combinations and spectral vegetation indices (SVIs) that are indicative of nitrogen nutritional condition and to analyze the accuracy of different spectral parameters for remote estimation of nitrogen status temporally. A study was conducted during 2010-11 at Agricultural Research Station, Northwest A & F University, Yangling, China, to determine the relationship between leaf hyperspectral reflectance (350-1075 nm) and leaf N contents in the field-grown corn (*Zea mays* L.) under five nitrogen rates (0, 60, 120, 180, and 240 kg/ha pure nitrogen) were measured at key developmental stages. The fitting of linear and nonlinear regressions models between leaves total nitrogen and the spectral of original reflectance were made. The accuracy of nitrogen nutrition diagnosis among the single (R) and dual (R1+R2) waveband spectral reflectance and spectral vegetation indices including, the spectral ratio (SR) in the green, red and infrared, NDVI, GNDVI, and SAVI were compared. Chose the highest determination of coefficient (R<sup>2</sup>) model and lowest RMSE and RRMSE at each growth stage, took the smaller as the best model. The results showed that there were good fitting between nitrogen contents and their single spectrum parameters at R450, R550, R630, R710 at 10-12 leaf, followed by silking, tasseling, and early dent stage, respectively. The relationship among the dual spectrum parameters and leaf nitrogen was better with R550+R710 at early dent stage of the corn crop. Spectral ratios in the NIR/Red with R810/R670 showed highest R<sup>2</sup> and lowest RMSE at 10-12 leaf and silking stage followed by NIR/Green with R780/R740 and NIR/NIR with R810/R670 and at silking stage and 10-12 leaf stages respectively. Overall GNDVI showed the highest R<sup>2</sup> and lowest RMSE values among all the SVIs at 10-12 leaf stage (0.88, 1.75), silking stage (0.80, 2.02) followed by NDVI while SAVI was the best indicator of nitrogen contents during early stage of the crop (at 6-8 leaf stages). The results indicated that leaf nitrogen status can be best predicted at 10-12 leaf stage and silking stage by using SVIs indices with GNDVI, tasseling (NDVI), 6-8 leaf stages (SAVI), early dent stage (R550+R710, NIR/Red). The study results showed that leaf hyperspectral reflectance can be used for real time, more reliable and quick monitoring of corn leaves nitrogen status and important tool for N fertilizer management in precision agriculture.

#### 8887-54, Session PS

### Monitoring and analysis of degradation using remote sensing in semi-arid lands of gash agricultural scheme, Eastern Sudan

Majdaldin Rahamtallah Abualgasim, GWT-TUD GmbH (Germany); Elmar Csaplovics, Technische Univ. Dresden (Germany); Osunmadewa Babatunde Adeniyi, GWT-TUD GmbH (Germany)

Agriculture is considered the backbone of the Sudanese national economy, approximately 80% of exports come from agricultural products and about 60% of the manpower works in the agricultural field activities. Almost half of Sudan's population live in rural areas and depend of their livelihood on the agricultural products for themselves and for their animals. Gash agricultural scheme (GAS) is considered one of many important agricultural schemes in Sudan, and one of the pilot schemes in eastern Sudan, the scheme located in Kassala state, Eastern Sudan, it was constructed to helps in stabilize the poor nomads, and to increase the rural development in the gash area and the areas around it for growing cotton as cash crop and other crops for local consumption. The scheme located in semi-arid region, where the human activities such as livestock overgrazing by nomads has influenced the ecological pattern of the area thereby resulting to loss of natural vegetation, reduction of ground water via a low of rainfall trend and decrease in clay soil, encroachment of sand which accelerate desert condition and invasion of unfavourable mesquite tree. The scheme has undergone to a shocking deterioration before two decades as a result of above factors in addition to periods of drought which suffered the country, which led to the deterioration of resources and decreased the cultivated land and hence led to decreased of the scheme productivity. This study is attempted to monitor, assess and to analysis the impacts of land degradation process and variation of land use land cover in the situ of study specifically in the cultivated area of the scheme. To achieve that, and to extract information for overall condition which occurred in the area, free cloudy Multi-temporal remotely sensed data Landsat imageries MSS, TM, ETM+ and ASTER for the years 1972,1987,1999 and 2010 respectively, acquisition in dry season to mitigate the seasonal fluctuation, were used covering the situ of study, combining with GIS techniques. Some correction methods have been done e.g. re-sampling and rectification, radiometric, geometric and atmospheric corrections to removed distortions and removal of differentiate in geographical location, using both Envi and Erdas softwares. Comparison of Both of object orient classification (OOC) via multiresolution segmentation rules using the recent eCognition technique and maximum likelihood classification (MLC) using Erdas imagine, integration with GIS technique to identify land cover land use classes namely: High dense mesquite trees (HDM), low dense mesquite trees (LDM), clay soil (cultivated) (CS), fine stabilized sand (FSS) and mobile sand (MS). To statistical analyze the final results using SPSS package and visual interpretation with verification of ground truth points to finalize the results and creation the final maps. The final results revealed that there were drastic change occurred during the period of the study, showed that a rapid increased of stabilized (25.89, 31.40, 55.71 and 24.87%) and mobile sand (14.62, 20.27, 24.85 and 17.13%) while decreased of clay soil (24.22, 23.28, 15.73 and 11.6), this observed that decreased in cultivated land over time, the results also observed of increased of mesquite trees (13.66, 9.73, 18.85 and 20.17%) invasion and expansion elsewhere as a result of miss use of irrigation water. This study demonstrates that remote sensing has ability to estimating and assessing degradation and impacts whereas the conventional method provides only areal reference in semi arid zone.

#### 8887-55, Session PS

### Evaluation of land ecological environment in Zhoushan islands by remotely sensed impervious surfaces

Xiao Ping Zhang, Delu Pan, Jianyu Chen, The Second Institute of Oceanography, SOA (China); Peng Chen, Yonghong Jia, Wuhan University (China)

Urbanization and urban sprawl have become a major concern throughout the coastal zones of China. During the past 20 years, Zhoushan islands are subject to rapid and increasing changes with

the implement of cross-sea bridge between Zhoushan and Ningbo city. The natural landscape of Zhoushan City is replaced by large amounts of impervious surfaces such as paved roads, driveways, parking lots, buildings, rooftops, to name a few. The expansion of impervious surfaces can affect urban hydrological cycle, surface runoff, water quality, local climate and biological diversity through the construction. Evaluation of the influences of anthropogenic activities to land ecological environment is crucial to urban development of in Zhoushan islands. In this paper, the Landsat TM images of 1986, 1995, and 2006 were utilized. Combining the normalized difference impervious surface index (NDISI) and complement of vegetation fraction, we derived impervious surfaces images. High resolution data of SPOT5 and aerial photographs were used to verified impervious surfaces maps, with correlation coefficient falling above 0.6 and mean relative error (MRE) controlled in 15%. Specifically, considering the spectral features of brine pan, tidal zone, water and dry land easily confused with impervious surfaces in islands, preprocessing of masks were added to extract fine impervious surfaces. Then to access land ecological environment of islands based on impervious surfaces, an integrated indicator (S) was introduced to discuss the change of underlying surfaces influenced by humans in Zhoushan islands. Here, the concept of VOR (Vigor, Organization, Resilience) was borrowed to set three parts of S. For each island (subset of the study area), percentage of impervious surfaces areas (ISA) accounting for Zhoushan islands was taken to record the V. The product of the average impervious surface coverage and the level of area ratio was the O. R was assigned, according to the contribution of different land use types to island ecosystem. Finally, the results showed that: (1) ISA of Zhoushan islands are remarkably increasing, from 19.2 km<sup>2</sup> in 1986 to 58.2 km<sup>2</sup> in 2006. (2) The levels of imperviousness for total areas in 1986, 1995, and 2006 were 2.73%, 4.20%, and 8.27% respectively. (3) The value of S for the whole research area was 0.66, 0.61, and 0.50 respectively for 1986, 1995, and 2006. (4) It was indicated that land ecological environment was variously disturbed by human activities. Among Changbai Island and Changzhi Island had little change, keeping a high ecological health value, and while Jintang Island, Xiushan Island, Damao Island and Zhoushan Island displaying a general downtrend from 1986 to 2006. (5) Further, we found that factors of island size, spatial location with Zhoushan, economic policy that constructing the major island and to emigrate from minor islands contributed to the faster increment in ISA for each island. Results from this research can be used by policymakers for island management, planning, and for ecological and hydrological modeling to determine the effect of the increasing ISA on coastal environments in urban development of Zhoushan islands.

#### 8887-56, Session PS

### Simulation and forecasting changes of typical lakes in Nam Co Lake in Tibetan Plateau using remote sensing data (1980-2020)

Yanhong Wu, Liping Lei, Bing Zhang, Institute of Remote Sensing and Digital Earth (China)

Climate changes are expected to seriously affect the water resources of the Tibetan Plateau. Inland lakes that are widely distributed on the Tibetan Plateau have minimum impact of human activities and are an important component of the water supply in China. A series of satellite-based environmental data archives including variation of snow cover, vegetation phenology and lake level, together with the in situ observation data were used to monitor and simulate the variation of typical lake basins in Tibetan Plateau for the period 1980-2010. Nam Co Lake is the highest lake in the central Tibetan Plateau and there was no any meteorological observation station or hydrological station in the basin before 2005. We chose Nam Co Lake as a typical study region and our results are including:

(1) We provides a method for estimating the lake water storage based on historical meteorological records from 1976 to 2009, remote sensing images scattered in this period, in situ bathymetric survey, and GIS techniques, and presents a comprehensive 34-year analysis of intra-annual and inter-annual variations of Nam Co Lake water storage.

(2) A series of satellite imagery-based environmental data archives including variation of snow cover, vegetation phenology and lake level in Nam Co Lake Basin, were mapped.

(3) Simulation of lake level variation (1980-2010) has been conducted through modeling at a monthly time step for the first time and the contemporaneous water storage series was acquired, based on the satellite altimetric data, meteorological data and the in-situ bathymetric survey data.

(4) Water balance in the Nam Co Lake Basin during 1980-2010 is calculated, and the positive water budget affected by climate warming led to the increase of water storage during 1980 to 2010. This is of particular importance in terms of global climate change because of a severe gap in the knowledge of the short, mid and long term implications on the hydrological system in Tibetan Plateau.

(5) Scene analysis for the coming 10 years is conducted through forecasting the lake level at a monthly time step. The increasing trend is acquired and different amplitude is implied according to future climate scenarios.

The comprehensive analysis of the lakes in Tibetan Plateau indicate that there is the spatial difference for the enlarging or shrinking status of the lakes in TP. Satellite observations, which are publically available and of high quality, are a powerful tool for monitoring the state of the lakes in TP, as well as other ungauged, remote and hard to access regions. The inland lakes which depend on the rainfall and river supply in the basin are shrinking, while the lakes which depend on glacial meltwater supply are enlarging. Climate change is an important factor promoting the lake variation.

#### 8887-57, Session PS

### Poyang Lake wetland classification using time series Envisat ASAR data and Beijing-1 imagery

Lin Wang, Chinese Academy of Fishery Sciences (China) and Institute of Remote Sensing (China) and Poyang Lake Ecological Research Station for Environment and Health (China); Peng Gong, Tsinghua Univ. (China) and Univ. of California, Berkeley (United States); Iryna Dronova, Univ. of California, Berkeley (United States); Yingren Li, Chinese Academy of Fishery Sciences (China)

Beijing-1 images and ENVISAT ASAR images were used in the classification of wetland aquatic macrophytes in terms of aquatic plant functional types (PFTs) over the Poyang Lake region, China. On the one hand, the speckle noise filtering, sensor systematic calibration within the same polarization or between different polarizations, and accurate geo-registration were applied to the time-series SAR data. As a result, time-series backscattering data, here referred to as permittivity curves were obtained. On the other hand time series indices, here referred to as phenological curves, derived from time-series Beijing-1 images in the classification experiment. Based on these two curves, a rule-based classification strategy was performed to extract wetland information from the combined SAR and optical data. In the rule based wetland classification method, DEM data, submersion time index, temporal Beijing-1 images, time series normalized difference vegetation index (TSNDVI) images, principal component analysis (PCA) and temporal ratio of ASAR time series images were used. In addition, a decision tree based method was used to map the wetlands. Some conclusions reached included that: (1) after the above mentioned preprocessing of ASAR data, it is possible satisfactorily to separate different aquatic plant functional types; (2) hydrophytes from different PFTs exhibit distinct phenological, structural, moisture and roughness characteristics due to the impact of the annual inundation of Poyang Lake wetland; (3) More accurate results have been obtained with the rule-based method than the decision tree (DT) method. Producer's accuracies and user's accuracies calculated from test samples in the classification results indicate that the DT method has the potential for mapping aquatic PFTs with overall producer's accuracies exceeding 80% and higher user's accuracies for aquatic bed wetland PFTs. A comparison of producer's accuracies and user's accuracies from the rule-based classification increased from 3% to 12% and 7% to 26% for different aquatic PFTs.

8887-58, Session PS

### Monte Carlo method based radiative transfer simulation of stochastic open forest generated by circle packing application

Shengye Jin, Masayuki Tamura, Kyoto Univ. (Japan)

Monte Carlo (MC) method is an exceptional application for simulating radiative transfer regime of the Solar – Atmosphere - Landscape system. Moreover, for accurate computation of the radiation distribution over a complex landscape configuration, ex. a forest area for instance, MC method is desirable. For its robust to the complexity of the 3-D scene altering and accurately performance, MC method is most commonly employed for simulating canopy radiative transfer regime as the validation source of other radiative transfer models. In MC radiative transfer modeling within vegetation, one basic step is the canopy scene set up. 3-D scanning application was used for representing canopy structure as accurately as possible, but this is time consuming. Botanical growth function was called for modeling the single tree growing, but cannot express impaction among trees. L-System is also function controlled tree growth simulation model, but costs computing memories. Additionally, we only model the current tree pattern rather than tree growth when we simulate the radiative transfer regime. Therefore using regular solid pattern like ellipsoidal, cone, cylinder etc. to indicate single canopy is a much more constructive way. Allowing for the allelopathy phenomenon in some open forest optical image that each tree has its own 'domain' repels other trees. Simply, the projection of the canopies should not be overlapped. According to this assumption a stochastic circle packing algorithm was developed to generate the 3-D canopy scene. The canopy coverage (%) and the tree amount (N) of the 3-D scene were declared at first, similar with a random open forest image. According to them, we randomly generated each canopy radius (rc). Then set the circle central coordinate on XY-plane as well as to keep circles separated from each other by the circle packing algorithm. To model the individual tree, Ishikawa's tree growth regressive model (1989) was employed to set the tree parameters like: age (Ag), DBH (dt), tree height (H). However, we do not have the relationship between canopy height (Hc) and trunk height (Ht). Therefore we assumed the proportion between Hc and Ht is a random number in the range from 2.0 to 3.0. De Wit's leaf angle distribution functions (1965) were used within the canopy. Finally the canopy BRDF was simulated using MC method. The MC algorithm from the study of North (1996) is summarized as following steps. (1) The initialization of the photon with a position (r0), source direction (Omega0) and intensity (I0), respectively. (2) To simulate the free path (s) of a photon with the condition of (r', Omega, I'). (3) Calculate the new photon position  $r = r' + s\Omega$ . (4) New scattering direction (Omega) determination after collision at r. (5) Calculate the new intensity  $I = Gama(r, \Omega \rightarrow \Omega') I'$ , the Gama (r, Omega' -> Omega) denotes the conditional probability of scattering from direction Omega' to a unit solid angle about Omega, given that a collision occurs at point r. (6) accumulate the intensity I of photon left canopy in bin corresponding to angle Omega, otherwise redo from step (2), until I smaller than a threshold. (7) Repeat from step (1), for each photon.

8887-59, Session PS

### Using the ratio of optical channels in satellite image decoding in monitoring biodiversity of boreal forests

Yurj P. Rozhkov, State Nature Reserve Olekminsky (Russian Federation); Maria Kondakova, Hydrochemical Institute (Russian Federation)

Determination of the index of vegetation gives information about the productivity and biomass of vegetation and allows to estimate the state of the stand. Moreover, the calculation of vegetation index is carried out around the images and allows mapping for this indicator. However, it is an integral indicator. It doesn't decrypt the contribution of various tree species, age, crown density, etc. to it.

The index of vegetation determination, which made for summer and autumn satellite images, allowed to divide areas of forest, composed of deciduous, conifer-fall and conifers species. Therefore, it is possible to differentiate the pine, spruce, pinus sibirica forests on the one

hand, and birch, larch, alder forests on the other. Using of a tool for the synthesis of optical channels (Stack images) allows to combine in a single multispectral image results of the determination of vegetation indices, which made in different months.

The use of tools or subtract the difference between channels (Image Difference) is another way to differentiate between forest types and to assess his condition. The difference between pictures taken in July, September and October was calculated. The difference was calculated in pair July-September, July - October, September-October on all three channels (R, G, B). The calculation of the ratio between the first channel of one image and the first channel of the second shot is produced, then between the second and third channels of the same pair. Synthesis of a combined image of the nine pan layers with the aid of a tool Stack Images provides a multispectral image of the 9 channels.

Pinus sibirica forests and pine flood plain forests in the valley Amga river have dense undergrowth and high crown density. Therefore it has the lowest value ratios of channels for all three months (for all nine columns). Siberian dwarf-pine (Pinus pumila) elfin wood also keeps the needles fall. Therefore the values in 4-9 columns are small and slightly different from the values of 1-3 columns. In contrast from the dense Pinus sibirica forests and wet pine forests, the values of channels proportions for Pinus sibirica forests mostly positive. The crown cover is considerably less than that for the first two types of forest. Siberian dwarf-pine (Pinus pumila) elfin wood is characterized by a high ratio in the first column from 34 to 45. This is less than for the grassy spaces and wetlands, but more than that for forests.

From the values of the differences between channels, It becomes possible to estimate the proportions of pine and larch, crown density in mixed forests. Than the thick stands, the lower the value of the difference. In the dense forest with well-developed understory values of the difference channels often have negative values. Conversely, the less stands, with large edges, the higher the value of the difference between channels.

8887-60, Session PS

### 11-year variability of summer snow cover extent over Himalayas

Jung-Mok Ha, Kyung-Soo Han, Jae-Il Cho, Chang-Suk Lee, Kyoung-Jin Pi, In-Hwan Kim, Jae-Hyun Ryu, Eun-Bin Park, Pukyong National Univ. (Korea, Republic of)

Snow is a component of the Cryosphere which has played an important role in Earth energy balance. Northern hemisphere snow cover extent (SCE) has steadily decreased since 1980 and in recently the trend of SCE is sharply decreased. Because Himalaya region's shows most significant changes except for the Arctic, we analyzed this region for SCE. We used Moderate Resolution Imaging Spectroradiometer (MODIS) snow product from 2001 to 2011 in august. Analysis was made by considering some conditions (region, elevation, longitude and climate) which can affect the changes in SCE. The entire SCE in Himalaya for 11 years has steadily increased(+55,098?). Trends for SCE in western region has increased(+77,781?), But trend for central and eastern have decreased -3,453?, -19,230?, respectively. According to elevation increases, the ratio of snow in each study area is increased. In 30°N-35°N SCE shows increased trend, 27°N-28°N shows decreased trend. In tundra climate, trends for SCE are similar to regional analysis. whereas the result in tropical climate's trend was increased. these performed result shows different side for change of SCE depending on each condition. The result of this study were similar to the rapid decline of the northern hemisphere SCE area in recent. The result of this study can be used to help management to water budget in Central-Asia country located to Himalayas

8887-61, Session PS

### Variations of spectral signature profiles of wet and dry targets for supporting the detection of water-leakages using satellite data

Athos Agapiou, Kyriakos Themistocleous, Dimitrios D. Alexakis, Nikolas Kourtis, Cyprus Univ. of Technology (Cyprus);

Apostolos Sarris, Foundation for Research and Technology-Hellas (Greece); Paraskevi Perdikou, Frederick Institute of Technology (Cyprus); Chris Clayton, Southampton University, Faculty of Engineering and the Environment (United Kingdom); Helena Phinikaridou, Andreas Manoli, Water Development Department (Cyprus); Diofantos G. Hadjimitsis, Cyprus Univ. of Technology (Cyprus)

Satellite data may be used as a valuable tool for the detection of water pipeline leakages in semiarid areas. However the use of multi-temporal satellite images for this purpose can be problematic since reflectance values may change due to phenological changes of plants, radiometric errors during the pre-processing of satellite data, etc. It is therefore important to establish a spectral signature library with "ground truth data" for different scenarios of water leakages in a control site minimizing potential other errors. For this purpose the GER 1500 spectroradiometer was used for measuring the reflectance values of three different targets: soil, vegetation and asphalt. The targets were doused with a specific amount of water and then several spectroradiometric measurements were taken. The narrowband reflectance values were then re-scaled to spectral bands of Landsat 5 TM and spectral signature variations were highlighted for all targets before and after moisture level was increased. Using these data, threshold values were defined in order to be used for multispectral satellite data analysis. Indeed, this information was used for detection of water leakages using Landsat 5 TM images, in pipelines in Cyprus.

## 8887-62, Session PS

### The thermal inertia approach to map soil water content under sparse vegetation

Antonino Maltese, Fulvio Capodici, Goffredo La Loggia, Univ. degli Studi di Palermo (Italy); Chiara Corbari, Marco Mancini, Politecnico di Milano (Italy)

Assessment of soil water content is of utmost importance in evaluating crop water requirement and productivity in agricultural sciences. Moreover, evaluating the spatial distribution of soil moisture could improve the effectiveness of agronomic practices.

However, standard point-based techniques (i.e., thermo-gravimetric method or reflectometry techniques) involve on-site operators and are time expensive.

It is possible to retrieve the spatial distribution of the soil water content from thermal inertia using remotely sensed data, as demonstrated in several applications.

The main difficulty in using these models is their limited applicability only to bare soils.

Recently a variation of the thermal inertia approach to map surface soil water content on bare and sparsely vegetated soils has been setup on an agricultural experimental field. In particular, a methodology has been proposed to attenuate the solar radiation (at the top of the canopy) to the one reaching the soil through an extinction factor; thus allowing achieving accurate results also on sparsely vegetated soils.

Within this paper in situ data were acquired in June 2011 and 2012 on two different fields of maize and sunflowers located in an experimental field in Barrax (Spain), both at their early growing stages. The low fractional cover characterizing both fields allows applying the widely used formulation of the thermal inertia. Advanced Hyperspectral Scanner (AHS) airborne imager provided images in the Visible/Near Infrared and Thermal Infrared bands, both in day and night time.

Previous results demonstrated that the vegetation cover correction is required even with low fractional cover; indeed, not applying this correction would result in strong overestimation. This paper aims to further validate the model on independent datasets aiming to confirm the reliability of the vegetation cover correction. The validation was carried out applying the model both on in situ and remotely sensed data.

## 8887-63, Session PS

### Remote sensing of viral infection of pepper plants (*Capsicum annuum* L.) using hyperspectral reflectance data

Dora D. Krezhova, Space Research and Technology Institute (Bulgaria); Svetla Maneva, Nikolai M. Petrov, Plant Protection Institute (Bulgaria)

The evaluation of plant quality is important for the production of grains, fruits and vegetables in industry, as well as tracking the effects of diseases, climate changes, and other adverse factors on the environment. Nowadays spectral remote sensing techniques allow presymptomatic monitoring of changes in the physiological state of plants with high spectral resolution. In this respect, spectral reflectance has proved its potential by detecting stress-related changes in the pattern of light emission from plant leaves. Vegetation analysis using remotely sensed data requires knowledge of the structure and function of vegetation and its reflectance properties. Spectral behavior of vegetation depends on the nature of the vegetation itself, its interactions with solar radiation and other climate factors, and the content of chemical nutrients and water. The spectral properties of the leaves directly relate with the surface characteristics, leaf structure, and chlorophyll content.

This research has been aimed to monitor and detect presence of stress in young pepper plants (*Capsicum annuum* L.) caused by viral infection with Cucumber Mosaic Virus (CMV) using hyperspectral leaf reflectance data. In Bulgaria CMV is one of the widest spread pathogens, causing the biggest economical losses in vegetable production.

Leaf spectral reflectance data was collected by a portable fiber-optics spectrometer in the visible and near infrared spectral ranges (450-850 nm). The pepper plants of two cultivars, Sevia and Ostrion, were investigated. They were grown in a greenhouse under controlled conditions. The plants from each cultivar were divided into six groups. The first group consisted of healthy (control) plants. At growth stage 4-6 expanded leaf, the second group was inoculated with CMV. The other four groups were treated with growth regulators: MEIA (beta-monomethyl ester of itaconic acid), ??? (benzo(1,2,3)thiadiazole-7-carbothioic acid-S-methyl ester), Spermine, and Phytoxin. On the next day, the plants of these four groups were inoculated with CMV. The viral concentrations in the plants were determined by the serological method Double antibody sandwich enzyme-linked immunosorbent assay (DAS-ELISA). All analyses were performed on the 7th and 14th day after the inoculation.

The differences between the reflectance spectra of infected and healthy leaves were analyzed in the most informative for green plants spectral ranges: green, red, red edge, and near infrared. Statistical significance of the differences was assessed by means of Student's t-criterion. On the 7th day no visual changes in the leaves occurred but a decrease of spectral reflectance was established in the green and red ranges for all groups of treated plants. The statistical analysis of data measured on the 14th day indicates an increase of the number of statistically significant differences between spectral reflectance of healthy and treated plants. A shift of the red edge position to the blue region was observed for the case of treatment only with CMV. The growth regulator MEIA is with the best preventing action on the leaves. The correlation of the results from spectral analyses and the DAS-ELISA findings for presence of CMV demonstrates the efficiency and sensitivity of this remote sensing technique for reliable diagnosis of viral infection and injuries of plants.

## 8887-64, Session PS

### Hyperspectral chlorophyll fluorescence technique for early detection of plant disease

Dora D. Krezhova, Space Research and Technology Institute (Bulgaria); Svetla Maneva, Plant Protection Institute (Bulgaria)

The interest of remote sensing of induced chlorophyll fluorescence of terrestrial vegetation arose by the link of photosynthetic efficiency which could be exploited in large scale. Fluorescence technologies can find place in areas such as biochemistry, medicine, in the analysis of organic compounds, as well as for monitoring of plants

status and functioning to help in making timely decisions in ecology and sustainable agriculture. In this study chlorophyll fluorescence technique was applied to establish the effect of viral infection with Cucumber Mosaic Virus (CMV) on young pepper plants (*Capsicum annum* L.).

Hyperspectral chlorophyll fluorescence data were measured by a portable fibre-optics spectrometer in the spectral range 600–900 nm where the main part of the emitted from leaves fluorescence radiation is concentrated. As a source of actinic light a LED with the maximum of the light output at 470 nm was used. The tested leaves were dark adapted before measurements and the excited fluorescence signal was measured from the abaxial leaf surface. The control of the spectrometer and the acquisition and processing of data were carried out by means of specialized software.

Pepper plants of two cultivars Sevria and Ostrion were investigated. All plants were grown in greenhouse under controlled conditions (temperature 25°C, illumination 3500–4000 luxes and photoperiod 16/8 hours day and night). A part of the plants of each cultivar was the control (healthy). The other plants were divided into five groups. At growth stage 4–6 expanded leaf the plants from the first group were infected with CMV. The plants from the other groups were treated with four growth regulators: MEIA (beta-monomethyl ester of itaconic acid), ??? (benzo(1,2,3)thiadiazole-7-carbothioic acid-S-methyl ester), and preparations Spermine and Phytoxin. On the next day, the pepper plants of these four groups were inoculated with CMV.

Spectral measurements were performed on the 7th and 14th day after the inoculation. The changes in the course of the fluorescence spectra and the statistical significance of the differences between normalized spectra of control and treated plants were established. The Student t-criterion was applied in five characteristic wavelengths in the spectral range 600–900 nm. Statistically significant differences between data means of the control and treated with growth regulators and treated only with CMV plants at the first two wavelengths on the forefront of the fluorescence spectra (650–740 nm) were ascertained. The growth regulator MEIA provoked stronger inhibition of CMV; it induced a systemic acquired resistance. The average curve of the fluorescence spectra of the plants treated only with CMV differed most significantly against the others. These results and their correlation with the results from the spectral reflectance analysis in the visible and near infrared ranges (650–850 nm) and from the serological analysis (DAS-ELISA) on the same plants for the presence of CMV imply that the chlorophyll fluorescence technique is a promising tool for express and reliable diagnosis of viral infections.

## 8887-65, Session PS

### Comparing the new generation WorldView-2 to hyperspectral image data for species discrimination

Khalid M. Mansour, Univ. of KwaZulu-Natal (South Africa) and Univ. of El-Fashir (Sudan); Onesimo Mutanga, Univ. of KwaZulu-Natal (South Africa)

An instrument concept called the Birefringent Imaging Doppler Wind Interferometer (BIDWIN) is being validated in the Atmospheric and Space Physics Lab at the University of New Brunswick in collaboration with COM DEV Ltd (Ottawa, Canada) to determine its capabilities for measuring Doppler wind fields in the Earth's nightglow. The instrument is adapted from a similar approach used to obtain two dimensional images of high speed (~1000 m/s) flow fields in plasmas at the Australian National University. For that application the precision of the wind measurements was not explored in detail. With BIDWIN, the intent is to obtain ~ 5 m/s precision on each bin of a CCD image of the wind field. An examination of the instrument concept and sensitivity of the wind measurements made using this approach is undertaken to determine the feasibility of this criterion. The BIDWIN has the advantage over other instruments that can be used for a similar purpose (such as the field widened Michelson interferometer and Fabry-Perot interferometer) in that it has no moving parts, has a large throughput, is light weight and is relatively cheap to construct. In this paper, the instrument concept is presented and the instrument is described using Jones matrices. The non-ideal instrument effects are also explored. Measurements taken using a proto-type of the instrument constructed in the lab at the University of New Brunswick are compared to the Jones matrix model and are used to verify the instrument concept.

## 8887-66, Session PS

### Estimating catechin concentrations of new shoots in the green tea field using ground-based hyperspectral image

Chanseok Ryu, Gyeongsang National Univ. (Korea, Republic of); Masahiko Suguri, Shi-bum Park, Mikio Umeda, Kyoto Univ. (Japan)

Tea is one of the most widely consumed beverages in the world. It is good and important source of many phytochemicals, such as catechins, caffeine, free amino acids, flavones, vitamins and minerals. Especially catechins have received a great deal of attention due to their many biological activities such as antioxidative and antitumour activities. The catechins (EC, ECG, EGC and EGCG) are colorless, astringent, water soluble compounds and constitute up to 30% on a dry weight basis. In the past few years, many different methods of analysis had been employed to identify some chemical compositions in tea. Although NIR or Vis/NIR spectroscopy technique has many advantages, these methods are only useful after harvesting because it is difficult to distinguish between the old leaves and new shoots before harvesting. Moreover the quality of green tea is mainly determined during the growth period, but previous studies have focused on the post-harvesting quality. Therefore it is necessary to identify the information about the quality of new shoots in the field to control the quality of green tea before harvesting. In this study, catechin concentration was established by a ground-based hyperspectral imagery using partial least squares regression (PLSR) analysis based on the reflectance of new shoots in the field.

The acquired image was separated into two parts: 1) new shoots and 2) others using the difference between NDVI and GreenNDVI. The reflectance of only new shoots regions was divided by the reflectance of reflect-board regions and defined it the reflectance. Using the reflectance and the chemical analysis of each catechin, each model was validated by the one leave out cross-validation. The accuracy and precision of the model was estimated by the coefficient of determination (R<sup>2</sup>), root mean square error (RMSE) and relative error (RE). It was possible to explain more than 78.5 % of each and each type of catechin (free and ester) using the hyperspectral reflectance of new shoot except a few catechins. The precision and accuracy (RE) were not changed or improved in the ester type of catechins (ECg and EGCg) but not in the free type of catechins (EC and EGC) compared with each catechins. The mutual prediction which means that each vegetation data was predicted by the other year's model was analyzed to check the possibility of year-invariant. In the mutual prediction, the accuracy was suitable compared with it of the validation except EGC and free type of catechins.

## 8887-68, Session PS

### Retrieve leaf area index from HJ-1 CCD Image based on support vector regression and physical model

Jingjing Pan, Hua Yang, Wei He Sr., Peipei Xu, Beijing Normal Univ. (China)

Many biophysical parameters of vegetation, have nonlinear relations with its spectral reflectance, and it can be simulated by canopy reflectance models, PROSAIL for instance. Through certain inversion method, some biophysical parameters can be retrieved from the spectral reflectance acquired by remote sensing. In this paper, a retrieval of Leaf Area Index from HJ-1 CCD Image based on Support Vector Regression and PROSAIL is conducted. Canopy's bi-directional property makes multi-angle inversion a hot spot, and angle information can effectively improve the precision. The retrieval of LAI using Support Vector Regression up to now can be concluded into two groups: one is the empirical regression between NDVI and LAI. Once the relationship is built, the biophysical parameters then can be extracted; the other is the use of multi-angle images, because of BRDF effect we can get different spectral reflectance at different viewing angles, and if we simulate the angular reflectance into physical model, the inversion precision would be higher. While multi-spectral images, for example, HJ-CCD, only have certain observation angle per pixel, the utilization of angular information would count much in the inversion process. Our research is composed of 3 parts?Data simulation using PROSAIL, model optimization with SVR, and finally

the inversion and the validation against field measured data. In the retrieval, our forward model is PROSAIL. It's a 1D turbid medium radiative transfer model, with which we can simulate both spectral and directional reflectance at given parameters. The input parameters for PROSAIL are set by a certain value or a distribution based on related articles and the field environment in which we measure LAI using LAI-2000. To test the noise resisting ability of SVR, we build 3 samples of HJ - CCD data with its spectral response function at different observation angles and three levels of Gaussian noise, 2%, 5% and 10%, respectively. After the data simulation, Support Vector Regression is then used to get the relationship between reflectance, observation angles and LAI. In the nonlinear situation, SVR uses kernel functions to construct mapping from low dimensional space to high dimensional space, which decidedly enhances the separability of data. Generally, SVR is composed of 3 parameters - meta-parameter,  $\gamma$ -insensitive loss and the kernel parameter. In this paper, we choose form of  $\gamma$ -SVR and the kernel function is Radial Basis Function (RBF). Meta-parameter is decided as the range of the training data, and the other two parameters are followed by a parameter selection process. The parameter selection process is conducted by a 5-fold cross validation to find the optimal parameters. After fitting validation data into SVR model, R2 and RMSE between retrieved LAI and original LAI are calculated. At 2%, 5% and 10% levels of Gaussian noise, the R2 are 0.9746, 0.9574 and 0.9323, and the corresponding RMSE are 0.2462, 0.3076 and 0.3965. Compared with the inversion result by the look-up table method using the same data, SVR has better performance on noise resisting and inversion precision. Finally, the satellite inversion comes. As HJ-CCD provides discrete angles every 34 lines or columns, we use a 3D spline interpolation with ArcGIS to get continuous angles. The trained model of SVR is used to retrieve LAI with HJ-CCD data, which includes reflectance, interpolated viewing angles. The validation data is measured with LAI-2000 in a winter wheat farm at Xinxiang, Henan, China. R2 and RMSE are also used to do the evaluation. The result shows that the method used in this study is of high inversion precision and is applicable to retrieve LAI with HJ - CCD image.

#### 8887-69, Session PS

### Estimation of wheat LAI by assimilating remote sensed data into crop model

Xiaohua Zhu, Lingling Ma, Lingli Tang, ChuanRong Li,  
Academy of Opto-Electronics (China)

Leaf Area Index (LAI) is a key parameter for characterizing the structure and the functioning of vegetation. Remote sensing technology is an important way for estimating regional scale LAI. Due to the restrictions of satellite operating cycle, remote sensing inversion results are temporal discontinuity. Process model can simulate continuous and long time series LAI data. However, influenced by parameterization scheme, atmosphere-driven conditions and process model initial state, the model simulation will cause unreasonable results. LAI estimation by remote sensing technology or by process model simulation, each have its own advantages and disadvantages (Yannick et al., 2012; Dorigo et al., 2007). So it is important to use multi-source data or multi-methods to estimate LAI and improve the estimation accuracy.

Data assimilation, using multi-source information to directly or indirectly participate in to improve the trajectory of process model simulation, improves the estimation accuracy of surface parameters and realizes the complementary advantages between the model simulation and remote sensing observations. In recent years, data assimilation technology is well applied in the research of atmospheric, oceanic, etc, and also attracted the attention of scholars in land surface research (Wang et al., 2010; Zhang et al., 2010; Fang et al., 2010). And in many researches of data assimilation, the application of prior knowledge has attracted the attentions of scholars (Yannick et al., 2012). The prior knowledge here means the field data, spatial information and temporal knowledge. In study of coupling crop growth model with radiative transfer model, spectral library data used as prior information was introduced into the cost function to achieve optimal LAI (Wang et al., 2010). In research of real-time retrieval of LAI from MODIS time series data, Xiao et al., (2011) extracted temporal knowledge from MODIS LAI products to construct a dynamic model for providing short-range forecast of LAI, then, they used Ensemble Kalman Filter techniques to update LAI when there is a new observation. The studies above have considered the application of prior knowledge, such as field data, temporal information, but still

less to consider the influence of the surface spatial heterogeneity and the introduction of spatial knowledge into regional assimilation research (Tian et al., 2002). At the same time, phenology information (temporal knowledge) as a characterization of crop growth process is an important temporal prior knowledge. If phenology information is introduced into the crop model simulation to optimize the model sensitive parameters, the accuracy of real-time simulation can be effectively improved.

On the basis of previous work, an assimilation scheme based on temporal and spatial knowledge is proposed in this paper. The assimilation scheme is implemented in two directions, seen as Figure 1. One is the temporal direction, in which the parameters of crop model are calibrated, the other one is the spatial direction, in which the spatial information extracted from different resolution data is taken into account during inversion. Based on parameter "LAI", the crop growth model WOFOST (Boogaard et al., 1998) and the reflectance model ACRM (Kuusk, 2001) are combined in this assimilation scheme by Kalman Filter (KF).

#### 8887-70, Session PS

### Spectral reflectance pattern as a method for potato crop characterization

Mohamed Aboelghar, National Authority for Remote Sensing and Space Sciences (Egypt)

Crop discrimination through satellite imagery is still problematic. Accuracy of crop classification for high spatial resolution satellite imagery in the intensive cultivated lands of Egyptian Nile delta is still low. Therefore, the main objectives of this research is to determine the optimal hyperspectral wavebands in the spectral range of (400-2500 nm) to discriminate between four different varieties of Potato crop (Diamond, Everest, Mondial and Rosetta) that are commonly used in old and new cultivated lands of Egypt and to propose detailed spectral reflectance characterization for these four varieties which will enable more accurate surveying of these varieties through satellite imagery. Hyperspectral ground measurements of ASD field Spec3 spectroradiometer was used to monitor the spectral reflectance profile during the period of the maximum growth stage of the crop. After accounting for atmospheric widows and/or areas of significant noise, a total of 2150 narrow bands in 400-2500 nm were used in the analysis. Spectral reflectance was divided into six spectral zones: blue, green, red, near-infrared, shortwave infrared-I and shortwave infrared-II. One Way ANOVA and Tukey's HSD post hoc analysis was performed to choose the optimal spectral zone that could be used to differentiate the different varieties. Then, linear regression discrimination (LDA) was used to identify the specific optimal wavebands in the spectral zones in which each variety could be spectrally identified. The results of Tukey's HSD showed that NIR is the best spectral zone in the discrimination between the four varieties. The other five spectral zones showed close spectral characterizations between at least two varieties. The results of (LDA) showed that the wavelength zones (713:1349, 1656:1691 nm) were the optimal to identify Diamond variety, (712:715, 1596:1699, 1700:1754 nm) were the optimal to identify Everest variety, (350:712, 1421:1656, 1696:1799, 1951:2349 nm) to identify Rosetta variety while very narrow waveband (714:717 nm) was found to be effective in identifying Mondial variety. An average of thirty measurements for each variety was considered in the process. These results will be used in machine learning process to improve the performance of the existing remote sensing software's to estimate Potato crop acreage. The study was carried out in El-Behirah governorate of Egypt.

#### 8887-71, Session PS

### Spatial variability of sorghum grain yield: site-specific relations of growth factors to irrigation and N-fertilization

Yousef Y. Aldakheel, King Faisal Univ. (Saudi Arabia)

The implementation of precision agriculture techniques for water and nitrogen fertilization management has the potential for improving water and fertilization use efficiencies in the use of such input. This study was aimed to investigate the effect of variable water application rates and variable nitrogen fertilization in a uniform field defined from information on measured soil properties on grain sorghum in eastern

Saudi Arabia. This is achieved by relating vegetation indices like NDVI (Normalized Difference Vegetation Index), SAVI (Soil Adjusted Vegetation Index), NDRE (Normalized Difference Red Edge) to growth indicators, such as leaf area index (LAI), chlorophyll content, and plant height.

The results of this study showed that there were significant differences between irrigation water treatments, fertilization and vegetation indices, in terms of growth stand and grain yield. This indicates that there is a strong relationship between vegetation indices and maps of spatial distribution of soil moisture content and N-fertilization in the field.

According to this study, information on seasonally steady factors such as soil texture is valuable in identifying management zones for water and fertilizer application. Water and fertilizers management should be complemented by in-season management of seasonally unsteady factors such as soil NO<sub>3</sub> N on grain yield.

## 8887-72, Session PS

### Increased agricultural production by managing irrigation and drainage water using mathematical modelling

A. F. M. Afzal Hossain, Institute of Water Modeling (Bangladesh); Muhammad Hassan Bin Afzal, Univ. of Dhaka (Bangladesh)

Bangladesh is an agriculture based country with huge population and per capita land is limited. Agriculture is the largest sector of Bangladesh economy, the largest source of employment, and the largest water user. Plenty of water during monsoon creates flood whereas too little surface water during dry season generates drought in some parts of the country. In order to get the self sufficiency in food, agricultural production needs to be increased, among others, by bringing potential cultivable area under irrigation along with improved water management and reduction of flooding and drainage where justified. In the next 25 years the population of the country is expected to increase by 40%. The agricultural land will be reduced by about 17% (NWMP, 2001). This increase of population will increase the rice demand in the next 25 years by about 29%. The changes in the agricultural area have important implications for food productions as the reduced area implies an increase in cropping intensity on the remaining land. Development of agriculture through irrigation, drainage and flood control has got priority in the national development plans to attain food sufficiency. The central strategy for the water resources development in the field of agriculture would be optimum utilization of water resources conjunctively to increase area under effective cultivation. As such, new irrigation projects wherever feasible need to be implemented for the improvement in agricultural productivity. The command area development (CAD) of the existing irrigation projects to be implemented to bring more area under irrigation and free from drainage to increase production.

Since 1996 IWM has been providing modelling support in irrigation and drainage management. It has been observed that in many irrigation and drainage projects, benefits have been achieved after implementation of IWM's suggestions in irrigation projects. After implementation of model study results in Meghna Dhonagoda Irrigation Project (MDIP), the command area coverage as well as the food production has been increased from 30% to 90%, Teesta Barrage Project(TBP) phase-1 become flood free and irrigation water can reach to almost every canal resulting annual gain from increased paddy is US\$ 37.5 million. The hydrological modelling has become now a proven tool in the water resources management aspects like irrigation and drainage management. The benefit of using the modelling tools for optimum utilization of water resources in irrigation and drainage management of two CAD projects e.g. MDIP and TBP have been discussed in this paper.

## 8887-73, Session PS

### Seasonal spectral response patterns of winter wheat canopy for crop performance monitoring

Rumiana Kancheva, Georgi Georgiev, Space Research and Technology Institute (Bulgaria)

Agricultural monitoring is an essential and continuously spreading application area of remote sensing observations. Valuable information on crop condition and development processes is derived from the analysed remotely sensed data. In agriculture, mapping farm-land use, crop area estimates, and spatial and temporal distributed information on crop growth are preconditions for improving the efficiency of agricultural policies and management. This is especially important in the context of site-specific precision agriculture running. Remote sensing monitoring is a major source of relevant data. Much research is being carried out on vegetation phenology issues. These issues are related to using remotely sensed data for phenology monitoring, assessment of vegetation types distribution, predicting ecosystems, quantifying the carbon budget, evaluation of year-to-year spatial and temporal variations of vegetation seasonality, and the dependence of these variations on environmental factors. Monitoring phenology and taking into account phenological events are a crucial element in vegetation data interpretation. In agriculture, the timing of seasonal cycles of crop activity is important for species classification and evaluation of crop development, growing conditions and potential yield. However, the correct interpretation of remote sensing data along with the increasing demand for high reliability of the derived information require precise ground-truth study of the seasonal performance of different species, knowledge of the phenology-resolved behaviour of the spectral response, and establishment of time-dependent relationships with crop vigour and productivity. For this reason, we have carried out detailed ground-based experiments to investigate the multispectral response of winter wheat at different phenological stages and to relate reflectance patterns to crop seasonal growth performance and yield. The goal is to quantify crop seasonality by establishing empirical relationships between plant biophysical and spectral properties in different ontogenetic periods. The implementation of various vegetation indices for monitoring crop seasonal dynamics, health condition, and yield potential has been examined. Empirical phenologically-specific relationships have been established which allow tracking of plant development from seasonal multispectral data, assessment of crop condition and yield prediction at different portions of the growth cycle. The performance of spectral features to effectively monitor plant development and distinguish crop health condition has been tested. Relating plant spectral and biophysical variables in a phenology-based manner has allowed crop diagnosis and predictions to be made multiple times during plant ontogenesis.

## 8887-74, Session PS

### Estimating potential soil erosion for environmental services in a sugarcane growing area using multisource remote sensing data

Betty A. Mulianga, Kenya Sugar Research Foundation (Kenya); Agn s B gu  D.D.S., CIRAD (France); Margareth Simoes, EMBRAPA (France); Pierre Todoroff, Pascal Clouvel, CIRAD (France)

Characterization of landscape heterogeneity is crucial in estimation of potential soil erosion to ascertain environmental services provided by main land uses to the ecosystem. Remote sensing techniques have proved successful in characterization of landscapes when integrated with ground data and expert knowledge. In this study, we used the characterized map to investigate whether sugarcane production provides a soil erosion control service to Kibos-Miwani ecosystem. This is a rain-fed sugarcane production region with favourable lake basin climate and located in the first sugar belt of Kenya. Data used included a 30 m Landsat time series images acquired between November 2010 and February 2012, a 10 m multispectral SPOT image acquired in October 2011, a 30m digital elevation model (DEM) and ground observations. Ground observation data was collected using the Mobile Mapper CX through a stratified random sampling approach and included soil samples for analysis of soil physical properties (bulk density, hydraulic conductivity, porosity and soil moisture content); land use and crop management practices. The land cover map was then produced by mixing information from the high resolution SPOT image, to delineate field limits, and from the Landsat time series NDVI data extracted for each of the fields. Based on ground observations, two methods were adopted for classification of the temporal Landsat NDVI data: (i) object based classification of crop fields based on training data in R software and (ii) pixel based



supervised classification of natural vegetation after masking the fields using the maximum likelihood classifier in Erdas software. The Fuzzy-based dynamic soil erosion model (FuDSEM) utilized the classified land cover together with the slope, aspect, curvature and soil physical properties to compute the potential soil erosion for each field. FuDSEM has the advantage of being spatially explicit and temporally dynamic compared to other models and was able to utilize data at landscape scale in this study. Results on classification show an overall accuracy of over 80% with a spatially heterogeneous land cover map. This heterogeneity is consistent with the variable management practices that commence with land preparation to harvesting and trash management. Results on potential soil erosion were consistent with crop management practices, presenting low values in sugarcane fields and significant values in fields with other crops. These results have shown a high level of interaction between phenomena in this landscape which is relevant for analysis on environmental impacts of heterogeneous systems. Remote sensing approach has successfully exemplified the objective of this study. We infer that interaction of sugarcane with other land uses introduces spatial heterogeneity which offers soil and water retention as an environmental service for enhanced agricultural productivity to the ecosystem. We therefore recommend the use of these approaches in similar studies.

### 8887-75, Session PS

#### Estimation of maximum air temperature using COMS data in Northeast Asia

Jae-Hyun Ryu, Kyung-Soo Han, Pukyong National Univ. (Korea, Republic of); Jae-Il Cho, Pukyong National Univ. (Korea, Republic of); Chang-Suk Lee, In-Hwan Kim, Kyoung-Jin Pi, Pukyong National Univ. (Korea, Republic of); Jung-Mok Ha, Eun-Bin Park, Pukyong National Univ. (Korea, Republic of)

Air temperature ( $T_a$ ) plays important role for the circulation of energy and water between the surface and atmosphere.  $T_a$  was accurately measured from ground observation stations. However, the number of ground observation stations is limited, and  $T_a$  is influenced from temporal and spatial change. In this study,  $T_a$  was estimated using satellite data from April 2011 to March 2012 in the Northeast Asia where consist of the various ecosystem. States of surface and atmosphere were considered through Normalized Difference Water Index (NDWI) and the differences of brightness temperature values of 11  $\mu\text{m}$  (TBB1) and 12  $\mu\text{m}$  (TBB2). Dataset was divided into nine cases that had seasonal characteristics according surface states (NDWI) and atmosphere states (TBB1-TBB2).  $T_a$  was acquired from 174 ground observation stations, and multiple regression equation of each case was consisted of LST, NDVI, TBB1-TBB2. The weighting region was set to be within 8.33% of total density from boundary area of cases in order to reduce the errors that can occur due to the small value. The weighting was applied as distance from the nearest four points. The spatial representativeness of estimated  $T_a$  was determined as 9 by 9 window size. R-squared of estimated  $T_a$  from satellite was 0.94, RMSE was 2.98 K, Bias was 0.56 K.

### 8887-76, Session PS

#### Aalto spectral imager calibration and qualification for a CubeSat flight

Heikki H. Saari, Kai H. Viherkanto, Antti Näsilä, Christer Holmlund, Jussi H. Mäkynen, Tapani Antila, Rami Mannila, VTT Technical Research Ctr. of Finland (Finland)

VTT Technical Research Centre of Finland has developed tunable piezo Fabry-Perot Interferometer (PFPI) based miniaturized hyperspectral imager which can be operated from light weight Unmanned Aerial Vehicles (UAV). The concept of the hyperspectral imager has been published in the SPIE Proc. 7474, 8174 and 8374. Now there is a space flight opportunity in the Finnish Aalto-1 CubeSat student nanosatellite for the Aalto-1 spectral imager (AaSI) instrument. This has spurred development of the PFPI module design for improvements with respect to temperature and vibration immunity. A space qualification activity for the PFPI module consisting of performance tests in thermal vacuum cycling conditions and vibration tests has been performed. The PFPI wavelength calibration

has a temperature dependence, which is mitigated by software temperature compensation and onboard wavelength calibration using the band limiting filter edges. Optimisation of the PFPI gap control loop for the operating temperature range and vacuum conditions was performed. The AaSI design realized with commercial of the shelf (CoTS) parts is described. The AaSI has a  $10^\circ \times 10^\circ$  field of view and delivers a  $512 \times 512$  pixel data cube consisting of ca 20 bands of 10-30 nm spectral resolution in the 500-900 nm range. The mass of the instrument is 500 g. Calibration and verification of the AaSI development model is described. The main goal of the mission is to demonstrate spectral performance in orbit. The activity is funded by the European Space Agency.

### 8887-77, Session PS

#### Remote sensing terminology: past experience and recent needs

Rumiana Kancheva, Space Research and Technology Institute (Bulgaria)

The paper is devoted to terminology issues referring to all aspects of remote sensing research and application areas. Terminology is a key issue for a better understanding among people. Inconsistent or erroneous terminology can be a barrier to the dissemination of ideas and information. Terminology accuracy is essential during technical meetings and during all phases of international cooperation. It is important as well in education, knowledge and experience exchange, publication activities and etc.. In our rapidly changing technological world, new terms emerge almost every day. It is crucial to keep up with the latest quantitative and qualitative developments and novelties of the terminology in advanced fields such as space science and technology. This is especially true in remote sensing and geoinformatics which have wide and ever expanding applications in various domains. The importance of the correct use of remote sensing terms refers not only to people working in this field but also to experts in many disciplines who handle remote sensing data and information products. Researchers, professionals, students and decision makers of different nationalities should fully understand, interpret and translate into their native languages any term, definition or acronym found in articles, books, proceedings, specifications, documentation, etc. Remote sensing terminology issues are directly relevant to the world-wide policies for international cooperation in scientific and application areas putting a particular accent on Earth observations and environmental problems of global significance. It is not less important that users of remote sensing products have to be well familiarized with the relevant terms and definitions. With this motivation, considering the importance of the matter and believing that the growing remote sensing community is an essential part of the today's information society, we draw the attention on the recent needs and peculiarities of the creation of specialized bilingual and multilingual dictionaries and glossaries of remote sensing terms. Our vision about the principles, structure and topic content of entries, the process of expanding and updating of a remote sensing bilingual glossary is presented in the paper. This vision builds upon previous national and international experience and makes use of on-going activities on the subject. Details are presented about the work in progress on the preparation of an English-Bulgarian defining dictionary focusing on Earth remote sensing observation, environmental monitoring and integration with other geoinformation technologies. Our belief is that the elaboration of suchlike materials in this specific, spreading and most perspective field of human expertise is of great practical importance.

### 8887-78, Session PS

#### Urban vegetation land covers change detection using multi-temporal MODIS Terra/Aqua data

Maria A. Zoran, National Institute of Research and Development for Optoelectronics (Romania); Adrian I. Dida, Transilvania University of Brasov (Romania) and Faculty of Forest Sciences (Romania); Ovidiu M. Ionescu, Transilvania Univ. of Brasov (Romania) and Faculty of Forest Sciences (Romania)

In the last decades the availability of global remote sensing data sets

has provided a modern tool of studying the patterns and dynamics of urban land cover. Urban vegetation, known as green space that includes vegetated areas such as parks or forest stands, and isolated trees growing along streets, in street medians, or private property, is a critical issue for both a healthy population as well as for city economy. Urban vegetation land cover change is a direct measure of quantitative increases or decreases in sources of urban pollution and the dimension of extreme climate events and changes that determine environment quality. Spatio-temporal monitoring of urban vegetation land cover changes is a very important task for establishing the links between policy decisions, regulatory actions and subsequent land use activities. Former studies incorporating two-date change detection using Landsat TM/ETM data had limited performance for urban biophysically complex systems applications. In this paper, we describe recent results using data from NASA's Moderate Resolution Imaging Spectroradiometer to study urban vegetation land cover dynamics. This study explored the use of time-series MODIS Terra/Aqua Normalized Difference Vegetation Index (NDVI) and Leaf Area Index (LAI), data to provide change detection information for metropolitan area of Bucharest in Romania. Training and validation are based on a reference dataset collected from IKONOS high resolution remote sensing data. The mean detection accuracy for period 2002-2012 was assessed to be of 89%, with a reasonable balance between change commission errors (21.7%), change omission errors (28.5%), and Kappa coefficient of 0.69. Annual change detection rates across the urban/periurban areas over the study period (2002-2012) were estimated at 0.78% per annum in the range of 0.45% (2002) to 0.75% (2012). Vegetation dynamics in urban areas at seasonal and longer timescales reflect large-scale interactions between the terrestrial biosphere and the climate system. As a result, phenology has recently emerged as an important topic with relevance to a wide array of climate and ecological research including regional and global carbon modeling, ecological assessment, and agroforest monitoring. Accurate information is essential for estimation of changes in surface energy balance and atmospheric greenhouse gas emissions, and Urban Heat Island function at local and regional scale as well as urban land cover/use dynamics in frame of global warming.

#### 8887-79, Session PS

### Urban thermal environment and its biophysical parameters derived from satellite remote sensing imagery

Maria A. Zoran, Roxana S. Savastru, Dan M. Savastru, Marina-Nicoleta Tautan, National Institute of Research and Development for Optoelectronics (Romania); Laurentiu V Baschir, National Institute of R & D for Optoelectronics (Romania)

Urban growth can profoundly alter the urban landscape structures, ecosystem processes, and local climates. Timely and accurate information on the status and trends of urban ecosystems is critical to develop strategies for sustainable development and to improve urban residential environment and living quality.

Multispectral, multitemporal and multiresolution satellite remotely sensed data are useful tool for land cover/use changes study associated with urban growth, and to retrieve land surface biogeophysical parameters, such as vegetation abundances, built-up indices and land surface temperatures, which are good environmental indicators of conditions of urban ecosystem. By integrating high-resolution and medium-resolution satellite imagery with other geospatial information, have been investigated several land surface parameters including impervious surfaces and land surface temperatures for Bucharest metropolitan area in Romania. In frame of global warming, the field of urbanization and urban thermal environment are important issues among scientists all over the world. This paper investigated the influences of urbanization on urban thermal environment as well as the relationships of thermal characteristics to other biophysical variables in Bucharest metropolitan area of Romania based on satellite remote sensing imagery Landsat TM/ETM+, time series MODIS Terra/Aqua data and IKONOS acquired during 1990-2012 period. Vegetation abundances and percent impervious surfaces were derived by means of linear spectral mixture model, and a method for effectively enhancing impervious surface has been developed to accurately examine the urban growth. The land surface temperature (LST), a key parameter for urban thermal characteristics analysis, was also retrieved from thermal infrared band

of Landsat TM/ETM+ and from MODIS Terra/Aqua datasets. Based on these parameters, the urban growth, urban heat island effect (UHI) and the relationships of LSTs to other biophysical parameters have been analyzed. Results indicated that the metropolitan area ratio of impervious surface in Bucharest increased significantly during two decades investigated period, the intensity of urban heat island and heat wave events being most significant. The correlation analyses revealed that, at the pixel-scale, LSTs possessed a strong positive correlation with percent impervious surfaces and negative correlation with vegetation abundances at the regional scale, respectively. This analysis provided an integrated research scheme and the findings can be very useful for urban ecosystem modeling.

#### 8887-80, Session PS

### Isolating and interpreting parcels from remote images as administrative census data

Luis García-Torres, Instituto de Agricultura Sostenible (Spain)

A methodology to isolate semi-automatically agrarian parcels from remotely sensed images and classifying its cropping systems and other land uses has been developed. Parcel micro-images individualization, spectral band average measurement extraction, and vegetative indices calculation for each parcel were automatically achieved through CROPCLASS® software implementation. Cropping systems classification was achieved based from multitemporal images taken over the growing season. We have validated this procedure using a series of seven GeoEye-1 satellite images taken over Ventillas area (Cordoba, Southern of Spain), taken throughout the growing season. The classification of cropping systems for each parcel was executed using CRT Decision Trees analysis. Census agri-environment administrative data of an area can be partially elaborated through multitemporal remote images applying the patented CROPCLASS® procedure (in process).

Agricultural land use information is updated routinely in many cropland regions in USA and Europe through farmer communications or ground visit of administrative inspectors to selected field. This process is tedious, time consuming, and therefore economically expensive. The use of remote sensing and the implementation of CROPCLASS procedure described below will facilitate this process, greatly reducing the field visits, which is the most expensive part of the traditional approach, and in addition providing images for verification and future studies.

#### 8887-81, Session PS

### Land surface emissivity retrieval from airborne hyperspectral scanner thermal infrared data over different land surfaces

Gaixia Gao, Academy of Opto-Electronics (China); Xiaoguang Jiang, Graduate Univ. of Chinese Academy of Sciences (China); Yonggang Qian, Academy of Opto-Electronics (China); Hua Wu, Bohui Tang, Institute of Geographical Sciences and Natural Resources Research (China); Zhaoliang Li, Institute of Agricultural Resources and Regional Planning (China)

Land surface emissivity (LSE) is a key parameter for characterizing the land surface, and is vital for a wide variety of surface-atmosphere studies. LSE is also a key parameter for estimating accurately land surface temperature (LST), which is important for global-change studies, estimation of radiation budgets, heat-balance studies and control for climate models. LSE retrieval from thermal infrared (TIR) data is the only way for acquiring LSE at wide spatial and temporal scale. However, the measured radiance by thermal infrared sensor is always affected by LSE, LST and atmospheric effect. Even the atmospheric contamination can be removed from measured radiance; LSE retrieval from space is underdetermined since there is one more unknown than the number of independent measurements. To make the solution deterministic, during the two most recent decades, a number of methods have been developed in literature regarding the estimation of LSE from TIR data. These methods include the classification-based method, the NDVI-based method, the day/night method, the temperature-independent spectral indices (TISI) method

and the temperature emissivity separation (TES) method.

The Dual-use European Security IR Experiment (DESIREX) campaign has been carried out in 2008 over the city of Madrid (Spain), and airborne hyperspectral scanner (AHS) data with high spatial resolution (4m) have been collected. The calibration of the AHS sensor was found to have a good performance for each thermal band, and the comparison between the brightness temperatures measured by the AHS and these simulated from in situ measurements to the sensor height level showed a bias of 0.1K and a RMSE of 1.0K. This provides an excellent opportunity for evaluating the performance of the TES method over different land surfaces. This paper retrieved LSEs of land surfaces over the city of Madrid, Spain from airborne hyperspectral scanner (AHS) thermal infrared data using temperature emissivity separation (TES) method. Therefore, after atmospheric correction, the TES algorithm is directly applied to the AHS images in bands 72, 73, 75-79. And then six different kinds of urban surfaces: asphalt, bare soil, granite, pavement, shrub and grass pavement, were selected to evaluate the performance of the TES method in urban areas. The results demonstrate that the six urban surfaces have similar curve shape of emissivity spectra, with the lowest emissivity in band 73, and highest in band 78. The LSE for bare soil varies significantly with spectra, approximately from 0.90 in band 72 to 0.98 in band 78. Among the six urban surfaces, the LSE for grass has the smallest spectral variation, approximately from 0.965 in band 72 to 0.974 in band 78, and the shrub presents higher LSE than other surfaces in bands 72, 73, 75-77, but a little lower in bands 78 and 79. Furthermore, the LSE discrepancies for different surfaces are obvious in band 73, this illustrates that it is more suitable to distinguish different surfaces using the LSEs in this channel. In addition, it is demonstrated that the grass presents the lowest LST, approximately 307 K, while the asphalt presents the highest LST, approximately 324.5K. The LSTs for asphalt, granites and pavement surfaces are all larger than that for grass and shrub.

## 8887-82, Session PS

### Monitoring gully erosion at Nyaba river of Enugu state southeastern Nigeria, using remote sensing

Virginia U. Okwu-Delunzu, Enugu State Univ. of Science and Technology (Nigeria); I. C. Enete, Nnamdi Azikwe Univ. (Nigeria); A. S. Abubakar, Federal Univ. of Technology (Nigeria); S. Lamidi, Univ. of Nigeria (Nigeria)

Erosion is a gradual and continuous process of earth surface displacement caused by various agents of denudation. Although erosion is a natural process, it is also caused by some anthropogenic activities. The erosion rate of an area at any given point in time is dependent mainly on climate factors which includes; precipitation, temperature, seasonality, wind speed and geological factors which includes; sediment or rock type, porosity or permeability, and the slope (gradient) of land. The physical aspects of the erosive force experienced in gullies are mainly dependent on the local prevailing climate condition. In this study, remotely sensed (satellite imagery) data was used in the analysis of gully erosion progression at Nyaba River in Enugu urban. It is aimed at mapping and monitoring gully erosion at the study site. The study area is Nyaba River located in Enugu urban, the political and administrative headquarters of Enugu state.

The methodologies employed include; data acquisition from field observation and satellite images; and data processing and analyses using ilwis 3.2 and Arc GIS 9.3 software. The total area of gullies for each year of study was calculated in square meters. The result showed that gully progressed from 578,713,735 meters in 1986 to 1,002,819,723 in 2011. Prediction showed also that the magnitude of the gully area is expected to increase as the years go by. The forecast put the expected coverage of gully erosion at Nyaba River to be 45,210,440 square meters by the year 2040.

In the light of this, some recommendations were made. They include: constant monitoring to detect early stages of gully formation; regulation of grazing of pasture in the area; restriction of sand mining from the river bank and construction of water ways to stabilize river flow.

In conclusion, monitoring clearly showed that there was a geometric progression in gully formation at Nyaba over years. And the expansion was aided by anthropogenic activities going on in the area than natural factors.

## 8887-20, Session 5

### Estimating snow albedo patterns in a Mediterranean site from Landsat TM and ETM+ images

Rafael Pimentel, Javier Herrero, Ctr. Andaluz de Medio Ambiente (Spain) and Grupo de Dinámica Fluvial e Hidrología (Spain); María José Polo-Gómez, Grupo de Dinámica Fluvial e Hidrología (Spain) and Ctr. Andaluz de Medio Ambiente (Spain)

The water present in the snowpack constitutes a basic resource in mountainous areas. In Mediterranean regions this is especially relevant due to the semiarid character of the climate. Therefore it is essential to know the behavior and evolution of the snow layer, which is not always simple due to the high spatiotemporal variability of the snowmelt/accumulation cycles. Snow albedo plays an important role in the mass and energy balance formulation. It affects to the shortwave radiative flux (0.3 to 2.5  $\mu\text{m}$ ), quantifying the amount of solar radiation absorbed and reflected by the snowpack. But snow albedo is not homogeneous throughout this spectral range. In semiarid areas, besides, the particular climatic conditions enhance the spatiotemporal variability of the snow albedo during the snow season, increasing its difficulty to be measured and monitored. Satellite remote sensing is a powerful tool to measure the snow albedo evolution, since these sources are able to capture the variability of albedo in each of the three domains: time, space and frequency. However, several factors, such as the atmospheric effects, the degree of isotropy, the spectral interval of the narrow band sensors, and the geometry between sun and sensor in rugged terrain, make it difficult its adequate estimation.

The aim of this work is to analyze the trend in the albedo evolution throughout the year and provide modeling with an estimation of this evolution without requiring external data. The study was carried out in Sierra Nevada Mountains (Southern Spain). They form a linear mountain range parallel to the shoreline of the Mediterranean Sea, with altitudes ranging from 1500 to 3500 m. Ten years of Landsat-5 and Landsat-7 Thematic Mapper images were analyzed to determine this trend in the albedo evolution. The broadband snow albedo for each image was derived from narrowband albedo, which is obtained from each one of the bands of the Landsat image series. Atmospheric and topographic corrections were applied on each band data. The presence of snow was firstly determined at each pixel by means of the calculation of the normalized difference snow index (NDSI), and then a narrowband to broadband conversion was performed.

The obtained trend allows reproducing the snow albedo evolution in an easy way in the modeling process. Moreover, some simulations of the different snow properties were also derived to evaluate the accuracy of this new representation.

## 8887-21, Session 5

### Accuracy of fuzzy burned area mapping as a function of the aerosol parameterization of atmospheric correction

Saidiazar Ramin, Politecnico di Milano (Italy) and Istituto per il Rilevamento Elettromagnetico dell'Ambiente (Italy); Daniela Stroppiana, Pietro A. Brivio, Mirco Boschetti, Mariano Bresciani, Claudia Giardino, Istituto per il Rilevamento Elettromagnetico dell'Ambiente (Italy)

Mediterranean Forests are every year affected by wildfires which have a significant effect on the ecosystem. Mapping burned areas is an important application field of optical remote sensing techniques and several methodologies have been developed and applied in order to reach the highest accuracy. Burned areas exhibit a wide range of spectral characteristics which depend on the characteristics of the site and of the fire event (e.g., pre-fire vegetation type and conditions, background soil, fire severity, and post-fire processes) and of the observation conditions (e.g., atmospheric conditions, geometry of acquisition, and time between image acquisition and fire date). Spectral Indices (SIs), which are computed from the remote sensing reflectance, have been widely exploited for burned area mapping (Bastarrika et al., 2011); we recently proposed an algorithm for mapping burned area from Landsat TM/ETM+ data which is based on SIs and fuzzy set theory. The algorithm has been applied over different regions of the Mediterranean area and provided satisfactory results

(Stroppiana et al., 2009). However, the robustness of the algorithm can significantly depend on the pre-processing of the optical remotely sensed data. In particular, atmospheric correction plays an important role in the variability of surface reflectance, hence on the variability of the SIs thus likely affecting the accuracy of the burned area maps. Therefore, we focused our research interest on the assessment of the accuracy of burned area maps as a function of the atmospheric correction. The primary objective of our research is to evaluate the robustness of the fuzzy burned area mapping algorithm with respect to atmospheric correction of the input optical remotely sensed data. We carried out an experiment on one Landsat TM/ETM+ image acquired over a study area in Portugal on August 12th, 2003; in 2003 Portugal has been seriously and extensively affected by forest fires during summer. In this paper we present the first results of the analysis of the sensitivity of atmospheric correction depending on different models of aerosols and concentration of Aerosol Optical Thickness (AOT). The atmospheric correction is carried out by means of 6S (Second Simulation of a Satellite Signal in the Solar Spectrum) code (Vermeote et al., 1997, 2000) which provides surface reflectance values. The study has considered a range of AOT values (from 0.20 to 0.55) combined with both the "Continental" and the "Maritime" models for correcting the atmospheric effect of the Landsat TM-5 scene. The surface reflectance images output from the 6S code have been used as input data for running the fuzzy burned area mapping algorithm. The accuracy of the output burned area maps has been assessed by comparison with burned area perimeters independently extracted from Landsat TM data. The results show that atmospheric correction affects to some extent the variability of the fuzzy output burned area maps in particular, the distribution of the fuzzy output values over the burned areas. Although results are preliminary, they encourage us to test the approach over different regions of the Mediterranean environment to evaluate its robustness.

#### 8887-22, Session 5

### ARIN (R) procedure for the normalization of multitemporal remote images through vegetative pseudo-invariant features

Luis García-Torres, Instituto de Agricultura Sostenible (Spain); Juan-José Caballero-Novella, David Gomez-Candón, Montse Jurado-Expósito, Institute for Sustainable Agriculture, CSIC (Spain)

An Automatic Relative Image Normalization (ARIN®) method was developed to normalize multitemporal remote images based in vegetative pseudo-invariant features (VPIFs), as following: 1) defining the same parcel for each selected VPIF in each multitemporal image; 2) extracting the VPIF spectral bands data for each image; 3) calculating the correction factor (CF) for each image band to fit it to the same expected values, normally for each band the average of the series; 4) obtaining the normalized images by transforming each original image band through the corresponding CF linear functions. ARIN® software was developed to automatically achieve the previously described procedure.

We have validated ARIN using a series of six GeoEye-1 satellite images taken over the same Southern of Spain scene in 2010, from early April to October, at about 4 weeks interval. Three VPIFs were chosen: citrus orchards (CIT), riparian trees (POP) and Mediterranean forest trees (MFO). The VPIFs spectral band correction factors (CFs) to implement the ARIN linear normalization procedure largely varied among spectral bands for any given image and among images for any given spectral band. The correlation coefficients between the CFs among VPIFs for any spectral band and overall all bands are over 0.83 and significant at  $P=0.95$  or higher. For the ARIN normalized images, the range and standard deviation of any spectral bands and vegetation indices values were considerably reduced as compared to the original images, regardless the VPIF or the combination of VPIFs selected for normalization, which proves the method efficacy. Moreover, ARIN method was easier and efficient than the absolute calibration QUAC method, and somehow similarly efficient as the highly tunable FLAASH, in which solar position and weather calibration parameters are required.

#### 8887-23, Session 5

### Details of the use of NIR reflectance as a tool for crop monitoring

Fermin Pascual-Ramirez, Jacovo Morales-Morales, Marcos Perez-Sato, Delfino Reyes-Lopez, Benemérita Univ. Autónoma de Puebla (Mexico)

The use of information obtained by remote sensing has been suggested to model the behavior of crops through the use of vegetation indices (IV) due to its qualities spatial sampling, temporal and radiometric. In this study, we examined the growth cycle of Sugarcane (*Saccharum officinarum* L.) using a traditional IV and spectral information in the near infrared region (NIR) to check its use as a tool for monitoring the state of development. The study was conducted in the Morelos state's sugarcane region, using a register field verified during the period 2010-2011. In the development of work employed a group of 25 satellite images ETM+ sensor, with information in the spectral region of the NIR and Red (R). The imagery covered temporally the end of one season and all of the next season. Before to extract information, we did proceedings for radiometric, atmospheric and BRDF corrections. After that, using this information, we calculated the Top of Atmosphere reflectance and Normalized Difference Vegetation Index (NDVI). NIR information and NDVI calculations were taken at the level of individual pixels within intercomparable plots, later to make global statistics plots level of interest. For this purpose we developed a software for extract información and store it in a local GeoDatabase using PostGIS. We analyzed the information, first at pixel level, relating the value of NIR and NDVI with the state of development of crops verified on field. After, this information was analyzed on on multi-temporal point of view during crop development. For this purpose, for each pixel we had graphed values of Julian Days, with values of NIR and NDVI, and locate different stages of the crop on the time and variation on values obtained. Similar process were conducted but with generalized information at plots of level, using an average value for all pixels located into plots. The results showed a similar behavior between NDVI and reflectance of the NIR by relating to the state of development of the crop in clear sky conditions. Furthermore, with analyzed information derived, it was found that the utility of NDVI decreases when cloudiness problems occur even in small amounts, while the reflectance information from NIR band can be used for purposes of modeling development cultivation under these conditions. We conclude that the NIR information can be used reliably even in cloudy conditions for modeling the state of development of sugar cane cultivation. This information can be used as a tool for monitoring crops and for yield predictions purpose.

#### 8887-24, Session 6

### EO4Water (Earth observation technologies for rural water management): a case study of transferability of satellite-based irrigation advisory services between two agricultural areas

Francesco Vuolo, Nikoluas Neugebauer, Univ. für Bodenkultur Wien (Austria)

Austria is very rich in water with annual average precipitations of 1200 mm. However, Eastern provinces are characterized by semi-arid climate conditions, with annual precipitations of less than 550 mm (about 250-300 mm from May to September). Crops such as vegetables, maize and sugar beet require between 200 and 600 mm of water for kg dry matter. For summer crops with high biomass potential this can reach a total water demand for the growing period of around 800 mm, which clearly cannot be provided by precipitation under current climatic conditions. In this region, increased demand for high quality food, sustainability of local production, and market development strategies, is stimulating the application of tools for more efficient and effective irrigation water use. Tests have been carried out to regulate irrigation based on soil water content measurements performed at plant or field scale. However, current solutions are only implemented at a very local and/or experimental level and they are not available for everybody.

The potentiality of satellite-based techniques in supporting the

management of water resources is nowadays widely recognized. They can provide detailed knowledge about the amount of water required by crops at a given development stage and in specific climatic conditions.

EO4Water (Earth observation technologies for rural water management) is a research project funded by the Austrian Space Applications Programme (ASAP) to apply satellite technologies for mapping crop water needs. The project development and implementation focused on the Marchfeld area, one of the major crop production areas of Eastern Austria. This work reports on the results of two experimental campaigns conducted in the growing season 2012 and 2013 using multi-temporal time series of DEIMOS-1 satellite sensor data. Our roadmap for transferability of technologies between different agricultural areas will be provided.

#### 8887-25, Session 6

### Strategic system development toward biofuel, desertification and crop production monitoring in continental scales using satellite-based photosynthesis models

Daijiro Kaneko, Remote Sensing Environmental Monitor, Inc. (Japan)

Carbon sequestration by photosynthesis is a fundamental and powerful approach to achieve carbon dioxide reduction as a measure against global warming. Many researchers have developed carbon fixation models for forest and grassland areas. Nevertheless, validation of the photosynthesis rate (PSN) remains in the validation stages of estimation accuracy because of the conventional flux scheme of surface energy imbalance in the atmospheric boundary layer. The application of carbon sequestration by photosynthesis is a hopeful step towards alleviating such environmental concerns as carbon storage, bio-energy, desertification, and crop production management.

Bio-fuels, renewable fuels used to reduce fossil-fuel consumption, are sustainable fuels such as bio-ethanol produced from glucose or starch, biodiesel produced by trans-esterification of seed oils from *Jatropha* derived by afforestation, and soybean oils. The latter can stabilize grain prices and maintain secure planting areas.

Land-cover classification using remote sensing extracts distributions of forests, grassland, and croplands. Grassland belts can provide signals related to the degradation of semi-arid lands through severe dust-storms in spring. Governments expect to re-cover rough lands with plants over desert areas to halt the spread of dust-storms over Beijing and Tianjin and even to limit air contaminant particles over the Seoul and Tokyo metropolitan areas. The proposed environmental system extracts suitable lands for a Clean Development Mechanism (CDM), as situated in semi-arid belts caused by Hadley downward convection. NDVI, PSN, surface pressure, and wind distributions indicate that the dust-storms originate from the Taklimakan and Gobi deserts in Mongolia.

Where the price of Certified Emission Reduction (CER) or EUA falls to less than 5 Euros /t, the author increases cost-performance by including bio-diesel in CDM projects. This paper reviews Japanese *Jatropha* projects and world biodiesel research activities. The author also emphasizes multiple benefits of afforestation/reforestation (A/R) projects such as beneficial impacts of carbon fixation, water resource management, erosion, combating desertification as well as bio-diversity.

Regarding crop production applications, industrialization in developing countries achieved through direct investment by economically developed nations raises their income, resulting in increased food demand. Last year, China began to import rice as it had in the past with grains of maize, wheat, and soybeans. Important agro-potential countries make efforts to cultivate new crop lands in South America, Africa, and Eastern Europe. Trends toward less food sustainability and stability are continuing, with exacerbation by rapid social and climate changes.

Operational monitoring of carbon sequestration by herbaceous and bore plants converges with efforts at bio-energy, crop production monitoring, and socio-environmental projects such as CDM, A/R, combating desertification, and bio-diversity.

The author has been developing a thematic monitoring structure, the RSEM system, which relies upon satellite-based photosynthesis models over several continents for operational support in environmental fields mentioned above. Validation methods stand not

on FLUXNET but on carbon partitioning validation (CPV). The models demand continuing parameterization. The entire frame system has been built using meteorological data supplied by NCEP/ECMWF Reanalysis, but the model accuracy remains insufficient except for that of paddy rice. The author shall produce a support system that incorporates global environmental forces.

#### 8887-26, Session 6

### The predictive models for estimating above ground biomass and stand volume of oil palm plantations using Landsat TM

Nazlin Asari, Mohd Nazip Suratman, Jasmee Jaafar, Univ. Teknologi MARA (Malaysia)

Oil palm agricultural tree crops have been extensively studied in the aspect of botanical and cultivation due to its socio-economic and commercial values. Malaysia is known as the world's top producer of palm oil with current planted area of plantations around 4.69 million ha. There is an abundance potential of biomass including oil palm in the country. Despite the importance of oil palm to the country, an accurate and reliable assessment method in resource availability is lacking. Therefore, the need for more efficient method of inventory is an impetus of this research into supplementing ground-based survey with information from satellite remote sensing. Remote sensing technology offers a cost-effective ways to monitor natural resources. The frequency of remote sensing data acquisition couple with the availability of data for extensive area increases its attractiveness for inventory and monitoring purposes. The objectives of this study are 1) to determine the relationships between spectral radiance recorded by Landsat TM and oil palm stand variables and 2) to develop the predictive models for estimating AGB and stand trunk volume of oil palm plantations by combining ground data and Landsat TM data. This study was conducted in the selected oil palm plantations in Selangor, Malaysia. The field stand parameters collected include stand age, oil palm trunk radius, height, diameter at breast height (DBH), density, crown width and crown closure. Parameter variables related to AGB and stand volume include Landsat TM bands and several vegetation indices such as simple ratios, Normalized Difference Vegetation Index (NDVI), Infrared Index (IRI), Enhanced Vegetation Index (EVI), Atmospherically Resistant Vegetation Index (ARVI), Principal Component Analysis (PCA) and Tasseled Cap Transformation.

#### 8887-27, Session 6

### Forest biomass estimation from the fusion of C-band SAR and optical data using wavelet transform

Md Latifur Rahman Sarker, Univ. Teknologi Malaysia (Malaysia)

Forest biomass estimation is essential for greenhouse gas inventories, terrestrial carbon accounting and climate change modelling studies. Although a lot of effort has been made in estimating biomass using both field-based and remote sensing techniques, no universal and transferable technique has been developed so far to quantify biomass carbon sources and sinks due to the complexity of the environmental, topographic and biophysical characteristics of forest ecosystems.

This study investigated the potential of SAR (RADARSAT-2 dual polarizations) and optical (AVNIR-2) image fusion for biomass estimation using wavelet transform. Six different types of wavelets (haar, daubechies, symlet, coiflet, biorthogonal and discrete meyer) were tested with different rules and three decomposition levels for four different image combinations of SAR and optical data. The highest accuracy ( $r$ ) of 0.84 was obtained from the fusion of NIR & HV polarization data, compared to 0.70 ( $r$ ) from the NIR band alone. The accuracy was further improved to 0.88 ( $r$ ) using texture measurements of the fused image. The results indicated a substantial improvement of biomass estimation from the fused images, and this accuracy is very promising, especially when using only one fused image in the high biomass situation of the study area, and gives a clear message to the research community that biomass estimation can be improved using the fusion of SAR and optical data due to their complementary information. Furthermore this fusion process can significantly reduce the saturation problem of optical and SAR data for biomass estimation.

8887-28, Session 7

## Using spatio-temporal Markov model for flood mapping : the case study of Yialias River in Cyprus

Dimitrios D. Alexakis, Cyprus Univ. of Technology (Cyprus); Aristeidis G. Koutroulis, Manolis Grillakis, Technical Univ. of Crete (Greece); Athos Agapiou, Kyriacos Themistocleous, Cyprus Univ. of Technology (Cyprus); Ioannis Tsanis, Technical Univ. of Crete (Greece); Diofantos G. Hadjimitsis, Cyprus Univ. of Technology (Cyprus)

Flooding is one of the most common natural disasters worldwide. This paper strives to highlight the hydrological effects of multi-temporal land use changes in flood hazard. The study area is Yialias River located in the broader region of Nicosia - Cyprus. The certain area has suffered from several flood disasters in the recent past. Initially, the land cover regime of the study area (last 20 years) was thoroughly studied using multi-temporal satellite images of either medium or high resolution (Landsat, ASTER, GeoEye-1) and implementing sophisticated classification methodologies such as Object oriented analysis and Support Vector Machine (SVM). Land use / Land (LULC) cover maps for the periods of 1990, 2000 and 2010 were developed. All these maps were incorporated in the CA-Markov chain analysis model and the LULC map of 2020 was constructed. The Markov Chain analysis describes the probability of land cover change from one period to another by developing a transition probability matrix between  $t_1$  and  $t_2$ . The CA component of the CA-Markov model allows the transition probabilities of one pixel to be a function of the neighboring pixels. Following, hydrological analysis was performed using the Hydrological Modeling System (HEC-HMS). HEC-HMS is designed to simulate the precipitation-runoff processes of dendritic watershed systems. This includes large river basin water supply and flood hydrology, and small urban or natural watershed runoff. The HEC-HMS model was setup in distributed mode, enabling the utilization of the spatial information of the land use via the Curve Number coefficient. Thus, the 2020 LULC map was incorporated in the hydrological model in order to predict the hydrological behavior of the catchment area for the next decade. The results were compared with the present hydrological regime and denoted the future increase of runoff due to the predicted extensive urban sprawl phenomenon.

8887-29, Session 7

## Dynamic characterization of the vegetation using remote sensing for hydrological modelling at basin scale

Elisabet Carpintero García, IFAPA Ctr. Alameda Del Obispo (Spain); María José Polo Gómez, Grupo de Dinámica Fluvial e Hidrología (Spain); María Patrocinio González-Dugo, IFAPA Ctr. Alameda Del Obispo (Spain)

Satellite remote sensing may provide distributed series of spectral properties of the vegetation with different spatial and temporal resolution for its dynamic characterization, but they do not always satisfy the requirements of some of the pursued applications. These limitations can be overcome with the use of image integration techniques, which allow the combination of sensors with different characteristics taking advantage of all of them. This work presents the monitoring of the vegetation cover in a Mediterranean watershed, the Guadalfeo River basin, by means of using both Landsat and MODIS data to meet the spatiotemporal scale appropriate for its hydrological modelling. An initial evaluation of the spectral differences between both sensors in this area is performed and, based on the results, an integration algorithm is proposed.

The Guadalfeo River basin, with an area around 1300 km<sup>2</sup>, is located on the southern slope of Sierra Nevada Mountains (Spain). The interaction of the alpine climate at the high mountains with the neighbour coastal influence from the Mediterranean Sea results in a large variety of climate conditions in a reduced area. It presents a heterogeneous distribution of rainfall due to orographic effects, with an average value around 800 mm in the source, and less than 450 mm in the coastal region. These conditions cause a high variability of vegetation types and cover fractions.

In this work, the temporal variations of the vegetation cover fraction are evaluated using a series of Landsat and MODIS images, taking advantage of the higher spatial resolution of the former versus the higher time resolution of the latter. The implications of the spatial and temporal scale differences between both sensors in an area characterized by the heterogeneity of environmental factors are also discussed. A preliminary study of the deviations of NDVI and ground cover fraction between concurrent data of both sensors is performed, analysing its relationship with basin topography and land cover. Thereafter, an integration algorithm was applied and validated to obtain synthetic NDVI images at the spatial resolution of Landsat data with MODIS sensor time steps. Two different methods, the Temporal Adaptive Reflectance Fusion Model (STARFM) algorithm (Gao et al., 2006) and a modification of TsHARP approach (algorithm for sharpening thermal imagery) (Agam et al., 2007) were tested in this study area.

The comparison between Landsat and MODIS parameters revealed NDVI deviations varying between 2-5% and ground cover fraction deviations between 3-6% on average. It was not possible to establish a direct relationship between ground cover fraction deviations from both sensors and basin topography, nor a clear relationship with vegetation types was found. However, higher deviation repeatedly corresponded with the vegetation types with higher ground cover fractions, conifers and quercus, with ground fraction cover deviation values of 10% and 7%, respectively. Some temporal patterns of NDVI deviations were found, especially significant during the summer (with  $r^2$  around 0.7). Finally, the integration algorithm successfully reflected the heterogeneity of the vegetation in the study area, and accurately predicted NDVI values at an effective spatial resolution close to that of Landsat images.

8887-30, Session 7

## Spatial processing techniques for satellite altimetry applications in continental hydrology

Philippe Maillard, UFMG (Brazil) and Observatoire Midi-Pyrénées (France); Stéphane Calmant, Ctr. d'Etudes Spatiales de la Biosphère (France)

Radar-based satellite altimetry is a well recognized measuring technique with good precision for oceanographic applications. For continental hydrology, the use of satellite altimetry is complicated by a number of factors such as river width, satellite crossing angle, returning wave shape and noise from the river banks or islands. These factors make precision vary significantly. Still, the perspective of having time series of water level can facilitate the monitoring of river behavior and improve hydrologic models. The satellite crossing points can be made into "virtual gauging stations" that can complement the existing network of land stations. This article describes a series of spatially explicit processing to correct or exclude point altimetry measurements not related to water levels. While some processing take advantage of a priori information such as the average river width at the satellite crossing point, the center line of the river and a digital elevation model, others are based on pattern recognition techniques to characterize the shape described by the sequence of points. The centerline of the river is used to rearrange the points according to their distance to the river while the river width and the digital elevation model are used to infer on the possibility of having river banks affecting the measurements. Other problems like "satellite signal hooking" are caused by the satellite recording strong off-nadir backscatter that yields falsely low water levels. These are dealt with by testing the shape of the point sequence which can describe a downward second degree polynomial curve. All these factors are corrected by determining a weight for each point in the crossing sequence of measurements. These processing approaches have been combined into a single tool called VHSTOOL. The method is tested on a 1000 km stretch of the São Francisco River in Brazil for which 13 in situ gauges are available, some of which very close to satellite crossing points. Data from Envisat cover the 2003-2010 period while the recently launched Altika satellite has provided data for a few months in 2013. The "ice1" product was used for both Envisat and Altika. Validation was not carried out with absolute measurements since official water level data are only measured relative to the local gauge position. Instead, a linear regression was computed between the satellite altimetry data and the in situ gauge data and yielded coefficient of determination above 0.95. The results show that significant improvements in precision can be obtained with the

combination of processing when comparing with regular automatic averaging techniques. In fact, the quality of the data series is very close to the precision attained by manual means that make use of visual interpretation to select the points to be averaged and typically result in offsets between 10 and 50 cm. Altika data has only been available since March 2013 but already promises to improve precision, especially for small rivers.

## 8887-31, Session 7

### Wetland change detection with remote sensing and quantitative analyses of hydrological driving factors

Hou Peng, Ministry of Environmental Protection (China)

Since wetland is water-dominated ecosystem, and similar remote sensing image features of hill shade, old residential area and wetland make it difficult to gain the wetland information and accurately detect wetland change. With the help of spatial analyses function in geographical information system software, the hill shade is simulated at the solar radiation conditions according with remote sensing image acquired. This paper successfully uses this DEM simulation method to remove the influence of hill shade on wetland. Because there is the similar digital number scope of old residential areas and wetlands in urban region, the digital number is replaced with surface reflectance to extract urban wetland information, and old residential area influences on the wetland is wiped off. Urban wetland is exactly extracted with normalized difference water index and its change is accurately detected with Landsat TM images acquired at 1991 and 2007. According to urban wetland features, wetland change and natural or social driving factors are closely tied together by wetland hydrology change. So that, according to the wetland water budget theory, taking hydrology factors in wetland water budget equation as the main index, together with the society, hydrology and meteorology statistic data, this research quantitatively analyzes the contribution of natural and human driving factors to wetland change. Natural factors are the main reasons for wetland change, the decrease of precipitation, surface water inflows and the increase of evaporation are negative contribution to wetland maintenance, about 39.22%, 14.05% and 11.85% respectively, the decrease of surface water outflows is positive contribution, about 12.75%. To the human factors, urban sprawl is negative contribution, about 3.42%, however, technology progress is positive contribution, about 25.55%, and helpful to protect wetland and reduce the negative contribution of urban sprawl.

## 8887-33, Session 8

### Correcting the influence of vegetation on surface soil moisture indices by using hyperspectral artificial 3D-canopy models

Daniel Spengler, Theres Kuester, Helmholtz-Zentrum Potsdam Deutsches GeoForschungsZentrum GFZ (Germany); Annett Frick, LUP - LUFTBILD UMWELT PLANUNG GmbH (Germany); Hermann J. Kaufmann, Helmholtz-Zentrum Potsdam Deutsches GeoForschungsZentrum GFZ (Germany)

Surface soil moisture content is one of the key variables used for many applications including hydrology, meteorology and agriculture. Hyperspectral remote sensing provides effective methodologies for mapping soil moisture content over a broad area by different indices such as Normalised Soil Moisture Index (Haubrock et al. 2005, 2008) and Soil Moisture Gaussian Modelling (Whiting et al. 2004). Both indices achieve a high accuracy for non-vegetation influenced soil samples, but are limited in case of the presence of vegetation. Increase of the vegetation cover leads to non-linear variations of the indices.

In this study a new vegetation correction methodology based on canopy reflectance simulation and combining a soil moisture index and a vegetation index is presented consisting of several processing steps. Firstly hyperspectral reflectance data are classified and masked in terms of crop type and growth stage. Actual the crop types winter wheat, winter rye and winter barley are implemented. For this purpose a Maximum Likelihood Classification based on spectral features is performed. The basic set of features is calculated of statistical functions like mean value and standard deviation as well as ratio,

absorption depth and coefficients of polynomial approximations. The classification result defines the potential vegetation types and growth stages of the hyperspectral image. Based on this information 3D plant models are selected from a database to simulate typical canopy reflectance data by Monte Carlo Raytracing considering variations in the canopy structure (e.g. plant density and distribution) and the soil moisture content for actual solar illumination and sensor viewing angles.

A vegetation correction function is developed, based on calculated soil moisture indices and vegetation indices of the simulated canopy reflectance data. The variations of the soil moisture indices in dependence of the vegetation cover represented by a vegetation index of the simulated data are analysed and related to soil moisture values. Finally this function is applied on hyperspectral image data.

The method is tested on multitemporal hyperspectral image data such as AISA DUAL, HySpex and APEX of the test site Fichtwald in Northeast Germany. The results will be presented and discussed in terms of validation, limitation and optimisation.

## 8887-34, Session 8

### Data assimilation of surface soil moisture, temperature and evapotranspiration estimates in a SVAT model over irrigated agriculture in semi-arid areas: what is best to constraint evapotranspiration predictions?

Adrien Tavernier, Lionel Jarlan, Ctr. d'Etudes Spatiales de la Biosphère (France); Salah Er-Raki, Univ. Cadi Ayyad (Morocco); Guillaume Bigeard, Ctr. d'Etudes Spatiales de la Biosphère (France); Saïd Khabba, Univ. Cadi Ayyad (Morocco); Amina Saaidi, Direction de la Météorologie Nationale (Morocco); Lepage Michel, Jonas Chirouze, Gilles Boulet, Ctr. d'Etudes Spatiales de la Biosphère (France)

A good estimation of latent heat flux is of prime importance in agriculture to improve the management of the irrigation water inputs. Soil-Vegetation-Atmosphere Transfer models (SVAT) solve the energy and water budget of the soil-vegetation-atmosphere continuum to predict the evolution of this key variable. Data assimilation is a way to improve the prediction of the different state variables of SVATs models by minimizing the difference between an observation indirect proxy of the evapotranspiration and the modeling predictions.

The context of the study deals with semi arid regions and more precisely in the Haouz plain, part of the Tensift basin near Marrakesh in Morocco. In the surrounding of this city, irrigation for agriculture represents more than 85% of the water consumption. Different data assimilation techniques (2DVAR, Ensemble Kalman Filter, Particle Filtering) have been implemented in the ISBA model (Interaction Soil Biosphere Atmosphere see J.Noilhan & S.Planton, 1989 / J.Noilhan & J.F.Mahfouf, 1996) on two sites of wheat and olive orchard. The results show that the basic parametrization of the model using global and spatialized data like the ecoclimap data base (S.Faroux et al, 2012) are not adapted to semi-arid region. A sensitivity analysis and a calibration procedure are first carried out using a stochastic multicriteria (L.A.Bastidas et al, 1999) approach and a genetic algorithm, respectively. Results show an overall bias reduction between observed and predicted evapotranspiration on both sites. In the view of using remote sensing products, the different product combinations that could be retrieved from remote sensing data (surface soil moisture, surface temperature and evapotranspiration) are evaluated and a sensitivity analysis to satellite repetitivity is carried out.

## 8887-35, Session 8

### Enhancing TIR Image Resolution via Bayesian Smoothing for IRRISAT Irrigation Management Project

Paolo Adesso, Univ. degli Studi di Salerno (Italy); Fulvio Capodici, Univ. degli Studi di Palermo (Italy); Guido D'Urso, Univ. degli Studi di Napoli Federico II (Italy); Maurizio Longo,

Univ. degli Studi di Salerno (Italy); Antonino Maltese, Univ. degli Studi di Palermo (Italy); Rita Montone, Rocco Restaino, Gemine Vivone, Univ. degli Studi di Salerno (Italy)

Nowadays, there is a growing attention to the efficient use of natural resources for the anthropic activities. In this context the Italian project IRRISAT [1] is devoted to Irrigation Management that, also due to the climate changes, is at the centre of several research programs in the world.

In order to monitor the water resources of large areas, remotely sensed data (largely used in many agricultural applications) are of paramount importance for the continuous and detailed tracking of several physical properties. In particular Thermal InfraRed (TIR) channels are very useful to estimate the so-called "thermal inertia" [2], that is a key feature to evaluate several quantities suitable for Irrigation Management, such as the "soil moisture" [3].

However, the desirable conjunction of high spatial and temporal resolutions is impossible to reach for any real sensor, because it results in conflicting requirements. Accordingly, in recent times, considerable research efforts have been devoted to integrate data at high acquisition rate with those provided by sensors with small pixel sizes.

In the particular context of Irrigation Management, the slow dynamics involved in agricultural applications allow to relax the real-time requirement in obtaining high space-time resolution thermal information. In that case the estimation accuracy can be improved by using Bayesian smoothing techniques [4].

More in detail, the idea is to employ all the remotely sensed data, characterized by both high spatial/low temporal and high temporal/low spatial resolution, that are available for the area of interest in a certain time interval (e.g. one day). Then the construction of high space/high time resolution image sequence is performed by resorting to the "fixed-interval" smoothing approach [5].

In the present work we assess the performance of this procedure through a comparison with classical filtering strategies (see e.g. [6]) carried out by experiments based on real remotely sensed data.

#### References

- [1] IRRISAT project: <http://www.irrisat.it/>
- [2] J.A. Sobrino, M.H. El Kharraz, J. Cuenca, N. Raissouni, "Thermal inertia mapping from NOAA-AVHRR data", *Advances in Space Research*, Volume 22, Issue 5, 1998, Pages 655-667, ISSN 0273-1177, 10.1016/S0273-1177(97)01127-7.
- [3] J. Van doninck, J. Peters, B. De Baets, E.M De Clercq, E. Ducheyne, N.E.C. Verhoest, "The potential of multitemporal Aqua and Terra MODIS apparent thermal inertia as a soil moisture indicator", *International Journal of Applied Earth Observations and Geoinformation*, Volume 13, Issue 6, 2011, Pages 934-941.
- [4] D. Simon, "Optimal State Estimation", Wiley-Interscience, 2006
- [5] J.E. Wall, A.S. Willsky, N.R. Sandell "On the fixed-interval smoothing problem" *Stochastics*, Vol. 5, Iss. 1-2, 1981, Pages 1-41.
- [6] P. Addesso, R. Conte, M. Longo, R. Restaino, G. Vivone, "A sequential Bayesian procedure for integrating heterogeneous remotely sensed data for irrigation management", *Proc. SPIE Remote Sensing 2012*, Edinburgh (UK), 24 - 27 September 2012, vol. 8531, pp. 85310C-1 - 85310C-10.

## 8887-36, Session 8

### Soil water content monitoring: a verification of thermal inertia approaches

Antonino Maltese, Fulvio Capodici, Univ. degli Studi di Palermo (Italy); Guido D'Urso, Univ. degli Studi di Napoli Federico II (Italy); Paolo Addesso, Maurizio Longo, Rita Montone, Rocco Restaino, Gemine Vivone, Univ. degli Studi di Salerno (Italy)

Soil water content is a soil status condition directly connected with soil evaporation and plant transpiration processes. These are related to the soil water content within the root zone, which is readily available to evapotranspiration.

Most methods to estimate actual evapotranspiration only indirectly accounts for the wetness of the soil surface. Thus, in agricultural sciences, the assessment of the spatial distribution of soil water

content could be of utmost importance in evaluating crop water requirement.

Water content of the upper part of the soil can be determined applying the thermal inertia approach on optical images matched with thermal infrared ones. Indeed, in spite of the limitation due to possible cloud cover, this approach takes on great interest as a source of information on soil water content.

Even if, the coupling between thermal inertia and soil moisture is not straightforward, actual and apparent thermal inertia can be converted to water content of the upper part of the soil when soil thermal properties are known.

Thermal inertia is based on the one-dimensional thermal diffusion differential equation relating the temperature variation, over a homogeneous half-space of constant thermal properties, with the temperature variation over time were.

Thermal inertia formulation has been rigorously retrieved on bare soil, even if, it was also verified on soils partially covered by vegetation. However, reliable assessments can be achieved once estimated the actual solar radiation reaching the soil through the canopy. This latter can be evaluated through an extinction factor.

The research is focused to determine the simpler operational approach providing reliable results over time.

To this aim, different formulations of the thermal inertia were tested:

- the apparent thermal inertia (this basic approximation solely requires surface albedo and a night-day surface temperature pair);
- the thermal inertia assuming a constant phase difference (this methodology uses a single ground measurement, being the time of maximum surface temperature);
- the thermal inertia assuming a spatially distributed phase difference (this approach requires at least three thermographies).

Moreover, the first and second order approximations of the Fourier series expansion of the thermal diffusion equation were tested.

Thermal inertia has been evaluated on agricultural areas of two regions of South Italy (Campania and Sicily) using MODIS images. Within this regions two micro-meteorological stations were installed to validate the soil water content estimates at different depths over the time.

## 8887-37, Session 8

### Multisensor characterization of subsurface structures in a desert plain area in Egypt with implications for groundwater exploration

Magaly Koch, Boston Univ. (United States); Ahmed Gaber, Port Said Univ. (Egypt); Mohamed H. Geriash, Suez Canal Univ. (Egypt); El-Sayed A. Zaghoul, Sayed M. Arafat, National Authority for Remote Sensing and Space Sciences (Egypt); Mostafa Abubakr, Boston Univ. (United States)

A desert plain, NW of Aswan in Egypt, is currently being investigated to develop new techniques of multisensor data integration for groundwater exploration. A combination of multispectral, thermal and microwave data obtained from space (ASTER and PALSAR) and supported by ground measurements (GPR, field spectroradiometry and magnetometry) were used to investigate surface sediment characteristics of the El-Gallaba Plain area. This desert plain once hosted an ancestral river system long before the Nile even existed. Nowadays the fluvial deposits are largely covered by aeolian and gravelly sands and thus only detectible with radar and thermal images.

The methodology consisting of 1) processing multi-spectral and thermal bands of ASTER imagery covering the El Gallaba plain area for identifying main surface covers, especially gravelly (fluvial) soils, and migrating sand dunes / sand sheets, 2) fusing optical (ASTER) with radar (PALSAR single polarization) data for spectral and textural classification, 3) correlating land surface temperature (LST) derived from ASTER thermal bands with surface material properties derived from SAR data, 4) validating satellite borne thermal and radar products with ground penetrating radar (GPR) and magnetic measurements at selected sites to determine layering and degree of homogeneity of the unconsolidated material and depth to the basement rock, and 5) correlating average LST with average backscatter signal strength of main surface sediment materials as identified on the classified ASTER/PALSAR fused image (sand dunes, sand veneer, gravel, alluvial sands and clays etc.).



Results show two broad strips of thermal cooling anomalies arranged in a linear fashion and diagonally crossing the alluvial basin. Spectral signatures collected along the linear LST anomalies show generally higher reflectance values (higher albedo) than the surrounding sediments. In arid environments, evaporation is minimal due to extremely low soil water content. Thus the cooling anomalies and high albedo are an indication of lower surface sediment emissivity (low heat storage capacity) than the surrounding warmer areas. Furthermore, the homogeneity of the sediments within the linear LST anomalies was measured with a ground penetrating radar using 250 MHz shielded antenna. The 12 GPR profiles across the LST anomalies confirmed that the near-surface sediments (up to 10 m depth) consist of thin horizontal layers of sandstone with very low gravel content. They show very different textural and compositional characteristics with respect to the surrounding areas suggesting that they were deposited under different depositional environments. A linear graben-like structure could be a proper depositional basin to host such loose and homogenous sandstone layers. Thus 12 magnetic profiles with 1.5 km average length were acquired across these linear LST anomalies to investigate deep seated structures. The processed magnetic profiles confirmed the existence of graben-like structures and a maximum depth to the basement of 150 m in the middle section and shallower depths toward the edges of the LST anomalies. Consequently, these structurally controlled linear basins could be promising areas for ground water accumulation and exploration in the El-Gallaba Plain of the Western Desert in Egypt.

#### 8887-40, Session 9

### Retrieving water productivity parameters by using Landsat images in the Nilo Coelho irrigation scheme, Brazil

Antônio H. Teixeira, Embrapa Monitoramento por Satélite (Brazil); Hélio L. Lopes, Univ. Federal do Vale do São Francisco (Brazil); Fernando Braz T. Hernandez, UNESP (Brazil); Morris Scherer-Warren, Agência Nacional das Águas (Brazil); Ricardo G Andrade, Embrapa Monitoramento por Satélite (Brazil)

The Nilo Coelho irrigation scheme, located in the semi-arid region of Brazil, is highlighted as an important agricultural irrigated perimeter. The natural vegetation has been progressively replaced by commercial fruit crops inducing a loss of biodiversity. The water consumption from the introduced irrigated crops under the Brazilian semi-arid region exceeds those from Caatinga species, the natural vegetation inside this naturally dry region. Considering the scenario of this fast land use change, it is important the development and application of suitable tools to quantify the trend of the water productivity parameters on a large scale. To analyze the land use change effects inside this perimeter, the large scale values of biomass production (BIO) and actual evapotranspiration (ET) were quantified from 1992 to 2011, under the naturally driest conditions along the year. Monteith's radiation model was applied for estimating the absorbed photosynthetically active radiation (APAR), while the SAFER (Simple Algorithm For Evapotranspiration Retrieving) algorithm was used to retrieve ET. Another model based on the surface resistance to water transfer ( $r_s$ ) was applied for a simplified vegetation classification. The highest incremental BIO values happened during the years of 1999 and 2005, as a consequence of the largest agricultural areas inside the perimeter, when the average differences between irrigated crops and natural vegetation were more than 70 kg ha<sup>-1</sup> d<sup>-1</sup>. Considering all analysed period, BIO values for natural vegetation represented 40% of those for irrigated crops. Comparing the average ET rates of 1992 (1.6 mm d<sup>-1</sup>) with those for 2011 (3.1 mm d<sup>-1</sup>), it was verified that the extra water consumption was doubled as a result of the increments of irrigated areas along the years, what means a flux reduction for São Francisco river downstream water users in the Brazilian semi-arid region. More uniformity along the years on both water productivity parameters occurred for natural vegetation, evidenced by the lower values of standard deviation when comparing to irrigated crops. The heterogeneity of ET values under irrigation conditions are due to the different species, crop stages, cultural and water managements. The models applied at the irrigation perimeter level with Landsat images are considered to be suitable for quantifying the land use change effects on vegetation and water variables in the Brazilian semiarid region; however, to transfer them to other agro-ecosystems, probably, the original regression coefficients of the equations should be calibrated and validated.

#### 8887-41, Session 9

### Towards a near real-time remote sensing based agricultural monitoring system for the MENA region

Rasmus M. Houborg, Matthew F. McCabe, King Abdullah Univ. of Science and Technology (Saudi Arabia); Martha C. Anderson, Feng Gao, Mitchell A. Schull, Carmelo Cammalleri, Agricultural Research Service (United States); Christopher R. Hain, Univ. of Maryland, College Park (United States); Tugrul M. Yilmaz, Agricultural Research Service (United States)

Satellite remote sensing has the potential to offer spatially and temporally distributed information on land surface characteristics, which may be used as inputs and constraints for estimating land surface fluxes of carbon, water and energy. Enhanced satellite-based monitoring systems for aiding local water resource assessments and agricultural management activities are particularly needed for the Middle East and North Africa (MENA) region. The MENA region is an area characterized by limited fresh water resources, an often inefficient use of these, and relatively poor in-situ monitoring as a result of sparse meteorological observations. To address these issues, an integrated modeling approach for near real-time monitoring of land surface states and fluxes at fine spatio-temporal scales over the MENA region is presented. This approach is based on synergistic application of multiple sensors and wavebands in the visible to shortwave infrared (VSWIR) and thermal infrared (TIR) domain. The agricultural monitoring system uses the Atmosphere-Land Exchange Inverse (ALEXI) model and associated flux disaggregation scheme (DisALEXI), the REGularized canopy reFLECTance (REGFLEC) model, and the Spatial and Temporal Adaptive Reflectance Fusion Model (STARFM) in conjunction with model reanalysis data and multi-sensor remotely sensed data from polar orbiting (e.g. Landsat and MODerate resolution Imaging Spectroradiometer (MODIS)) and geostationary (MSG; Meteosat Second Generation) satellite platforms to facilitate time-continuous (i.e. daily) estimates of field-scale water, energy and carbon fluxes. Within this modeling system, TIR satellite data provide information about the sub-surface moisture status and plant stress, obviating the need for precipitation input and a detailed soil surface characterization (i.e. for prognostic modeling of soil transport processes). REGFLEC represents a regularized radiative transfer framework for utilizing at-sensor VSWIR observations directly for retrieving leaf area index and leaf chlorophyll, that in turn function as useful proxies for vegetation density, crop development, nutrient availability and photosynthetic function. For this specific application, REGFLEC vegetation parameters are embedded within a new leaf-scaled carbon assimilation and transpiration sub-model of the two-source energy balance land surface representation. The STARFM fusion methodology blends aspects of high frequency (spatially coarse) and spatially fine resolution sensors and is applied directly to flux output fields to facilitate daily mapping of fluxes at sub-field scales. A complete processing infrastructure to automatically ingest and pre-process all required input data and to execute the integrated modeling system for near real-time agricultural monitoring purposes over targeted MENA sites is being developed, and initial results from this concerted effort will be discussed.

#### 8887-42, Session 9

### Multitemporal analysis of the relationship between production parameters and vegetation index in vineyard

Tanino Santangelo, Rosario Di Lorenzo, Goffredo La Loggia, Antonino Maltese, Univ. degli Studi di Palermo (Italy)

The use and timing of many agronomical practices such as the scheduling of irrigation and harvesting are dependent on accurate vineyard sampling of qualitative and productive parameters. Crop forecasting also depends on the ability to representatively sample vineyard performance. Moreover, growers want to be confident that the herbaceous phase is characterized in a robust manner because the cellular division determines the final size of the berry.

This manuscript summarizes almost ten years of precision viticulture in Sicily (Italy); six spectroradiometric and agronomic campaigns were carried out between 2002 and 2012 in the "Tenute Rapitalà"

farm. These datasets were collected in the frameworks of a PhD research work, and two research projects (namely the DIFA project “Digitalizzazione della Filiera Agro-Alimentare” and AVIGERE project “Applicazione della viticoltura di precision ad alcune aziende siciliane per il risparmio energetico e l’ecocompatibilità”). High-resolution images were acquired from satellites and airborne platforms. Satellite images include QuickBird, World View 2 and GeoEye multispectral images, whereas airborne images were acquired using a Duncan multispectral camera.

In situ data encompasses production parameters (plant production, and berry and bunch weight) of selected red cultivars such as Nero D’Avola and Syrah, during the ripening phenological phase. Production parameters were related to remote sensing derived Normalized Difference Vegetation Index.

These relationships have several operational uses: 1) estimation of the total production at the harvest; 2) production characterization within the vineyard plot; 3) diversification of agricultural practices to improve the productive efficiency.

The research aims to assess how robust are the prediction models. In particular: 1) if the spectral response is consistent from year to year, and between similar varieties, 2) if the relationships have to be recalibrated each year.

Results show that production parameters and vegetation indexes are usually linearly related with determination coefficients ranging between 0.6 and 0.7. These relationships slightly change on yearly basis. However, an evident effect due to the rows orientation and solar-sensor geometry characterizes the retrieved reflectance, thus influencing also the vegetation index. This could partially explain the differences between the calibrated relationships.

## 8887-43, Session 9

### Estimation of maize LAI by assimilating remotely sensed data into crop model

Xiaohua Zhu, Academy of Opto-Electronics (China)

Leaf Area Index (LAI) is a key parameter for characterizing the structure and the functioning of vegetation. Remote sensing technology is an important way for estimating regional scale LAI. Due to the restrictions of satellite operating cycle, remote sensing inversion results are temporal discontinuity. Process model can simulate continuous and long time series LAI data. However, influenced by parameterization scheme, atmosphere-driven conditions and process model initial state, the model simulation will cause unreasonable results. LAI estimation by remote sensing technology or by process model simulation, each have its own advantages and disadvantages (Yannick et al., 2012; Dorigo et al., 2007). So it is important to use multi-source data or multi-methods to estimate LAI and improve the estimation accuracy.

Data assimilation, using multi-source information to directly or indirectly participate in to improve the trajectory of process model simulation, improves the estimation accuracy of surface parameters and realizes the complementary advantages between the model simulation and remote sensing observations. In recent years, data assimilation technology is well applied in the research of atmospheric, oceanic, etc, and also attracted the attention of scholars in land surface research (Wang et al., 2010; Zhang et al., 2010; Fang et al., 2010). And in many researches of data assimilation, the application of prior knowledge has attracted the attentions of scholars (Yannick et al., 2012). The prior knowledge here means the field data, spatial information and temporal knowledge. In study of coupling crop growth model with radiative transfer model, spectral library data used as prior information was introduced into the cost function to achieve optimal LAI (Wang et al., 2010). In research of real-time retrieval of LAI from MODIS time series data, Xiao et al., (2011) extracted temporal knowledge from MODIS LAI products to construct a dynamic model for providing short-range forecast of LAI, then, they used Ensemble Kalman Filter techniques to update LAI when there is a new observation. The studies above have considered the application of prior knowledge, such as field data, temporal information, but still less to consider the influence of the surface spatial heterogeneity and the introduction of spatial knowledge into regional assimilation research (Tian et al., 2002). At the same time, phenology information (temporal knowledge) as a characterization of crop growth process is an important temporal prior knowledge. If phenology information is introduced into the crop model simulation to optimize the model sensitive parameters, the accuracy of real-time simulation can be effectively improved.

On the basis of previous work, an assimilation scheme based on temporal and spatial knowledge is proposed in this paper. The assimilation scheme is implemented in two directions, seen as Figure 1. One is the temporal direction, in which the parameters of crop model are calibrated, the other one is the spatial direction, in which the spatial information extracted from different resolution data is taken into account during inversion. Based on parameter “LAI”, the crop growth model WOFOST (Boogaard et al., 1998) and the reflectance model ACRM (Kuusk, 2001) are combined in this assimilation scheme by Kalman Filter (KF).

## 8887-44, Session 10

### Estimating surface energy fluxes over an Andalusian Dehesa ecosystem using a thermal-based two-source energy balance model and validation with flux tower measurements.

Ana Andreu, Instituto de Investigación y Formación Agraria y Pesquera (Spain); William P. Kustas, Agricultural Research Service (United States); María José Polo-Gómez, Grupo de Dinámica Fluvial e Hidrología (Spain); Martha C. Anderson, Agricultural Research Service (United States); Maria Patrocinio González-Dugo, Instituto de Investigación y Formación Agraria y Pesquera (Spain)

The dehesa, the most widespread agroforestry land-use system in Europe ( $\approx 3$  million ha), is recognized as an example of sustainable land use and for his importance in rural economy (Diaz et al., 1997; Plieninger and Wilbrand, 2001). It consists in a widely-spaced oak forest (mostly *Quercus ilex* L.), combined with crops, pasture and shrubs. It has a Mediterranean climate with severe periodic droughts. Understanding the hydrological, atmospheric and physiological processes affecting the ecosystem will improve its management and conservation. In particular, monitoring of the evapotranspiration (ET) is critical for assessing ecosystem condition or health, especially in this water-limited environment. Remote sensing from satellites can provide spatial information required for the ET analysis from local to regional scales.

In such semi-arid sparse canopy-cover landscapes, thermal-based energy balance techniques which distinguish soil/substrate and vegetation contributions to the radiative temperature and radiation/turbulent fluxes have proven to be highly reliable. In particular, the two-source energy balance (TSEB) model by Norman et al. (1995) and Kustas and Norman (1999) has shown to be robust for a wide range of partially-vegetated landscapes. Its application in the Dehesa ecosystem is challenging due to the complexity of the canopy structure, having sparse tree cover, with large areas of grass and bare soil substrate strongly influencing the radiative and turbulent exchanges.

For the evaluation of TSEB model over this environment, an energy flux measurement system has been installed in an Andalusian Dehesa (Santa Clotilde,  $39^{\circ}56' N$ ;  $5^{\circ}46' W$ , 260 m a.s.l) with 1 km homogeneous fetch in all directions. To ensure that satellite spatial resolution is similar to local fetch, a footprint analysis using two models (Schuepp et al., 1999; Kormann and Meixer, 2001) has been done, showing that peak contribution area is within 500 m and over 75% of the source-area is within 1 km of the tower. The fully corrected turbulent fluxes has a daily energy-balance closure with the available energy of 86% on average which is similar to other eddy covariance measurements over a variety of landscapes (Li et al., 2004; Leuning et al., 2005; Foken, 2008; Hendricks Franssen et al., 2010). Accounting for the storages terms as usually performed for forested ecosystems (e.g. Foken et al., 2006) had a minor affect on closure, probably due to the low fractional cover of the tall canopy ( $fc=0.19$ ).

The TSEB model was evaluated in the study area during 2012 summer season, using as an input Landsat 7 TM images and meteorological data from a local station. The half-hourly fluxes estimates were compared with the flux tower measurements, and found to be within the uncertainty in the eddy covariance measurements when considering closure. This area has the typical pattern of dry systems, with high sensible heat flux (H) reaching the maximum in the middle of the afternoon and low latent heat values (LE), increasing over the day. Soil heat flux (G) is not negligible even on a daily time scale, being at least 10% of net radiation (Rn). This is consistent with the climatic

conditions, with low rates of soil water and high temperatures, with the humidity controlling the partition of the available energy between turbulent fluxes (Entekhabi and Rodriguez-Iturbe, 1994).

8887-45, Session 10

## Assessing daily actual evapotranspiration through energy balance: an experiment to evaluate the self-

### preservation hypothesis with acquisition time

Antonino Maltese, Fulvio Capodici, Giuseppe Ciraolo, Goffredo La Loggia, Antonio Motisi, Univ. degli Studi di Palermo (Italy)

An operational use of the actual evapotranspiration retrieved by remote sensing approaches requires the integration of instantaneous fluxes to daily values. This is commonly achieved under the hypothesis of daytime self-preservation of the evaporative fraction.

In this study, it was evaluated the effect of this assumption on estimate daily evapotranspiration from proximity sensing images acquired at hourly intervals.

To assess the reliability of the results, the observations made by a flux tower on a homogeneous olive trees orchard were analysed (A. Consiglio farm). The farm is located in the north-western part of Sicily.

The SEBAL model was applied on the study area by means of images acquired during a clear day of August 2009 through a FLIR A320G thermal camera and a Tetracam MCA II multispectral camera installed on a balloon. Images were characterized by very high spatial resolution (the coarser resolution was approximately 50 cm). Thus, images describe the orchard at sub-plant scale, whereas the model should provide reliable results at least at plant scale.

Hence, the experiment aims to analyse two effects: 1) the consistency of the self-preservation hypothesis for daily estimates of the latent heat flux from hourly assessments at different times of the day; 2) the effects of the spatial resolution of the inputs on the estimates.

To evaluate the effects of the spatial resolution original image were downscaled at plant scale (2 and 5 m) and coarser resolutions (10 and 20 m).

To assess the reliability of the results, the observations made by a flux tower on a footprint at semi-hourly interval were compared to the estimates of the hourly actual latent heat flux and daily evapotranspiration.

Results show that the best estimates are obtained with a spatial resolution comparable to the average size of the canopy with images taken approximately at 10 UTC.

8887-46, Session 10

## Evaluation of remote sensing evapotranspiration as a proxy of semi-arid rangeland production

Francesco Nutini, Consiglio Nazionale delle Ricerche (Italy); Alberto Crema, Giacinto Manfron, Istituto per il Rilevamento Elettromagnetico dell'Ambiente (Italy); Davide Cinquanta, Univ. degli Studi di Milano (Italy); Mirco Boschetti, Istituto per il Rilevamento Elettromagnetico dell'Ambiente (Italy); Stefano Bocchi, Pietro Alessandro Brivio, Univ. degli Studi di Milano (Italy)

In seminatural environment such as rangeland areas, where the vegetation production relies on the dynamic of natural variables more than human activities, the capability to monitor vegetation behaviour and assess biomass production are crucial.

Since the firsts satellite images were made available, these data were exploited to obtain proxies of vegetation biophysical parameters to be used in natural resources monitoring especially in the analysis of wide natural areas where field measurements are lacking and difficult to be acquired.

Recent research works on semi-arid rangelands have focused their attention on the estimation of actual evapotranspiration (ET) from

remotely sensed data.

Since the ET is strongly linked to the vegetation status, being water availability the major limiting factor of vegetation growing in semi-arid areas, it has been proposed by scientific community as a proxy for modelling/estimating the biomass production.

In this paper a method for estimating actual ET based on energy balance formulation, at a daily time-span from different data sources is presented. The study area is located in the Sahelian region of Niger, where field measurements of grassland biomass over 92 sites for the period 1998-2009 and satellite derived high resolution land cover (LC) are available.

The goals of the present work are to i) analyze temporal variations and spatial patterns of the estimated actual ET in relation to land cover and land cover change and ii) to evaluate the ET as a proxy of biomass production.

Remote sensing model input are vegetation index (VI), surface temperature and albedo, these data have been obtained from MODIS imagery (products MOD09A1, MOD11A2 and MOD43B respectively), whereas the incoming solar radiation has been estimated derived by ECMWF (European Centre for Medium-Range Weather Forecasts) data.

Preliminary results demonstrate how the spatial variability of ET is related to the patterns of land use and land cover (Shrublands, Cultivated lands, Natural herbaceous vegetation and Bare areas) derived by Landsat TM. The analysis of spatially distributed rainfall estimation (RFE) allowed also to interpret the interannual variation of the ET parameter.

Time series analysis of VI retrieved from MODIS data have been also exploited to detect the phenological phases of the Start growing season (SoS) and of the End of growing season (EoS) in a spatially distributed way. The yearly behaviour of VI allowed us to characterize different sahelian eco-climatic regions by phenological features and to highlights the variations between years due to the weather fluctuations.

Finally, the phenological information were used to integrate the seasonal variation of ET along the growing season (?ET) in order to perform a comparison with end of season biomass field data.

The manuscript discusses the utility of remote sensing actual ET estimation to monitoring rangeland production and provides an analysis of the correlation between ?ET and field data along the study area and within different years. The ET performances in pasture production monitoring, are also compared with other remote sensed proxies of biomass proposed by scientific community such as NDVI (peak value and cumulate) and DMP (Dry Matter Productivity) .

8887-47, Session 10

## Application of MODIS images for modelling the energy balance components in the semi-arid conditions of Brazil

Antônio H. Teixeira, Embrapa Monitoramento por Satélite (Brazil); Morris Sherer-Warren, Agência Nacional de Águas (Brazil); Hélio L. Lopes, Univ. Federal do Vale do São Francisco (Brazil); Fernando Braz T. Hernandez, UNESP (Brazil); Ricardo G. Andrade, Embrapa Monitoramento por Satélite (Brazil)

In the Brazilian semi-arid region, irrigated agriculture has replaced the natural vegetation, being important the quantification of the energy exchanges between the mixed agro-ecosystems and the low atmosphere. The bands 1, 2, 31 and 32 from 10 MODIS images together with 10 agro-meteorological stations were used, covering the period of 2010 to 2011, for modelling the large scale radiation and energy balance components in the Petrolina municipality, Brazil. Previous field measurements in irrigated crops and natural vegetation, were used to develop equations for surface albedo (?0), using the bands 1 and 2, and for surface temperature (T0), using the bands 31 and 32. ?0, NDVI and T0 were the basic input remote sensing parameters necessary for using together with reference evapotranspiration data (ET0), to model the latent heat flux (?E) and surface resistance to water fluxes (rs) on a large scale. The daily net radiation (Rn) was retrieved from ?0, air temperature (Ta) and transmissivity (?sw), allowing the quantification of the sensible heat flux (H) by residual in the energy balance. With a threshold value for rs during the driest conditions along the year, it was possible to separate the irrigated crops from natural vegetation (Caatinga) to evaluate the

behaviour of the vegetation variables and the daily energy partition along the year. The  $\rho$  values for Caatinga were in average 90% of those for irrigated crops with the highest ones occurring during the rainy period from November to April. On the other hand, the mean NDVI values for irrigated crops were 43% higher than those for natural vegetation.  $T_0$  values were lower under irrigation conditions with an averaged difference between the two kind of vegetation being 1.8 K, however not distinguished irrigated conditions as well as the NDVI values did. Considering all periods along the year the averaged fractions of  $R_n$  partitioned as H and  $\rho E$ , were 31 and 78%, for irrigated crops and natural vegetation, respectively, while as  $\rho E$  the corresponding values were 69 and 22%. Although there were raises and declines of these fractions along the year, depending on the environmental conditions, it was observed heat advection from the dry to irrigated plots, with  $\rho E$  exceeding  $R_n$  by 9% in July. The models tested here can subsidize the monitoring of the energy exchanges between the mixed agro-ecosystems in the Brazilian semiarid, under conditions of fast climate and land use changes.

8887-48, Session 10

### Carbon cycling of European croplands: a framework for the assimilation of optical and microwave Earth observation data

Andrew Revill, The Univ. of Edinburgh (United Kingdom)

No Abstract Available

8887-49, Session RJS

### Multi-temporal classification of TerraSAR-X data for wetland vegetation mapping

Julie Betbeder, Sébastien Rapinel, Thomas Corpetti, Univ. Rennes 2 (France); Eric Pottier, Univ. de Rennes 1 (France); Samuel Corgne, Laurence Hubert Moy, Univ. Rennes 2 (France)

Whilst wetlands play a key role in controlling flooding and nonpoint source pollution, sequestering carbon, and providing an abundance of ecological services, knowledge of the flora and fauna of these environments is patchy, and understanding of their ecological functioning is still insufficient for a reliable functional assessment on areas larger than a few hectares.

Remotely sensed data are often used to identify water areas and vegetation types to delineate, characterize and monitor wetland areas to account for inter- and intra-annual variations. SAR data provide a reliable alternative to optical images, whose accessibility is limited due to the presence of cloud cover. Indeed, SAR imagery in single, dual, or quad polarizations has proved its ability to map flooded vegetation and open water in wetlands (Evans & Costa, 2013). Moreover, high-spatial resolution SAR sensors as TerraSAR X and RADARSAT-2 allow identifying the dominant backscattering mechanism associated with the flooded vegetation. However, their ability to differentiate vegetation formations based on their phenological and flooded status, at a fine scale is still unknown.

Thus, the objective of this study is to evaluate multitemporal TerraSAR-X imagery to map precisely the distribution of vegetation formations within wetlands, in determining seasonally flooded areas of wetlands.

The investigated area is a Long Ecological Research site named 'Plaine Fougères', localized on the southern part of the Bay of Mont-Saint-Michel, France. It is referenced in the LTER-Europe (lterEurope.net) and the ILTER networks (<http://osur.univ-rennes1.fr/zoneatelier-armorique/>). This study focuses on the Sougéal marsh which is entirely made up of grazing land.

A series of six dual-polarization TerraSAR-X images (HH/VV) were acquired in 2012 during dry and wet seasons. In parallel, surveys and ground measurements were conducted on the study site to calibrate and validate image processing methods. Data preprocessing included speckle filtering and geocoding process. A  $2 \times 2$  coherency matrix was firstly extracted from the raw images to investigate the single and double bounce scattering mechanisms associated with the presence of open water and flooded vegetation, respectively. The Shannon entropy, which corresponds to the sum of two contributions related

to the intensity and the degree of polarization (Lee and Pottier, 2009), was then calculated to identify the flooded vegetation formations and monitor non-flooded vegetation phenology. Each of these variables presents a temporal variation that depends on wetland flooding status and vegetation roughness. Therefore classifying these time series may be of great interest for the identification of wetland status. The classification process is based on Support Vector Machines (SVM) techniques where a specific kernel, adapted to the comparison of vectors of time series, is used. In practice the training samples were issued from the field campaigns.

The results show that vegetation formations are identified with a very good accuracy ( $Kappa > 0.90$ ) from the classification of temporal profiles derived from the TerraSAR-X images. Moreover, the analysis of the relationship established between vegetation formations and the surface hydrodynamic of the wetland should contribute to predict the vegetation colonization and wetland evolution.

Evans, T.L., Costa, M. (2013). Landcover classification of the Lower Nhecolândia subregion of the Brazilian Pantanal Wetlands using ALOS/PALSAR, RADARSAT-2 and ENVISAT/ASAR imagery, Remote Sensing of Environment, 128, 118-137.

Lee J.S., Pottier, E. (2009). Polarimetric Radar Imaging: From basics to applications, CRC Press, Taylor & Francis editor, 397 pages, Jan. 2009, ISBN: 978-1-4200-5497-2.

8887-50, Session RJS

### Coupling X-Band COSMO-SkyMed and optical DEIMOS-1 data for NDVI retrieval: model calibration and validation on two test areas

Fulvio Capodici, Univ. degli Studi di Palermo (Italy); Guido D'Urso, Univ. degli Studi di Napoli Federico II (Italy); Antonino Maltese, Giuseppe Ciraolo, Univ. degli Studi di Palermo (Italy)

Sustainability of modern agriculture requires the knowledge of spatial and temporal variability of vegetation biomass to optimize management of land and water resources.

Diversely from optical imaging, the temporal resolution of observations from active sensors, such as SAR, is not limited by sky cloudiness; if carefully validated, it may be used in combination with optical imageries to provide a more continuous monitoring of agricultural surfaces.

Several new SAR missions (e.g., ALOS-PALSAR, COSMO-SkyMed 1 and 2, TerraSAR-X, TerraSAR-X2, Sentinel 1) acquiring at X-, C- and L-bands and dual polarization capability, are characterized by a short revisit time (from 12 h to ~10 days) and high spatial resolution (<20 m). The satellites could provide suitable data for operative crop monitoring.

The new COSMO-SkyMed (owned by Italian Space Agency-ASI) opened new opportunities to develop agro-hydrological applications representing a valuable source of data for operational use. Although X-band is not the most suitable to model agricultural and hydrological processes, an assessment of vegetation development could be achieved combining optical vegetation indices (VIs) and SAR backscattering data.

Within this framework, even if some research efforts have been recently carried out in addressing biomass or vegetation water content using X-band images, the use of SAR data to reproduce 'optical' vegetation indices, such as the normalized difference vegetation index (NDVI) is an important task because this is a key-input data in both mass and energy exchange models of soil-vegetation-atmosphere systems (e.g., SWAP and SEBAL).

Recently two models to infer a VI from  $\rho$  have been setup. One of these achieved accurate results in VI retrieval at a certain time using  $\rho$  (VISAR), once known the NDVI derived from optical images (VIopt) at a reference time.

This paper aims to further validate this model through two independent dataset.

The model setup using COSMO-SkyMed and optical DEIMOS-1 data acquired over the Sele plain (Campania, Italy) has been further validated using a dataset of 2 COSMO-SkyMed images and 2 Landsat 7 SLC-off images acquired in the south-western part of Sicily (Italy) between 8 and 28 August 2011.

Determination coefficients of the validation set were similar that those

of the calibration set. Results confirm that VISAR obtained using the combined model is a suitable surrogate of Vlopt if estimated at parcel scale.

This study is carried out in the framework of the COSMOLAND project (Use of COSMO-SkyMed SAR data for LAND cover classification and surface parameters retrieval over agricultural sites) funded by the Italian Space Agency (ASI).

8887-51, Session RJS

## Integration of multispectral and C-band SAR data for crop monitoring applications

Lorenzo Ianni, Ramses A. Molijn, Ramon F. Hanssen,  
Technische Univ. Delft (Netherlands)

Reliable large-scale mapping of the crop type and crop health has a key role in economical and political (near)real-time strategies, as well as in maintaining a sustainable ecological status, improving soil conservation and water resource management. Remote sensing systems provide to scientists and stakeholders the unique capability of observing the land on a constant time basis at broad scale. It was shown indeed that several bio-physical crops features can be inferred from the spectral information at microwave and optical frequencies, i.e. indicators of the vegetation (biomass volume, height, shape and orientation) and soil conditions (soil moisture, roughness, composition). It is also common knowledge that the diversity introduced by multi-temporal observations and multiple sensor configurations benefits both crop classification and parameter estimation in a significant way. The multi-temporal information is in particular important for crop classification since different crops respond with different temporal signatures, whereas multi-angle and multi-sensor information are used to yield more robust biomass and soil moisture estimates. Data availability should be therefore considered the central issue in agricultural land characterization. Several works have been committed at searching for more insight in this regard, trying to exploit to the utmost extent all the datasets at disposal. However, only few efforts were spent in defining an operational way to deal with possible missing information. The availability of spaceborne SAR information is in fact currently limited by the scarce number of satellites available, while optical imagery, especially in tropical and subtropical regions, is critical due to cloud cover. The present work aims therefore to provide a detailed analysis on the uncertainty achieved by multi-angle polarimetric SAR and multispectral imaging indicators for different dataset combinations. The analysis is carried out on the AgriSAR 2009 dataset, which comprises multi-angle C-Band Radarsat-2 Fine Quad-Pol images, Rapideye acquisitions, and extensive in-situ measurements used for validation for three sites in Spain (Barrax), Netherlands (Flevoland) and Canada (Indian Head). The SAR image series are composed by 8 images collected during the most significant part of the crop season for a wide range of ascending and descending modes. The images have been slightly post-processed applied to emulate the Sentinel-1 IW mode quality. A semi-empirical model is adopted to assimilate the different SAR angle measurements for crop characterization and the Rapideye acquisitions have been used to calibrate/cross-validate the SAR model. Crop classification is then performed on a field basis through standard ML technique. Both the raw channel covariances and the retrieved bio-physical indicators are used to this aim. The uncertainty related to estimation of soil parameters (biomass and soil moisture) and the error in crop classification for different data availability is analyzed with particular reference to optical information but also to a partial use of the RS2 beams and polarizations (RS2 quad-pol rather than S1 dual-pol). Considerations on the operational use of remote sensing in areas affected by critical weather conditions will be hence presented.

# Conference 8888: Remote Sensing of the Ocean, Sea Ice, Coastal Waters, and Large Water Regions 2013

Tuesday 24–24 September 2013

Part of Proceedings of SPIE Vol. 8888 Remote Sensing of the Ocean, Sea Ice, Coastal Waters, and Large Water Regions 2013

8888-1, Session 1

## Effect of denoising on assimilation of SAR data

Zahra Ashouri, K. Andrea Scott, Univ. of Waterloo (Canada);  
Thomas G. Carrieres, Environment Canada (Canada)

Operational ice-ocean discrimination from SAR imagery is usually based on human interpretation of the imagery. As the Arctic warms, and shipping increases, there is motivation to introduce automatic interpretation of these images for efficiency and consistency. Various approaches have been developed towards automatically discriminating ice from open water in SAR imagery. The methods typically incorporate backscatter intensity, second order texture statistics, and sometimes ancillary information, such as weather conditions.

The assimilation of Synthetic Aperture Radar (SAR) data in an operational data assimilation system for the purpose of estimating sea ice properties is one approach that can be used to discriminate ice from open water in SAR imagery. The assimilation of data to estimate sea ice concentration usually relies on passive microwave data, which has a resolution of 5-50km. Including SAR data, with a resolution on the order of 100m, in the assimilation should significantly improve the representation of small scale details in the analysis. One of the areas where SAR data can provide key information regarding the details of the ice cover is in the marginal ice zone. However, automatic interpretation of the images in this area is challenging due to sensitivity of the backscattered signal to changing surface conditions and speckle noise. For SAR images of sea ice, texture can be used to discriminate ice from open water. Texture can be described using the Grey Level Co-occurrence Matrix (GLCM). The GLCM is a matrix whose entries ( $c_{ij}$ ) contain the probability that a pixel of grey level  $j$  occurs at displacement  $\Delta x$  in direction  $\Delta y$  from a pixel with grey level  $i$  in a chosen window of an image. In order to extract information regarding the texture of an image, various properties of the GLCM matrix are calculated. Here three complementary texture features are chosen, contrast, entropy and correlation.

The presence of noise is unavoidable in SAR images. The source of this noise in SAR imagery is the coherent returns of the transmitted signal, scattered on the surface. The objective of this work is to evaluate the use of an image denoising algorithm in a data assimilation system which is estimating sea ice concentration. Two cases have been considered; one assimilating SAR data using texture features and the other one having a denoising step prior to the calculation and assimilation of texture features. In this study the median filter was applied because it preserves edges and it is also fairly simple.

The results show that denoising the image prior to assimilating it has a positive impact on the fit between the observations and both the ice concentration background state and analysis in observation space. The impact is small, which may be a limitation associated with the linear forward model being used to map the ice concentration from the background state to the texture feature space. This will be investigated further in the full paper, and an alternative forward model may be explored. Results from the assimilation will be verified against independent data or image analyses from the Canadian Ice Service.

8888-2, Session 1

## Recent 10-year Changes and the Prediction of Arctic Sea Ice: A Multivariate SARIMA approach

Jihye Ahn, Yang Won Lee, Pukyong National Univ. (Korea, Republic of)

In recent years, Arctic sea ice extent has significantly declined, and it had the lowest ratings ever recorded in the summer of 2012. The environment of Arctic is very important for the global environment and human society because it is sensitive as sea ice varies and keeps the Earth's cool or warm climate. So we need continuous monitoring of Arctic sea ice to understand and predict the process

of climate changes. Therefore, the purpose of this study is to analyze the temporal changes of Arctic sea ice using time-series statistical methods with satellite remote sensing data. Continuous monitoring of sea ice is not easy because its observation is limited in polar regions which are difficult to approach from the ground, and distribution ranges are very extensive so it is being mainly observed by means of satellite remote sensing. There are satellite-based sea ice products from GOES-R/ABI, Terra/MODIS and Aqua/MODIS sensor, etc. The algorithms for estimating sea ice include three components: (1) NDSI(Normalized Difference Snow/Ice Index), (2)reflectance of the near-infrared or visible channel, and (3)surface temperature of ice. We analyze the temporal changes of Arctic sea ice extent for 10 years on the daily basis using MODIS sea ice products observed in daytime with a high spatial resolution. The factors affecting the creation, variation(growth or decline), and movement of ice are known as temperatures, winds, waves, currents, and stream water, etc. In consideration of these factors, we employ the ARIMA(Autoregressive Integrated Moving Average) model for time-series statistical analyses of the Arctic sea ice changes. The ARIMA model can predict the time-series changes of an Earth environmental phenomenon with the help of the meteorological variables. It is thought of as a very reliable prediction method for time-series data. Especially, this study uses a Multivariate Seasonal ARIMA model that reflects multiple meteorological variables and seasonality to explain and predict the temporal changes of the Arctic sea ice. If the ARIMA model is properly set, the time-series pattern of the Arctic sea ice will be quantified and it is possible to predict the future time-series using the model. This study is expected to provide a clue to the changes of Arctic sea ice in relation to the changes of weather and climate.

8888-3, Session 1

## Arctic environment monitoring using new satellite data from Suomi NPP VIIRS

Yi Luo, Environment Canada (Canada)

The Arctic environment is changing dramatically since the last decade, while the satellite remote sensing has provided a unique and indispensable approach for monitoring such change in a way almost without spatial and temporal gaps. The Canadian Ice Service (CIS) intends to ingest and use all valuable data for Arctic sea ice mapping and forecasting, and the recently available data from Suomi NPP VIIRS is on the top list. Different from current popular visible/infrared sensors such as MODIS, the VIIRS has more bands sampled at a higher spatial resolution of 375m. Its polar orbit track with its extra wide cross-track swath of about 3040km enables most Arctic area to be observed at multiple times a day. Also its unique Day-and-Night band makes it possible to acquire night-time imagery without need of solar illumination. This is specifically useful for Arctic monitoring during the polar winter. The CIS has developed an in-house VIIRS raw data ingesting and processing system based on a near-real time frame. Data from different sources, i.e. several ground stations or data distribution centers, are received and combined. They are re-projected into a polar map and various kinds of imagery are produced for operational analysis. Additional products such as cloud mask and daily mosaic are also produced to help analyst on ice and cloud discrimination and large area ice/open water mapping. The preliminary results show the new data can offer detailed ice information, especially along coast area or around small islands. It can also offer thin ice and melt ponds information to which other sensors like the microwave is not sensitive. It is able to optimally present important sea ice features such as ice concentration and ice edge. The new data show great potentials for operational service of ice analysis and ice modeling.

## 8888-4, Session 1

### Improved exploration of Fishery Resources through the integration of remotely sensed merged sea level anomaly, chlorophyll concentration and sea surface temperature

Kanmani Shanmuga Priya R. Rajkumar, Indian Institute of Remote Sensing (India)

The promise of satellite remote sensing technology for marine research and management has been recognized since 1960s. The capabilities of evolving satellite remote sensing technology, combined with conventional data collection techniques, provide a powerful tool for efficient and cost effective management of living marine resources. Fishes are the valuable living marine resources producing food, profit and pleasure to the human community. Variations in oceanic condition play a role in natural fluctuations of fish stocks. The Satellite Altimeter derived Merged Sea Level Anomaly (MSLA) results in the better understanding of ocean variability and mesoscale oceanography and provides good possibility to reveal the zones of high dynamic activity. This study comprised the synergistic analysis of signatures of SEAWIFS derived chlorophyll concentration, National Oceanic and Atmospheric Administration-Advanced Very High Resolution Radiometer (NOAA-AVHRR) derived Sea Surface Temperature and the monthly Merged Sea Level Anomaly data derived from Topex/Poseidon, Jason-1 and ERS-1 Altimeters for the past 7 years during the period from 1998 to 2004. The overlapping Chlorophyll, SST and MSLA were suggested for delineating Potential Fishing Zones (PFZs). It was observed that SST and MSLA signatures are covarying and also the Chlorophyll and MSLA signatures are inversely related with each other. It was found that negative MSLA areas with high Chlorophyll and relatively low SST are cool denser nutrient rich water which is an indicator of the presence of phytoplankton. The Chlorophyll and SST images were found to be often incomplete with blanked out areas where there are no data because of cloud cover and persisted for days to week while MSLA signatures of respective features persisted for longer duration. Hence, the study used Altimeter derived MSLA as an index for long term variability detection of fish catches along with Chlorophyll and SST images and the maps showing PFZs of the study area were generated. The real time Fishing statistics of the same duration were procured from FSI Mumbai. The catch contours were generated with respect to peak spectra of chlorophyll variation and trough spectra of MSLA and SST variation. The vice-a-versa patterns were observed in the poor catch contours. The Catch Per Unit Effort (CPUE) for each fishing trail was calculated to normalize the fish catch. Based on the statistical analysis the actual CPUEs were classified at each probable MSLA depth zones and plotted on the same images.

## 8888-5, Session 2

### Inter-calibration of Metop-A and Metop-B scatterometers using ocean measurements

Anis Elyouncha, Xavier Neyt, Royal Belgian Military Academy (Belgium)

A method of inter-calibration has been developed recently at the Royal Military Academy of Belgium.

This method was successfully applied to ERS-1/ERS-2 and ASCAT-A/ERS-2 C-band scatterometers. The method is based on combining different targets (ocean, sea ice and rainforest) and associated geophysical models.

In this paper, the focus is on the ocean measurements. Calibration of the scatterometer over ocean is widely used for monitoring and correction of the backscattering coefficients. The method is based on the assessment of the difference between the measured and the simulated backscatter using NWP winds and geophysical model functions (GMF's) such as CMOD5. The method provides the instrument bias against the GMF. It was found that this bias varies spatially and temporally. This temporal and spatial variation of the bias could lead to discrepancies of up to 0.1 dB, which is significant compared to the calibration accuracy (0.2 dB). This adds to the bias (instrument drift) an artificial error which is due to the misfit of the input wind distribution. It is shown that this discrepancy is due to the sensitivity of the GMF to the wind speed distribution and this consequently yields the calibration over ocean to be sensitive to the wind speed distribution.

In this paper, the inter-calibration method is applied to Metop-A and Metop-B scatterometers data. Additionally, the bias obtained from the ocean is compared to other targets i.e., rainforest and sea ice. The wind speed distribution variation in time and space is analyzed. The sensitivity of the calibration over the ocean to the wind speed distribution variation is assessed. Finally, a method is proposed to mitigate this variation and thus reduces the misfit error.

## 8888-6, Session 2

### Measuring marine oil spill extent by Markov Random Fields

Miguel Moctezuma Flores, Univ. Nacional Autónoma de México (Mexico); Flavio F. Parmiggiani, Istituto di Scienze dell'Atmosfera e del Clima (Italy); Ludwin Lopez Lopez, Univ. Nacional Autónoma de México (Mexico)

The Deepwater Horizon oil spill of the Gulf of Mexico in the spring of 2010 was the largest accidental marine oil spill in the history of the petroleum industry. An immediate request, after the accident, was to detect the oil slick and to measure its extent: SAR images were the obvious tool to be employed for the task.

This paper presents a processing scheme based on Markov Random Fields (MRF) theory. MRF theory describes the global information by probability terms involving local neighborhood representations of the SAR backscatter data. The random degradation introduced by speckle noise is dealt with a pre-processing stage which applies a nonlinear diffusion filter. Spatial context attributes are structured by the Bayes' equation derived from a Maximum-A-Posteriori (MAP) estimation. The probability terms define an objective function of a MRF model whose goal is to detect contours and fine structures. The Markovian segmentation problem is solved with a numerical optimization method.

The scheme was applied to an Envisat/ASAR image over the Gulf of Mexico of May 9, 2010, when the oil spill was already fully developed. The final result was obtained with 40 recursion cycles, where, at each step, the segmentation consists of a 3-class label field (open sea and two oil slick thicknesses). Both the MRF model and the parameters of the stochastic optimization procedure will be provided, together with the area measurement of the two kinds of oil slick.

## 8888-7, Session 2

### Analysis of spaceborne SAR monitoring capabilities for coastal areas bathymetry with COSMO-SkyMed and Alos data

Alfredo Renga, Giancarlo Rufino, Univ. degli Studi di Napoli Federico II (Italy); Marco D'Errico, Seconda Univ. degli Studi di Napoli (Italy); Antonio Moccia, Univ. degli Studi di Napoli Federico II (Italy); Valentina Boccia, University of Naples "Federico II" (Italy); Maria Daniela Graziano, CO.RI.S.T.A. (Italy); Cesare Aragno, Kell S.r.l. (Italy); Simona Zoffoli, Agenzia Spaziale Italiana (Italy)

Accurate measurements of sea floor morphology are essential for monitoring and control of geo-morphological risk in coastal regions (e.g. warp analysis and forecasting of potential flooding effects). They can also support measurements for marine pollution monitoring and can be useful in underwater coastal archaeological applications, for supporting the researches or monitoring the sites. The basic concept of SAR-based bathymetry is that, for all practical purposes, SAR signals are not able to penetrate sea surface and echoed signals from sea are actually sea surface echoes. Microwave signals emitted by SAR are able to penetrate into seawater only to a depth which is negligible in comparison to the electromagnetic wavelength, which is typically shorter than a few tens of centimetres. Therefore, the key-point of any SAR-based bathymetric technique is that bathymetric data retrieval from SAR images must be based on indirect processes with sea floor morphology sensed through the effects it may have on sea surface. In particular, two different techniques exist: wave-based techniques, which rely on the ability of local bathymetry to modify the characteristics of sea surface (swell or gravity) waves, and current-based techniques, which rely on the ability of underwater bottom morphology to influence sea surface currents.

In the present paper the results of SAR4BAT project, funded by Italian Space Agency with Kell srl as prime contractor and University of Naples as technical consultant, are reported. It is aimed at the development of SAR-based products for coastal area bathymetry intended as the measurement of the morphology of sea floor and then the identification of the relevant bathymetric features. The peculiarity of this research is the application and adaptation of SAR-based bathymetric data retrieval techniques, typically applied in open waters showing strong tidal currents or significant wave motions over sandy sea beds, in the Mediterranean basin (Gulf of Naples), which is characterized by a prevalently rocky sea floor and by different water dynamics.

The paper, after a state-of-the-art analysis of SAR-based bathymetric techniques, will report on the selection of specific algorithms and the error budget analysis which has been performed to identify critical aspects of algorithms application with particular emphasis on wind, waves, and current conditions. The range of suitable depths for SAR-based bathymetry has been identified, sensitivities and water depth uncertainties due to waves characteristics have been defined, values of current velocity and wind speed for correct SAR-based bathymetric data retrieval have been selected, detectable underwater features have been characterized and SAR data specifications have been determined. Then, bathymetric data have been retrieved by processing SAR data of COSMO/SkyMed and ALOS and results validated with pre-existing nautical maps obtained with conventional bathymetric retrieval methods is performed.

## 8888-8, Session 2

### Laboratory investigation of short wind wave breaking modulation in the long surface wave field

Victor V. Bakhanov, Nikolai A. Bogatov, Alexei V. Ermoshkin, Aleksandr A. Kandaurov, Olga N. Kemarskaya, Daniil A. Sergeev, Yulia I. Troitskaya, Institute of Applied Physics (Russian Federation)

Both the modulation of short wind wave breaking in the long surface wave field and the occurrence of breaking in the presence of a long wave were thoroughly investigated with X- and Ka-band scatterometers in horizontal and vertical polarizations, a system for video recording of rough water surface by web camera, and string wave recorder.

Laboratory experiments were carried out in the IAP RAS wind-wave complex mounted in the large thermostratified tank. The wind speed ranged from 12.5 m/s to 20.1 m/s in reference to a standard height of 10 m. A long surface wave at two frequencies 0.9 Hz or 1.1 Hz was generated by wave maker located in the channel, the wave-maker oscillation amplitudes were 10 mm, 20 mm, 30 mm, and 50 mm. The probing angles of X- and Ka-band scatterometers amounted to 60 deg. from nadir. A string wave recorder that recorded parameters of surface waves longer than 3 cm was located near the measuring area. We also used a system for video recording of rough water surface by web camera. The camera was mounted so that the measuring area of radar and string wave recorder was in its sweep. The presence or absence of breaking was recorded on video record of web camera.

A single record length was 3 min. At the beginning of each realization, we observed only wind waves at an assigned wind speed without a long surface wave. Surface-wave wavemaker was switched on at the 50th s and the long wave was generated. In this time interval of the record, we considered the evolution of the interaction between wind and long surface waves. At the final stage we examined the interaction of wind waves and the long wave initially generated by wavemaker and then completely formed under the action of wind.

Measurement results in experiments with long wave and wind are compared with measurement results with the long wave in the absence of wind. If the amplitudes of the long wave and waves generated both by the long wave and wind are close, we conclude that it is the same long wave but in the presence of wind waves. It is found that breaking is absent in all realizations with the long wave without wind. Thus we can predetermine the influence of the long wave on wind waves, in particular, on modulation of short wind wave breaking.

It is shown that at relatively weak wind without a long wave breaking is absent; in the presence of a long wave breaking is observed. At high wind speeds breaking is observed both with and without a long wave.

The presence of long wave intensifies breaking. At relatively weak wind breaking is mainly observed on the front slope of the long wave. At stronger wind, the breaking observation area extends but also remains at the front slope of the long wave.

## 8888-9, Session 2

### Satellite SAR and in situ observations of water eutrophication areas

Stanislav A. Ermakov, Institute of Applied Physics (Russian Federation) and Russian State Hydrometeorological Univ. (Russian Federation) and Nizhny Novgorod State Univ. (Russian Federation); Jose da Silva, Univ. do Porto (Portugal); Ivan Kapustin, Institute of Applied Physics (Russian Federation) and Russian State Hydrometeorological Univ. (Russian Federation); Irina Sergievskaya, Tatiana Lazareva, Institute of Applied Physics (Russian Federation); Olga Shomina, Institute of Applied Physics (Russian Federation) and Nizhny Novgorod State Univ. (Russian Federation)

Development of remote sensing methods for characterization of intensive algae bloom is an urgent problem for the ecology of the ocean and inland waters. Alpers et al (2003) from the analysis of satellite optical and radar images of the ocean have concluded that algae bloom can be detected by radar arguing that phytoplankton produces biogenic films which result in the reduced radar backscattering. First direct proof of the relation between radar backscattering, biogenic films and phytoplankton have been obtained by Ermakov et al. (2013), and the physical mechanisms of radar backscatter depression were suggested based on damping of short wind waves due to elastic surface films and enhanced effective water viscosity.

This paper presents results of new detailed studies of the problem of remote sensing of algae bloom. Field observations were carried out on the Gorky Water Reservoir from board a ship and from a small motor boat and were co-located and nearly simultaneous with TerraSAR-X image acquisition. Radar backscattering was measured from a ship with an X-band scatterometer, and acoustical scattering due to phytoplankton and the current velocity profiles were recorded with an acoustic Doppler Current Profiler (ADCP) Workhorse Sentinel 600 kHz from the motor boat, moving parallel to the ship track. Water samples and samples of biogenic films were collected from the boat and analyzed in laboratory. Phytoplankton volume concentration was measured with an optical sensor in YSI 6600 probe, as well as using traditional methods of counting of phytoplankton cells. Analysis of characteristics of biogenic films sampled with a net method was carried out with a parametric wave method developed at IAP RAS which allowed us to retrieve the film elasticity and the surface tension coefficient. The parametric wave method was also applied to estimate the effective water viscosity in the presence of phytoplankton. Radar backscatter profiles were retrieved from TerraSAR-X images along the ship tracks and were found to be consistent with X-band scatterometer data. SAR backscatter reduction as well as reduced scatterometer signal intensity were detected in the areas of enhanced phytoplankton concentration. Based on retrieved values of the effective water viscosity, the film elasticity and the surface tension coefficient theoretical calculations of radar backscatter as a function of phytoplankton concentration were performed. The theory was shown to be in good agreement with observations.

The work has been supported by the Russian Foundation of Basic Research (Projects RFBR 12-05-31237, 11-05-00295, 13-05-97058,, 13-05-97043), the Program RAS Radiophysics, and by the Russian Government (Grants No. 11.G34.31.0048 and 11.G34.31.0078).

## 8888-10, Session 3

### Analysis of historical MERIS and MODIS data to evaluate the impact of dredging to monthly mean surface TSM concentration

Laura Raag, Liis Sipelgas, Rivo Uiboupin, Tallinn Univ. of Technology (Estonia)

Dredging operations in coastal waters affect water quality through



an increase in suspended matter concentration. Total Suspended Matter (TSM) can be determined by the backward scattering of light in the visible region, which is retrieved using satellite data. We studied the changes of TSM distribution in Estonian coastal sea with special interest in Muuga and Paldiski bay, where two biggest harbors of Estonia are located. The purpose of current study was to examine the suitability of remote sensing data to detect the turbidity differences caused by dredged sediments and to evaluate the impact of monthly mean dredging amount to the surface TSM concentration retrieved from satellite images. We used MERIS Full Swath Geo-located (FSG) products with 300m resolution and MODIS band data with 250m resolution from years 2006-2010 in our analysis. For calculation of TSM concentration MERIS images were further processed using the Case-2 waters processors available in BEAM software. Outputs of C2R and FUB processors were validated with in situ measurements of TSM at the time of dredging operation. Analysis showed reliable correlation between satellite data and in situ TSM measurements,  $r_2$  was 0.43 for FUB processor and 0.47 for C2R processor.

For conversion of MODIS band 1 (B1) reflectance data to TSM concentration an empirical algorithm was established. Firstly we used "dark pixel" methodology for correction of atmospheric disturbances. Using the whole dataset statistically reliable correlation ( $r_2=0.43$ ) between TSM from water sample and MODIS B1 reflectance was obtained. Our analysis of in situ measured scattering coefficient data showed that increase in Chlorophyll a (Chl a) concentration (when the phytoplankton particles become dominant in water indicating bloom conditions) changes the shape of in situ scattering spectrum and also the relationship between in situ scattering and TSM. Therefore, we also found correlations separately for two situations 1) MODIS B1 vs. TSM in case Chl a <5mg m<sup>-3</sup> and 2) MODIS B1 vs. TSM in case Chl a >5mg m<sup>-3</sup>. The  $r_2$  for low chlorophyll situation was 0.67 and  $r_2$  for the high Chl a conditions was 0.63. The separation relying on dominant particles origin gave slightly better result. In the Baltic Sea the chlorophyll content exceeds 5 mg m<sup>-3</sup> quite often - in case spring, summer and autumn bloom. Daily Chl a data from ship of opportunity measurements (Ferrybox systems) that operate on passenger's ferries between Tallinn and Helsinki are available operationally (on-line). Thus, the Chl a concentration was determined from on situ measurements and different conversion coefficient were selected according to current situation before processing the MODIS images to TSM concentration.

The average TSM maps in the harbor region were calculated from MERIS and MODIS using validated conversion algorithms for further analysis of environmental impact. The maps covered different timeframes: annual mean, monthly mean, season mean, dredging period mean and non-dredging period mean. These maps were compared to the monthly mean dredging cubage. Comparison revealed that in case of monthly mean dredging cubage more than 5250 m<sup>3</sup> the changes in monthly mean TSM maps can be detected.

### 8888-11, Session 3

#### Operational multi-angle hyperspectral remote sensing for feature detection

Charles R. Bostater Jr., Florida Institute of Technology (United States)

Remote sensing results of land and water surfaces from airborne and satellite platforms are dependent upon the illumination geometry and the sensor viewing geometry. Correction of pushbroom hyperspectral imagery can be achieved using bidirectional reflectance factor (BRF) information of known image features using ground based measurements from goniometers and/or from a newly designed linear translation sensor platform system. Imagery and hyperspectral signatures from a (a) newly designed goniometer system is described and (b) from a multi-angle translation imaging system are demonstrated using hyperspectral pushbroom imagery. Results are presented in a manner in order to describe how ground based measurements can be applied to operational airborne hyperspectral imagery and satellite multispectral system imagery. Features analysis from the systems is exploited to help determine surface and subsurface feature detection based using radiative transfer considerations.

### 8888-12, Session 3

#### Retrieval of solar-induced fluorescence spectral shape of oil slicks from the infilling of solar Fraunhofer lines

Valentina Raimondi, Lorenzo Palombi, Donatella Guzzi, David Lognoli, Vanni Nardino, Ivan Pippi, Istituto di Fisica Applicata Nello Carrara (Italy); Francesco Petroni, Sitael (Italy)

Fluorescence techniques are regarded as particularly valuable for the early detection of oil spills and their classification on the basis of their fluorescence typical spectral shape. Among these techniques, the fluorescence lidar is considered as particularly effective and reliable, since it is able to detect oil under water surface, in water-oil emulsions and also on different backgrounds (seawater, weeds, ice, etc.) and can operate from airborne platform. The deployment of fluorescence lidars for oil spill detection, however, is presently limited to an airborne platform, mainly due to the need of a laser as an excitation source. This leads to an increase in the overall payload budgets in terms of weight, consumption and dimensions.

Hence, the development of a method based on passive measurements of the solar-induced fluorescence of oils can be of great interest since it would not require the deployment of any excitation source. In addition, it could open several unexplored opportunities, such as its deployment from satellite platforms to gain a synoptic monitoring of oil spills at global scale for strategic planning, the study of oil spill spreading dynamics, etc. on long-time scale.

In this paper we present the spectral behaviour of the solar induced fluorescence of an oil slick, reconstructed from its radiance spectrum acquired in eight selected spectral windows of the visible spectrum from about 389 nm to 659 nm. Each spectral window was chosen to cover one or more solar Fraunhofer absorbing lines so as to retrieve the in-filling due to the oil fluorescence contribution induced by the solar irradiance. Measured Fraunhofer lines were chosen within the solar ones avoiding the telluric ones to demonstrate the feasibility of the measuring method from airborne or spaceborne platform. Solar lines, compared with telluric lines, requires simpler atmospheric model to evaluate ground solar irradiance and, besides, the measured signal is not affected by re-absorption effects in the lines.

For each spectral window, oil fluorescence infilling and reflectance was evaluated by the comparisons with the incident sun irradiance spectrum measured in the same conditions. Fluorescence and reflectance spectral shapes were evaluated within each measured spectral windows by applying a spectral fitting method (SFM) and polynomial modelling. Finally, solar-induced fluorescence data were used to reconstruct the fluorescence spectrum of the oil.

### 8888-13, Session 3

#### From multi-sensor tracking of sea surface films to mesoscale and sub-mesoscale sea surface current fields

Benjamin Seppke, Martin Gade, Leonie Dreschler-Fischer, Univ. Hamburg (Germany)

The knowledge about mesoscale and sub-mesoscale sea surface current fields is of high interdisciplinary interest, since it results in a better understanding of ocean-atmosphere interactions. However, many available numerical model results are of resolutions, which are too coarse to investigate mesoscale and sub-mesoscale turbulent features like eddies, particularly in coastal waters. In this work we present the results of tracking biogenic and anthropogenic surface film signatures on multi-sensor satellite images (SAR and multispectral images) to estimate the local sea surface current field. The main advantage of this approach is that the resolution of the derived current fields depends mainly on the resolution of the images, which have been used for tracking.

Due to the large temporal distance between two acquisitions of a scene and the high variability of the tracked sea surface films, classical tracking methods, e.g. feature based or Optical Flow methods may not be applicable to successfully track the imaged signatures of the surface films. In this work, we use our former developed generic framework, which ensures the applicability and increases the stability of the results for well-known tracking and Optical Flow algorithms. With this framework, it is e.g. possible to compute the sea

surface current field using Optical Flow approaches even for large spatiotemporal distances and with partial scene coverage.

We present and compare the results of different tracking algorithms by means of tracking biogenic sea surface films. The investigated areas are the Baltic Sea and the Black Sea. We present the use of Landsat TM, SeaWiFS, ERS-2, TerraSAR-X and RADARSAT-2 data for the derivation of sea surface currents. The resolution of the images used varies from moderate to fine resolution, which allows the derivation sea surface current fields of moderate to fine resolutions.

The sea surface current fields, which can be derived using the different well-known algorithms within the proposed generic framework, correspond well with those provided by numerical models for the investigation area of the Baltic Sea. For the Black Sea, field studies have been performed in 2011 and 2012 as a part of the joint German/Russian DTeddie project, which is funded by ESA/CSA-SOAR under license no. 5074. Here the derived current fields correspond well with in-situ measurements, which have been acquired during the field studies. In addition, the results yield interesting interpretations for the visible turbulent structures in which the surface films are aggregated with respect to their role in the sea surface current field.

### 8888-14, Session 3

#### Assessment of fine scale IOP variability over a wide range of environmental conditions in the Ligurian Sea using in situ lidar and volume scattering measurements

Fraser R. Dalgleish, Harbor Branch Oceanographic Institute (United States); Michael S. Twardowski, WET Labs., Inc. (United States); Anni K. Vuorenkoski, Harbor Branch Oceanographic Institute (United States); Nicole Stockley, WET Labs., Inc. (United States); Bing Ouyang, Harbor Branch Oceanographic Institute (United States)

Identifying and quantifying small scale physical and biological processes within natural waters requires techniques for real-time characterization of inherent optical properties (IOPs) as synoptically as possible. Conventional beam attenuation sensors use a very small sample volume and must therefore be moved laterally and vertically to resolve spatial distributions of IOPs. Furthermore, the process of sampling with these sensors can significantly perturb particles, with boundary layer shear forces disturbing naturally occurring structures and therefore obscuring our understanding.

To enable unobtrusive measurement of these natural phenomena, a fine structure underwater imaging lidar (FSUIL), which rapidly projects an array of closely spaced, narrow, collimated laser pulses into the water column to produce time-resolved backscatter profiles with fine spatial and temporal resolution was recently developed at Harbor Branch Oceanographic Institute (Fort Pierce, FL). The system was extensively field tested during the NATO Ligurian Sea LIDAR & Optical Measurements Experiment (LLOMEX) cruise in March 2013, which was conducted during the Spring bloom conditions. Throughout a wide range of environmental conditions, the FSUIL was deployed on an in situ profiler obtaining depth-overlapping profiles from near surface down to the lower thermocline. Deployed concurrent to the FSUIL was the Multi-Angle Scattering Optical Tool (MASCOT) instrument package, developed by WET Labs Inc. (Narragansett, RI) to allow for side-by-side IOP measurement, including high update rate volume scattering function (VSF) measurements between 10° and 170° in 10° intervals.

The measured VSF, beam attenuation and absorption coefficients, are being analyzed in relation to the experimental lidar waveforms and a time-resolved radiative transfer model in order to develop a robust calibration methodology for the FSUIL. This is necessary in order to assess the utility of such a system in deriving accurate beam attenuation measurements from inversion of the lidar waveforms. In addition, the combination of the data generated by the MASCOT sensor package and the FSUIL sensor package is being used to assess the small scale variability in IOPs over the wide range of environmental conditions that were encountered.

### 8888-15, Session 4

#### Polarization of light in shallow waters

Alexander Gilerson, Amir Ibrahim, Jan Stepinski, Alberto Tonizzo, Carlos Carrizo, Samir Ahmed, The City College of New York (United States)

Both direct measurement and numerical simulations have been used to study the polarized nature of the light in the ocean since for about last 60 years. Polarization in the underwater light field is of great importance for aquatic creatures having polarization vision, which utilize its signals for a variety of purposes including navigation, communication and camouflaging. In the water column, pelagic silvery fish camouflages by reflecting the underwater polarized light; benthic creatures living in shallow waters, on the other hand, are able to produce a wide variety of body patterns both for camouflage and signaling. It was showed before that the polarized patterns are a concealed communication channel and they can be used as such channel while camouflaged. Polarization of light is also extremely important in various remote sensing techniques and in the underwater imaging.

In deep open ocean waters bottoms can be neglected and the polarization in water is largely determined by the water column and the atmosphere. However, neglecting bottoms in shallow bottoms make any numerical experiments very inaccurate. There, the light reflecting from the bottom significantly contributes to the intensity measured near the surface. Furthermore, because the bottom is not a plane of rock but rather an irregularly spaced, varicolored, underwater forest, its albedo is very difficult to measure directly. Quite a number of studies have dealt with the hyperspectral effects of optically shallow bottoms on above and underwater upwelling radiance, however none of them has considered the polarization of light in the field.

In this study, we report some of the first comprehensive results of hyperspectral measurements of the polarized light fields in shallow waters from field experiment which took place in benthic waters around the Florida Keys. These measurements were conducted together with measurements of water inherent optical properties, which made possible to compare them with simulations of the polarized light field using a vector radiative transfer program.

The upwelling polarized radiance distribution in these shallow waters is examined using CCNY hyperspectral multi-angular polarimeter for a variety of different benthic surfaces and it is compared to the polarized radiances simulated by vector radiative transfer RayXP code. It is shown that the assumption of an unpolarized Lambertian bottom in the numerical calculations gives good qualitative agreement with the experimental measurements. The results suggest that polarization camouflage might not be a requirement for benthic creatures, since the polarization of the light reflected from the oceanic bottoms is nearly zero. On the other hand, the angle of linear polarization is not affected by the presence of any type of benthic surface, implying that it can be used as hidden communication channel and as an effective way of orientation.

Impact of the bottom reflectance on polarized remote sensing is also analyzed. Recent results of in water measurements using a full Stokes vector imaging camera will be presented as well.

### 8888-16, Session 4

#### Evaluation of ocean color data processing schemes for VIIRS sensor using in-situ data of coastal AERONET-OC sites

Samir Ahmed, Alexander Gilerson, Soe Hlaing, Robert Foster, The City College of New York (United States); Alan Weidemann II, U.S. Naval Research Lab. (United States); Robert A. Arnone, The Univ. of Southern Mississippi (United States); Menghua Wang, National Oceanic and Atmospheric Administration (United States)

In the processing of Ocean Color (OC) data from sensor data recorded by the Visible Infrared Imaging Radiometer Suite (VIIRS) aboard JPSS-Suomi satellite, NASA Ocean Biology Processing Group (OBPG) is deriving a continuous temporal calibrations based on the on-board calibration measurements for the visible bands, and then reprocessing the full mission to produce a continuously calibrated sensor data record (SDR) product. In addition, a vicarious calibration

during SDR to OC Level-2 processing is applied. In the latest processing (version 2012.2), the vicarious calibration is now derived from the Marine Optical Buoy (MOBY) data, whereas previously it was derived from a sea surface reflectance model and climatology of chlorophyll-a concentration. An effort is currently underway for the reprocessing of OC data for the entire VIIRS mission with lunar-based temporal calibration and updated vicarious gains. In addition, NOAA, in fulfillment of its mission for the processing of the environmental data products from sensor data records has been implementing the Interface Data Processing Segment (IDPS) developed by Raytheon Intelligence and Information Systems, which has gained beta status for evaluation. As these processing schemes continue to evolve, monitoring the validity and assessments of the VIIRS ocean color products are necessary, especially for coastal waters to evaluate the consistency of processing and calibration schemes. In this context, the ocean color component of the Aerosol Robotic Network (AERONET-OC) has been designed to support long-term satellite ocean color investigations through cross-site measurements collected by autonomous multispectral radiometer systems deployed above water. As part of this network, the Long Island Sound Coastal Observatory (LISCO) near New York City and WaveCIS in the Gulf of Mexico expand those observational capabilities with continuous monitoring as well as (for the LISCO site) additional assessment of the hyper-spectral properties of coastal waters. In investigations carried out over a period of almost a year, with VIIRS datasets from two coastal AERONET-OC sites, it has been observed that the VIIRS sensor can capture well the seasonal and temporal variations in the nLw data, exhibiting significant correlations with in-situ data (R equal to 0.968 and 0.977 for LISCO and WaveCIS respectively). For the WaveCIS site, VIIRS nLw data retrieval is improved with the version 2012.2 processing schemes, reducing the retrieval biases at every wavelength. However, that it is not the case for the LISCO site which is closer to the coast (with typically more turbid water conditions), which exhibits more frequent occurrences of negative water-leaving radiance retrievals, and underestimation of VIIRS nLw data. Furthermore, while strong consistency is observed between nLw data retrieved from VIIRS and MODIS, aerosol optical thickness,  $\tau_a$ , data also exhibits significant correlation but with substantial overestimations. These results imply that impacts of vicarious calibration procedures are not the same for sites closer to coasts with different water and atmospheric (increased fine mode aerosols) conditions, and suggest the need to take these factors, including impacts of aerosol model selection on atmospheric correction procedures, with inputs from comparisons between AERONET-OC and satellite atmospheric data, in consideration.

#### 8888-17, Session 4

### CDOM retrieval using measurements of downwelling irradiance

Kathrin Linnemann, Technische Univ. München (Germany); Peter Gege, Deutsches Zentrum für Luft- und Raumfahrt e.V. (Germany); Sebastian Rößler, Thomas Schneider, Arnulf Melzer, Technische Univ. München (Germany)

As it can strongly influence the availability of light, coloured dissolved organic matter (CDOM) affects the function of lake ecosystems. The absorption of CDOM increases exponentially with decreasing wavelengths. In the blue wavelength domain this absorption overlays with the absorption of phytoplankton pigments and thus affects primary production. Therefore reliable methods are required for the monitoring of CDOM concentration. Large fluctuations induced by the water surface make the determination of CDOM by means of in situ radiation measurements quite difficult. A new method using downwelling irradiance was tested for applicability in four selected lakes of the Bavarian Easter Lake district, which consists of 19 naturally connected freshwater lakes of different trophic levels. Surrounded by bog the Easter Lake district can be influenced by high CDOM input, which can prevent phytoplankton blooms. The software WASI includes an irradiance model that separates between the direct and diffuse part of the incident light in order to handle the strong variability of the underwater light field. It is capable to retrieve water constituents. During field campaigns the intensity of the downwelling irradiance (Ed) was measured using a RAMSES ACC VIS device. Depending on the Secchi depth measurements were made up to depths of 4.5 meters with depth intervals of 0.5 meters. To eliminate the influence of remaining bottom reflection, the locations for the measurements and samples were chosen guided by the greatest

depth of each lake. Simultaneously, water samples were taken in three depths (0.5 m, 2 m and Secchi depth). The water samples were filtered using 0.45  $\mu\text{m}$  pore-size cellulose-acetate filters and subsequently the absorption of CDOM was derived in the range from 190 to 900 nm using photometric absorption measurements. Concentration (defined as absorption coefficient at 440 nm) showed differences between the selected lakes and ranged from 0.31 to 1.43  $\text{m}^{-1}$  with a mean standard deviation of 0.07  $\text{m}^{-1}$ . These laboratory measurements from water samples were compared to CDOM concentration obtained by inverse modelling of downwelling irradiance measurements using WASI. A total of four datasets containing 450 Ed spectra was analysed. For sensor depths lower than 1.5 m large uncertainties were observed. The measurements in 2 m depth and at Secchi depth yielded good correlation between water sample and WASI derived data ( $R^2 = 0.87$ ), with a mean standard deviation of 0.05  $\text{m}^{-1}$  for the determined CDOM concentrations. This new method is an alternative to laboratory analysis of water samples for in situ measurements of CDOM concentration.

#### 8888-18, Session 4

### Remote sensing of sea surface features by optical RTI images

Victor I. Titov, Victor Bakhanov, Alexander Luchinin, Institute of Applied Physics (Russian Federation); Irina Repina, A.M.Obukhov Institute of Atmospheric Physics Russian Academy of Sciences (Russian Federation); Emma Zuikova, Institute of Applied Physics (Russian Federation)

The complex of optical devices for monitoring of sea surface by optical RTI images (range-time-intensity images) constructed from optical profiles of sea surface was developed.

The RTI image is optical analog of side-looking radar image of sea surface but having higher spatial resolution and some possibility for remote sensing of sea roughness. It is possible to form RTI images with range from some tens meters to kilometers depending on spatial resolution needed and height of optical device above sea level. The complex of original optical devices for recoding of RTI images using the linear array of CCD-photodiodes is created.

Complex consists of four synchronized optical devices operated under various polarization of light and directions of observations.

The optical device specifications:

Swath width: from 50m to tens of kilometers;

Resolution (geometrical): from 3cm and more depending on swath width;

Frame repetition: 18.7 Hz;

ADC frequency: 38 KHz;

Number of points in swath: 2000;

Spectral range of light: 0.46 – 0.6 microns;

Polarization of light: vertical and horizontal.

It is possible to develop multi-channel complex of such optical devices for various spectral diapasons and polarization of light. The optical complex can be installed on a shore, ship and aerial carrier.

Processing of signals, which are optical cross sections of the surface image, consists in correction of perspective distortion and construction of spatially-temporal images of the surface in the coordinates: range – time – intensity RTI images, and in analysis of obtained images.

The investigations of water surface features in internal reservoirs and various regions of world's oceans and seas during last years were conducted by optical complex. The structure of energy waves and swells, wave's breaking, ship waves and ship wakes, manifestations of near surface wind fields, eddies, manifestations of subsurface processes (currents, internal waves, features of bottom relief), oil slicks were recorded and analyzed. The classification of water surface features by its origin was developed. Derived data of optical monitoring of sea surface may serve for future investigations of sea surface features.

8888-19, Session 4

### Monitoring long-term ocean health using remote sensing: a case study of the Bay of Bengal

Lim Jin Yi, Universiti Teknologi Malaysia (Malaysia); Md Latifur Rahman Sarker, Univ. Teknologi Malaysia (Malaysia); Lei Zhang, The Hong Kong Polytechnic Univ. (Hong Kong, China); Eko Siswanto, Research Institute for Global Change (Japan); Ahmad Mubin, Saadah Sabarudin, Universiti Teknologi Malaysia (Malaysia)

Oceans play a significant role in the global carbon cycle and climate change, and the most importantly it is a reservoir for plenty of protein supply, and at the center of many economic activities. Ocean health is important and can be monitored by observing different parameters, but the main element is the phytoplankton concentration (chlorophyll-a concentration) because it is the indicator of ocean productivity. Many methods can be used to estimate chlorophyll-a (Chl-a) concentration, among them, remote sensing technique is one of the most suitable methods for monitoring the ocean health locally, regionally and globally with very high temporal resolution.

In this research, long term ocean health monitoring was carried out at the Bay of Bengal considering three facts i.e. i) very dynamic local weather (monsoon), ii) large number of population in the vicinity of the Bay of Bengal, and iii) the frequent natural calamities (cyclone and flooding) in and around the Bay of Bengal. Data (ten years: from 2001 to 2010) from SeaWiFS and MODIS were used. Monthly Chl-a concentration was estimated from the SeaWiFS data using OC4 algorithm, and the monthly sea surface temperature was obtained from the MODIS sea surface temperature (SST) data. Information about cyclones and floods were obtained from the necessary sources and in-situ Chl-a data was collected from the published research papers for the validation of Chl-a from the OC4 algorithm. Systematic random sampling was used to select 70 locations all over the Bay of Bengal for extracting data from the monthly Chl-a and SST maps. Finally the relationships between different aspects i.e. i) Chl-a and SST, ii) Chl-a and monsoon, iii) Chl-a and cyclones, and iv) Chl-a and floods were investigated monthly, yearly and for long term (i.e 10 years). Results indicate that SST, monsoon, cyclone, and flooding can affect Chl-a concentration but the effect of monsoon, cyclone, and flooding is temporal, and normally reduces over time. However, the effect of SST on Chl-a concentration can't be minimized very quickly although the change of temperature over this period is not very large.

8888-20, Session PS

### New method for extracting internal wave parameters from SAR image

Kaiguo Fan, The Second Institute of Oceanography, SOA (China); Xingxiu Yu, Linyi Univ. (China); Bin Fu, Xilin Gan, The Second Institute of Oceanography, SOA (China)

This paper introduce a new method for extracting internal wave parameters from SAR image based on the microwave scattering imaging model for oceanic surface features and internal wave synthetic aperture radar (SAR) imaging mechanism. Wind fields are gotten from NCEP reanalysis data. The thermocline depth and sea density are estimated from the Levitus data. The surface current induced by the internal wave is simulated according to the KDV equation. Then the microwave scattering imaging model for oceanic surface features is applied to solve the action balance equation and the radar cross section induced by the internal wave can be calculated. The wind speed and internal wave depth are modified using the dichotomy method step by step which causes the simulation radar cross sections close to those measured from the SAR image. Finally, the wind speed, thermocline depth, the phase speed and the amplitude can be obtained. This measure is tested on the example of an ERS-2 image near Dongsha Island acquired at 14:40 on 23 June, 1998. The results conclude that after four iterative calculations the simulated radar cross section between the dark and bright band is about 3.26dB.

8888-21, Session PS

### Model of airborne imaging system with complex modulated beam of illumination, adaptive to wavy surface

Alexander G. Luchinin, Institute of Applied Physics (Russian Federation)

New principles of design of imaging system through the rough surface are offered. These principles allow to lower negative influence of surface wavy and multiple scattering in water on the spatial resolution. The system model in which the image of underwater objects is formed at by means of angular scanning by an illumination beam is considered. Image distortions in such system are caused basically by random changes of a refraction angle of a laser beam on a surface and can be eliminated, if the true direction of an input of a beam in water is known. We suggest taking the information on refraction angle of a beam from angular distribution of backscattering signal of water layer. Such information can be received by means of receivers with sensitivity linearly vary across the field of view. The knowledge of true position of a beam of illumination on object allows receiving the image not deformed by wavy.

We suggest reducing influence of multiplayer scattering in water by means of application of high-frequency modulation of beam power and the matched processing in reception system. Use of a complex signal modulation allows keeping the good resolution on depth and the resolution in a horizontal plane to rise. Thus, the combination of a method of definition of a refraction angle of a beam and modulation of a beam by a high-frequency complex signal gives an essential gain in the resolution of airborne imaging system.

We have derived the equations for an average estimation of an angle of refraction of a beam and for an estimation variance. These equations are used for calculation an estimation variance for different observation conditions. Examples of such calculations are resulted. We have derived the equation for modulation transfer function of imaging system, taking into account effects from adaptive compensation of a refraction angle and high-frequency modulation of a beam. On the basis of this equation the achievable gain (in comparison with usual imaging systems) in the resolution for various conditions on a surface, optical properties of water and a range of modulation of an illumination beam is estimated. Numerical examples with reference to typical marine conditions are given. The self similar solution of the radiation transfer equation in small angle approach taking into account time dispersion of photons was used.

8888-22, Session PS

### Imitation model validation of HF-band signal backscattering from sea surface

Vladimir T. Lobach, Michael V. Potipak, Southern Federal Univ. (Russian Federation)

Despite the highly developed technology of remote sensing, the developing of more efficient algorithms for sea surface parameters remote monitoring is actual. This requires a series of field experiments during which it is quite difficult to keep similar conditions. For such studies we proposed phenomenological model of scattering HF-band signals on the sea surface. It is based on the Huygens-Fresnel principle, which most fully allows take into consideration all sorts of electromagnetic wave backscattering "local effects". This paper assesses the quality of the imitation model by comparing the simulation results and experimental data. The estimation of standard errors of height and the mean waves measurements are given.

8888-23, Session PS

### Directional ocean wave spectra extracted from the dual-polarization SAR imagery

Lin Ren, Jingsong Yang, Juan Wang, Gang Zheng, Peng Chen, The Second Institute of Oceanography, SOA (China); Jianyu Chen, Second Institute of Oceanography SOA (China)

Synthetic Aperture Radar(SAR) can measure the directional ocean

wave spectra from the image spectra based on the SAR-ocean mapping relation. To remove the speckle noise of the image spectra and the 180-degree ambiguity of wave propagation direction, the image cross spectra for different time but same scene imagery was proposed to retrieve the wave spectra and analyze the wave direction. Based on the cross spectra technology, Single-Look Complex (SLC) SAR imagery utilized the different looks formed from the same image to extract the wave spectra. Is the cross spectra technology adapted for other cases for the same scene but different observation conditions like different polarizations? This paper tries to use the cross spectra for dual-polarization SAR imagery to extract the wave spectra. RADARSAT-2 can provide the high-resolution quad-polarization (HH, VV, HV and VH) imagery, whose HH and VV polarization data are chosen to validate the method mentioned above in this paper.

Firstly, we propose the new SAR-ocean mapping relation between the dual-polarization cross spectra and the wave spectra. It slightly modifies from the classical quasi-linear mapping relation proposed by Hasselmann and treats the velocity bunching modulation the same as the classical one. The difference is mainly manifested in the fact that it simultaneously contains HH and VV polarization model of tilt and hydrodynamic modulation.

Secondly, we calculate the cross spectra for the dual-polarization data. From the calculated spectra, the signal noise ratio (SNR) of cross spectra are apparently higher than the one of single-polarization. It is apparently due to the fact that the cross spectra have the stronger wave information but not the reduction of speckle noise. The cross spectra of dual-polarization have the similar pattern with the single-polarization for the real part. The real part of the cross spectra are used to extract the wave spectra based on the new mapping relation. We adopt an iterative method to retrieve the wave spectra, which remain the 180-degree ambiguity of wave propagation direction yet.

Thirdly, the imaginary part of cross spectra of dual-polarization are used to analyze the wave direction. We find that the imaginary part of cross spectra have positive and negative value. The positive peak of imaginary part corresponds to the dominated wave propagation direction, which can remove the 180-degree ambiguity. The principle of removing the 180-degree ambiguity for cross spectra is originally based on the fact that different time SAR images of the same imaged scene are misregistered. But for the principle of dual-polarization, we are under study.

Finally, we make the comparisons between the extracted wave spectra from the RADARSAT-2 quad-polarization imagery and measured buoy data in terms of significant wave height (swh), wave length and wave direction. The relative errors of swh and wave length are less than 15% and the root mean square error (rmse) is less than 20-degree. Preliminary results show that the dual-polarization (HH and VV) data have the ability of extracting the wave spectra and removing the 180-degree ambiguity based on the cross spectra technology.

8888-24, Session PS

## Spectral imaging AOTF spectrometer for World Ocean observation

Alexey V. Perchik, Bauman Moscow State Technical Univ.  
(Russian Federation)

### Introduction

There are a lot of different methods for World Ocean monitoring. One of them is a spectral images analysis. Spectral analysis gives us information about water pollution, bioproductivity, ecological situation and other parameters of observing water surface.

Acousto-optical spectrometers without spatial resolution are widely used in World Ocean monitoring applications these spectrometers allows to study spectrum data of dispersion and fluorescence radiation in different spectral ranges from UV to IR. There are a lot of methods for spectrum data analysis that can be applied to spectral image processing. Also acousto-optical imaging spectrometers are widely used in microscopy for biological and medical applications such as luminescence spectroscopy, photoluminescence diagnostics of tumors, bioluminescence research.

Acousto-optical tunable filter (AOTF) based imaging spectrometer that allows defining spectral contrast areas on water surface in the regions of interest is described in this paper.

### Physical principle

Acousto-optical tunable filter are based on crystals, generally tellurium dioxide or quartz, with optical properties that are altered in the presence of an acoustic wave (elasto-optical effect). When an acoustic wave propagates through the crystal it induces regions of compression and relaxation in lattice structure of crystal that causes fluctuations of refractive index. This induced structure plays a role of diffraction grating for incident light, controlled by frequency of sound wave. Changing frequency of RF signal on piezoelectric transducer bonded to acousto-optical crystal allows selecting wavelength of light that passes through filter

### Technical characteristics and features

Imaging spectrometer consists of high resolution double AOTF-based monochromator, black and white CCD based camera and optical system.

Acousto-optical monochromator determines the basic characteristics of the imaging spectrometer.

In our setup we used double non-collinear monochromator which contains two paratellurite (TeO<sub>2</sub>) filters and three polarizers (input, intermediate, and output) made of calcite (CaCO<sub>3</sub>).

It provides following optical characteristics: spectral range from 430 to 780 nm with 2 nm bandwidth; input AOTF aperture is round shaped with 8 mm diameter; field of view 3 degrees; spatial resolution is about 800x800 elements.

Basic advantages of using AOTF are following: high optical throughput combined with rather high spectral resolution, two-dimensional imaging and fast random spectral access.

Imaging spectrometer RF signal generator and CCD camera controlled by computer. Software is based on National Instruments highly productive development graphical programming environment LabVIEW with NI Vision module. This software allows realizing various adaptive algorithms of image processing utilizing unique random spectral access property of AOTF.

Using double AOTF allows us to obtain images on different wavelengths without any spectral drift, scaling in two orthogonal directions or non-linear distortions. Double-AOTF monochromator eliminates the spectral drift effect due to compensation of the image shift caused by the first AOTF with equal opposite shift produced by the second filter. Image

position with respect to CCD matrix is the same at any wavelength. Also double AOTF provides rather narrow band pass and strong suppression of out-of-band pass radiation.

### Conclusion

Acousto-optical imaging spectrometer based on double AOTF is an instrument for World Ocean monitoring with suitable characteristics and high quality spectral imaging for ecological monitoring applications.

8888-25, Session PS

## In-orbit optical performance analysis for geostationary ocean color imager using integrated ray tracing technique

Eunsong Oh, Korea Institute of Ocean Science & Technology (Korea, Republic of); Dongok Y. Ry, Jinsuk Hong, Sug-Whan Kim, Yonsei Univ. (Korea, Republic of)

In recent remote sensing researches, one of the essential techniques is how to estimate the current and future status of satellite on the orbit. Integrated Ray Tracing (IRT) method, what we report in this paper, has been developed as the state-of-art end-to-end simulation technique. We focus on the IRT technique for the Geostationary Ocean Color Imager (GOCI) which was launched on June 2010. IRT simulation technique deals with 3D modeling of GOCI flight model as well as the entire space environments among the Sun, the Earth, and the GOCI. The Earth model as a target system is constructed with using Digital Elevation Map (DEM) data and considering the optical properties of target surface such as BSDF (Bi-directional Scattering Distribution Function). Trial simulation runs for the GOCI imaging performance were focused on the combined slot images and MTF. First, we investigated GOCI in-orbit MTF performance with the slanted knife edge method applied to an East coastline image of the Korea peninsula covering 38.04N, 128.40E to 38.01N, 128.43E. The ray tracing simulation results showed 0.34 in MTF mean for near

IR band image while the GOCl image obtained 9th Sep, 2010 and 15th Sep, 2010, were used to produce 0.34 at Nyquist frequency in MTF. Second, stray-light effect from unwanted reflected bright source for GOCl is estimated in the realistic simulation. With integrated ray tracing technique, we estimated how much the stray light according to the targets suggested clouds affects near-by slot image. Two ways including East-West and North-South effect were progressed at each slot. In addition, the spectral results for 8 bands were compared with varying filter wheel mechanical structure and glass material characteristic. Last, we compared Normalized Difference Vegetation Index (NDVI) generated from real and simulated image in Korean peninsula. Comparing results were performed to verify the DEM model included in IRT technique, and to support remote sensed results with GOCl data in the technical field. These study results prove that the GOCl optical performance is well within the target performance requirement, and that the IRT end-to-end simulation technique introduced here can be applicable for high accuracy simulation of remote sensing.

## 8888-26, Session PS

### Determining sea surface heights using small footprint airborne laser scanning

Anti Gruno, Tallinn Univ. of Technology (Estonia); Aive Liibusk, Estonian Univ. of Life Sciences (Estonia); Artu Ellmann, Tallinn Univ. of Technology (Estonia); Ants Vain, Tõnis Oja, Estonian Land Board (Estonia); Harli Jürgenson, Estonian Univ. of Life Sciences (Estonia)

Small footprint airborne laser scanning (ALS) is widely used to collect topographic data over large areas. ALS point clouds provide high resolution datasets for variety of scientific and engineering applications, e.g. geomorphology, geodynamics and forestry. ALS can also be used for monitoring coastal processes. For many marine applications, however, the sea surface heights (SSH) are often requested. Satellite altimetry (SA) has been used to monitor SSH globally. But in regional scale, especially in the coastal areas and enclosed water bodies, the usability of SA is limited due to poor accuracy. Alternatively, our experiments have demonstrated that the water surface in the nadir range can be registered using small footprint ALS. Therefore, a special case study was carried out to analyze SSH determination from ALS measurements. Three profile-wise ALS measurements were carried out in the eastern shores of the Baltic Sea. Along ALS tracks 100 m wide corridors from ALS point cloud were formed. Shorter wavelength signals, like sea wave oscillation, were removed by a moving averaging filter. The achieved SSH were verified against a high resolution regional geoid model in conjunction with high-frequency tide gauge observations. Comparisons revealed that the ALS-based sea level-corrected SSH agree with the regional geoid model within a decimeter. Thus, small footprint ALS measurements could be applied to determine SSH in regions where SA has limited quality, e.g. in coastal areas and enclosed water bodies.

# Conference 8889: Sensors, Systems, and Next-Generation Satellites XVII

Monday - Thursday 23–26 September 2013

Part of Proceedings of SPIE Vol. 8889 Sensors, Systems, and Next-Generation Satellites XVII

8889-1, Session 1

## Overview of Japanese Earth observation programs (*Invited Paper*)

Haruhisa Shimoda, Tokai Univ. (Japan)

Five programs, i.e. TRMM, ADEOS2, ASTER, GOSAT, and GCOM-W1 are going on in Japanese Earth Observation programs. PR on TRMM and ASTER on EOS-Terra are operating well except SWI channels of ASTER. ASTER SWI channels have stopped the operation because of a refrigerator failure in 2009. ADEOS2 was failed, but AMSR-E on Aqua was operating until 14, Oct. 2011. AMSR-E has stopped at that time because of the antenna driving mechanism's torque increase. Now, AMSR-E instrument has been on from March 2012 without antenna rotation and antenna rotation has been started from Dec. 2012 with 2rpm. GCOM-W1 was launched on May, 2012. GCOM-W1 carries AMSR2. The orbit is A-train and has higher resolution than AMSR-E. GOSAT was launched on 23, Jan., 2009. GOSAT carries 2 instruments, i.e. a greenhouse gas sensor (TANSO-FTS) and a cloud/aerosol imager (TANSO-CAI). TANSO-FTS is a Fourier transform spectrometer (FTS) and covers 0.76 to 15  $\mu$ m region with 0.2 cm<sup>-1</sup> resolution. TANSO-CAI is a 5 channel push broom scanner to observe aerosols and clouds. Both sensors are operating well. SMILES was on JEM of ISS. SMILES is a sub-millimeter limb sounding instrument using super conducting mixer and measures stratospheric ozone and related compounds. Unfortunately, SMILES stopped its operation on 21, April, 2010. ALOS was launched on 24, Jan., 2006 and stopped on 22, April, 2011 by power anomaly. ALOS carried three instruments, i.e., PRISM, AVNIR-2 and PALSAR. PRISM is a 3 line panchromatic push broom scanner with 2.5m IFOV. AVNIR-2 is a 4 channel multi spectral scanner with 10m IFOV. PALSAR is a full polarimetric active phased array SAR. Next generation satellites will be launched in 2013-2017 timeframe. They are GCOM-C1, GPM core satellite, EarthCare, ALOS2 and ALOS3. GCOM-C1 will carry SGLI. SGLI has polarization channels. GCOM-C will be launched on 2016. GPM is a joint project with NASA and will carry two instruments. JAXA is developing DPR. DPR has Ka band channel in addition to Ku band channel. GPM will be launched on 2014. Another project is EarthCare. It is a joint project with ESA and JAXA is going to provide CPR with NICT. EarthCare will be launched on 2015. ALOS F/O is composed by 2 satellites like GCOM. One is called ALOS-2 and will carry L-band SAR while the other is called ALOS-3 and will carry optical sensors. ALOS-2 will be launched on 2013.

8889-2, Session 1

## Onboard electrical calibration of the ASTER VNIR

Fumihiko Sakuma, Masakuni Kikuchi, Japan Space Systems (Japan); Hitomi Inada, NEC TOSHIBA Space Systems, Ltd. (Japan)

The Advanced Space-borne Thermal Emission and Reflection Radiometer (ASTER) is one of the five sensors on the NASA's Terra satellite on orbit since December 1999. ASTER consists of three radiometers, the Visible and Near InfraRed (VNIR), the Short-Wave InfraRed (SWIR) and Thermal InfraRed (TIR) whose spatial resolutions are 15 m, 30 m and 90 m, respectively. Unfortunately the SWIR image data are saturated since April 2008 due to the offset rise caused by the cooler temperature rise, but VNIR and TIR are taking Earth images of good quality. VNIR and TIR experienced responsivity degradation while SWIR showed little change. From the lamp calibration, the band 1 decreased the most among three VNIR bands and 31 % in thirteen years. VNIR has the electrical calibration mode to check the healthiness of the electrical circuits after the charge coupled device (CCD). Four voltage levels from line 1 to line 4, which are from 2.78 V to 3.10 V, are input to the CCD in the onboard calibration sequence and the output digital numbers (DN) are detected in the images. These input voltages are monitored as telemetry data and have been stable up to now. Using the electrical calibration we can check stabilities of the offset, gain ratio and gain of VNIR. The output level of the line1 input is close to the offset level which is measured at night. The trend of the line 1 output is compared to the offset level. They are

similar but are not exactly the same. The trends of the even pixel and odd pixel are the same so the partly saturated offset levels of the odd pixel is corrected by using the even pixel trend. The gain ratio trend shows that the ratio is stable. But the ratio values are different from the prelaunch value. The difference comes up to 10 % for the band 2. When the gain ratio is different, it affects the result of the vicarious calibration because the onboard calibration is measured with the normal gain whereas the vicarious calibration often measures with the high gain. The cause of the responsivity degradation of VNIR is not known but one of the causes might be the change of the electric circuit. The band 3 gain shows 17 % decrease whereas the gain changes of the band 1 and band 2 are 5 % and 7 %, respectively. The responsivity decrease after 1500 days since launch might be controlled by the electric circuit change.

8889-3, Session 1

## Current status of the Global Change Observation Mission 1st Water 'SHIZUKU' (GCOM-W1) and the advanced microwave scanning radiometer 2 (AMSR2)

Misako Kachi, Keiji Imaoka, Takashi Maeda, Kazuhiro Naoki, Arata Okuyama, Marehito Kasahara, Norimasa Ito, Japan Aerospace Exploration Agency (Japan); Taikan Oki, The Univ. of Tokyo (Japan) and Japan Aerospace Exploration Agency (Japan); Haruhisa Shimoda, Tokai Univ. (Japan) and Japan Aerospace Exploration Agency (Japan)

Japan Aerospace Exploration Agency (JAXA) launched the Global Change Observation Mission 1st - Water (GCOM-W1) or "SHIZUKU" (meaning "droplet" in Japanese) in 18 May 2012 (JST) from JAXA's Tanegashima Space Center. GCOM-W1 is not a name of single satellite mission. It is a part of global and long-term observation program with two complementary medium-sized satellites (GCOM-W and GCOM-C series) and three generations (10-15 years) for stable data records. The GCOM-W1 satellite has joined to NASA's A-train orbit since June 29, 2012 to succeed observation by the Advanced Microwave Scanning Radiometer for EOS (AMSR-E) and to provide combined utilization with other A-train satellites. The Advanced Microwave Scanning Radiometer 2 (AMSR2) onboard GCOM-W1 has started its scientific observation since July 3, 2012.

The Advanced Microwave Scanning Radiometer 2 (AMSR2) on board the GCOM-W1 satellite is multi-frequency, total-power microwave radiometer system with dual polarization channels for all frequency bands. Basic concept of AMSR2 is almost identical to that of AMSR-E: conical scanning system with large-size offset parabolic antenna, feed horn cluster to realize multi-frequency observation, external calibration with two temperature standards, and total-power radiometer systems. AMSR2 continues AMSR-E observations of water vapor, cloud liquid water, precipitation, SST, sea surface wind speed, sea ice concentration, snow depth, and soil moisture.

AMSR-E on the NASA's Aqua satellite was launched in May 2002 and halted its scientific observation on October 4, 2011. AMSR-E, however, has restarted observation in slow antenna rotation rate since December 4, 2012 for cross-calibration with AMSR2.

For validation of AMSR2 standard products and development of some research products, JAXA implements two types of activities in cooperation with other researchers and projects. The first category is utilizing the existing ground observation networks maintained by operational agencies and instantaneous observations by other satellites and instruments. For example, validation of sea surface temperature and sea surface wind speed is implemented by using those data provided by various buoy systems operated, and validation of precipitation is implemented in collaboration with the Tropical Rainfall Measurement Mission (TRMM) and the Global Precipitation Measurement (GPM) projects, which carries the space-borne precipitation radar. The other one is implementation of specific field campaigns and monitoring focusing on specific parameters in collaboration with other projects, especially for land surface variables, such as snow depth and soil moisture content.

JAXA has started distribution of AMSR2 brightness temperature

products to public since January 24, 2013 after initial calibration/validation period through the GCOM-W1 Data Providing Service (<https://gcom-w1.jaxa.jp/>). The system has been in operation since August 2011 in order to distribute AMSR2 standard products along with AMSR and AMSR-E standard products. Registered users can also use sftp or http protocols to download data without searching. Validation of geophysical parameters is still underway toward their public release scheduled in May 2013.

## 8889-4, Session 1

### On-orbit status of TANSO on GOSAT over 4 years

Kei Shiomi, Shuji Kawakami, Hiroshi Suto, Akihiko Kuze, Masakatsu Nakajima, Japan Aerospace Exploration Agency (Japan)

The Greenhouse Gases Observing Satellite (GOSAT) is a Japanese mission to monitor greenhouse gases such as CO<sub>2</sub> and CH<sub>4</sub> from space. The GOSAT was launched on 23 January 2009 and obtains normal operation data over 4 years. On-board science instruments consist of the Fourier Transform Spectrometer (TANSO-FTS) and the Cloud and Aerosol Imager (TANSO-CAI). The FTS covers wide wavelength range from SWIR to TIR by simultaneous observations with high spectral resolution of 0.2 cm<sup>-1</sup>. The FTS has 3 polarized SWIR bands, which are 0.76, 1.6 and 2.0 microns of O<sub>2</sub>, CO<sub>2</sub>, and CH<sub>4</sub> absorptions. The TIR band observes from 5.5 to 14.3 microns, which includes CO<sub>2</sub>, CH<sub>4</sub>, O<sub>3</sub> and H<sub>2</sub>O absorptions. The FTS observes globally with grid points of 10 km IFOV by separate pointing. The CAI is carried 4 radiometers of 0.38, 0.67, 0.87, and 1.60 microns to detect cloud and aerosol interference in the FTS IFOV with high spatial resolution and wide swath of 1000 km.

The GOSAT is operated successfully and acquired observation data over 4 years. The calibration accuracies are evaluated in annual trends. The radiometric accuracies of the SWIR bands are monitored by the solar diffuser, lunar calibration and stable calibration sites (Railroad valley and Sahara desert) by comparison of other coincident satellite data and simulated radiance using in-situ field experiment data. The TIR radiances are optimized by the polarized calibration using polarization reflectance and transmittance of the optical components and emissivity of the on-board blackbody. The radiometric accuracy of the TIR band is evaluated by comparison of other coincident satellite sensor such as AIRS. The geometric accuracies are monitored the GCPs on reference image and coastline database continuously. The Level 1 product is updated to the latest version V160.160 in May 2013. This presentation shows the calibration results of TANSO FTS and CAI after 4 year operation.

## 8889-5, Session 2

### CO<sub>2</sub>, CH<sub>4</sub>, and other trace gases retrieved from thermal infrared spectra of GOSAT satellite

Naoko Saitoh, Chiba Univ. (Japan); Ryoichi Imasu, The Univ. of Tokyo (Japan)

A thermal infrared spectrum emitted from the earth includes many absorption bands of atmospheric gases such as water vapor, carbon dioxide, ozone, methane, and so on. A Japanese satellite, Greenhouse gases Observing Satellite (GOSAT) is a sun-synchronous orbital satellite that was developed by the National Institute for Environmental Studies (NIES), the Ministry of the Environment (MOE), and the Japan Aerospace Exploration Agency (JAXA) for global observations of greenhouse gases (GHG). The GOSAT was successfully launched on 23 January 2009 and has been making observations continuously, including both nadir and off-nadir measurements, for about four years since its launch. It carries two sensors: the Thermal And Near infrared Sensor for carbon Observation Fourier transform spectrometer (TANSO-FTS) and the TANSO-Cloud and Aer-osal Imager (TANSO-CAI) [Kuze et al., 2006]. The TANSO-FTS consists of four spectral bands: Band 1 (0.75-0.78 μm), Band 2 (1.56-1.72 μm), Band 3 (1.92-2.08 μm), and Band 4 (5.5-14.3 μm). The maximum optical path difference of the TANSO-FTS is ±2.5 cm; thus, the full width at half maximum of the instrumental line shape (spectral resolution) is approximately 0.2 cm<sup>-1</sup>. GOSAT is unique in that it can simultaneously observe column

amounts and profiles of carbon dioxide and methane in the same field of view. This study focuses on the Band 4 thermal infrared (TIR) spectra.

We have been developing an algorithm for retrieving GHG and other trace gases from the GOSAT TIR spectra. We adopted a non-linear Maximum a Posteriori (MAP) method with linear mapping [e.g., Rodgers, 2000; Saitoh et al, 2009]. The latest version of the GOSAT Level 1B (L1B) radiance spectra, the version 150.150 at this time, is improved compared to the previous versions, but still has a bias judging from comparisons with other coincident satellite spectral data such as the Atmospheric Infrared Sounder (AIRS); the bias is largest at around 14-15 micron band that includes carbon dioxide strong absorption lines, which results in a high bias in mid-tropospheric carbon dioxide concentration retrieved. In order to overcome the spectral bias problem, we assumed that the magnitude of the bias in the TIR L1B spectra correlates with its radiance and utilized the correlation for the spectral bias correction. In our algorithm, we treated surface temperature and surface emissivity as spectral bias correction parameters and re-tri-ieved them simultaneously with gas retrieval. We used 7-8 micron band for methane retrieval and 10 and 14-15 micron bands for carbon dioxide retrieval; in our algorithm, temperature, water vapor, ozone, and nitrous oxide were retrieved simultaneously. Although the above-mentioned bias correction was applied, some biases were still seen in the retrieved concentrations; therefore, we carefully selected the channel datasets for the retrieval especially at 14-15 micron band. This study assesses the accuracy and precision of carbon dioxide, methane, and other trace gas concentrations retrieved by the de-veloped algorithm. We also discuss the effect of a priori covariance setting on the re-tri-ieval and the difference in temperature and water vapor concentration between re-tri-ieved and analytical data.

## 8889-6, Session 2

### The current status of GOSAT-2: mission and sensor system

Masakatsu Nakajima, Hiroshi Suto, Kazuhiko Yotsumoto, Masashi Abe, Akihiko Kuze, Kei Shiomi, Japan Aerospace Exploration Agency (Japan)

GOSAT was launched almost 4 years ago and the data processing algorithm have been improved a few times based on the calibration and validation activities and these activities have resulted in the improvements of the accuracy of the net flux of the carbon dioxide as well as the one of the concentrations.

GOSAT has accomplished the global observation of the greenhouse gases whose accuracy is highest ever for any observations from space with involvement of the information of the boundary layer. But the accuracy of the GOSAT measurements is not enough for the operational uses such as the political purpose. And it has been required to improve the observation performance such as signal to noise ratio, the number of the useful data and the density of the observation points.

So Japan's three parties, Ministry of the Environment(MOE), National Institute for Environmental Studies(NIES) and JAXA which have led the GOSAT project have studied the requirements for the greenhouse gases observations from space. And we decided the mission requirements for the GOSAT-2 from the view points of the contribution to the policies on the climate changes such as the decision of the emission reduction targets based on the scientific facts, the monitor of the emission reduction efforts and so on.

The principal requirements are measuring the Carbon Dioxide concentration with the accuracy of 0.5 ppm at 500km and 2,000km mesh spatial resolution over the land and ocean, respectively and 1 month average, estimating the net flux with the error of 100% and to contribute to the detection of the anthropogenic emission of the greenhouse gases.

And we have studied the mission instruments which were possible to satisfy these mission requirements.

To achieve these targets, GOSAT-2 will continuously adopt the Fourier Transform Spectrometer (FTS) as the instrument to measure the carbon dioxide and methane, and will equip the imager to compensate the FTS data.

The performance of these instruments will be improved, for example the new observation band to measure the carbon monoxide will be added to FTS and the pointing angle in the along track direction will be extend from 20 degrees of GOSAT to 40 degrees to expand the observation area over the ocean where the sun glint is observed.



In addition to these improvements, we had considered to adopt the multi photo diodes and to reduce the diameter of the footprint to increase the number of the effective data. But we had to give up the adoption of these methods from the view points of the technical issues of the signal to noise ratio and optical cross talk. And instead of the adoption of these methods, GOSAT-2 will equip the function to avoid the clouds using the images obtained by the monitor camera whose optical axis is adjusted coaxially with the line of sight of FTS.

In this presentation, the results of the studies of the mission instruments and satellite system and the specification and development schedule will be shown.

## 8889-7, Session 2

### ALOS-2 current status and operation plan

Shinichi Suzuki, Yukihiro Kankaku, Yuji Osawa, Japan  
Aerospace Exploration Agency (Japan)

The Advanced Land Observing Satellite-2 (ALOS-2) will succeed to the radar mission of the ALOS "Daichi" which had contributed to cartography, regional observation, disaster monitoring, and resources surveys for more than 5 years until its termination of operation in May 2011. The state-of-the-art L-band Synthetic Aperture Radar (SAR) called PALSAR-2 onboard ALOS-2 will have enhanced performance in both high resolution (1m \* 3m at finest in the Spotlight mode) and wide swath (up to 490km in the ScanSAR wide mode), compared to ALOS / PALSAR. It will allow comprehensive monitoring of disasters. Wider bandwidth and shorter revisit time will give better conference for INSAR data analysis such as crustal deformation and deforestation.

The SAR antenna consists of 5 panels with total 1,080 radiation elements driven by 180 Transmit-Receive-Modules (TRMs) in order to steer and form a beam in both range and azimuth direction. In order to reduce range ambiguities, PALSAR-2 is capable to transmit up or down chirp signal alternatively and has phase modulation with zero or pi as well. And, in order to achieve high coherence of ScanSAR-ScanSAR InSAR, the timing is aligned at the first bursts among different ScanSAR observations, and then the beam overlap ratio for sub-swath pairs is more than 90 %.

The Proto Flight Test (PFT) of ALOS-2 has been conducted since June 2012, and the Thermal Vacuum test was completed in November 2013. As the result of Thermal Vacuum test, the thermal design of satellite system and equipped components was verified. In parallel, the PFT of PALSAR-2 had been conducted since March 2012. The Thermal Vacuum Test vibration test, deployment test were completed. As the result of RF impulse response measurement, the resolutions of each imaging modes were verified. As of April 2013, ALOS-2 system is preparing for the Vibration test, Acoustic test and Electromagnetic Compatibility test. After the End-to-End test including the ground system, ALOS-2 will be transported to JAXA Tanegashima Space Center for launch.

The initial commissioning phase of ALOS-2 is planned for six months which are comprised of LEOP (Launch and Early Orbit Phase) and initial Cal/Val phase. During the LEOP, all components will be tested with direct downlink via X-band and data relay communication with JAXA's DRTS (Data Relay Test Satellite). During the initial Cal/Val phase, the data of PALSAR-2 will be verified and calibrated by using Corner Reflectors and Geometric Calibrator at ground. Also the data acquisition during the commissioning phase will be consistent with the systematic acquisition strategy prepared for the routine operation. The LEOP operation procedures and the initial commissioning plan are now being prepared.

This paper describes the current status and operation plan of ALOS-2.

## 8889-8, Session 2

### Status of Japanese Global Precipitation Measurement (GPM) Mission

Misako Kachi, Riko Oki, Takuji Kubota, Takeshi Masaki, Satoshi Kida, Yuki Kaneko, Kinji Furukawa, Takeshi Miura, Masahiro Kojima, Japan Aerospace Exploration Agency (Japan); Toshio Iguchi, National Institute of Information and Communications Technology (Japan); Yukari N. Takayabu, The Univ. of Tokyo (Japan) and Japan Aerospace Exploration

Agency (Japan); Kenji Nakamura, Dokkyo Univ. (Japan) and Japan Aerospace Exploration Agency (Japan)

The Global Precipitation Measurement (GPM) is a mission led by the Japan Aerospace Exploration Agency (JAXA) and the National Aeronautics and Space Administration (NASA) under collaboration with many international partners, who will provide constellation of satellites carrying microwave radiometer instruments. Main target of the GPM mission is generation and dissemination of global map of precipitation rate with high frequency and accuracy, and the GPM Core Observatory will provide a reference standard to other constellation of satellites. The Dual-frequency Precipitation Radar (DPR) on board the GPM Core Observatory was developed by JAXA and National Institute of Information and Communications Technology (NICT), and consists of Ku-band (13.6GHz) and Ka-band (35.5GHz) precipitation radars to measure light rainfall and snowfall as well as moderate-to-heavy rainfall. The integration of DPR onto the Core Observatory was successfully completed in May 2012 at NASA Goddard Space Flight Center. The GPM Core Observatory is scheduled to be launched in early 2014 from JAXA's Tanegashima Space Center. JAXA also provides the Global Change Observation Mission (GCOM) 1st - Water (GCOM-W1) named "SHIZUKU," as one of constellation satellites. The GCOM-W1 satellite was launched in 18 May, 2012 from JAXA's Tanegashima Space Center, and brightness temperature products of the Advanced Microwave Scanning Radiometer 2 (AMSR2) on board the GCOM-W1 satellite have been released to public since January 2013, and geophysical parameter products including precipitation are scheduled in May 2013. JAXA also promotes collaboration studies in Japan and Asian countries, and public relations activities to extend potential users of satellite precipitation products.

The Japanese GPM research project conducts scientific activities on algorithm development, ground validation, application research including production of research products.

The DPR and DPR/GMI combined Level 2 algorithms are being developed by Japan-U.S. Joint GPM Algorithm Team. Algorithms for national products, such as global rainfall map algorithm, are being developed by each GPM partner including JAXA and NASA. JAXA also develops the Global Rainfall Map product as national product to distribute hourly and 0.1-degree horizontal resolution rainfall map. All standard algorithms including Japan-US joint algorithm will be reviewed by the Japan-US Joint Precipitation Measuring Mission (PMM) Science Team (JPST) before the release. All algorithms for at-launch code were submitted to both JAXA and NASA for end-to-end tests in each mission operation system.

Pre-launch validation activities have been conducted by both Japan and U.S. sides in order to contribute to the development and improvement of algorithms. JAXA has implemented several field campaign experiments using two field-portable Ka-band radars since 2011 in Okinawa, Tsukuba, Mount Fuji, Nagaoka, and Sapporo.

## 8889-9, Session 2

### EarthCARE/CPR design results and PFM performance

Yoshihisa Aida, Japan Aerospace Exploration Agency (Japan)

The Earth Clouds, Aerosols and Radiation Explorer (EarthCARE) mission is joint mission between Europe and Japan for the launch year of 2015. Mission objective is to improve scientific understanding of cloud-aerosol-radiation interactions that is one of the biggest uncertain factors for numerical climate and weather predictions. The EarthCARE spacecraft equips four instruments; an ultra violet lidar (ATLID), a cloud profiling radar (CPR), a broadband radiometer (BBR) and a multi-spectral imager (MSI), for synergistic observation. Japan aerospace exploration agency (JAXA) is responsible for development of the CPR in this mission, under joint cooperation with National Institute of Information and Communications Technology (NICT). The CPR will be the first space-borne W-band Doppler radar. Major CPR specifications are; minimum radar sensitivity of -35dBZ, radiometric accuracy of <2.7 dB, and Doppler velocity measurement accuracy of <1m/s. They require highly accurate pointing knowledge in orbit and high power source with large and accurate antenna dish. Additionally a new ground calibration technique to determine CPR pointing is also being progressed towards the launch.

Currently, Development phase has been completed with tests using engineering model to confirm its compliances of design, performance and reliability. Critical Design Review (CDR) for CPR was held on March 2013.

## 8889-10, Session 2

### Ground-based demonstration experiment of imaging SWIR-FTS for space-based detection of air pollution and greenhouse gases

Tadashi Imai, Hiroshi Suto, Jumpei Murooka, Akihiko Kuze, Ryota Sato, Japan Aerospace Exploration Agency (Japan)

Fourier transform spectrometer (FTS) has many advantages, especially for greenhouse gases and air pollution detection in the atmosphere, because a single instrument can provide wide spectral coverage and high spectral resolution with highly stabilized instrumental line function for all wavenumbers. Several channels are usually required to derive the column amount or vertical profile of a target species. Near infrared (NIR) and shortwave infrared (SWIR) spectral regions, such as the 0.7-2.5  $\mu\text{m}$  bands, are very attractive for remote sensing applications. The GHG and CO precursors of air pollution have absorption lines in the SWIR region, and the amounts of these species and the sensitivity against change in the amounts in the boundary layer is high enough to measure mole fractions near the Earth surface. One disadvantage of conventional space-based FTS is the spatial density of effective observation. To improve the effective numbers of observations, an imaging FTS coupled with a two-dimensional (2D)-camera was considered. At first, a mercury cadmium telluride (MCT)-based imaging FTS was considered. However, an MCT-based system requires a calibration source (black body and deep-space view) and a highly accurate and super-low temperature control system for the MCT detector. As a result, size, weight, and power consumption are increased and the cost of the instrument becomes too high. To reduce the size, weight, power consumption, and cost, a commercial 2D indium gallium arsenide (InGaAs) camera can be used to detect SWIR light. To demonstrate a small imaging SWIR-FTS (IS-FTS), an imaging FTS coupled with a commercial 2D InGaAs camera was developed. In the demonstration, the CH<sub>4</sub> gas cell was equipped with an IS-FTS for the absorber to construct the spectra in the SWIR region. The spectra of CH<sub>4</sub> of the IS-FTS demonstration model were then compared with those of traditional FTS. The spectral agreement between the traditional and IS-FTS instruments was very good.

Further, a feasibility design study of space-based IS-FTS for use on the International Space Station, a low-earth orbit satellite, or a geostationary satellite will be started.

In this presentation we introduce the result of demonstration experiment, tentative mission objectives of space-based IS-FTS in a low-earth orbit and a geostationary orbit, and preliminary result of the feasibility design study.

## 8889-11, Session 3

### NASA Earth science missions (*Invited Paper*)

Steven P. Neeck, Stephen M. Volz, NASA Headquarters (United States)

NASA's Earth Science Division (ESD) conducts pioneering work in Earth system science, the interdisciplinary view of Earth that explores the interaction among the atmosphere, oceans, ice sheets, land surface interior, and life itself that has enabled scientists to measure global and climate changes and to inform decisions by governments, organizations, and people in the United States and around the world. The ESD makes the data collected and results generated by its space missions accessible to other agencies and organizations to improve the products and services they provide, including air quality indices, disaster management, agricultural yield projections, and aviation safety. Through partnerships with national and international agencies, NASA enables the application of this understanding. The ESD's Flight Program provides the spacebased observing systems and supporting ground segment infrastructure for mission operations and scientific data processing and distribution that support NASA's Earth system science research and modeling activities. The Flight Program currently has 17 operating Earth observing space missions, including the recently launched Landsat Data Continuity Mission (LDCM). The ESD has 16 more missions planned for launch over the next decade. These include first and second tier missions from the 2007 Earth Science Decadal Survey, Climate Continuity missions to assure availability of key data sets needed for climate science and applications, and small-sized competitively selected orbital missions and instrument

missions of opportunity utilizing rideshares that are part of the Earth Venture (EV) Program. The recently selected Cyclone Global Navigation Satellite System (CYGNSS) microsatellite constellation and the Tropospheric Emissions: Monitoring of Pollution (TEMPO) instrument are examples. In addition, the International Space Station (ISS) is being increasingly used to host NASA Earth observing science instruments. An overview of plans and current status will be presented.

## 8889-12, Session 3

### Global precipitation measurement (GPM) L-6

Steven P. Neeck, Ramesh K. Kakar, NASA Headquarters (United States); Ardeshir A. Azarbarzin, Arthur Y. Hou, NASA Goddard Space Flight Ctr. (United States)

The Global Precipitation Measurement (GPM) mission will advance the measurement of global precipitation, making possible high spatial resolution precipitation measurements. GPM will provide the first opportunity to calibrate measurements of global precipitation across tropical, mid-latitude, and polar regions. The GPM mission has the following scientific objectives: (1) Advance precipitation measurement capability from space through combined use of active and passive remote-sensing techniques; (2) Advance understanding of global water/energy cycle variability and fresh water availability; (3) Improve climate prediction by providing the foundation for better understanding of surface water fluxes, soil moisture storage, cloud/precipitation microphysics and latent heat release in the Earth's atmosphere; (4) Advance Numerical Weather Prediction (NWP) skills through more accurate and frequent measurements of instantaneous rain rates; and (5) Improve high impact natural hazard (flood/drought, landslide, and hurricane hazard) prediction capabilities. The GPM mission centers on the deployment of a Core Observatory carrying an advanced radar / radiometer system to measure precipitation from space and serve as a reference standard to unify precipitation measurements from a constellation of research and operational satellites. GPM, jointly led with the Japan Aerospace Exploration Agency (JAXA), involves a partnership with other international space agencies including the French Centre National d'Études Spatiales (CNES), the Indian Space Research Organisation (ISRO), the U.S. National Oceanic and Atmospheric Administration (NOAA), the European Organisation for the Exploitation of Meteorological Satellites (EUMETSAT), and others. The GPM Core Observatory is currently being prepared for shipment to Japan for launch. Launch is scheduled for February 2014 from JAXA's Tanegashima Space Center on an H-IIA launch vehicle.

## 8889-13, Session 3

### NASA's Earth venture cyclone global navigation satellite system (CYGNSS) mission: designed to provide the science data to better understand the genesis and intensification of tropic cyclones

Randall J. Rose, Southwest Research Institute (United States); Christofer Ruf, Univ. of Michigan (United States)

Since 1990 there has been essentially no improvement in the accuracy of a tropical cyclone's intensity prediction, while their track forecasts have improved in accuracy by ~50%. Forecasters can now predict almost exactly where the storms will make landfall, but routinely fail to predict strength of the storm when it gets there. Principle deficiencies of current tropical cyclone intensity forecasts lie primarily with inadequate observations and modeling of the inner core. The inadequacy in observations results from two causes: 1) Much of the inner core ocean surface is obscured from conventional remote sensing instruments by intense precipitation in the eye wall and inner rain bands. 2) The rapidly evolving (genesis and intensification) stages of the TC life cycle are poorly sampled in time by conventional polar-orbiting, wide-swath surface wind imagers.

NASA's recently awarded Earth science mission, the Cyclone Global Navigation Satellite System (CYGNSS) has been designed to address tropical storm intensity forecast deficiencies by combining the all-weather performance of GNSS bi-static ocean surface scatterometry with the sampling properties of a satellite constellation. CYGNSS

will demonstrate how micro-satellite technology can be applied to provide low cost solutions to fill capability voids in existing large-scale observatories.

An overview will be presented of the CYGNSS mission, its science objectives, and how the use of a micro-satellite constellation results in sampling properties that are markedly improved beyond conventional wind speed observatories.

### 8889-14, Session 3

#### On the ozone mapper profiler suite Nadir sensor data record

Chunhui Pan, Univ. of Maryland, College Park (United States); Xiangqian Wu, Fuzhong Weng, National Oceanic and Atmospheric Administration (United States); Richard H. Buss, Raytheon Co. (United States); Lawrence E. Flynn, National Oceanic and Atmospheric Administration (United States)

OMPS is the latest advanced hyper-spectral sensor suite that continues a 30 year heritage of global ozone monitoring by providing Earth atmosphere ozone data to the Suomi-NPP/JPSS program. Launched on 28 October 2011, OMPS opened its aperture door on 26 January 2012, began the Earth observation mission, continuing until now, more than one year in operation. During the past year, OMPS has collected all types of orbital calibration and science data that have allowed us to understand better the two Nadir sensors' on-orbit performances, and consequently to establish the baseline calibrations during the early orbital checkout of the instruments. From studies that we have conducted so far since the launch, this paper defines the current status of the OMPS Nadir sensor data records (SDRs); evaluates the orbital sensors' performances; as well as verifies updates to the data processing ground system and to the orbital calibration sequences. Our results suggest that OMP Nadir orbital performance meets the project requirements; that the modified calibration sequences are suited to determine the sensors' characteristics; and that the Nadir sensors are capable of collecting higher resolution data, which will benefit both the operational and research needs of the OMPS user community.

### 8889-15, Session 4

#### Overview of ESA Earth observation missions (*Invited Paper*)

Roland Meynart, European Space Research and Technology Ctr. (Netherlands)

No Abstract Available

### 8889-16, Session 4

#### The EUMETSAT Polar System-Second Generation (EPS-SG) Micro-Wave and Sub-millimetre Wave Imaging Missions

Christophe Accadia, Peter Schluessel, Pepe L. Phillips, European Organisation for the Exploitation of Meteorological Satellites (Germany); J. Julian W. Wilson, EUMETSAT (Germany)

The EUMETSAT Polar System (EPS) will be followed by a second generation system, EPS-SG, in the 2020 timeframe and contribute to the Joint Polar System being jointly set up with NOAA. The satellites will fly, like Metop, in a sun synchronous, low earth orbit at 820 km altitude and 09:30 local time of the descending node, providing observations over the full globe with revisit times of 12 to 24 hours, depending on instrument.

Among the various missions relevant to EPS-SG, there are the Microwave Imager (MWI) and the Ice Cloud Imager (ICI). The MWI frequencies are from 18 GHz up to 183 GHz. All MWI channels up to 89 GHz are measured with both V- and H polarizations. The primary objective of the MWI mission is to support Numerical Weather Prediction at regional and global scales. The MWI will provide

continuity of measurements for some heritage microwave imager channels (e.g. SSM/I, AMSR-E), but will also include additional channels like the 50-55 / 118 GHz bands.

The ICI will provide measurements over the sub-millimetre spectral range contributing to an innovative characterization of clouds over the whole globe. The ICI has channels at 183 GHz, 243 GHz, 325 GHz, 448 GHz and 664 GHz with single polarisation, with two window channels (243 GHz and 664 GHz) with V and H polarization. ICI's primary objectives are the support to climate monitoring and validation of ice clouds modelling and parameterization in weather and climate models through the retrieval of ice cloud products.

The presence of sounding channels on MWI like the 50-55 and 118 GHz bands will provide more information on cloud and precipitation over sea and land. This set of channels was already tested on the NAST-M airborne radiometer, but it is the first time that will be implemented in an operational mission.

ICI will contribute to better characterize the essential climate variable ice water path (IWP) due to its sensitivity to the amount of cloud ice in the sub-millimetre frequency range, while measurements at different frequencies will sample the ice particle size distribution providing information on particles' size.

### 8889-17, Session 4

#### The Multi-Viewing, -Channel, -Polarisation Imager (3MI) of the EUMETSAT Polar System - Second Generation (EPS-SG) Dedicated to Aerosol Characterisation

Thierry Marbach, Pepe L. Phillips, European Organisation for the Exploitation of Meteorological Satellites (Germany); Antoine Lacan, Peter Schluessel, EUMETSAT (Germany)

The EUMETSAT Polar System (EPS) will be followed by a second generation system, EPS-SG, in the 2020 timeframe and contribute to the Joint Polar System being jointly set up with NOAA. The satellites will fly, like Metop, in a sun synchronous, low earth orbit at 820 km altitude and 09:30 local time of the descending node, providing observations over the full globe with revisit times of 12 to 24 hours, depending on instrument.

The EPS-SG Multi-Viewing Multi-Channel Multi-Polarisation Imaging mission (3MI) is a push-broom radiometer dedicated to aerosol characterisation for climate monitoring, atmospheric composition, and more specifically air quality and numerical weather prediction. The purpose of the 3MI is to provide multi-spectral (from 410 to 2130 nm), multi-polarisation (-60°, 0°, and +60°), and multi-angular (10 to 14 views) images of the Earth top of atmosphere (TOA) outgoing radiance to accurately measure the aerosol load and thereby resolve the directional anisotropy and to characterise the microphysical properties. Although the 3MI design will be based on the POLDER missions (3 instruments flown since 1996), the new instrument will provide substantial innovations by measuring over an extended spectral range and with higher spatial resolution.

Although aerosol characterisation is the primary application, 3MI will further support observation of cloud microphysical properties, water vapour load, Earth radiation budget, and land-surface characteristics all of which will benefit from the enhanced directional and polarisation measurements.

The 3MI also contributes to artefact correction of other EPS-SG sensors METImage, Sentinel-5, and IASI-NG by providing anisotropy and polarisation information on scattered radiation from aerosols and cirrus clouds. Likewise, the synergy with these instruments will support 3MI with beneficial cross-calibration. Indeed 3MI will not have an onboard calibration and its radiometric performance will rely on vicarious calibration.

### 8889-18, Session 4

#### The MetOp second generation 3MI instrument

Ilias G. Manolis, European Space Research and Technology Ctr. (Netherlands); Semen Grabarnik, Jérôme Caron, European Space Agency / ESTEC (Netherlands); Jean-Loup Bézy, Marc

Loiselet, Maurizio Betto, Hubert Barre, Graeme Mason, Roland Meynart, European Space Research and Technology Ctr. (Netherlands)

Since 2006, the European contribution to operational meteorological observations from polar orbit has been provided by the first generation of Meteorological Operational (MetOp) satellites. The MetOp Second Generation (MetOp-SG) series of satellites will provide continuity and enhancement of these observations in the timeframe of 2020 to 2040.

The MetOp-SG programme is being implemented in collaboration with EUMETSAT. ESA develops the prototype MetOp-SG satellites (including associated instruments) and procures, on behalf of EUMETSAT, the recurrent satellites (and associated instruments). EUMETSAT is responsible for the overall mission, funds the recurrent satellites, develops the ground segment, procures the launch and LEOP services and performs the satellites operations. The corresponding EUMETSAT Programme is termed the EUMETSAT Polar System – Second Generation or EPS-SG.

ESA is responsible for instrument design of five missions, namely Microwave Sounding Mission (MWS), Scatterometer mission (SCA), Radio Occultation mission (RO), Microwave Imaging mission (MWI) and Multi-viewing, Multi-channel, Multi-polarisation imaging mission (3MI). Two parallel, competitive phase A/B1 studies for MetOp Second Generation (MetOp-SG) will be concluded in May 2013. The final implementation phases (B2/C/D) are planned to start beginning of 2014.

This paper will present the instrument main design elements of the 3MI mission, primarily aimed at providing aerosol characterization for climate monitoring, Numerical Weather Prediction (NWP), atmospheric chemistry and air quality. The 3MI instrument is a passive radiometer measuring the polarised radiances reflected by the Earth under different viewing geometries and across several spectral bands spanning the visible and short-wave infrared spectrum.

The paper will present the main performances of the instrument and will highlight the performance improvements, with respect to its heritage derived by the POLDER instrument. 3MI features several improvements in terms of number of spectral channels and spectral range coverage (see Table 1), swath as well as ground spatial resolution.

The engineering of some key performance requirements (multi-viewing, polarisation sensitivity, etc.) will also be discussed. The results of the feasibility studies will be discussed together with the programmatics for the instrument development.

Several pre-development activities have been initiated to retire any risk and to demonstrate the ultimate performances of the 3MI optics. The preliminary results from those activities (most notably on AR coatings, filters and polarisers) will be presented. Key technologies involved in the 3MI instrument design and implementation are considered to be: the optical design featuring aspheric optics, the implementation of broadband AR coatings featuring low polarisation and low de-phasing properties over a wide range of angles of incidence, the development of polarisers with acceptable performances over a wide spectral range as well as spectral filters with good uniformities over a large clear aperture.

## 8889-19, Session 5

### Sentinel-2: next generation satellites for optical land observation from space

Stefan Bursch, Roland Gessner, Wilhelm Gockel, Cornelius Haas, Gunn Schweickert, Mario Welsch, Heinz Sontag, EADS Astrium GmbH (Germany)

Within the Global Monitoring for Environment and Security programme (GMES) jointly initiated by the European Space Agency (ESA) and the European Union (EU), the two first Sentinel-2 satellites, which constitute the next generation of Earth observation satellites for optical land monitoring from space, are undergoing assembly, integration and tests in the facilities at Astrium for a launch of the first satellite planned in 2014. Sentinel-2 will feature a major breakthrough in the area of optical land observation since it will for the first time enable continuous acquisition of all land surfaces world-wide thus providing the basis for a truly operational service. Flying in the same orbital plane and spaced at 180°, two satellites, designed for an operational lifetime of 12 years each, will acquire all land surfaces in only 5 days. Images are acquired in 13 spectral channels from Visible-to-Near

Infrared (VNIR) to Short Wave Infrared (SWIR) with a swath of 290 km on ground and a spatial resolution up to 10 m. The data ensure continuity to the existing data sets produced by the series of SPOT and Landsat satellites, and will further provide detailed spectral information to enable derivation of biophysical or geophysical products. Excellent image quality performances are achieved with geo-location of near real time data better than 20 m, thanks to an innovative instrument design in conjunction with a high-performance satellite AOCS subsystem centered around a 2-band GPS receiver, high-performance star trackers and a fiber optic gyrometer. To cope with the high data volume on-board, data are compressed using a state-of-the-art wavelet compressing scheme. Thanks to a powerful mission data handling system built around a newly developed very large solid-state flash memory, on-board compression losses will be kept to a minimum. The Sentinel-2 satellite design features a highly flexible operational concept, allowing downlinking of mission data either to a nominal X-band core ground station network, selected user ground stations or via an optical inter-satellite link to a geostationary EDRS relay satellite. Different priority schemes can be selected in flight to allow transmission of critical data with the shortest possible latency. The system is designed for a high degree of autonomy allowing for pre-programming of the operational schedule for 15 days in advance without intervention from ground. Apart from the nominal imaging mode, the satellites also feature a calibration mode to support regular in-orbit radiometric calibration of the instrument with a sun diffuser. Overall, Sentinel-2 designed for a very high availability of >97% is expected to fulfill the requirements of a fully operational system for multispectral Earth observation.

The activities are being performed under an ESA contract. Support by the European Union is gratefully acknowledged.

## 8889-20, Session 5

### Overview of sentinel-2

Valérie Fernandez, European Space Agency (Netherlands); Philippe Martimort, European Space Research and Technology Ctr. (Netherlands); Francois Spoto, Omar Sy, Paolo Laberinti, European Space Agency (Netherlands)

GMES is a joint initiative of the European Commission (EC) and the European Space Agency (ESA), designed to establish a European capacity for the provision and use of operational monitoring information for environment and security applications. ESA's role in GMES is to provide the definition and the development of the space- and ground-related system elements. GMES Sentinel-2 mission provides continuity to services relying on multi-spectral high-resolution optical observations over global terrestrial surfaces. The key mission objectives for Sentinel-2 are: (1) To provide systematic global acquisitions of high-resolution multi-spectral imagery with a high revisit frequency, (2) to provide enhanced continuity of multi-spectral imagery provided by the SPOT series of satellites, and (3) to provide observations for the next generation of operational products such as land-cover maps, land change detection maps, and geophysical variables. Consequently, Sentinel-2 will directly contribute to the Land Monitoring, Emergency Response, and Security services. The corresponding user requirements have driven the design towards a dependable multi-spectral Earth-observation system featuring the Multispectral Instrument with 13 spectral bands spanning from the visible and the near infrared to the short wave infrared. The spatial resolution varies from 10 m to 60 m depending on the spectral band with a 290 km field of view. This unique combination of high spatial resolution, wide field of view and large spectral coverage will represent a major step forward compared to current multi-spectral missions. The mission foresees a series of satellites, each having a 7.25-year lifetime over a 20-year period starting with the launch of Sentinel-2A foreseen in 2014. During full operations two identical satellites will be maintained in the same orbit with a phase delay of 180° providing a revisit time of five days at the equator. This presentation will concentrate on the development status of the two satellite flight models and on further plans to prepare for the launch and in orbit commissioning phase of the first satellite.

8889-21, Session 5

**The multispectral instrument of the Sentinel-2 PFM program results**

Vincent Chorvalli, Francis Delbru, Stéphane Espuche, EADS Astrium (France); Cornelius Haas, EADS Astrium GmbH (Germany); Philippe Martimort, European Space Research and Technology Ctr. (Netherlands); Valérie Fernandez, European Space Agency (Netherlands); Volker Kirshner, European Space Research and Technology Ctr. (Netherlands)

The presentation provides an outlook of the S2 MSI PFM program status and test results.

Sentinel-2 will provide a permanent record of comprehensive data to support services such as: risk management (floods and forest fires, subsidence and landslides); European land-use/land-cover state and changes; forest monitoring; food security/early warning systems; water management and soil protection; urban mapping; natural hazards; and terrestrial mapping for humanitarian aid and development. In the Sentinel-2 mission programme, Astrium in Friedrichshafen is responsible for the satellite's system design and platform, as well as for satellite integration and testing. Astrium Toulouse will supply the MultiSpectral Instrument (MSI), and Astrium Spain is in charge of the satellite's structure pre-integrated with its thermal equipment and harness. The industrial core team also comprises Jena Optronik (Germany), Boostec (France), Sener and GMV (Spain).

Sentinel-2 is designed to image the Earth's landmasses from its orbit for at least 7.25 years. Its on-board resources allow to prolong the mission by extra five years. The 1.1-metric-ton satellite will circle the Earth in a sun-synchronous, polar orbit at an altitude of 786 kilometres, fully covering the planet's landmasses in ten days. The first satellite is expected to be launched in 2014 and the second satellite is expected to be ready for launch in 2015.

The multi-spectral instrument (MSI) will generate optical images in 13 spectral channels in the visible and short-wave infrared spectral ranges down to a resolution of 10 meters with a swath of 290 kilometers.

The instrument ProtoFlight Model (PFM) program is approaching to the end with the instrument qualification testing sequence. Before reaching this final validation activity, several steps have already been achieved demonstrating the outstanding performances of the MSI. Already, major steps paving the way of the MSI PF qualification have been passed:

- the MSI EM test campaign completion and related lessons learned,
- the VNIR and SWIR focal planes alignment and exhaustive testing,
- the alignment of the telescope,
- the precise alignment of the focal planes on the telescope
- the validation of main optical performances at ambient

Main achievements of 2 years of integration and test will be presented providing an overall picture of the MSI performances before entering the final qualification test campaign. Special focus will be made on test specificities related to the large swath and numerous spectral bands embedded on the MSI.

8889-22, Session 5

**Overview on GMES Sentinel-3 optical mission, development, products and calval preparation**

Jens Nieke, European Space Research and Technology Ctr. (Netherlands); Philippe Goryl, ESRIN (Italy); Constantin E. Mavrocordatos, Craig Donlon, Bruno Berutti, European Space Research and Technology Ctr. (Netherlands)

The Global Monitoring for Environment and Security (GMES) programme decided to develop the Sentinels as first series of operational satellites in order to meet specific Earth observation user needs. The series of Sentinel-3 satellites will provide global, frequent and near-realtime ocean, ice and land monitoring. It continues Envisat's altimetry, the multispectral, medium-resolution visible and infrared ocean and land-surface observations of ERS, Envisat and Spot, and includes enhancements to meet the operational revisit

requirements and to facilitate new products and evolution of services. In this paper the status of the Sentinel-3 satellite and optical payload is presented. Further the dedicated calibration and validation activities regarding the sea and land surface temperature radiometer (SLSTR) and ocean and land colour radiometer (OLCI) are then reviewed. Calibration and validation (calval) activities are based on the heritage gained from ENVISAT MERIS and AATSR experience and cover pre-launch, in-orbit commissioning and operational measures for the Sentinel 3 satellites.

8889-23, Session 6

**The ocean and land colour imager (OLCI) design and performance**

Yves Delclaud, Jean-Bernard Riti, Thierry Garnier, Thales Alenia Space (France); Jens Nieke, European Space Research and Technology Ctr. (Netherlands)

The Ocean & Land Colour Imager (OLCI) is a high accuracy optical payload selected for the Sentinel 3 component of the Global Monitoring for Environment & Security (GMES) mission, to provide ocean and land data continuity with the previous ESA Envisat missions. Based on the very successful opto-mechanical and imaging design of MERIS, the OLCI instrument is a quasi-autonomous, self contained, visible-near-infrared push-broom imaging spectrometer.

The development of the instrument is currently in its phase C/D, i.e., camera and instrument of the engineering model has been accomplished and results from the camera flight model are available.

The paper highlights the technical and programmatic challenges of the project, and provides first results from the FM camera test activities.

8889-24, Session 6

**The Sentinel-3 microwave radiometer**

Ulf Klein, Bruno Berruti, Constantin E. Mavrocordatos, European Space Research and Technology Ctr. (Netherlands); Marc Bergada, EADS CASA Espacio (Spain)

The microwave radiometer observations are used to correct the delay of the radar altimeter signal due to the water vapour contained in the Earths atmosphere. It measures the brightness temperature at 23.8 GHz and 36.5 GHz covering a bandwidth of 200 MHz in each channel. Conceptually it is a balanced Dicke radiometer for brightness temperatures below the Dicke load temperature. The balancing is achieved by means of a noise injection circuit. For brightness temperatures higher than the Dicke load temperature a conventional Dicke mode is used. The radiometer employs a single offset reflector of 60 cm in diameter and two separate feeds for the two channels. Calibration is achieved through a dedicated horn antenna pointing at the cold sky. The radiometer electronics unit consists of the radiometer processing module that provides the interface to the satellite main computer and the radio-frequency front end that contains the amplifiers, filters and the calibration/redundancy switch assembly. A block diagram of the MWR is depicted in Figure 8 and a sketch of the whole instrument is shown in Figure 1.

The accuracy of the tropospheric path correction of the Altimeter signal is expected to have an accuracy of 1.2 – 1.5cm. This delay is influenced by both the atmospheric integrated water vapour content and by liquid water. In addition, MWR measurement data could be useful for the determination of surface emissivity and soil moisture over land, for surface energy budget investigations to support atmospheric studies and for ice characterization. In the frame of the operational Sentinel 3 these kind of products are a secondary objective only.

Some of the main characteristics of the Sentinel-3 MWR are listed in the following Table.

Frequencies	23.8 / 36.5 GHz
Bandwidth	200 MHz
Radiometric Noise	0.45 K*
Radiometric Stability	0.6 K
Radiometric accuracy	3 K
3-dB footprint ?	23.2 / 16.7 km

Beam efficiency (2.5 HPBW)	93.5 / 95.8 %
Mass	24.5 kg
Power consumption	34 W
Calibration cycle	≈1/h
Dicke frequency	78.5 Hz
Integration time	150 ms
Main characteristics of the Sentinel-3 MWR (* without blanking)	

The Radiometer Electronics Unit (REU) consists of the Radio Frequency Front End (RFFE) and the Radiometer Processing Module (RPM). The RFFE is located as close as possible to the measurement feed to optimize the length of the waveguides and thus the radiometric performance. It contains the amplifiers, switches and other performance determining elements. The RPM contains the thermal control, the RFFE control, the power supplies and provides the electronic interface to the platform. The REU includes a mode to blank the receiver inputs when the radar altimeter emits its pulses to avoid potential disturbances.

The antenna assembly consists of the main reflector that has a diameter of 60 cm, the two measurement feeds and the sky horn.

The antenna assembly receives the noise temperature emitted by the objects within the antenna field of view. Discrimination between the different measurement frequencies is done by using different feed horns, covering each a separate frequency band. A separate sky measurement is provided by means of a dedicated sky horn. In this way, the satellite can continue the regular nadir measurements without the need of any maneuvers to turn over the satellite to look at cold sky. The different frequencies received the sky horn, are separated by a wave guide diplexer. The signals received by the feeds are guided towards the receiver electronics by means of waveguides. The physical temperatures of the different sections of the antenna assembly are measured and sent to the Radiometer Processing Module (RPM) of the REU.

## 8889-25, Session 6

### The TROPOMI instrument: first H/W results

Robert Voors, Johan de Vries, Dutch Space B.V. (Netherlands); Nick C. J. van der Valk, TNO Science and Industry (Netherlands); Ianjit Bhatti, David M. Woods, Surrey Satellite Technology Ltd. (United Kingdom); Ilse Aben, Ruud Hoogeveen, SRON Netherlands Institute for Space Research (Netherlands); Pepijn Veefkind, Quintus Kleipool, Koninklijk Nederlands Meteorologisch Instituut (Netherlands)

The Tropospheric Monitoring Instrument, TROPOMI, is a passive UV-VIS-NIR-SWIR spectrograph, which uses sun backscattered radiation to study the Earth's atmosphere and to monitor air quality, on both global and local scale. It follows in the line of SCIAMACHY (2002) and OMI (2004), both of which have been very successful. OMI is still operational. TROPOMI is scheduled for launch in 2015. Compared with its predecessors, TROPOMI will take a major step forward in spatial resolution and sensitivity. The nominal observations are at 7 x 7 km<sup>2</sup> at nadir and the signal-to-noises are sufficient for trace gas retrieval even at very low albedos (2 to 5%). This allows observations of air quality at sub-city level.

TROPOMI combines the broad wavelength range from SCIAMACHY from UV to SWIR and the broad viewing angle push-broom concept from OMI. This enables daily global coverage in combination with good spatial resolution. At moderate spectral resolution (0.25-0.6 nm) in the UV-VIS-NIR-SWIR wavelength range, TROPOMI will measure O<sub>3</sub>, NO<sub>2</sub>, SO<sub>2</sub>, BrO, HCHO, H<sub>2</sub>O, CO and CH<sub>4</sub> tropospheric columns. Cloud information will come from the O<sub>2</sub>A band in the NIR. TROPOMI will yield an unprecedented accuracy of the tropospheric products compared with instruments currently in orbit.

TROPOMI has reached CDR status and production of flight model units has started. Flight detectors have been produced and detector electronics is expected to be finished by mid-2013. The instrument control unit is undergoing extensive tests, to ensure full instrument functionality. Early results are promising and this paper discusses these H/W results as well as some challenges encountered during the development of the instrument.

TROPOMI is the single payload on the Sentinel-5 precursor mission which is a joint initiative of the European Community (EC) and of the

European Space Agency (ESA). The 2015 launch intends to bridge the data stream from SCIAMACHY/OMI and the upcoming Sentinel 5 mission, with a scheduled launch date of 2019/2020. TROPOMI is funded jointly by the Netherlands Space Office and by ESA. Dutch Space is the instrument prime contractor. Dutch Space and TNO are working as an integrated team for the UVN module. SSTL are responsible for the SWIR module with a significant contribution from SRON. KNMI and SRON are responsible for ensuring the scientific capabilities of the instrument.

## 8889-26, Session 6

### Progress in the hyperspectral payload for PRISMA programme

Marco Meini, SELEX ES Ltd. (Italy); Fabrizio Battazza, Roberto Formaro, Agenzia Spaziale Italiana (Italy); Alessandro Bini, SELEX Galileo S.p.A. (Italy)

The PRISMA (PRecursore IperSpettrale della Missione Applicativa) Programme is an ASI (Agenzia Spaziale Italiana) hyperspectral mission for Earth observation based on a mono-payload single satellite: an Italian Consortium is in charge to realize the mission; Selex ES has the full responsibility of the hyperspectral payload composed by a high spectral resolution spectrometer optically integrated with a medium resolution panchromatic camera.

The optical design permits to cover the wavelength range from 400 to 2500 nm and it is based on high transmittance optical assemblies, including a reflective common telescope in Three-Mirror Anastigmat (TMA) configuration, a single slit aperture, a panchromatic camera (700-900 nm) and a spectrometer having two channels (VNIR and SWIR), each one using a suitable prism configuration and spectrally separated by a beam splitter, conceived to minimize the number of optical elements. High performance MCT-based detectors represent the core of the instrument. To provide the required data quality for the entire mission lifetime (5 years), an accurate and stable calibration unit (radiometric and spectral) is integrated, for the in-flight instrument calibration. The thermal design has been based on a passive cooling system: a double stage radiator, suitable oriented and protected from unwanted heat fluxes, high performance heat pipes and an operational heaters network represent the solution adopted to achieve the required thermal stability.

\*marco.meini@selex-es.com; phone +39 055 8950689; fax +39 055 8950616; selex-es.com

## 8889-27, Session 6

### EnMAP hyperspectral imager: design, technology and predicted performance

Bernhard Sang, Brian Heider, Markus Erhard, Bettina König, Kayser-Threde GmbH (Germany); Christoph Straif, Jan Grosser, Christian Chlebek, Deutsches Zentrum für Luft- und Raumfahrt e.V. (Germany); Hermann J. Kaufmann, Helmholtz-Zentrum Potsdam Deutsches GeoForschungsZentrum GFZ (Germany)

The Environmental Mapping and Analysis Program (EnMAP) is a German space based hyperspectral mission which has successfully passed CDR in 2012 and will be launched in 2017. The space segment is being realized by Kayser-Threde GmbH as the prime contractor to the German DLR Space Administration. It consists of a 3 axis stabilized platform hosting a single hyperspectral payload. Hyperspectral imaging is performed in a dual push broom configuration from a sun synchronous low earth orbit covering the wavelength range from 420nm to 2450nm at 30m ground sampling distance in Nadir configuration. With a swath of 30km and 30° across track pointing capability a 4 day global accessibility is achieved. A total of up to 5000km along track can be recorded and downlinked per day for a spectral configuration of 230 channels with an average spectral sampling interval of 6.5nm in the visual near infra-red (VNIR) and 10nm in the short wave infra-red range (SWIR).

The paper will present the key requirements together with the EnMAP space segment design with focus on the newly developed payload and critical technologies. A novel optical design concept employing curved prisms was chosen to implement the two low distortion high

throughput spectrometers, the combined entrance slit of which is made of a micro-mechanical slit and field separating unit. Two application specific focal planes are used to record the upwelling radiance for the VNIR and SWIR spectral ranges. To ensure consistent high quality data products a sophisticated thermal control system provides stable temperatures for all critical elements. Calibration data can be generated in-orbit for system linearity, offset and physical response characteristics as well as for spectral referencing with the help of three on-board calibration units.

A structural thermal demonstrator of the instrument optical unit and the thermal control system was tested for confirmation of structural and thermal performance. Furthermore the critical technology elements have been manufactured and tested in engineering models (EM) to ratify the technology and design. System performance predictions based on the results of the EM tests will be presented to demonstrate the system's ability to fulfill the key requirements such as signal to noise ratio, image quality and various line of sight related parameters.

## 8889-28, Session 6

### FLORIS: phase A status of the fluorescence imaging spectrometer of the Earth Explorer mission candidate FLEX

Stefan Kraft, Jean-Loup Bézy, Umberto Del Bello, Rene Berlich, Matthias Drusch, Antonio Gabriele, Bernd Harnisch, Roland Meynart, Pierluigi Silvestrin, European Space Research and Technology Ctr. (Netherlands)

The Fluorescence Explorer (FLEX) mission is currently subject to feasibility (Phase A) study as one of the two candidates of ESA's 8th Earth Explorer opportunity mission. The FLuORescence Imaging Spectrometer (FLORIS) will be an imaging grating spectrometer onboard of a medium sized satellite flying in tandem with Sentinel-3 in a Sun synchronous orbit at a height of about 815 km. FLORIS will observe vegetation fluorescence and reflectance within a spectral range between 500 and 780 nm. It will thereby cover the photochemical reflection features between 500 and 600 nm, the Chlorophyll absorption band between 600 and 677 nm, and the red-edge in the region from 697 to 755 nm being located between the Oxygen A and B absorption bands.

By this measurement approach, it is expected that the full spectrum and amount of the fluorescence radiance can be retrieved, and that atmospheric corrections can efficiently be applied. FLORIS will measure Earth reflected spectral radiance at a relatively high spectral resolution of ~0.3 nm around the Oxygen absorption bands. Other spectral areas with less pronounced absorption features will be measured at medium spectral resolution between 0.5 and 3 nm. FLORIS will provide imagery at 300 m resolution on ground with a swath width of 150 km. This will allow achieving global revisit times of less than one month so as to monitor seasonal variations of the vegetation cycles. The mission life time is expected to be at least 4 years. The fluorescence retrieval will make use of information coming from OLCI and SLSTR, which are onboard of Sentinel-3, to monitor temperature, to detect thin clouds and to derive vegetation reflectance also outside the FLORIS spectral range.

In order to mitigate the technological and programmatic risk of this Explorer mission candidate, ESA has initiated two comprehensive bread-boarding activities, in which the most critical technologies and instrument performance shall be investigated and demonstrated. The breadboards will include representative optics and dispersive elements in a configuration, which is expected to be very close to the instrument flight configuration. This approach follows the guideline to reach, before it goes into the implementation phase, a technology readiness level of 5. It thereby requires a demonstration of predicted performance in a configuration, where the basic technological components are integrated with reasonably realistic supporting elements such that it can be tested in a simulated environment.

We will report, within the limits of the competitive nature of the industrial study, on the currently running or planned preparatory activities. We will present the mission configuration, the imposed instrument requirements and the identified instrument concepts as derived by the Phase A studies.

## 8889-29, Session 7

### Status of MODIS on-orbit calibration and characterization (*Invited Paper*)

Xiaoxiong Xiong, NASA Goddard Space Flight Ctr. (United States); Brian Wenny, Sigma Space Corp. (United States); Amit Angal, Science Systems and Applications, Inc. (United States); Vincent V. Salomonson, The Univ. of Utah (United States)

Since launch, Terra MODIS has successfully operated for more than 13 years and Aqua MODIS for nearly 11 years. High quality science data products have been continuously produced from sensor calibrated radiance and reflectance, or the Level 1 (L1B) data products, and distributed to users worldwide for a broad range of studies of the earth's land, ocean, and atmospheric properties and their changes over time. MODIS observations are made in 20 reflective solar bands (RSB) and 16 thermal emissive bands (TEB). The RSB are calibrated using data collected from its on-board solar diffuser and lunar observations, and the TEB are calibrated by an on-board blackbody (BB). On-orbit changes in the sensor's spectral and spatial characteristics are monitored by an on-board spectroradiometric calibration assembly (SRCA). This paper presents an overview of both Terra and Aqua MODIS on-orbit operations, calibration activities, and methodologies applied from launch to present, and reports the current instrument status. It provides a summary of sensor on-orbit radiometric, spectral, and spatial calibration and characterization performance. In addition, this paper illustrates on-orbit changes in sensor characteristics and correction strategies applied to maintain instrument calibration and level 1B (L1B) data quality, and discusses lessons that could benefit future calibration efforts for both MODIS and other earth-observing sensors.

## 8889-30, Session 7

### MODIS and VIIRS lunar observations and applications

Xiaoxiong Xiong, James Butler, NASA Goddard Space Flight Ctr. (United States); Amit Angal, Science Systems and Applications, Inc. (United States); Jon Fulbright, Sigma Space Corp. (United States)

The MODIS has successfully operated on both the Terra and Aqua spacecraft since their launch in December 1999 and May 2002, respectively, and the first VIIRS has operated on-board the S-NPP spacecraft since its launch in October 2011. The VIIRS instrument was designed and built with strong MODIS heritage. MODIS has 36 spectral bands with wavelengths ranging from 0.41 to 14.5 microns and VIIRS has 22 spectral bands, covering wavelengths from 0.41 to 12.2 microns. Both MODIS and VIIRS carry a similar set of on-board calibrators (OBC), which include a solar diffuser (SD), a solar diffuser stability monitor (SDSM), and a blackbody (BB). Because of this, instrument on-orbit operation and calibration approaches and strategies developed for MODIS have also been used for VIIRS. In addition to calibration data collected from sensor on-board OBC, lunar observations are regularly scheduled and performed by both MODIS and VIIRS in support of their on-orbit calibration and characterization for the reflective solar bands (RSB). This paper provides an overview of MODIS and VIIRS lunar observations and applications. It describes the strategies developed to schedule and implement lunar calibration events and discusses the methods used to derive sensor on-orbit calibration and characterization parameters. Specific applications presented in this paper include monitoring sensor radiometric calibration stability and tracking sensor spatial characterization performance in terms of the band-to-band registration (BBR).

## 8889-31, Session 7

### Sentinel-2 diffuser on-ground calibration

Emmanuel Mazy, Univ. de Liège (Belgium); Fabrice Camus, Vincent Chorvalli, EADS Astrium (France); Isabelle Domken, Anouk Laborie, Sara Marcotte, Yvan G. Stockman, Univ. de Liège (Belgium)

The Sentinel-2 multi-spectral instrument (MSI) will provide Earth

imagery in the frame of the Global Monitoring for Environment and Security (GMES) initiative which is a joint undertaking of the European Commission and the Agency. MSI instrument, under Astrium SAS responsibility, is a push-broom spectro imager in 13 spectral channels in VNIR and SWIR. The instrument performances depend on in-flight calibration with sunlight through a quasi Lambertian diffuser. The on-ground calibration of the diffuser BRDF is mandatory to fulfil the in-flight performances.

The diffuser is a 779 x 278 mm<sup>2</sup> rectangular flat area in Zenith-A material. It is mounted on a motorised door in front of the instrument optical system entrance. The diffuser manufacturing and calibration is under the Centre spatial of Liege (CSL) responsibility.

The CSL has designed and built a completely remote controlled BRDF measurement bench able to handle large diffusers in their mount. As the diffuser is calibrated directly in its mount with respect to a reference cube, the error budget is significantly improved. The BRDF calibration is performed directly in MSI instrument spectral bands by using dedicated band-pass filters (VNIR and SWIR up to 2200 nm). Absolute accuracy is better than 0.5% in VNIR spectral bands and 1% in SWIR spectral bands. Performances were cross checked with other laboratories.

The first MSI diffuser for flight model was calibrated end of 2012 and beginning of 2013 on CSL BRDF measurement bench. The calibration of the diffuser consists mainly in thermal vacuum cycles, verification of BRDF degradation after environmental tests, BRDF uniformity characterisation over the entire useful area and BRDF angular characterisation into a large observation angular configuration. Performances are discussed in terms of BRDF degradation after environmental tests, uniformity over pupils for each spectral band and dependence with incidence and observation angular configurations. A mathematical model of the diffuser BRDF is built for each spectral band. Discussion over the accuracy of the fitted model is also introduced. The total amount of measurement for the first flight model diffuser corresponds to more than 17500 BRDF acquisitions.

Additional measurements are also performed on samples to verify thermo-optical properties (mainly in terms of total reflectance) and BRDF polarisation sensitivity.

The whole calibration campaign performed at CSL on the MSI instrument diffuser shows the importance to calibrate diffusers directly on its own mechanical mount and with respect to reference frame optically accessible.

## 8889-32, Session 7

### Sentinel 2: implementation of the means and methods for the CAL/VAL commissioning phase

Thierry L. Trémas, Cécile Dechoz, Sophie Lacherade, Ctr. National d'Études Spatiales (France); Philippe Martimort, Claudia Isola, European Space Research and Technology Ctr. (Netherlands); Julien Nosavan, Beatrice Petrucci, Ctr. National d'Études Spatiales (France)

In partnership with the European Commission and in the frame of the Copernicus program (previously GMES), the European Space Agency (ESA) is developing the Sentinel-2 optical imaging mission devoted to the operational monitoring of land and coastal areas.

The Sentinel-2 mission is based on a satellites constellation deployed in polar sun-synchronous orbit. While ensuring data continuity of former SPOT and LANDSAT multi-spectral missions, Sentinel-2 will also offer improvements such as a combination of global coverage with a wide field of view (290km), a high revisit (5 days with two satellites), a high resolution (10m to 60m) and multi-spectral imagery (13 spectral bands in visible and shortwave infra-red domains).

The Centre National d'Études Spatiales (CNES) supports ESA to insure the cal/val commissioning phase during the firsts 3 months in flight.

This paper provides, first, an overview of the Sentinel-2 system and the image products delivered by the ground processing: the Level-0 and Level-1A, respectively raw compressed and uncompressed data, the Level-1B, including radiometric corrections, the Level-1C that provides ortho-rectified top of atmosphere reflectance. The ground sampling distance of Level-1C product will be 10m, 20m or 60m depending on the band.

Then the paper will present the ground segment, presently under preparation at CNES. It will operate the follow-up of the satellites

performances, and the production of the first files. The rule and the architecture of each device will be explained. GPP, the Ground Processor Prototype, will be the core of the ground system. From Level-0 files and sets of Satellite Ancillary Data, it will produce the different Level-1 files. At this step will be introduced the radiometric corrections and geometric processing that takes advantage of a Global Reference Image database (GRI), accurately geo-referenced, to correct the physical geometric model of each recorded image.

While GPP is devoted to the production of Level-1 files, the analyses of data are delegated to supplemental means. The "radiometric unit" will be in charge of fine calibration of the gains, dark currents, monitoring of image quality. At this level will be compared the results of calibrations set with the on-board diffuser and on natural sites like deserts. The "geometric unit" will deal with the best way to reach an accuracy of location of 12.5 meters. These analyses will allow the making out of GIPP (Ground Image Processing Parameters), a set of calibration parameters loaded up to the satellite. The calibration operations are applied on-board.

A supplemental device, MACCS (Multisensor Atmospheric and Cloud Screening Correction), will be introduced. MACCS will process Level-1C files to produce Level-2A files in which ground reflectances are computed.

All these softwares are included in a higher level structure : the TEC-S2 (Technical Expertise Center for Sentinel 2) . This unit will rule a data base in which will be collected the different files essential for the production of Level 1 products. TEC-S2 will command the other programs and will insure the exchanges with the whole sentinel 2 Ground Segment.

## 8889-33, Session 7

### Calibration plan for the sea and land surface temperature radiometer (SLSTR)

David L. Smith, Tim J. Nightingale, Hugh Mortimer, Kevin F. Middleton, Caroline V. Cox, Christopher T. Mutlow, Brian J. Maddison, Science and Technology Facilities Council (United Kingdom)

The Sea and Land Surface Temperature Radiometer (SLSTR) to be flown on ESA's Sentinel-3 mission is a multi-channel scanning radiometer that will continue the 21 year datasets of the Along Track Scanning Radiometer (ATSR) series. As its name implies, measurements from SLSTR will be used to retrieve global sea surface temperatures to an uncertainty of <0.3K traced to international standards. To achieve these low uncertainties requires an end to end instrument calibration strategy that includes pre-launch calibration at subsystem and instrument level, on-board calibration systems and sustained post launch activities.

SLSTR shares many features from the ATSR sensors including: thermal infrared spectral bands at 12, 10.8, 3.7 microns that are cooled using a Stirling cycle cooler, VIS-SWIR bands at 1.6, 0.87, 0.66 and 0.555 microns measuring solar reflected radiation, a dual view allowing the same terrestrial scene to be viewed through two atmospheric paths, a nadir view and an along-track view at 55° zenith angle, two black-body sources to provide continuous calibration of the infrared channels, and a diffuser based VISCAL source for calibrating the solar reflectance bands. In addition SLSTR has bands at 1.375 and 2.25 microns for improved cloud detection, a 1400km nadir view and 750km inclined view for improved coverage. A more detailed description of SLSTR and its expected performance will be described the paper by Coppo et al.

The starting point for the calibration plan is the calibration model for the instrument that defines how the sensor data is to be converted to radiometric units and identifies the key sources of uncertainty in the measurements. This model forms the basis of the level-1 processing algorithms and identifies the key parameters to be measured needed to characterise and calibrate the SLSTR instrument.

The authors describe the preparations for the pre-launch calibration activities including the spectral response, instrument level alignment tests, solar and infrared radiometric calibration.

Because SLSTR measures thermal infrared radiation, it is necessary to perform the pre-launch calibration tests in a vacuum chamber with the instrument surrounded by temperature controlled panels to ensure that the radiometric environment is known. A purpose built calibration rig has been designed and built at RAL space that will accommodate the SLSTR instrument, infrared calibration sources and alignment



equipment. The calibration rig has been commissioned and results of these tests will be presented.

Finally the authors will present the planning for the on-orbit monitoring and calibration activities to ensure that calibration is maintained. These activities include vicarious calibration techniques that have been developed through previous missions, and the deployment of ship-borne radiometers.

## 8889-70, Session PS

### TDRS satellite application to LEO satellite data link

Hu Jiang, Shanghai Institute of Microsystem and Information Technology (China); Xuemin Shen, Shanghai Institute of Technical Physics (China); Wenbin Gong, Shanghai Engineering Center for Microsatellites (China); Jinpei Yu, Shanghai Institute of Microsystem and Information Technology (China)

With the development of space technologies, satellite-based data link is becoming more and more popular due to its wide coverage. However, it needs tens of LEO satellites, short for Low Earth Orbiting satellites, to cover the whole Earth in real time. Therefore it requires huge investment to fulfill such an engineering. If several TDRS satellites, short for Tracking and Data Relaying Satellites, are included, the engineering investment might as well be acceptable. Herein, simulations of coverage and some particular performances are presented in three cases, i.e., a single LEO satellite plus one TDRS satellite, a single LEO satellite plus two TDRS satellite, a single LEO satellite plus three TDRS satellite. Simulations have shown that in the case of one LEO satellite and one TDRS satellite, the revisiting period is 5726s, which will shorten the revisiting period by 57%; the encounter frequency between one LEO and one TDRS is 11 times daily; the average duration for every encounter is 2128s. The performances of one LEO satellite and two TDRS satellites are presented as followings: the revisiting period is 2819s, which will shorten the revisiting period by 79%; the encounter frequency among one LEO and two TDRS is 23 times daily; the average duration for every encounter is 2049s. The performances of one LEO satellite and two TDRS satellites are presented as followings: the revisiting period is 1780s, which will shorten the revisiting period by 87%; the encounter frequency among one LEO and two TDRS is 34 times daily; the average duration for every encounter is 2067s. The above simulations have indicated TDRS satellites can greatly improve LEO satellite coverage and related performances.

For china customers, the space orbits of TDRS are limited by either geographical positions or by orbital space regulation in equator. Such limitations make sparsely-distributed LEO satellites global real-time data link difficult, especially above western hemisphere. LEO satellite data link above some of the western hemisphere has to be retarded. Delayed data link are hardly acceptable for some emergency rescues. Before the constellation of tens of LEO communication satellites is deployed in space, it might be a good choice to realize LEO satellite data link via TDRS satellites for China users.

## 8889-71, Session PS

### ALSAT-2A solar array in orbit performances after 32 months

Nacera Larbi, Mehdi Attaba, Fethi Bouchiba, Ctr. National des Techniques Spatiales (Algeria); Eric Beaufume, EADS Astrium (France)

ALSAT-2A is the second Algerian earth observation satellite build by the Algerian Space Agency and the first spacecraft of Astrium's AstroSat-100 family. The spacecraft design is based on the Myriade platform and its power subsystem consists of high-efficiency GaAs/Ge triple junction solar cells with up to 26% efficiency at beginning of life (BOL), Li-ion battery, power conditioning & distribution unit and harness. The purpose of a power subsystem is to ensure reliable delivery of electrical power compatible with payload under all foreseeable operational states, environments effect, and during all mission phases. The power subsystem is unarguably the most critical subsystem on a satellite. Reliability, efficiency and continuous

operation of the power subsystem is essential to the successful fulfillment of ALSAT-2A mission, a failure even a brief interruption in the source of power can have catastrophic consequences for the spacecraft. Therefore, the design of the power system reflects the need of autonomous operation, independent from all other subsystems. Even immediately following the launch, the power subsystem requires no intervention from the ground station. In this context, this paper outlines the in-orbit performances of ALSAT-2A solar array from its launch on July 2010 until March 2013. The health and state of ALSAT-2A solar array is monitored via three main telemetries: current (IGS), voltage (VGS) and temperature (TGS). However, the solar array power (PGS) is not a direct telemetry but a ground calculated parameter which indicates the power supplied instantly. As the environmental conditions in space are very harsh, with extreme temperatures ranging coupled with solar radiation, the 32 months solar array telemetry data will be analyzed and discussed in function of satellite power consumption. These factors change from orbit to orbit and even within the same orbit. All spacecraft available observations show a nominal solar array state since its voltage, current and temperature are within the expected values.

## 8889-72, Session PS

### Flight experience of 329K star tracker

Ivan S. Kruzhilov, Moscow Power Engineering Institute (Russian Federation); Victor I. Fedoseev, Vladimir V. Kuniaev, Geofizika-Cosmos (Russian Federation); Gennadiy P. Titov, Sergey V. Latincev, Oleg V. Shevlyakov, JSC "Academician M.F. Reshetnev" Information Satellite Systems" (Russian Federation)

The report is dedicated to 329K star tracker flight tests on Luch-5A and Luch-5B satellites launched to a geostationary orbit in December 2011 and November 2012 respectively.

329K is a wide-field star tracker with a field of view of 22°17 degrees. The CCD-matrix is used. Photo-sensitive and optical behavior of the star tracker guarantee that in 96% cases, at least 4 stars fall within the instrument's field of view. Stars are sensed on the basis of analysis of their reciprocal angular distances. The instrument operation result is delivery of an orientation matrix assigning transition from the star tracker coordinate system to the inertial geocentric coordinate system.

In order to explore specifications of instruments, daily test measurement sessions were held. During these sessions, data came from the orbit containing information on operation of the instrument – its orientation matrix, information on stars having been sensed and other specification. It is to analysis of these data that this report is dedicated, focusing on 329K sensor accuracy and photometric performance.

Random components of errors of change of three Euler angles making up a sequence of rotations around OX, OY, OZ axes were used as accuracy performance subject to estimation. Traditionally, the star tracker optical axis coincides with the OZ axis, therefore, the first two Euler angles preset the accuracy of the instrument line of sight and the third angle – the error of rotation around the line of sight. Due to limitedness of the star tracker field of view, the third angle error exceeds that of the first two angles.

As the actual orientation matrix value is not known, the actual value of Euler angles is not known either. Due to this, in the course of the instrument flight data processing, a method of approximated estimate of actual values of orientation angles was used. The idea of the method is based on the fact that the satellite orientation in the orbit is changed gradually whereas the instrument errors are mainly accidental. Due to this, the actual value of orientation angles may be obtained by data cleaning. The method used for data analysis is based first of all on deletion of the straight-line trend determined by the method of least squares and subsequent deletion of several harmonic low-frequency components using Fourier transformation.

Photometric performance of the star tracker and the star catalogue corresponding to it imply correspondence of the level of signal coming from a star as picked up by the instrument and calculated on the basis of its stellar magnitude in the work star catalogue.

The work star catalogue was calculated using a special method considering the instrument spectral response. This method is based on calculation of color indices of stars using stellar brightness in standard photometric stripes (U, B, V, R, I, J, H) of 2MASS, Tycho, Tycho-2 and other catalogues.

8889-73, Session PS

**Design and realization of the miniature long-life integrative coded sun sensor**

Yanan Mo, Jian Cui, Yuan Zhao, Ran Chen, Xin Liu, Beijing Institute of Control Engineering (China)

This paper describes the research activity at the Beijing institute of control engineering about the miniature long-life integrative coded sun sensor. Sun sensor is the main part of control system in spacecraft. The coded sun sensor is applied in all kinds of spacecraft because it has high accuracy, high reliability and long life time. The research on Coded Sun Sensor started from about 20 years ago in CAST and have about 300 flight products until now. But as the developing of techniques of optical machining an IC, the miniaturization design is possible and necessary. The optical system of the miniature coded sun sensor is composed with a semi-column silex glass, a cube silex with Gray coded shape on the bottom and an integrative silicon battery with 14 cells. The sun line forms a light spot through the slit on light system on the coded plate. The sensor determines the orientation of sun through the position of light spot. With the limitation of the diameter of sun plate the accuracy of only 0.5° can be realized with 8-bit Gray code in FOV of 128°. To achieve high accuracy of 0.05° the subdivision technique must be adopted. Compared with the sensor based on APS or CCD which outputs 1024×1024 8-bit data in one frame, the coded sun sensor outputs only 14 current signals. High speed CPU and large RAM are not necessary and the design of signal processing circuit are simpler. To achieve higher accuracy the algorithm can be designed with less cost of hardware. For example the CODDIC algorithm is used to calculate the subdivision angle on the cost of only 500 gates of FPGA. As shown in Fig 1, the optical system is integrated with the signal processing circuits in one mechanical house. An FPGA is introduced to generate the control signals and calculate the sun incidence angles. Flexibility board connecting different parts makes the product more compact. It uses RS422 interface to communicate with central computer. The performance of the miniature long-life integrative coded sun sensor is listed as below : FOV 124°×124°, accuracy 0.05°(3?), resolution 14?, power consumption 0.5W, update rate 40Hz, mass 475g, designed life-time 15 years. It has been adopted in new platform of Remote Sensing Satellite of CAST. The first flight will be at 2015.

8889-74, Session PS

**Primary mirror alignment and assembly for a multispectral space telescope**

Wei-Cheng Lin, Shenq-Tsong Chang, Instrument Technology Research Ctr. (Taiwan); Sheng-Hsiung Chang, Chen-Peng Chang, National Space Organization (Taiwan); Yu-Chuan Lin, Po-Hsuan Huang, Instrument Technology Research Ctr. (Taiwan); Ting-Ming Huang, Instrument Technology Research Ctr (Taiwan)

For a currently developing multispectral space Cassegrain telescope with clear aperture of 450 mm, the primary mirror is Zerodur and lightweighted as the ratio about 50 % to meet both thermal and weight requirement. For this mirror, it is critical to reduce the astigmatism caused from the gravity effect, bonding process and the deformation from the mounting to the main structure of the telescope (main plate). In this article, the primary mirror alignment, assembly process and the optical performance test for the primary mirror assembly are presented. The mechanical shim is the interface between the iso-static mount and main plate. It is used to compensate the manufacture errors of elements and differences of local co-planarity errors during alignment. The thickness of the mechanical shim is determined by the coordinate measuring machine (CMM) to prevent the stress while iso-static mount is integrated to main plate.

After primary mirror assembly, an optical performance test method called bench test with a novel algorithm is used to analyze the astigmatism caused from the gravity effect, form error from manufacture and the deformation from the mounting or supporter. In an effort to achieve the requirement for the tolerance in primary mirror assembly, the astigmatism caused from the gravity effect and the deformation from the mounting are found less than P-V 0.02 λ at 633 nm. The results of these demonstrations indicate that the designed mechanical ground supported equipment (MGSE) for

the alignment, alignment and assembly processes meet the critical requirements for primary mirror assembly of the telescope.

8889-75, Session PS

**Analysis and design of grazing incidence x-ray optics for pulsar navigation**

Fuchang Zuo, Jianwu Chen, Liansheng Li, Zhiwu Mei, Beijing Institute of Control Engineering (China)

As a promising new technology for deep space exploration because of its autonomous capability, pulsar navigation has attracted extensive attentions from academy and engineering domains. By comparing pulse arrival time measured on-board the spacecraft with predicted pulse arrival time at some reference location, the spacecraft position can be determined autonomously. The pulsar navigation accuracy is determined by the measurement accuracy of TOA (Time of Arrival) of the X-ray photon based on pulsar timing data, which can be enhanced by increasing the effective detection area, decreasing the background noise, and thereby improving SNR of the observed pulse profile through design of appropriate optics. The energy spectrum range of soft X-ray suitable for pulsar navigation is 0.1-10keV, the effective focusing of which can be primarily and effectively realized by the grazing incidence reflective optics due to the optical property of X-ray. Particularly, the Wolter-I configuration grazing incidence optics is adopted and investigated in the paper.

The Wolter-I optics, originally proposed based on a paraboloid mirror and a hyperboloid mirror, has long been widely developed and employed in X-ray observatory. The incoming X-ray photons are reflected under small angles of incidence in order not to be absorbed and are focused by double reflection off a parabolic and then a hyperbolic surface. Some differences, however, remain in the requirements on optics between astronomical X-ray observation and pulsar navigation. The design of an X-ray telescope suitable for navigation will be a compromise between angular resolution, collecting area and weight of the system.

In this paper, the requirements on aperture, effective area and focal length of the grazing incidence optics were firstly analyzed and presented based on the characteristics, such as high time resolution, large effective area and low angular resolution, of the pulsar navigation. Furthermore, on the basis of this, the preliminary design of optical system and overall structure, as well as the stray light baffle and diaphragm, was implemented for the Wolter-I grazing incidence optics. With optical and FEA simulation methods, system engineering analysis on grazing incidence optics was finally performed to analyze the impacts of surface roughness, assembly errors and environmental effects (heat and gravity) on the imaging quality, focal length and focusing performance, providing basis and guidance for fabrication of the Wolter-I grazing incidence optics.

8889-76, Session PS

**X-ray photon arrival time tagging error analysis and simulation for pulsar navigation**

Jianwu Chen, Liansheng Li, Fuchang Zuo, Zhiwu Mei, Beijing Institute of Control Engineering (China)

X-ray pulsar provides stable, predictable and unique signatures, which are attractive for spacecraft navigation. The fundamental measurable quantity is the arrival time of an observed pulse at the detector on the spacecraft. The arrival time is measured with respect to the onboard clock to high precision. A time difference between the photon arrivals at the spacecraft and the solar system barycenter can be generated. This time accuracy leads range determination accuracy.

An X-ray pulsar timing instrument based on semiconductor detectors is assigned to detect the X-ray photon. Each photon detected must be time stamped to a precision such that the uncertainty in the time tagging is small compared to the statistical error in the pulsar measurement. The time tagging error arises from the detector and the pulse processing chain. First, for the large area detector, the time required to collect charges depends on the location of the incidence photon. The time resolution is limited by the spread of electron drift times for photons interacting at various distances from the central collecting anode. This rise time uncertainty will introduce time jitter,

which increases with the detector area. Second, the rise time of the amplifier output pulse varies with bandwidth. For high precise X-ray photon timing, a fast shaping time is preferred; however, this would introduce more noise, resulting in more time uncertainty. Third, the timing error caused by the time stamping circuit is non-ignorable. Moreover, the pulse amplitude is determined by the incidence photon energy, which is related to the rise time. Considering these factors, we find that the time tagging error is dominated by the design parameters at low count rate. The contribution of the detector time resolution increases rapidly as the shaping time constant reduces at high count rate. A correction program is performed to improve the time tagging accuracy at various photon energies and count rates, so as to minimize the random error.

The accuracy of the navigation is determined by the SNR of the observed pulse profile, which is created by large amount photon detection. However, the relation between the arrival time accuracy and the pulse profile SNR is still obscured. We model the arrival time of each photon in a pulse profile with random offset. A simulation is performed to evaluate the impact of the offset amplitude on the pulse profile SNR. A higher SNR is expected when the offset is reduced. However, it is hard to enhance the SNR to some extent when the offset is small enough.

The time tagging error sources are analyzed in this paper. A correction program is proposed to improve the time tagging accuracy for various energies and count rates. Moreover, the relation between the time tagging uncertainty and the pulsar profile SNR or the navigation accuracy is modeled and simulated.

#### 8889-77, Session PS

### New class of monolithic sensors for low frequency motion measurement and control of spacecrafts and satellites

Fabrizio Barone, Fausto Acernese, Gerardo Giordano, Rocco Romano, Univ. degli Studi di Salerno (Italy)

This paper describes a new mechanical application of the Watt-linkage for the development and implementation of a new class of mono/triaxial sensors aimed to low frequency motion measurement and control of spacecrafts and satellites. The basic element of these sensors is the one dimensional UNISA seismometer/accelerometer based on the classic Watt-linkage configured as Folded Pendulum monolithic FP sensors, suitably geometrically positioned. The triaxial sensor is, therefore, compact, light, scalable, tunable instrument (frequency < 100 mHz), with large band (at least  $10^{-7}$  Hz - 10 Hz), high quality factor ( $Q > 14000$  in vacuum) with good immunity to environmental noises, guaranteed by an integrated laser optical readout, and, not less important fully adaptable to the specific requirements of the application. The measured sensitivity curve is in very good agreement with the theoretical ones (at least  $10^{-12}$  m/sqrt(Hz) in the band (0.1 - 10 Hz). Applications of dedicated versions of this sensor already exist in the field of earthquake engineering, geophysics and civil engineering requiring large band-low frequency performances coupled with high sensitivities.

#### 8889-78, Session PS

### The extended Maxwell Garnett formula for carbon-nanotube-doped nematic liquid crystal for remote sensing application

Kevin Yu-Chia Huang, National Cheng Kung Univ. (Taiwan)

A numerical effort for modeling the dielectric behavior of the novel binary mixture of nematic liquid crystal and carbon nanotube (NLC:CNT) has been carried out using the Maxwell Garnett theory. The CNTs are treated as conductive anisotropic inclusions while the NLCs as dielectric isotropic or anisotropic matrix depending on temperature. Thus, the numerical expressions for the dielectric anisotropy for the scenarios of aligned CNTs in the NLC matrix of either nematic or isotropic phases have been derived, and the results show that the Debye parameter of CNT at optic limit seems to be the decisive factor in the enhancement of the dielectric anisotropy of the nematic system. Due to the unique anisotropic characteristics of the composite, NLC:CNT holds promise for a dual-mode remote sensing application under the controllable external field.

#### 8889-79, Session PS

### Supercontinuum-source-based facility for evaluation of hyperspectral imagers

Yu Yamaguchi, Yoshiro Yamada, Juntaro Ishii, National Metrology Institute of Japan (Japan)

Radiometric pre-launch calibration of earth observing multispectral sensors such as ASTER was performed traceable to defining fixed-point blackbodies of the International Temperature Scale of 1990. The next Japanese earth observing hyperspectral/multispectral imager mission, the HISUI (Hyper-spectral Imager SUite) mission, is currently underway. The HISUI hyperspectral sensor will have 185 bands, 57 of which are in the visible and the near infrared and the remaining 128 in the short wavelength infrared, covering the spectral range from 400 nm to 2500 nm.

In order to guarantee the observed data with its high spatial and wavelength resolution, in addition to ensuring traceability to ITS-90, it is necessary to evaluate the difference of the spectral sensitivity among the detector devices arrayed two-dimensionally and correct spectral and spatial misregistrations and the effect of stray light. Since there are tens of thousands of detectors in the two-dimensional-array sensor, they have to be evaluated in parallel, instead of point by point, with the special technique for the hyperspectral sensor. Hence, the new calibration system which has high radiance with the spatial uniformity and widely tunable wavelength range is required instead of conventional lamp systems which have poor power to calibrate arrayed devices at once.

In this presentation, a supercontinuum-source-based system for calibration of hyperspectral imagers and its preliminary performance are described. Supercontinuum light is white light with continuous and broad spectra, which is generated by nonlinear optical effects of ultrashort pulse lasers in photonic crystal fibers. Using the system, the relative spectral responsivity, spectral and spatial misregistrations and the stray light of a hyperspectral imager, which is consist of a polychromator and two-dimensionally arrayed CCD, are measured.

#### 8889-80, Session PS

### A new polarimetric SAR calibration method based on calibrators

Ping Zhang, Institute of Remote Sensing and Digital Earth (China)

The accurate calibration of polarimetric SAR system is essential to the quantitative application and analysis of full polarimetric SAR data. We analyze the impact on polarimetric calibration after superresolution polarimetric SAR method processing. A practical polarimetric calibration method is proposed using one standard trihedral calibrator, one dihedral calibrator and two polarimetric active radar calibrators (PARC).

The paper presents the simulation experiment. We simulate an uncalibration polarimetric SAR image with some targets, including trihedral calibrator, dihedral calibrator and polarimetric active radar calibrators (PARC). The proposed calibration method is applied to correct the distortion matrix. The analysis is given about the variation of channel imbalance and channel crosstalk after calibration.

#### 8889-34, Session 8

### Absolute radiometric characterization of the transfer radiometer unit of RASTA in the UV, VIS and NIR spectral range

Dieter R. Taubert, Jörg Hollandt, Christian Monte, Physikalisch-Technische Bundesanstalt (Germany); Peter Gege, Thomas Schwarzmaier, Karim Lenhard, Andreas Baumgartner, Deutsches Zentrum für Luft- und Raumfahrt e.V. (Germany)

The German Aerospace Centre (DLR) is operating the Calibration Home Base (CHB) as a facility for the radiometric calibration of airborne hyperspectral sensors and field spectrometers [1], the calibration concept relying on the application of both absolutely

calibrated source- and detector-based radiometric transfer standards. Following this concept, DLR has designed a new and dedicated radiance standard (RASTA) [2], its setup consisting of a high-stability 1000 W FEL-type tungsten halogen lamp illuminating a reflectance standard in a well defined geometry.

Recently, to provide a source-based SI traceability to the CHB facility, RASTA has been calibrated at the Physikalisch-Technische Bundesanstalt (PTB) with respect to its spectral radiance in the wavelength range from 350 nm to 2.5  $\mu\text{m}$  employing two independent calibration methods with relative standard uncertainties ( $k=1$ ) ranging from 0.8 % to 7.5 % depending on wavelength [3]. To provide redundancy to the source-based calibration and to take advantage of the superior stability of detector-based radiometric transfer standards, the RASTA design includes a multiple detector unit, the so-called transfer radiometer.

This transfer radiometer is built up of five individual filter radiometers (FRs), each consisting of a detector, a dedicated amplifier and an associated temperature controller. Three of these FRs use silicon photodiodes as detectors and coloured optical glass filters as wavelength selecting elements with centre wavelengths at 400 nm, 550 nm and 850 nm. The remaining two FRs are of broad-band design without any filters, applying a standard-type and a long-wavelength-type InGaAs photodiode for covering the wavelength range from 850 nm to 1.7  $\mu\text{m}$  and 850 nm to 2.5  $\mu\text{m}$ , respectively.

The measurement of the spectral irradiance responsivity of each of these FRs was performed at the spectral comparator facility of PTB [4]. In the wavelength range from 250 nm to 1.7  $\mu\text{m}$ , this was accomplished by comparison with absolutely calibrated transfer detectors, traceable to the primary detector standard, the cryogenic radiometer. In the wavelength range from 1.7  $\mu\text{m}$  to 2.5  $\mu\text{m}$  a relative calibration was done by applying a thermopile-detector with a previously characterized, spectrally flat absorbing layer. The instrumentation, the comparison procedure and the calibration results including a detailed uncertainty analysis will be presented.

[1] P. Gege et al., "Calibration facility for airborne imaging spectrometers", ISPRS Journal of Photogrammetry & Remote Sensing 64 (2009) 387-397

[2] T. Schwarzmeier et al., "The radiance standard RASTA of DLR's calibration facility for airborne imaging spectrometers", Proceedings SPIE, 2012, Edinburgh, Scotland

[3] D. R. Taubert et al., "Providing radiometric traceability for the Calibration Home Base of DLR by PTB", Proceedings of IRS2012, Berlin, Germany

[4] D. R. Taubert et al., "Improved calibration of the spectral responsivity of interference filter radiometers in the visible and near infrared spectral range at PTB", Metrologia 40, (2003) S35-S38

## 8889-35, Session 8

### Calibration of a monochromator using a lambdameter

Thomas Schwarzmaier, Peter Gege, Andreas Baumgartner, Karim Lenhard, Deutsches Zentrum für Luft- und Raumfahrt e.V. (Germany)

The German Aerospace Center (DLR) operates the Calibration Home Base (CHB) as a facility for the calibration of airborne imaging spectrometers and for field spectrometers. For spectral measurements in the wavelength range from 350 to 2500 nm, a monochromator illuminated by quartz tungsten halogen lamps (QTH) is used as light source. For accurate calibration results, precise knowledge of the monochromator characteristics is essential. The standard procedure for wavelength characterization uses low-pressure gas discharge lamps with spectrally well-known emission lines. The monochromator's grating is rotated in small steps around the expected position of one spectral line and measurements of the relative light intensity are taken using a radiometer. By fitting a Gaussian curve through these intensity values, the angular position of the grating can be calculated for each spectral line. This procedure needs to be done with several spectral lines to get a reliable calibration. With this method highly accurate results are obtained, but the lamps must be exchanged and hundreds of measurements undertaken. Because of this, the calibration of a monochromator in the wavelength range of 350 to 2500 nm usually takes some days. A much faster way for monochromator characterization is the now developed method using a lambdameter. Lambdameters are instruments designed to

measure single spectral lines with a very good accuracy. The used model "GWU Lambda Scan" has a spectral accuracy of  $5 \times 10^{-5}$  (+/- 0.0125nm @ 500nm). The method was developed using a 1-meter focal length monochromator McPherson Model 2051 and a grating with 600 grooves/mm. The fiber of the lambdameter was fixed in front of the monochromator output slit. The position of the lamp remained unchanged, so a re-adjustment was not necessary and uncertainties caused by adjustment errors were avoided. To select a wavelength, the grating of the monochromator is turned by a stepper motor. For the described characterization, measurements with the lambdameter were taken distributed over the grating's entire angular range. To get a wavelength calibration for the monochromator, a polynomial was fitted to the data points. With this polynomial the step number of the stepper motor can be calculated for every wavelength in the covered wavelength range. These measurements show that a wavelength accuracy of 0.1 nm or better is possible with this setup. The limiting factor is the repeatability of the monochromator and not the applied methodology. As the new method is much more time efficient than the conventional and the accuracy is even better, it provides a good alternative.

## 8889-36, Session 8

### Stray light testing of the PROBA V payload

Yvan G. Stockman, Univ. de Liège (Belgium); Matteo Taccola, European Space Research and Technology Ctr. (Netherlands); Didier P. Beghuin, LAMBDA-X sa (Belgium); Jorg Versluys, OIP N.V. (Belgium); Michael Francois, European Space Research and Technology Ctr. (Netherlands); L Aballea, A Baeke, OIP (Belgium); E Mazy, ML Hellin, S Marcotte, Univ de Liège (Belgium)

The Centre Spatial de Liege in Belgium (CSL) developed a stray light test facility for In Field and Out of Field of View straylight characterization of small Earth observation satellites. The first tested satellite is PROBA V, a small Belgium satellite dedicated to replace the SPOT VGT on SPOT missions. The test results demonstrate that the stray light performance of both PROBA V and the test facility are excellent and are in line with the model predictions. The new facility is designed for in-field and far field straylight characterization: intensities dynamic range up to  $10^{-8}$  for in-field and up to  $10^{-10}$  for far field straylight in the visible to SWIR spectral ranges. Moreover, from previous straylight test performed at CSL, vacuum conditions are needed for reaching the  $10^{-10}$  rejection requirement mainly to avoid air/dust diffusion. To fulfill these requirements the straylight facility is built in one of CSL vacuum chamber located in a class 100. The large dynamic range required is achieved by using a high radiance point source allowing small diverging collimated beam. A lot of care is taken in the design of the collimator focal plane to provide a highly purely collimated luminance.

Previous articles have presented the principle, the concept and a detailed analysis of the facility for straylight characterization of EO satellites. This paper goes a step forward with the presentation of actual results obtained on PROBA V EO satellite. The achieved results are put in parallel to the modeled computed values.

## 8889-37, Session 8

### Stray light calibration of the DAWN framing camera

Gabor Kovacs, Budapest Univ. of Technology (Hungary); Holger Sierks, Michael L. Richards, Pablo Gutierrez-Marques, Andreas Nathues, Max-Planck-Institut für Sonnensystemforschung (Germany)

Sensitive imaging systems with high dynamic range onboard spacecraft are susceptible to ghost and stray-light effects. During the design phase, the Dawn Framing Camera was laid out and optimized to minimize those unwanted, parasitic effects. However, the requirement of low distortion to the optical design and use of front-lit focal plane array indicated certain potential issues. This paper presents the ground-based and in-flight procedures characterizing the potential stray-light artifacts. The in-flight test used the Sun as the stray light source, at different angles of incidence. The spacecraft was commanded to point predefined solar elongation positions,

and long exposure images were recorded. The PSNIT function was calculated by the known illumination and the ground based calibration information.

In the ground based calibration, several extended and point sources were used with long exposure times in dedicated imaging setups. The tests revealed that the major contribution to the stray light is coming from the ghost reflections between the focal plan array and the band pass interference filters. Various laboratory experiments and computer modeling simulations were carried out to quantify the amount of this effect, including the analysis of the diffractive reflection pattern generated by the imaging sensor. The accurate characterization of the detector reflection pattern is the key to successfully predict the intensity distribution of the ghost image. Based on the results, and the properties of the optical system, a novel correction method is suggested to apply in the image processing pipeline. The effect of this correction procedure is also demonstrated with the first images of asteroid Vesta.

## 8889-38, Session 9

### Characterization results of the TROPOMI-SWIR detector

Ruud Hoogeveen, SRON Netherlands Institute for Space Research (Netherlands); Robert Voors, Dutch Space B.V. (Netherlands); Mark S. Robbins, Surrey Satellite Technology Ltd. (United Kingdom); Paul J. J. Tol, Toncho Ivanov, SRON Netherlands Institute for Space Research (Netherlands)

The TROPOMI Earth observing instrument is the single payload on board ESA's Sentinel-5 Precursor mission. It is the successor of the Sciamachy instrument (ESA ENVISAT) and the OMI instrument (NASA EOS/Aura), and combines the best of both instruments. TROPOMI copies the push broom observation geometry of OMI allowing for daily global coverage due to its instantaneous field of view of 110 degrees, or 2500 km swath on ground. From Sciamachy the 2305 - 2385 nm SWIR-3 observational band is copied by which methane and carbonmonoxide is observed.

This paper reports on the development of the Front-End Electronics (FEE) unit of the SWIR detector module and detailed characterization of the 1000x256 SWIR Saturn detector array produced by Sofradir (F) as measured with the FEE. The detailed characterization comprises not only the regular properties such as dark current, noise and photo-response, but also more complex characteristics including non-linearity, memory, etc. Performance evaluation of the detection module was carried out against all operational parameters: detector temperature (135 - 150 K), bias voltage and integration time. Thanks to the detector characterization program, the operational clocking of the detector could be optimized, resulting in significantly improved performance.

## 8889-39, Session 9

### The sea and land surface temperature radiometer (SLSTR) detection assembly design and performance

Peter Coppo, SELEX Galileo S.p.A. (Italy); Carmine Mastrandrea, Moreno Stagi, Luciano Calamai, Marco Barilli, Selex ES Ltd. (Italy); Jens Nieke, European Space Research and Technology Ctr. (Netherlands)

The SLSTRs are high accuracy radiometers selected for the Sentinel-3 space component of the GMES (Global Monitoring for Environment and Security) mission. They will provide climatological data continuity following on previous ESA environmental missions (ENVISAT, ERS2 and ERS1) that embarked respectively AATSR, ATSR-2 and ATSR. After 10 years of Service the ENVISAT platform was lost in early 2012 and AATSR operations stopped. The SLSTR instrument represents the successor to the AATSR family and is expected to be launched in 2014. The S3 mission foresees a series of satellites, each having a 7.5-year design lifetime, over a 20-year period starting with the launch of Sentinel-3A in April 2014 and of Sentinel-3B at least 6 months later. During full operations two identical satellites will be maintained in the same orbit with a phase delay of 180°.

Each SLSTR has an improved design respect to the previous (A)ATSRs

affording large near nadir and oblique view swaths (1400 and 740 km) for global coverage of Sea and Land Surface Temperature (SST/LST) with a daily revisit time (with two satellites) appropriate for both climate and meteorology (1 km spatial resolution). Clouds screening and other products are implemented via the double spatial resolution (0.5 km) visible and SWIR channels. Moreover two additional fire channels have been included using dedicated elements within the detectors to monitor high temperature events such as forest fires.

SLSTR comprises two physical units: first the Optical Scanning Unit, which forms the main instrument structure holding telescopes, calibration units, radiators, detection assembly comprising FPA, Front End Electronics (FEE) and the cooling system (cryo-cooler plus its electronics); second the Control & Processor electronics unit which controls all subsystems and manages the data interface with the satellite.

Two dedicated telescopes and rotating scan mirrors (with encoders to provide pointing knowledge) generate the two viewed swaths, combined optically at the prime focus by a fast switching flip mirror which is synchronised with the scan mirrors with a dedicated electronic. This technology is housed in the Opto-Mechanical Enclosure (OME). The Focal Plane Assembly (FPA) spectrally separates eleven channels (3 VIS, 3 SWIR, 2 MIR, 3 TIR) with dichroics and dedicated optics. There are nine Detector Units (DUs) each of one has a precision optical filter to define the spectral response of the nominal channels. The two fire channels (1 MIR and 1 TIR) are implemented within the same DUs as the nominal ones, but they use different pixels and/or electronic gains.

The IR and SWIR channels optics/detectors are cooled to about 85 K by an active mechanical cryo-cooler with vibration compensation, while the separately housed VIS channels need to be run at a stable ambient temperature.

This paper describes the opto-mechanical design and the expected electro-optical performance of the Focal Plane Assembly and the FEE, designed and manufactured by Selex-ES. The mathematical model predictions will be compared with experimental data acquired in the vacuum chamber in flight representative thermal conditions or in laboratory to demonstrate and validate the system level requirements.

## 8889-40, Session 9

### Infrared detector units for SLSTR of GMES Sentinel-3 mission

Holger Höhnemann, Markus Haiml, Lothar Mester, Richard Wollrab, AIM INFRAROT-MODULE GmbH (Germany)

Within the ESA/EC GMES program AIM INFRAROT MODULE GmbH was selected to provide the six infrared detector units (IR-DU) for the sea and land surface temperature radiometer (SLSTR) instrument onboard of the Sentinel-3 satellites. For the six different infrared channels six different detector units were developed. The short-wave infrared (SWIR) channels S4, S5, S6 and the mid-wave infrared (MWIR) channel S7 have been realized with MCT photo-voltaic (PV) quantum detectors with silicon read-out circuit (ROIC). The thermal infrared (TIR) channels S8 and S9 have been realized with MCT photo-conductive (PC) elements. All channels share a common housing design with individual spectral filter and individual flex cable.

The development of the IR-DUs was based on more than 35 years heritage in HgCdTe (MCT) sensor technology and cryogenic packaging and assembly processes at AIM.

Particular design drivers of the project have been the high detector operation temperature above 85K resulting in a mixed PV / PC detector concept with front-side illumination for all channels. Low photon flux requirements for the SWIR channels have been addressed by CTIA input stages, whereas the high photon flux requirements for fire detection have been addressed by BDI input stages. Out-of-band rejection in the filter design and stray light suppression has been addressed a specifically optimized coating and assembly processes to black the edge regions of the filter. High filter transmission of >90% and low anti-reflection coating (ARC) transmission losses of less than 3% for all PV channels have been achieved. A total quantum efficiency of 70%-80%, including filter transmission and ARC has been achieved for all PV channels. PC devices with high sensitivity and good homogeneity even at elevated temperatures have been provided. Finally, specific cryogenic flex-cables with sufficient analog video bandwidth, low cross-talk and low thermal conductivity have been developed.

24 flight models have been delivered in 2012 to the customer for Sentinel 3A and Sentinel 3B satellites.

## 8889-41, Session 9

### VNIR back illuminated CMOS focal plane

Ralf Reulke, Andreas Eckardt, Horst Schwarzer, Holger Venus, Deutsches Zentrum für Luft- und Raumfahrt e.V. (Germany); Christian Neumann, Fabian Gansmann, Bernhard Sang, Kayser-Threde GmbH (Germany)

The Institute of Optical Sensor Systems (OS) of the German Aerospace Center (DLR) has more than 30 years of experience with high-resolution imaging technology. It was selected to realize the visible/near infra read (VNIR) focal plane for the German hyperspectral mission EnMAP (Environmental Mapping and Analysis Program). This paper introduces the key requirements of the EnMAP VNIR focal plane and points to the design drivers. High resolution imaging spectrometry requires sophisticated solutions both for the detector and its operation as well as for the hardware and mechanics. The design of the focal plane including the CMOS detector technology and the derived system structure are presented. Key features essential for a reliable and stable high performance operation are entitled and explained in detail. Examples are the detector architecture with multiple parallel on chip analog to digital conversion, the mechanical design supporting pixel position stability in the sub micro meter region as well as the detector temperature stabilization technique required to allow long term radiometric stability. An engineering model of the focal plane has been realized and characterized extensively using analytical methods as well as a set of electro-optical tests. The measured performance on the engineering model is presented and shows the excellent performance very close to the predicted values. Results on quantum efficiency, linearity of the detector, pixel response non-uniformity (PRNU) and dark current noise will be presented. For this purpose specially calibrated integrated spheres are used that allow traceability of the measured data. Using the obtained data the system performance can be modeled to a high precision in system level simulations.

## 8889-42, Session 9

### The PRISMA hyperspectral imaging spectrometer: detectors and front-end electronics

Massimo Camerini, Mauro Mancini, SELEX ES Ltd. (Italy); Enrico Fossati, SELEX Galileo S.p.A. (Italy); Fabrizio Battazza, Roberto Formaro, Agenzia Spaziale Italiana (Italy)

Two detectors, SWIR and VNIR, and relevant front-end electronics were developed in the frame of the PRISMA project, an hyperspectral instrument for the earth observation. The two detectors were of the MCT type and, in particular, the VNIR was realized by Sofradir by using the CZT substrate removal to obtain the sensitivity in the visible spectral range. The use of the same ROIC permitted to design an unique front-end electronics. Two test campaigns were carried out: by Sofradir, only on the detectors, and by Selex ES, by using the PRISMA flight electronics. This latter tests demonstrated that was possible to obtain the same detector performance, with respect of those ones obtained by a ground setup, with a flight hardware in terms of noise, linearity and thermal stability.

## 8889-43, Session 9

### ENMAP SWIR FPA: design cooling system, performance, and test results

Markus Haiml, Luis-Dieter Haas, Dominique Hübner, Stefan Rutzinger, Richard Thôt, Sebastian Zehner, AIM INFRAROT-MODULE GmbH (Germany); Christian Neumann, Bernhard Sang, Kayser-Threde GmbH (Germany)

Within the German hyperspectral satellite mission EnMAP (Environmental Mapping and Analysis Program) AIM INFRAROT-MODULE GmbH is sub-contracted by KAYSER-THREDE GmbH for

the development and production of the 0.9-2.5 $\mu$ m SWIR focal plane assembly (FPA). The SWIR FPA consists of an MCT IR sensor with highly sensitive CTIA input stage, sealed in a compact vacuum dewar, a long-life pulse tube cryo-cooler with flexure bearing compressor, cooler drive and control electronics (CCE), and detector control electronics (DCE). This development relies on AIM heritage in design, production and qualification of infrared sensor assemblies for space applications. As of 2012, AIM has delivered 26 IR-sensor flight models (FM) for ESA and international space programs. All design and MAIT activities for the EnMAP SWIR FPA are done in-house, except CCE and DCE. Cooler drive power electronic hybrids are procured from a space experienced supplier and the DCE development is fully sub-contracted.

The 1024x256 pixel detector has a 24x32  $\mu$ m pixel pitch, which leads to an optical active area of 25x 8mm<sup>2</sup>. The silicon readout integrated circuit (ROIC) is optimized for measurement of low photon fluxes with frame rates of up to 250 fps for the full 1024x256 array. Due to the high dynamic nature of spectral data each of the 256 spectral lines can be set individually into a low or high gain mode or turned off for on-chip data reduction by dropping irrelevant spectral lines. The EnMAP application operates the SWIR FPA with 150 active spectral lines at 230 fps and 7.5 MHz pixel clock.

This paper describes the FPA key requirements, system interfaces, and EnMAP specific design optimizations. Particular focus of the presentation is the electro-optical performance, cryo-cooler details and corresponding life-time test status, and environmental vibration test results from the SWIR FPA structural model. Detailed key parameter test results from the engineering model (EM), including temporal readout noise (TRON), linearity, quantum efficiency (QE), spectral response, homogeneity, dark current, and stability will be addressed.

Finally, an overview of our latest development on SWIR detector technology is presented.

## 8889-81, Session 9

### Acceptance and first post-launch results of the 3000 pixel SWIR array on the Proba-V satellite

Koen van der Zanden, Xenics NV (Belgium); Jorg Versluys, OIP N.V. (United States); Tanja Van Achteren, VITO NV (Belgium); Michael Francois, European Space Research and Technology Ctr. (Netherlands); Jan P. Vermeiren, Xenics NV (Belgium)

No Abstract Available

## 8889-44, Session 10

### SWIR space detectors and future developments at Sofradir

Cédric Leroy, Nicolas Jamin, Bruno Fièque, SOFRADIR (France)

Based on a large experience, Sofradir is conducting major space programs covering all the wavelength range from visible to VLWIR as Sentinel projects in the frame of the GMES program or MTG detectors development and manufacturing for the future European meteorological satellites of third generation.

Among all the space activity, a large part of the programs are based on SWIR detectors (with extension in visible spectral range on some of them). Thus the well-known Saturn and Neptune VISIR or SWIR detectors are widely used in numerous space applications at Sofradir to answer these needs. More recently, Sofradir developed in the frame of an ESA contract a new 1kx1k VISIR – SWIR detector with 15  $\mu$ m pixel pitch for future space missions.

In this paper, the last results on space programs involving VISIR – SWIR detectors are presented and discussed. A particular emphasis is also made on the new 1k? VISIR – SWIR detector for space applications which is presented with its performances.

8889-45, Session 10

**MTF optimization of MCT detectors**

Lilian Martineau, Laurent Rubaldo, Fabien Chabuel, SOFRADIR (France); Olivier Gravrand, CEA-LETI-Minatec (France)

Spatial applications are challenging IR technologies to obtain the best system performances. Usually, in these applications, there is the need for trade-off between the signal to noise ratio (SNR) and the spatial response. The merit function for the latter performance is the modulation transfer function (MTF). The MTF optimization requires an understanding of detector physics and the use of evaluation tools.

This paper describes the optimization of an n-on-p Mercury Cadmium Telluride (MCT) pixel design by the making of a MTF mathematical model. Several calculation approximations on the detector physics have to be applied to establish this MTF model. They were justified by comparison to a full finite element MTF model. MTF measurements on retinas were also required to validate this model. Evaluated detectors operated at a focal plane temperature around 77K in all the MCT bands (SWIR, MWIR, LWIR and VLWIR) with precise IR channels ranging from 1.3 to 13  $\mu$ m. Retinas were based on photovoltaic HgCdTe arrays hybridized to a standard Sofradir silicon CMOS readout circuit. Moreover several variants of pixels were designed and implemented on the detection circuit in order to evaluate the effect of the shape and the size of the pixel sensitive area, but also the impact of a guard ring. Depolarisation issue of the illuminated pixel during measurement was avoided by design consideration.

Experimental MTF values were obtained with the classical moving knife edge measurement for all IR bands. In the case of one dimensional measurement, a knife edge image is focused onto the detector and scanned over the pixel under test while the pixel signal is recorded. This signal corresponds to the one dimensional sensible area called the Line Spread Function (LSF). A Fast Fourier Transform (FFT) processing of this signal provides the global MTF of both detector and bench (the product of the bench and pixel MTF). The MTF of the pixel is obtained by dividing the global MTF by the bench MTF determined during the calibration. Special care was taken to evaluate precisely the MTF bench function to have the optimum accuracy for pixel MTF measurement.

Thanks to special care to the optical calibration of the bench, the MTF model was compared with various measurement results. This allows to precise the impact of varying the mercury composition or the cut-off wavelength of MCT material, the illumination wavelength, the focal plane temperature, the implantation size and the effect of the detection circuit substrate removal. Finally this model can be used to design, in a predictive manner, the pixel active area of an atypical MTF response function.

8889-46, Session 10

**High performance multispectral TDI CCD image sensors**

Yichun Luo, Charles R. Smith, Nixon O, Melanie Ledgerwood, Sukhbir Kullar, Teledyne DALSA (Canada)

We developed a TDI image sensor that includes four multispectral bands (B1-B4 zone) and one panchromatic band (P zone) in an integrated, compact package. The B zones have a horizontal resolution of 3k columns, and with a pixel size of 28  $\mu$ m x 28  $\mu$ m. The P zone has a horizontal resolution of 12k columns, and with a pixel size of 7  $\mu$ m x 7  $\mu$ m. The large pixel size of B zones enables them to differentiate the colours of the target by their spectral reflectance signatures even under extremely low light intensity, while the small pixel size and the large pixel number of broad band zone (P zone) provides high resolution images within a wide spectrum range. By utilizing a particularly designed hybrid optical filter, the sensor is able to collect blue, green, red, and near infrared images with only negligible optical cross talk. The sensor uses selectable outputs and data rate: 2 or 1 outputs running at 16.5 MHz (B1-B4) per output, and 8 or 4 outputs running at 33 MHz (P) per output. Special design features minimize electrical and optical cross talk between the image zones, and achieve a low signal noise:  $\leq 85$  e- in B zone, and  $\leq 35$  e- in P zone. To acquire spectral reflectance signatures with good fidelity, the image sensor must be very sensitive to weak light in some spectral bands and cannot be over exposed to light in other spectral bands. To satisfy this requirement, the sensor is designed to show a balanced responsivity in all the image zones. Over all, the sensor demonstrates

an outstanding performance, providing exceptional images that are crucial for remote sensing applications. A part of the sensor test result is shown in the table below.

8889-47, Session 10

**Investigations on performance of electron multiplied CCD detectors (EMCCDs) after radiation for observation of low light star-like objects in scientific space missions**

Harald Michaelis, Thomas Behnke, Stefano Mottola, Andrej Krimlowski, Belinda Borgs, Deutsches Zentrum für Luft- und Raumfahrt e.V. (Germany); Andrew D. Holland, XCAM Ltd. (United Kingdom); Michael Schmid, Ingenieurbüro Schmid (Germany)

The DLR Institute of Planetary Exploration has proposed a novel design of a space instrument accommodated on a small satellite bus (SSB) that is dedicated to the detection of inner earth objects (IEOs) from a low earth orbit (LEO).

The instrument design is based on a focal plane consisting of electron multiplied CCDs (EMCCD) operating at high frame rates for compensation of the spacecraft's pointing jitter at very low effective readout noise. The CCD detectors operate at a nominal operating temperature of -80°C and at a frame rate of 5fps.

It is well known, that CCD detectors are prone to space radiation. However, EMCCD, designed to detect very low light levels of a few electrons, have not yet been used in space. Therefore, investigations have been initiated and performed by DLR for evaluation of the performance of EMCCDs before and after radiation. The main scope of the investigations was the characterization of the charge transfer efficiency (CTE) at low light levels because of its key impact on the detection performance. The non-ionizing dose effects of space high energy particle radiation on the detector were simulated by 60MeV protons at two different fluence levels. The low light-CTE was measured with point light sources without and with background-light.

8889-48, Session 10

**High resolution, high bandwidth global shutter CMOS area scan sensors**

Naser Faramarzpour, Matthias Sonder, Binqiao Li, Teledyne DALSA (Canada)

Global shuttering, sometimes also known as electronic shuttering, enables the use of CMOS sensors in vast range of applications. Teledyne DALSA Global shutter sensors are able to integrate light synchronously across millions of pixels with microsecond accuracy. Each pixel in these arrays includes a PPD for light collection and a separate sense node for signal readout. A transfer gate (shutter) controls the simultaneous transfer of photo generated charge from PPDs to sense nodes. In concurrent operation, while the sense node values are being read-out, PPDs integrate the next frame signal. The maximum frame rate that the sensor can achieve is limited by how fast the contents of the sense nodes in the array can be read out of the sensor.

Teledyne DALSA offers 5 transistor global shutter pixels in variety of resolutions, pitches and noise and full-well combinations. One of the recent generations of these pixels is implemented in 12 mega pixel area scan device at 6  $\mu$ m pitch, with up to 60 dB dynamic range at 70 frames per second. These square pixels include microlens and optional color filters. These sensors also offer exposure control, anti-blooming and high dynamic range operation by introduction of a drain and a PPD reset gate to the pixel. By draining the PPD charge within the frame time, the effective exposure can be controlled from the full frame time down to 10 microseconds.

The state of the art sense node design of Teledyne DALSA's 5T pixel offers exceptional shutter rejection ratio. The architecture is consistent with the requirements to use stitching to achieve very large area scan devices. Improvements have also been made to both pixel process and device functionality to improve dark performance in these devices, with hot pixel counts of less than 5ppm.

Parallel or serial digital output is provided on these sensors using on-chip, column-wise analog to digital converters. Flexible ADC bit depth combined with windowing (adjustable region of interest, ROI) allows these sensors to run with variety of resolution/bandwidth combinations. The low power, state of the art LVDS I/O technology allows for overall power consumptions of less than 2W at full performance conditions.

Making use of microlens on top of the high fill factor layout of these 5T pixels result in Effective QE of more than 35% in the full visible range peaking at 65% at about 600nm light wavelength. The reduced stack height of silicon dioxide and metal layers on the silicon surface used in the specialized process results in improved angular response dependency. At 600nm wavelength the MTF is about 0.4 for this pixel.

## 8889-49, Session 10

### CMOS image sensors optimised for GEO observation

Michel Bréart de Boisanger, Franck Larnaudie, Olivier Saint-Pe, EADS Astrium (France); Pierre Magnan, Institut Supérieur de l'Aéronautique et de l'Espace (France); Paul Jerram, e2v technologies plc (United Kingdom)

CMOS Image Sensors (CIS) arrays have well proven their capabilities to address the growing need of space imaging from the GEO orbit within the visible and near infrared spectral bands. The main interesting features of CIS detectors for such applications are: smearing-free capability, small pixel pitches even with large charge handling capacity, fine tuning of QE and MTF, low power dissipation, exposure control and good radiation behaviour. This paper will present new results obtained by our team in the field of development of such 2D arrays, including large format detectors (up to 12 million pixels), front and back side illuminations, 3T and 4T pixels, microlenses and different types of epitaxial layers/thicknesses. Radiometric and geometric characterisation results obtained for various devices with dedicated test benches will be presented.

## 8889-50, Session 11

### An earth imaging camera simulation using wide-scale construction of reflectance surfaces

Kiran Murthy, Skybox Imaging, Inc. (United States); Alexandra H Chau, Skybox Imaging (United States); Minesh B. Amin, MBA Sciences, Inc. (United States); Dirk Robinson, Skybox Imaging, Inc. (United States)

Developing and testing advanced ground-based image processing systems for earth-observing remote sensing applications presents a unique challenge that requires advanced imagery simulation capabilities. These image processing algorithms must be robust to a wide range of geometric, radiometric, atmospheric, and scene conditions. Thus, the simulation must be able to generate millions of photo-realistic images that reasonably span the wide variety of operating conditions.

This paper presents an earth-imaging multispectral framing camera simulation system called PayloadSim (PaySim) for generating terabytes of simulated photorealistic imagery. Previous camera simulation methods fall into two general categories: those that use 2-D scenes and those that use high-fidelity 3-D scenes. 2-D scene simulations assume a flat earth and use high-resolution orthoimagery to simulate photorealistic imagery. 3-D scene simulations ray trace high-fidelity 3-D reflectance scenes illuminated by multiple light sources, similar to rendering methods in computer graphics. 2-D scene simulation is very efficient, but less accurate in representing geometry and radiance. 3-D scene simulation is more accurate at the expense of computational costs, as well as the cost of manual scene construction. PaySim is designed as a hybrid of these two approaches by leveraging a novel method for automatically and efficiently constructing 3-D reflectance scenes by draping orthorectified imagery over a geo-registered Digital Elevation Maps (DEMs). In addition, the ortho-imagery and DEMs used by PaySim are widely available over the globe, which allows for the construction of 3-D scenes over the entire earth.

PaySim's modeling chain is presented in detail, with emphasis given to the techniques used to achieve computational efficiency. To accelerate the simulations and minimize the memory footprint during scene construction, DEM and imagery tiles are constructed as a pre-processing step. During the pre-processing, an anti-rendering function is applied to the imagery to undo the effects of gamma correction and convert the image into a reflectance map. The anti-rendering function is based on parametrically fitting the digital numbers associated with known features, such as trees or asphalt, to their reflectances. An optimized ray tracing model is then utilized to trace image pixel rays to this reflectance map, and is combined with radiative transfer codes to generate a top-of-atmosphere radiance map. Clouds are simulated by modifying the in-band reflectances using a second ray tracing step to a 2-D cloud-only reflectance scene. Lastly, the digital-optical imagery chain is simulated, including optical blurring, ground smear, and noise effects. A GridEngine-based cluster deployment of this system is presented, which leads to orbit-real time image generation where a single orbit worth of imagery can be simulated within an orbital period of 98 minutes.

The diversity of imagery that can be produced by PaySim has enabled Skybox Imaging to design and robustly test space- and ground-based image processing algorithms prior to launch. In addition, the tool has enabled the production of realistic sample data for early customer engagement, as well as full-scale real-time image production rehearsals via the cluster-deployed version of the sim. Examples of simulated imagery of Skybox's first imaging satellite are shown.

## 8889-51, Session 11

### Compare and contrast next generation climate monitoring architectural alternatives from three different perspectives: suggesting logical collaborative paths forward

Douglas B. Helmuth, Lockheed Martin Space Systems Co. (United States)

Collecting the earth's climate signatures over the next 30 years is a priority for many world governments and international organizations. Implementing a solution requires bridging from today's scientific missions to 'operational' constellations that are adequate to support the future demands of decision makers, scientific investigators and global users for trusted data. Earlier efforts parsed out 'operational' constellation components - this paper will compare/contrast architectural alternatives from three different perspectives.

First, the heavily securitized NPOESS architecture, while undone by requirements growth and collaborations that were not sustained; still a well considered (ambitious) constellation construct to learn from.

Second, the earth climate observations identified by GCOS in ECV's (essential climate variables) measured from space-based sensors with global implementation in sufficient coverage and quality to ensure the needs of major global & international organizations (UNFCCC & IPCC).

Third, the application of a rule-based system of architecting earth observation satellite systems, for comparison against existing architectures to gain insights and make recommendations for global architectures by assessing the value of alternatives and effectively exploring the trade space.

These three architectural references are instructive by their breadth of solution space(s) and boundary conditions. Creative 'graphic science' representation(s) will be exploited, to suggest logical collaborative paths forward and elicit (provoke) identification of and responses from shareholders..

## 8889-52, Session 11

### LOCUS: low cost upper atmosphere sounder

Daniel Gerber, RAL Space (United Kingdom); Bruce M. Swinyard, RAL Space (United Kingdom) and Univ. College London (United Kingdom); Brian N. Ellison, RAL Space (United Kingdom); John M. C. Plane, Wuhu Feng, Univ. of Leeds (United Kingdom); Nimal Navarathinam, Stuart J. Eves, Rachel Bird, Surrey Satellite Technology Ltd. (United Kingdom)



We present the mission concept for LOCUS, a low cost sounder for the upper atmosphere. LOCUS is to provide a low cost space mission to observe terahertz frequency (THz) atomic and molecular transitions to trace and monitor important chemical species in the Mesosphere (55 - 90 km) and lower thermosphere (90 - 120 km), a region known as the MLT. Observations show that in some places the mesosphere is cooling up to 30 times faster than the troposphere is warming. Although not fully understood, this can partly be attributed to processes which are linked to climate change either directly (increased greenhouse gas concentrations in the middle atmosphere, stratospheric ozone depletion) or indirectly (changes in meridional circulation patterns, gravity wave spectrum). Despite the uncertainty, it therefore provides a highly geared indicator of global climate change. Given its importance, it is surprising that the chemistry of the MLT has not been well studied to date by space based platforms. The reason for this is that the best probes of the important chemical species (atomic O, OH, HO<sub>2</sub>, NO etc.) lie in the THz range for the MLT and the corresponding detection technology is relatively immature and perceived as expensive to deploy in comparison to other wavebands. However, recent technical advances in heterodyne receivers, especially in the area of Quantum Cascade Lasers (QCLs) used as local oscillators and planar Schottky frequency mixers and high-speed digital signal processing, mean that payload resource demands (mass power and volume) are being significantly reduced and are evolving towards compliance with smaller space borne missions. An initial science study funded by the Centre for Earth Observation Instrumentation (CEOI) in the UK has resulted in the definition of science requirements for such a mission, as well as an instrument concept that can deliver on the science objectives. In the framework of the study, radiative transfer simulations have been performed with the reference forward model (RFM) to assess the line strengths of the species O, OH, HO<sub>2</sub>, NO, CO and O<sub>2</sub> in frequency regimes open to exploitation by QCL and Schottky mixer technology. Based on this work, the following selection of four micro windows that meet both the scientific and technological requirements is proposed.

Band	Centre	Primary Target Species	Secondary Target Species
Band 1	4.7 THz	O	O <sub>3</sub>
Band 2	3.5 THz	OH	CO
Band 3	1.1 THz	NO, CO	H <sub>2</sub> O, O <sub>3</sub>
Band 4	0.8 THz	O <sub>2</sub> (Pointing)	O <sub>3</sub> , H <sub>2</sub> O

A detailed receiver layout for the four channels was designed, and a satellite platform has been identified to accommodate the mission. The LOCUS concept is currently further investigated, with the aim of a potential in orbit demonstration in the future. Here, we present the results of the science study, as well as an overview of the mission concept and instrument design.

## 8889-53, Session 11

### On-ground evaluation of MTG Image Navigation and Registration (INR) performances

Thomas Chambon, Vincent Soullignac, Francis Olivier, Philippe Tanguy, Thales Alenia Space (France)

In the frame of the future European satellite mission Meteosat Third Generation (MTG), Thales Alenia Space, as satellite prime contractor, is responsible for the design, validation and monitoring of the geometric image quality. This program undertaken by ESA, is the first 3-axis stabilized geo-stationary meteorological mission in Europe and represents therefore a technical challenge for the European industry. Moreover, the variety of the embarked instruments (one imaging and one sounding mission) as well as their demanding required performances make the project particularly complex.

All final products delivered by the MTG mission will be geolocated on-ground by the so-called Image Navigation Registration (INR) process. MTG requirements concerning geolocation and geometric image quality are particularly constraining and demand therefore a robust navigation process.

The MTG INR process is based on a Kalman filter that estimates a set of parameters that model the global behaviour of the instrument line-of-sight and are used in the computation of every sample geolocation. This filter processes observables (e.g landmarks, stars) extracted from the instrument acquired images as well as auxiliary data such as orbit, attitude or scan mirror measurements.

The paper presents the high-fidelity engineering tool which has been developed to assess and analyze the future INR performances of the system. Compared to previous Meteosat generations based on spinning satellites, the 3-axis stabilisation required by the sounding and lightning imagery missions increases the complexity of the INR model prediction by inducing high-frequency perturbations. A dedicated tool is thus required for the simulation of the real behaviour of the line-of-sight, including perturbations from all contributors, and its on-ground estimation by the INR process.

In order to estimate the INR filter behaviour, realistic sets of observables used for the geolocation estimation process are simulated. Being the inputs of the filter, these observables are therefore a key simulation step and the core of the performance assessment model. The simulation takes into account all error sources affecting the pointing knowledge of each MTG instrument such as thermo-elastic deformations, micro-vibrations, orbit estimation errors or instrument scan and spacecraft attitude knowledge performances, as well as uncertainties linked to the observation detection process. After simulating the navigation process over the images, the tool evaluates the geometric performances according to the metrics defined in MTG system requirements.

The simulations predict the INR behaviour depending on various operational conditions to estimate the overall system performances or perform system trade-offs. It is then possible to dissociate the contribution of each perturbation to the final performances and to tune the INR filter with respect to the behaviour of the satellite. These performance assessment campaigns are therefore a key step in the project cycle.

## 8889-54, Session 11

### High rejection VNIR-SWIR beam splitter for the multispectral instrument of Sentinel 2

Vincent Moreau, AMOS s.a. (Belgium); Marc Lappschies, Optics Balzers Jena (Germany); Fabrice Camus, EADS Astrium (France); Volker Kirschner, ESA-ESTEC (Netherlands); Cornelius Haas, EADS Astrium (Germany)

The Sentinel 2 mission shall ensure the continuity and enhancement of Landsat and SPOT data and sustain operational land services in the frame of the Global Monitoring for Environment and Security (GMES) initiative. Sentinel-2 is designed to image the Earth's landmasses from its orbit for at least 7.25 years.

The Multi-Spectral Instrument (MSI), delivered by Astrium Toulouse, will provide high resolution imagery in 13 spectral channels extending from the Visible Near Infrared (VNIR, 400-1100 nm) to the Short Wave Infra-Red (SWIR, 1100-2500 nm) range, down to a resolution of 10 meters with an image width of 290 kilometers.

A dichroic splitter device is located in back-focal path of the telescope. It allows splitting the incoming optical beam between VNIR and SWIR focal planes. It shall ensure an extremely high rejection, better than 1:1000, between both ranges while introducing negligible aberrations in reflected (VNIR) and transmitted (SWIR) paths. The splitter assembly consists of a wedged dichroic filter plate and a wedged compensator plate mounted in a common frame. Both plates are made of fused silica (Infrasil) and polished to  $\lambda/40$ . The major challenges reside in the design complexity of the dichroic coating and in the deposition process control to ensure the required high uniformity of performances through the large aperture.

The paper presents the final spectral and optical performances of this challenging sub-system. It also discusses the main difficulties that have been overpassed during the development and qualification phase.

Ion assisted deposition (IAD) technique has been used for the coating of the beam splitter faces. The layers generated this way have a packing density near the ideal value of 1. Compared to conventionally generated layers, this brings about a higher refractive index of the layers, prevents the layers almost completely from water absorption, and produces amorphous, hard, low-loss and durable layers. It allows complex thin-film designs with far more than 100 layers, any deposit thickness and very thin deposits (needle layers).

The thickness of growing layers have been monitored and controlled in real time by spectroscopic probe install in the chamber.

On the dichroic coating, a reflectance of about 99% has been measured over the full VNIR domain. The uniformity of the spectral performances is better than 0.5% over the plate area (300mm x 100

mm) and the polarization sensitivity is lower than 0,5%.

The transmittance of the splitter assembly is higher than 95% in the three SWIR bands.

Compensation of the bending induced by the residual stress in the coating has allowed achieving a surface error of only 5 nm RMS over the aperture sub-pupils. A perfect stability of the properties after radiation, humidity and thermal vacuum cycling test confirms the excellent durability of the coating.

## 8889-55, Session 12

### 3D wind field from spaceborne Doppler radar

Yvon Lemaître, Nicolas Viltard, Lab. Atmosphères, Milieux, Observations Spatiales (France)

Numerous space radar missions are presently envisioned to study tropical rain systems. Among them, the DYCECT (Dynamique, énergie et Cycle de l'Eau dans la Convection Tropicale) mission, a French proposal (submitted to CNES), could embark a Doppler radar (W-band or Ka-band) with scanning possibilities onboard a low-orbiting satellite. This instrument could be implemented in addition to a Passive Microwave Radiometer (PMR), and eventually an improved ScaraB-like broadband radiometer, and a lightning detection instrument. This package will document the ice microphysics and the heat and radiative budgets. Since the microphysics and the water and energy budgets are strongly driven by the dynamics, the addition of a Doppler radar with scanning possibilities could provide valuable information (3D wind and rain fields) and a large statistic of such a critical information over the entire tropics and for all the stages of development. These new information could be used to better understand the tropical convection and to improve convection parameterization relevant for cloud and climate models and associated direct applications such as now-casting and risk prevention. The present study focuses on the feasibility of such 3D wind field retrieval from spaceborne radar. It uses a simulator of some parts of the spaceborne radar in order i) to evaluate the sensitivity of the retrieved wind fields to the scanning strategies and sampling parameters, and to the instrumental and platform parameters and ii) to determine the best parameters providing the most accurate wind fields.

## 8889-56, Session 12

### Design heritage for a compact atmospheric imager

Joseph Mobilia, Lockheed Martin Advanced Technology Ctr. (United States); John B. Kumer, Alice L. Palmer, Lockheed Martin Space Systems Co. (United States); Kevin A. Sawyer, Yalan Mao, Jack Mix, Theodore C. Nast, Charles S. Clark, Roel Vanbezooijen, David L. Chenette, Lockheed Martin Advanced Technology Ctr. (United States)

The geoCARB sensor uses a 4-channel slit-scan push broom slit-scan infrared imaging grating spectrometer to measure the absorption spectra of sunlight reflected from the ground in narrow wavelength regions. The instrument is designed for flight at geostationary orbit to provide continual monitoring of greenhouse gas over continental scales, several times per day, with a spatial resolution of a few kilometers. The sensor provides multiple daily maps of column-averaged mixing ratios of CO<sub>2</sub>, CH<sub>4</sub>, and CO over the regions of interest, which enables flux determination at unprecedented time, space, and accuracy scales. The geoCARB sensor development is based on our experience in successful implementation of advanced, space deployed optical instruments for remote sensing. A few recent examples include the Atmospheric Imaging Assembly (AIA) and Helioseismic and Magnetic Imager (HMI) on the geostationary Solar Dynamics Observatory (SDO), the Space Based Infrared System (SBIRS GEO-1) and the Interface Region Imaging Spectrograph (IRIS), along with sensors under development, the Near Infrared camera (NIRcam) for James Webb, and Global Lightning Mapper (GLM) and Solar UltraViolet Imager (SUVI) for the GOES-R series. The Tropospheric Infrared Mapping Spectrometer (TIMS), developed in part through the NASA Instrument Incubator Program (IIP), provides an important part of the strong technological foundation for geoCARB. The presentation discusses subsystem heritage and technology

readiness levels for these subsystems. The system level flight technology readiness and methods used to determine this level are presented along with plans to enhance the level.

## 8889-57, Session 12

### Validation and simulation examples of an end-to-end simulator for optical imaging systems

Peter Coppo, Leandro Chiarantini, SELEX Galileo S.p.A. (Italy); Luciano Alparone, Univ. degli Studi di Firenze (Italy)

A software tool for a simplified end-to-end simulation of data products from spaceborne and airborne visible, near-infrared and short-wave infrared imaging spectrometers, starting from either synthetic or airborne hyperspectral data, has been developed and tested. Such a simulator is conceived as a preliminary aid tool (during phase 0?A) for the specification and early development of new Earth observation optical instruments, whose compliance to user's requirements is achieved through a process of cost/performance trade-off.

The proposed simulator is based on three different core modules: the reflectance scenario simulator, the atmospheric simulator, and the instrument simulator. High spatial/spectral resolution images with low intrinsic noise and the sensor/mission specifications are used as inputs for the simulations.

Some simulation examples of hyperspectral and panchromatic images for existing and future design instruments are also reported in this paper showing the tool capabilities for simulating target detection scenarios, data quality assessment with respect to classification performance and class discrimination, impact of optical design on image quality, and 3D modelling of optical performances.

The Selex-ES simulator, as compared with other existing image simulators for phase C/D projects of space-borne instruments, implements all modules necessary for a complete panchromatic and hyper spectral image simulation, and it allows excellent flexibility and expandability for new integrated functions because of the adopted IDL-ENVI software environment.

The modeling adopted for the simulator is validated and assessed through the matching of synthesized spectra, both radiance and reflectance, to true spectra measured on an agricultural clay bare soil by means of a hand-held point spectrometer and an airborne instrument developed and manufactured by Selex ES. In particular the validation test has been performed for clay soil mapping at ground and airborne level. A simulation of the same clay map at satellite scale has been also tried demonstrating a more than acceptable agreement notwithstanding the coarser spatial resolution as compared to the airborne scale.

## 8889-58, Session 12

### Miniaturized hyperspectral imager calibration and UAV flight campaigns

Heikki Saari, VTT Technical Research Ctr. of Finland (Finland); Ilkka Pölonen, Heikki A. Salo, Univ. of Jyväskylä (Finland); Eija Honkavaara, Teemu Hakala, Finnish Geodetic Institute (Finland); Christer Holmlund, Jussi H. Mäkyinen, Rami Mannila, Tapani Antila, Altti Akujärvi, VTT Technical Research Ctr. of Finland (Finland)

VTT Technical Research Centre of Finland has developed Tunable Fabry-Perot Interferometer (FPI) based miniaturized hyperspectral imager which can be operated from light weight Unmanned Aerial Vehicles (UAV). The concept of the hyperspectral imager has been published in the SPIE Proc. 7474, 8174 and 8374. This instrument requires dedicated laboratory and on-board calibration procedures which are described. During summer 2012 extensive UAV Hyperspectral imaging campaigns in the wavelength range 400 – 1000 nm at resolution range 10 – 40 nm @ FWHM were performed to study forest inventory, crop biomass and nitrogen distributions and environmental status of natural water applications. The instrument includes spectral band limiting filters which can be used for the on-board wavelength scale calibration by scanning the FPI pass band center wavelength through the low and high edge of the operational wavelength band. The procedure and results of the laboratory and on-

board calibration tests will be presented. A summary of the performed extensive UAV imaging campaign during summer 2012 will be described and the guide lines for future development are outlined.

## 8889-66, Session 13

### GeoCARB image navigation and registration performance

Roel W. H. van Bezooijen, John B. Kumer, Charles S. Clark, Harald J. Weigl, Ketao Liu, Lockheed Martin Space Systems Co. (United States)

The geoCARB sensor uses a 4-channel slit-scan infrared imaging grating spectrometer to measure the absorption spectra of sunlight reflected from the ground in narrow wavelength regions. The instrument is designed for flight at geostationary orbit to provide continual monitoring of greenhouse gas over continental scales, several times per day, with a spatial resolution of a few kilometers. The sensor provides multiple daily maps of column-averaged mixing ratios of CO<sub>2</sub>, CH<sub>4</sub>, and CO over the regions of interest, which enables flux determination at unprecedented time, space, and accuracy scales. The Tropospheric Infrared Mapping Spectrometer (TIMS), developed in part through the NASA Instrument Incubator Program (IIP), provides an important part of the strong technological foundation for geoCARB. The paper discusses the hardware implementation selected to enable high precision image navigation and registration (INR) as well as the INR technique used for mapping the geoCARB optical footprints on to the earth's surface.

The instrument acquires data in a step and stare mode with 4.08 s stare (integration) time and 0.34s step time on 1016 footprints spaced by 2.7 km at sub satellite point (SSP) in the NS direction along the slit. The slit is stepped in 3 km EW increments. Accurate knowledge of the instrument line of sight is obtained through use of a dual-head star tracker system (STS), high-precision optical encoders for the two scan mirrors, a GPS receiver, and a highly stable common optical bench to which the instrument components, the scan mirror assembly, and the heads of the STS are kinematically mounted.

The contribution of the 4 Hz STS to the INR error in the NS and EW direction is limited to 0.25 and 0.37 km, respectively at the SSP. While attitude disturbances due to jitter and solar array flex of the communication satellite hosting geoCARB affect spatial resolution, we show that the effect on INR is negligible due to the frequencies and amplitudes involved. Solar array flex typically causes sinusoidal motion with amplitudes up to 0.0025° at a frequency ranging from 0.1 to 0.5 Hz, while jitter causes motions from 0.0003 to 0.003° at multiple frequencies greater than 10 Hz. To compensate for diurnal alignment variation of the instrument relative to the STS, the instrument performs 8 star sightings per day. Use of coastline ID improves geo-location accuracy by 30% allowing for an INR accuracy of 0.37 and 0.49 km in the NS and EW direction, respectively.

By studying the systematics in coastline error variation, it is anticipated that, following considerable post-processing, both the diurnal alignment error and STS bias error (which repeats every sidereal day) can be identified, allowing improvement of the accuracy by another 35%.

In addition to describing the INR method, the paper quantifies all error sources and describes how each of them affects overall INR accuracy. These error sources include: STS error, star sighting error, encoder error, scan mirror bearing wobble, residual diurnal alignment error, alignment uncertainty of scan mirror axes, mirror alignment uncertainty, mirror home position uncertainty, coastline ID error, and GPS position error.

## 8889-67, Session 13

### Raytheon high-bandwidth, large-angle, reactionless fast steering mirror

Islam Shawki, Andrew Bullard, Raytheon Co. (United States)

Raytheon Space and Airborne Systems (SAS) has designed, built and tested a 3-inch diameter fast steering mirror (FSM) for space application. This 2-axis FSM operates over a large angle (over 10 degree range), has a very high servo bandwidth (over 3.3 KHz closed loop bandwidth), has nanoradian class noise, and has micro-radian line of sight accuracy. The FSM maintains excellent performance

over large temperature ranges (which includes wave front error) and has very high reliability with the help of fully redundant angle sensors and actuator circuits. The FSM is capable of achieving all its design requirements while also being reaction-compensated. The reaction compensation is achieved passively and does not need a separate control loop. The FSM has undergone various environmental testing which include exported forces and torques and thermal vacuum testing that support the FSM design claims. This paper presents the mechanical design and test results of the mechanism which satisfies the rigorous vacuum and space application requirements.

## 8889-68, Session 13

### Development of a compressive sampling hyperspectral imager prototype

Alessandro Barducci, Donatella Guzzi, Cinzia Lastris, Vanni Nardino, Paolo Marcoionni, Ivan Pippi, Istituto di Fisica Applicata Nello Carrara (Italy)

Compressive sensing, aka compressive sampling (CS), is a new technology that investigates the chance to sample signals at a lower rate than that dictated by the traditional sampling theory, such as the Nyquist-Shannon theorem. This option is connected to a specific signal property which is called sparsity. A sparse signal doesn't convey the information amount predicted by the traditional sampling theory, regardless of the maximum frequency contained in its spectrum. Therefore, some mathematical representation of a sparse signal must exist in which the number of non-trivial elements (coefficients) is less than that originated by a non-sparse signal. Usually, such representation is an Integral Transformation (IT) of the signal itself. The sparse mathematical representation admitted by the signal can be made accessible to a sensor, provided that a dedicated subsystem performs the involved IT before its measurement. When radiometric and spectroscopic signals are considered, an optical subsystem would be the natural choice for optically computing this transformation.

The main advantage of CS is that compression takes place during the sampling phase. Therefore, CS promises outstanding savings in terms of the ADC specs, data storage memory, down-link bandwidth, and electrical power absorption, paving the way to significant reductions of payload mass, volume, and cost of space missions. The possible impact of CS could be remarkable, motivating new investigations and research programs regarding this emerging technology. On the contrary, the main CS disadvantage is constituted by the intensive off-line data processing necessary to obtain the desired source estimation.

In this paper we summarize the CS architecture and its possible implementations for Earth observation, giving evidence of possible bottlenecks hindering this technology. We show that CS sensors require optical light modulators and 2dim detector arrays of high frame rate. The paper shows that the CS necessarily employs a multiplexing scheme, which in spite of traditional expectations gives rise to a noteworthy SNR disadvantage. We further describe the development of a sensor prototype at laboratory level that will be utilized for the experimental assessment of CS performance and the related reconstruction errors. This experimental test-bed adopts a push-broom imaging spectrometer with spectral resolution between 0.2 nm and 0.02 nm (FWHM) for generating a 2dim (space-spectrum) domain in the VIS-NIR spectral range. A beam-splitter at the output port of the spectrometer divides the light into two focal planes, one of which adopts the standard sampling while the other performs the CS. In this way it is possible to make a direct comparison between the CS reconstructed dataset and its expectation. The image on the CS arm is first modulated by a liquid crystal plate, then undersampled with a Silicon PhotoMultiplier (SiPM) 12x12 matrix that collects elements of the requested IT. SiPM acquisition is iterated while changing the pattern (integral kernel) of the spatial modulator, thus measuring several elements of the involved integral transform. The prototype is being developed within the framework of the ESA ITI-B Project titled "Hyperspectral Passive Satellite Imaging via Compressive Sensing".

8889-69, Session 13

### Assessment of FLD-based algorithms for the retrieval of vegetation solar-induced fluorescence from the in-filling of the telluric O2-A and O2-B lines

Lorenzo Palombi, Paola Di Ninni, Donatella Guzzi, David Lognoli, Vanni Nardino, Ivan Pippi, Valentina Raimondi, Istituto di Fisica Applicata Nello Carrara (Italy)

The well-known FLD (Fraunhofer Line Discriminator) method consists in the detection of the infilling, due to the contribution of a fluorescent target, in the Fraunhofer lines of solar irradiance. In these lines, the radiance is lower in comparison with the offline radiance, and it is thus easier by an inline-offline comparison to decouple the weak fluorescence signal from the measured radiance. Recently, the method has aroused a growing interest for vegetation remote sensing at global scale from satellite by using the telluric O2-A and O2-B bands, respectively at 760 nm and 687 nm, as also envisaged by the ESA Earth Explorer FLEX (Fluorescence EXplorer) mission.

This study evaluates the performances of different algorithms for the retrieval of solar induced fluorescence of vegetation in both the telluric O2-A and O2-B bands by taking into account the main technical specifications of a passive spectroradiometer for airborne remote sensing. In particular, we evaluated the performances of three different algorithms amongst those already applied by the scientific community: two of them are based on the use of two or three spectral bands (sFLD and 3FLD methods), while the third one exploits the information content of all the spectral channels in certain bands by applying a polynomial model fluorescence and reflectance (SFM method). These were applied to a synthetic set of fluorescence data corresponding to different types of vegetation. The main technical specifications of the spectroradiometer have been outlined in terms of three different airborne operating scenarios, addressing different flight altitudes and speeds chosen on the basis of typical platforms suitable for operation from low-medium altitudes.

The results underlined that the high spectral resolution of the instrument plays a fundamental role for the determination of the value of fluorescence with a good precision and accuracy, as expected. Nevertheless, the extraction of the value of fluorescence in the O2-A band is less critical than in the O2-B band and, specifically, it is less sensitive to the spectral resolution of the spectroradiometer. Even at low spectral resolutions, however, the retrieval algorithms based on polynomial fitting provided better results than methods based on the use of spectral bands.

8889-59, Session 14

### Design and realization of linear APS-based sun sensor

He Liang, Fu Jian Zhang, Xin Z. Lv, Chengwu Yu, Zhong Jin Jia, Beijing Institute of Control Engineering (China)

Linear APS-based sun sensor is a kind of sun sensor based on a linear Active Pixel Sensor (APS) with low power consumption, small size, and small mass. It is integrated with optical, mechanical and electronic technologies. The main function of Linear APS-based sun sensor is to measure the solar aspect angle about two axis directions, determining the attitude of spacecraft. It is composed of four major parts: a mask with a N-shape diaphragm aperture, electronic system, mechanical structure and software. The angle measurement principle of linear APS-based sun sensor is introduced in this paper. With only one 2048x1 linear image sensor, the sun sensor can get the two axis sun position information. The image of the solar is projected on the linear image sensor through a N-shape aperture in front of it. Each slit of the N-shape aperture is 70 μm in width and the width is equivalent to 10x1 pixels of the APS array. The information of the image position can be calculated through a centroid algorithm. By comparing the central position of solar image on APS at a time with the central position of solar image when the solar aspect angle is zero, we can get the solar aspect angle. This paper analyzes the sources of systematic errors and some specific solutions proposed help to reduce systematic errors. The compensation algorithm in the software designed makes the sun sensor meet the accuracy requirements. The performance characteristics are as follows: FOV ±64° x ±64°, the accuracy of θ-axis is better than 0.02°(3σ) in the FOV of less than 45°, and better

than 0.03°(3σ) in other FOV, the accuracy of φ-axis is better than 0.03°(3σ) in the whole FOV. The power consumption is 1W. The mass is 0.42kg. The update rate: 10Hz. Linear APS-based sun sensor was successfully carried by satellite in orbit in October 2012. On-orbit testing showed that it operates normally and the data curves tells the accuracy meets requirements.

8889-61, Session 14

### A carbon dioxide radiance model of the earth planet using the conical earth sensor data

Loulou Deng, Zhiwu Mei, Zhijun Tu, Jun Yuan, Ting He, Wei Yi, Beijing Institute of Control Engineering (China)

Climate Modeling results show that about 50% of the Earth's outgoing radiation and 75% of the atmospheric outgoing radiation are contained in the far infrared. Generally the earth is considered as a 220~230K black body, and the peak value of the Earth's outgoing radiation is around the wavelength of 10 micron. The atmospheric outgoing radiation are contained with five spectral intervals: the water vapor band from 6.33 to 6.85 microns, the ozone band from 8.9 to 10.1 microns, the atmospheric window from 10.75 to 11.75 microns, the carbon dioxide band from 14 to 16 microns, and finally the rotational water vapor band from 21 to 125 microns. The properties of the carbon dioxide band is stable than other bands which has been chosen for the work spectrum of the earth sensors. But the radiation energy of carbon dioxide band is variety and it is a function of latitude, season and weather conditions. Usually the luminance of the Earth's radiation (14 to 16 μm) is from 3 to 7 W/m<sup>2</sup>Sr.

Earth sensor is an important instrument of the Attitude and Orbit Control System (AOCS), and it is sensitive to the curve of the earth's and atmospheric outgoing radiation profile to determine the roll and pitch angles of satellite which are relative to nadir vector. Most earth sensors use profile data gathered from Project Scanner taken in August and December 1966.

The earth sensor referred in this paper is the conical scan earth sensor which is mainly used in the LEO (Low Earth Orbit) satellite. A method to determine the luminance of earth's and atmospheric outgoing radiation (carbon dioxide) using the earth sensor is discussed in this paper. When the conical scan sensor scan from the space to the earth, a pulse is produced and the pulse value is scale with the infrared radiation luminance. Then the infrared radiation luminance can be calculated. A carbon dioxide radiance model of the earth's and atmospheric outgoing radiation is obtained according the luminance data about with different latitudes and seasons which are measured from the conical scan earth sensors of ZY-1 satellite.

When the carbon dioxide radiance model has been collected, it can be fed directly to the earth sensors to improve their accuracy. It also can be supplied for the research of the content and distribution of carbon dioxide in the atmosphere.

8889-63, Session 14

### Design concepts for mechanical architecture of geo imaging payloads

Anup Vora, J. Rami, Naimesh R. Patel, H. H. Mavani, Chirag P. Dewan, Space Applications Ctr. (India)

Indian Space Research Organization, ISRO carries the core responsibility of realizing satellite missions in India. For last more than two decades, it has flown several imaging instruments in geostationary orbit catering mainly to meteorological needs of the country. This orbit has been used for better imaging opportunities in terms of temporal resolution by India in VHRR and CCD payloads launched in INSAT-2, 3 and Kalpana satellites. Imager and Sounder payloads of INSAT-3D are also realized in the same manner with a better imaging capability in terms of spatial resolution.

Each payload has unique features in terms of orbital constraints, optical aperture, layout, resolution, number of spectral channels, focal plane design, field scanning strategy, size and mass constraints, spacecraft interface, launch configuration, launch loads and enhancement from capability of predecessors. Sounder has special arrangement to acquire narrow spectral channel through filter wheel.

Mechanical design is governed by above features in general and driven through various challenges across the realization cycle, like need of thermal control under large temperature excursions, optical sensitivity, very stringent thermo-elastic stability of the instrument, material choices, kinematic mounting of optical elements, alignment of all the optical and focal plane elements as well as mechanisms, stress free payload mounting, testability and electronic package design.

All these challenges are met through a systematic design, analysis, development, integration and testing efforts within the system specifications and schedules. They are supported by development of various ground support equipments and particular model philosophy.

This paper explains how these design needs are met to arrive at an acceptable mechanical architecture and qualified for space use. Future high resolution missions are also briefly discussed.

#### 8889-64, Session 14

### **Spectral response function effects on surface reflectance and NDVI measured with CCD cameras of HJ-1A/B small satellite constellation**

Wenjuan Zhang, Bing Zhang, Zhengchao Chen, Lianru Gao, Hao Zhang, Institute of Remote Sensing and Digital Earth (China)

On September 6th, 2008, HJ-1A/B, the small satellite Constellation for Environment and Disaster Monitoring, was successfully launched in China. HJ-1A/B is composed by two small satellites named as Satellite-A (HJ-1A) and Satellite-B (HJ-1B). A multispectral sensor was carried on HJ-1A and another onboard on HJ-1B to obtain images including blue, green, red and near-infrared(NIR) band. Two CCD cameras in a multispectral sensor were mosaiced together to make the swath width reach 700km. All the four CCD cameras have a approximate design. They were named as HJ-1ACCD1, HJ-1ACCD2, HJ-1BCCD1 and HJ-1BCCD2. Under the cooperation of the two satellites and the wide swath, the revisit-period of the HJ-1A/B multispectral imager less than 48 hours.

This paper reports on the sensitivity of normalized difference vegetation index (NDVI) and surface reflectance due to differences in spectral response functions (SRF). All the four CCD cameras onboard HJ-1A/B small satellite constellation were included in the paper. To encompass a potential range of variability in surface reflectance and NDVI, a set of representative spectra for various surface targets were compiled, and the 6S radiative transfer model was employed to simulate the TOA signal in different atmospheric conditions(water vapor, aerosol, and ozone). It is shown that for identical atmospheric state and similar surface spectral reflectance, the NDVI and spectral reflectance are sensitive to the sensor's SRF. Compared to HJ-1ACCD1, the relative differences in reflectance among the CCD cameras range from -4.35% to 12.5% for red channel, from -1.89% to 0.81% for NIR channel, from -0.03% to 7% for surface NDVI, and from -0.22% to 4.7% for TOA NDVI. The most significant difference was observed for the HJ-1BCCD1 for NDVI. Consistent results about NIR channel were obtained with the HJ-1BCCD1 and HJ-1BCCD2. Variability of the SRF effect among different atmospheric state is very small in general. A good linear relationship between the four CCD cameras with various surface targets and weather conditions. Linear regression models are provided for spectral and NDVI correction with respect to HJ-1ACCD1.

#### 8889-82, Session 14

### **Research on complicated imaging condition of GEO optical high-resolution remote sensing satellite**

Linghua Guo, ENYU GAO, DIANJUN WANG, China Academy of Space Technology (China); Biru Wang, Hebei Univ. of Science and Technology (China)

The requirement for high time and space resolution of optical remote sensing satellite in disaster, land resources, environment, marine monitoring and meteorology observation, etc is getting urgent and strict. For that reason, a remote sensing satellite system solely located in MEO or LEO cannot operate continuous observation and Surveillance. GEO optical high resolution earth observing satellite in the other hand can keep the mesoscale and microscale target under continuous surveillance by controlling line of sight (LOS), and can provide imaging observation of an extensive region in a short time. The advantages of GEO satellite such as real-time observation of the mesoscale and microscale target, rapid response of key events, have been recognized by lots of countries and become a new trend of remote sensing satellite. As many advantages as the GEO remote sensing satellite has, its imaging condition is more complicated. Many new characteristics of imaging observation and imaging quality need to be discussed. We analyze each factor in the remote sensing link, using theoretical analysis and modeling simulation to get coefficient of each factor to represent its effect on imaging system. Such research achievements can provide reference for satellite mission analysis and system design.

# Conference 8890A: Remote Sensing of Clouds and the Atmosphere XVIII

Wednesday - Thursday 25–26 September 2013

Part of Proceedings of SPIE Vol. 8890 Remote Sensing of Clouds and the Atmosphere XVIII; and Optics in Atmospheric Propagation and Adaptive Systems XVI

8890-35, Session PS

## Measurements of PM<sub>2.5</sub> in megacity

Makiko Nakata, Itaru Sano, Sonoyo Mukai, Kinki Univ. (Japan)

Osaka is located on the main island of Japan. Osaka Prefecture, which includes Osaka City and 42 other municipalities, has a population of 8.8 million and a total land mass of about 1,890 square kilometers. Although Osaka is Japan's second smallest prefecture by size, its population represents 7% of the entire nation, making it the second most populous prefecture after Tokyo. The greater Osaka metropolitan area covers a total of 7,800 square kilometers within a radius of 50 to 60 km from the center of Osaka. The population exceeds 17 million, making it one of the biggest metropolitan areas in the world. Our observation site is located in eastern Osaka. Eastern Osaka lies along the foot of the chain of mountains from Mt. Ikoma to the Kongozan. The area is known for manufacturing technologies for small and medium enterprises. Then clear atmosphere with few small particles is not too often and usually polluted particles from diesel vehicles and industries are suspended in this area. Furthermore pollutants carried by winds from China are adding to the pollution of the atmosphere. In the winter of 2013, the Chinese environment protection ministry said that up to a quarter of China was covered with thick fog. Especially problematic are fine particle called PM<sub>2.5</sub>, whose diameter is 2.5 micrometers or less. The problem has become particularly acute, raising health concerns in neighboring parts of Asia including Japan. A noticeable change in characteristics of particulate matter was observed in Japan when pollutant air was transported from China. In this work, we focus on the variation of particulate matter around Higashi-Osaka located on the east side of Osaka, the second-largest city in Japan. We take advantage of simultaneous observations on the campus of Kinki University in Higashi-Osaka. Radiometric data supplied by a Cimel instrument were analysed using a standard AERONET (Aerosol Robotics Network) processing system. An SPM (suspended particulate matter) sampler set up at the same AERONET site on the roof of a building at Kinki University about 50 m above sea level. We also set up a standard LIDAR (Light Detection and Ranging) network governed with NIES (National Institute for Environmental Studies) at the same site. The SPM sampler provides particle information about the concentrations of PM<sub>2.5</sub>, PM<sub>10</sub> and OBC separately. To investigate the change of size and composition of particulate matter, we analyse the particulate matter with a scanning electron microscope (SEM) coupled with an energy-dispersive X-ray analyser (EDX). We used sampling data from the SPM sampler. The component analysis shows that the rate of sulphur increases when pollution suffered from China.

8890-36, Session PS

## Analysis of the relation between GPS tropospheric delay and intense precipitation

Pedro J. Benevides, João Catalão, Pedro Miranda, Maria J. Chinita, Univ. de Lisboa (Portugal)

The electromagnetic signal transmitted by the global navigation and positioning systems (GNSS) suffers a delay which is mainly caused by the water vapor existing in the atmosphere. Estimating the delay affecting the signal propagation between the satellites and the station receivers, separating from other error sources, it is possible to estimate the water vapor column on the troposphere above each station. The GNSS atmospheric processing has been developed in the past several years providing measures of integrated water vapor with similar precision comparing with the usual observation methods like radiosondes or radiometers. The main advantages over these classical methods are all weather condition, greater spatial resolution and almost continuous temporal monitoring given by the GNSS stations, allowing a better characterization of the atmospheric water vapor variability. The torrential precipitation caused occasionally by some atmospheric instability phenomena can lead to several damages in artificial structures sometimes causing deaths. The aim of this study is to characterize the 3D water vapor field on the troposphere over time by GNSS techniques (Tomography). It is expected that can also come

to assist in the Nowcasting particularly in the prediction of severe meteorological phenomenon.

For this study, several events of strong, intense and short precipitation, observed in the Lisbon region were analyzed. The chosen dates are: 15 March, 18 to 19 May and 14 to 15 August of 2012. The choice of these periods was based on the analysis of hourly precipitation given by a synoptic meteorological station located on Lisbon center. This region is monitored by a network of 13 GNSS stations covering an area of 100 squared kilometers. Data crossing with precipitation data was done by observing the hourly precipitation data given by the closest meteorological stations (up to 40 regionally distributed) from each GNSS station. The relationship between the GPS precipitable water vapor (PWV) and the hourly accumulated precipitation was evaluated over the time (1D closest GPS-meteorological station plots) and spatially (2D maps) interpolated over the GNSS and meteorological stations. It was verified that there were a high and sudden increment of the GPS PWV prior to a severe precipitation event. The PWV increment starts 6 to 9 hours before the rain event and the value has increased between 47% and 64% relatively to the PWV value observed previously. This effect will be studied taking into account the seasonal variation of the GPS signal. In this study is shown that GPS data have good potential for forecasting severe rain events or high moisture flux situations.

Acknowledgements: Fundação para a Ciência e Tecnologia (FCT), Portugal, for the PhD Grant SFRH/BD/80288/2011 and for the financial support Project SMOG (PTDC/CTE-ATM/119922/2010)

8890-37, Session PS

## Detecting climate signatures with high spectral resolution infrared satellite measurements

Daniel H. DeSlover, David C. Tobin, Henry E. Revercomb, Robert O. Knuteson, Univ. of Wisconsin-Madison (United States)

Upwelling atmospheric infrared radiances can be accurately monitored from high spectral resolution satellite observations. The high spectral resolution nature of these measurements affords the ability to track various climate relevant parameters such as window channels sensitive to surface temperature and clouds, channels with higher sensitivity to trace gases including CO<sub>2</sub>, CH<sub>4</sub>, SO<sub>2</sub>, HNO<sub>3</sub>, as well as channels sensitive only to upper tropospheric or lower stratospheric temperature.

NASA's Atmospheric Infrared Sounder (AIRS) provides a data record that extends from its 2002 launch to the present. The Infrared Atmospheric Sounding Interferometer (IASI) onboard Metop- (A launched in 2006, B in 2012), as well as the Joint Polar Satellite System (JPSS) Cross-track Infrared Sounder (CrIS) launched in 2011, complement this data record. Future infrared sounders with similar capabilities will augment these measurements into the distant future.

We have created a global data set from the aforementioned satellite observations. Our analysis yields a channel dependent approach that can be further constrained in terms of diurnal, seasonal and geographic limits, with measurement accuracies of better than a few tenths of degree Kelvin. In this study, we have applied this concept to obtain a better understanding of long-term stratospheric temperature trends. We will present a survey of temperature trends for spectral channels that were chosen to be sensitive to stratospheric emission. Results will be shown for tropical, mid-latitude and polar stratospheric observations.

8890-38, Session PS

## Development a computation code of radiation simulation based on the superposition method

Masayoshi Yasumoto, Kinki Univ. (Japan); Sonoyo Mukai,

Kyoto College of Graduate Studies for Informatics (Japan);  
Itaru Sano, Makiko Nakata, Kinki Univ. (Japan)

Retrieval of atmospheric aerosol characteristics from satellite data, i.e. aerosol remote sensing, is based on the light scattering theory. The aerosol properties are estimated by comparing satellite measurements with the numerical values of radiation simulations in the Earth atmosphere-surface model.

It is well known that real ground surface of the Earth is complicated. Then radiation simulations in the Earth atmosphere-surface system for aerosol remote sensing should consider the appropriate reflection function at the ground surface. In other words, it is necessary to take into account the BRDF (bidirectional reflectance distribution function) for the bottom ground surface, when the aerosol properties are retrieved from the satellite data.

The BRDF depends upon the structure and/or vegetation of the ground surface. In this work, the ground surface is assumed to be interpreted by such a semi-empirical kernel driven BRDF as Ross-Li model.

The superposition method is applied for the radiation simulations in the present atmosphere-surface system. The superposition method is available for variable reflecting-surface model. Because the upward reflectance at the top of atmosphere from the atmosphere-surface system can be calculated by summing up the numbers of reflection at the reflecting bottom surface, once the scattering and transmission functions (i.e. S- & T- functions defined by Chandrasekhar) have been obtained for free atmosphere.

This computation code, named REESIT-SM, is practically applied for Aqua/MODIS data.

## 8890-39, Session PS

### Focused sunrays and forest fire danger: new concept

G. V. Kuznetsov, N. V. Baranovskiy, Tomsk Polytechnic Univ.  
(Russian Federation)

Estimation of forest fire danger has traditionally been based on historical fire weather climatology. This presentation describes a new concept for an improved estimation of forest fire danger, which takes into account the possibility of forest fuel ignition as a result of focused sun's light. For example, glass containers, their splinters and large drops of coniferous trees pitch can be fire hazard due to their potential for focusing the sun's rays (under favorable conditions) and, consequently for setting forest fuel ablaze. Our analysis of numerous observational reports suggests that the forest fuel ignition process can be described by system of the non-stationary nonlinear equations of heat conductivity and diffusion with corresponding initial and boundary conditions. To solve these equations, we apply well-established numerical methods. This presentation includes model results and their comparison with available observational constrains together with suggestions for using remote sensing data.

## 8890-1, Session 1

### LACROS: the Leipzig aerosol and cloud remote observations system (*Invited Paper*)

Johannes Bühl, Leibniz Institut für Troposphärenforschung  
(Germany); Patric Seifert, Leibniz-Institut für  
Atmosphärenphysik e.V. (Germany); Ulla Wandinger, Holger  
Baars, Thomas Kanitz, Jörg Schmidt, Alexander Myagkov,  
Ronny Engelmann, Annett Skupin, Birgit Heese, Andre Klepel,  
Dietrich Althausen, Albert Ansmann, Leibniz Institut für  
Troposphärenforschung (Germany)

LACROS combines the strengths of a multitude of measurement systems. It includes active remote sensing instruments, (e.g., multiwavelength Raman/polarization lidar PollyXT, 1064 nm Jenoptik Ceilometer, wind Doppler Lidar Wili with focus on updraft and downdraft motions at cloud base, and a Mira36 cloud radar) and passive ones (e.g. HATPRO Microwave Radiometer with two infrared radiometers, sun-sky-AERONET photometer, all-sky-imager). While the active remote sensing instruments deliver column information, the passive instruments mostly yield column integrated values. A

distrometer mounted next to the radar assists the interpretation and calibration of the radar measurements. All systems can be placed within a 15 m radius to achieve maximum agreement between the different observation volumes.

LACROS is usually located at Leipzig, Germany but it is designed to be mobile and has recently been deployed in field experiments (e.g. HOPE, April-May 2013, near Cologne, Germany). When located at Leipzig additional instruments, for example the highly sophisticated Dual-Field of View MARTHA lidar, the BERTHA HSRL lidar and SAEMS (Spectral Aerosol Extinction Monitoring System), accompany the measurements of LACROS. Wherever deployed, it is an operational CLOUDNET and AERONET station. For Europe, both networks (and the EARLINET facility at Leipzig) are coordinated under the European Union's ACTRIS (Aerosols, Clouds and Trace Gases Research InfraStructure) project. The main goal of LACROS is presently the investigation of aerosol-cloud-turbulence/dynamics interaction with focus on heterogeneous ice formation (ice formation in water clouds). To gain statistical significant results in this field the cooperation with other research supersites (Cabauw, Chilbolton, Jülich, Lindenberg, Paris, Potenza) is crucial and already established for example within ACTRIS, EARLINET and CLOUDNET.

Lidar and radar complement each other because they are sensitive to different kinds of particles. Both instruments are most sensitive for particles in the size range of the operating wavelength, which is about 0.3...2 micron for lidars and 8 mm for the Mira36 cloud radar. This makes the lidar ideal for sensing aerosol particles and small (just activated) cloud droplets while the radar delivers best signals when bigger cloud droplets (>30 µm), drizzle- / rain droplets or falling ice particles are present. The consecutive connection and combined interpretation of all measured parameters is then a difficult task and will be a major research focus within the next years. Combining the particle terminal fall velocities and depolarization information measured by PollyXT Raman lidar, Wili Doppler lidar and Mira36 cloud radar allows to retrieve information about particle sizes and shapes. For this purpose the Doppler lidar can be used to correct the vertical wind offset or deliver information about small particles not visible to the radar.

## 8890-2, Session 1

### Tropospheric IWV profiles estimation through multifrequency signal attenuation measurements between two counter- rotating LEO satellites: performance analysis

Luca Facheris, Fabrizio Cuccoli, Univ. degli Studi di  
Firenze (Italy); Enrica Martini, CNIT c/o Dept. of Information  
Engineering and Mathematical Sciences, University of Siena  
(Italy)

The Normalized Differential Spectral Attenuation (NDSA) approach was introduced by us years ago with the purpose to define a tool for tropospheric water vapor sounding utilizing a couple of counter-rotating LEO satellites (one carrying a transmitter, the other a receiver) in a limb geometry. It relies on the conversion of a spectral parameter (the so-called spectral sensitivity S), into the Integrated Water Vapor (IWV) along the radio link established between the two LEO satellites.

S at a given frequency  $f_0$  is a function of the attenuations undergone by two tones simultaneously transmitted at relatively close frequencies  $f_0 - Df/2$  and  $f_0 + Df/2$ , where the spectral separation  $Df \ll f_0$ . A multifrequency approach is however needed to provide an equivalent accuracy for IWV at all tropospheric heights.

The interest toward NDSA was mainly related to two characteristics: 1) the tight relationship between S and IWV and 2) the differential and normalized approach that made the IWV estimates less sensitive to tropospheric scintillation effects. Previous studies, reported also in former SPIE Remote Sensing Symposia, showed that under certain conditions of SNR and scintillation power, NDSA could provide good estimates up to 10 km through S measurements in the Ku/K bands.

For various reasons, however, such past activities left open some issues that we are currently facing through an on-going ESA study (ANISAP), jointly with new ones that deserved to be treated in order to get the complete theoretical understanding of the NDSA potential. These are:

1) to finalize the analysis of the accuracy of the IWV-S relations and of

the IWV estimates above 10 km by exploiting multiple NDSA channels in the K-Ku and M (179-182 GHz) band;

2) to focus on the potential of NDSA channels in the 27-36 GHz band for estimating the Integrated Liquid Water (ILW) and correcting the IWV estimates made in the Ku-K bands;

3) to devise an algorithm for the derivation of turbulence parameters (vertical profiles of the refractive index structure function and value of the outer scale length) from high resolution radiosonde profiles;

The first two points were rather important and have been discussed in [1], while the third was actually critical. In fact, previous performance analyses were carried out assuming an exponential scintillation profile that, besides being a single-parameter model, was not related to the simulated atmosphere used for performance evaluation. It could however provide information about the maximum level of scintillation tolerable for a given SNR at the receiver. The newly developed procedure has been tested on a set of radiosonde data corresponding to different latitudes, seasons and times and includes anisotropic irregularities, which can contribute to amplitude scintillation in the higher troposphere, modeled by introducing an ellipsoidal spectrum as a generalization of the conventional von Karman spectrum. In this paper, we show the multi-frequency NDSA performance up to 15 km altitude accounting for signal impairments (scintillation at all frequencies plus thermal noise) and based on the new study outcomes extended to the M band, including also the liquid water detection and the correction of IWV.

[1] L. Facheris, F. Cuccoli, S. Schweitzer: Assessing the relations between spectral sensitivity and integrated water vapor for NDSA processing applied to a radio link between two LEO satellites, SPIE Proceedings Vol. 8534, Remote Sensing of Clouds and the Atmosphere XVII; and Lidar Technologies, Techniques, and Measurements for Atmospheric Remote Sensing VIII, 2012

#### 8890-4, Session 1

### Atmospheric trace gas profiles from Suomi-NPP cross track infrared sounder

Xu Liu, NASA Langley Research Ctr. (United States)

The Cross-track Infrared and Microwave Sounder Suite (CrIMSS) was successfully launched onboard of Suomi National Polar-orbiting Partnership (S-NPP) in October 2011. The CrIMSS consists of the Advanced Technology Microwave Sounder (ATMS) and Cross-track Infrared Sounder (CrIS) instruments. A Principal Component-based Radiative Transfer Model (PCRTM) has been developed to explore the abundant information from both the nominal and the full resolution CrIS spectra. The nominal resolution CrIS spectra have three bands with spectral resolutions of 0.625 cm<sup>-1</sup> for band 1, 1.25 cm<sup>-1</sup> for band 2, and 2.5 cm<sup>-1</sup> for band 3. The full resolution CrIS data have a spectral resolution of 0.625 cm<sup>-1</sup> for all three bands and are processed in a special mode of the CrIS operations. An optimal estimation physical retrieval method has been used to retrieve atmospheric trace gas profiles from the CrIS spectra. The impact of the spectral resolution on the trace gas profile retrieval performances will be discussed.

#### 8890-5, Session 1

### Monitoring of nitrogen dioxide, ozone and halogens radicals in Antarctica

Daniele Bortoli, Univ. de Évora (Portugal) and Institute of Atmospheric Sciences and Climate (Italy); Fabrizio Ravegnani, Istituto di Scienze dell'Atmosfera e del Clima (Italy); Maria Joao T. Costa, Univ. de Évora (Portugal); Silvia Genco, Istituto di Scienze dell'Atmosfera e del Clima (Italy); Pavan Kumar S. Kulkarni, Rui Mendes, Univ. de Évora (Portugal); Manuel Anton, Univ. de Extremadura (Spain); Giorgio Giovanelli, Istituto di Scienze dell'Atmosfera e del Clima (Italy); Ana Maria Silva, Univ. de Évora (Portugal)

Monitoring of atmospheric compounds at high latitudes is a key factor for a better understanding of the processes driving the chemical cycles of ozone and related chemical species. In this frame, the GASCOD (Gas Analyzer Spectrometer Correlating Optical Differences) equipment is installed at the Mario Zucchelli Station

(MZS - 74.69S, 164.12E) since December 1995, carrying out observations of nitrogen dioxide and ozone. The recent advances in sensor technologies and processor capabilities, suggested the setup of a new equipment, based on the same optical layout of the 'old' GASCOD, with enhanced performances and improved capabilities for the measurements of solar radiation in the UV-visible spectral range (300-700nm). The efforts accomplished, allowed for the increase of the investigated tracers. Actually, mainly due to the enlargement of the covered spectral range and to the adoption of a CCD sensor, in addition to the nitrogen dioxide (NO<sub>2</sub>) and ozone (O<sub>3</sub>) compounds, others species can be monitored with the new instrumental setup such as bromine, chlorine and iodine oxides (BrO, ClO and IO). The innovative equipment called GASCODNG (GASCOD New Generation) was installed at MZS during the 2012/2013 Italian Antarctic expedition, in the framework of the research projects SAMOA (Automatic Station Monitoring Antarctic Ozonosphere) and MATAGRO (Monitoring Atmospheric Tracers in Antarctica with Ground Based Observations) funded by the Italian and Portuguese Antarctic programs respectively.

In this paper a brief description of the new equipment is provided, highlighting the main improvements with regard to the 'old' one. Furthermore the full dataset (1996 - 2012) of NO<sub>2</sub> total columns, obtained with the GASCOD installed at MZS, are compared with the data obtained with satellite borne equipments (GOME, SCIAMACHY and OMI). The periods covered by the comparison are: 1996-2003 - GASCOD/GOME; 2002-2010 - GASCOD/SCIAMACHY and 2004-2012 - GASCOD/OMI. The best fits of the GASCOD datasets over the different satellites time series give satisfactory results presenting determination coefficients (R<sup>2</sup>) in the range 0.68 ~ 0.93.

Finally, the first results retrieved from the measurements of the GASCODNG during the Summer expedition 2013 are presented, and discussed.

#### 8890-6, Session 1

### Remote sensing monitoring of the global ozonosphere

Fabrizio Ravegnani, Silvia Genco, Daniele Bortoli, Istituto di Scienze dell'Atmosfera e del Clima (Italy)

The use of CFCs, which are the main responsible for the ozone depletion in the upper atmosphere and the formation of the so-called "ozone hole" over Antarctic Region, was phase out by Montreal Protocol (1989). CFC's concentration is recently reported to decrease in the free atmosphere, but severe episodes of ozone depletion in both Arctic and Antarctic regions are still occurring. Nevertheless the complete recovery of the Ozone layer is expected by about 2050, assuming the full compliance of the Montreal Protocol and its amendments as well as the absence of un-accounted effects.

The ozonosphere protects the biosphere from the harmful effects of UV radiation (in particular the UV-B radiation), therefore the decreasing of the stratospheric ozone concentration can lead to harmful effects like increasing of skin cancer and also alteration of marine ecosystem.

Recent simulation of perturbations in stratospheric chemistry highlight that circulation, temperature and composition are strictly correlated and they influence the global climate changes. In fact chemical composition plays an important role in the thermodynamic of the atmosphere, as every gaseous species can absorb and emit in different wavelengths, so their different concentration is responsible for the heating or cooling of the atmosphere. Consequently changing in temperature gradients can create anomalous circulation in atmosphere.

Therefore long-term observations are required to monitor the evolution of the stratospheric ozone layer. Measurements from satellite remote sensing instruments, which provide wide coverage, are supplementary to selective ground-based observations which are usually better calibrated, more stable in time and cover a wider time span. The combination of the data derived from different space-borne instruments calibrated with ground-based sensors is needed to produce homogeneous and consistent long-term data records. These last are required for robust investigations and especially for trend analysis.

Here, we perform a review of the major remote-sensing techniques and of the principal datasets available to study the evolution of ozone layer in the past decades and predict future behavior. Trend analysis for selected tracers and major physical parameters involved in stratospheric chemistry and dynamics will be presented and discussed.



8890-7, Session 1

## Spectral reference data of molecules relevant to Earth's atmosphere: impact of European metrology research on atmospheric remote sensing

Olav Werhahn, Andrea Pogány, Javis A. Nwaboh, Viktor Werwein, Volker Ebert, Physikalisch-Technische Bundesanstalt (Germany)

The European metrology research has seen a tremendous change in focus on research impacting specific fields of application. The European Metrology Research Programme (EMRP) [1] in its different calls on environment and energy subjects has revealed a lot of new metrology projects devoted to problems, applications, and stakeholder needs in atmospheric sensing, pollution management, air quality assessments, and new energy technologies. Two of these projects are focusing on metrology for air quality and on metrological aspects of spectral reference data for atmospheric monitoring [2, 3]. We will present the potentials of metrological infrared spectroscopy to measurement needs in atmospheric sensing, describe current deficiencies regarding the quality of spectral reference data and show some examples of new initiatives to improve upon the current situation. Both supported by our group, they include the development of a European infrastructure for traceable spectral reference data and the development of field-employable spectrometric transfer standards. However, in the presentation this is demonstrated by means of standardized measurement approaches we are developing and by new measurement results regarding H<sub>2</sub>O, CO<sub>2</sub>, and N<sub>2</sub>O molecular line parameters, like line strengths and pressure broadening coefficients. Further molecular species are currently being interrogated by us. All of them are key to the earth atmosphere's understanding as well as to the interpretation of observed atmospheric spectra, as such recorded in remote sensing applications. Molecular line data are required to process raw spectra in order to extract column concentrations or local emission rates of specific analytes. Without molecular line data, all instruments were to calibrate frequently by means of certified reference gas mixtures which were to keep available onboard throughout the instrument's life time. At present, many instruments use line data from managed line collections like HITRAN and GEISA [4, 5]. These comprise paramount information on many thousands of lines for many different molecular species, but, modern remote sensing applications like CO<sub>2</sub> emission monitoring by satellites tend to significantly tighten data quality objectives and thus require improved data quality that go beyond the present data bases. In this presentation we will show how metrology attempts to benefit this aim.

[1] The EMRP is jointly funded by the EMRP participating countries within EURAMET and the European Union. <http://www.emrponline.eu> .

[2] Metrology for chemical pollutants in air (MACPoll, project code ENV01), <http://www.macpoll.eu> .

[3] Spectral reference data for atmospheric monitoring (EUMETRISPEC, project code ENV06), <http://www.eumetrispec.eu> .

[4] Rothman LS, Gordon IE, Barbe A, Benner DC, Bernath PF, Birk M, et al. The HITRAN 2008 molecular spectroscopic database. *J Quant Spectrosc Radiat Transf* 2009; 110(9-10):533-572.

[5] Jacquinet-Husson N, Crepeau L, Armante R, Boutammine C, Chédin A, Scott NA, et al. The 2009 edition of the GEISA spectroscopic database. *J Quant Spectrosc Radiat Transf* 2011; 112:2395-2445.

8890-8, Session 1

## Retrievals of atmospheric CO<sub>2</sub>, CH<sub>4</sub> and optical path modifications from the GOSAT observations

Andrey I. Bril, Sergey Oshchepkov, Tatsuya Yokota, Yukio Yoshida, Isamu Morino, Osamu Uchino, Dmitry A. Belikov, Shamil Maksyutov, National Institute for Environmental Studies (Japan)

We present retrievals of the column-averaged dry air mole fraction of atmospheric carbon dioxide (XCO<sub>2</sub>) and methane (XCH<sub>4</sub>), which were derived from the radiance spectra measured by Greenhouse gases Observing SATellite (GOSAT) in the short wave infrared (SWIR) region.

We have applied new version of the Photon path-length Probability Density Function (PPDF) -based algorithm [1] to estimate XCO<sub>2</sub> and PPDF parameters. These parameters serve to allow for optical path modification due to atmospheric light scattering and they are retrieved simultaneously with CO<sub>2</sub> concentration using radiance spectra from all available GOSAT SWIR bands (oxygen A-band, 1.6- $\mu$ m, and 2.0- $\mu$ m CO<sub>2</sub> absorption bands). This permits satellite data processing under non-negligible light path modification, thereby substantially increasing the number of successfully retrieved atmospheric greenhouse gases observations.

Three dimensional PPDF model was applied for the atmospheric light scattering correction. This model permits an arbitrary number of gas layers and assumes three atmospheric layers within which the photon trajectories can be modified. These latter overlapping layers serve to describe light path modification by Rayleigh light scattering and combined Rayleigh and aerosol light scattering. Main retrieved PPDF parameters include layer altitudes, layer relative reflectivity, and scaled first moment of the PPDF describing multiple reflection and scattering of light within the layers.

For the methane abundance retrieval from 1.67- $\mu$ m absorption band we applied optical path correction based on PPDF parameters from 1.6- $\mu$ m CO<sub>2</sub> absorption band. Similarly to widely used CO<sub>2</sub>-proxy technique, this correction assumes identical light path modifications in 1.67- $\mu$ m and 1.6- $\mu$ m bands. However, PPDF-based approach is believed to offer some advantages over proxy technique: the proxy technique needs modeled XCO<sub>2</sub> values to compute XCH<sub>4</sub>, whilst the PPDF-based approach does not use any prior assumptions on carbon dioxide concentrations.

Both carbon dioxide and methane GOSAT retrievals were validated using ground-based Fourier Transform Spectrometer (FTS) measurements provided by the Total Carbon Column Observing Network (TCCON). For XCO<sub>2</sub> we found sub-ppm station-to station bias (GOSAT versus TCCON); single-scan precision (one-sigma) of mostly below 2 ppm (0.5%); correlation coefficient for the Northern Hemisphere TCCON stations above 0.8. We found XCH<sub>4</sub>, single-scan precision below 1 % and correlation coefficient above 0.8.

We analyzed XCO<sub>2</sub> and XCH<sub>4</sub> GOSAT-PPDF retrievals for 26 months of GOSAT operation from June 2009 that included more than one million single scans. In addition to the analysis of the observations over 12 TCCON stations we focused on the data under conditions of strong optical path modifications due to atmospheric light scattering (e.g. over-desert and sun-glint observations). We estimated temporal and spatial trends (inter-annual XCO<sub>2</sub> and XCH<sub>4</sub> growths, seasonal cycles, latitudinal gradients) and compared them with modeled data as well as with other GOSAT retrieval algorithms.

1. S. Oshchepkov, A. Bril, T. Yokota, et al. *Applied Optics*, 52, 1339-1350 (2013)

8890-9, Session 2

## Long-term detection of mixing layer height by integration of ceilometer and radio-acoustic sounding system measurements

Klaus Schäfer, Stefan Emeis, Michael Tuma, Carsten Jahn, Maria Hoffmann, Karlsruher Institut für Technologie (Germany); Christoph Muenkel, Vaisala GmbH (Germany)

The mixing layer height (MLH) is an important factor which influences exchange processes of ground level emissions. The continuous knowledge of MLH is supporting the understanding of processes directing air quality. If the MLH is located near to the ground, which occurs mainly during winter and night-time, air pollution can be high due to a strongly limited air mass dilution.

From April 2008 until July 2010 different methods for long-term continuous remote sensing of MLH are operated simultaneously in Augsburg. The Vaisala ceilometer CL31 is used which is an eye-safe commercial mini-lidar system. The ceilometer measurements provide information about the range-dependent aerosol concentration; gradient minima within this profile mark the borders of mixed layers. Special software for these ceilometers with MATLAB provides routine retrievals of lower atmosphere layering from vertical profiles of laser backscatter data. A RASS (Radio-Acoustic Sounding System) from Metek is applied which detects the height of a turbulent layer characterized by high acoustic backscatter intensities due to thermal fluctuations and a high variance of the vertical velocity component as well as the vertical temperature profile from the detection of

acoustic signal propagation and thus temperature inversions which mark atmospheric layers. This is the input for a software-based determination of MLH.

These data are integrated if the MLH results of both remote sensing methods complete each other to get continuous information about MLH. The procedure includes algorithms to take RASS but not ceilometer information during cloudiness and fog as well as to avoid strong jumps in MLH information if the lowest layer is not detected during some time by ceilometer.

## 8890-10, Session 2

### **Influence of mixing layer height measured by ceilometer upon traffic-related air pollution in urban area**

Klaus Schäfer, Stefan Emeis, Hong Ling, Carsten Jahn, Maria Hoffmann, Karlsruher Institut für Technologie (Germany); Christoph Muenkel, Vaisala GmbH (Germany)

Ceilometers are applied by KIT/IMK-IFU to detect layering of the lower atmosphere continuously. This is necessary because not only wind speeds and directions but also atmospheric layering and especially the mixing layer height (MLH) influence exchange processes of ground level emissions. It will be discussed how the ceilometer monitoring information is used to interpret the traffic-related air pollution near the ground.

The information about atmospheric layering is continuously monitored in Augsburg by uninterrupted remote sensing measurements with the Vaisala ceilometer CL31 which is an eye-safe commercial mini-lidar system. Special software for this ceilometer with MATLAB provides routine retrievals of lower atmosphere layering from vertical profiles of laser backscatter data. The path-averaged concentrations of NO, NO<sub>2</sub>, O<sub>3</sub> and HCHO are measured with a DOAS (Differential Optical Absorption Spectroscopy) in Augsburg across main traffic roads since March 2012. Ground-based (Airport Augsburg) and radiosonde (Oberschleißheim) measured meteorological data are taken from the German National Meteorological Service (DWD).

The weather situations are characterized, the meteorological influences upon air pollutant concentrations like wind speed and wind direction are studied and the correlations of ceilometer MLH with traffic-related air pollutant concentrations are determined. The meteorological characteristics for high traffic-related air pollution are shown.

## 8890-11, Session 2

### **Investigation of boundary layer dynamics, dust and volcanic ash clouds with laser ceilometer**

Christoph Munkel, Vaisala GmbH (Germany); Klaus Schäfer, Stefan Emeis, Karlsruher Institut für Technologie (Germany)

The main purpose of eye-safe laser ceilometers is regular reporting of cloud base height, vertical visibility, and cloud cover. These instruments operate unattended in harsh weather conditions. The application of state-of-the-art electronics increases the quality of backscatter profiles and thus qualifies modern ceilometers for applications beyond cloud base detection. These include the automated characterization of the boundary layer structure, determination of the layering as e.g. height of the mixing layer, monitoring of dust and volcanic ash clouds, and estimations of the melting layer height and of particulate matter concentration.

This presentation concentrates on the ability of the Vaisala ceilometers CL31 and CL51 to monitor structure and dynamics of elevated aerosol layers. The single lens optics of these instruments that uses the inner part of the lens for transmitting and its outer part for receiving light provides sufficient overlap of the transmitter light cone and the receiver field-of-view over the whole measuring range. This provides an improved near-range performance compared to two lens systems and allows reliable detection of very low nocturnal stable layers below 200 m not seen by other instrument types.

The long-term measuring stability and robustness of these ceilometers enables their application in campaigns monitoring climate change

effects. That is why three of the German Terrestrial Environmental Observatories (TERENO) run by the Karlsruhe Institute of Technology are equipped with CL51 ceilometers. These observatories are dedicated to gain information about the effects of regional climate change on the coupled C and N cycles. The Technical University of Denmark (DTU) utilizes the high near-range sensitivity of the CL51 to study arctic cloud formation at Station Nord, Greenland. Recent applications include site assessment for solar energy applications in the Arabic Peninsula, where sunlight is often partly blocked by dust and sand, and monitoring of Sahara dust cloud events over Germany.

The measuring examples presented from these sites show the different types of elevated aerosol layers and their dynamic evolution. A European COST action has been proposed to discuss the ability of such data to improve numerical weather predictions. Backward trajectory calculations with the HYSPLIT trajectory model provided by the NOAA Air Resources Laboratory have been carried out to investigate possible sources of such layers, including eruptions of the Eyjafjallajökull and Puyehue-Cordón Caulle volcanoes, that have been monitored by a CL31 ceilometer in Augsburg, Germany, and by a CL51 ceilometer at the German Antarctic research base Neumayer Station III.

## 8890-12, Session 2

### **A static birefringent interferometer for the measurement of upper atmospheric winds**

Jeffery A. Langille, William E. Ward, William A. Gault, Univ. of New Brunswick (Canada); Alan D. Scott, Driss Touahri, COM DEV Canada (Canada); Andrew Bell, EMS Aviation (Canada)

An instrument concept called the Birefringent Imaging Doppler Wind Interferometer (BIDWIN) is being validated in the Atmospheric and Space Physics Lab at the University of New Brunswick in collaboration with COM DEV Ltd (Ottawa, Canada) to determine its capabilities for measuring Doppler wind fields in the Earth's nightglow. The instrument is adapted from a similar approach used to obtain two dimensional images of high speed (~1000 m/s) flow fields in plasmas at the Australian National University. For that application the precision of the wind measurements was not explored in detail. With BIDWIN, the intent is to obtain ~ 5 m/s precision on each bin of a CCD image of the wind field. An examination of the instrument concept and sensitivity of the wind measurements made using this approach is undertaken to determine the feasibility of this criterion. The BIDWIN has the advantage over other instruments that can be used for a similar purpose (such as the field widened Michelson interferometer and Fabry-Perot interferometer) in that it has no moving parts, has a large throughput, is light weight and is relatively cheap to construct. In this paper, the instrument concept is presented and the instrument is described using Jones matrices. The non-ideal instrument effects are also explored. Measurements taken using a proto-type of the instrument constructed in the lab at the University of New Brunswick are compared to the Jones matrix model and are used to verify the instrument concept.

## 8890-13, Session 2

### **Capability and limitations in measuring atmospheric nitrogen dioxide column amounts by means of the MKIV Brewer spectrophotometers**

Henri Diémoz, Agenzia Regionale per la Protezione dell'Ambiente della Valle d'Aosta (Italy) and Univ. degli Studi di Roma La Sapienza (Italy); Vladimír Savastíouk, International Ozone Services Inc. (Canada); Anna Maria Siani, Univ. degli Studi di Roma La Sapienza (Italy)

In 1985, an automated Brewer ozone spectrophotometer was modified to add capability to measure visible radiation in the 450 nm region and thus retrieve atmospheric nitrogen dioxide (NO<sub>2</sub>) besides ozone and sulphur dioxide. Since then, more than 60 MKIV Brewer spectrophotometers are in operation worldwide and long-term NO<sub>2</sub> records were collected at several sites, both in the direct-sun and zenith-sky geometries, using the original algorithm developed by Environment Canada.

As shown by Barton (2007) and Cede (2006), the latter with regards to the MKIII Brewer instruments operating in the UV, some atmospheric constituents (mainly the oxygen dimer and water vapor) and other species (ozone, aerosols, Rayleigh scattering and spectrally-flat factors) already accounted for in the retrieval algorithm can potentially interfere at the operational selected wavelengths. Also, Brewer zenith-sky estimations are affected by the Ring effect and both direct-sun and zenith-sky geometries may be sensitive to the effective temperature of the atmospheric NO<sub>2</sub> and even slight wavelength misalignments of the monochromator.

To evaluate the influence of the various effects on NO<sub>2</sub> measurements, a MKIV Brewer #066 was accurately characterized and the resulting data were used along with a radiative transfer model (libRadtran). The contribution of each factor was analytically determined in the case of the standard Brewer retrieval algorithm, which is based on irradiance measurements at five different wavelengths. Introducing an additional wavelength, making use of the slit regularly employed for the mercury calibration, may lead to relevant improvements in the signal-to-noise ratio or, as an alternative, in removing the contribution of interfering species (e.g. O<sub>4</sub>). The impact of such a modification were quantitatively assessed.

Two solutions are then proposed to further improve the retrieval of NO<sub>2</sub> with MKIV Brewer spectrophotometers. The first method uses eleven wavelengths for each measurement ("Umkehr-like technique"), thus increasing the number of equations in the retrieval algorithm and allowing the determination of the columnar abundances of other influencing species. Conversely, the second method consists in finding an optimal setting of the monochromator, displacing the diffraction grating, in order to reduce the contribution of interfering factors. Capability and limitations of both techniques were assessed.

Furthermore, great improvements were found when using recently laboratory-measured cross-sections and Rayleigh optical depth calculations instead of the obsolete data supplied to the standard Brewer NO<sub>2</sub> algorithm (e.g. NO<sub>2</sub> cross-sections by Johnston, 1976).

The practicability of measuring the oxygen dimer and water vapor at suitable wavelengths in the allowed spectral range, as well as the effective temperature of nitrogen dioxide, was also investigated. It was found that good measurements of O<sub>4</sub> using the absorption band at 477 nm, which are valuable both in aerosol applications and for cloudscreening purposes, can be performed with the MKIV Brewer spectrophotometers, while the H<sub>2</sub>O signal is too weak compared to the instrumental noise. Finally, the effect of NO<sub>2</sub> temperature is colinear with the NO<sub>2</sub> cross-section, thus making the separation of the two effects not possible.

The results of this study may be of help in upgrading the MKIV Brewer algorithm for the retrieval of NO<sub>2</sub> column amounts. Accurate reprocessing of raw data from several long-term series registered worldwide will then be possible.

## 8890-14, Session 2

### Optimum interpolation algorithms for ABI multiple channel radiance downscaling processing

Haibing Sun, I. M. Systems Group, Inc. (United States); Walter Wolf, National Oceanic and Atmospheric Administration (United States); Thomas S. King, Shanna Sampson, I. M. Systems Group, Inc. (United States); Eric S. Maddy, Science and Technology Corp. (United States)

The Advanced Baseline Imager is the primary instrument on GOES-R for imaging Earth's weather, climate, and environment, it will provide over 65% of all the mission data products currently defined. ABI will be able to view the Earth with 16 different spectral bands, including two visible channels, four near-infrared channels, and ten infrared channels. The GOES-R ABI is designed to observe the western hemisphere in various time intervals at 0.5, 1, and 2 km spatial resolutions in visible, near-infrared (IR), and IR wavelengths, respectively. For most of the present ABI present retrieval algorithms, the collocated/co-registered radiance dataset at 2 km resolution of all of the bands are required. This requires re-sampling the radiance data from 0.5 or 1 km to 2 km for ABI visible and near-IR bands (2 or 1, 3 & 5 respectively).

The BACKUS-GILBERT (BG) method has been employed by various authors to spatially co-register and invert various data sets while accounting for different spatial and error propagation behaviors. In

particular, the earth science remote sensing community has employed BG for footprint-matching between various satellite data channels (usually in the microwave spectrum).

In this paper, spatial resolution characteristic of the ABI fixed grid level1b radiance data are discussed. Basing on the BACKUS-GILBERT (BG) method, an optimum interpolation algorithms developed for ABI multiple channel Radiance Down-scaling Processing is present.

## 8890-15, Session 2

### GOMOS one-step retrieval algorithm

Janne Hakkarainen, Marko Laine, Johanna Tamminen, Finnish Meteorological Institute (Finland)

Global Ozone Monitoring by Occultation of Stars (GOMOS) is a limb-viewing satellite instrument onboard the Envisat platform, that was in operation during 2002-2012. During these years GOMOS observed about 880 000 vertical profiles of ozone, NO<sub>2</sub>, NO<sub>3</sub> and aerosols. Half of these measurements were made during night time.

The GOMOS measurement principle is relatively simple based on the stellar occultation technique. The challenge of the stellar light as a light source is the low signal-to-noise ratio and that the quality of the measurements varies from star to star. The operative GOMOS retrieval algorithm works in two parts: the spectral inversion and the vertical inversion. In the first part, horizontally integrated line densities of O<sub>3</sub>, NO<sub>2</sub>, NO<sub>3</sub> and aerosols are retrieved simultaneously using a combination of absolute and differential cross sections. In the second part, profiles are retrieved from these horizontally integrated line densities at different tangent altitudes. In the latter part, Tikhonov regularization is applied to compensate uncorrelated scintillation effects as well as the low signal-to-noise ratio.

In this paper, we present an alternative retrieval algorithm for GOMOS satellite measurements. The presented algorithm is based on the so called one-step approach where both spectral and vertical inversions are executed simultaneously. This approach has several attractive features and it is statistically more sound than the operative algorithm. In particular, the one-step approach allows the better use of smoothness prior information and, unlike in the operative algorithm, the prior given to one specie affects also the other species as well. This feature is critical when going near the detection limit, especially in the upper troposphere lower stratosphere (UTLS) region. The main challenge in GOMOS one-step algorithm is to find the correct smoothness priors for the different species and altitudes.

In this paper, we give a technical description of the one-step retrieval algorithm. We discuss the statistical validity and the role of priors in the algorithm. In addition, different numerical techniques to solve the one-step inversion problem and the limitation in speed are discussed.

As a case study, we consider the GOMOS measurements in Arctic region during the exceptional ozone depletion conditions in spring 2011. It is shown how the quality of the ozone profiles can be improved by introducing the one-step algorithm and how requiring smoothness of aerosol profile will also affect the ozone retrievals. The improvement is drastic in the lower stratosphere at 15-20 km altitude. The retrieved profiles are also compared against the ozone soundings made in Sodankylä measurement site in northern Finland.

## 8890-16, Session 2

### Use of satellite data for air quality applications in northern China

Stefanie Schrader, Karlsruhe Institut für Technologie (Germany); Irina N. Sokolik, Georgia Institute of Technology (United States); Bernhard Vogel, Heike Vogel, Peter Suppan, Klaus Schäfer, Stefan Norra, Karlsruhe Institut für Technologie (Germany)

Mineral dust has a significant impact on air quality by reducing visibility and causing adverse health effects on humans such as increased respiratory symptoms and decreased lung function. Ground-based monitoring of PM<sub>10</sub> and PM<sub>2.5</sub> is the common metric used for assessing air quality degradation. Because of vast dust sources in Northern China and Mongolia, a limited number of existing ground-based sites across this region renders air quality monitoring

difficult. Information about air quality within these regions can only be gained by the use of models or satellite data. The goal of this study is to determine satellite value-added information from four different satellite sensors for improving air quality modeling on regional scale and in the Beijing metropolitan area.

We examine MODIS-Aqua, OMI, MISR and CALIPSO lidar aerosol products over Northern China during a severe dust episode in the spring of 2011. During this episode large amounts of mineral dust were transported from the Chinese and Mongolian deserts towards the densely urbanized Chinese coastal area, affecting Beijing.

OMI light-absorbing aerosol index and aerosol optical depth (AOD) from MODIS Deep Blue and MISR were used to characterize the spatiotemporal variability of mineral dust. AOD data gives information about main dust sources and transport pathways of the mineral dust from the sources to the downwind location of the Beijing metropolitan area. The satellite retrieved AOD was also used to validate modeled AOD from the mesoscale weather and aerosol model system COSMO-ART. However these satellite sensors provide no information about the vertical distribution of aerosols which is important for air quality assessment. To provide better understanding of the linkage between total column AOD retrieved from passive satellite sensors and near-ground PM10, we analyze the vertical profile of AOD measured by CALIPSO lidar. The CALIPSO lidar system provides the unique opportunity to get information about the vertical distribution of different types of aerosols. The amount of near surface mineral dust which is most relevant in terms of air quality studies can be determined. In addition, CALIPSO AOD profiles were compared against COSMO-ART modeling results. Using satellite and COSMO-ART data, we assess the contribution of mineral dust to PM10 and air quality degradation for the considered episode in the dust sources and the Beijing urban area.

### 8890-17, Session 2

## The principle of fragmentary spectrum registration for acousto-optical spectrometers based on differential optical absorption spectroscopy

Alexander V. Fadeyev, Vitold E. Pozhar, Vladislav I. Pustovoit, Scientific and Technological Ctr. for Unique Instrumentation (Russian Federation)

In this paper, a new approach for spectral analysis with use of acousto-optical spectrometers (AOS) is proposed and analyzed. The analytical method, named fragmentary spectrum registration (FSR), is based on the unique AOS capability of fast (10<sup>-9</sup>s) random spectral access (RSA). The method is the most efficient for the objects exhibited sparse spectral structure.

The proposed method is based on differential optical absorption spectroscopy (DOAS), which deals with a limited set of spectral differential features (lines) of an object. The use of acousto-optical spectrometers allows detection of only those spectral channels, which are necessary for a complete determination of an object. It gives a substantial (up to 100 times) reduction of detection interval in comparison with the record time of total spectrum. This is particularly important for the tasks such as rapid analysis of multi-component mixtures, in which an instrumental error of each spectral channel (for example noise variations) can affect the accuracy of calculation of all the controlled substances.

To determine the optimal set of spectral channels to be controlled, we have developed an optimization procedure which is a part of the proposed FSR-approach. We have considered a mathematical problem of finding an appropriate criterion and developed all the stages of optimization algorithm to find the set of characteristic features of the measured substances.

It has been developed a software model of an acousto-optical spectrometer in a function of gas analyzer. The model simulates all the main measuring functions according to real-life situations. The use of optimization procedure provides reduction of the total measurement time and provides decrease of measurement error for mixtures containing substances with similar spectral features. It has been shown experimentally that the developed procedure can reduce the measurement time dramatically or reduce up to 2.5 times the error of measurement results (depending on the noise level) at a fixed total measurement time for concentrations varying from common background level up to industrial emissions level. For

numerical experiments, we have used the spectra recorded by the trace gas monitoring system GAOS (gas analytical optical system) based on acousto-optical spectrometer, which provides simultaneous real-time detection of such pollutants as simple oxides (NO<sub>2</sub>, SO<sub>2</sub>, H<sub>2</sub>CO) and aromatic hydrocarbons (C<sub>6</sub>H<sub>6</sub>, C<sub>6</sub>H<sub>5</sub>CH<sub>3</sub>, C<sub>6</sub>H<sub>5</sub>OH, etc.). The developed software package enables the calculation and determination of the optimal set of spectral channels, which ensures short time detection (1 min. for the mixture of 5 substances). It makes possible variation of the set of channels during the registration process and thus provides an opportunity to implement the adaptive spectral analysis algorithms.

As an additional software procedure, we have developed an algorithm of qualitative analysis based on the statistical method of independent component analysis (ICA). Its basic function is to estimate the possible loss of important information during the spectral selection procedures. The use of the FSR method in combination with this algorithm gives new adaptive properties to gas analysis systems based on acousto-optical spectrometers (as well as to any other RSA-systems).

Some implementations of the FSR method combined with ICA-based algorithm for constructing RSA-based real-time adaptive systems are considered.

### 8890-18, Session 3

## Contemplating synergistic algorithms for the NASA ACE Mission (*Invited Paper*)

Gerald G. Mace, The Univ. of Utah (United States)

ACE is a proposed Tier 2 NASA Decadal Survey mission that will focus on clouds, aerosols, and precipitation as well as ocean ecosystems. The primary objective of the clouds component of this mission is to advance our ability to predict changes to the Earth's hydrological cycle and energy balance in response to climate forcings by generating observational constraints on future science questions, especially those associated with the effects of aerosol on clouds and precipitation. ACE will continue and extend the measurement heritage that began with the A-Train and that will continue through Earthcare. In particular, ACE will continue the detailed vertical profiling of aerosol, cloud, and light precipitation properties into a second decade and will allow for the documentation of changes in certain key characteristics of the hydrological cycle over this extended period of time thereby enabling the examination of such change to dominant modes of variability that occur on annual to decadal time scales.

ACE planning efforts have identified several data streams that can contribute significantly to characterizing the properties of clouds and precipitation and the physical processes that force these properties. These include dual frequency Doppler radar, high spectral resolution lidar, polarimetric visible imagers, passive microwave and submillimeter wave radiometry. While all these data streams are technologically feasible, their total cost is substantial and likely prohibitive. It is, therefore, necessary to critically evaluate their contributions to the ACE science goals. We have begun developing algorithms to explore this trade space. Specifically, we will describe our early exploratory algorithms that take as input the set of potential ACE-like data streams and evaluate critically to what extent each data stream influences the error in a specific cloud quantity retrieval. For instance, we will investigate to what extent passive microwave measurements contributes to deriving liquid water content profiles when combined with Doppler radar.

### 8890-19, Session 3

## Automated cloud classification using a ground based infra-red camera and texture analysis techniques

Emal Rumi, Campbell Scientific Ltd. (United Kingdom); David Kerr, Jeremy M. Coupland, Loughborough Univ. (United Kingdom); Andrew Sandford, Mike Brettle, Campbell Scientific Ltd. (United Kingdom)

Clouds play an important role in influencing the dynamics of local and global weather and climate conditions. Continuous monitoring of clouds is vital for weather forecasting and for air-traffic control. Convective clouds such as Towering Cumulus (TCU) can develop into Cumulonimbus clouds (CB). CB clouds are associated with

thunderstorms, turbulence and atmospheric instability. They may produce lightning and other dangerous severe weather conditions, such as strong gusts and hail. Human observers periodically report the presence of CB and TCU clouds during operational hours at airports and observatories; however it is expensive and time limited. Advances in remote sensing instrumentation have provided various means of satellite or ground-based sensing, including radar and sky imaging using visible cameras. Robust, automatic classification of cloud type using ground-based instrumentation can provide valuable information such as in meteorological monitoring, aviation services and other safety critical applications. Modern infrared imaging devices offer the advantage of continuous, real-time (24/7) data capture and the representation of cloud structure in the form of a thermal map, which can greatly help to characterise certain cloud formations. The work presented here utilised a ground based infrared (8-14)  $\mu\text{m}$  imaging device mounted on a pan/tilt unit for capturing high spatial resolution sky images. Images were captured at 320x240 pixel resolution at between 26 and 76 degrees of zenith angle, to avoid spurious thermal signatures from buildings or other objects near the horizon. A set of nine spatially adjacent images were then stitched together to form a panoramic, high resolution image of a section of the sky with a field of view of approximately 62 x 46 degrees. These composite images were then processed to extract 45 separate textural features using statistical and spatial frequency based analytical techniques. These features were used to train a weighted k-nearest neighbour (KNN) classifier in order to determine cloud type at each observed sky section. Ground truth data were obtained by inspection of images captured simultaneously from a visible wavelength colour TV camera at the same installation, with approximately the same field of view as the infrared device. These images were classified by a trained cloud observer into a total of 8 cloud types, including TCU, CB, and clear sky. Results from the KNN classifier gave an encouraging success rate. An overall probability of detection (POD) of 90% was achieved, with a false alarm rate (FAR) of 15%.

### 8890-20, Session 3

#### Remote sensing of water clouds temperature with an IR camera on board the ISS in the frame of JEM-EUSO Mission

Susana Briz, Isabel Fernández-Gómez, Irene Rodríguez Muñoz, Univ. Carlos III de Madrid (Spain); Antonio J. de Castro González, Universidad Carlos III de Madrid (Spain); Fernando López Martínez, Univ. Carlos III de Madrid (Spain); Guadalupe Sáez Cano, María Dolores Rodríguez Frías, Univ. de Alcalá (Spain)

The Extreme Universe Space Observatory (EUSO) is an astronomical telescope that will be hosted by the Japan Experiment Module (JEM) on the International Space Station (ISS). The final objective of this instrument is to detect Ultra High Energy Cosmic Rays (UHECR) and retrieve their properties. However, the JEM-EUSO telescope will not look into the space but to Earth since it will use the Atmosphere as detector. The cosmic rays impact on the atmospheric nuclei and generate secondary particles which produce a cascade of secondary particles. This phenomenon is called 'Extensive Air Shower'. These showers develop and propagate in the atmosphere, excite nitrogen molecules which emit UV fluorescence light. The JEM-EUSO telescope will measure this light from which cosmic ray properties are inferred.

However, the UV radiation interferes with the atmosphere and the clouds. Therefore it is extremely important to detect if there are clouds in the FOV of the telescope. Moreover, the exact cloud top height is crucial for a proper interpretation of the air shower.

In order to measure the cloud top height an IR camera is being designed. It will provide the cloud top temperature from which the height can be retrieved. The camera design is constrained by JEM-EUSO requirements. The most important restrictions among others are the instrument weight and the data rate leading to a bi-spectral camera option with 1 microns-wide bands centered at 10.8 and 12 microns.

The cloud top temperature is retrieved from radiometric information. After the calibration procedure, the IR camera will provide temperature values (brightness temperature). However, this temperature will not be the cloud temperature since the radiance emitted by the cloud is partially absorbed by the atmosphere. Therefore the radiance that

impinges the camera is not exactly the radiance emitted by the cloud. For this reason, algorithms to consider atmospheric effects are needed in order to obtain a better cloud temperature accuracy.

The bi-spectral design of the IR camera has allowed us to develop a Split Window Algorithm to retrieve the temperature of water clouds from the brightness temperatures provided by the IR camera in the bands aforementioned.

The algorithm has been checked in synthetic scenarios at pixel level. The simulations used to generate the scenarios have been carried out with clouds at different levels (i.e. different temperatures) and with diverse atmospheres obtained by changing the vertical profiles of temperature and relative humidity. The results show that the algorithm is able to retrieve the temperature with accuracy much better than the required one by the JEM-EUSO mission of 3K.

The algorithm has also been tested in 2D real scenarios (MODIS images). MODIS measures radiance in 36 spectral bands and provides many products such as brightness temperatures in different bands, cloud top temperature, cloud phase, etc. The algorithm has been applied to MODIS brightness temperatures in bands 31 and 32 which are similar to these ones of the IR camera. The temperatures retrieved by the algorithm are in a very good agreement with the cloud top temperatures given by

MODIS.

### 8890-21, Session 3

#### Two-stage algorithm for cloud detection with ZY-1 02C multispectral measurements

Ye-Yao Wang, National Environmental Monitoring Ctr. (China); Wei-Min Wang, Lijun Yang, Hong Liang, China National Environmental Monitoring Ctr. (China)

Optical remote sensing observations often are the primary data source for many studies and applications in large scale, even in tropical regions. Frequent clouds over moist tropical regions often cause difficulty in obtaining good-quality high-resolution images. Different cloud styles and shadows make it hard to be masked on the images. The ZY-1 02C satellite, where multi-spectral and panchromatic imagers were on-boarded, was launched on 22 Nov. 2011. The objective of this satellite is to acquire data contributing for earth resources and environmental monitoring, as well as for applications such as land use and disaster reduction. The multi-spectral imager has three wavebands, centered at 0.55 micrometer (green), 0.66 micrometer (red) and 0.83 micrometer (near infrared), at a spatial resolution of 10 meters. Panchromatic band, centered at 0.68 micrometer, has a spatial resolution of 5 m and is not used.

In this study, a two-stage algorithm is presented to detect cloud and cloud shadow for ZY-1 02C multi-spectral measurements. First, maximum and minimum filters with a moving window size of 5 by 5 pixels are operated on ZY-1 02C multi-spectral measurements. Optimal thresholds are selected by spatial statistics and visual examination. Pixels in maximum-filtered images with a grey level higher than the given thresholds ( $T_c$ ) are labeled as potential cloud. In contrast, pixels in minimum-filtered images with a grey value lower than the given thresholds ( $T_s$ ) are considered as potential shadow. Then, the contextual are used to mask out errors with potential cloud and shadow (e.g. vegetation canopy-cast shadow, road and bare soil etc.) in previous stage. A window size of 3 by 3 centered at each potential cloud position is searched. If no potential shadow is found the potential cloud is rejected. Meanwhile, each potential shadow also is tested to get the final cloud/shadow mask. Two ZY-1 02C multi-spectral images acquired over Pearl River Delta, a subtropical region in South China, are used to validate the two-stage algorithm. The research result indicates that, two-stage algorithm developed in this study has successfully detected the cloud and shadow on ZY-1 02C multi-spectral images.

### 8890-22, Session 3

#### Estimation of a radiative transfer model in the longwave spectral range: sensitivity study and application to real cases

Michaël Sicard, Santi Bertolín, Univ. Politècnica de Catalunya (Spain); Marc Mallet, Univ. de Toulouse (France) and Ctr.

National de la Recherche Scientifique (France); Philippe Dubuisson, Univ. de Lille 1 (France); Adolfo Comerón, Univ. Politècnica de Catalunya (Spain)

The aerosol radiative effect in the longwave spectral range is often neglected in atmospheric aerosol forcing studies, hence very few research is conducted in this field at local scale, and even lesser at regional scale. However, strong absorbing aerosols, like mineral dust, can have a small, but non-negligible heating effect in the longwave which can slightly counteract the aerosol cooling effect in the shortwave. The objective of this research is to perform a sensitivity study of an aerosol radiative transfer model as a function of dust particle properties. The model used is GAME [Dubuisson et al., 1996] which can compute the radiative forcing of aerosol layers in both the shortwave and the longwave regions under different input conditions. Preliminary radiative forcing simulations in the longwave have already shown an important sensitivity to the following parameters: aerosol size and refractive index, aerosol vertical distribution, humidity, surface temperature and albedo. Before developing the sensitivity analysis, the aerosol radiative transfer model is validated by comparing its outputs with previous published results. Finally, a real event of a strong mineral dust intrusion observed by means of lidar and sun-photometer will also be presented in terms of shortwave and longwave radiative forcing.

8890-23, Session 3

### Gas plume characterization from infrared airborne hyperspectral sensors at high spatial resolution using 3D spatial a priori information

Pierre-Yves Foucher, Ramzi Idoughi, Laurent Poutier, Xavier Briottet, ONERA (France)

The air pollution is a very important issue for industrialized society, both in terms of health (respiratory diseases, allergies...) and in terms of climate change (global warming and greenhouse gas emissions). Anthropogenic sources, especially industrial, emit into the atmosphere gases and aerosols, which play an important role in atmospheric exchanges. However emissions are poorly estimated as most of existing space sensors have a limited spectral range but also a too low spatial resolution. The use of the new hyperspectral airborne sensors as SYSIPHE sensor developed by Onera from visible to the thermal infrared opens the way to new development to improve gas and aerosol plume characterisation.

Hyperspectral imagery in the VIS-NIR and SWIR domains from airborne acquisitions has proven the gain brought by such technique to estimate aerosols and some gaseous species (methane, Carbone dioxide...) over biomass burning or thermal power plant. Unlike SWIR, in the thermal domain (MWIR-LWIR), where are found the signatures of the majority of gas plume, temperature plays an important role. In addition, intrinsically, only the integrated amount of gas column can be detected and gas signal is convolved by ground signature, atmospheric species characterization from airborne observation becomes very challenging. In the last ten years, several works provide linear formalism or bayesian method to detect and quantify gaseous species over industrial site. These methods are based on the differential signature between a clean pixel and a polluted pixel under strong hypothesis. Their main limitations are the heterogeneous environment impact on the performances of these methods and such technique does not take into account the spatial and vertical extent of the plume which can lead to strong errors on thermal contrast.

In this work, a new method for characterizing gas plumes is presented to overcome such limitations using a multi-pixels approach and 3D spatial constraint from chemical transport model (CTM). This method is based on a non linear optimal estimation algorithm using an accurate formalism of cloud gas radiative impact taking into account vertical plume heterogeneity in term of concentration and temperature. The multi-pixel regularisation approach includes spatial 3D shape plume properties from CTM and bayesian information of ground properties. It includes a ground classification of the scene, in order to take account the soil's heterogeneity and the intra-class variability. Then, for each class an appropriate analysis will be followed, to initialize the multi-pixel iterative algorithm. Finally, we use synthetic scenes of industrial area, and airborne acquisitions to validate the method.

8890-24, Session 3

### Aerosol information over Osaka during DRAGON Japan experiment

Itaru Sano, Sonoyo Mukai, Kinki Univ. (Japan); Brent N. Holben, NASA Goddard Space Flight Ctr. (United States); Makiko Nakata, Kinki Univ. (Japan); Nobuo Sugimoto, National Institute for Environmental Studies (Japan)

The distributed regional aerosol gridded observation networks (DRAGON)-Japan experiment was made from March to May in 2012. Seven AERONET instruments were deployed in Osaka area as well as two mountain sites during the period. This high dense AERONET sun/sky radiometer network gives us detail aerosol information over the city.

This work intends to estimate aerosol optical thickness (AOT) over large city Osaka in Japan. Estimating local aerosol distribution is important for understanding local air quality such as PM<sub>2.5</sub>. Our aerosol retrieval method is based on the radiative transfer calculations in the Earth atmosphere surface system with various aerosol conditions. The estimated AOT distribution is validated with the measurements of DRAGON Japan experiment.

8890-25, Session 3

### Temporal variability of aerosol properties during TCAP: Impact on radiative forcing

Evgueni I. Kassianov, James Barnard, Mikhail Pekour, Larry K. Berg, Pacific Northwest National Lab. (United States); Jerome Fast, Pacific Northwest National Lab (United States); Joseph J. Michalsky Jr., National Oceanic and Atmospheric Administration (United States); Kathleen O. Lantz, Cooperative Institute for Research in Environment Sciences (United States); Gary Hodges, National Oceanic and Atmospheric Administration (United States) and Cooperative Institute for Research in Environment Sciences (United States)

Ground-based remote sensing and in situ observations of aerosol microphysical and optical properties have been performed during summertime (June-August, 2013) in the frame of the Two-Column Aerosol Project (TCAP; <http://campaign.arm.gov/tcap/>), which was supported by the U.S. Department of Energy's (DOE's) Atmospheric Radiation Measurement (ARM) Program (<http://www.arm.gov/>). The overall goal of the TCAP field campaign is to study the evolution of optical and microphysical properties of atmospheric aerosol transported from North America to the Atlantic and their impact on the radiation energy budget. During TCAP, the ground-based ARM Mobile Facility (AMF) was deployed on Cape Cod, an arm-shaped peninsula situated on the easternmost portion of Massachusetts (along the east coast of the United States) and generally downwind of large metropolitan areas. The AMF site (at 41.87°N; 70.28°W) was equipped with numerous instruments for sampling aerosol, cloud and radiative properties, including a Multi-Filter Rotating Shadowband Radiometer (MFRSR), a Scanning Mobility Particle Sizer (SMPS), an Aerodynamic Particle Sizer (APS) and the three-wavelength nephelometer. In this study we present an analysis of diurnal and day-to-day variability of the column and near-surface aerosol properties obtained from remote sensing (MFRSR data) and in situ measurements (SMPS, APS, nephelometer data), respectively. In particular, we show that the observed diurnal variability of the MFRSR aerosol optical depth is strong and comparable with that obtained previously from the AERONET climatology in Mexico City, which is expected to have larger aerosol loading. Moreover, we illustrate how the variability of aerosol properties impacts the direct aerosol radiative forcing at different time scales.

8890-26, Session 4

### Application of MAIAC high spatial resolution aerosol retrievals over Po Valley (Italy)

Barbara Arvani M.D., Univ. degli Studi di Modena e Reggio Emilia (Italy); Robert B. Pierce, NOAA / NESDIS Office of

Satellite Operations (United States); Alexei Lyapustin, NASA Goddard Space Flight Ctr. (United States); Yujie Wang, Univ. of Maryland (United States); Sergio Teggi, Grazia Ghermandi, Univ. degli Studi di Modena e Reggio Emilia (Italy)

Particulate matter (PM) is one of the major pollutants studied and monitored as it affects air quality especially the urban areas worldwide. PM particles vary in size and composition. It remains suspended in the air for different period of time and it is generated by both natural and anthropogenic sources. PM with aerodynamics diameters of 10  $\mu\text{m}$  or less is the responsible agent of serious human health effects. Because of this, PM assessment is an important aspect all around the world: many environmental protection agencies are working for a continuous monitoring and assessment of air pollution from surface based stations and for improving the techniques for better results. Today, the use of satellite aerosol measurements to study urban air quality is one of the most important and developed aspects of research. The Moderate Resolution Imaging Spectroradiometer (MODIS) AOD data retrieved at 0.55  $\mu\text{m}$  with a spatial resolution of 10 km have been considered in this work. MODIS, on board of Terra and Aqua satellite, supply daily near-global coverage data. Yet the 10 km resolution of MODIS – AOD product is inadequate for studying spatial distribution of aerosols in urban areas. Nowadays, new data processing methodologies allow the achievement of a better spatial resolution, with a consequent increase of the applicability of Earth Observation data for urban studies. Recently, a new Multi-Angle Implementation of Atmospheric Correction (MAIAC) algorithm was developed for MODIS which provides AOD data at 1 km resolution. The area studied in this work is the Po valley area (northern Italy). Air pollution is an important concern in this valley as it is one of the main industrialized and populated areas of the country. The studied domain is characterized by a relative limited extension, of about 46000  $\text{km}^2$ . Population and industrial activities are located in a large number of urban areas distributed on the valley. Thus in the Po valley, the 10km spatial resolution of MODIS AOD product is too large and inadequate for air quality studies at the urban scale. To mitigate this problematic aspect, we refined the spatial resolution of MODIS AOD product. This has been accomplished by introducing the recently developed MAIAC algorithm over the Po valley. The high-resolution MAIAC aerosol product brings new information about distribution of aerosol sources; its strength is to improve information on air quality assessment by MODIS AOD data retrieved. The MAIAC high-resolution data are requested in different applications including air quality. In this work, the use of MAIAC data at 1 km permitted us to proceed with the examination of the relationship between PM10 concentrations measured at the ground based stations and AOD retrieved data, for 2012 over the studied area. The results suggested that the correlation PM10 – AOD obtained using MAIAC – MODIS AOD data, with increased spatial resolution are used is stronger than that obtained using the standard MODIS-AOD product.

#### 8890-27, Session 4

### Ground-based high resolution Fourier transform spectrometer and its application in Beijing

Dongdong Fan, DFH Satellite Co., Ltd. (China)

The B3M-FTS instrument, inherited from ACE-FTS and PARIS, is built by Canadian ABB and Beijing Vision Sky Aerospace Co., Ltd. The B3M is a complete stand-alone spectrometer designed to operate from the ground in moderate environment. It can acquire atmospheric spectra with the Sun as back illumination. This instrument is an adapted version of the classical Michelson interferometer using an optimised optical layout, and it is a high-resolution infrared Fourier transform spectrometer operating in the 750 to 4100 $\text{cm}^{-1}$  spectral range.

The sort of spectrometer has several interesting advantages such as: a)selectable spectral resolution; b) number of spectral elements is independent of number of detector element(s) and c) well behaved spectral line shape. Using the sun as target, the solar radiance and the infrared absorption signals is measured at high resolution (0.02  $\text{cm}^{-1}$ ) that contain useful information on atmospheric constituents at clear daytime in the ground.

In this paper, the instrument concept of a compact, portable, high-resolution Fourier transform spectrometer is introduced, some test results of the instrument such as ILS and SNR are presented. A signal-to-noise ratio (SNR) better than 100 will be achieved, with a

field-of-view (FOV) of 1.25 mrad and an aperture diameter of 100 mm. Sample atmospheric absorption spectra and corresponding retrieval results measured by the FTS are given. The success of atmospheric composition profile retrieval using the FTS measurements provides an useful way to understand the atmospheric chemistry, and validates the feasibility of atmospheric composition remote sensing using high-resolution FTS.

The B3M-FTS, with a spectral resolution of 0.028 $\text{cm}^{-1}$  and SNR over 100:1, provides the capability to monitor the atmospheric composition changes by measuring the atmospheric absorption spectra of solar radiance. Lots of measurements have been acquired at the Olympics atmospheric observation super-station. Up to now, the VMRs of near 10 trace gases have been retrieved. The success of atmospheric composition profile retrieval using the FTS measurements makes the further application of FTS type payload possible in China in the near future.

#### 8890-28, Session 4

### Retrieval of water cloud top and bottom heights and the validation with ground-based observations

Makoto Kuji, Nara Women's Univ. (Japan)

It is of great interest to investigate the optical, microphysical, and geometrical properties of clouds that play crucial role in the earth climate system. Water clouds are generally optically thick and consequently have a great cooling effect on earth-atmosphere radiation budget. The water clouds usually exist in a lower troposphere where aerosol-cloud interaction occurs frequently, and then cloud droplet size variation influences reflection of solar radiation as well. Further, a cloud layer height is one of the key properties that determine downward longwave radiation and then surface radiation budget. In this study, top height, geometrical thickness and bottom height of a water cloud layer are investigated as cloud geometrical properties in particular.

Several studies show that observation data of some spectral regions including oxygen A-band, enables us to retrieve the cloud geometrical properties as well as the optical thickness, the effective particle radius. In this study, an algorithm was developed to retrieve simultaneously the cloud optical thickness, effective particle radius, top height, geometrical thickness and then bottom height of a cloud layer with the spectral observation of visible, near infrared, thermal infrared, and oxygen A-band channels.

This algorithm was applied to Advanced Earth Observing Satellite ? II / Global Imager (ADEOS-II / GLI) dataset so as to retrieve global distribution of cloud geometrical properties. The retrieved results around Japan were compared with other observation such as ground-based active sensors, which suggests this algorithm work for cloud system over ocean at least although the cloud bottom height was underestimated. The underestimation is attributed to cloud inhomogeneity at this stage and is investigated in detail. Based on this preliminary result, I further applied it to a global dataset and have obtained an initial result. I will continue the global analyses and their validation studies so as to contribute to surface radiation budget and cloud physics studies eventually. In addition, the algorithm will be also applicable to dataset observed with the Global Change Observation Mission 1st-Climate / Second generation Global Imager (GCOM-C1 / SGLI) that Japan Aerospace Exploration Agency (JAXA) has a plan to launch in a few year.

#### 8890-29, Session 4

### Analytical model and spectral correction of vibration effects on Fourier transform spectrometer

Irina Shatalina, Politecnico di Milano (Italy); Frederic Schmidt, Univ. Paris-Sud 11 (France); Bortolino Saggin, Politecnico di Milano (Italy); Nicolas Gac, Matthieu Kowalski, Univ. Paris-Sud 11 (France); Marco Giuranna, Istituto di Fisica dello Spazio Interplanetario (Italy)

Sensitivity to mechanical vibrations of Fourier Transform Spectrometers is a well-known phenomenon. Vibration generated

spectral distortions are especially critical for FTS devoted to atmospheric studies (e.g. Planetary Fourier Spectrometer onboard Mars Express 2003), as the gas composition determination is based on the matching of spectral features deriving from absorption bands that for the low concentration element are comparable with the instrument spectral noise. The adopted techniques aiming at the reduction of the vibration sensitivity (such as the constant optical path step sampling based on reference laser signal trigger), suffer of limitations in the practical implementation: time delays in the acquisition chain and cyclical fluctuations of optical misalignments lead to residual vibration induced modulations of the interferogram and eventually to the so-called ghosts in the spectra. Moreover as it is often impossible to measure the vibrations during the FTS measurement, the position and magnitude of these ghosts cannot be evaluated. Up to now the adopted ghost reduction techniques are mostly based on the averaging of spectra, being the disturbance phase randomly distributed.

This paper presents an innovative data treatment technique able to deal with undesired spectral distortions of unknown nature allowing the single spectrum correction. Such a technique would increase the spatial resolution of the mapping process by avoiding the need of spectral averaging and becomes crucial when the desired information is linked to a particular mapping area associated to an individual spectrum.

As first step of our study we analyze the ghost nature and mechanisms of their formation in detail. The result is the explicit mathematical description of the interferogram modulations generated by the mechanical vibrations. The obtained model allows implementing the second step of the research i.e. the post-processing algorithm.

The proposed approach of vibration effect correction is based on the semi-blind deconvolution method – an iterative numerical algorithm of the series of consecutive deconvolutions. The general problem of the data post-processing was subdivided into three separate sub-problems: definition of the vibration kernel, recovering of the original spectrum from the distorted one and the results validation.

We tested this technique on the data from the PFS. The key-point of the procedure was the kernel determination. The lack of information about the vibrations and their nature is the main difficulty: frequency, intensity and phase with respect to the main signal interferogram are only statistically known from PFS calibration measurements that are performed at most once per orbit. The iterative procedure of kernel definition was performed on smoothed spectral data, each iteration loop including constrained deconvolutions of measured distorted spectrum with signal and kernel estimates. Proposed general constraints were the ones of spectrum smoothness and kernel sparsity. The final deconvolution step was performed on the unsmoothed data, with the aim to retrieve the original spectrum from the distorted one.

Efficiency of this technique strongly depends on the initial guesses for the semi-blind deconvolution input. Also the correct definition of the deconvolution constraints is important. Utilization of additional information about the expected spectral features (e.g. some gas absorption bands, regions of detector low responsivity, any known vibration components, etc.) makes proposed algorithm more robust.

Finally the algorithm proved to be consistent according to the selected efficiency criteria (coming from the available general information about the signal spectral shape).

#### References

- [1] V. Formisano et al., "The Planetary Fourier Spectrometer (PFS) onboard the European Mars Express mission," *Planetary and Space Science*, Vol. 53, (2005).
- [2] B. Saggin, L. Comolli, and V. Formisano, "Mechanical disturbances in Fourier spectrometers," *Applied Optics*, Vol. 46, (2007)
- [3] L. Comolli, and B. Saggin, "Evaluation of the sensitivity to mechanical vibrations of an IR Fourier spectrometer," *Review of Scientific Instruments*, Vol. 76, (2005).
- [4] M. Giuranna et al., "Calibration of the Planetary Fourier Spectrometer short wavelength channel," *Planetary and Space Science*, Vol. 53, (2005).

#### 8890-30, Session 4

### MicroMIMA FTS: design of spectrometer for Mars atmosphere investigation

Irina Shatalina, Bortolino Saggin, Diego Scaccabarozzi, Roberto Panzeri, Politecnico di Milano (Italy); Giancarlo Bellucci, Istituto Nazionale di Astrofisica (Italy)

This paper is devoted to the miniaturized Fourier Transform Spectrometer "MicroMIMA" (micro Mars Infrared MApper) design. The instrument has been designed for spectral characterization and monitoring of the Martian atmosphere, bound to investigate its composition, minor species abundances and evolution during time. The spectral resolution of MicroMIMA is of 2 cm<sup>-1</sup> (with the option to be extended up to 1 cm<sup>-1</sup>) that allows to recognize the spectral features of the main elements of interest in the atmosphere and in particular to assess methane abundance with ppb resolution.

The optimal instrument configuration has been set in order to achieve the highest sensitivity in the 2 to 5 μm spectral range, along with the reduction of possible noise, i.e. the Signal-to-Noise Ratio (SNR) has been used as figure of merit. The optimization has been carried-out under the constraints of instrument mass, power and spectral resolution.

The theoretical SNR has been maximized starting from the analytical expressions for Noise Equivalent Spectral Radiance. NESR reduction was achieved by means of the optical layout geometry optimization and by selection of optical elements that offer highest efficiencies for the instrument wavenumber range of interest. Afterwards for the proposed optical layout we performed evaluation of the theoretical SNR for different application cases: laboratory observations by the instrument on the Earth and actual acquisition of Martian atmosphere spectrum during the mission.

At the first step the typical terrestrial spectrum has been assumed as signal and the theoretical SNR evaluated for a perfectly aligned instrument under different incident radiation conditions (accounting also for different meteorological conditions). The obtained results with SNR level above 1.5x10<sup>5</sup> have shown the high efficiency of the instrument for the in-lab observations.

As second step the expected SNR during the Martian observations has been evaluated, taking the spectrum of the Solar Black Body radiation as the approximate Martian spectrum. The determined SNR levels were higher than 5x10<sup>4</sup> even using NESR measured in laboratory conditions.

The third step of the instrument performances evaluations was focused on the trace gas detection capability of the instrument. The critical point in the analysis of the atmospheric composition is the identification of the abundance of special gases even at low concentrations; methane is an example being it also a byproduct of biological activity. The evaluation of the SNR in the absorption band identification activity has been performed for the methane detection with the expected gas concentration varying around 10-20 ppbv [1, 2]. The evaluation of the SNR, using the expected depth of the methane absorption band as signal, has proved the instrument capability of gas detection with the required resolution.

#### References

- [1] V. Formisano, S. Atreya, T. Encrenaz, N. Ignatiev, M. Giuranna, "Detection of Methane in the Atmosphere of Mars", *Science*, Vol. 306 (2004).
- [2] A. Geminali, V. Formisano, G. Sindoni "Mapping methane in Martian atmosphere with PFS-MEX data", *Planetary and Space Science*, Vol. 59 (2011).
- [3] B. Saggin, E. Alberti, L. Comolli, M. Tarabini, G. Bellucci, S. Fonti, "MIMA, a miniaturized infrared spectrometer for Mars ground exploration: part III, thermomechanical design", *Sensors, Systems, and Next-Generation Satellites XI*, Proc. of SPIE Vol. 6744, 67441S, (2007)



8890-31, Session 4

## Assessing satellite based PM<sub>2.5</sub> estimates against CMAQ model forecasts

Lina Cordero, The City College of New York (United States); Nabin Malakar, Yonghua Wu, City College of New York (United States); Barry M. Gross, Fred Moshary, The City College of New York (United States); Mike Ku, New York State Dept. of Environmental Conservation (United States)

Fine particulate matter with particle diameters < 2.5 microns (PM<sub>2.5</sub>) has been linked to respiratory and pulmonary difficulties and for this reason, strong concentration guidelines have been developed by the EPA to limit exposure. Efforts to connect surface PM<sub>2.5</sub> to satellite retrieval of Aerosol Optical Depth (AOD) have been made based on statistical approaches connecting AIRNow PM<sub>2.5</sub> measurements and satellite AOD for different seasons and geographic regions. However, this approach does not account for complex aerosol behavior including Planetary Boundary Layer dynamics. In another approach, the use of models are an attempt to account for such factors as RH modification, aerosol speciation inhomogeneity and complex Planetary Boundary Layer (PBL) height dynamics. For example, a Global Model (GEOS-CHEM) is used to estimate on a daily basis, the spatial relationship between forecast PM<sub>2.5</sub> and column path AOD which can then be used with satellite AOD estimates. This approach has been developed as part of IDEA (Infusing satellite Data into Environmental air quality Applications) and real time spatial maps of PM<sub>2.5</sub> based on this methodology have been made operational. However, one difficulty with the GEOS-CHEM approach is the poor spatial resolution symptomatic with global models with a spatial resolution of 2.5 degrees.

To improve on this, the WRF/CMAQ model is a high resolution algorithm which accounts for physically based meteorological factors and surface boundary conditions including emission inventories to estimate particulate concentrations and vertical distributions.

In this presentation, we focus on a detailed assessment of both the regression based satellite retrieval algorithms and the GEOS-CHEM based approach to the WRF/CMAQ model outputs. In making this comparison, it is well known that strong biases in the PM<sub>2.5</sub> model exist and manifests themselves on seasonal periods. However, in making a relevant comparison with regression based satellite estimates, a suitable regression based post-analysis can be made to the CMAQ PM<sub>2.5</sub> in comparison to EPA AQS surface network station measurements for seasonal and diurnal periods to better understand the relative merits of satellite based and model based PM<sub>2.5</sub> estimates.

As part of our analysis, we first explore the baseline performances of both the CMAQ model and the satellite based regression approach to provide robust estimators for PM<sub>2.5</sub> measured against the EPA AQS surface network. In particular, we find that the CMAQ based approach after post-processing results in a significantly more robust retrieval for all seasonal cases although summer comparisons are much closer as can be expected from the improved mixing of aerosols in the PBL and improved satellite AOD performance due to better solar geometry. Unfortunately, the computer processing makes the full WRF/CMAQ retrievals difficult. In addition, the GEOS-CHEM approach's performance is actually less accurate than the satellite based regression algorithm which seems to be a function of the model limitations. In particular, we explore the question of model limitations by reducing the spatial resolution of CMAQ retrievals. In particular, we find significant degradation as we reduce the CMAQ resolution to GEOS-CHEM values. In addition, we explore climatological PM<sub>2.5</sub>/AOD factors from CMAQ as an alternative approach which may reduce computational limitations.

8890-32, Session 4

## Uncertainty quantification in aerosol optical thickness retrieval from Ozone Monitoring Instrument (OMI) measurements

Anu Määttä, Marko Laine, Johanna Tamminen, Finnish Meteorological Institute (Finland); Pepijn Veefkind, Koninklijk Nederlands Meteorologisch Instituut (Netherlands)

The space borne measurements provide a global view of atmospheric

aerosol distribution. The Ozone Monitoring Instrument (OMI) on board NASA's EOS-Aura satellite is a Dutch-Finnish nadir-viewing solar backscatter spectrometer measuring in the ultraviolet and visible wavelengths. OMI measures several trace gases and aerosols which affect the air quality and climate. The OMI aerosol measurements are also used for example for detecting volcanic ash plumes, wildfires and transportation of desert dust.

The operational OMI multi-wavelength aerosol algorithm OMAERO derives aerosol characteristics including aerosol optical thickness (AOT) and single scattering albedo. The algorithm uses a number of microphysical aerosol models representing varying atmospheric aerosol conditions. In the retrieval, the candidate aerosol models are fitted to the observations in the least-squares sense. The unknown AOT is finally determined from the best fitting aerosol model.

Here we present a methodology for quantifying the uncertainty in the aerosol model selection and its influence to the retrieved AOT. Our approach is based on Bayesian approach, and therefore all unknowns and quantities involved are treated as random variables. The observed information is combined with a priori information and the solution is expressed as a posterior probability distribution.

The pre-calculated aerosol models are simplifications of the real aerosol conditions in the atmosphere. If this discrepancy between aerosol models and the reality is not taken into account, the posterior probability distribution of unknown AOT becomes unrealistically narrow, resulting misleading confidence. However, this additional uncertainty can be taken into account in the statistical analysis. We have used a Gaussian process to characterize this model error (often called model discrepancy). The Gaussian process is a stochastic process that is defined by its mean and covariance function. The covariance function has been estimated by studying ensembles of residuals of aerosol model fits. By including this model discrepancy in the retrieval problem the posterior distribution of AOT will have more realistic uncertainty level.

In practice, there can be more than one aerosol model that fit the observations equally well. By applying a Bayesian model averaging technique, the weighted average of posterior distributions over the best models is obtained and the uncertainty related to the model selection can be taken into account, also.

This presentation describes a methodology for improving the uncertainty quantification in remote sensing of aerosols. We characterize the uncertainty originating from the pre-calculated aerosol models and from the aerosol model selection. These uncertainties are included in the uncertainty estimate of the unknown model parameter. The retrieved AOT is given as a probability density function that describes the confidence level of the AOT within the best aerosol models. Real examples of applying the methodology for retrieving AOT from Ozone Monitoring Instrument are presented.

8890-33, Session 4

## Development of 3D Earth system scattering model with ray tracing method

Dongok Ryu, Sug-Whan Kim, Sehyun Seong, Yonsei Univ. (Korea, Republic of)

(TBD) In this study, we report a ray-tracing based Earth scattering system model with 3 principle sub-components i.e. land, sea and atmosphere. Atmospheric specular and scattering algorithms uses MODTRAN radiative transfer codes for 50 horizontal distributions with their input characteristics using the GIOVANNI database. Land surface distributions constructed with the 30-arcsec (1 km) resolution coastal line and extended 22 kinds of vegetation distribution map data from the Global Ecological Zone (GEZ) database. The 22 scattering properties of land surface uses bidirectional reflection distribution function (BSDF) models converted from annually observed directional parameter data which is characterized with 3 different scattering components in MODIS and POLDER3 missions. The ocean sphere surface model has combination of wind speed dependent sun-glint scattering and spectral Lambertian scattering. The ray tracing is computed from a sun model(Kurucz) as light sources to the Earth system scattering model in real scale computation 3D space. The ray paths and their characteristics such as radiant power and direction are computed as they experience reflection, refraction, transmission, absorption and scattering. The details of simulation computation, the resulting calculations are discussed together with future plan. (TBD)

# Conference 8890B: Optics in Atmospheric Propagation and Adaptive Systems XVI

Monday 23–23 September 2013

Part of Proceedings of SPIE Vol. 8890 Remote Sensing of Clouds and the Atmosphere XVIII; and Optics in Atmospheric Propagation and Adaptive Systems XVI

8890-40, Session 5

## Measuring non-Kolmogorov turbulence

Szymon Gladysz, Detlev Sprung, Karin Stein, Fraunhofer-Institut für Optronik, Systemtechnik und Bildauswertung (Germany)

We have performed a series of experiments aiming at understanding the statistics of deep turbulence over cities. Our focus is “urban” turbulence because we are interested in the usefulness of adaptive optics for free-space optical communications over urban areas. Our “last mile problem” is that urban turbulence is significantly stronger, in the sense of shallower power spectrum, compared to the classic Kolmogorov turbulence. This places significant challenges for adaptive optics systems.

That data were collected over a 2.5 km horizontal path, at a height of approximately 20 m over the town of Ettlingen (40.000 inhabitants). The experimental setup consisted of a Shack-Hartmann wavefront sensor and an imaging camera that simultaneously recording wavefront-, and focal-plane data, respectively. From the wavefront sensor we have measured temporal power spectra of the phase and of the Zernike polynomials. From the images we have estimated power spectra and auto-correlations of image motion. We have also used the Shack-Hartmann sensor as a “super-DIMM” and measured the differential angle-of-arrival variance which we also compared with the Kolmogorov model.

Substantial and consistent disagreement was found between the data and the Kolmogorov model. All the employed methods yielded similar level of disagreement suggesting another model for turbulence statistics has to be employed for “close-to-rooftops” propagation.

The suggested turbulent statistic model is compared to optical turbulence monitored at our “close to ideal”, rural permanent measurement site in northwestern Germany. The integrated optical turbulence over a horizontal path of 75 m is measured close to the ground with a scintillometer. Its vertical distribution is monitored in the atmospheric surface layer between 4 and 64 m with 4 sonic anemometers. The dependency of turbulence statistics on height and atmospheric stability is analyzed. The results are discussed with respect to the conditions of the measurements of urban turbulence.

8890-41, Session 5

## A comparison of slant-path scintillometry, sonic anemometry and high speed videography for vertical profiling of atmospheric turbulence in the surface layer

Derek J. Griffith, Council for Scientific and Industrial Research (South Africa); Lufuno Vhengani, Arshath Ramkilowan, Council for Scientific and Industrial Research Chapter (South Africa); Detlev Sprung, Fraunhofer-Institut für Optronik, Systemtechnik und Bildauswertung (Germany)

The optical effect of atmospheric turbulence greatly inhibits the achievable range of Detection, Recognition and Identification (DRI) of targets when using imaging sensors within the surface layer. Since turbulence tends to be worst near the ground and decays with height, the question often arises as to how much DRI range could be gained by elevating the sensor. Because this potential DRI gain depends on the rate of decay of turbulence strength with height in any particular environment, there is a need to measure the strength profile of turbulence with respect to height in various environments under different atmospheric and meteorological conditions. Various techniques exist to measure turbulence strength, including scintillometry, sonic anemometry, Radio Acoustic Sounding Systems (RASS) and the analysis of point source imagery. These techniques vary in absolute sensitivity, sensitivity to range profile, temporal and spatial response, making comparison and interpretation challenging. We describe a field experiment using multiple scintillometers, sonic anemometers and point source videography to collect statistics on

atmospheric turbulence strength at different heights above ground. The environment is a relatively flat, temperate to sub-tropical grassland area on the interior plateau of Southern Africa near Pretoria. The site in question, Rietvlei Nature Reserve, offers good spatial homogeneity over a substantial area and low average wind speed. Rietvlei was therefore chosen to simplify comparison of techniques as well as to obtain representative turbulence profile data for temperate grassland. A key element of the experimental layout is to place a sonic anemometer 15 m above ground at the centre of a 1 km slant-path extending from ground level to a height of 30 m. An optical scintillometer is operated along the slant-path. The experiment layout and practical implementation are described in detail and initial results are presented.

8890-42, Session 5

## Characterization of optical turbulence at telescope dome level affecting the solar observatory at the Mount Teide

Detlev Sprung, Erik Sucher, Fraunhofer-Institut für Optronik, Systemtechnik und Bildauswertung (Germany)

Optical turbulence represented by the structure function parameter of the refractive index  $C_n^2$  is regarded as one of the main causes of image degradation of ground-based astronomical telescopes operating in visible or infrared wavelengths. Especially it affects the attainable spatial resolution. Therefore since 15th September 2012 the optical turbulence was monitored between the German solar telescope domes at the Observatory in Tenerife /Canary Islands / Spain. It comprises the solar telescope GREGOR and the vacuum tower telescope VTT mounted on two 30 m high towers. Between the two towers at the level of the telescope domes  $C_n^2$  was measured using a Laser-Scintillometer SLS40 (Scintec, Rottenburg, Germany). The horizontal distance of the measurement path was 75 m. The first results of the measurements starting in September 2012 are presented and analyzed regarding simultaneous measured meteorological data of wind, temperature and humidity. Daily and seasonal variations are shown and discussed.

8890-43, Session 5

## Characterizing inertial and convective optical turbulence by detrended fluctuation analysis

Gustavo Funes, Ctr. de Investigaciones en Óptica, A.C. (Argentina); Eduardo Figueroa, Pontificia Univ. Católica de Valparaíso (Chile); Damián Gulich, Ctr. de Investigaciones en Óptica, A.C. (Argentina); Luciano Zunino, Ctr. de Investigaciones en Óptica, A.C. (Argentina) and Univ. Nacional de la Plata (Argentina); Darío G. Pérez, Pontificia Univ. Católica de Valparaíso (Chile)

Atmospheric turbulence is usually simulated at the laboratory by generating convective free flows with hot surfaces, or heaters. It is tacitly assumed that propagation experiments in this environment are comparable to those usually found outdoors. Nevertheless, it is unclear under which conditions the analogy between convective and inertial turbulence is valid; that is obeying Kolmogorov isotropic models. For instance, near-ground-level turbulence often is driven by convective shear ratchets deviating from established inertial models. In this case, a value for the structure constant can be obtained but it would be unable to distinguish between partial (convective) and fully developed turbulence.

We have performed a conceptually simple experiment of laser beam propagation through two types of artificial turbulence: isotropic turbulence generated by a device known as turbulator [Proc. SPIE textbf{8535}, 853508 (2012)], and convective turbulence by controlling the temperature of electric heaters. In both cases, a thin laser beam

propagates along the turbulent path, and its wandering is registered by a position sensor detector.

During the experiment we have changed the temperature on each device to obtain a wide range of turbulence conditions.

The strength of the optical turbulence, in terms of the structure constant, is obtained from the wandering variance and is expressed as a function of the temperature difference between the cold and hot sources in each setup. We compare the time series behaviour for each turbulence with increasing turbulence strength estimating the Hurst exponent ( $H$ , a well known quantifier of memory effects) through detrended fluctuation analysis (DFA). Refractive index fluctuations are inherently fractal; this characteristic is reflected in its spectra power dependence---in the inertial range, it decays as  $2H+1$ . This fractal behaviour is translated to time series of optical quantities, like the wandering, by the occurrence of long-range correlations. The DFA has proven to be useful for revealing the extent of these long-range correlations in time series. By analyzing with this technique the wandering time series, we are able to correlate the turbulence strength to the value of  $H$ . Preliminary results reveal the existence of saturation to different Hurst exponents depending on the type of turbulence. The findings obtained can be useful for modelling purposes.

8890-44, Session 6

### Evaluation of refractive index structure

No Abstract Available

8890-45, Session 6

### Validation of MATISSE background images and cloud simulations: comparing results with MODIS satellite images

Caroline Schweitzer, Fraunhofer-Institut für Optronik, Systemtechnik und Bildauswertung (Germany); Claire Malherbe, ONERA (France); Norbert Wendelstein, Fraunhofer-Institut für Optronik, Systemtechnik und Bildauswertung (Germany)

Conducting measurements with a satellite based sensor can become critical in terms of time consumption during the mission planning as well as during the instrumentation phase. Being able to predict the effectiveness of a space based sensor for a certain application, e. g. special earth surface observations, can help reduce the expenses. The simulation software MATISSE (developed by ONERA) is able to reproduce not only spectral characteristics of terrestrial and atmospheric backgrounds, but also sensor based ones. With the help of such a tool, spectral radiance images as seen from a space based field of view can be modeled, thus making a satellite mission dispensable in some cases. Advantages of the simulation process are obvious: a higher variety and flexibility in fields of orbit height, wavelength, cloud formations and geographical as well as seasonal or even diurnal dependencies can be obtained. To ensure the quality of MATISSE simulations, validations have already been carried out concerning sea radiances and different ground cover types. Using the latest version of the modeling software, simulations of the terrestrial background are evaluated for spectral bands, where reflectance is the dominant factor. Furthermore, a comparison between a MODIS image and clouds resulting from MATISSE computations carried out by ONERA will be presented for spectral bands, where thermal effects are prevailing. Both of the results show a good correlation between the measured MODIS image and the MATISSE simulation.

8890-46, Session 6

### Propagation of shot-pulsed partially coherent laser beams

Olga V. Tikhomirova, Viktor A. Banakh, Iya Zaloznaya, V.E. Zuev Institute of Atmospheric Optics (Russian Federation)

The results of analysis of propagation of short-pulsed optical partially coherent Gaussian beams in a homogeneous medium are presented. Analysis was performed based on the solution of wave parabolic

equation for density of electric field for different diffraction conditions on a transmitting aperture. It is shown that for any Fresnel number of the aperture diameter and initial wave front curvature radius the diffraction broadening of a pulsed beam is less than that for a continuous wave beam. Diffraction broadening of a pulsed beam decreases with a decrease of the pulse duration, and in the limit of zero pulse duration (?-pulsed beam) the diffraction broadening of a beam is absent.

The task of atmospheric backscattering of short pulsed partially coherent optical beams is formulated. The coherency of a field of backscattered pulsed optical beam is analyzed. It is shown that the spatial coherence of a backscattered pulsed beam, focused at the scattering layer, becomes worth with a decrease of the pulse duration.

The results of study of vorticity of the optical singular short-pulsed beams are discussed as well.

8890-47, Session 6

### Density oscillations generated by vortex rings and their effect on scintillation of a Gaussian beam

Fedor V. Shugaev, Evgeni N. Terentiev, Ludmila S. Shtemenko, Lomonosov Moscow State Univ. (Russian Federation); Oxana A. Nikolaeva, Lomonosov Moscow State Univ (Russian Federation)

Density oscillations in the vicinity of vortex rings in air have been investigated. As known, vortical structures play an important role in turbulence. The calculations were fulfilled on the basis of the Navier-Stokes equations. We used series expansions of unknown functions in powers of a parameter which characterizes vorticity. As a result, we got a non-uniform system of parabolic differential equations with constant coefficients. The solution is presented in the form of multiple integrals which have been evaluated with the aid of Korobov method. The frequency of oscillations depends only on the dimensions and the shape of the ring in the case of small vorticity (weak turbulence). If the vorticity is large (strong turbulence), the frequency depends not only on the ring shape, but also on the value of vorticity. We analyzed oscillations generated by rings with circular cross-section whose diameter varied from 0.001 mm to 10mm. It is interesting to note that first of all the amplitude of oscillations increases, reaches its maximum and then decreases up to zero. The range of ring sizes includes inertial range and dissipation range. Thus we can find statistical properties of the flow where there is an ensemble of vortex rings and fulfill modeling of turbulence. The spectrum of oscillations in the case of an ensemble of rings was investigated, too. Using these data we modeled the propagation of a Gaussian beam through the turbulent atmosphere. To accomplish this, we used the solution to the problem of a Gaussian beam propagation in non-uniform gas. This solution can be written in analytic form. We considered intensity fluctuations (scintillations) of the beam after the passage through the non-uniform region which contains vortex rings.

We have analyzed some ill-posed problems (e.g., that of super-resolution) connected with image restoration. In such cases if the input data are slightly changed, the solution may vary considerably. The proposed procedure is as follows. We have a set of experimental data (result of measurements) and an instrument function whose accuracy is known. We change the instrument function in such a manner that it will be reversible one within the limits of accuracy. The procedure enables to solve some problems referring to the turbulent atmosphere. Numerical results are given.

8890-48, Session 7

### Imaging through atmospheric turbulence for laser based C-RAM systems: an analytical approach

Ivo Buske, Wolfgang Riede, Deutsches Zentrum für Luft- und Raumfahrt e.V. (Germany); Jürgen Zoz, MBDA Germany (Germany)

High Energy Laser weapons (HEL) have unique attributes which distinguish them from limitations of kinetic energy weapons. Its inherent precision strike capability and ability to engage while looking

at the target are the most distinguishing attributes. There's a long history about gas and chemical laser which were driven by the Cold War environment. Currently HEL developments are focused on solid-state laser or FEL technology [1].

HEL weapon's engagement process typical starts with identifying the target and selecting the aim point on the target through a high magnification telescope. The lethality depends on the thermal effects that the laser induced at the target surface. During the beam on target dwell time the laser has to follow the aim point with high accuracy. The laser beam can be delivered with the speed of light but the impact on structures and materials is a time dependent process. One scenario for such a HEL system is the countermeasure of rockets, artillery or mortar (RAM) objects to protect ships, camps or other infrastructure against terrorist attacks. The operator is in instantaneous control of this process while looking at the target being engaged. This is complementary to fire and forget approach of gatling gun systems using a hail of bullets to increase the probability of impact.

For target identification and especially to resolve the aim point it is significant to ensure high resolution imaging of RAM objects. During the whole ballistic flight phase the knowledge about the expectable imaging quality is important to estimate and evaluate the countermeasure system performance. Hereby image quality is mainly influenced by unavoidable atmospheric turbulence.

The tracking task requires a high speed and high sensitive megapixel imaging camera connected to an objective with a focal length about 1-3 m. Analytical calculations have been taken to analyze and evaluate image quality parameters during an approaching RAM object. In general, Kolmogorov turbulence theory was implemented to determine atmospheric coherence length, seeing angle, strehl ratio or isoplanatic angle. The image acquisition is distinguishing between long and short exposure times to characterize tip/tilt image shift and the impact of high order turbulence fluctuations. Two different observer positions are considered to show the influence of the selected sensor site. Furthermore two different turbulence strengths are investigated to point out the effect of climate or weather condition.

It is well known that atmospheric turbulence degenerate image sharpness and creates blurred images. During the start phase near the horizontal line of sight image resolution will be not sufficient to hold the point of impact on RAM object. Image stabilization techniques or adaptive optics can be applied to compensate low order atmospheric turbulence effect. Investigations are done to estimate the effectiveness of simple tip/tilt systems or low order adaptive optics for laser based C-RAM systems.

[1] Cook, "High-energy laser weapons since the early 1960s", Opt. Eng. 2.2013

## 8890-49, Session 7

### High-resolution imaging through strong atmospheric turbulence

Stuart M. Jefferies, Douglas A. Hope, Univ. of Hawai'i (United States); Michael Hart, The Univ. of Arizona (United States); James Nagy, Emory Univ. (United States)

We discuss how high-resolution imaging through strong atmospheric turbulence requires both maximizing the transmission of information through the optical system and accurate estimation of the observed wave front over a wide range of spatial frequencies.

We show that both requirements can be met by observing with a dual channel system where one channel employs aperture diversity and the other an imaging Shack-Hartmann wave-front sensor. The imagery from this setup is processed using a blind restoration algorithm that combines the strengths of the multi-aperture phase retrieval and multi-telescope, multi-frame blind deconvolution techniques: it also captures the inherent temporal correlations in the observed phases. This approach, which strengthens the synergy between image acquisition and post-processing, provides near-diffraction-limited imagery at unprecedented levels of atmospheric turbulence. The approach also allows for the separation of the phase perturbations from different layers of the atmosphere. This characteristic offers potential for a beaconless wave-front sensor and for the accurate restoration of images with fields of view substantially larger than the isoplanatic angle. The proposed approach also has application for high-dynamic range imaging.

## 8890-50, Session 8

### Solar adaptive optics at the Observatorio del Teide, Tenerife

Dirk Soltau, Thomas Berkefeld, Kiepenheuer-Institut für Sonnenphysik (Germany); Dirk Schmidt, National Solar Observatory (United States); Oskar von der Lühse, Kiepenheuer-Institut für Sonnenphysik (Germany)

Observing the Sun with high angular resolution is difficult because the turbulence in the atmosphere is strongest during day time. In this paper we describe the principles of solar adaptive optics exemplified by the two German solar telescopes VTT and GREGOR at the Observatorio del Teide. With these systems we obtain near diffraction limited images of the Sun. Ways to overcome the limits of conventional AO by applying multiconjugate adaptive optics (MCAO) are shown.

## 8890-51, Session 8

### Compensation of laser beam initial wave front aberrations using backscattered radiation as a signal for adaptive control

Viktor A. Banakh, V.E. Zuev Institute of Atmospheric Optics (Russian Federation)

At high altitudes the impact of atmospheric turbulence on laser beam propagation is small and aberrations of the beam initial wave front play a prevailing role in a beam broadening and reducing the power of registered laser radiation at the receiving plane. This poses the problem of minimizing the distortions of the beam wave front at the transmitting aperture. To compensate the initial wave front aberrations the adaptive system can be used with a flexible mirror controlled by a signal from the beam wave front sensor.

In this paper it is shown that atmospherically backscattered laser beam radiation can be used as a signal for adaptive control of a flexible mirror instead of a wave front sensor signal. The results of computer simulation which demonstrate feasibility of this technique of adaptive control are presented. The results of concept prove laboratory and atmospheric experiments on adaptive control based on backscattered signal are discussed. It is shown that for wave front aberrations, considered in the experiments, adaptive control of a flexible mirror based on a beam backscattered radiation provides for the compensation of the main part of the preset aberrations.

## 8890-52, Session 8

### Characterization of the holographic wavefront sensor for free-space optical communications

Andreas Zepp, Szymon Gladysz, Fraunhofer-Institut für Optronik, Systemtechnik und Bildauswertung (Germany)

The main components of the holographic wavefront sensor (HWFS) are a holographic diffraction pattern and an intensity-sensitive device like a photodiode array. With this basic setup the wavefront of an incoming laser beam is decomposed into its fundamental modes, e.g. the Zernike basis functions. The main advantage of HWFS is that the decomposition of the wavefront is realized in hardware and, in principle, could be executed at the speed of light. Therefore, HWFS is highly suitable for applications with high temporal requirements. Especially in the field of horizontal beam propagation through the atmosphere HWFS is a promising alternative to the most popular Shack-Hartmann sensor. Unlike in HWFS, the measurement of aberrations in the Shack-Hartmann sensor is highly influenced by scintillation: the obscuration or saturation of large parts of the sensor's pupil can lead to a significant failure rate of the wavefront reconstruction process. On the other hand, HWFS is, in principle, insensitive to scintillation.

We are studying the effectiveness of HWFS for measuring the first few low-order aberrations. In literature a value of 10% Strehl ratio has been assumed as a threshold of usefulness of adaptive-optics correction for laser communications. We want to check whether such a value can be achieved through the use of HWFS for compensation

of laser beams over long horizontal paths.

We realized HWFS by recording an analog multiplex hologram. This multiplex consists of two interference patterns for every aberration type we want to measure with the sensor. A convergent wave is taken as object beam, focused on a specific object point. As reference beam a wave with the negative amplitude of an aberration is applied, and then with the positive amplitude. These calibrations are carried out for any Zernike mode of interest while changing the location of the object point.

We analyzed the sensor's response to incoming laser beams with defined wavefront aberrations. The test wavefronts were aberrated with the deformable mirror DM-52-15 by ALPAO. Of special interest is the response of HWFS to partial obscurations of the pupil. We present corresponding experimental and simulation results. Furthermore, we analyzed the influence of tip/tilt on the sensor's accuracy. The effect of a tilted laser beam on HWFS is a misalignment of the reconstructed spots. In this case the use of small photodiodes for intensity measurement – a configuration recommended for tip/tilt-free beam, can lead to error-prone measurements. While HWFS in itself could operate at the speed of light, sensitivity can become an issue for very short integration times. We are also investigating this point.

### 8890-53, Session 8

#### Adaptive optical focusing of laser beam in turbulent atmosphere with use fluctuating reference source

Lidiia A. Bolbasova, Vladimir P. Lukin, V.E. Zuev Institute of Atmospheric Optics (Russian Federation)

Turbulent distortions in the real atmosphere leading to reduce power and energy of radiation, spatial coherence and brightness of laser beam, an increase in its angular divergence. All these characteristics of the laser radiation determine the effectiveness of lasers applications in many areas, such as location, navigation systems, communication, and space technology. The adaptive focusing of a laser beam through a turbulent atmosphere is investigated in the work. We consider the reference source with a random position (position fluctuations of its center of gravity) for laser radiation focusing on the object. The wavefront tilts (or the fluctuations of the position of the center of gravity in the laser beam) are the most important components of phase fluctuations and approximately 80% of the energy of phase fluctuations are concentrated in random tilts of the wavefront. The problem of focusing of coherent optical radiation through the atmosphere can arise in practice when energy is transporting to a sufficiently large remote object. The reference source can be formed by radiation reflected from the object to which coherent laser radiation should be focused. The methods used for determining the phase on the basis of coherent and non-coherent reference radiations were described early. The analytical calculations are performed. Distributions of the averaged intensity of the coherent laser beam focused in a turbulent medium by means of adaptive phase correction with the use of a point reference source with random center are calculated. The laser beam focused with the use of adaptive correction with phase conjugation algorithm and the spherical wave with a fluctuating radiation center as reference source. The distribution of the averaged intensity of the focused coherent radiation beam on the basis of the Huygens–Fresnel principle is studied. The approach considered here can be used in cases with coherent and non-coherent illuminations. We have made the attempt of estimation the adaptive focusing of coherent laser radiation efficiency from the viewpoint of energy concentration and transfer. The Strehl ratio as the parameter of efficiency is used. Results of adaptive focusing with moving and motionless reference sources are compared. It is demonstrated that a point reference source with a random position of the center can be an effective tool for adaptive focusing of radiation beams. A comparison results of analysis shows that correction with the use of a point source with a fluctuating position is a fairly effective tool of energy concentration on the system axis, as compared with a non-adaptive system for the following reasons: the mean position of the fluctuating illuminating source is located on the optical axis, and such adaptive correction eliminates higher aberrations and focuses the beam as a whole.

### 8890-54, Session 8

#### A new method to measure atmospheric turbulence

Régis Barillé, Univ. d'Angers (France); Darío G. Perez, Pontificia Univ. Católica de Valparaíso (Chile); Ewelina Ortyl, Sonia Zielinska, Wroclaw Univ. of Technology (Poland); Yohann Morille, Univ. d'Angers (France)

A new optical system able to measure the influence of a turbid medium on laser beam propagation is proposed. This system is similar to a holographic recording with only a single beam used to imprint informations.

The first objective of the system is to simultaneously obtain several characteristics of the turbulence induced on a laser beam by measuring its impact during propagation in the turbulent environment. The hologram inscribed on the surface by a single laser beam propagated into the turbulent medium is perturbed. The second objective of the study is to integrate information on short or long term in order to have an integrated value of this effect and save the information.

This measurement is based on the inscription of a surface relief grating (SRG) on a photochromic thin film by a laser beam. The material self-organize at the surface under the effect of a laser light to produce a surface pattern in the form of a diffraction grating. Azo molecules of the thin film material photoisomerize by repeating trans-cis-trans isomerizations induced by light absorption and lead to a surface mass transport.

The spatial regular structuration on the surface is modified by the turbulence and analyzed by two different methods. One is direct and qualitative in real time with optical visualization of the pattern induced by the laser diffracted on the surface grating changes by a CCD camera. The other one is quantitatively. In this case a complementary study might be done in parallel by scanning the surface pattern with an AFM and analysed it two different analysis. The first analysis use the 2D Radon transform (RT) and we obtain a 2-D totality of 1-D projections in  $RT(\theta, r)$ , formed by using integration along lines with normal, sloped values of  $\theta$  with  $r$  the length of the normal from the origin to the line and  $\theta$  the angle the normal forms with respect to the x-axis? A more sophisticated analysis uses a Multifractal Detrended Fluctuation Analysis (MDFa) after surface characterization and image processing. In both cases a relation between the refractive index structure parameter changes  $Cn2$  as a function of the surface parameters extracted is obtained.

Time registration of the grating on the surface can integrate changes in turbid medium on a long term period. The device can also be erased for reuse for further measurements.

This new optical system has the advantage to use a single beam to remotely inscribe a grating and store informations.

# Conference 8891: SAR Image Analysis, Modeling, and Techniques XIII

Wednesday - Thursday 25–26 September 2013

Part of Proceedings of SPIE Vol. 8891 SAR Image Analysis, Modeling, and Techniques XIII

8891-7, Session PS

## Tomographic SAR inversion by generic log-barrier algorithm: the second order cone programming approach

Filippo Biondi, Ministro Della Difesa (Italy); Nazzareno Pierdicca, Univ. degli Studi di Roma La Sapienza (Italy); Piero Ciotti, Univ. degli Studi dell'Aquila (Italy)

**Abstract** – In Multi-Baseline SAR tomography vertical resolution is directly proportional to the synthetic height aperture antenna. In order to avoid the problem of obtaining aliased inverted tomographic results it is necessary to collect a sufficient number of repeat-pass observations that are distributed along the vertical synthetic aperture interval according with the sampling theorem. Such a procedure introduces additional problems, such as the temporal decorrelation phenomena when using a number of passes spanning a long timeframe. Consequently, it's often necessary to design tomographic SAR acquisition geometries using the fewest number of repeated active radar tracks. To adequately compensate the consequences of the undersampled configuration, it's therefore necessary to process the acquired data with advanced signal processing techniques that can work properly in forested environments, characterized to have both point and distributed targets. In order to process data collected over forest by the SAR Tomography technique in the above described configuration, it is necessary to implement algorithms that work for both point and distributed targets. Compressed Sensing (CS) signal processing techniques based on the minimization of the  $l_1$  norm in most of the cases are unable, in the continuous environmental condition, to correctly estimate scattering targets parameters, whereas they are generally excellent methods for processing isolated point scatterers. This paper considers the Convex Optimization (CVX) tomographic solution in order to process multi-baseline data-sets with forested environments, in a Fourier under-sampled configuration. The CVX Second Order Cone Programming Solution (SOCPs) has been tested by a generic log-barrier algorithm, through a successfully computational bottleneck Newton calculation. This technique is validated on point and distributed targets critically analyzing the radiometric consistency response of other classical Fourier, Linear CS and SOCP CS based tomographic inversion procedures.

8891-23, Session PS

## Experimental extraction of sub-pixel resolution in RADAR images via amplitude, phase and polarization readouts

Zeev Zalevsky, Sara Cohen, Bar-Ilan Univ. (Israel)

The Synthetic Aperture Radar (SAR) image resolution is determined by the synthetic aperture length in the azimuth direction and by the linear frequency modulation (LFM) pulse bandwidth in the range direction. Hence the azimuth resolution can be improved by creating larger synthetic aperture. On the other hand the ability to improve range resolution has technological limit, because it requires a rise in the sampling frequency. Therefore super-resolution processing for SAR images is desired for image applications as interpretation and target detection. A common approach for sub-pixel separation uses polarimetric SAR and performs coherent target decomposition to distinguish the different scattering components within each resolution cell.

The technique presented herein uses additional characteristics of the SAR data to increase the ability to identify sub-resolution information. It uses polarization state, phase and amount of backscattered power in order to distinguish different sub-pixels combinations.

The application presented in this paper is based on full-polarization, complex SAR data, created by L-band airborne RADAR. The proposed concept is demonstrated via experiments involving airborne SAR RADAR capable of polarimetry and angle extraction.

Polarization, phase and magnitude expected values were experimentally used to characterize the different 2 X 2 sub-pixel combinations and to separate among them. The predicted values were compared to real values extracted from experimental SAR data.

Although only partial sub pixel identification of targets was experimentally demonstrated, yet the results indicate a potential in performing separation by magnitude and polarization. The proposed technique can further be improved by using several SAR images of the experimental scene and comparing the outcome coming from analyzing each one of them separately.

8891-26, Session PS

## A new detection method of oil rig in SAR imagery

Peng Chen, Jingsong Yang, The Second Institute of Oceanography, SOA (China); Lin Ren, Second Institute of Oceanography SOA (China)

It's difficulty for simple space-borne SAR to identify oil rigs effectively in single pass SAR image. One method of oil rig detection is using multi-temporal SAR images. Some papers had do some research on it. In this paper, we use interferometry SAR image to detect the oil rigs. We get the correlation coefficient image from the In-SAR data, and using the histogram of correlation coefficient image, a Constant False Alarm Rate (CFAR) algorithm is imported to detect the oil rigs. The Probabilistic Neural Network (PNN) is used to get the shreshold of detection. The test result shows that sea coherent target detection in the coherent coefficient image is efficacious.

8891-27, Session PS

## SAR data analysis in mineral ore utilization

G. A. Shanmugha Sundaram, Amrita Vishwa Vidyapeetham Univ. (India)

Current practices of mining for mineral-rich ores rely heavily on the use of massive, heavy earth-mover equipment that follow an open-cast approach as a first step in the extended series of processing the raw ore into manufacturing-grade metal. SAR signals are particularly polarization-tuned to the exact composition of the scatterer, which in this application is metal-rich in content. The mining process involves creating large-scale heaps of the metallic ore in the vicinity of the mining area, that can be potentially hazardous to the entire operation on account of the likelihood to massive landslides. Additionally, the rate of utilization is one more vital element in understanding the productivity of any operational mine. Analysis of SAR imaging information, by way of relevant pre-processing stages on the images followed by implementation of a robust change-detection step, shall offer a quantitative understanding as regards the functional aspects of the metal-mining activity.

8891-28, Session PS

## Radar clutter as an indicator for vegetation classification: vegetation classification using a single dual polarimetric TSX-1 image

Marina Hetz, Dan G. Blumberg, Stanley R. Rotman, Ben-Gurion Univ. of the Negev (Israel); Roe Enbar, Ariel Benou, Ben-Gurion University of the Negev (Israel)

This work investigates the ability to classify different vegetation types covering a semi-arid Mediterranean vegetated area using single-polarization SAR image from the TerraSAR-X (TSX-1) satellite. Based on statistical moments such as mean, standard deviation (STDEV), skewness and kurtosis, we found textural differences useful for the classification of the vegetation types. The research site, located near

Zafit Hill, Israel, includes several different vegetation types such as pines and cypress forests with shrubs as an underlying vegetation layer (understorey), olive orchards, eucalyptus clusters, natural grove areas with the presence of stones and smooth rocks, a wet cotton field, and smooth agricultural fields after harvest. In each vegetation type area, 40 equal polygons (10\*10 pixels each) were identified on an optical image and defined (by hand) on the TSX-1 image; 280 polygons in total were identified. The aforementioned statistical parameters were produced for each polygon, and co-variance matrices of combinations of two, three, or all four parameters together were produced. It was found that using the Mahalanobis distance of the mean-STDEV-skewness combination after applying a mode filter (5\*5 in size) was the best way to classify the vegetation types in the research area.

## 8891-29, Session PS

### Estimating the surface age of arid-zone alluvial fans using spaceborne radar data

Guy Hetz, Ben-Gurion Univ. of the Negev (Israel); Amit Mushkin, Geological Survey of Israel (Israel); Dan G. Blumberg, Ben-Gurion Univ. of the Negev (Israel); Gidi Baer, Geological Survey of Israel (Israel)

Alluvial fans and deposits constitute important recorders of tectonic and climatic signals and thus, geologic age is a common and pivotal component in many quantitative studies of recent tectonic activity, past climatic variations and landscape evolution studies. Numerical and relative dating techniques add to our ability to constrain surface ages in desert environments, but they also require large efforts and commitment of resources. Our study is based on a hypothesis demonstrated that surface roughness changes with age. Therefore, we propose the use of radar backscatter data that responds to surface roughness to obtain 'non-contact' quantitative surface age constraints.

This study was conducted on the alluvial fan of Nahal Shehoret that located in the Southern Arava rift valley. At the last step of the research the technique was tested in Nahal Raham as well as in Jordan. In this study ALOS-PALSAR radar data were used with L-Band (?=23) dual polarized (e.g., HH, HV), different incidence angles (e.g., 24°, 38°) and various resolutions (e.g., 6.25m, 12m), to show the best integration between the surface age and the radar backscatter. Regions of interest (ROIs) representing different age groups and different surface types were selected on the radar images. Absolute age of each ROI was taken from Porat et al. (2010) that used OSL (Optically Simulated Luminescence) technique. In order to identify the best parameters that vary with age, first and second order statistical parameters were calculated for each ROI and the variance of these parameters was examined. The same was done also for the different radar configurations such as incidence angles, polarization and resolution. The results show that the mean backscatter of each age group was found to be the best prediction parameter for the characterization of the surface roughness, as the surface become smoother, the mean backscatter becomes lower and vice versa. The HH- polarized image with ~38° incidence angle and 6.25 m resolution allowed separation of the different groups of the surface ages. These radar parameters allowed distinguishing significantly between groups on a scale of 4.6ka±07 to 330ka±30.

## 8891-30, Session PS

### Compact polarimetry evaluation for reconstruction of full polarimetric information in SAR RS

Mmaamar Abimouloud, Univ. des Sciences et de la Technologie Houari Boumediene (Algeria)

The goal of this work is to assess the potentials of CPSAR (compact polarimetric synthetic aperture radar) for remote sensing applications. This imaging technique comes as alternative mode for imaging SAR system to overcome limitations present with known classical modes. The compact polarimetry mode is a special case of dual polarimetry (DP). The word compact comes from the system design which is minimized while maximizing the polarimetric information. In fact, it consists in unique polarization in transmission and two orthogonal

polarizations in reception. the  $\pi/4$  mode is characterized by a linear transmission oriented at 45°, the  $\pi/2$  mode has circular transmission. After exploring some of the proposed techniques associated to CP imagery, as The approach proposed by Souyris who introduced the concept of using the CP acquisition to reconstruct pseudo FP information; then Nord enhanced the results by double bounce correction. Here We investigate the performance of CP dataset simulation and FP descriptors reconstruction on different target types. the application is then achieved on a data set of known region for the purpose of visual and ground truth knowledge evaluation.

the data set is quad pol acquisition acquired over the city of Algiers Algeria by the Canadian satellite RADARSAT-II in 2009.

## 8891-1, Session SJS1

### Simulation of imaging effects of very high resolution SAR systems

Harald Anglberger, Rainer Speck, Helmut Suess, Deutsches Zentrum für Luft- und Raumfahrt e.V. (Germany)

Current space borne synthetic aperture radar (SAR) systems like TerraSAR-X, COSMO-SkyMed or Radarsat-2 are able to provide users with high resolution image data of around one meter. Focusing on systems operating in the X-band, this value is not the end of possible improvements in resolution. There still lies a great potential in an increase of bandwidth of the radar signal itself and also in a significant enlargement of the synthetic aperture. From the technical point of view this certainly is a challenge, but could be possible for future space borne SAR missions already with current state of the art hardware. Actually, the technical realization of the SAR system is not the only obstacle to overcome. Especially the increase of Doppler bandwidth along the synthetic aperture requests special treatment and considerations in system design from a signal processing's point of view.

In this paper, methods and results are shown that are able to study critical aspects of very high resolution SAR imaging. Basically, the challenges can be summarized into two critical parts: the considerable reduction of the depth-of-focus on the one side and the strong reflectivity fluctuation of single scatterers along the synthetic aperture on the other side. Both aspects result in a loss of resolution. The amount of defocusing of scatterers that are out of the depth-of-focus is caused by the curvature of the very long orbital path in combination with the unknown offset of the scatterer from a given reference height. Thus, one solution to circumvent these effects is the usage of digital elevation models during SAR image reconstruction. In contrast, the fluctuation of an object's reflectivity along the synthetic aperture directly depends on the shape and material of the objects, which are physical characteristics and can therefore not be compensated. This means, that every single scatterer has his own distinctive reflectivity profile along the synthetic aperture and only provides a maximum amount of bandwidth that can be significantly lower than the theoretical one. To study effects of very high resolution SAR imaging, simulation methods have to be newly developed. Usually, SAR simulators approximate the system as being linear shift invariant. In this way the point spread function of the imaging system can be used to generate simulated SAR images in a very efficient way. Unfortunately, in the very high resolution case this assumption is not feasible anymore, because the point spread function is unique for every single scatterer in the scenery due to its characteristic history of reflectivity along the synthetic aperture and its offset from the reference height.

This paper shows methods that are able to realistically simulate these effects. This ability will be demonstrated not only for single point scatterers, but also for complex objects. Simulation results will be given for a varying geometrical resolution range, starting with parameters of existing sensors like TerraSAR-X and improving stepwise to higher resolutions.

## 8891-3, Session SJS1

### A change detection approach applied to COSMO-SkyMed images to characterize snow cover areas

Simonetta Paloscia, Simone Pettinato, Istituto di Fisica Applicata Nello Carrara (Italy)

The use of satellite data for a timely monitoring of the Earth's surface has become ever more appealing and effective in the last decades. Quantitative snow cover investigation can provide important information on global changes and water resource management, as well as flood and avalanche risk prevention. Optical sensors have been proven capable of monitoring snow cover in cloud-free conditions, and several systems have been developed for operational monitoring of snow parameters from remote sensing data. However, only microwave sensors are able to acquire data independently of daylight and in adverse weather conditions. In particular, spaceborne X-band SAR systems (COSMO-SkyMed and TerraSAR-X) can provide accurate localization of snow-covered areas, exploit high/low penetration in dry/wet snow and estimate of the snow water equivalent (SWE) in the case of dry snow. In general, backscattering coefficients higher than the snow-free case can be detected, by assuming that the backscattering enhancement is due to snow characterized by a SWE greater than 100mm and therefore able to contribute to the radar response at the X-band. In this paper, an experimental study on the characterization of snow cover areas on COSMO-SkyMed images is presented. Different data processing approaches are tested and experimentally compared:

1. Process multi-temporal SAR images to detect a backscattering change due to wet snow which typically ranges from -3 to -2dB with respect to snow-free soil.
2. Apply a classical change detection algorithm based on semi-automatic thresholding of the logarithm of the ratio image between two SAR images acquired at different dates.
3. Apply a non-parametric change detection algorithm on two-date SAR images based on mean-shift clustering.

It should be noted that the first approach requires geo-coded and radiometrically calibrated multi-temporal SAR images, the second approach needs accurate de-speckling and suffers from the trade-off between noise reduction and preservation of spatial resolution, while the third approach has been proven to be effective also on 1-look SAR image data at very high spatial resolution. Preliminary results on Single-Look-Complex CSK images (Himage data in Stripmap acquisition mode) acquired in September 2011, December 2011 and January 2012 on an alpine region in Northern Italy show that the results obtained by applying the third approach are very promising since they provide accurate localization of the snow covered areas and reduced false alarm rate with respect to the first two classical approaches. Experimental results on PingPong Stripmap images will be also presented in the final paper and objectively assessed by using ground truth data.

#### 8891-4, Session SJS2

### Multichromatic analysis of SAR images for target analysis

Fabio Bovenga, Consiglio Nazionale delle Ricerche (Italy); Dominique Derauw, Univ. de Liège (Belgium); Christian Barbier, Centre Spatial de Liège (Belgium); Fabio M. Rana, Alberto Refice, Nicola Veneziani, Consiglio Nazionale delle Ricerche (Italy); Raffaele Vitulli, European Space Research and Technology Ctr. (Netherlands)

The Multi-Chromatic Analysis (MCA) of SAR images relays on exploring sub-band images obtained by processing portions of range spectrum located at different frequency positions. The first application of MCA consisted in analyzing the phase obtained by coupling sub-images derived from interferometric pairs and performing both phase unwrapping as well as height computation on coherent pixels without spatial integration. Results obtained through theoretical modeling as well as by processing wideband SAR data acquired by TerraSAR-X (TSX) and COSMO-SkyMed (CSK) indicate that at least 300 MHz is required to provide reliable results. Further potential applications are possible. In particular, this work is aimed at investigating two promising aspects: the comparison between the frequency-persistent scatterers (PSfd) and the temporal-persistent Scatterers (PS), and the use of inter-band coherence of single SAR image for vessel detection.

The MCA technique introduces the concept of frequency-stable targets, i.e. objects exhibiting stable radar returns across the frequency domain. This concept is complementary to that of temporal stability, which is at the base of persistent scatterers interferometry (PSI) techniques. It is then natural to try to compare the two concepts, examining the assumptions which form the base of the two definitions, and evaluating the respective characteristics of the two populations,

with the final goal of ascertaining if any synergy can be identified between the two types of object, and how possibly to take advantage from the availability of both processing techniques. Both Spotlight and Stripmap TSX images acquired on the Venice Lagoon have been processed to identify PSfd as well as PS targets. Different populations have been analyzed to evaluate the respective characteristics and the physical nature of PSfd and PS.

Concerning the second aspect, coherence between sub-images of single SAR acquisition can be computed leading to a measurement of the spectral coherence. A simple model shows that, in the presence of a random distribution of surface scatterers, spectral coherence must be proportional to sub-band intersection of considered sub-images. Consequently, for this distribution of scatterers, spectral coherence should fall to zero when sub-bands are disjointed. This model is fully verified when observing measured spectral coherence on open sea areas corresponding well to the scatterer distribution under concern. If scatterers distribution departs from this basic distribution, spectral coherence may be preserved. It is especially the case in presence of manmade structures. Spectral coherence is shown to stay high and stable for point scatterers, whatever sub-images central frequency gap. We investigated the spectral coherence to perform vessel detection on sea background by using TSX Spotlight images acquired on Venice Lagoon. Sea background tends to lead to very low spectral coherence while this latter is well preserved on the targeted vessels, even for very small ones despite the inherent resolution loss of the process. A first analysis shows that all vessels observable in intensity images are easily detected in the spectral coherence images which can be used as a complementary information channel to still constrain vessel detection.

#### 8891-5, Session SJS2

### A novel multiband SAR data technique for fully automatic oil spill detection in the ocean

Fabio Del Frate, Daniele Latini, Alireza Taravat, Univ. degli Studi di Roma Tor Vergata (Italy); Cathleen E. Jones, Jet Propulsion Lab. (United States)

With the launch of the Italian constellation of small satellites for the Mediterranean basin observation (COSMO)-SkyMed and the German TerraSAR-X missions, the availability of very high-resolution SAR data to observe the Earth day or night has remarkably increased. Moreover, future SAR missions such as Sentinel-1 (C-band) are scheduled for launch in the very next years while additional support can be provided by Uninhabited Aerial Vehicle (UAV) SAR systems. Suitable and adequate image processing multi-band procedures are then necessary to fully exploit the huge amount of data available. As far as oil spill detection is concerned, it is known that one of the most critical issues for the implementation of a fully automatic processing chain is the image segmentation. In fact, the extraction of the dark spots in the image is the first of three necessary steps, the other two being its characterisation by using a set of features and the classification between oil spill and look-alike. Aside from the accuracy of the segmentation results, one of the most significant parameters for evaluating the performance in this context is the processing time which is necessary to provide the segmented image. This might be crucial both in emergency cases and when stack of images have to be elaborated in a raw. In this paper we present a new fast, robust and effective automated approach for oil-spill monitoring. A combination of Weibull Multiplicative Model (WMM), Pulse Coupled Neural Network (PCNN) and Multi-Layer Perceptron (MLP) techniques is proposed for achieving the aforementioned goals starting from data at different bands and spatial resolutions. One of the most innovative ideas is to separate the detection process into two main steps, WMM enhancement and PCNN segmentation. The complete processing chain has been applied to a data set containing C-band (ERS-SAR, ENVISAT ASAR), X-band images (Cosmo-SkyMed, TerraSAR-X) and UAVSAR L-band images for an overall number of more than 200 images considered.



8891-6, Session 1

## Detection of partially coherent scatterers in multidimensional SAR tomography: a theoretical study

Antonio Pauciullo, Istituto per il Rilevamento Elettromagnetico dell'Ambiente (Italy); Antonio De Maio, Univ. degli Studi di Napoli Federico II (Italy); Stefano Perna, Univ. degli Studi di Napoli Parthenope (Italy); Diego Reale, Gianfranco Fornaro, Istituto per il Rilevamento Elettromagnetico dell'Ambiente (Italy)

The development of advanced Differential Interferometric SAR (DInSAR) techniques [1],[2] represents a breakthrough for environmental risk analysis and security. Along this line are approaches such as Persistent Scatterers Interferometry (PSI) [3] and SAR Tomography [4],[5], also known as multi-D imaging. In the context of repeat-pass SAR Tomography, a problem is associated with the identification of scatterers characterized by high coherency properties over the time (Persistent Scatterers, PS). With reference to the imaging and monitoring of PS, the detection approach based on multi-D imaging outperforms the detectors derived in the PSI context, because of the use of both amplitude and phase information in the received data [6]. Anyway, since both detectors are based on the restrictive assumption of absence of decorrelation in the scatterer response, they may present performance losses when operating in real scenarios. To handle this problem, empirical solutions using an estimation of the data covariance matrix, performed via spatial averaging operation, have been proposed. Such approaches provide higher densities of detected scatterers, paid however with a loss of spatial resolution.

In this work the problem of detecting scatterers showing partial correlation properties in multidimensional SAR imaging is addressed, generalizing the detector in [6] where the absence of target decorrelation is assumed. The optimum detector is first derived according to the Neyman-Pearson criterion. Then, since it requires the knowledge of the power of both target and noise, a suboptimum detector is derived. Its performances in terms of both false alarm and detection probability are compared with that achieved by the receiver in [6]. Experiments on simulated data confirm that the new detector outperforms the old one if the target correlation is suitably accounted for.

### References

- [1] A. Ferretti, C. Prati, and F. Rocca, "Nonlinear Subsidence Rate Estimation Using the Permanent Scatterers in Differential SAR Interferometry", IEEE Trans. on Geosci. Remote Sens., Vol. 38, No. 5, pp. 2202-2212, September 2000.
- [2] P. Berardino, G. Fornaro, R. Lanari, and E. Sansosti, "A new Algorithm for Surface Deformation Monitoring Based on Small Baseline Differential SAR Interferograms", IEEE Trans. on Geosci. Remote Sens., Vol. 40, No. 11, pp. 2375-2383, November 2002.
- [3] A. Ferretti, C. Prati, and F. Rocca, "Permanent Scatterers in SAR Interferometry", IEEE Trans. on Geosci. Remote Sens., Vol. 39, No. 1, pp. 8-20, January 2001.
- [4] F. Lombardini, "Differential Tomography: a New Framework for SAR Interferometry", IEEE Trans. on Geosci. Remote Sens., Vol. 43, No. 1, pp. 37-44, January 2005.
- [5] G. Fornaro, D. Reale, and F. Serafino, "Four-Dimensional SAR Imaging for Height Estimation and Monitoring of Single and Double Scatterers", IEEE Trans. on Geosci. Remote Sens., Vol. 47, No. 1, pp. 224-237, January 2009.
- [6] A. De Maio, G. Fornaro, and A. Pauciullo "Detection of Single Scatterers in Multidimensional SAR Imaging", IEEE Trans. on Geosci. and Remote Sens., Vol. 47, No. 7, pp. 2284-2297, July 2009.

8891-8, Session 1

## 2D phase unwrapping using Markov random field based phase locked loops

Nazli Deniz Cagatay, German Aerospace Center (Germany); Mihai P. Datcu, Deutsches Zentrum für Luft- und Raumfahrt e.V. (Germany)

Phase unwrapping is the reconstruction, or estimation, of the absolute phase signal from its observed noisy wrapped samples. Phase locked loop (PLL) has already been proposed to unwrap the two dimensional (2D) interferometric phase [1, 2]. As opposed to common phase unwrapping methods dealing with the wrapped phase obtained by the  $\arg(\cdot)$  operator, PLL operates on the complex interferogram directly, and it continuously tracks and demodulates the phase of the input signal by integrating the estimation errors through a loop filter and an oscillator. Furthermore, from the Bayesian point of view, PLL output can be considered as the maximum a-posteriori (MAP) estimate.

On the other hand, the Markov random field (MRF) is a well-known appropriate statistical model for parameter estimation of images [3]. In this model, Markovianity condition states that the conditional probability of a state  $s$  in an  $M \times N$  lattice having the value of  $z_s$  depends only on the neighboring states. Based on this, in this work, an MRF based PLL is proposed to be used for 2D phase unwrapping.

In this approach, considering the second order neighboring pixels as the past based on the MRF model, error measures, i.e., the phase detector outputs of the PLL, from 8 neighboring samples are averaged to update the phase estimate of the current center pixel. Then, the current center pixel itself is used as the next reference input of the PLL. For a better noise suppression and tracking capability, a second order PLL is implemented.

The performance of the proposed approach is evaluated for i) a synthetic fractal Brownian surface (fBs), which is considered to be a proper model for 2D absolute phase [4], and ii) a real TerraSAR-X / TanDEM-X interferometric pair. For both synthetic and real data, the phase singularity points (residue points) are first detected and the residue maps are extracted. The generated fBs is corrupted by different levels of noise in order to observe the noise suppression capability of PLL based phase unwrapping. On the other hand, for the real data, the contribution of the flat earth phase is removed by interferogram flattening before phase unwrapping, so the phase variations are reduced. The results show that the proposed method performs quite well under proper sampling condition, i.e., no aliasing, and recovers the phase gradient successfully. In case of abrupt phase changes due to the topography of terrain, the success of unwrapping operation depends on the tracking speed of PLL. In other words, if the loop bandwidth of PLL is wide enough to track these abrupt phase changes, phase unwrapping will be successful. Otherwise, the unwrapping error caused by such a singularity point propagates through the integration path. Here, it is also important to consider the stability of the PLL and treat the trade-off between the noise suppression capability and tracking speed of PLL accordingly.

8891-9, Session 1

## End-to-end design consideration of a radar altimeter for terrain-aided navigation

Inchan Paek, Dongmin Park, Kyungju Yoo, Samsung Thales Co., Ltd. (Korea, Republic of); Joohwan Chun, KAIST (Korea, Republic of)

Radar altimeters have long been used for the terrain-aided navigation of aerial vehicles. However, there are little works published in the open literature on the joint design of the rear-end data processing part and the front-end signal processing part. The data processing is carried out with a tracker based either on the point estimator such as the Kalman filter or on the propagator of the probability density function (pdf) such as the particle filter. The measurement model which those trackers employ is usually the altitude of the land surface in the vertical descent direction plus additive zero-mean white Gaussian noise. Our present work hinges on the fact that this measurement model does not reflect the reality, the limitation of the current signal processing techniques with the radar altimeter.

The measurement generated from the signal processing part is usually the first echo return timing, which conveys the distance information between the vehicle and the closest terrain point. A major difficulty is that the pulse width cannot be made very short and therefore its pulse-limited illumination area covers a wide disk around the vertical descent point. Therefore, the first returned echo is usually not the altitude in the vertical descent direction, if the altimeter is used on mountainous surfaces or in the urban area with high-rise buildings.

Designers of the altimeter signal processor were of course, very well aware of this difficulty associated with the large resolution cell, Raney proposed to use the delay-Doppler altimeter (DDA), which essentially is the multi-look synthetic aperture radar (SAR) processing, with range

curvature correction. This approach can greatly reduce the along-track resolution cell size. The cross-track resolution, however, cannot be improved with the DDA technique. Jensen proposed to use the interferometric SAR (InSAR) to determine the angle of arrival (AOA) of the echo, with two antennas spaced by a half a wavelength. The resolution obtainable with an array antenna depends on its aperture size, and therefore a later proposal was to use two widely-spaced antennas, with an additional antenna in between, so that the three antennas form two co-prime baselines. These InSAR techniques however, do not give accurate measurements if the echo signal has a broad angular spread or has two or more AOAs. Therefore, the current state-of-the-art signal processing technique does not give accurate measurement.

Our approach is different from those previous efforts in that we focus on the tracker (rather than the signal processor) elaborating on its measurement model, noting that the purpose of our altimeter is not to acquire accurate altitude measurement but to collect reference data that are to be compared with the map on board. Namely we may use an ordinary radar altimeter, but model its measurement as a sum of the echo waveforms from the multiple scatterers in the pulse-limited illuminated disk. Therefore, the measurement is now a waveform (rather than the simple echo timing) that contains rich information such as noise level, signal level, leading slope, trailing slope as well as the echo timing. This measurement waveform is processed using a particle filter, and our technique can be used either with previous InSAR altimeters or with ordinary altimeters. The preliminary simulation results indicate that the position accuracy obtained with our approach in urban area with high-rise buildings is at least as good as with the complicated InSAR approach.

## 8891-10, Session 2

### Assessment of INSAR potential in simulating subsurface geological structure

Negin Fouladi Moghaddam, Chris Rudiger, Monash Univ. (Australia); Sergey Samsonov, Natural Resources Canada (Canada) and European Ctr. for Geodynamics and Seismology (Luxembourg); Jeffrey P. Walker, Mike Hall, Monash Univ. (Australia)

High resolution geophysical surveys, including seismic, gravity, magnetic, etc., provide valuable information about subsurface structuring but they are very costly and time consuming with non-unique and sometimes conflicting interpretations. Several recent studies have examined the application of DInSAR to estimate surface deformation, monitor possible fault reactivation and constrain reservoir dynamic behaviour in geothermal and groundwater fields. The main focus of these studies was to generate an elevation map, which represents the reservoir extraction induced deformation. This research study, however, will focus on developing methods to simulate subsurface structuring and identify hidden faults/hydraulic barriers using DInSAR surface observations, as an innovative and cost-effective reconnaissance exploration tool for planning of seismic acquisition surveys in geothermal and Carbon Capture and Sequestration regions.

By direct integration of various DInSAR datasets with overlapping temporal and spatial coverage we produce multi-temporal ground deformation maps with high resolution and precision to evaluate the potential of a new multidimensional MSBAS technique (Samsonov & d'Oreye, 2012). The technique is based on the Small Baseline Subset Algorithm (SBAS) that is modified to account for variation in sensor parameters. It allows integration of data from sensors with different wave-band, azimuth and incidence angles, different spatial and temporal sampling and resolutions. These deformation maps then will be used as an input for inverse modelling to simulate strain history and shallow depth structure.

To achieve the main objective of our research, i.e. developing a method for coupled InSAR and geophysical observations and better understanding of subsurface structuring, comparing DInSAR inverse modelling results with previously provided static structural model will result in iteratively modified DInSAR structural model for adequate match with in situ observations. The newly developed and modified algorithm will then be applied in another part of the region where subsurface information is limited.

## 8891-11, Session 2

### An algorithm for phase-offset evaluation in InSAR DEM generation

Stefano Perna, Univ. degli Studi di Napoli Parthenope (Italy) and CNR-IREA (Italy); Carmen Esposito, Istituto per il Rilevamento Elettromagnetico dell'Ambiente (Italy) and Univ. degli Studi del Sannio (Italy); Riccardo Lanari, Antonio Pauciuolo, Istituto per il Rilevamento Elettromagnetico dell'Ambiente (Italy); Christian Wimmer, Orbisat Remote Sensing (Brazil); Paolo Berardino, Istituto per il Rilevamento Elettromagnetico dell'Ambiente (Italy)

Generation of Digital Elevation Models (DEMs) can be carried out by means of the Synthetic Aperture Radar Interferometry (InSAR) technique [1][2][3], which exploits the phase difference (interferogram) between two focused SAR data relevant to the same illuminated area. Within the processing chain usually applied for InSAR DEM generation [1], one crucial step consists in the evaluation of the offset up to which the unwrapped interferometric phase is given after application of phase unwrapping procedures [1]. Such an offset, which is constant over the unwrapped interferogram, can be accurately calculated by using ground control points (GCPs) properly deployed over the illuminated area. However, use of GCPs involves accurate measurement of their precise position (typically by means of GPS ground-stations), thus resulting expensive in terms of costs and time. Moreover, in case of emergencies, such a kind of operation can be difficult, if not impossible. Thus, in some cases of practical interest, GCP-based algorithms cannot be applied for evaluation of the searched phase offset. Accordingly, some methods have been developed to circumvent this limitation [4][5][6][7].

In this paper, we present a novel procedure aimed at estimating such a phase-offset without using GCPs. The proposed method exploits an available external DEM with resolution and accuracy worse than those of the SAR DEM we are going to generate. More precisely, the algorithm evaluates first of all a raw phase offset with a least squares estimation exploiting the difference between the unwrapped interferogram and the synthetic phase computed by means of the external DEM. Thereafter, the algorithm calculates, with an iterative procedure, the correct phase offset exploiting the difference between the external DEM and the DEM generated with the initial raw-phase offset. The algorithm is very efficient and it has been tested on InSAR data acquired by two different X-band airborne SAR systems [8][9]. Comparisons with results achieved by using corner reflectors properly deployed over the test areas are also included.

#### REFERENCES

- [1] G.Franceschetti, R.Lanari, Synthetic Aperture Radar Processing, CRC PRESS, New York, 1999.
- [2] R.Bamler, P.Hartl, "Synthetic aperture radar interferometry," *Inverse Problems*, 14, R1-R54, 1998.
- [3] H.A.Zebker, R.M.Goldstein, "Topographic mapping from interferometric synthetic aperture radar observations," *J. Geophys. Res.*, 91, 4993, 1986
- [4] S.N. Madsen, H.A.Zebker, "Automated Absolute Phase Retrieval in Across-track Interferometry," *IGARSS*, 1992
- [5] J.C.Mura, M.Pinheiro, R.Rosa and J.Moreira, "A Phase-Offset Estimation Method for InSAR DEM Generation Based on Phase-Offset Functions," *Remote Sens.* 4, 745-761, 2012.
- [6] C.Rossi, F.R.Gonzalez, T.Fritz, N.Yague-Martinez, M.Eineder, "TanDEM-X calibrated Raw DEM generation," *ISPRS Journal of Photogrammetry and Remote Sensing*, Volume 73, 12-20, 2012.
- [7] G. Gatti, S. Tebaldini, M. Mariotti d'Alessandro, F. Rocca, "ALGAE: A Fast Algebraic Estimation of Interferogram Phase Offsets in Space-Varying Geometries", *IEEE Trans. Geosci. Remote Sens.*, 49, 6, 2011
- [8] S.Perna, C.Wimmer, J.Moreira, G.Fornaro, "X-Band Airborne Differential Interferometry: Results of the OrbiSAR Campaign Over the Perugia Area", *IEEE Trans. Geosci. Remote Sens.*, 46, 2, 2008
- [9] S. Perna et al, "Capabilities of the TELAER airborne SAR system upgraded to the multi-antenna mode", In *Proceedings IGARSS 2012 Symposium, Munich*, 2012.

8891-12, Session 2

**Decorrelation of L-band and C-band interferometry to volcanic risk prevention**

Eva Savina Malinverni, Anna Nora Tasseti, Univ. Politecnica delle Marche (Italy); David Sandwell, Univ. of California, San Diego (United States); Lucia Cappelletti, Università Politecnica delle Marche (Italy)

Synthetic aperture radar (SAR) has got nowadays several strong key features such as a fine spatial resolution/precision and a high temporal pass frequency. Moreover, the InSAR technique allows the detection, with an extreme accuracy, of ground deformations, both on large and small scale. This high potential technology can be invaluable to study volcanoes and the related natural hazard. Most volcanoes experience pre-eruption surface deformation. The broad and detailed spatial coverage of radar satellites, giving continuous and accurate deformation data in time and space, provides important information on magma migration and other processes at depth improving the understanding of volcanic processes and hence, the ability to predict and understand eruptions. As a downside, radar satellite measurements can be influenced by artifacts such as atmospheric effects or bad topographic data. Correlation, sometimes called coherence, gives a measure of these interferences, quantifying the similarity of the phase of two SAR images. Different approaches exist to reduce errors due to these artifacts but the main concern remains the possibility to correlate images with different acquisition times: snow-covered or heavily-vegetated areas produce seasonal changes on the surface. Sometimes in these conditions it is impossible to construct interferograms and assess ground deformations. It is important to understand when and why two images have a sufficiently high coherence to generate an interferogram. Generally, minimizing the time between passes partly limits decorrelation. Though, images of the area of interest with a short temporal baseline aren't always available and some artifacts affecting correlation are time-independent. This work aims at studying correlation of pairs of SAR images covering the Yellowstone caldera area (northern USA) and focuses on the influence of surface and climate conditions, especially snow coverage and temperature; furthermore, the effects of the acquisition band (the wavelength of the signal) on correlation are taken into account, comparing L-band and C-band images as a function of frozen and unfrozen conditions in the Yellowstone area. Snow depth and temperature data are the most effective parameters for this study. All the images of the chosen satellites (both ascending and descending) are selected considering the date of acquisition between a 4 years span possibly sampling all the seasons and with an area covering most of the caldera. Interferograms and correlation maps are generated using an open source software, GMTSAR. To isolate temporal decorrelation, pairs of images with the shortest baseline are preferably chosen. Correlation maps are analyzed in relation to snow depth and temperature. Results obtained with ENVISAT and ERS satellites (C band) are later compared with the ones from ALOS (L-band). The study shows how a longer wavelength performs better during winter time, when the surface is covered with snow and temperature is below zero. Both of the satellites, though, have a bad attitude towards wet snow: especially during spring and fall, coherence is so low that no information about phase can be retrieved. During summer months both L- band and C- band maintain a good coherence with L- band performing better over vegetated areas, supporting the result of previous studies.

8891-13, Session 2

**C/X-band SAR interferometry applied to ground monitoring: examples and new potentials**

Raffaele Nutricato, Davide O. Nitti, GAP S.r.l. (Italy); Fabio Bovenga, Alberto Refice, Janusz Wasowski, Consiglio Nazionale delle Ricerche (Italy); Maria Teresa Chiaradia, Politecnico di Bari (Italy)

Thanks to the all-weather, day-night capability to detect and quantify accurately small ground surface deformations, Synthetic Aperture Radar (SAR) Interferometry (InSAR) techniques are attractive for different areas of risk management such as monitoring of subsidence, volcanoes, tectonic movements, urban areas and infrastructure and

slope instabilities. In particular, multi-temporal InSAR (MTInSAR) techniques allow to detect and monitor millimetric displacements occurring on selected point targets exhibiting coherent radar backscattering properties. Application to different geophysical phenomena has been already successfully demonstrated.

Classical applications of the MTInSAR techniques has been carried out in the past on medium resolution data acquired by the ERS, Envisat (ENV) and Radarsat sensors. The new generation of high-resolution X-Band SAR sensors, such as TerraSAR-X (TSX) and the COSMO-SkyMed (CSK) constellation allows acquiring data with spatial resolution reaching metric/submetric values. Thanks to the finer spatial resolution with respect to C-band data, X-band InSAR applications appear very promising for monitoring single man-made structures (buildings, bridges, railways and highways), also isolated, thus giving more chances to provide displacement records in particular where C-band data show low density of coherent scatterers.

Moreover, thanks again to the higher resolution, it should be possible to infer reliable estimates of the displacement rates with a number of SAR scenes significantly lower than in C-band ?? within the same time span or by using more images acquired in a narrower time span. Finally, with shorter wavelengths the sensitivity to LOS displacements is increased together with the capability of detecting very low displacements rates (as the pre- and post-failure movements related to landslides).

We present the recent results of the application of a Persistent Scatterers Interferometry technique, namely the SPINUA (Stable Point INterferometry over Unurbanized Areas) algorithm, to data acquired by ENV, TSX and CSK on selected number of sites. Different applications cases will be considered from landslide monitoring to ground elevation computation. Results will be compared and commented with particular attention paid to the advantages provided by the new generation of X-band high resolution space-borne SAR sensors.

REFERENCES

- 1) F. Bovenga, J. Wasowski, D.O. Nitti, R. Nutricato, M.T. Chiaradia, "Using COSMO/SkyMed X-band and ENVISAT C-band SAR interferometry for landslides analysis", Remote Sensing of Environment, Volume 119, 16 April 2012, Pages 272-285, ISSN 0034-4257, 10.1016/j.rse.2011.12.013.
- 2) D. O. Nitti, F. Bovenga, R. Nutricato, F. Intini, M. T. Chiaradia, "On the use of COSMO/SkyMed data and Weather Models for interferometric DEM generation", European Journal of Remote Sensing, European Journal of Remote Sensing, Vol. 46, pp. 250-271, 2013. Doi: 10.5721/EuJRS20134614.
- 3) R. Nutricato, J. Wasowski, F. Bovenga, A. Refice, G. Pasquariello, D. O. Nitti, M. T. Chiaradia, "C/X-band SAR interferometry used to monitor slope instability in Daunia, Italy". Proceedings of the second World Landslide Forum, Rome, Italy, 03 - 07 October 2011.

8891-14, Session 2

**Monitoring of infrastructural sites by means of advanced multi-temporal DInSAR methods**

Andreas Vollrath, Francesco Zucca, Univ. degli Studi di Pavia (Italy); Salvatore Stramondo, Istituto Nazionale di Geofisica e Vulcanologia (Italy)

With the launch of Sentinel-1, advanced interferometric applications will become more applicable than ever. The foreseen standard Wide Area Product (WAP), with its higher spatial and temporal resolution than comparable SAR missions, will provide the basement for the use of new wide scale and multi-temporal analysis. By now the use of SAR interferometry methods with respect to risk assessment are mainly conducted for active tectonic zones, plate boundaries, volcanoes as well as urban areas, where local surface movements occur and enough pixels contain a stable phase.

This study in contrast aims to focus on infrastructural sites that are located outside cities and are therefore surrounded by rural landscapes. The stumbling block gave the communication letter by the European Commission with regard to the stress tests of nuclear power plants in Europe. It is mentioned that continuously re-evaluated risk and safety assessments are necessary to guarantee highest possible security to the European citizens and environment. This is also true for other infrastructural sites, that are prone to diverse geophysical hazards.

At this stage of the project, first results of the combined PSInSAR and SBAS approach will be presented for the industrial area around Priolo Gargallo in South East Sicily by using ENVISAT ASAR IM mode data from 2003-2010. This area is located between the Malta Escarpment fault system and the Hyblean plateau and is prone to earthquake and tsunami risk. It features a high density of oil refineries that are directly located at the coast.

The general potential of these techniques with respect to the SENTINEL-1 mission will be shown for this area and a road-map for further improvements is given in order to overcome limitations that refer to the influence of the atmosphere, orbit or DEM errors.

Further steps will also include validation and tectonic modeling for risk assessment. Subsequently, other sites of interest (e.g. nuclear power plants, chemical plants, toxic waste dump) will be considered as well.

## 8891-15, Session RJS

### Comparison of three algorithms for the retrieval of soil moisture from ASCAT data in the framework of the round robin exercise

Simonetta Paloscia, Emanuele Santi, Istituto di Fisica Applicata Nello Carrara (Italy)

The goal of the Round Robin project is to encourage the active participation of the international community in CCI soil moisture activities. It has been performed as a public and open process, which benefits from the knowledge of the research community that works with soil moisture data sets. Consequently, the soil moisture CCI project welcomes every researcher and institution with the will to participate and contribute with their algorithms to this exercise.

Within the framework of the CCI Soil Moisture project two separate Round Robins will be carried out: one is for algorithms to be applied to the ASCAT scatterometer measurements and the other one is for passive microwave AMSR-E observations from the 5-years period 2007 to 2011. Such intercomparisons are very useful to objectively assess similarities and differences between models and retrieval algorithms.

In this paper three retrieval algorithms applied to MetOp-ASCAT backscatter time series resampled over 150 sites, for the retrieval of soil moisture, have been compared. For model training, calibration, and validation a selection of datasets from the International Soil Moisture Network (ISMN) was used (Dorigo et al. 2011).

Not all datasets contained in the ISMN are considered for the Round Robin. Only surface layer (< 10 cm) measurements are used. Secondly, only stations that are operational during the period 2007 – 2011 are selected. The locations of the in situ soil moisture measurements used for the Round Robin represent a wide range of climate conditions, covering a wide variety of vegetation types and vegetation density classes.

The three algorithms which have been implemented and compared by using this available datasets are shortly described in the following:

1. Inversion algorithm based on two Artificial Neural Networks, one of them including the information on Lat/Lon for smoothing the effect of the climatic variability.
2. Inversion algorithm based on SVR methods using as input the backscattering coefficients for one, two and three incidence angles
3. Inversion algorithm based on Bayes methods, modeled on backscattering coefficients with one incidence angle and a non informative prior information.

The results showed a good agreement with the soil moisture datasets of the ISMN, in spite of the great distribution of the test areas worldwide in very different climatic zones and very wide range of vegetation covers. The correlation coefficients (R) ranged from 0.5 to 0.8 with rather low RMSE (around 4-6%, according to the different test areas).

Although these results should be considered preliminary, they are encouraging and further test and validation of the algorithm will be necessary for refining the results.

## 8891-16, Session RJS

### How far can be SAR considered a tool for mountain hydrology?

Giacomo Bertoldi, Claudia Notarnicola, Luca Pasolli, EURAC research (Italy); Stefano Della Chiesa, Georg Niedrist, Ulrike Tappeiner, EURAC research (Italy) and Univ. Innsbruck (Austria)

Accurate, spatially and temporally distributed information about soil moisture in mountain catchments is of great importance in hydrological applications, like floods prediction in case of extreme rainfall events, watershed management during dry periods, precision farming, as well as earth sciences, like climate change analysis and meteorology.

In the last two decades, the increasing number of space-borne sensors, and, in particular, microwave remote sensing sensors such as radiometers, scatterometers and Synthetic Aperture Radar (SAR), have been deeply exploited for the estimation of soil moisture content, thanks to the well-established sensitivity of microwave electromagnetic waves to the dielectric properties (and thus the water content) of soils. For this reason, soil moisture retrieval from remote sensing in alpine context is promising also to provide validation data for physically based hydrological models, and therefore improve their predictive capability. However, due to the extreme variability in topography, soil and vegetation properties of mountain areas, obtaining reliable predictions of soil moisture of fine-scale spatial and temporal patterns is still challenging.

In this contribution, we analyze the spatial and temporal dynamics of surface soil moisture (0 - 5 cm depth) of alpine meadows and pastures in the establishing Long Term Ecological Research area (LTER) "Mazia Valley" (South Tyrol – Italy), at different spatial scales and with different techniques: (I) a network of fixed stations; (II) field campaigns with mobile ground sensors; (III) soil moisture retrieval from 20-m resolution polarimetric RADARSAT2 SAR images, estimated using an advanced algorithm based on the Support Vector Regression (SVR) technique and the integration of ancillary information on land use and topographic proprieties; (IV) numerical simulations using the GEOtop hydrological model. The strength, the weaknesses and the consistency of the different estimation techniques are evaluated and, in particular, the GEOtop model is used to understand the physical controls of the observed patterns in RADARSAT2 products, and their consistency with respect to the catchment hydrological behaviour.

Results show that RADARSAT2 soil moisture estimation corresponds well to the spatial ground surveys, but shows different patterns with respect to the model, especially for irrigated meadows. In fact, RADARSAT2 patterns strongly reflect observed vegetation, soil type and topographic patterns. Model output shows smaller spatial variability with respect to the spatial ground surveys, and a stronger temporal variability, in agreement with the fixed station network. Differences are likely due to the strong sensitivity of the SAR signal to surface roughness and vegetation density and to the difficulties to know with sufficient spatial detail model parameters and irrigation amount. Therefore, results suggest that RADARSAT2 products have a good ability to reproduce small-scale (~ 20 m pixels size) soil moisture patterns, thus complementing the ability of the hydrological model to predict temporal variations of soil moisture. A further step of this work will be towards the integration of model results with remote sensing observations at different spatial scales.

## 8891-17, Session RJS

### Soil moisture retrieval from three-day repeat ERS-2/SAR data: comparison with ASCAT- and SMOS-derived estimates and in situ measurements

Luca Pulvirenti, Nazzareno Pierdicca, Fabio Fascaetti, Univ. degli Studi di Roma La Sapienza (Italy)

It is well-known that satellite microwave remote sensing allows obtaining frequent measurements of soil moisture (SM) and global coverage, thus representing a fundamental complement to in situ measurements. At microwave bands, a direct sensitivity to SM exists, because SM drives the soil dielectric permittivity. Sensors operating in the low-frequency portion of the microwave spectrum (L- to C-band) are able to measure SM within a suitable depth, although their

measurements (especially those at C-band) are affected by vegetation and soil roughness.

Both microwave passive radiometers and active radars can be used, with different swath width, spatial resolution and revisit time, to retrieve SM. Microwave radiometers (such as the L-band Soil Moisture and Ocean Salinity SMOS satellite) and scatterometers (as the C-band Advanced Scatterometer ASCAT on-board METOP), generally offer a temporal resolution which allows fulfilling the observing cycle requirement of a soil moisture product. However, they do not always fulfil the spatial resolution requirement, since the spatial resolution of these instruments generally ranges between 20 and 50 km. Conversely, the use of Synthetic Aperture Radar (SAR) systems to retrieve SM allows for the generation of soil moisture products with resolution varying from hundreds of meters to 1 km, but SAR temporal resolution was generally considered as a critical aspect for soil moisture applications, so far. However, the forthcoming European Space Agency (ESA) Sentinel-1 (S-1) mission will provide C-band radar data characterized by short revisit time (the two-satellite constellation will offer six days repeat, or less over Europe and Canada). This kind of data give also the opportunity to deal with the well-known ill-posedness of the problem of SM retrieval using SAR data, thus increasing the capability to produce reliable SM maps. This improvement of the quality of SAR-derived SM maps can be achieved by applying multitemporal inversion techniques which assume that the temporal scale of variation of soil roughness and vegetation is considerably slower than that of soil moisture.

Although S-1 data will be only available in the near future, some SAR data with short revisit time are already available. In fact, owing to a request from the cryosphere science community, during the last months of ERS-2 activity (in 2011), its orbit was lowered and, in this way, ERS-2 was able to acquire radar images every three days, rather than its previous 35-day cycle. Three-day ERS-2/SAR data represent a unique opportunity to apply a multitemporal approach to retrieve SM. This application has been carried out to the data acquired over Denmark throughout May and June 2011. Denmark observations have been chosen since in the area covered by ERS-2 images, in situ SM measurements provided by the International Soil Moisture Network (ISMN) are available.

In this study, the first outcomes of the comparison between ERS-2-derived estimates and in situ data are presented. To provide further insights on SM retrievals from satellite microwave data, SAR and ISMN SMs are also compared with the estimates provided by ASCAT and SMOS. To account for the different scales of the various SM data, SAR derived estimates are averaged over different spatial scales, for instance over the area in which ISMN stations are placed, or within the SMOS pixels. Both temporal and spatial correlations between the various SM data will be presented and discussed at the conference.

### 8891-18, Session RJS

## GNSS-R sensor sensitivity to soil moisture and vegetation biomass and comparison with SAR data performance

Simonetta Paloscia, Istituto di Fisica Applicata Nello Carrara (Italy)

In this paper the results obtained from an experiment focused on the capabilities of GNSS-R sensors for land applications are described. Indeed, most of GNSS-R activities were carried out over ocean, as the high conductivity and relatively homogeneous surface roughness, compared to typical land topography and land cover variability, would maximize the incoherent reflected signal strength.

The ESA project GRASS (GNSS Reflectometry Analysis for BiomaSS Monitoring) consisted in the analysis of direct and reflected bitstreams at both polarizations of a GNSS-R polarimetric sensor installed on an aircraft. The flight campaigns were complemented by extensive in-situ campaigns in order to measure key bio-geophysical parameters of soil and vegetation. Two experimental test-sites were covered: the agricultural area along the Elsa river of 'Ponte a Elsa' test-site, and the Forcoli test-site, a region with scattered poplar plots and forest areas.

It was observed that the LR reflection coefficient has a rapid response to terrain reflectivity changes, such as transitions between land and rivers, roads, and housing. The response of the RR reflection coefficient is not so evident; however, it can still be appreciated over highly reflective surfaces such as water bodies. This visual comparison of the reflectivity changes of specular points with respect to surface characteristics was used in order to validate the good performance of

the GNSS-R instrument and the data processing chain.

A more detailed comparison of the GNSS-R signals with the ground truth data was performed. For each campaign, a land-use map was used to distinguish the GNSS-R reflectivity measurements according to the land cover. It was noted that, as observed in a previous ESA project (LEIMON), both LR and RR reflection coefficients were sensitive to changes in the surface soil moisture, with a total variation of about 6 dB between the dry and wet seasons. It was also observed that changes in the surface roughness originated strong variation on the reflection coefficients. It has been observed that the RR reflection coefficient was generally very low for all surfaces, in the range -20/-25 dB, with an increasing trend with incidence angle. LR signal showed instead a lower dependence on the incidence angle and a higher sensitivity to surface characteristics, within an interval between -8/-17 dB. Typically LR reflection coefficient showed higher values on moist and smooth fields and lower values on rough and dry soils.

Regarding the sensitivity to vegetation, it was observed that the measured LR coefficients have a moderate power variation due to the presence of woody vegetation. It was observed that the LR coefficient experienced a monotonic decrease with increasing biomass, up to an estimated forest dry biomass of more than 150 t/ha. Both experimental and simulated data agreed that the sensitivity was of about 2.0dB/50t/ha of dry biomass. Furthermore, since the dominant component appeared to be the coherent one, the sensitivity was maintained up to 150 t/ha of dry biomass, for the Forcoli test site, which is well beyond the monostatic radar saturation point at L-band (about 50t/ha), usually indicated in literature. Of course, further data would be welcome to confirm this result and especially to explore wider biomass ranges.

### 8891-19, Session 3

## Combining polarimetric and contextual information using autoassociative neural networks

Ruggero G. Avezano, Fabio Del Frate, Univ. degli Studi di Roma Tor Vergata (Italy)

In the last decade there has been a considerable development of spaceborne SAR sensors. All the major space agencies are planning future SAR missions with polarimetric capabilities. However there is still a need to guide electromagnetic and statistics theories that take advantage of this kind of information towards operational applications.

The use of contextual information is also often required for automatic interpretation and target detection. In general, the selection of features is dependent on the kind of required analysis and ultimate application. However, the implementation of fast and reliable algorithms that exploit both polarimetric and contextual information can be limited by the increased dimensionality of the problem.

Principal Component Analysis (PCA) is a data analysis technique that relies on a simple transformation of recorded observation, stored in a vector, to produce statistically independent variables. Non-Linear PCA is commonly seen as a non-linear generalization and extension of standard PCA. If non-linear correlations between variables exist, NLPCA will describe the data with greater accuracy and/or by fewer factors than PCA.

The use of Autoassociative Neural Networks (AANN) to perform a NLPCA has been demonstrated. AANN operates by training a feedforward neural network to perform the identity mapping, where the network inputs are reproduced at the output layer. The central hidden layer is called textquotedblleft bottlenecktextquotedblright layer, containing fewer nodes than input or output layers. This topology forces the network to develop a compact representation of the input data.

In this work a combination of polarimetric and contextual information is performed using an AANN.

A set of polarimetric input features were chosen together with contextual descriptors in order to produce an information set having lower dimensionality that can be exploited in a classification problem.

The number of nodes of the hidden layers of the AANN strongly influences the training process and the compression of input information. This problem can be solved by using a simple grid search algorithm that varies recursively the number of nodes of the hidden layers and evaluates the respective error. The topology presenting the lowest error is then selected.

Two Fine Quad Radarsat-2 products of San Francisco and Rome areas

were selected as test sets. A vector of features extracted from the bottleneck layer is used as input to a classical NN classifier, evaluating the performance with respect to the input vector containing standard polarimetric and/or textural features.

### 8891-20, Session 3

## Dealing with flood mapping using SAR data in the presence of wind or heavy precipitation

Nazzareno Pierdicca, Luca Pulvirenti, Univ. degli Studi di Roma La Sapienza (Italy)

The potentiality of spaceborne Synthetic Aperture Radar (SAR) for flood mapping was demonstrated by several past investigations. The synoptic view, the capability to operate during both day time and night time and the sensitivity of the microwave band to water are the key features that make SAR data useful for monitoring inundation events. In addition, their high spatial resolution, which can reach 1m with the new generation of X-band instruments such as TerraSAR-X and COSMO-SkyMed (CSK), allows emergency managers to gather accurate information on the flood extent. CSK gives also the possibility of performing frequent observations of regions hit by floods, thanks to the four-satellite constellation.

Current research on flood mapping using SAR is focused on the development of automatic algorithms to be used in near real time applications. The approaches are usually based on the low radar return from terrestrial water bodies that generally behave as specular reflectors and appear dark in SAR images. It is well known that techniques searching for regions of low backscatter may fail in the presence of vegetation emerging from the water surface, or of flooded forests, since this these kinds of targets appear bright in SAR images because of the double bounce effect involving the water surface and stems or trees. However, even flooded bare soils can be difficult to detect in some meteorological conditions. Missed detection of flooded areas may occur when wind-induced waves cause the roughening of the water surface. This roughening causes, on its turn, an increase of the backscatter from water to a level similar to (or even higher than) that from surrounding non-flooded areas. Moreover, because of the multiplicative nature of speckle that affects SAR images, any increase in backscatter from the water surface produces also an increase of the level of noise in the flooded region. Actually, if X-band SAR data are used to map inundation, not only missed detection, but also false alarms may occur when searching for regions of low backscatter. In fact, some areas may appear dark because of artefacts caused by heavy precipitating clouds, since it has been demonstrated that the attenuation of the radar signal because of precipitation implies that the microwave radar signature of rain can be similar to that of water surfaces.

In this study, we deal with flood mapping when high winds or heavy precipitation are present at the time of the SAR observation of a flood. As for wind roughening of a water surface, several electromagnetic models have provided insights on the effects of wind on radar backscatter from ocean, but the effect on terrestrial water bodies is complicated by the variability of fetch and water depth. Here, an electromagnetic model able to simulate the backscatter from shallow waters as function of wind is used, and its outputs are compared to CSK observations of floods in the presence of high winds, as well as to some CSK images of lakes acquired in different wind conditions.

To deal with the effects of intense precipitation on X-band SAR data, a pre-processor able to detect flooded regions away from areas of heavy rainfall has been developed, using, as calibration data, the CSK images of the event that hit Northwestern Italy on November 2011.

### 8891-21, Session 3

## Phenomenology of fully polarimetric TerraSAR-X data

Jorge V. Geaga, Consultant (United States)

We have studied and reported on the eigenanalysis of complex single look and multilook fully polarimetric SIR-C data and fully polarimetric complex ISAR turntable data. We have presented formalism for the diagonalization of the Kennaugh(Stokes) matrices of individual single look complex fully polarimetric data. Three of the

transformation parameters for the diagonalization are the Huynen orientation, ellipticity and bounce parameters. The orientation and ellipticity parameters are shown to be the angular parameters of the fully polarized Stokes eigenvector of the Kennaugh matrix. We have extended the analysis to experimental fully polarimetric complex data from TerraSAR-X. We report on empirical observations from individual TerraSAR pixels. We report progress using a neural net scheme to isolate scattering signatures from ten terrestrial surface regions picked from six TerraSAR-X scenes. The feature set inputs to the neural net are from a feature set we have developed, the Krogager decomposition and the entropy/alpha/anisotropy decomposition of Cloude and Pottier.

### 8891-22, Session 3

## Asymmetric decomposition method for polarimetric SAR data using a modified four-component scattering model

Bin Zou, Ning Cao, Yan Zhang, Hongjun Cai, Harbin Institute of Technology (China)

For polarimetric SAR (PolSAR) information extraction, polarimetric target decomposition theorem is a typical method. Several decomposition methods have been proposed to identify the scattering characteristics based on polarimetric statistical characteristics. Freeman proposed a three-component scattering model for natural distributed areas. Based on Freeman decomposition method, Yamaguchi extended the three-component to a four-component scattering model. All these methods are based on the ensemble averaging of coherency or covariance matrix. The incoherently averaged PolSAR data contains 9 independent parameters as the second order statistics of polarimetric information. Freeman decomposition only accounts 5 parameters and an improved four-component decomposition method with rotation of coherency matrix proposed by Yamaguchi leaves unaccounted number as 2. In 2012, Yamaguchi further reduced the parameters from 9 to 7 by using double unitary transformation. Then all polarimetric information has been utilized in this G4U decomposition. This paper intends to propose an additional method that can fully utilize the polarimetric information without reducing the parameters of the measured data.

In the four-component decomposition, helix scattering mechanism is utilized in decomposition schemes to describe man-made structures in urban area. This paper analyzed the limitation of helix scattering mechanism in dealing with the non-reflection symmetric scattering cases. In the four-component decomposition model, the probability density function of rotation angle around the radar line of sight is assumed to be uniform. However, the measured data does not always fit such assumption. So the helix scattering component cannot deal with this situation. Then a general scattering term, named asymmetric scattering term, is proposed to take account of the non-reflection symmetric scattering information of man-made structures. This asymmetric scattering corresponds to the non-reflection symmetric condition that the co-polar and cross-polar correlations are not close to zero.

Using asymmetric scattering term to describe man-made structures in urban area, the covariance matrix can be decomposed into surface, double-bounce, volume and asymmetric scattering components. It has been found that the proposed decomposition model accounts all the 9 independent parameters of the covariance matrix.

The experiments are implemented using ESAR L-band polarimetric SAR data to validate the proposed decomposition method. The test area is close to Oberpfaffenhofen, Germany. The results of the four-component decomposition and the proposed decomposition are compared. The experiment confirms that the proposed method is effective in distinguishing different types of terrains. It can be found that double-bounce and asymmetric scattering are predominant in urban areas.

# Conference 8892: Image and Signal Processing for Remote Sensing XIX

Monday - Wednesday 23–25 September 2013

Part of Proceedings of SPIE Vol. 8892 Image and Signal Processing for Remote Sensing XIX

8892-1, Session 1

## Quality assessment of pan-sharpening methods

Gintautas Palubinskas, Peter Reinartz, Deutsches Zentrum für Luft- und Raumfahrt e.V. (Germany)

The quality of pan-sharpened image is usually quantified separately by various spectral and spatial quality measures mostly originating from image processing, what it makes quite difficult to rank different image fusion methods. A new Joint Quality Measure (JQM) is proposed which is based on the combination (averaging) of two Structural Similarity Image (SSIM) indices (one for spectral quality and another one for spatial quality) allowing comfortable selection of optimal parameters of a particular pan-sharpening method and comparison of different methods using a sole measure. Recent studies show, that the SSIM between original spectral bands and corresponding low pass filtered pan-sharpened bands is a quite well suitable measure (further called Quality for Low Resolution (QLR)) for spectral quality. Spatial quality is much more difficult to measure and none of the known measures can perform this task satisfactorily. We propose a new spatial quality measure - a SSIM between the intensity or mean image - calculated from the appropriately selected fused multispectral bands, and original panchromatic band, which will be called further Quality for High Resolution (QHR). This measure is much more physically reasonable than the measures based on separate spectral bands (e.g. SSIM between individual spectral band (narrow spectrum) and panchromatic band (wide spectrum)), because it compares data with approximately similar spectral responses (only bands which spectral responses are overlapping with spectral response of panchromatic band are considered). A simple average or product of these two measures: QLR and QHR would bias the result due to different ranges of the two measures (QHR usually exhibits lower values than QLR). Thus we propose a normalization of one of the measures before averaging (producing a joint quality measure (JQM)) based on a linear scaling transform. Minimum and maximum values for each of the measures (spectral and spatial) are derived separately from the quality assessment results of two pan-sharpening methods (or one method with two different parameter settings) exhibiting lowest and highest values for spectral and spatial quality measures. Additional margin of 10% added to these extreme values ensures the appropriate comparison or quality assessment of other pan-sharpening methods. Thus the proposed normalization of quality measures is data dependent what means it should be performed individually for each image/scene. But this is not a really great drawback because the normalization should be estimated only once per scene and a fast fusion method such as High Pass Filtering Method (HPFM) with different parameter settings can be used. Quality assessment of the five fusion methods: Component Substitution (CS), High Pass Filtering Method (HPFM), General Fusion Filtering (GFF), ARSIS variant (ATWT Model for Wavelet Fusion) and Gram-Schmidt (GS) pan-sharpening is performed for IKONOS and WorldView-2 satellite optical remote sensing data over the two cities: Munich and Melbourne. Experiments showed the superiority of the proposed JQM when compared with the two known joint measures: simple product of two different measures and Quality with No Reference (QNR) index. Moreover, the results are fully supported by the visual analysis of imagery and existing experience.

8892-2, Session 1

## Pansharpening of hyperspectral images: a critical analysis of requirements and assessment on simulated PRISMA data

Andrea Garzelli, Univ. degli Studi di Siena (Italy); Bruno Aiazzi, Istituto di Fisica Applicata Nello Carrara (Italy); Luciano Alparone, Univ. degli Studi di Firenze (Italy); Stefano Baronti, Massimo Selva, Istituto di Fisica Applicata Nello Carrara (Italy)

Pansharpening methods suitable for the spatial enhancement of hyperspectral images are critically discussed and assessed on simulated data from the upcoming PRISMA mission. In principle,

most of methods that can be used for spatial resolution enhancement of HS imagery may be inherited from MS pansharpening. HS pansharpening, however, is more complex than that of MS data, mainly for the following two reasons. Firstly, the spectral coverage of the panchromatic (Pan) image does not match the wavelength acquisition range of the HS bands. The lack spectral overlap may determine a low physical congruity between the short wave infra-red (SWIR) channels of HS and the Pan image. Thus, most of otherwise valuable MS pansharpening methods may become unsuitable for HS pansharpening. Secondly, the HS bands are designed to be high-SNR data, in order to be useful to specific tasks, like spectral unmixing. Pansharpening fusion may contaminate the high SNR of HS data with the lower SNR of the Pan data. In this sense, regardless of the number of bands, a Bayesian approach to fusion is attractive. Furthermore, the huge number of HS bands does not allow fusion methods based on local context, either in the original spatial domain or in a transformed domain, to be exploited. The spatial scale ratio (SR) between HS and Pan may not be a power of two, e.g.,  $SR = 3$  in the case of Hyperion data (30 m) and the panchromatic channel of ALI (10 m). For fusion methods based on multiresolution analysis (MRA), this implies redesigning all digital spatial filters.

Constraining the spectral angle of the original HS data is the key to achieve pansharpening of hyperspectral image data. To this aim, applying modulation-based pansharpening algorithms preserves the spectral consistency of fusion products to the original HS data. However, the extent of the modulating term is crucial for the spatial quality of fusion products (possible under/over-enhancement).

Experiments will be carried out on simulated hyperspectral and panchromatic data. A simulator has been designed to provide data with spatial and spectral characteristics similar to those provided by the PRISMA instruments. The data set that can be generated is constituted by a 5m<sup>2</sup>5m Pan image and a 30m<sup>2</sup>30m hyperspectral data cube. A 5m<sup>2</sup>5m hyperspectral data cube is also generated and represents the ground truth on which the results of the pansharpening algorithms can be validated.

Using simulated data allows quality assessment of pansharpening to be performed directly on a reference HS image at high spatial resolution, which is not available when real data are concerned. Also, the effectiveness of the existing quality indexes for pansharpening algorithms shall be verified, both in the presence of a reference image (Q2n index) and without a reference image (QNR index). The opportunity of applying a quality assessment protocol at degraded spatial scale will be also investigated, particularly for spatial scale ratios between HS and Pan images greater than four ( $SR = 6$ , for PRISMA data). As a general criterion concerning quality measurements, spectral consistency will be considered more important than spatial consistency.

8892-3, Session 1

## A new super resolution method based on combined sparse representations for remote sensing imagery

Feng Li, Lingli Tang, ChuanRong Li, Academy of Opto-Electronics (China); Yi Guo, Commonwealth Scientific and Industrial Research Organisation (Australia); JunBin Gao, Charles Sturt Univ. (Australia)

In the past few decades, global spaceborne/airborne payloads and observation data have been experiencing a rapid development. While pursuing high resolution payloads, it is also necessary to make full use of the present spaceborne/airborne payload resources by super resolution (SR). SR is a technique of restoring a high spatial resolution image from a series of low resolution images of the same scene captured at different times in a short period. Common SR methods, however, may fail to overcome the irregular local warps and transformation brought by platform vibration and air turbulence existing in low resolution remote sensing images. Moreover, it is difficult to setup a generalized prior for remote sensing images for Maximum a Posteriori based methods when solving the problem of super resolution. In this paper, irregular local warps and transformation within the low resolution remote sensing images will be solved by

combining an elastic registration method.

Compressive sensing has been a hot research direction since it was proposed years ago. It works well for sparse signals or sparse representations respect to a particular transform domain or basis, and L1 norm minimization method has become popular again in solving the ill-conditioned problem in compressive sensing. Because there are lots of pseudo high resolution images satisfying the degenerating model of the imaging procedure to create the observed low resolution images, SR is a typical ill-conditioned problem where sparse models are suitable. Therefore, L1 norm minimization method will be adopted in this paper for the SR restoration. Although L1 norm minimization can well preserve sparsity, a sparse representation problem for remote sensing images is yet to be solved. It is well known that different transform domains are good at providing sparse representation for particular types of input signal/images. For example, Wavelet transform is suitable for sparse representations for smooth content images; ridgelet transform can well represent global line structures; discrete cosine transform is excellent in representing either smooth or periodic content images. Nevertheless, it is difficult to find a general transform for all kind of images, especially, for remote sensing images where complex contents are present all the time. In this paper, combined sparse representation will be proposed for remote sensing images SR problem. We assume that a remote sensing image consists of two types of sub-images, for which we use the sparse representations in the space domain and the isotropic undecimated wavelet domain respectively. Four sub-scene of Canberra, the capital of Australia, of Landsat7 panchromatic data (spatial resolution of 30m) captured on four different dates are adopted as testing data. Experimental results show that the new method constructs a much better high resolution image (spatial resolution of 15m) than other common methods. As a plus, the combined sparse representation helps to decompose remote sensing images into sub-images. This method is promising for real applications of restoring high resolution images from current on orbit payloads.

8892-4, Session 1

### Linear spectral unmixing-based method including extended nonnegative matrix factorization for pan-sharpening multispectral remote sensing images

Moussa Sofiane Karoui, Ctr. des Techniques Spatiales (Algeria)

Multispectral imaging systems are currently one of the most important tools in the field of remote sensing. These imaging systems are designed to support many applications by providing a few relatively large spectral bands that detect information in specific combinations of desired domains of the spectrum.

Many current spaceborne sensors provide two different types of images: a low spatial resolution multispectral image and a high spatial resolution panchromatic image. The fusion methods of multispectral and panchromatic images are attractive in this framework, because they aim at producing unobservable fused multispectral image (classically referred to as pan-sharpened multispectral image) with high spatial resolution.

Most famous pan-sharpening methods of multispectral images are Projection/Transformation-Substitution-based methods, such as those based on Principal Component Analysis (PCA) and Gram-Schmidt (GS)-based method.

Recently, we have proposed Linear Spectral Unmixing (LSU)-based techniques for multi/hyperspectral images processing. LSU techniques consist of linearly unmixing remote sensing data into a collection of endmember (pure material) spectra and their corresponding abundance fractions. In this paper, we extend our techniques by proposing a new method for pan-sharpening multispectral remote sensing images. This new fusion method, which uses our recent developed Sparse Component Analysis (SCA)-based LSU approaches, is based on extended Nonnegative Matrix Factorization (NMF) for combining observable low spatial resolution multispectral and high spatial panchromatic data.

The proposed method first simultaneously unmixes low spatial resolution multispectral and high spatial resolution panchromatic data by using extended NMF to estimate the multispectral endmember spectra matrix and the high spatial resolution abundance fraction maps matrix. The unobservable pan-sharpened high spatial resolution multispectral image is then derived by multiplying these two matrices.

The proposed algorithm, inspired from standard NMF methods, consists in optimizing extended cost function by using joint standard and constrained multiplicative update rules.

The proposed algorithm, as standard NMF algorithms, is not guaranteed to provide a unique solution and its convergence point may depend on its initialization.

To avoid random initialization of the proposed algorithm, and as initialization phase, the initial estimated multispectral endmember spectra are calculated by our "2 Dimensions - Variance of Mixtures (2D-VM)" method. These initial spectra are used to derive the initial estimated low spatial resolution abundance fraction maps from low spatial resolution multispectral image by means of the Fully Constrained Least Squares (FCLS) method. The initial estimated one-value panchromatic spectra are derived from the initial estimated multispectral spectra by simply averaging the samples of the latter spectra over the panchromatic wavelength domain. The initial estimated low spatial resolution abundance fraction maps are upsampled to obtain the initial estimated high spatial resolution abundance fraction maps.

The optimization phase consists in jointly and repeatedly updating all initial matrices, according to the proposed standard and constrained update rules.

As a convergence criterion, the condition that the number of iterations exceeds a predefined maximum number of iterations is used.

The proposed method is applied to different real multispectral and panchromatic data sets with different spatial resolutions and different number of spectral bands. Spectral and spatial qualities of fused data are evaluated by frequently used criteria. Obtained results show that our method outperforms the PCA and GS-based standard literature methods.

8892-5, Session 1

### On non-uniform sampling for remote sensing optical images: the METEOSAT Third Generation rectification case study

Rebeca Gutiérrez, Dieter Just, European Organisation for the Exploitation of Meteorological Satellites (Germany)

The METEOSAT Third Generation (MTG) Programme will provide the geostationary platforms for operational meteorological data acquisitions over Europe in 2018-2030. The first MTG satellite will be launched end of 2018 and will host two imaging instruments: the Flexible Combined Imager (FCI) and the Lightning Imager. The FCI instrument has a heritage from the SEVIRI imager on the current METEOSAT Second Generation satellites (MSG), but with improved performance. It provides a full Earth coverage in 16 spectral bands every 10 minutes. For the Level 2 processing of FCI datasets, and in particular for the derivation of Atmospheric Winds, the FCI measurements have to be mapped on a constant reference grid – this process is referred to as rectification. The reference grid is defined by uniform azimuth and elevation angles as seen from a geostationary projection point. Rectification for the FCI implies, therefore, resampling of the acquired science samples to a fixed grid in a geostationary projection.

The rectification process of MTG is more challenging than the current implementation in MSG, because of tighter requirements, the use of a three-axis stabilized platform, and the scanning scheme applied to the FCI, which will be performed with a slow S/N step and a rapid alternating E/W and W/E scan. The classical interpolation formulas assume a uniform sampling spacing in the acquisition measurements. However, non-uniform sampling spacing is an expected feature of the FCI sampling acquisition. Platform micro-vibrations, focal plane distortions (e.g. rotation, axes non-orthogonality) and scan pattern implementation errors (e.g., pointing error of the mirror normal orientation, variations in the velocity of the E/W and W/E scans) result in the acquisition of non-uniform FCI samples, which need to be interpolated at the reference grid points. In such a case, the classical interpolation methods (linear, cubic, truncated Shannon) would cause in some cases significant rectification errors. Nevertheless, it has been shown that, for a band-limited signal and under certain conditions, the sampling theorem can be generalized for the case of non-uniform samples, thus opening a way to handle the sampling irregularities in the rectification process. The main focus is on interpolation algorithms that apply to signals which are band limited and that use a finite number of non-uniform samples, which is a practical constraint in our FCI processing.



This paper analyses the effect of non-uniform sampling in the FCI rectification process and aims to select and assess suitable resampling algorithms for the FCI Level 1 processing chain. We have selected and evaluated a number of interpolation techniques which are tailored to non-uniform resampling, including Lagrange-type interpolation, non-uniform Discrete Fourier Transform (NDFT), a particular method for uniform jittered samples and the general non-uniform sampling reconstruction formula for band-limited signals (Paley-Wiener-Levinson theorem). We have compared the performance of the selected non-uniform algorithms with several classical interpolation formulas using simulated FCI-like non-uniform samples. Analysis has been done for a nominal and a worst-case sample acquisition scenario. The presentation will show the results of our simulations with respect to the MTG requirements.

## 8892-6, Session 2

### Hyperspectral image restoration using wavelets

Behnood Rasti, Johannes R. Sveinsson, Magnus O. Ulfarsson, Jon Atli Benediktsson, Univ. of Iceland (Iceland)

Hyperspectral image restoration is considered in this paper. The decorrelation along the wavelength is done by an undecimated wavelet and in the spatial domain by an orthogonal wavelet. In doing so, a new linear model based on two dimensional orthogonal and one dimensional undecimated wavelets for hyperspectral images is given. The signal is restored with a sparse regularization. It can be shown that the minimization problem is separable. The regularization parameter is chosen automatically by Stein's Unbiased Risk Estimator (SURE). Thus, the proposed denoising method, called Wavelet Based Sparse Restoration (WBSR), is fully automatic. The denoising results show that WBSR outperforms PCABiShrinkage method [1] and 3D Shrinkage [2] based on Signal to Noise Ratio (SNR) in dB.

#### REFERENCES

- [1] Chen, G. and Qian, S.-E., "Denoising of hyperspectral imagery using principal component analysis and wavelet shrinkage," *IEEE Tran. Geoscience and Remote Sensing* 49, 973-980 (2011).
- [2] Basuhail, A. A. and Kozaitis, S. P., "Wavelet-based noise reduction in multispectral imagery," in *SPIE, Algorithms for Multispectral and Hyperspectral Imagery IV*, 3372, 234-240 (July 1998).

## 8892-7, Session 2

### Evaluation of a segmentation algorithm designed for an FPGA implementation

Kurt Schwenk, Maria von Schönemark, Felix Huber, Deutsches Zentrum für Luft- und Raumfahrt e.V. (Germany)

The following work has to be seen in the context of real-time on board image evaluation of optical satellite data. With on board image evaluation more useful data can be acquired, the time to get requested information can be decreased and new real time applications are possible. Because of the relative high processing power in comparison to low power consumption, FPGA technology has been chosen to be the adequate hardware platform for image processing tasks.

One fundamental part for image evaluation is image segmentation. It is a basic tool to extract spatial image information which is very important for many applications such as object detection. Therefore a special segmentation algorithm using the advantages of FPGA technology has been developed. The algorithm works on gray level data and is based on contour extraction.

The aim of this work is the evaluation of this algorithm. The first reason for the evaluation has been the determination of optimal algorithm parameters. Furthermore it should be investigated in which cases the algorithm is applicable and what the limits are. Finally, it should be tested how the algorithm performs in comparison with others.

Segmentation evaluation is a difficult task, which is rarely done objectively in literature.

The most common way for evaluating the performance of a segmentation method is still subjective evaluation, in which human experts determine the quality of the segmentation result.

This way is not in compliance with our needs. For us, the evaluation process has to fulfill the following requirements. The most important

point is that it provides a reasonable quality assessment. One other crucial point is that it is objective and easy to interpret. And finally the assessment process should be as simple as possible. To reach these requirements a so called segmentation accuracy norm (SA EQ) was created, which compares the difference of two segmentation results.

It is shown that this norm is capable for a first quality measurement. Due to its objectivity and simplicity, the algorithm has been tested on a specially chosen synthetic test model. In the test model environment, a simple square has to be separated from the background. To be more realistic, Gaussian noise of different levels has been added and the object contours have been smeared out to simulate border pixels. An analysis with Landsat 7 and Worldview 1 images has shown that the synthetic test model gives a good first approximation of the performance in real applications.

In this work, the most important results of the quality assessment will be presented. A filter characterization graph, describing the segmentation performance in dependency of the gray value difference between the fore and background object at various noise levels, will be presented.

On this basis, the impact of noise level and contour sharpness on the segmentation process is objectively and quantitatively shown. Finally the limits and a comparison with other algorithms are discussed.

## 8892-8, Session 2

### Comparison of an L1-regression-based and a RANSAC-based planar segmentation procedure for urban terrain data with many outliers

Dimitri Bulatov, Fraunhofer-Institut für Optronik, Systemtechnik und Bildauswertung (Germany); Jian Luo, Zhibin Deng, North Carolina State Univ. (United States); John E. Lavery, North Carolina State Univ. (United States) and U.S. Army Research Lab. (United States); Shu-Cherng Fang, North Carolina State Univ. (United States)

Planar segmentation is a key issue for a large number of applications, such as roof detail analysis for urban-terrain building modeling. The point clouds that are used as the basis for planar segmentation come from many sources, one of the cheapest of which is depth maps from optical images of urban terrain, taken by cheap cameras on light unmanned aerial vehicles (UAVs). The optical images are often of limited quality and the depth maps thus obtained are noise- and outlier-rich, and, since generation of the depth map involves discretization, they exhibit a larger uncertainty in the direction in which the camera is looking. These point clouds are the source of interest in this article because in order to process them, robust methods are needed. We concentrate on local methods, that is, those that calculate the normal vector of every point by considering its neighborhood. RANSAC (RANDOM SAMPLE CONSENSUS) has the reputation of performing well for point clouds contaminated by outliers. However, RANSAC often has large computation time and does not always degrade gracefully as the outlier percentage increases.

We propose here a planar segmentation procedure based on  $\ell_1$  regression as an alternative to a planar segmentation procedure based on the commonly used RANSAC. This procedure consists of 1) calculating the normal at each of the points by using planar  $\ell_1$  regression on a local xy-neighborhood of points around the given point, 2) clustering the normals thus generated using DBSCAN, 3) within each cluster, identifying segments (roofs, walls, ground) by DBSCAN-based-subclustering of the 3D points that correspond to each cluster of normals and 4) fitting the subclusters by planar  $\ell_1$  regression. The conventional RANSAC-based procedure, to which the  $\ell_1$ -regression-based procedure is compared, extracts the normal by fitting a plane to a large set of inliers among the points in the local xy-neighborhood around the given point and then proceeds by the same steps as in the  $\ell_1$ -regression-based procedure. Domain decomposition is used to handle data sets that are too large for handling as a whole.

Computational results for an artificial data set (two-segment roof with controlled Gaussian and Student t noise) and for a point cloud of a building complex obtained from a depth map of seven UAV-images are presented. In accuracy of segmentation, the RANSAC-based procedure outperforms the  $\ell_1$ -regression-based procedure for low noise but  $\ell_1$  regression strongly outperforms RANSAC for medium

and high noise. In most cases, the  $\ell_1$ -regression-based procedure is faster than the RANSAC-based procedure.

Finally, we outline the complete building reconstruction procedure into which the  $\ell_1$ -regression-based segmentation procedure will in the future be integrated. This building reconstruction procedure will be designed to analyze buildings with complicated structure for which elevation values have been generated from optical images by depth maps.

## 8892-9, Session 2

### Automatic urban road extraction on DSM data based-on fuzzy ART, region growing, morphological operations and Radon transform

Darlis Herumurti, Keiichi Uchimura, Gou Koutaki, Kumamoto Univ. (Japan); Takumi Uemura, Sojo Univ. (Japan)

In recent years, an automatic urban road extraction, as part of Intelligent Transportation research, has attracted the researchers due the important role for the next modern transportation where the digital road information system is a necessity. Urban area plays the main role in the transportation system where it contains complex road network as well as the property within it. In this work, we propose a new combination of fuzzy ART clustering, Region growing, Morphological Operations and Radon transform (ARMOR) for automatic extraction of urban road networks from digital surface model (DSM). The DSM data, which is based-on the elevation of surface, overcome a serious buildings shadow problem as in an aerial photo image. However, the challenges in urban road network on DSM data are non-road regions which have the similar road elevation, as well as the complex road network itself. The pre-processing includes the median filtering, transforming the DSM to grayscale image and enhancing the image contrast using adaptive histogram equalization (CLAHE). Since the different elevation between the road and the buildings, the thresholding technique yields a fast extraction of the initial road region. The threshold values are obtained from Fuzzy ART clustering of the geometrical points in histogram. The initial road region is then expanded using the seeded region growing, where the seeds are come from the perimeter of the initial road region. Though most of road regions are extracted, it still contains a lot of non-road area which have similar elevation with the road, such as: parking lot, empty ground and so on, and also the edge of the region is very rough, as well as a lot of small holes and small regions. A fast way to perform smoothing the road region is by employing the morphology closing operation using disk shape structuring element. And to remove a large region which mostly is a non-road, we perform a morphology erode operation, and we use structuring element with rectangle shape for this work, thus, it remains the large area detected, and these large areas are then subtracted from the road. Furthermore, the locations of straight line of the road in the image can be found by finding the locations of strong peaks in the Radon transform matrix. By selecting the regional max in the Radon matrix, we obtain the orientation which most likely is a road line. These orientations are then used in conjunction with a line shape structuring element for morphology opening operation as the road line detector. Finally, the road network is constructed based-on B-Spline from the skeleton of the extracted road. The skeleton is resulted from morphological thinning operation. The nodes of road network come from the end vertex, the join and between them. Then, the B-spline curve is drawn based on these nodes. The experimental of road extraction from Shinjuku and Sapporo urban, shows that the proposed method running faster and increases the quality and the accuracy average about 10% higher than the highest result of the compared method

## 8892-10, Session 2

### Soil surface roughness modeling: limit of global characterization in remote sensing

Olivier Chimi Chiadjeu, Edwige Vannier, Richard Dusséaux, Odile Taconet, LATMOS (France)

The potential of remote sensing imagery for assessment of soil surface roughness or moisture retrieving has been widely studied and applied. The scattering of microwaves depends on several surface

characteristics as well as on imagery configuration. It is acknowledged that roughness parameterization needs further improvements to reduce dispersion between surface characteristics, electromagnetic simulations and radar measures.

Many scientists use a global characterization of bare soil surface random roughness. Surface roughness is generally characterized by the autocorrelation function and by statistical parameters such as root-mean square of the heights, correlation length, roughness exponent or parameter  $Z_s$  [1-3]. Assuming an autocorrelation model and the hypothesis of Gaussian character of heights distribution, some authors have developed algorithms for numerical generation of soil surfaces that have the same statistical properties [4]. First, all agricultural surfaces do not have a Gaussian distribution of heights and second, this approach does not take into account morphological aspects of the soil surface micro-topography. Yet, these elements are fundamental in the development of hydrological models [5].

In the present study, a Digital Elevation Model (DEM) of natural seedbed surface was recorded by stereo photogrammetry. After estimating global parameters of this natural surface, we generated numerical surfaces of same characteristics by linear filtering. Big aggregates and clods were then captured by a contour-based segmentation method developed by Taconet et al. [6]. We show that two-dimensional autocorrelation functions of generated surfaces and of natural surface are close together. Nevertheless, the number and contours of segmented objects change from generated surfaces to natural surface. Generated surfaces show fewer and bigger segmented objects than in the natural case. Moreover, the shape of segmented objects is unrealistic in comparison to real clods, which have to be convex and of low circularity. Thus we clearly show that when describing surface roughness as a whole, some information related to micro-topographic objects is lost.

- [1] M. Zribi, M. Dechambre, "An new empirical model to retrieve soil moisture and roughness from Radar Data." *Remote Sensing of Environment*, Vol. 84, pp. 42-52, 2003.
- [2] O. Taconet and V. Ciarletti, "Estimation soil roughness indices on a ridge and furrow surface using stereo photogrammetry." *Soil Tillage Research*, Vol. 93, pp. 64-76, 2007.
- [3] G. Franceschetti, and D. Riccio, *Scattering, Natural Surfaces and Fractals*, Elsevier, 2007.
- [4] R. Dusséaux, E. Vannier, O. Taconet, G. Granet, "Study of backscatter signature for seedbed surface evolution under rainfall – Influence of radar precision". *Progress In Electromagnetics Research*, Vol. 125, pp. 415-437, 2012.
- [5] L. Borselli, D. Torri, "Soil roughness, slope and surface storage relationship for impervious areas." *Journal of hydrology*, Vol. 393, pp. 389-400, 2010.
- [6] O. Taconet, E. Vannier and S. Le Hégarat-Masclé, "A contour-based approach for clods identification and characterization a soil surface." *Soil Tillage Research*, Vol. 109, pp. 123-132, 2010.

## 8892-11, Session 3

### Dense registration of CHRIS-Proba and Ikonos images using multi-dimensional mutual information maximization

Claude Cariou, Kacem Chehdi, Univ. de Rennes 1 (France)

We investigate the potential of multidimensional mutual information for the registration of remote sensing images.

Image registration is an important tool for the preprocessing of images obtained from different modalities, especially in medical imaging and remote sensing. However, it is often performed using only scalar imaging modalities (e.g. panchromatic and radar intensity), and little work has been done on the registration of vectorial (multidimensional) modalities, such as multispectral images.

In this study, we devise a gradient flow algorithm which iteratively aligns two images, one being the reference image, and the other one being warped under some displacement map to optimise. Based upon the maximisation of the multidimensional mutual information with respect to the displacement map, our gradient flow extends the method of Hermosillo et al. (IJCV 50, 2002) by accounting for partial derivatives of the multivariate joint distribution and the multivariate marginal of the warp image with respect to each variable of the mutual information derivative. The resulting terms are shown to weight the band specific gradients of the warp image to provide

the current displacement map. Since these terms require a high memory storage even for a moderate number of bands, we propose in addition to compute them with an alternative method to classical histogram binning, based on the k-nearest neighbours approach. The proposed gradient flow also involves a 2-D filtering procedure of the displacement map in order to regularise the solution.

Experiments were conducted to assess the reliability of multidimensional mutual information measure for the registration of images issued from two Earth observation satellites, namely Ikonos and CHRIS-Proba. The area under study was the region of Baabdat, Lebanon (33°53'N, 35°40'E), with application to the detection of cedar pines. Since the ground spatial resolutions of the two images are very different (0.8 meters for Ikonos and 19 meters for CHRIS-Proba), their registration is a very challenging task, but one might expect that the multispectral information from CHRIS-Proba (18 bands) can compensate for its low spatial resolution. In order to keep a good spatial resolution, we downsampled the Ikonos image by a factor of 2, and upsampled the CHRIS-Proba image to align with the resampled Ikonos image at 1.6 meters using bicubic interpolation. For the Ikonos image, we chose the green and red channels, while we took bands 7 and 12 of the CHRIS-Proba image, respectively centered at 661.35nm (red) and 741.47nm (near infra-red) since they are assumed to hold the most relevant information for the targeted application. Therefore, in this example, four dimensional joint distributions had to be estimated. The solution was regularised by low-pass filtering the displacement map in the spectral domain, using a binary disk-shaped mask with diameter 5 centered at the origin of spatial frequencies.

A comparison with the registration results obtained for the computation of the mutual information from only two scalar modalities (both red channels of each image mentioned above) shows that using the multidimensional mutual information brings a significant gain in positional accuracy and is potentially suitable for multispectral remote sensing image registration.

### 8892-12, Session 3

#### A self-adaptive image registration method: from local learning to overall processing

Peng Ye, Na Li, Fang Liu, National Univ. of Defense Technology (China); Juhong Wu, Guirong Guo, ATR Lab (China)

##### 1. Objective

Image registration is a fundamental step for further applications like change detection and information fusion. Remote sensing images are usually large-size and rich of features. Different parts of a remote sensing image show different characteristics. Most previous image registration methods implement only one type of feature, similarity metric and optimization. It is more appropriate for different image parts to flexibly choose different features, similarity metrics or optimization methods. Moreover, using representative parts to obtain the overall transformation parameters would reduce the heavy computation load of registering the whole image.

In this work, the proposed is a novel image registration method which learns from local registration to drive the whole image registration. The method could choose the type of feature, similarity or optimization which is more suitable for the images under processing. The major contributions include: 1. building an image registration framework which could flexibly select features, similarity metrics, and optimization methods; 2. reducing registration computation load of large-size images; 3. It's a highly extendable tool with key steps like local region definition and precision assessment easily adjusted.

##### 2. Method:

Major steps of the proposed method are as follow:

a. Image representation by local region or initialization: choose corresponding feature-rich areas with hand or use a coarse feature registration method to locate possible corresponding anchor regions. The shape and adjustment of the region could be different and they are set as rectangle and fixed in this work.

b. Local registration: for corresponding local areas, each pair uses a different feature type with a different similarity metric and optimization method; the transformation models of all pairs are set as the same.

c. Learning from local registration results: results from local registrations are evaluated with pre-defined measures. Local area pairs with result far from others or low score of pre-defined measures are excluded as outlier areas. Those with good results are kept as anchor regions. Feature type, similarity metric and optimization

method from anchor regions are implemented on all areas and the type with highest score is chosen as the type for the final registration of the whole image.

d. Overall registration: registration on the whole image is conducted with corresponding control points, similarity measure and optimization method derived from local registrations. Therefore outliers of features are eliminated from registration of the whole image and the feature type, similarity measure and optimization method are more suitable for the whole image.

##### 3. Result and conclusion

Experiments on real remote sensing image pairs demonstrated the feasibility and superiority of the proposed method. The RMSE error of the proposed method is below 1 pixel and smaller than that of traditional methods. The time cost of the proposed method is less than that of traditional methods.

In conclusion, by learning from local registrations, our method gains control points with good accuracy, decreases the search space into smaller local area, and flexibly chooses feature type, similarity measure and optimization method which are more suitable for the image. The proposed method achieved better result with less computation energy.

### 8892-13, Session 3

#### Automatic SAR and optical images registration method based on improved SIFT

Chunyu Yue, Beijing Institute of Space Mechanics and Electricity (China); Wanshou Jiang, Wuhan Univ. (China)

With the rapid development of space technologies, remote sensing data intergration becomes increasingly urgent. The combination with SAR (Synthetic Aperture Radar) and visual sensor can not only provide complementary information of multisensor in space or time, but also realize continuous earth observation. The great differences between SAR and optical images caused by imaging mechanism barrier the feature extraction and matching, which make image registration the biggest difficulty for the intergration of the two. Therefore, the research on image registration of SAR and optical images is of practical meaning and theory value.

An automatic SAR and optical images registration method based on improved SIFT (scale invariant feature transform) is proposed in this paper. The registration method is a two-step strategy, which is from rough to accuracy.

Generally, there are rotation and scale differences between SAR and optical images, a rough rectification based on the geometrical relationship of images is realized. The geometry relation of images is constructed by the geographic information, and image is arranged based on the elevation datum plane to eliminate the rotation and resolution differences, which is also a rough rectification, and thereby, image rough registration is achieved.

Then, the method for feature extraction and matching with the improved SIFT is presented. A good many features are extracted by SIFT in SAR and optical images. As rotation difference is eliminated in images of flat area after rough registration, the number of correct matches and correct matching rate can be increased by altering the feature orientation assignment. SSIM is introduced as similarity measure of keypoint descriptor for matching SIFT features duo to the structure information contained in the SIFT feature. The threshold effect of matching result is analyzed, and some other similarity measures are also included for comparative analysis. At last, the optimization strategy for automatic rejection of wrong matches is produced. It is necessary to study on automatic rejection of wrong matches, for there are plenty of wrong matches after the original matching by SSIM. As rotation and resolution differences are eliminated in images of flat area after rough registration, correct matches have consistencies at parallax and rotation. Mapping the original matches to the parallax feature space and rotation feature space in sequence, which are established by the custom defined parallax parameters and rotation parameters respectively. Cluster analysis is applied in the parallax feature space and rotation feature space, and the relationship between cluster parameters and matching result is analyzed. Owing to the clustering feature, correct matches are retained.

Finally, the perspective transform parameters for the registration are obtained by RANSAC (Random Sampling Consensus) algorithm with

removing the false matches simultaneously. The whole process is done automatically. Experiments show that the algorithm proposed in this paper is effective in the registration of SAR and optical images with large differences.

8892-14, Session 3

## Automated search for livestock enclosures of rectangular shape in remotely sensed imagery

Igor Zingman, Dietmar Saupe, Univ. Konstanz (Germany);  
Karsten Lambers, Otto-Friedrich-Univ. Bamberg (Germany)

We introduce an approach for detection of rectangular patterns of variable sizes and proportions in gray scale images. Our work is motivated by the Silvretta Historica project that aims at automated detection of residues of livestock enclosures in remotely sensed images of alpine regions. These structures are composed of linear walls that frequently form approximately right angles.

An approach based on a local Hough transform can be used for detection of rectangles in images. To find the sides of a rectangle, which are considerably shorter than the size of an image, the local Hough transform is computed within a sliding window for each image point. A criterion had been proposed earlier for the detection of the four constrained peaks in the Hough space, which correspond to the four sides of a rectangle. The criterion is based on the properties of a rectangle, namely parallel and equal length opposite sides and right angles between adjacent sides.

In many practical applications, however, including the detection of livestock enclosures mentioned above, such a basic approach fails to detect fragmented or incomplete rectangular structures. In our approach, we propose a different criterion to find peak patterns that does not rely on equal length of opposite sides. This is crucial when parts of a rectangle may be absent, including the case of the complete absence of one of its sides. Moreover, we do not require the number of sides to four, thus allowing the searched structure to be a polygon with angles around either 90 or 180 degrees.

To reduce the number of false detections resulting from rectilinear structures that do not form a rectangle, we suggest adding a convexity constraint. Fortunately, convex configurations of lines in an image plane induce a specific distribution in the Hough space. Thus, the convexity constraint can be analyzed directly in the Hough space. Thereby, our method does not need to construct a list of linear segments in contrast to other convex grouping techniques.

Since it is computationally expensive to compute the local Hough transform at each point in the image, we first find sparse candidate points where the transform is further computed. We use candidate points on the ridges of the distance transform of the binary image of short linear segments. The values of the distance transform are also used to determine an appropriate size of an analysis window for each candidate point. Short linear segments with the attached orientation were detected using morphological operators. Availability of the orientation restricts mapping of a point in the image plane to a point in the Hough space, instead of mapping points to curves. The resulting distribution in the Hough space is much sparser, simplifying the search for meaningful peaks.

We experimentally tested our approach on a set of large images (aerial and GeoEye-1 satellite images of 0.5m resolution) that contain partially ruined livestock enclosures of approximately rectangular shape. The approach showed reliable results in finding groups of linear structures originating from the objects of our interest.

8892-15, Session 3

## A comprehensive analysis of earthquake damage patterns using high dimensional model representation feature selection

Gulsen Taskin Kaya, Istanbul Technical Univ. (Turkey)

Recently, earthquake damage assessment using satellite images has been a very popular ongoing research direction. Especially with the availability of very high resolution (VHR) satellite images, a quite detailed damage maps based on building scale has been produced, and various studies have also been conducted in the literature. As

the spatial resolution of satellite images increases, distinguishability of damage patterns becomes more crucial especially in case of using only the spectral information during classification. In order to overcome this difficulty, textural information needs to be involved in the classification to improve the visual quality and reliability of damage map. There are many types of textural information which can be derived from VHR satellite images depending on the algorithm used. However, extraction of textural information and evaluation of them have been generally a time consuming process especially if the region of interest is very large. Therefore, in order to provide a quick damage map, the most useful features describing damage patterns needs to be known in advance as well as the redundant features. In this study, a VHR satellite image after Iran, Bam earthquake was used to identify the earthquake damage. Not only the spectral information, the textural information was also used during the classification. For textural information, second order Haralick features were extracted from the panchromatic image for the area of interest using gray level co-occurrence matrix with different sizes of windows and directions. The most useful features representing the damage characteristic were selected with a novel feature selection method based on High Dimensional Model Representation (HDMR) giving sensitivity of each feature during classification. HDMR is a method that was recently proposed as an efficient tool to capture the input-output relationships in high-dimensional systems for many problems in science and engineering. The method proposes an expansion in order to model multivariate functions in such a way that the components of the expansion are ordered starting from a constant and gradually including terms like univariate, bivariate and so on. The basic underlying philosophy of HDMR is to generate an approximation scheme using the first few terms of the expansion usually up to the second order terms. HDMR expansion can be also regarded as hierarchically correlated function expansion in terms of the input variables. It is observed that the output of most physical systems often has negligible higher order correlations amongst the independent input variables. Most numerical experiments show that the third and higher order HDMR functions have very small impact on the output so it suffices to limit the approximation at the second order. The performance of the HDMR based feature selection algorithm was tested using SVM with a small region from Iran, Bam, and the performance of the algorithm was compared to SVM and random feature selection algorithm. The preliminary results showed that the earthquake damage can be extracted by using a few features instead of using all of them, and the HDMR based feature selection algorithms gives the highest classification accuracies with a few features compared to aforementioned feature selection algorithms.

8892-16, Session 4

## Preprocessing of hyperspectral images: a comparative study of destriping algorithms for EO1-Hyperion

Daniel Scheffler, Pierre Karrasch, Technische Univ. Dresden (Germany)

The use of hyperspectral remote sensing data arises in a lot of scientific fields. Many studies show the benefit of detailed spectral signatures in the fields of, inter alia, agriculture, geology or geomorphology. For such applications often signatures are used which are hardly different from each other. For this reason, the radiometric as well as the geometric calibration of hyperspectral remote sensing data is one of the most important steps of preprocessing.

In this study, data from the EO-1 Hyperion instrument were used. Besides atmospheric influences or topographic effects, the data represent a good choice in order to show different steps of the preprocessing process targeting sensor-internal sources of errors. These include:

- diffuse sensor noise
- striping effect
- smile effect
- keystone effect
- spatial misalignments between the detector arrays

For this research paper the authors focus on the striping effect by comparing and evaluating different algorithms, methods and configurations to correct striping errors.

The correction of striping effects is necessary because of the inaccuracy during the calibration of the detector array. Especially

the first 12 visual and near infrared bands (VNIR) bands and also a large number of the bands in the short wave infrared array are affected. Analyses by BINDSCHADLER AND CHOI (2003) show that for Hyperion data detector error standard deviations of up to 123 DN can be expected in the shortest wavelengths of the SWIR array (representing about 2 % of the global mean).

Altogether six destriping techniques were tested on the basis of a Hyperion dataset covering a Central Europe region.

- 1) Destriping based on ENVI Hyperion Tools: The ENVI-plugin Hyperion-Tools features a method called "Flag Mask Correction" offering a local-statistic algorithm which performs a simple linear interpolation between adjacent image columns.
- 2) Destriping based on ENVI-SPEAR-Tools – Vertical Stripe Removal: This method is also implemented in ENVI but only inadequately described in publications or manuals. However, an advantage may be the option to exclude certain areas from the corrections, e.g. very bright (clouds) or very dark image areas.
- 3) Destriping based on ENVI General Purpose Utilities – "Destripe": It's another ENVI implemented method which originally has been developed for the Landsat-MSS-sensor. Under certain conditions, this global-statistic algorithm is also applicable to Hyperion data.
- 4) Destriping based on a method by DATT (2003): This local-statistic approach analyses the mean and standard deviation of columns in a user defined window (filter width). If these parameters exceed a given threshold, a recalculation of the relevant column is carried out.
- 5) ERDAS Periodic Noise Reduction: This approach is part of the ERDAS Imagine Software package and was developed for the correction of periodical noise in the images.
- 6) Destriping using Wavelet Fourier Adaptive Filtering based on algorithm by PANDE-CHHETRI AND ABD-ELRAHMAN (2011; 2012): This algorithm is based on a combination of wavelet decomposition and frequency domain adaptive filtering.

Three main criteria were used to assess the quality of the different destriping algorithms.

- number and position of corrected image columns
- the amount of alteration to the sensor's initial signal
- visual impression

For the final evaluation, various analyses across all Hyperion channels were performed. The results show that some methods have almost no effect on the striping in the images. Other methods may eliminate the striping, but analyses show that these algorithms also alter pixel values in adjacent areas which were not disturbed by the striping effect.

In the scientific paper, the authors will present in-depth results of this comparative study with the goal to give recommendations on the usability of the different destriping methods.

References:

- Bindschadler, R., Choi, H., 2003. Characterizing and correcting Hyperion detectors using ice-sheet images. *IEEE Transactions on Geoscience and Remote Sensing*, Vol. 41(6), 2003, pp. 1189-1193.
- Datt, B., McVicar, T.R., Van Niel, T.G., Jupp, D.L.G., Pearlman, J.S., 2003. Preprocessing EO-1 Hyperion Hyperspectral Data to Support the Application of Agricultural Indexes. – *IEEE Transactions on Geoscience and Remote Sensing*, Vol. 41, No. 6, pp. 1246-1259.
- Pande-Chhetri, R., Abd-Elrahman, A., 2011. De-striping hyperspectral imagery using wavelet transform and adaptive frequency domain filtering. – *ISPRS Journal of Photogrammetry and Remote Sensing* 66 (2011), pp. 620–636.
- Pande-Chhetri, R., Abd-Elrahman, A., 2012. Filtering high-resolution hyperspectral imagery in a maximum noise fraction transform domain using wavelet-based de-striping. – *International Journal of Remote Sensing*, Vol. 34, No. 6, pp. 2216-2235.

## 8892-17, Session 4

### Wavelet based hyperspectral image restoration using spatial and spectral penalties

Behnood Rasti, Johannes R. Sveinsson, Magnus O. Ulfarsson, Jon Atli Benediktsson, Univ. of Iceland (Iceland)

In this paper, the penalized least squares with a novel spatial-spectral

penalty is used for hyperspectral image restoration. The new penalty is a combination of First Order Roughness Penalty (FORP) to enforce smoothness spectrally and a group lasso (GLASSO) to enforce sparsity spatially. A linear model based on two dimensional orthogonal wavelets for hyperspectral images is used. The minimization problem is solved using Alternating Direction Method of Multipliers (ADMM) [1]. The regularization parameters are chosen to get the optimum Signal to Noise Ratio (SNR). The proposed denoising method, called GLASSORP, is compared with Bivariate Shrinkage (BiShr) [2] and PCABiShrinkage [3]. The results shown that GLASSORP outperforms the other methods based on SNR in dB. The comparisons are for the Pavia University hyperspectral data set after adding different levels of zero-mean Gaussian noise to it.

#### REFERENCES

- [1] Eckstein, J. and Bertsekas, D. P., "On the Douglas-Rachford splitting method and the proximal point algorithm for maximal monotone operators," *Math. Program.* 55, 293-318 (June 1992).
- [2] Sendur, L. and Selesnick, I. W., "Bivariate shrinkage functions for wavelet-based denoising exploiting interscale dependency," *IEEE Trans. Signal Process.* 50(11), 2744–2756 (Nov.,2002).
- [3] Chen, G. and Qian, S.-E., "Denoising of hyperspectral imagery using principal component analysis and wavelet shrinkage," *IEEE Tran. Geoscience and Remote Sensing* 49, 973-980 (2011).

## 8892-18, Session 4

### Hyperspectral image segmentation using a cooperative nonparametric approach

Akar Taher, Kacem Chehdi, Univ. de Rennes 1 (France); Claude Cariou, Univ de Rennes 1 (France)

In this paper a new unsupervised nonparametric cooperative and adaptive hyperspectral image segmentation approach is presented. In this approach, the hyperspectral images are partitioned band by band in parallel, and then identical classification results between adjacent bands are grouped into subsets and evaluated, to get the final segmentation result. In this approach two unsupervised nonparametric segmentation methods are used in cooperation, namely the Fuzzy C-means (FCM) method, and the Linde-Buzo-Gray (LBG) algorithm, to segment each band of the image. The originality of the approach relies firstly on its adaptation to the type of regions in an image (textured, non-textured), and secondly on merging the results into subsets before validation process.

The proposed segmentation approach is composed of four steps:

The first step is the adaptive feature extraction, in which the image is divided into two types of regions, i.e. textured and non-textured, to adapt the feature extraction. The adaptive characterization of pixels, taking into account the textured or non-textured nature of region to which they belong, is an essential step before the classification. Indeed, the attributes dedicated to the description of regions with low variance do not have sufficient discriminating power for textured regions and vice versa.

The second step is the parallel cooperative pixel classification, in which the pixels in the textured and non-textured regions are processed independently and in parallel. The features extracted are injected into the two classification methods named above. These two methods are used in many applicative domains, and have shown their efficiency. Their common advantage is that they are both unsupervised and nonparametric. In our approach, the FCM and LBG methods are chosen to cooperate with each other, due to the complementary of their principle (fuzzy/hard decision).

The third step includes the management of results which is done at two levels, first by validating pixels which are coherently classified by the two methods, and then processing conflicting classification results using a genetic algorithm (GA). The objective function of the genetic algorithm depends on inter-class and intra-class disparities to evaluate and manage the conflicting pixels between the segmentation results.

The above three steps are applied on each band of the image independently.

The fourth step is the identification of similar pixels between the adjacent band classification results. In this step the results from the different bands are grouped in subsets, which are formed depending on the number of pixels that are classified to the same class in different bands. Then these subsets are processed independently to get one classification result for each of them. The same procedure

as in the third step is used to get the final result of the hyperspectral image.

This approach is tested on two applications using multispectral and hyperspectral images and shows its efficiency, namely cedar detection in the region of Beirut with a correct classification rate over 97%, and identification of invasive plants in Cieza (Spain) with a correct classification rate over 99%.

#### 8892-19, Session 4

### Hyperspectral image simulation over heterogeneous non-Lambertian rugged terrain

Alijafar Mousivand, Technische Univ. Delft (Netherlands); Wouter Verhoef, Univ. Twente (Netherlands); Massimo Menenti, Ben Gorte, Technische Univ. Delft (Netherlands)

In this paper, a modeling system for the simulation of optical hyperspectral images over heterogeneous non-Lambertian rugged surfaces is presented. The system is modeled at three different levels: the surface, the atmosphere and the sensor. The simulation begins with four surface reflectance factors modeled by the Soil-Leaf-Canopy radiative transfer model SLC at the top of canopy and propagate them through the effects of the atmosphere which is explained with seven atmospheric coefficients, derived from MODTRAN radiative transfer code. The top of the atmosphere radiance is then convolved with the sensor spectral and spatial responses.

The model requires textural information from the scene to be simulated including landuse map, soil and vegetation properties and digital elevation model and the geometry of the observation. Atmospheric visibility and water vapor content are used to define the atmospheric profile where the angular effects are taken into account across the scene and ultimately the characteristics of sensor are used to simulate sensor-like radiance.

The paper also provides a detailed account for BRDF effects, adjacency effects and the topography effects on the radiance simulation in which sky-view factor and non-Lambertian adjacent terrain reflectance are modeled precisely. The model has been tested over two different type of surfaces; a flat cropland area and a mountainous area for the simulation. Validation of the model is considered over the two test sites and results of the simulation for various configurations are included.

#### 8892-20, Session 4

### VST-based lossy compression of hyperspectral data for new generation sensors

Alexander N. Zemliachenko, Ruslan A. Kozhemiakin, Mykhail L. Uss, Sergey K. Abramov, Vladimir V. Lukin, National Aerospace Univ. (Ukraine); Benoit Vozel, Kacem Chehdi, Univ. de Rennes 1 (France)

Modern airborne and spaceborne hyperspectral sensors produce a lot of useful information for Earth surface monitoring but amount of acquired data is huge. Thus, there is a need for their compression before transferring, archiving, and dissemination. Even the best lossless compression techniques are often unable to provide a required compression ratio (CR). Thus, lossy compression has to be applied. Such methods should take into account noise properties in acquired data. Recent studies have clearly demonstrated that images acquired by new generation hyperspectral sensors are corrupted by noise which has signal-dependent nature. However, this fact is mostly ignored in design of lossy compression techniques.

Using real-life Hyperion data, we first demonstrate that signal-dependent component of the noise is dominant for most sub-band images. Then, we consider two approaches to lossy compression of sub-band images in component-wise manner. The first approach is direct application of the DCT-based coder AGU to each sub-band image with parameters individually adjusted to a given sub-band. The second approach presumes the use of variance stabilizing transform (VST), namely, generalized Anscombe transform. It is shown that in both cases it is possible to provide compression in the

neighborhood of optimal operation point (OOP). However, the results for the second approach are better and OOP (where introduced losses basically correspond to removal of the noise) is attained easier. Some peculiarities of performing VST for real-life data are discussed. In particular, they deal with the presence of negative values in sub-band images due to dark current noise.

A useful property of the second approach based on VST is that OOP for all sub-band images is produced for the same quantization step (QS) of the coder, namely,  $QS=3.5$  for the considered coder AGU (noise variance after VST is equal to unity in all sub-band images). Then, for component-wise compression, attained CR varies from 5..6 to 25 depending upon dynamic range and signal-to-noise ratio. This is considerably more than for lossless compression. However, the CR values can be considerably increased if spectral correlation of hyperspectral data is taken into account. This can be done by exploiting either 3D coders applied to data after VST or by compressing difference images. The latter way is considered in the paper. One or several sub-band images after VST are used as reference(s) whilst for other sub-band images difference images (with respect to reference one(s)) are obtained and compressed with the same QS as that one used for the reference image(s). This approach allows increasing CR by about two times compared to component-wise compression. The introduced losses remain at the same level. Thus, OOP is provided for all sub-bands of hyperspectral data irrespectively to dynamic range and signal-to-noise ratio in a given sub-band.

Examples of original images (for sub-bands where noise is visible) and compressed images (where noise filtering effect is observed) will be presented in the final paper. One advantage of the proposed approach is that noise suppression due to lossy compression remains practically the same for image fragments with different local mean values.

#### 8892-21, Session 5

### Estimating the number of endmembers in hyperspectral imagery using hierarchical agglomerate clustering

Jee-Cheng Wu, Heng-Yang Wu, Gwo-Chyang Tsuei, National Ilan Univ.. (Taiwan)

In a hyperspectral image, one pixel always contains a mixture of the several reflected spectra because of spatial resolution limits and ground material distribution. A classical spectral un-mixing involves two steps: identifying the unique signatures of the endmembers (i.e. pure materials) and estimating the proportions of endmembers for each pixel by inversion. However, the key to successful spectral un-mixing is indicating the number of endmembers and their corresponding spectral signatures. Currently, Noise Whitened Harsanyi, Farrand, and Chang (NWHFC) and hyperspectral signal subspace identification by minimum error (HySime) are the two well-known eigenvalue-based methods for estimating the number of endmembers in hyperspectral image. Nevertheless, in a realistic situation, the two methods are not only sensitive to noise in the image but also difficult to separate signal sources which may include unknown anomalous or interferers.

In this paper, we propose a two-stage process to estimate the number of endmembers. At the preprocessing stage, the principal component analysis is used to transform the original L-spectral bands to feature bands. Then, based on the eigenvalues of the covariance matrix, we use the first q-feature bands ( $q \ll L$ ) and q-dimensional convex hull to select a group of vertex pixels in the image as candidate endmember pixels.

At the hierarchical agglomerate clustering stage, the processing includes six steps. In step 1, two parameters are set. The minimum number, tol, is a threshold of a cluster, which makes us avoid finding anomalies or interferers; and the angle,  $\theta$ , is used to aggregate the vertex pixels into a subgroup of pixels and a cluster of pixels. In step 2, we select the vertex pixel, which has the largest magnitude of pixel vector as an initial endmember. In step 3, similarity is measured between the selected pixel vector and the group pixel vectors using the spectral angle mapper (SAM). Then, based on the predefined angle, each of the group pixels will be aggregated into a subgroup pixel or a cluster pixel. In step 4, if the number of the subgroup pixels is larger than the predefined number, the group pixels will be replaced by the subgroup pixels. Otherwise, the algorithm will be terminated and the number of the clusters is the number of endmembers. In step 5, if the number of the cluster pixels is larger than the predefined

number, the selected pixel is set as the endmember. And a new endmember pixel can be found by applying orthogonal subspace projection (OSP) to the subgroup pixel vectors with the one most different from the already selected pixel vectors. Otherwise, a new pixel will be found, and it has the largest magnitude of pixel vector in the subgroup pixels because anomaly or interferer pixel is found. In step 6, we return to the step 3.

The proposed method was carried with both synthetic and real images for estimating the number of endmembers. The results demonstrate that the proposed method can be used to estimate more reasonable and precise number of endmembers than the two published methods.

## 8892-22, Session 5

### Boundary constraints for singular value decomposition of spectral data

John H. Gruninger, Hoang Dothe, Spectral Sciences, Inc. (United States)

Singular value decomposition (SVD) and principal component analysis enjoy a broad range of applications, including, rank estimation, noise reduction, classification and compression. The resulting singular vectors form orthogonal basis sets for subspace projection techniques. The procedures are applicable to general data matrices. Spectral matrices belong to a special class known as non-negative matrices. A key property of non-negative matrices is that their columns/rows form non-negative cones, with any non-negative linear combination of the columns/rows belonging to the cone. This special property has been implicitly used in popular rank estimation techniques known as virtual dimension (VD) and hyperspectral signal identification by minimum error (HySime). Data sets of spectra reside in non-negative orthants. The subspace spanned by a SVD of a set of spectra includes all orthants. However SVD projections can be constrained to the non-negative orthants. In this paper two types of singular vector projection constraints are identified, one that confines the projection to lie within the cone formed by the spectral data set, and a second that only restricts projections to the non-negative orthant. The former is referred to here as the inner constraint set, the latter the outer constraint set. The outer constraint set forms a broader cone since it includes projections outside the cone formed by the data array. The two cones form boundaries for the cones formed by non-negative matrix factorizations (NNF). Ambiguities in the NNF lead to a variety of possible sets of left and right non-negative vectors and their cones. Analysis of the constraints leads to general non-negative factorizations, and to within scene end-member identification and band selection. The paper presents the constraint set approach and illustrates it with applications to within scene endmember selection, band selection and NNF ambiguity.

The essence of the approach is outlined here for columns of a non-negative matrix,  $A$ . The column inner cone of  $A$  is defined as  $A_p$  for all vectors  $p \geq 0$ . Any spectral vector represented by  $A_p$  is a non-negative linear combination of the columns of  $A$  and lies within the cone. The outer cone is defined as  $A_f$  for all vectors  $f$  that satisfy  $Af \geq 0$ . For the outer cone  $f$  can have negative elements, the only requirement is that the resultant vector is nonnegative. In this work, these inner and outer left cones are defined in terms of the SVD of  $A=WSVT$ . The inner cone is defined as  $Wc$  with the vector  $c$  satisfying  $Vs^{-1}c \geq 0$ . The outer cone is defined by  $Wd$  for all vectors  $d$  that satisfy  $Wd \geq 0$ . Within scene endmembers are extreme points of the inner cone while general NNF vectors are extreme points of a cone lying between the inner and outer cone. The traditional approaches to finding endmembers is replaced by eliminating redundancies in inequalities expressed in terms of the left and right singular vectors of the matrix  $A$ .

## 8892-23, Session 5

### Improving the efficiency of MESMA through geometric unmixing principles

Laurent Tits, Katholieke Univ. Leuven (Belgium); Ben Somers, VITO NV (Belgium); Rob Heylen, Univ. Antwerpen (Belgium) and Univ. of Florida (United States); Paul Scheunders, Univ. Antwerpen (Belgium); Pol Coppin, Katholieke Univ. Leuven (Belgium)

Spectral Mixture Analysis is a widely used image analysis tool with

many applications. Yet, one of the major issues with this technique remains the lack of ability to properly account for the spectral variability of endmembers or ground cover components that occur throughout an image scene. Endmember variability is most often addressed using iterative mixture cycles in which different endmember combination models are compared for each pixel, i.e. each pixel is unmixed numerous times with different mixture models or endmember combinations. The model with the best fit is assigned to the pixel. Typical examples are Multiple Endmember Spectral Mixture Analysis (MESMA) and Monte Carlo Unmixing (AutoMCU). The drawback of these iterative mixture analysis cycles is the computational burden which often hampers the operational use. In an attempt to address this issue we proposed a new geometric based methodology to more efficiently evaluate different endmember combinations in iterative mixture analysis methods, and more specifically in MESMA. This geometric unmixing methodology has a two-fold benefit. First of all, geometric unmixing allows a fast and fully constrained unmixing, which was previously infeasible in MESMA due to the long processing times of the available fully constrained unmixing methods. Secondly, whereas the traditional MESMA explores all the different endmember combinations separately, and selects the most appropriate combination as a final step, our approach selects the best endmember combination prior to unmixing, as such increasing the computational efficiency of MESMA. To do so, we built upon the equivalence between the reconstruction error in least-squares unmixing and spectral angle minimisation in geometric unmixing. For a two endmember mixture, the best possible representation of a mixed pixel  $y$  is the perpendicular projection of  $y$  on the line between the two endmembers ( $y'$ ). The distance between  $y$  and  $y'$  is equal to the residual error or modelling error. For two-endmember combinations, this perpendicular distance can be translated to the angle between the vector  $y$ -endmember 1 and the line between the two endmembers. This geometric approach was tested on both a simulated dataset based on field measurements and a HyMap image from Berlin, Germany, and compared with the results from both MESMA and the traditional Fully Constrained Least Squares Unmixing (FCLSU). Constrained unmixing provided higher accuracies compared to the unconstrained results of MESMA, while the processing time of geometric unmixing was similar to MESMA. With the inclusion of the proposed endmember combination selection technique, the computation time decreased by a factor between 5 and 8.5, depending on the size and organisation of the libraries. The spectral angle can as such be used as a proxy for model fit, enabling the selection of the proper endmember combination from large spectral libraries prior to unmixing. Geometric unmixing thus provided a mean for (i) fully constrained unmixing in MESMA, which was previously infeasible due to the long processing time required by FCLSU (around 100 times slower than geometric unmixing in this study), and (ii) improving the computational efficiency of MESMA.

## 8892-24, Session 5

### Extraction of spatial features in hyperspectral images based on the analysis of differential attribute profiles

Nicola Falco, Univ. degli Studi di Trento (Italy) and Univ. of Iceland (Iceland); Jon Atli Benediktsson, Univ. of Iceland (Iceland); Lorenzo Bruzzone, Univ. degli Studi di Trento (Italy)

Remote sensing hyperspectral images (HSI) are characterized by a high spectral resolution, where each pixel can be seen as a detailed representation of the spectral reflectance of the materials presented on the ground. This characteristic makes these data suitable for a detailed classification with the possibility to distinguish land-cover classes with similar spectral signatures. Moreover, the new generation of hyperspectral sensors are able to provide images with an improved spatial resolution. In this scenario, the spatial context information, which is represented by the neighborhood pixel system, becomes an important information source for distinguishing different objects on the ground. However, the exploitation of this information source increases the complexity of the classification process. Recent improvements in mathematical morphology provided new techniques such as the Attribute Profiles (APs)<sup>1</sup> and the Extended Attribute Profiles (EAPs) that can effectively model the spatial information in remote sensing images. However, one of the main drawbacks of these techniques is the selection of the optimal range of values related to the family of criteria adopted to each filter step, which is difficult to identify if prior knowledge of the investigated area is not available. Another important

issue, which arises when hyperspectral images are considered, is related to the high dimensionality of the profiles, which results into a very large number of features and thus in the Hughes phenomenon.

In this work, a novel strategy is proposed for extracting spatial information from hyperspectral images based on Differential Attribute Profiles (DAPs) but previously DAPs have been shown to be suitable in extracting and characterizing structures in VHR image analysis and in change detection. A DAP is generated by computing the derivative of the AP; it shows at each level the residual between two adjacent levels of the AP. By analyzing the multilevel behavior of the DAP, it is possible to extract geometrical features corresponding to the structures within the scene at different scales. Our proposed approach for extraction of spatial information from hyperspectral images is in two steps. The first step uses a homogeneity measurement to identify the level  $L$  in which a given pixel belongs to a region with a physical meaning. The second step is to fuse the geometrical information of the extracted regions into a single map considering their level  $L$  previously identified. The process is repeated for different attributes building a stack of spatial features whose dimensionality is much lower with respect to the ones of the original AP.

The experiments are carried out on an hyperspectral image acquired by the ROSIS sensor on the area of the university of Pavia, Italy. Firstly, the APs considering different attributes are computed and the related DAPs are derived and analyzed. The extracted spatial features are then fused and provided as input to an SVM classifier. The preliminary results are promising, showing the effectiveness of the proposed method in extracting spatial features related to the physical structures present in the scene.

## 8892-25, Session 5

### Affinity propagation for large size hyperspectral image classification

Mariam Soltani, Kacem Chehdi, Claude Cariou, Univ. de Rennes 1 (France)

Clustering of large scale data is an important issue for the processing of remote sensing images. Motivated by the application requirements, we used a recent clustering method called Affinity Propagation (AP). AP takes as input measures of similarity between pairs of data points to classify. Real-valued messages are exchanged between data points until a high quality set of exemplars and corresponding clusters gradually emerge. AP's major advantage is its robustness during the optimization process, since it is based on a continuous optimization problem. At the beginning, all the data points are considered as candidate exemplars, and the AP progressively generates clusters centered around surviving exemplars. This algorithm does not face initialization issues and provides a quasi global optimization. Therefore, it has been successfully used in many applications in various disciplines such as colour image segmentation, proteins clustering, initial training set selection in active learning, keyphrase extraction, representative image extraction, and supervised dimensionality reduction.

When using the AP, one may face computing problems. On the one hand, this algorithm controls only the number of clusters in an implicit way from a given Preference parameter. This latter is usually initialized as the median value of the similarity matrix, which often gives an over partitioning of the data set. On the other hand, when dealing with large sets, its computing complexity is quadratic and severely hinders its use into large scale remote sensing images.

In this paper we propose a classification approach which attempts to solve the above problems in the context of large scale hyperspectral image clustering.

Our approach is composed of two steps. Firstly, we start by dividing the hyperspectral image into non-overlapping blocks in order to parallelize the processing. For each block a first level of data aggregation is applied, based on a nearest neighbours rule using the  $L_1$  distance (i.e. that presents a high similarity). For the set of image blocks, this aggregation is performed in a parallel manner. This step makes the AP stable and invariant under a change of the block size and uses less memory since a full similarity matrix is not required.

The second step consists on applying the AP to the set of all the exemplars which are selected from the above blocks. To estimate the number of clusters, we introduce, in a dichotomic manner, an evaluation criterion of a partition that takes into account the inter-class and intra-class variance.

This approach is tested on multispectral and hyperspectral images and shows its efficiency. We show in this paper the results of two applications. The first one is the detection of cedar pines from an Ikonos multispectral image taken over Beirut, Lebanon (3273x3000 pixels, 3 bands). The correct detection rate for this application is nearly 96%. The second application is the classification of invasive and non-invasive plants from the analysis of an hyperspectral scene taken over Cieza, Spain (1000x1000 pixels, 62 bands), providing a correct classification rate over 95%.

## 8892-26, Session 6

### Hyperspectral image classification using a spectral-spatial sparse coding model

Ender Oguslu, Old Dominion Univ. (United States); Guoqing Zhou, Guilin Univ. of Technology (China); Jiang Li, Old Dominion Univ. (United States)

In this paper, we present a sparse coding based spectral-spatial classification model for hyperspectral image (HSI) datasets. The proposed method consists of four steps: 1) Dictionary learning. In this step, we constructed spectral-spatial patches from HSI datasets to learn a set of basis functions using the sparse coding framework. 2) Encoding. For each pixel in HSI datasets, we projected data onto the basis functions to achieve a new representation for the pixel. The projection can be done in a number of ways. We utilized the soft thresholding scheme for this purpose. 3) Dimensionality reduction. The new representation usually has a very high dimensionality requiring a large amount of computational resources. We utilized two methods to reduce the dimension of the new representation. First, the numbers of basis functions were reduced by the Kernel principle component analysis (PCA) algorithm. Second, the size of new pixel representations was further reduced by the  $l_1/l_q$  regularized multi-class logistic regression technique, resulting in compact feature representations for classification and 4) Classification. In the classification step, we used a linear support vector machine (SVM) to discriminate different types of land cover. We applied the proposed algorithm to a HSI dataset collected at the Kennedy Space Center (KSC) and compared our algorithm to a recently proposed method, Gaussian process maximum likelihood (GP-ML) classifier. Experimental results show that the proposed method can achieve significantly better performances than the current state-of-the-art with a compact pixel representation, leading to more efficient HSI classification systems.

## 8892-27, Session 6

### Classification of hyperspectral images with binary fractional order Darwinian PSO and random forests

Pedram Ghamisi, Univ. of Iceland (Iceland); Micael S. Couceiro, Univ. de Coimbra (Portugal); Jon Atli Benediktsson, Univ. of Iceland (Iceland)

In the paper, a novel approach for spectral and spatial classification of hyperspectral remote sensing images is proposed. The proposed approach is based on extended morphological profiles (EMP) [1], random forest classifiers (RF) [2], and a new binary optimization algorithm. The key novelties of the paper are listed below.

i) Proposal of a new binary optimization algorithm, denoted as BinAry fracTioNal orDer Darwinian Particle Swarm Optimization (BANDED-PSO), with tuned convergence and sub-optimal avoidance capabilities for feature selection of hyperspectral images;

ii) Development of a novel spectral and spatial classification framework for efficient feature selection from stacked vector including raw hyperspectral bands and EMP.

The work-flow of the proposed spectral and spatial classification method is as follows:

- i. The most effective bands of the input data set are selected by using the new optimization algorithm called BANDED-PSO
- ii. In parallel, EMP is derived from the input data and optimized by BANDED-PSO.
- iii. The most effective features from i and ii are gathered into one stacked vector.



iv. The stacked vector from iii are classified using Random Forest classifier and final classification map is produced.

Due to the novelty regarding the BANDED-PSO, a brief description is introduced. The goal is to overcome the curse of dimensionality by selecting the optimal  $L_E$  bands from  $L$  input bands which maximize the overall classification accuracy. The BANDED-PSO is a binary extension of the PSO [3] which is based on natural selection and the Grünwald-Letnikov fractional order definition. At each step, the fitness function (overall accuracy of the classification of a cross validation set) is used to evaluate the particle success. Each particle's position will be represented as a  $L$ -dimension binary vector ( $L$  is the number of bands in the input data) which 0 and 1 demonstrates the absence and presence of one band, respectively.

The whole population is divided into several swarms with competitive behaviour. To model each swarm, each particle moves in a multidimensional space according to the position and velocity, values which are highly dependent on local best and global best information. It is noteworthy that the velocity dimension, as well as the position dimension, correspond to the total number of bands of the image. Moreover, the velocity of a particle turns out to be related to the probability of changing its state, thus presenting particles' position in binary values, i.e., 0 or 1.

The proposed spectral and spatial classification method is tested on the widely used ROSIS Pavia University data set and improves the overall classification accuracy of the raw data set (Spectral), EMPs, and Spectral+EMPs by 11, 4 and 5 percent, respectively.

[1] J. A. Benediktsson, J. A. Palmason, and J. R. Sveinsson, "Classification of hyperspectral data from urban areas based on extended morphological profiles," *IEEE Trans. Geosci. Remote Sens.*, vol. 43, no. 3, pp. 480–491, Mar. 2005.

[2] L. Breiman, "Random forests," *Mach. Learn.*, vol. 45, no. 1, pp. 5–32, 2001.

[3] J. Kennedy, R. Eberhart, "Particle Swarm Optimization" *Proceedings of IEEE International Conference on Neural Networks*. IV. pp. 1942–1948, 1995 doi:10.1109/ICNN.1995.488968

## 8892-28, Session 6

### Smoothing parameter estimation framework for Markov random field by using contextual and spectral information

Hossein Aghighi, John C. Trinder, The Univ. of New South Wales (Australia)

In order to understand a scene in a remotely sensed image, humans use the spatial and visual information through observation. This information is necessary to enable interpretation of the image by humans or by computer vision system. The most common method to find the optimal solution for image data incorporating contextual visual information is a Markov random field (MRF). The labeling for a site in MRF is related to the interaction between labels of the site and its neighbors via a neighborhood system.

Through the definition of an energy function in MRF, the performance of the model depends on smoothing parameters which are the weights that determine relative contributions of the spectral and spatial energy. It has been demonstrated that a too large value of the smoothing parameter causes over-smoothing and a too small value does not fully use the spatial information in the MRF model. So, the motivation for this research comes from concerns of the balance between spatial and spectral energies for the purpose of maximizing the classification accuracy.

This paper deals with the development of a new robust two-step method to determine the smoothing parameter, incorporating spatial and spectral features. Spatial information is calculated using the co-occurrence matrix and the spectral information is extracted by some class separability indexes. Multispectral images obtained by WorldView-2 satellite were employed in this research.

In the first step, a support vector machine (SVM) as the state-of-the-art technique with sigmoid kernel function was used to provide a vector of multi-class probabilities and class labels. The summation of the maximum of the probability of each pixel and its 8 neighbors are calculated and assigned to the central pixels. By using the summation of the probability of each pixel, the pixels of each class are sorted and then an equal proportion of the pixels of each class with the highest probability is selected. The class code of the selected pixels and

their neighbors are extracted from the classified map and spectral information from the multispectral image. These pixels are used to calculate the co-occurrence matrix and class separability indexes.

In the second step, the data set of the selected pixels and information from their neighbors are used to model contextual and spectral information. The distribution of co-occurring classes is calculated based on the selected pixels and their neighbors' class codes. According to the unequal class covariance matrices of the spectral bands, the mean vector and covariance matrix for each class are estimated by using the spectral information of the selected pixels of that class. Then, class separability is determined using the divergence, transformed divergence, Bhattacharyya distance and Jeffries-Matusita distance.

Finally, the different smoothing parameters are calculated and the supervised MRF method is applied to produce the thematic map of the WorldView-2 satellite images. The validation of the MRF is done by a pixel-based method and the quality of the obtained MRF map is assessed by computing the kappa coefficient. The results show that MRF algorithm performance depends on the availability of correct parameter estimates.

## 8892-29, Session 6

### Road extraction from satellite images by self-supervised classification and perceptual grouping

Eda Sahin, ASELSAN Inc. (Turkey); ?Ikay Ulusoy, Middle East Technical Univ. (Turkey)

APPROACH: A road centerline extraction method, which is based on classification, is proposed. The training set is obtained from the image itself automatically. The steps of the approach can be listed as follows: 1. Seed Point Extraction, 2. Classification, 3. Morphological Operations, 4. Perceptual Grouping

1. Seed Point Extraction: The ACE (Anti-parallel Centerline Extraction) algorithm is proposed by Doucette et al. [1] to extract road center points by finding the midpoints of the edges of the roads. After finding the midpoints, small connected-components are eliminated from the response. In this paper, instead of directly using the ACE results as the training data, the perceptual grouping method is used to link fragmented line segments by using Gestalt principles. First, line segment labeling is performed to determine pixel locations of a connected line. After labeling, line segments that are close to each other and have similar angles are grouped. Then, gaps between grouped segments are filled to construct a higher level road structure. The lines smaller than a predefined line length are erased from the seed point image. Finally, the pixels between road centers and the corresponding edges are also added to the training set.

2. Classification: The features of the training set are modeled by Gaussian Mixtures. Gaussian mixture is selected as the modeling method in order to include different road types of the input image in the same model. We used HSV color bands as features and the road pixels are determined as a result of the classification.

3. Morphological Operation: Morphological operations are used to obtain a compact and noise free classification result before the result is used for topology construction. Thinning is performed and the skeleton of the road network is generated.

4. Topology Construction: Perceptual grouping algorithm is also used for topology construction. After grouping the lines, the ones shorter than a minimum connected line threshold are removed from the image.

EXPERIMENTS: The results of the proposed algorithm are compared with the algorithm proposed by Doucette et al. [1]. The steps of our algorithm are same as theirs. 20 high resolution satellite images with 1m resolution and 1024 x 1024 size are used for evaluation purposes. Correct road center lines are manually labeled by experts and used for performance computation. Performance metrics (correctness, completeness, quality) are calculated by defining a buffer width of 5 pixels around the manually labeled data and the outputs of the algorithms. The performance comparison is as follows:

Correctness, completeness, quality of the proposed algorithm are 57.13, 40.00, 32.29 respectively. Similarly, correctness, completeness, quality of the compared algorithm are 17.45, 16.94, 7.83 respectively.

#### REFERENCES

[1] Doucette, P. Agouris, and A. Stefanidis, "Automated Road Extraction from High Resolution Multispectral Imagery",

Photogrammetric Engineering & Remote Sensing vol. 70, no. 12, pp. 1405–1416, 2004.

8892-30, Session 6

## Extraction and refinement of building faces in 3D point clouds

Melanie Pohl, Dimitri Bulatov, Jochen Meidow, Fraunhofer-Institut für Optronik, Systemtechnik und Bildauswertung (Germany)

Due to the fast progress in sensor technology in the recent years, a huge amount of high resolution data of urban terrain, such as aerial photos and videos, laser scans etc., has been captured and is available for a wide use. Semantically-based representation of urban terrain is needed to pre-process and compress sensor data; such virtual models can be used for simulation and navigation in 3D urban terrain, imaging and planning of cities, disaster management and tactical reconnaissance.

The first important milestones on the way from sensor data to a virtual model of the scene comprise extraction of the ground, buildings and vegetation, as well as building outlining; these milestones have been accomplished within our previous work and, therefore, results on building detection and their outlines by closed, piecewise orthogonal polygons can be assumed.

The next level of abstraction concerns roof detail analysis of individual buildings. The contribution of this work is a four-step procedure for roof planes extraction. At first, small elevated objects – like chimneys – are detected with hot spot operators, modeled separately and excluded from further consideration. For large point clouds, a more precise modeling of different roof structures benefits from separation of complex buildings into single parts. Therefore, in the second step of our procedure, the building points are projected into the ground plane, after which two main groups of methods were tested. In the one group, ground polygons are subdivided along their diagonals into simpler sub-polygons. The other group operates on binary masks of the underlying building. In that case, we use morphologic operations and segmentation methods. In the third step, extraction of dominant planes is carried out by one of two main algorithms, namely, RANSAC and J-linkage, applied on the measured 3D points of adequate confidence in the whole building part. These methods allow handling even very noisy data with many outliers. The iterative error minimization and support set computation are carried out for each dominant plane. The last step consists of re-fining the previously determined planes. Due to noisy data and the influence of different thresholds, we use the parallelism and perpendicularity constraints of planes and line segments of the footprint to refine the planes simultaneously. The applicability of these hypothetical constraints is verified by statistical tests and the Gauss-Newton method is used to solve the optimization problem.

The proposed methods are tested on several data sets. At first, we use a synthetic data set to prove the principle of the algorithm basically and to analyze its behavior dependent on the underlying building model and its roof structure. To make sure the methods are also suitable for real data, we consider two different urban areas. One of them is represented by a noisy data set of points extracted from depth maps while the other one is made up by a superposition of four laser scans.

8892-31, Session 7

## Multisource oil spill detection

Arnt B. Salberg, Siri O. Larsen, Maciel Zortea, Norwegian Computing Ctr. (Norway)

Current oil spill detection methodology, as well as operational services, use mainly single frequency, single polarization SAR images only, e.g., C-band VV- or HH-polarization. In such imagery, the oil slicks are often clearly visible; however, one of the main challenges is to discriminate oil spills from lookalikes. Typically the lookalikes arise from e.g. low-wind patterns, biogenic materials (e.g. algae or bacteria), upwelling, ocean-currents, weather fronts, or rain cells. The challenge is that several conditions result in dark slicks in the SAR image.

The goal of this paper is to improve oil spill detection by the use of other information sources, including optical data and ocean-color

products, wind and ocean-current data, and automatic identification systems (AIS). The focus is on deriving methodology for multisource automatic oil spill detection. The oil spill detection algorithm consists of three main parts: 1) detection of dark spots; 2) extraction of features corresponding to the dark spots; and 3) classification of dark spots as oil spills or lookalikes.

The SAR image is the main data source of the proposed oil spill detection approach. From this image potential oil spills are identified by first detecting dark spots in the SAR image. Then, for each dark spot, corresponding features are extracted from both the SAR image and the multisource data. These features include:

- (i) Dark spot shape features.
- (ii) SAR image features related to contrast, border gradient and homogeneity.
- (iii) Contextual features related to the number and distribution of neighboring dark spots.
- (iv) Optical features and ocean-color products derived from near-time optical data (e.g. Modis).
- (v) Wind features (both SAR-based wind and model-based wind).
- (vi) AIS features (e.g. nearest distance from the AIS tracks to the segmented dark spots).

The aim of the classification stage is to classify the dark spots into two groups: oil slicks and lookalikes. The classifier consists of two parts. First a statistical classifier based on some of the shape and SAR image intensity features is applied to suppress obvious lookalikes, and then a confidence estimation strategy that also exploits the multisource features, is applied to assign a confidence measure to the remaining dark spots. Dark spots with a confidence measure above a defined level are classified as potential oil slicks.

The proposed multisource oil spill detection methodology is applied to a set of Radarsat-2 (HH-polarization, scan SAR narrow) and Envisat ASAR (VV-polarization, wide swath) image covering European waters. The results show that both wind and AIS data are effective for reducing the number of false alarms. However, for effective use of AIS an oil spill drift model should also be applied. The importance of ocean-color products was not clear, as many of the products like e.g. chlorophyll are not tailored to detect surface slicks.

An automatic algorithm can be considered to be a good alternative to manual inspection when large ocean areas are to be inspected. However, the use of multisource data is regarded to be necessary for effective use of automatic oil spill detection.

8892-32, Session 7

## Joint processing of Landsat ETM+ and ALOS-PALSAR data for species richness and forest biodiversity monitoring

Sara Attarchi, Technische Univ. Bergakademie Freiberg (Germany); Richard Gloaguen, Technische Univ. Bergakademie Freiberg (Germany) and Helmholtz Institute Freiberg of Resource Technology (Germany)

Optical remote sensing data is commonly used for estimating biophysical characteristics of forest like tree biodiversity and species richness. Recent advances in radar remote sensing technology, raise significant interest to take advantage of complementary nature of optical and radar data. This paper proposes an approach combining Landsat ETM+ and ALOS -PALSAR (Advanced Land-Observing Satellite- Phased Array L-band Synthetic Aperture Radar) data for biodiversity and species richness monitoring. Inventory data from one part of Hyrcanian forest in north of Iran is used as field data.

Visible and infrared ETM+ bands, indices, band ratios and textures information as well as HH, HV backscattering, their decomposition elements (alpha angle, entropy and anisotropy) and SAR texture are extracted. We use Partial Least Square Method (PLS) to find the best components to describe the biodiversity indices and species richness in study area. We show how tree biodiversity is related to information derived from ETM+ and PALSAR data ( $R^2=0.62$ ). Also the effects of every component on the variation of biodiversity and species richness are shown. ETM+ reflectances, decomposition elements and texture from PALSAR can describe approximately 60% of biodiversity. The results of multi source monitoring of tree biodiversity and species richness are promising and worth further investigation.

8892-33, Session 7

## Recurrent neural networks for automatic clustering of multispectral satellite images

Petia Koprinkova-Hristova, Kiril Alexiev, Bulgarian Academy of Sciences (Bulgaria); Denitsa Borisova, Georgi Jeleu, Space Research and Technology Institute (Bulgaria); Valentin Atanassov, Space Research and Technology Institute - Bulgarian Academy of Sciences (SRTI-BAS) (Bulgaria)

In the present work we applied a recently developed procedure for multidimensional data clustering to processing of spectral satellite images. The main aim is to discover points with similar characteristics. This was done by clustering of the resulting image. Multispectral data from Landsat 7 Enhanced Thematic Mapper Plus (ETM+) instrument are used in this work. The core of our approach lays in projection of multidimensional image to a two dimensional space. For this purpose it is proposed to use extensively investigated type of recurrent artificial neural networks (RNN) called "Echo state network" (ESN). It incorporates a randomly generated recurrent reservoir with sigmoid nonlinearities of neurons outputs (usually hyperbolic tangent). The procedure for reservoir improvement called Intrinsic Plasticity (IP) is aimed at its entropy maximization. In fact IP training stabilizes even initially unstable reservoirs. Experimentally together with improved stability the IP tuned ESN reservoirs possess also better clustering abilities that naturally opens the possibility to apply them for multidimensional data clustering. Based on investigated effect of IP improvement of ESN reservoir we propose a procedure for multidimensional data clustering. We consider combinations between steady states of each two neurons in the reservoir as numerous two-dimensional projections of the original multidimensional data fed into ESN input. These low dimensional projections can be used next for data clustering. Two approaches to choose a proper projection among the all possible combination between neurons were investigated. The first one is based on the calculation of two-dimensional density distributions of each projection, determination of number of their local maxima and choice of the projection with biggest number of these maxima; then the chosen projection is clustered using subtractive clustering algorithm that is a procedure that determines position and number of clusters without preliminary knowledge of their number. The second one applies subtractive clustering to each projection and the one with maximum number of clusters is chosen. We also compared the results obtained using different number of neurons in the ESN reservoir. The obtained number and position of clusters of a multi-spectral image of a mountain region in Bulgaria is compared with the classification of the region landscape. The bigger is the number of reservoir neurons the bigger was the number of discovered clusters. It is observed that the shadows in the part of the clustered images mask the real objects but in the case of smaller number of clusters a small part of image is put into the wrong cluster. In the case of bigger clusters number, the wrongly clustered parts number decreased since now they belong to another cluster. However in the case of smaller number of clusters the slopes are better outlined. In case of more clusters it appears that they are related to the real land covers in the region.

8892-34, Session 7

## Data mining and model adaptation for the land use and land cover classification of a Worldview 2 image

Lidice C. Nascimento, Carla B. M. Cruz, Univ. Federal do Rio de Janeiro (Brazil); Elizabeth M.F.R. Souza, Universidade Federal do Rio de Janeiro (Brazil)

The studies about forest fragmentation have increased since the past 3 decades, together with the increase of the discussion about conservation and preservation. In this way, the landscape and land use maps are important tools for this analysis, as well as other remote sensing techniques. The object oriented analysis classifies the image according to patterns as texture, color, shape, and context. In this way, the aim of this paper is to describe data mining techniques and results of a heterogeneous area, as the Silva Jardim city in Rio de Janeiro state - Brazil. The landscape of the study area has predominantly forest and pastures. However, there is also urban areas, water bodies, agriculture and also some shadows as objects

to be represented. The analyzed image was from the Worldview2 satellite, from 2010. However the available bands were the visible one, and the Near Infrared (NIR), named 1 to 4. The attributes chosen to be mined were: brightness; entropy (all directions and layers 1, 2, 3, 4); maximum difference; average layers 1, 2, 3, 4; NDVI; standard deviation layers 1, 2, 3, 4. To identify which value and attribute is necessary to the classification, data mining technique has been used, because it looks for patterns inside the data, helping us to learn about the most important information which characterize the classes. This technique also helps to accelerate the process. In this way, the land use and land cover classification was made using the values that data mining software (WEKA) has provided (NDVI, maximum difference, entropy layer 1 and all directions) with a Kappa index of 0.9403, using the classify method J48. Afterwards, this classification was analyzed, and the verification was made by the confusion matrix, which was generated through the creation of random points shapefile in ArcGIS 9.3, being possible to evaluate the classification accuracy (58,89%). The objects pasture and urban areas were classified as agriculture. The best classification results were in classes "water" and "forest" which have more homogenous reflectance. Because of that, the model has been adapted, in the classes "water" and "forest" in order to create a model for the most homogeneous classes, and in the future continue the modeling process in the most heterogeneous classes. As result, 2 new classes have been created: "shadow" and "dark forest". It is important to highlight the role of the earth surface. The study area is rough, which can create shadow areas depending on the position of the Sun. Also, some values were changed and some attributes, which were not chosen in the mining process, added. For example brightness, to identify dark areas. In the end, the accuracy of the classified classes was 89,33%, however this result doesn't show some errors which are still on the model. Although the data mining is a good tool to accelerate the classification process, it is still important to adapt the model by the specialist. It is important to highlight this is not a conclusive paper; there are still many steps to develop in the mining process, especially in highly heterogeneous surfaces.

8892-35, Session 7

## Application of genetic programming and Landsat multi-date imagery for urban growth monitoring

Khelifa Djerriri, Ctr. National des Techniques Spatiales (Algeria); Malki Mimoun, Univ. de Sidi-Bel-Abbes (Algeria)

The development of automatd and semi-automted techniques to extract useful information from multi-date satellite imagery was always a main concern to researchers in the field of remotely sensed image processing. Thus, several techniques have been proposed since the early 70s as possible alternative to reduce human integration and saving technicians from interpreting and digitizing hundreds of areas by hand.

Thematic information extraction using supervised classifications such as neural networks, statistical methods, SVMs and kNN, which have been traditionally considered as black box methods are difficult to understand; otherwise the using of simple, easy to memorize and often comprehensible mathematical models such band-ratios and indices are one of the widely used techniques in remote sensing for the extraction of particular land-cover/land-use like urban and vegetation areas. The results of these models generally only need the definition of adequate threshold to discriminate between the class of interest and the background.

Genetic programming (GP) is essentially considered to be a variant of evolutionary algorithms (EAs) that uses tree representation to codify individuals (possible solutions). The original goal of GP, as its name implies, was the evolution of computer programs, mathematical expressions or rule-based systems. GP individuals are usually seen as parse trees, where leaves correspond to terminal symbols (variables and constants) and internal nodes correspond to non-terminals (operators and functions). GP is a flexible and powerful evolutionary technique and it can be configured to promote the evolution of comprehensible classifiers by setting a maximum tree depth or including a size penalty in the fitness function.

Most critics of using bio-inspired algorithms in general and EAs in particular, concern their expensive time cost. However thanks to nowadays high performance computing machines, processing time can be reduced considerably, in addition GP can easily parallelized through evaluating the population of solutions in parallel. Such

parallelization can be even done on personal computers through low-cost GPU-based parallel computing.

In our study the Landsat TM imagery has been chosen as data source to monitor urban growth from space. The Landsat program offers the longest continuous scientifically valuable free datasets, which were widely used for studying land cover change and human influences on the land surface since the mid-eighties. The Program will continue to obtain valuable data and imagery through the recently launched Landsat Data Continuity Mission (LDCM), which is the new satellite in the Landsat series.

In our work a GP based approach has been adopted to evolve simple mathematical expression to extract urban areas. The model is built from a single Landsat TM image by using a basic set of operators between multi-spectral bands (addition, subtraction, multiplication and division) and maximizing a fitness function based on the using of the M-statistic, which assesses the degree of discrimination between the urban and non-urban pixel groups. A high value of M criterion denotes that the classes are well separated and that the two regions are relatively easy to discriminate. Many other fitness functions from the literature functions can be used to guide the evolution.

The model was constructed from the Landsat 5 TM image acquired in 2006 by using training samples extracted with the help of a Quick-bird high spatial resolution satellite image acquired the same day as the Landsat TM image over the city of Oran, Algeria. The model has been tested to extract urban areas from multi-date series of Landsat TM imagery acquired respectively in the years: 1984, 2003 and 2011. The generalization capacity of the obtained model has been analyzed, evaluated and compared to results from GP-based models built with different fitness functions and to results from other supervised classification techniques.

## 8892-51, Session PS

### Detection of region of interest based on visual saliency analysis in high spatial resolution remote sensing images

Libao Zhang, Bingchang Qiu, Xianchuan Yu, Beijing Normal Univ. (China)

Compared with the traditional low spatial resolution remote sensing images, the high spatial resolution images have extraordinary amount of data, clear details and abundant texture information. Detection of region of interest (ROI) is one of the most popular applications applied to high spatial resolution remote sensing images. Traditional approaches to detect of ROIs in high spatial resolution remote sensing images commonly include procedures of classification and segmentation. However, most of the classification methods need a prior knowledge model which is highly influential to detection results and hard to build. In addition, global searching is an essential part of both classification and segmentation procedures, which is time-consuming and storage-expensive. In this paper, an efficient visual saliency analysis method based on bottom-up visual attention mechanism is proposed to detect the ROIs in a high spatial resolution remote sensing image. First, this new method reduces the spatial resolution of the input high spatial resolution remote sensing image by subsampling. Second, it can extract color, intensity and orientation information from the subsampled remote sensing image and create spatial scales using dynamic Gaussian pyramid. Third, a linear "center-surround difference" operation is used between different levels of the pyramid to compute multi-scale visual saliency and generate several feature maps. Fourth, a new feature competition strategy is employed to attach different weights to different feature maps according to the size and saliency of the salient regions. Finally, the final saliency map is computed as the addition of these feature maps. The detected visual saliency regions are described using threshold segmentation, which improves the accuracy and the speed of detection. Experimental statistics have shown that the proposed method is computational efficient and provide more visually accurate detection results.

## 8892-52, Session PS

### Observation of aerosol properties at Saga using GOSAT product validation lidar

Hiroshi Okumura, Takeru Kawasaki, Taiga Akaho, Saga

Univ. (Japan); Osamu Uchino, Isamu Morino, Tatsuya Yokota, National Institute for Environmental Studies (Japan); Tomohiro Nagai, Tetsu Sakai, Takashi Maki, Akihiro Yamazaki, Meteorological Research Institute (Japan); Kohei Arai, Saga Univ. (Japan)

Global warming has become a very serious issue for human beings.

So far, the number of ground-based carbon dioxide observation points has been limited, and they have been distributed unequally throughout the world.

Greenhouse gas Observation SATellite (GOSAT) enables the precise monitoring of the density of carbon dioxide by combining global observation data sent from space with data obtained on land, and with simulation models. In addition, observation of methane, another Greenhouse gas, has been considered.

For validation of GOSAT data products, we have continued ground-base observation with Fourier Transform Spectrometer (FTS), aerosol lidar and ozone-DIAL lidar at Saga University, JAPAN since March, 2011.

In these equipment, aerosol lidar system is a monostatic and has a Nd:YAG laser for its light source.

The system has 4 different wavelength channels, parallel and perpendicular (senkrecht) polarized channel at 532[nm], 1064[nm] and 607[nm] for Raman shift caused by nitrogen molecules.

For analysis of this aerosol lidar data, not only acquired lidar data but also meteorological data are required.

We automatically obtain the following meteorological or image data for aerosol data analysis:

- 1) Ground-level meteorological data from Saga city AMeDAS station every 10 minutes;
- 2) GPS Sonde upper-air meteorological data from Fukuoka city AMeDAS station twice (00Z and 12Z) a day;
- 3) images taken by a Skyview camera established on the roof of the building adjacent to the aerosol lidar are acquired every 5 minutes in daytime;
- 4) meteorological satellite (MTSAT) IR image data are acquired every hour.
- 5) Skyradiometer data every 10 minutes in daytime;

Ground-level meteorological data, GPS Sonde upper-air meteorological data are used for estimation of extinction coefficient caused by Rayleigh scattering. The US standard atmosphere model is used for estimation of extinction coefficient above the stratosphere.

Skyview camera images and meteorological satellite IR image data are required to confirm clouds above lidar.

Skyradiometer data are required to analyze optical thickness, volume spectrum and complex refractive indexes.

In this study, observation results of yellow sands, PM<sub>2.5</sub> caused by East Asian air pollution obtained from aerosol lidar are reported. Seasonal or annual tendency of backscattering ratio, wavelength dependency, depolarization and lidar ratio are also shown.

## 8892-53, Session PS

### Evaluation of the radiometric properties of infrared imaging Fourier-transform spectrometers

Mariusz Kastek, Military Univ. of Technology (Poland); Martin Chamberland, Telops (Canada); Tadeusz Piatkowski, Military Univ. of Technology (Poland); Philippe Lagueux, Telops (Canada); Rafal Dulski, Military Univ. of Technology (Poland); Vincent Farley, Telops (Canada); Piotr Trzaskawka, Military Univ. of Technology (Poland)

The imaging spectroradiometer Hyper-Cam offered by Telops is based on infrared imaging Fourier-transform spectrometer technology to provide high spectral resolution and to enable high accuracy radiometric calibration. The Hyper-Cam, a man portable sensor, provides hyperspectral data cubes of up to 320x256 pixels at 0.35 mrad spatial resolution over the 8-12 μm spectral range at spectral resolutions of up to 0.25 cm<sup>-1</sup>. The Hyper-Cam has been used in several field measurements, including demonstration of standoff chemical agent detection. One key feature of the Hyper-Cam is

its ability to provide calibrated measurements. The quality of the calibrated measurements will be presented in this paper as well as the analysis of radiometric parameters of infrared imaging Fourier-transform spectrometer (IFTS). The Hyper-Cam sensor is offered as medium (MWIR) or long wave (LWIR) infrared sensor. However, only the results for long-wave Hyper-Cam (LWIR) will be presented. The principle of operation, construction and technical specifications of the Hyper-Cam LWIR spectrometer are described in the paper.

The results of the measurements of selected radiometric parameters of Hyper-Cam device will be presented. The measurements will be conducted in the Institute of Optoelectronics on a test stand fitted with highly-stable, extended standard radiation sources. The method used to determine the selected radiometric parameters will be presented and the analysis of the related measurement results will be included. Sensitivity, spectral resolution and radiometric stability as obtained during field and laboratory measurements will be presented and discussed.

## 8892-55, Session PS

### Comparison on accuracy of image matching between lossy JPEG compression and lossy JPEG 2000 compression

Ryuji Matsuoka, Kokusai Kogyo Co., Ltd. (Japan) and Tokai Univ. (Japan); Mitsuo Sone, Noboru Sudo, Hideyo Yokotsuka, Tokai Univ. (Japan); Naoki Shirai, Kokusai Kogyo Co., Ltd. (Japan)

The recent increase in number of pixels of images acquired by a digital camera encourages one to utilize it for not only photogrammetry but also remote sensing. A large number of pixels of an image bring difficulties in dealing with it. Therefore, lossy image compression before recording an image in a digital camera is still required. Almost all the recent digital cameras have the built-in function of lossy JPEG compression. On the other hand, although JPEG 2000, which is the successor to JPEG, is superior in compression performance to JPEG, lossy JPEG 2000 compression has not yet come into use in a digital camera. Although image matching is conducted for image registration and stereo measurement in remote sensing, few papers have reported on comparison of image matching accuracy between lossy JPEG compression and lossy JPEG 2000 compression.

This paper reports an experiment conducted in order to compare lossy JPEG compression and lossy JPEG 2000 compression on the accuracy of image matching. The experiment was conducted by using 54 color images of diverse textures and diverse tones of color on the assumption that image matching utilizes a pair of images reconstructed from image data which are lossily compressed in an ordinary digital camera. Lossy JPEG compression was executed with a set of compression parameters utilized in the lens-interchangeable digital camera Canon EOS 20D, while lossy JPEG 2000 compression was executed in the way as the file size of a piece of JPEG 2000 compressed image data was the same file size of the corresponding JPEG compressed image data. Moreover, we prepared another set of JPEG and JPEG 2000 compressed image data which were lossily compressed with the compression ratios of 6.5 and 13.0 which are expected for an ordinary color image when it is compressed in the EOS 20D. Image matching was carried out by least squares matching in the experiment. The least square matching is a popular area-based matching method in digital photogrammetry and would be able to estimate a corresponding position with sub-pixel accuracy. All three color components R, G and B have been utilized in the least squares matching.

When the file size of a piece of JPEG 2000 compressed image data was the same as that of a piece of JPEG compressed image data, the experiment results clearly showed that the compression performance of lossy JPEG 2000 compression would be superior to that of lossy JPEG compression on image quality as to pixel value in RGB color space as several papers on comparison of various image compression techniques reported. On the contrary, the results did not necessarily indicate that lossy JPEG 2000 compression would be able to provide more accurate matching results than lossy JPEG compression when the file size of a piece of JPEG 2000 compressed image data was the same as that of a piece of JPEG compressed image data. Furthermore, the results demonstrated that the degradation of matching accuracy by using JPEG or JPEG 2000 compressed image data with the compression ratio of 13.0 would be too large to be ignored.

## 8892-56, Session PS

### GOES Imager IR channel to channel co-registration correction program

Zhenping Li, SGT, Inc. (United States); Michael G. Grotenhuis, National Oceanic and Atmospheric Administration (United States); Timothy J. Schmit, Xiangqian Wu, National Environmental Satellite, Data, and Information Service (United States); Tony Schreiner, Jim P. Nelson, Univ. of Wisconsin-Madison (United States); Fangfang Yu, Sam M. Chen, Hyre Bysal, National Environmental Satellite, Data, and Information Service (United States)

The channel-to-channel co-registration is an important performance metric for the GOES Imager, and large co-registration error could have a significant impact on the reliability of derived products that rely on the combinations of the multiple IR channels. Example products include the cloud mask, fog and fire detection. This is especially the case for GOES-13, in which the co-registration error between channel 2 (3.9 micrometer) and 4 (10.7 micrometer) could be as large as 1 pixel along the East-West direction. Characterization results show significant large co-registration errors along the East-West direction for both GOES13 and 14, while the errors are generally smaller along the North-South direction. Furthermore, all co-registration errors have a 24 hour periodic behavior. The GOES Imager IR Channel to Channel Co-Registration Correction Program (GII4C) currently being implemented in NOAA GOES ground system consists of two components, an algorithm to characterize the IR channel to channel co-registration error and an image resampling algorithm to re-project the image in one of the IR channels so that it is better aligned with the other IR channels. The key to both components is the Fast Fourier Transformation Resampling algorithm (FFTR), which is shown to be generally reversible, and efficient enough that meets the real time processing requirement in the GOES ground system. The evaluation of the resampled images shows no degradation of the image quality, and the reliability of most of the derived products that utilize the combinations of the IR channels has improved significantly with the resampled images.

## 8892-57, Session PS

### Geometric correction of airborne radar image data, and overlay with map data and satellite

Philippe Durand, Luan Jaupi, Dariush Ghorbanzadeh, Conservatoire National des Arts Métiers (France); Jean-Paul Rudant, Univ. Paris-Est Marne-la-Vallée (France)

Comparison of satellite data, from different sensors reveals a specific problem. Data can be more or less noisy, but especially the geometry of their acquisition requires corrections for comparisons between them.

In this paper we demonstrate how highly deformed radar images can be geometrically corrected and compared to map data coming from numerical models and also with data coming from SPOT satellite. Radar images that we use, come from the sensor airborne radar Varan, which is used for data acquisition campaign in the South-East of France. Applications include both structural geology, land cover and the study of the coastline. First, we discuss specific issues related to radar imagery. The problem of speckle: multiplicative noise is added to the landscape which may be flat or have landforms. We propose a solution to rectify radar image in the geometry of a numerical terrain model. To achieve this, we construct a radar image synthesis encoding all flight parameters of aircraft or satellite which allows to perceive field geometry of radar imagery. From this method, it is possible to simulate radar image of aircraft or satellite missions as ERS1 or ERS2. Satellite images acquired on areas of complex landscapes are of course much more distorted than those acquired from airborne radar. Finally, we can consider other comparisons: we then apply the superposition of radar data and SPOT images of terrains with or without landforms. Further, we discuss also how our methodology can reduce calculations in pretraitement phase and the improvement that it allow on final results. The results allow a fine expertise in the field. The application of our method in field of geology permit us to identify changes in landscape and locate them precisely where the data do not allow visible.

Its applications in coastland use allows to follow the underwater objects such drift oyster beds . In some cases, it is necessary to take some precautions: the speckle is not always an inconvenience and its disposal can disappear also valuable information:the granulometry information. The noise can indeed be seen as the size of particles which is added to information: the filter from the mathematical morphology allows fine segmentations of housing and urban roads. In this situation also, the image registration between aerial photographs and radar images can be very useful.

8892-58, Session PS

### Pixel Response Non -Uniformity Correction for Multi-TDICCD Camera based on FPGA

Guofang Zhai, Beijing Institute of Space Mechanics and Electricity (China)

To solve a non-uniformity problem of multi Time Delay and Integration Charge Couple Device (TDICCD) mosaic camera, a non-uniformity correction algorithm is proposed and implemented on a Field-Programmable Gate Array (FPGA) platform. Firstly, the generation and definition of non-uniformity are introduced; several regular non-uniformity correction methods are discussed. Secondly, the correction algorithm is designed. Finally, considering the fix-point processing ability of FPGA, the correction algorithm is optimized properly, and implemented on FPGA. Testing results indicate that the non-uniformity can be decreased obviously for 3-TDICCD mosaic camera's images with the proposed correction algorithm at 96 TDI stage, proving that this correction algorithm is with high real-time performance, good engineering realization and satisfaction of the requirements of the target system.

In wide-view-field and high-resolution electro-optical systems, single CCD can not satisfy the measure precision and view width, so multi-CCD must be assembled for satisfaction of demands. time delay and integration CCD(TDICCD) is a new kind of optical imaging device which developed with the use of CCD. Compared with original CCD, TDICCD is more sensitive to light and has higher Signal-to-Noise Ratio (SNR).Therefore, multi-TDICCD mosaic cameras are employed in the field of remote sensing popularly in recent years. However, with the increasing demand for the development of high quality remote sensing image techniques, the problem of pixel response non-uniformity is becoming a key issue. In order to get optimal image, it's essential to do some research on pixel response non-uniformity for multi-TDICCD mosaic cameras.

Based on the analysis of TDICCD single channel response non-uniformity, a novel correction algorithm is introduced in this paper, which is two-point correction and compensating gain correction method for single channel and multi channel of single TDICCD, compensating offset correction method for multi TDICCD. Finally, the correction algorithm is implemented on the FPGA hardware platform.

8892-59, Session PS

### Research on unmanned aerial vehicle (UAV) remote sensing and its applications for natural disasters management in China

He Huang, Siqun Yang, Lei Wang, Wei Wu, Juan Nie, Haixia He, Wei Zhang, Yan Cui, Feng Xu, Qi H. Wen, Fan Chun Bo, Tong Tang, Ping Wang, Li Ling Ling, National Disaster Reduction Ctr. of China (China)

Both satellite remote sensing and airborne remote sensing images are main data used for natural disasters management. The unmanned aerial vehicle (UAV) remote sensing is one category of airborne remote sensing. At present, the unmanned biplane and unmanned helicopter are always employed as the platforms of the unmanned aerial vehicle to obtain the airborne remote sensing data. The airborne remote sensing data have the advantages of high spatial resolution, low costing, flexibility, real-time image transmission, high-risk area detection, etc. Thus, the UAV remote sensing technology becomes an important spatial data acquisition tool in natural disasters management in China for its capability of information collection in dangerous environments with no risk to flight crews. The National Disaster Reduction Center of China (NDRCC), which is the decision making support agency for China disaster management, has

established a mechanism for the UAV remote sensing application.

First, the UAV remote sensing application mechanism of NDRCC was introduced in this paper. Then we focused on the data processing flow of the UAV remote sensing data in natural disasters emergency management. Furthermore, the UAV remote sensing images application effects on housing loss monitoring, slope point monitoring, victim settlements monitoring, blockage road monitoring in Qinghai Yushu earthquake disaster (2010), Gansu Zhouqu debris flow disaster (2010), and Yunnan Yingjiang earthquake disaster (2011) had been analyzed. Finally, we analyzed and summarized the positives and negatives of the UAV remote sensing technology in emergency relief, comprehensive loss assessment, and post-disaster reconstruction in occurrence of sudden natural disaster.

8892-60, Session PS

### Multi-source remote-sensing image matching based on epipolar line and least squares

Peng Chen, Wuhan Univ. (China) and The Second Institute of Oceanography, SOA (China); Zhihua Mao, Jianyu Chen, The Second Institute of Oceanography, SOA (China); Xiaoping Zhang, State Key Laboratory of Information Engineering in Surveying Mapping and Remote Sensing (China); Zifeng Li, State Key Lab. of Information Engineering in Surveying Mapping and Remote Sensing (China)

In remote sensing image applications, the image matching is a very key technology, its quality directly related to the quality of the subsequent results. This paper studied an improved SIFT features matching method for multi-source remote-sensing image registration based on GPU computing, epipolar line and least squares, its main purpose is to take both accuracy and efficiency into consideration. This method is firstly based on tonal balanced methods(such as histogram matching method, image information entropy method, the mean variance method, Wallis filtering method) matching, and then extracts SIFT features based on the GPU computing technology, and then matches feature points based on epipolar line and least squares matching method with RANSAC method, finally analies error sources of SIFT mismatch, researchs an improved SIFT mismatch reduce strategy.

The experimental results prove that the method can effectively improve the efficiency and precision of SIFT feature matching. Tonal balanced can effectively increased SIFT points.86 feature matching points were extracted with Wallis tonal balanced method while 58 were extracted before tonal balanced.The GPU acceleration technology can obviously improve the efficiency of SIFT feature matching. For the same images with the size of 4272 \* 4272, it shorten the time close to 10 times. Epipolar line and least squares matching method, can effectively solve the situation of scare points. SIFT mismatch reduce strategy can effectively remove SIFT mismatch, thereby improving the accuracy of SIFT feature matching. Flat areas and mountain areas were used respectively in this experiment with two groups of different source remote sensing images (SAR and optical image) as the experimental data, the flat region matching accuracy can reach 0.99 pixel, mountainous area were 1.9 pixels. It shows that the method can meet the specified requirements.

8892-62, Session PS

### Estimating urban surface component from Landsat-5 TM data using spectral index model and sub-pixel model

QingNi Huang, Zhiqiang Cao, China Meteorological Administration (China); Xiaohuan Xi, Institute of Remote Sensing and Digital Earth (China)

Recently, growing interest in urban ecological systems promote development of urban remote sensing. Meanwhile, urban land cover features are so complex which challenges the identifying and quantifying urban land cover types. A great amount of research has been carried out on distinguishing and quantifying urban components such as impervious surface, vegetation, soil and water. The object

of this paper is to examine and to compare the effectiveness of two approaches for extracting urban components from Landsat TM data based on spectral index models (including NDVI, NDBI, NDBal and MNDWI) and sub-pixel model (including SUBPIX algorithm and SVM algorithm). The accuracy assessment was carried out using high resolution Land Use and Land Cover based on evaluation indicators including product accuracy (PA), user accuracy (UA), overall accuracy (OA) and overall Kappa coefficient (OK). Results indicated that SUBPIX algorithm produced the worst result which underestimated the selected signatures. And for spectral index models, it showed a good distinction for vegetation and water (accuracy larger than 90%) while for impervious surface and half-naked soil this method manifested a relatively weak capability (less than 86%). The SVM model yielded a better result with an OA of 94.09% and an OK of 92.12%. In addition, a hybrid method of combining SVM and spectral index model was performed and it got a best result with an OA of 98.88% and an OK of 98.5%. The results of the research suggested that SVM had better capability in handling the mixed-pixel problem especially hybrid approach of SVM and spectral index models.

8892-63, Session PS

### Study of spectrally segmented PCA for feature extraction of hyperspectral data

Lord N. Prabhu, Manoj K. Arora, Balasubramanian Raman,  
Indian Institute of Technology Roorkee (India)

The hyperspectral remote sensing data provides a huge volume of data in visible, near infrared and short wave infrared regions of EMS in hundreds of narrow and contiguous bands. This helps in discrimination of vegetation species, study of minerals and soil types, etc. Indeed, the hyperspectral data are rich in spectral information but at times the data in various bands may be highly correlated. Therefore, Principal Component Analysis (PCA) is generally applied to decorrelate the data such that the components that carry useful information are selected without any significant loss of data. However, PCA operates on global statistics and thus it may overlook the local variances that are helpful for the detection of small objects/targets. Therefore, segmented PCA may be appropriate in hyperspectral data processing as the data have the property in which the correlations between neighboring spectral bands are generally higher than for bands further apart, with high correlations appearing in blocks. Typically, the segments are formed by computing the correlation between the bands. This approach may be appropriate when the ultimate aim of hyperspectral data processing is produce a general land use land cover classification. For a specific application such as vegetation mapping, built-up area assessment, military target detection, it would be more expedient to segment the data based on the spectral characteristics of the targeted class. In this paper, the segmented PCA has been extended to produce segments on the basis of spectral reflectance curve of a given class. Here, focus has been placed on vegetation type. Peaks and lows of the spectral reflectance curve form the basis of generating the segments. The PCA is then applied to data in each segment individually to pick a set of components from each segment. The selected components are then used in the classification process to produce a vegetation classification using Support Vector Machines. The performance of the suggested approach shall be evaluated with conventional PCA as well as segmented PCA based on correlation matrix.

8892-64, Session PS

### Effect of attribute variation on the extraction quality of objects from high resolution remote sensing data

Mohit Srivastava, Manoj K. Arora, Indian Institute of  
Technology Roorkee (India)

Pixel based classification techniques are appropriate for producing land use land cover classification from medium spatial resolution remote sensing data. The object based image analysis (OBIA) appears attractive in producing land use classification from high spatial resolution remote sensing data, as these take into account spectral, spatial and textural characteristics of the data and classes to be mapped. Additionally, the OBIA has been found useful in extraction of individual objects and targets. For example, urban feature extraction, military target detection etc. Typically, an OBIA process involves

segmentation, attribute selection and classification. Once the data have been segmented, a number of attributes for each segment can be recorded. At times, the number of these attributes is very large. Thus, many of the attributes may not be useful in extracting the desired targets and hence may be redundant. It may therefore be expedient to select a few attributes that describe the data characteristics useful for a given application.

The aim of this paper is to investigate the effect of various attributes for the object extraction using an ROC curve approach. The decision tree classifier has been used for object extraction using the selected attributes. The high spatial resolution data from Quick-bird sensor acquired over the city of Chandigarh, India has been used as experimental data. The image has been segmented using multiresolution region growing technique in eCognition software.

Further, the decision tree classifier has been used to calculate the gain ratio of every attribute for each class. Every attribute had been providing a rank based on their gain ratio. Statistically ranked attributes, provided based on their importance, has been further used for extraction of eight classes, namely; residential metallic and nonmetallic road, grass land, trees, bare land, water body and shadow. The ranks of an attribute may vary for each class. Object has been extracted via decision tree classifier using ranked attributes, starting from highest ranked single attribute to the least ranked all attributes one by one.

The true detection rate (TDR) and false alarm rate (FAR) values have been calculated for each set of attributes used for the object extraction and the receiver operating characteristic (ROC) curves have been drawn (Maxion and Roberts, 2004). Further, it has been noted that ROC curve is an upward rising curve, lies between point (0, 0) and point (1, 1). The extreme point (1, 1) shows that the extraction is highest but at same time, error is also high, thus extraction quality is low. While, at origin (0, 0), both values are low hence produces worst quality, however, the point closer to (0, 1) represents the highest accuracy.

Further, it has been found that both TDR and FAR values are high when extraction has been done with few highest ranked attributes. While by adding some more attributes, high TDR value with low FAR value has been achieved and shows highest extraction quality of object, the TDR becomes low by further inclusion of more attributes for object extraction. It has also been observed that shape of ROC curves appear different for different objects, which represents the variation in extraction quality of objects. From the result, it has been interpreted that highest extraction quality for all objects has been obtained with suitable attributes, and lies between TDR ranging from 0.35 to 1.0. Whereas, quality goes down when extraction has been done using all attributes, and it appears with TDR ranges of 0.02 to 0.11. Thus, it can be concluded that optimal extraction quality has been achieved with some required attributes while it is worst with all attributes. In addition to this, it is also noted that there have variation in the number of attributes for extracting the object with highest quality.

8892-65, Session PS

### Kernel-based linear spectral mixture analysis via multiple kernels

Keng-Hao Liu, Yen-Yu Lin, Chu-Song Chen, Academia Sinica  
(Taiwan)

Linear spectral mixture analysis (LSMA) has been received wide attentions for spectral unmixing in remote sensing community. Three representative LSMA techniques, Least Squares Orthogonal Subspace Projection (LSOSP), Non-negativity Constrained Least Squares (NCLS) and Fully Constrained Least Squares (FCLS) were successively developed for this purpose. Recently, the LSMA techniques were further extended to the Kernel-based LSMA (K-LSMA) to resolve the linear non-separability issue occurred in multispectral and hyperspectral image classification. The K-LSMA algorithms have shown the strength on processing heavily-mixed data, however, there are some remained issues which restricts the practicality and implementation of K-LSMA. For instance, how to select an appropriate kernel function that generates more discriminant ability for classification, and how to select corresponding parameters are the long standing problems. Empirical and trial-and-error based testing are the most common solutions. This kind of issues have been investigate in machine learning society for classification problem. Recently, multiple kernel learning (MKL) is a new topic which has

been arouse considerable attention. The MKL assumes that the high dimension feature space is combined with several individual feature subspace such that it uses a combination of kernels instead of one in its algorithm. The MKL has brought good success in general classification problems, but its spirit has not been explored to the spectral-unmixing in remote sensing society. Inspired by such intention, this paper develops a promising technique, called Multiple Kernel-based LSMA (MK-LSMA), which can introduce a set of basis kernels into the unmixing framework instead of being restricted to adopt a single one. The MK-LSMA takes advantages of the concept of multiple kernel learning, where the different representations or features of data in high dimensional Hilbert space are able to be adopted for classification at the same time. More specifically, the MK-LSMA allows us to use different kernel types with a wide range of kernel parameters such that it g provide better generalization ability. Also, our proposed framework can also automatically find the optimized weightings for each basis kernel through an iterative procedure by minimizing the unmixing error, and the abundance fractions can be simply estimated by LSMA or K-LSMA without utilizing optimization algorithms such as quadratic programming (QP). The derivation shows that both LSMA and K-LSMA are the special cases of MK-LSMA. The experiments indicate that the MK-LSMA contributes to the selection of kernel parameters, and the unmixing results conducted on real multispectral and hyperspectral images demonstrate that the MK-LSMA indeed has potential to achieve better unmixing/classification performance than the K-LSMA.

8892-66, Session PS

### A method to correct the smile effect based on the combination correction of radiometric and spectrum

Chuncheng Zhou, Xinhong Wang, Lingling Ma, Academy of Opto-Electronics (China)

The hyperspectral imageries obtained from dispersive imaging spectroscopy systems often contain significant cross-track spectral curvature nonlinearity disturbances, known as the smile/frown effect, which is due to the change of dispersion angle with field position. The smile effect must be corrected because the across-track wavelength shift from center wavelength alters the pixel spectra and reduces the application effect of classification and target recognition. There are several methods to correct the smile effect such as moving linear fitting and interpolation (Goodenough et al., 2003), column mean adjusted in radiance space (Goodenough et al., 2003), column mean adjusted in MNF space (Goodenough et al., 2003) and trend line smile correction (Dadon et al., 2010). These methods don't take into account the fact that the smile effect is woven together with the sensor radiation characteristic, just processing spectra distortion to correct the smile effect would renewably lead to radiometric distortion of the radiometric correction image. The effective method to correct the smile effect must combine radiometric correction with spectrum correction. This paper analyzes the CCD radiation model with these conditions of the inconsistent radiation characteristic of CCD array and the dispersion angle changing with field position, then presents a method to correct the smile effect based on the combination correction of radiometric and spectrum. An experiment is conducted and the new method is compared with several traditional methods. The results show that the smile effect can be effectively removed by the proposed method, and meanwhile the radiometric correction result is finely reserved.

8892-67, Session PS

### Estimation of optical properties of aerosols and bidirectional reflectance from PARASOL/POLDER data over land

Takashi Kusaka, Kanazawa Institute of Technology (Japan)

When monitoring target areas covered with vegetation in a global scale, it is very useful to estimate the vegetation index using the surface anisotropic reflectance, which is dependent on both solar and viewing geometries, from satellite data. The PARASOL/POLDER observes the reflectance and polarization of a target quasi-simultaneously in multi-viewing angles at wavelengths of 490nm, 670nm and 865nm and so POLDER data provide enough

information to estimate optical properties of aerosols and the surface reflectance. In this study, the algorithm for estimating optical parameters of Atmospheric aerosols such as the optical thickness ( $\tau$ ), the refractive index ( $N_r$ ), index of Junge power-law ( $a$ ) and the bidirectional reflectance ( $R$ ) from only the radiance and polarization at the 865nm channel received by the PARASOL/POLDER is described. Ground-based polarization measurements of light ray reflected by the grassland were made, using the multi-spectral polarimeter, PSR1000, developed by Opt Research Corporation, Japan. As a result, it was found that degrees of polarization of the reflected light by the grassland are very low values at the 865nm channel. This indicates that the contribution of the surface reflectance to the polarized radiance received by the satellite is small. Aerosol properties such as  $\tau$ ,  $N_r$  and  $a$  in an atmosphere were estimated, by comparing only polarized radiances received by the POLDER with those computed by the radiative transfer code (6sV-1.0B code). Since aerosol properties in the atmosphere were determined, the bidirectional reflectance can be easily derived from the total radiance received the POLDER. In this study, the bidirectional reflectance given by the Ross-Li BRDF model was used. This BRDF model is defined as a sum of three terms, isotropic scattering term (fiso), volume-scattering term (fvolKvol( $\theta, \theta, \phi$ )) and geometric-optical term (fgeoKgeo( $\theta, \theta, \phi$ )), where Kvol is the RossThick kernel and Kgeo is the LiSparse kernel, and  $\theta$  is solar zenith angle,  $\theta$  is viewing zenith angle and  $\phi$  is relative azimuth angle. We first used the 6SV-1.0B code to compute total radiances at the top of atmosphere for typical values of Lambertian reflectance (fiso) under geometric conditions given in POLDER data and then determined inversely the value of fiso from the measured radiances by means of the least square method. In this case, values of fvol and fgeo were assumed to be zero. After that, the estimated value of fiso was fixed and values of fvol and fgeo were estimated from total radiances received by the POLDER.

The estimation algorithm developed in this study was applied to PARASOL/POLDER data over the Japanese islands taken on April 28, 2012. The estimated optical thickness of aerosols was checked with those given in the AERONET managed by NASA and fvol and fgeo of the estimated BRDF were compared with those of vegetation measured from the radio-controlled helicopter. Consequently, it is shown that this algorithm provides reasonable values for aerosol properties and surface bidirectional reflectances.

8892-69, Session PS

### Bartlett algorithm modification for energy spectrum assessment of optical radiation

Arseny Zhdanov, Oleg D. Moskaletz, St. Petersburg State Univ. of Aerospace Instrumentation (Russian Federation)

This research is conducted in order to develop a spectral device for instant remote sensing. The spectral device should process radiation from sources, direct contact with radiation of which is either impossible or undesirable. Such sources include jet blast of an aircraft. Moreover, this device should instantly process radiation from distant sources. This can be useful in metallurgy and textile industry. In proposed spectral device optical radiation is guided out of unfavorable environment via a piece of optical fiber with high negative dispersion. Dispersion properties of optical fiber allow using it as a key element of proposed spectral device.

In this paper stationary in time optical radiation energy spectrum assessment is proposed using a modified Bartlett algorithm. Original Bartlett algorithm is based on power sample spectrum calculation on the series of following samples with duty cycle  $Q = 1$ . Bartlett algorithm modification is a significant increase in duty cycle ( $Q \gg 1$ ) of stationary process samples. Proposed algorithm is to be realized basing on complex sample spectra calculation using a piece of optical fiber as a dispersive system. Dispersion properties application to acquire sample optical spectra causes that time function of a single sample spectrum has much longer duration than the original sample. This is the reason to modify the Bartlett algorithm.

Power spectrum assessment consists of the following optical radiation processing stages:

1. Forming samples of optical radiation with necessary duration.
2. Complex sample spectrum calculation basing on the dispersion properties of optical fiber.
3. Quadratic detection of acquired complex sample spectra.
4. Summation of delayed power sample spectra.



Significant increase of duty cycle  $Q$  means that separate samples of analyzed radiation are uncorrelated in time. This allows considering set of separate samples as an ensemble of  $N$  stochastic process realizations. Temporal stationarity condition allows acquiring a big number of sample spectra from a single realization. This allows acquiring power spectrum assessment with necessary properties.

In this paper we perform mathematical analysis of optical radiation processing using modified Bartlett algorithm. A complex sample spectrum is described as convolution of window spectrum function and complex spectral function of optical radiation. Power spectrum is considered as product of complex spectrum and its complex conjugate with certain phase shift due to temporal position of window functions. Spectral slot of modified Bartlett algorithm matches the spectral slot of original Bartlett algorithm. This confirms allowability of Bartlett algorithm modification.

8892-70, Session PS

### Region of interest coding for high spatial resolution remote sensing image using adaptive direction lifting integer wavelet

Libao Zhang, Bingchang Qiu, Xianchuan Yu, Beijing Normal Univ. (China)

For the high spatial resolution remote sensing images, efficient storage and transmission is in great demand. Region of interest coding (ROI) is one of the best solutions between the efficient compression performance and the high quality reconstruction for the high spatial resolution remote sensing image. It allows a region of interest of the remote sensing image can have a better quality than the rest at any decoding bit-rate. In this paper, a new region of interest coding based on adaptive direction lifting integer wavelet transform is proposed. First, a new adaptive direction lifting integer wavelet transform (ADIWT) is proposed to reconstruct effectively the non-horizontal and non-vertical high-frequency information of the ROIs in a high spatial resolution remote sensing image. Second, the most significant bitplanes of ROIs are shifted up above the maximum background (BG) bitplane, which ensures that the most important ROI coefficients are coded and transmitted at a higher priority than BG. Second, the most significant bitplanes of BG coefficients and general significant bitplanes of ROI coefficients are shifted up by bitplanes alternating scaling method, which enables the flexible adjustment of compression quality in ROI and BG. Finally, the SPECK coding algorithm is used to encode all bitplanes according to the scaling order. The experimental results on the high spatial resolution remote sensing images show the presented method supports ROI coding of both arbitrary shape and arbitrary scaling without shape coding. Additionally, it can reduce the high frequency wavelet coefficients more effectively, and improve the quality of the reconstructed ROIs of the remote sensing image.

8892-71, Session PS

### MIMO Radar Arrays with Minimum Redundancy: A Design Method

Andreas J. Kirschner, Uwe Siart, Johanna Guetlein, Juergen B. Detlefsen, Technische Univ. München (Germany)

Coherent MIMO radar systems with co-located antennas, form monostatic virtual arrays by discrete convolution of a bistatic setup of transmitters and receivers. Thereby, a trade-off between maximum array dimension, element spacing and hardware efforts exists. Minimum redundancy arrays aim at a hardware reduction with signal reconstruction by exploiting the Toeplitz characteristics of the signal covariance matrix. This paper presents a possible algorithm to find MIMO array setups of maximum dimension with minimum redundancy.

8892-72, Session PS

### The remote sensing image retrieval based on multi-feature

Jianbo Duan, Caihong Ma, Shibin Liu, Jing Zhang, Institute of Remote Sensing and Digital Earth (China)

With the rapid development of remote sensing technology and variety of earth observation satellites have been successfully launched, the volume of image datasets is growing exponentially in many application areas. The Content-based image retrieval (CBRSIR), as an efficient means for management and utilization of the information in image database from the viewpoint of comprehension of image content, is applied on the remote sensing images retrieval. However, one kind of features always can't express the image content exactly. So, a multi-feature retrieval model based on three color features and four texture features is proposed in this paper. The experiment results show that the multi-features model can improve the retrieval results than other model just by each singular feature.

8892-73, Session PS

### Visual appearance of wind turbine tower at long range measured using imaging system

Ove K. S. Gustafsson, Sebastian Möller, Swedish Defence Research Agency (Sweden)

Wind turbines affect the visual appearance of the landscape. In landscapes as for instance the woodland of Dalecarlia, just south of the midpoint of Sweden, the fear is that the visual intrusion will be too negative and impact the important tourist trade. The landscape analysis, developed by municipalities around Lake Siljan, limited expansion of wind power, due to the strong visual impression of wind turbine towers.

In order to facilitate the assessment of the visual impact of wind turbine a view, from Tällberg, over the ring of height on the other side of Lake Siljan, has been photographed every ten minutes for a year, with some interruptions (a total of 34,727 images, i.e. about 65% of the possible number during a year). Four wind power plants are possible to see in the photos, three of them have been used in the assessment of visual impression.

This contribution presents a method to assess visibility of wind turbine towers from photographs, measuring situation (location and equipment) as well as the analytical method and results of the analysis. Since no manual analysis of those many images was reasonable a method of tracking significant structures in the image were used together with contrast comparison between the objects (target) and the background. The comparison between image taken and a naked eye restricted the number of images analyzed to day time images. The response of the comparison has to settle the visual impact out of the visual appearance. This demand a limit of the exposure time, aperture size and detector sensitivity for sorting of image in to groups of no visible wind turbine tower or with visible wind turbine tower.

The contrast between the detector signal on the tower and detector signals from detector beside the tower, both adjusted by the ratio of camera settings gives the normalized contrast. A limit of this measured normalized contrast defined number of images that show when the tower is visible or not. The limit is set by comparing examples of images with different contrast ratios.

Using his method the wind turbine towers are possible to see in about 48% of analyzed images taken during daytime with the used camera equipment. During the summer months the towers were apparent in 49% of the images and the equivalent number for the winter months was 46%. In about 66% of the pictures, taken during the night, was at least one red warning light possible to see on the four wind turbine towers.

One conclusion of this work is that the method to assess the visibility of digital photographs and translate it into the equivalent of a normal eye can only provide an upper limit for visual appearance.

8892-74, Session PS

### Non-uniformity correction for multi-TDICCD mosaic camera on FPGA

Guofang Zhai, Yun Cheng, Beijing Institute of Space Mechanics and Electricity (China)

To solve a non-uniformity problem of multi Time Delay and Integration Charge Couple Device (TDICCD) mosaic camera, a non-uniformity correction algorithm is proposed and implemented on a Field-Programmable Gate Array (FPGA) platform. Firstly, the generation

and definition of non-uniformity are introduced; several regular non-uniformity correction methods are discussed. Secondly, the correction algorithm is designed. Finally, considering the fix-point processing ability of FPGA, the correction algorithm is optimized properly, and implemented on FPGA. Testing results indicate that the non-uniformity can be decreased obviously for 3-TDICCD mosaic camera's images with the proposed correction algorithm at 96 TDI stage, proving that this correction algorithm is with high real-time performance, good engineering realization and satisfaction of the requirements of the target system.

In wide-view-field and high-resolution electro-optical systems, single CCD can not satisfy the measure precision and view width, so multi-CCD must be assembled for satisfaction of demands. Time delay and integration CCD (TDICCD) is a new kind of optical imaging device which developed with the use of CCD. Compared with original CCD, TDICCD is more sensitive to light and has higher Signal-to-Noise Ratio (SNR). Therefore, multi-TDICCD mosaic cameras are employed in the field of remote sensing popularly in recent years. However, with the increasing demand for the development of high quality remote sensing image techniques, the problem of pixel response non-uniformity is becoming a key issue. In order to get optimal image, it's essential to do some research on pixel response non-uniformity for multi-TDICCD mosaic cameras.

Based on the analysis of TDICCD single channel response non-uniformity, a novel correction algorithm is introduced in this paper, which is two-point correction and compensating gain correction method for single channel and multi channel of single TDICCD, compensating offset correction method for multi TDICCD. Finally, the correction algorithm is implemented on the FPGA hardware platform.

## 8892-36, Session 8

### Extended image differencing for change detection in UAV video mosaics

Günter Saur, Wolfgang Krüger, Fraunhofer-Institut für Optronik, Systemtechnik und Bildauswertung (Germany)

Change detection is one of the most important tasks when applying unmanned aerial vehicles (UAV) for video reconnaissance and surveillance. Here we address changes of short time scale, i. e. the observations are taken in time distances from several minutes up to few hours. Each observation is a short video sequence corresponding to the near-nadir overflight of the UAV over the interesting area and the relevant changes are e. g. recently parked or moved vehicles.

To cope with local misalignment of image structures we extended in a precious work the change detection approaches by a local neighborhood search. The algorithms had been applied to several examples covering both urban and rural scenes. The local neighborhood search in combination with intensity and gradient magnitude differencing clearly improved the results. Extended image differencing performed better than both the correlation based approach and the multivariate alternation detection (MAD).

Our present work extends the change detection on single video frames to video mosaics. A precise image-to-image registration combined with a robust matching approach is needed to stitch the video frames together to a mosaic. Additionally this matching algorithm is applied to mosaic pairs in order to align them to a common geometry. The resulting registered video mosaic pairs are the input of the change detection procedure based on extended image differencing. A change mask is generated by an adaptive threshold applied to a linear combination of difference images of intensity and gradient magnitude.

The change detection algorithm has to distinguish between relevant and non-relevant changes. Examples for non-relevant changes are stereo disparity at 3D structures of the scene, changed length of shadows, and compression or transmission artifacts. The special effects of video mosaicking like geometric distortions and artifacts at moving objects, have to be considered too. In our experiments we analyze the influence of these effects on the change detection results by considering

1. video mosaic pairs of several scenes,
2. corresponding single video frames in comparison to the mosaics,
3. image examples with synthetic errors e. g. by misalignment or noise.

The results show that for video mosaics this task is more difficult than for single video frames. On the other hand video mosaics cover a larger scene space and the computed change mask is useful for

interactive image exploitation. In a further step, the algorithms will be adapted to be used in a semi-automatic work-flow for the ABUL video exploitation system of Fraunhofer IOSB.

## 8892-37, Session 8

### Detection of damage to building side-walls in the 2011 Tohoku, Japan earthquake using high-resolution TerraSAR-X images

Fumio Yamazaki, Chiba Univ. (Japan); Wen Liu, Wen Liu, Tokyo Institute of Technology (Japan); Takashi Nonaka, Tadashi Sasagawa, PASCO Co. (Japan)

Optical satellite images have been widely used to detect building damage due natural disasters in the world. However, since optical satellites images are mostly acquired from the vertical direction, they can observe only the roofs of buildings. Building damage such as to side-walls or mid-story collapse is often overlooked because the upper surfaces of buildings do not change too much in the vertical view. Hence in this study, the use of high-resolution SAR intensity images is considered with the aid of side looking nature of SAR.

In the 11 March 2011 Tohoku, Japan earthquake, a large number of buildings were collapsed or severely damaged due to repeated tsunamis. One of the important aspects of tsunami effects on buildings is that the damage is concentrated to their side-walls and lower stories, which is difficult to observe from vertical images. Therefore, this paper proposes the method to detect this kind of building damage from the change in layover and radar shadow in high-resolution SAR intensity images.

Multi-temporal TerraSAR-X images acquired by the StripMap mode with HH polarization covering the Sendai-Shiogama Port and the Fukushima Daiichi Nuclear Power Plant were employed to detect building damages due to tsunamis and hydrogen explosions after the 2011 Tohoku, Japan earthquake. For the TerraSAR-X images including the Sendai-Shiogama Port, the backscattering coefficients in the layover areas of individual buildings were extracted and then, the average value of the backscattering coefficient in each layover area was calculated for the pre-event and post-event SAR images. Comparing these values before and after the event, the average value was seen to reduce in the post-event image due to the reduced backscatter from building side-walls.

For the Fukushima Nuclear Power Plant, two TerraSAR-X images before and after the explosions were employed. We calculated the changes of the backscattering coefficients in layover and radar-shadow areas. Due to the explosions of two reactor buildings, their radar shadow areas were reduced and hence their backscattering coefficients were increased in the areas for the post-event SAR image. On the contrary, there was almost no change in radar-shadow for a non-exploded reactor building. The changes in layover areas were difficult to observe in the Fukushima Nuclear Power Plant due to steel frames, which appeared after the explosion and had strong backscatter. These examples demonstrated the usefulness of high-resolution SAR images to detect severe damage to building side-walls and lower parts from the changes of the backscattering coefficient in layover and radar-shadow areas.

## 8892-38, Session 8

### Connectivity constraint-based sequential pattern extraction from Satellite Image Time Series (SITS)

Andreea Maria Julea, Institute of Space Science (Romania); Nicolas Méger, Univ. de Savoie (France)

The temporal pixel values evolution in SITS is considered a criterion for the characterization, discrimination and identification of terrestrial objects and phenomena. Due to the exponential behavior of sequences number when specialization increases, Sequential Data Mining (SDM) techniques need to be applied. The huge search and solution spaces imply the use of constraints according to user's knowledge and expectation.

This work is focused on efficient SITS extraction of evolutions which fulfill frequency and connectivity constraints. The pixel level approach is unsupervised and follows the steps of Knowledge Discovery

from Databases process. As preprocessing step, the pixel values are re-quantized and the resulting values are symbolized, obtaining symbolic evolutions of pixels that constitute the Sequences Base, the input for the SDM process. The DM techniques for the SITS analysis were introduced by authors in 2006, by using anti-monotone support constraint. The extracted Frequent Sequential Patterns, FSP, surpassing a support threshold are relevant for the user.

The spatial aspect of the data was taken into account, in 2010, by introduction of the Average Connectivity constraint, that leads to the extraction of Grouped Frequent Sequential Patterns, GFSP, a concept with proved capability for preliminary description and localization of terrestrial events. The connectivity measures characterize the pixels tendency to form objects. They repose on Local Connectivity, LC, (number of liaisons of a given pixel with surrounding pixels in 8NN consideration). The previously used measure of Average Connectivity, AC, gives the mean number of liaisons that a pixel has with the pixels sharing the same evolution. The corresponding constraint leads by FSP filtering to the GFSP.

The improvements made in this work regard the use of anti-monotone measures as Global Connectivity, GC, and Minimum Support Related Connectivity, MSRC. The corresponding anti-monotone constraints can be pushed directly into the extraction, increasing the process efficiency due to the pruning property. A constraint based on LC measure, calculated with a variable dimension sliding window, is used to eliminate the isolated or weakly connected pixels. A comparative analysis of results obtained with different combinations of constraints is presented.

Connectivity measures, describing a supplementary feature for extracted patterns, improve their description quality. Passing from the distribution of support ranked to GC ranked patterns, for a good fitting, we must replace the power law with superposition of exponential or power expressions, which shows a stratified structure expressing a special self-organization aspect.

The AC measure intrinsically carries information about the nature of geometrical shapes. For a given shape, AC measure is practically invariant to translation and rotation but variable with scaling. The developed function AC(area) can offer a parameter depending on shape that is possible to apply in automatic shape recognition.

At the level of post processing techniques, the extracted patterns are temporally and spatially localized and a preliminary clustering based on alignment of similar or different length pattern is discussed. The effects of described improvements are analyzed on extracted GFSP from optical and radar SITS data.

## 8892-39, Session 8

### Fusion of satellite and aerial images for identification and modeling of nature types

Arnt B. Salberg, Norwegian Computing Ctr. (Norway); Lars Erikstad, Maciel Zortea, Norwegian Institute for Nature Research (Norway)

Nature systems are often very detailed spatially structured as a result of a multitude of environmental gradients and will in many cases form highly complex patterns in detail. The ability to identify nature types (habitats) is strongly related to the spatial level of the observation and the spatial character of environmental attributes related to them. Many nature type description systems are not designed to be easily mapped using remote sensing. Practical use of nature type description systems, however, requires methods that are cost effective, and in this respect remote sensing may play an important role.

In this paper we propose a framework for fusion of very high resolution optical aerial images, satellite images (optical or SAR) and other ancillary data (e.g. a digital elevation model) for identification and modeling of nature types typically present in mountain vegetation.

Aerial photos form the basis of our analysis. Due to the very high resolution provided by the aerial photos, the detailed mosaic of the vegetation may be mapped. In order to extract the vegetation mosaic we segment the aerial photos into polygons that are spectrally or structurally homogeneous. The segmented image typically consists of many thousands of polygons. However, the RGB-channels provided by the aerial photos are often not sufficient for identification and modeling of the nature types of interest due to the high spectral variation within many of the nature types, or the dependency on other non-visible features.

To enhance the identification and modeling of the segmented polygons, we exploit additional information provided by the satellite and ancillary data. In particular, the temporal dimension of the satellite data enables us to model the phenological signature of the vegetation, and to determine important nature features related to the spatial and temporal distribution of snow. Information contained in non-RGB spectral bands (e.g. NIR, red edge) provides more information about the spectral characteristics of the polygons, and SAR data provide information about soil moisture and may be used to identify polygons corresponding to marsh areas. All information about a given polygon is collected in a feature vector.

We demonstrated the data fusion methodology by analyzing data collected at a study site in the Norwegian mountain area Dovrefjell. The following data sources were acquired: Aerial photos, SPOT-5, AVNIR-2, Landsat-5 TM, Radarsat-2 quad-pol and a lidar-based digital elevation model. From in-situ observations, areas with known land cover and nature types were identified and used for training and validation. The results showed that the proposed data fusion methodology provided improved identification and modeling capabilities compared to using only aerial photos or single source satellite data.

The proposed methodology has a potential for improved analysis of nature systems, especially the temporal component is important for identification of many mountain-based nature types that are strongly dependent on both the length and stability of the snow cover. Sentinel-2 is expected to be particularly useful for such fine-scale snow cover mapping.

## 8892-40, Session 8

### A robust nonlinear scale space change detection approach for SAR images

Berk Sevilimis, Osman Erman Okman, Fatih Nar, Can Demirkesen, SDT A.S. (Turkey); Müjdat Çetin, Sabanci Univ. (Turkey)

Multitemporal remote sensing images have been actively utilized to infer dynamics of regions being monitored and change detection analysis has been a key concept of aiding several disciplines such as environmental monitoring and urban planning. In this paper, we propose a nonlinear scale space change detection approach in Synthetic Aperture Radar (SAR) images. Our method is based on Maximally Stable Extremal Region (MSER) analysis of scale space change images to locate regions of various changes incurred by natural phenomena and/or human activities. To this end, a slightly modified variant of the log-ratio image is obtained. This variant takes into account the multiplicative behavior of speckle noise and considers the possibility of having both appearance and disappearance of regions from one image to the other. Feature Preserving Despeckling (FPD) is applied to the resultant log-ratio image. The advantage of applying FPD is two-fold; first it helps further reduce speckle noise through minimizing a cost function having a data fidelity criterion as well as terms enhancing and preserving point-based and region-based features. Secondly, utilizing different parameter choices, and hence exploring different trade-offs between speckle reduction and detail preservation through FPD, leads to the construction of a nonlinear scale space. In order to properly detect and recover regions of change having different levels of contrast with respect to their surroundings, MSERs are found in each scale space image. Two different decision level fusion strategies of the extracted MSERs, namely fusion through voting and selective scale fusion, are introduced. The performance of the proposed method is evaluated on both real multitemporal high resolution TerraSAR-X images and on synthetically generated multitemporal images composed of shapes with several orientations, sizes and intensity levels representing a variety of possible changes. One of the main outcomes of this approach is that different objects having different sizes and levels of contrast with their surroundings appear as stable regions at different scale space images thus the fusion of results from scale space images appear to yield a good overall performance.

8892-41, Session 9

### Investigating vegetation spectral reflectance for detecting hydrocarbon pipeline leaks from multispectral data

Bashir Adamu, Kevin J. Tansey, Michael J. Bradshaw, Univ. of Leicester (United Kingdom)

Traditionally, monitoring and investigating hydrocarbon leakages in pipeline environments involves surveillance on foot, by flown aircraft etc. and field sampling for laboratory analysis, these are time consuming and expensive and can be very restricted in time and space. Previous studies have shown that vegetation spectral characteristics from hyperspectral image data for monitoring of hydrocarbon (HC) contaminated sites for remediation or clean-up has been promising. Hence, this study will build on the existing approaches using multispectral rather than hyperspectral image data (both medium and high resolution) to investigate hydrocarbon contaminated sites using vegetation health and solar reflectance data along pipeline routes in the Nigeria's oil producing (Niger Delta) region. The techniques which are not fully explored by researchers in a developing country like Nigeria will focus on comparing the vegetation spectral reflectance of contaminated and non-contaminated sites from multispectral data of different temporal period of the study sites. To aid the investigation of these HC contaminated sites and improve the outcome of the results, ancillary datasets (oil pipeline map, date of spill and GPS locations) will be integrated with the satellite image data for modelling possible leaked sites. A classification algorithm (artificial neural network) will be used to detect and map changes in the multispectral image data over a time series. Initial results of this study indicated changes in the spectral reflectance of vegetation between two different image acquisition dates (Landsat 1986 and SPOT 5 2006) and between contaminated and non-contaminated sites. Though the scale or magnitude of the change cannot be determined at this stage, thus visual and statistical interpretation and further analysis of the spectral characteristics from the multitemporal image data of contaminated and non-contaminated sites will be undertaken using vegetation health indices such as the normalized difference vegetation index (NDVI).

8892-42, Session 9

### The development of a remote sensing system with real-time automated horizon tracking for distance estimation at sea

Abdulquadir L. Baruwa, Adrian Evans, Univ. of Bath (United Kingdom); Roy Wyatt, Seiche Measurements Ltd. (United Kingdom)

Marine activities that produce significant amount of underwater noise, for example geophysical surveys, are often obliged to employ various forms of mitigation measures to safeguard marine mammals during the survey operation [1]. A standard form involves defining a mitigating zone, for example a radius of 500m around the source, and then taking actions whenever a marine mammal is identified within this zone e.g. delay or suspension of operation. During daylight hours Marine Mammal Observers (MMO) are employed to visually monitor the mitigation zone. When an MMO identifies a marine mammal on the sea surface, they must estimate its distance from the noise source, to determine whether it is in the mitigation zone. In addition to problems caused by poor visibility due to fog, sea mist and swells, estimating distance at sea with the naked eyes is very difficult and is often inaccurate.

Although often used, unsophisticated distance estimation methods, such as using sighting stick, are not very accurate or precise [2] and can result in unnecessary, and expensive, delays to geophysical surveys. To provide more accurate distance estimates, this paper details the image processing techniques developed for a new system to assist the MMO visual monitoring by providing accurate, real-time distance information. The system employs High Definition cameras overlooking the mitigation zone for visual monitoring, coupled with bespoke Real-time Automated Distance Estimation at Sea (RADES) software. Compared to previous methods, RADES provides a fully automated, real-time computer vision system. It has five main image processing stages:

1. Camera calibration using multiple poses of a planar object;

2. Single image dehazing of foggy sea images;
3. Horizon detection based on a trous wavelet transform and tracking using extended Kalman filter;
4. Pixel localisation and graphic overlay of line on image demarking the edge of the mitigation zone;
5. Video stabilisation using the position of the horizon eliminating the need of expensive gimbals.

RADES estimates distance to a point at sea by calculating the angle between the horizon and the waterline of that point from a known height. It uses the real-world angle between the horizon and the edge of the mitigation zone to find its pixel position in the image and then uses graphics to overlay a line demarking the edge of the mitigation zone on each frame, before displaying them in real-time to a screen.

The operation of RADES requires a robust horizon detection stage. This is achieved by first applying a wavelet-based edge detector [3] to the dark channel image. To localise the horizon position, a modified version of the method based on wavelet transform singularity analysis introduced in [4] is proposed. A shift invariant a trous wavelet transform is used to keep spatial features localized. A single image dehazing algorithm, tuned for sea images, is employed in the pre-processing stage to deal with fog and sea mists, which can mask the horizon and cause the algorithm to underestimate its position. Finally, the system facilitates remote visual monitoring through real-time relay of images to an onshore monitoring station via a satellite link. Results from sea trials showing the effectiveness of the system will be presented.

References

- [1] C. R. Weir and S. J. Dolman, "Comparative Review of the Regional Marine Mammal Mitigation Guidelines Implemented During Industrial Seismic Surveys, and Guidance Towards a Worldwide Standard," *Journal of International Wildlife Law Policy*, vol. 10, no. 1, pp. 1–27, Jan. 2007.
- [2] J. Gordon, "Measuring the range to animals at sea from boats using," *Journal of Applied Ecology*, vol. 38, no. 4, pp. 879–887, 2001.
- [3] J. W. Hsieh, M. T. Ko, H. Y. M. Liao, and K. C. Fan, "A new wavelet-based edge detector via constrained optimization," *Image and Vision Computing*, vol. 15, no. 7, pp. 511–527, 1997.
- [4] B. Qi, T. Wu, H. He, and T. Hu, "Real-Time Detection of Small Surface Objects Using Weather Effects," *Computer Vision—ACCV 2010, Lecture Notes in Computer Science Volume 6494*, pp. 27–38, 2011.

8892-43, Session 9

### On board processing procedures for the solar orbiter: METIS coronagraph

Maurizio Pancrazzi, Mauro Focardi, INAF - Osservatorio Astrofisico di Arcetri (Italy); Michela C. Uslenghi, INAF - IASF Milano (Italy); Gianalfredo Nicolini, INAF - Osservatorio Astronomico di Torino (Italy); Federico Landini, INAF - Osservatorio Astrofisico di Arcetri (Italy); Marco Romoli, Univ. degli Studi di Firenze (Italy); Ester Antonucci, Silvano Fineschi, INAF - Osservatorio Astronomico di Torino (Italy); Giampiero Naletto, Piergiorgio Nicolosi, Univ. degli Studi di Padova (Italy) and Consiglio Nazionale delle Ricerche (Italy); Daniele Spadaro, INAF - Osservatorio Astrofisico di Catania (Italy); Vincenzo Andretta, INAF - Osservatorio Astronomico di Capodimonte (Italy)

Solar Orbiter is an ESA space mission devoted to improve the knowledge of those effects nowadays still not fully understood on the physical mechanisms underlying the behaviour of our star, like the coronal heating process and the solar wind acceleration. The mission has a peculiar trajectory that will bring the S/C close to the Sun up to 0.28 AU, exploiting the opportunity to follow up our star as close as never before. METIS, one of the instruments selected to be part of the Solar Orbiter payload, is a coronagraph that will investigate the inner part of the heliosphere performing imaging in the visible band and in the hydrogen Lyman  $\gamma$  line @ 121.6 nm. METIS will be able to simultaneously operate the two detectors: an Intensified APS for the UV channel and an APS for the visible light, and a Liquid Crystal Variable Retarder (LCVR) plate, for broadband visible polarimetry. They will be operated by means of the centralised management unit of the

instrument, the MPPU, acronym of METIS Processing and Power Unit. This payload subsystem hosts a microprocessor that implements, thanks to the application software, all the needed functionalities to fully control the instrument subsystems and its own processing capabilities. Both sensors will be readout at high rate and the acquired data shall undergo through a preliminary on-board processing to maximize the scientific return and to provide the necessary information to validate the results on ground. Operations as images summing and cosmic rays monitoring will be fundamental not only to mitigate the effects of the main sources of noise on the acquired data, but also to maximize the data volume to transfer to the spacecraft in order to fully exploit the limited bandwidth telemetry downlink. Being Solar Orbiter a deep-space mission, some METIS procedures have been designed to provide to the instrument an efficient autonomous behaviour in case of an immediate reaction is required as for arising transient events or occurrence of safety hazards condition.

One of the most interesting targets of the mission is represented by the observation and evolution of solar flares and Coronal Mass Ejections (CMEs). These sudden events are connected with the release of enormous amount of energy and solar particles into the heliosphere and are, for their intrinsic nature, not easily predictable and therefore their observation cannot be scheduled in advance. METIS will implement an on-board algorithm for the automatic detection of this kind of events in order to promptly react and autonomously adapt the observing procedure.

## 8892-45, Session 9

### A spectral water index based on visual bands

Essa Basaeed, Harish Bhaskar, Mohammed Al-Mualla, Khalifa Univ. of Science, Technology and Research (United Arab Emirates)

Classifying water bodies in remote sensing images is useful in a number of applications including environmental monitoring, map updating, coastal planning, and maritime surveillance. The availability of well-registered multi-spectral remote sensing images is a challenge. In general, visual bands are highly available when compared to other bands. In addition, other sensor specific inadequacies make post-processing a difficult task, as in the occasional mis-registration of the NIR band in DubaiSat-1. The currently available water indices are efficient and effective but rely significantly on non-visual bands. Considering the aforementioned challenges, there is an increasing need for water classification strategies that exploits visual bands alone. Besides water indices, generic classification methods, both supervised and unsupervised, can be used for water classification. Supervised methods require per-image training and generalizing these methods to different images is not straight forward. Unsupervised methods, on the other hand, can separate an image into classes with no training required. However, the output of these methods requires further processing in order to determine which class represents water. Finally, other water classification methods exist but require computationally expensive pre-processes such as segmentation or transformation of input data.

In this paper, a novel water index is proposed that exploits spectral characteristics of water in visual bands. The proposed method is inspired from the analysis of the total attenuation response characteristics due to scattering and absorption of surface of water bodies. It models the interrelationship between spectral reflectance of water bodies across the spectrum of visual bands. In addition, the proposed method uses a non-linear normalization procedure that renders strong emphasize on small changes in lower digital numbers whilst guaranteeing that the segmentation process remains highly image-independent. The paper also suggests several improvements to generic supervised classification methods for a better classification of water.

For the purpose of evaluation, the proposed method is tested on Dubai Sat-1 images and compared with supervised classification methods such as maximum-likelihood, parallelepiped, and density slicing classification methods. Without loss of generality, the proposed method can be extended to imagery data from other satellites imposing similar spectral characteristics. In the first group of experiments, classification accuracy is evaluated on a single image from which the training set is selected. In the second set, classification accuracy is evaluated on a mosaic of segments retrieved from four images. In order to measure the generalization of methods, the training set in the second test is retrieved from images that are not part of

the test set. The results of both experiments are presented using a confusion matrix. The proposed method outperformed other methods in both experiments; it resulted in 96.8%, 85.5%, and 0.89 in the first and 83.2%, 92%, and 0.805 in the second for user's accuracy, producer's accuracy, and Kappa coefficient, respectively.

Analysis has indicated that the proposed method has the advantages that it is accurate and efficient, requires no global knowledge of the scene under investigation, can be implemented in parallel processing, and does not require training or pre-processing of input data.

## 8892-46, Session SJS1

### Robust tie points selection for InSAR image coregistration

Takieddine Skanderi, Boulerbah Chabira, Univ. des Sciences et de la Technologie Houari Boumediene (Algeria); Afifa Belkacem, Univ. des Sciences et de la Technologie (Algeria); Aichouche Belhadj Aissa, Univ. des Sciences et de la Technologie Houari Boumediene (Algeria)

Image coregistration is an important step in SAR interferometry which is a well-known technique for DEM generation and earth surface displacement monitoring. Due to the huge size of these images, a practical and widely used automatic coregistration algorithm is based on selecting a number of tie points in the master image and looking for the correspondence of each point in a search window in the slave image using template matching technique. The characteristics of these points, their number and their distribution have a great impact on the reliability of the estimated transformation. In our work, we propose a method for automatic selection of suitable tie points that are well distributed over the common area without decreasing the desired tie points' number. In contrast to many methods which are used in the most available software (e.g. sarscape, NEAST and RAT) where the points are selected in a grid form, in our method the points are selected based on their Harris cornerness measure which characterizes the shape of the autocorrelation function and the measure used in the template matching is the Normalized Cross Correlation, NCC, between the amplitude images. The auto-correlation is a good estimate for the cross-correlation and a good tie point is where the NCC has a distinctive peak. This is exactly what Harris operator detects. To insure a good distribution, we select the tie points from the points detected by Harris depending on their cornerness (the greatest first); after selecting a tie point, the cornerness of the remaining Harris points are multiplied by a spatially radially increasing function centered at the selected point in such a way that eliminates all the points in a neighborhood of a radius determined from the size of the common area and the desired number of points. This is repeated until the desired number of points is selected. For reliability purpose, after the template matching, any tie point which has NCC less than a given threshold or at the border of the search window is eliminated. This will decrease the number of the selected tie points and influence their distribution. The number of the eliminated points depends on the imaged area. If the area contains moving targets like ships, which are good candidates for template matching (they are detectable by Harris in general), or it has a low coherency between the two acquisitions, a great number of tie points will be eliminated. To avoid this problem and to make the algorithm more robust, we have combined the correspondence point detection (template matching step) with the tie point selection step. i.e. when a Harris point is taken as a candidate for a tie point, we search its correspondence, if it is found then we take it as a tie point, otherwise, this point is not selected and we proceed to the next candidate Harris point. In this manner the desired number is selected and the distribution is assured. Our method is tested on three ERS1/2 and two RADARSAT-2 interferometric pairs, on the whole images and on patches where some are taken around the harbor of Algiers where they contain a lot of ships.

## 8892-47, Session SJS1

### A new heterogeneity scale to improve anisotropic diffusion based speckle filters in SAR images

Rohit K. Chatterjee, Birla Institute of Technology (India); Avijit Kar, Jadavpur Univ. (India)

The noise like quality characteristic of SAR images, known as speckle become most critical impediment for automatic segmentation and classification of targets. For last thirty years many adaptive speckle filters were proposed, such as Lee, Kuan, Frost, GMAP etc. All these classical filters are single stage i.e. repeated use of them causes blurring of image features (e.g. edges or textures) and generates artefacts. But iterative use of filters are required for desired amount of smoothing. Failure of traditional filters to retain features upon iteration is due to failure to measure scene heterogeneity optimally.

Perona and Malik (P-M) proposed an Anisotropic Diffusion (AD) equation which iteratively diffuses gray values by preserving edges and other features. Black et al developed a robust statistical interpretation of AD. Depending on Black's work Chatterjee and Kar proposed a robust speckle filter named as ROSRAD and a heterogeneity scale based on Otsu's thresholding algorithm. This paper is an extension to the work, here we propose a different heterogeneity scale, and this is robust and performs better for speckle noise distribution.

Heterogeneity scale:

In classical filters CV in homogeneous region (C0) is used as a heterogeneity scale i.e., gray values below this scale must be smoothed. Obviously, it is not a trivial task to find a homogeneous region automatically. For automatic estimation of C0, Yu and Acton proposed a robust scale  $C0(t) = (\frac{1}{\sqrt{2}})MAD(\log I_{st})$ , where  $MAD(x) = \text{median}(|x - \text{median}(|x|)|)$  and  $\frac{1}{\sqrt{2}} = 1.4826$ . In spite of its robustness, MAD takes a symmetric view on dispersion, because one first estimates a central value (the median) and then attaches equal importance to positive and negative deviations from it, which does not seem to be a natural approach at asymmetric distributions. which does not seem to be a natural approach at asymmetric distributions like speckle. Experimentally we found that on iteration MAD converges towards zero, i.e. smoothes the image features. Chatterjee and Kar replace C0 by Otsu's threshold, though it is optimal, but not robust.

Our proposed robust scale (RHM) is given by

$$T = \text{med} \{ (L + H) \}$$

where  $\text{med}(x)$  is median of the sample  $x$ ,  $t$  is the iteration and  $L$  is the median of all gray values less than the threshold  $T$ ,  $H$  is the median of all gray values greater than the threshold  $T$ , i.e.

$$L = \text{med}(\{i | i < T\}) \text{ and } H = \text{med}(\{i | i > T\})$$

$i$  all image pixels up to gray level  $i$ . On iteration this robust scale converges to a non-zero value for an image with heterogeneous structures.

To compare performance of RHM with other AD filters we used two performance measures, namely Pratt's Figure of Merit and Structural similarity metric (SSIM). Experiment shows that RHM gives better results than other AD based speckle reducing filters.

## 8892-48, Session SJS1

### Label co-occurrence matrix for the detection of urban areas in high-resolution SAR Images

Na Li, National Univ. of Defense Technology (China) and Univ. degli Studi di Trento (Italy); Lorenzo Bruzzone, Univ. degli Studi di Trento (Italy); Zeng-Ping Chen, Fang Liu, National Univ. of Defense Technology (China)

The characterization of urban environments in SAR images is becoming increasingly challenging with the increased spatial ground resolutions. In this paper we address the problem of detecting and extracting built-up areas in SAR images characterized by a geometrical resolution in the order of few meters. Due to the coherent acquisition process and thus to the presence of speckle, single pixel value is not sufficient for characterizing the objects present in a scene. Texture features are considered, and the grey level co-occurrence matrix (GLCM) is a well-known and widely used one in remote sensing applications. However, the number of quantization levels severely affects both the reliability of the estimation of the joint statistic and the computation load. In the remote sensing literature there are only few qualitative guidelines on how tuning the tradeoff between the number of quantization levels used and the information loss.

In this paper, we propose a label co-occurrence matrix (LCM) to detect and extract built-up areas from high resolution SAR images. The major contributions of this work include: (1) the number of quantization levels in GLCM is replaced by the labels of backscattering classes

derived through a fuzzy clustering technique when calculate the co-occurrence matrix; (2) the functions of the joint labels possibilities distribution substitute the estimation of the second-order joint grey-levels conditional probability density functions.

In SAR images having a geometrical resolution of few meters (e.g. 3 m), urban scenes are roughly speaking characterized by three main types of backscattering: i) low intensity, which corresponds to shadows, roads, possible presence of water, etc.; ii) medium intensity, which corresponds to possible presence of vegetation, grassland, etc.; iii) high intensity, which is mainly due to roof, façade and corner reflectors associated with buildings or to human infrastructures. Inspired by the above-mentioned observations, the proposed LCM technique for the detection and the extraction of urban areas is based on three steps. Firstly, we apply clustering to the SAR image for partitioning it into three (or more, depending on the considered image and on its specific resolution) backscattering classes. This is done by means of the Spatial Fuzzy C-Means (SFCM) clustering algorithm. Then the two (or more) classes with lower grey values are merged together in order to emphasize the presence of strong backscattering contributions related to building and human infrastructures. Accordingly, each pixel can belong to built-up class or not with a certain membership value. Secondly, similarly to the traditional GLCM algorithm, we calculate the co-occurrence matrix by using the labels of the class of backscattering of each pixel and the membership values in a sliding window. Then we extract texture features from the matrix. Among various texture features, autocorrelation and entropy moment are selected, which proved empirically to well discriminate the built-up areas from other land-cover types. Finally, we apply similarity classifier defined in the general Lukasiewicz structure to identify and detect the built-up areas.

Experiments have been carried out on TerraSAR-X images acquired on Nanjing, China (2.75-m), and on Barcelona, Spain (3-m), respectively. The accuracy obtained by the use of the proposed LCM textural measures is compared with that obtained by the traditional GLCM. Qualitative and quantitative results point out the effectiveness of the proposed technique for texture extraction in identifying and detecting built-up areas.

In conclusion, LCM can effectively discriminate built-up areas from other land-cover types and is robust to the backscattering variation in the scenes thanks to the simple approach used for driving the computation of the co-occurrence matrix.

## 8892-49, Session SJS2

### A semi-automatic approach for estimating bedrock and surface layers from multichannel coherent radar depth sounder imagery

Jerome E. Mitchell, David J. Crandall, Geoffrey C. Fox, Indiana Univ. (United States); John D. Paden, Ctr. for Remote Sensing of Ice Sheets (United States)

We have developed an active contours method (called level sets) for estimating surface and bedrock layers in polar radar imagery using minimal human input, which an operator simply draws a quick, coarse ellipse around each boundary. For each layer, a 2D embedding functions,  $\phi$ , is initialized to an ellipse, so that its zero level set contains the contour of interest. Each ellipse has a center  $(u_1, v_1)$  and radii  $a$  and  $b$ .

$$(u - u_1)^2/a^2 + (v - v_1)^2/b^2 = 1$$

We define a function,  $f(u, v)$ , to be zero for all points  $(u, v)$  lying on the ellipse. Therefore,

$$f(u, v) = (u - u_1)^2/a^2 + (v - v_1)^2/b^2 - 1 = 0$$

and an initial embedding function

$$\phi_{t=0}(x, y) = f(u, v)$$

The level set evolves iteratively in a direction normal to a gradient and is determined by a partial differential equation (Hamilton-Jacobi) in order to minimize the cost function,

$$g(l) = 1/(1 + |G_{\phi} \cdot \nabla \phi|)^2,$$

where  $G_{\phi}$  represents a Gaussian kernel of standard deviation  $\sigma$  and  $l$  representing the segmented bedrock and surface image. This cost function is minimized as it is inversely proportional to the gradient and acts as an edge stopping function with the gradient being maximum at object edges.

The value of embedding the embedding function  $\varphi_{t+1}$  at any instant  $t+1$  is expressed as

$$\varphi_{t+1} = \varphi_t + l \frac{\partial \varphi}{\partial t},$$

where  $\varphi_t$  is the value at instant  $t$  and  $l$  is the gradient descent step size.

As the function  $\varphi$  evolves with time, the shape of its zero level set changes from an ellipse to the exact bedrock and surface topology. However, some numerical instabilities, such as sharp or flat shapes may occur, which may lead to computational inaccuracies and an improper result. A traditional way to avoid this problem focuses on using re-initialization to reshape  $\varphi$  periodically after a number of iterations. The reinitialization function used is:

$$\frac{\partial \varphi}{\partial t} = S(1 - |\varphi|),$$

where  $S(\cdot)$ , a sign function using initial value of  $\varphi$  may be expressed as  $S(\varphi) = \varphi / \sqrt{\varphi^2 + (\Delta x)^2}$

Evolution of  $\varphi$  automatically stops when its zero level set reaches the bedrock and surface layers because the cost function is minimized.

Although our method is depended on manually defining a simple ellipse for surface and bedrock layers, it saves a considerable amount of time from identifying complicated contours. Our approach will be applied to 827 ice thickness radar images and will be evaluated using the mean squared error with respect to hand-labeled ground-truth and a similar technique using a hidden markov model.

## 8892-75, Session SJS2

### A system for the automatic classification of Earth continental ice subsurface features in radar sounder data

Ana-Maria Ilisei, Lorenzo Bruzzone, Univ. degli Studi di Trento (Italy)

The continuous melting of the glaciers at the Earth polar caps motivates scientists to carry on exhaustive investigations on the ice subsurface structure and dynamics. These studies are performed by analyzing images of the ice cross-section (radargrams) acquired by radar sounder (RS) instruments operated at the Earth polar caps. In order to efficiently analyze the large amount of radargrams that RS can acquire, it is required to develop automatic techniques that could support the investigation of the ice subsurface on very large scales. However, the development of automatic techniques for the study of the Earth continental ice subsurface has not been sufficiently addressed in the literature.

In order to fill this gap, we propose a system for the automatic classification of the ice subsurface features visible in RS radargrams acquired at the Earth polar regions: layers of ice, the bedrock underlying the ice stratigraphy and noise regions located above and below the bedrock scattering area [1]. The proposed classification system aims to automatically classify samples of the radargram that belong to the aforementioned target classes. It is made up of 3 main components: 1) data preprocessing, 2) feature extraction and 3) automatic classification with machine learning methods. The preprocessing step aligns the columns of the original radargram with respect to a reference coordinate computed on the bases of the knowledge of the elevation of the platform with respect to the WGS-84 system and the two-way travel time between wave transmission and reception. The feature extraction represents the core of the proposed system. The objective at this stage is to extract from the aligned radargram discriminant features for classification purposes. Such features are identified after a detailed analysis of the statistical distribution of the radar signal (following the approach proposed in [2]) and of the spatial distribution and the relational properties of the ice subsurface features both in the azimuth and range directions. Consequently, the following features were identified as significant for the considered problem:

- the amplitude data, i.e., the values of the samples in the aligned radargram,
- the values of the parameters of the theoretical statistical distribution that best fits samples inside a rectangular sliding window over the amplitude data. Parameter values are estimated using the Maximum Likelihood estimation approach,
- the texture of the radargram in terms of entropy computed on a rectangular sliding window over the amplitude data that has been quantized on  $N$  levels,

- the range position of the subsurface features computed for each column of the radargram as the relative distance with respect to the surface,

- the statistical distance between the distribution of the samples of the target and of the noise computed with the Kullback-Leibler (KL) divergence measure [3] inside the sliding window over the amplitude data,

- relational features computed on the bases of a segmentation algorithm applied to a statistical map of the radargram generated on the bases of the KL divergence.

The automatic classification module takes as input the extracted features and performs classification by exploiting machine learning techniques based on Support Vector Machine (SVM) [4].

For space constraints, further details about the motivation of the choice of the SVM and its analytical description will be provided in the full paper

The proposed system has been validated on a dataset made up of 8 radargrams acquired in sequence over a distance of 400km by the airborne-mounted MultiCoherent Radar Depth Sounder (MCoRDS) [5] in Antarctica. Several experiments have been performed by varying the samples used by the SVM in the training, validation and test phases. The average accuracy computed on the test samples on 10 such experiments is equal to 98.85%. This result along with qualitative analyses of the corresponding classification maps (which will be provided in the full paper) confirm the effectiveness of the proposed automatic classification system.

References:

- [1] R. Drews, "Layer disturbances and the radio-echo free zone in ice sheets," *The Cryosphere*, vol. 3, no. 2, pp. 195–203, 2009.
- [2] A. Ferro and L. Bruzzone, "Analysis of radar sounder signals for the automatic detection and characterization of subsurface features," *IEEE Transactions on Geoscience and Remote Sensing*, vol. 50, no. 11, pp. 4333–4348, November 2012.
- [3] J. Lin, "Divergence measures based on the Shannon entropy," *IEEE Transactions on Information Theory*, vol. 37, no. 1, pp. 145–151, January 1991.
- [4] L. Bruzzone and C. Persello, *Approaches based on Support Vector Machines to Classification of Remote Sensing Data*, vol. 4, chapter 3.2, pp. 329–352, C.H. Chen, World Scientific, 2009.
- [5] L. Shi, "Multichannel Coherent Radar Depth Sounder for NASA Operation Ice Bridge," in *IEEE International Geoscience and Remote Sensing Symposium (IGARSS)*, July 2010, pp. 1729–1732.

Monday - Wednesday 23–25 September 2013

Part of Proceedings of SPIE Vol. 8893 Earth Resources and Environmental Remote Sensing/GIS Applications IV

8893-1, Session 1

## Quantification of anthropogenic and natural changes in oil sands mining infrastructure land based on RapidEye and SPOT5

Ying Zhang, Canada Ctr. for Remote Sensing (Canada)

The infrastructure development of natural resources mining alters local land surface in various spatial scales related the human activities such as exploration, production and transportation. Quantification of these anthropogenic and reversed changes on the land surface related to natural resources development activities is a key information collection component for better understanding sustainability implications of the changes and hence for development of effective sustainable management strategies. Multi-spectral high resolution imagery data from SPOT5 and RapidEye were used for extraction and quantification of the anthropogenic and natural changes for a case study of Alberta bitumen (oil sands) mining located in the Western Boreal Plains near Fort McMurray, Canada, where two test sites representative of the major Alberta bitumen production extraction processes, open pit and in-situ extraction, were selected. A hybrid approach combined pixel- and object-based target detection and extraction, including a Change Vector Analysis method, has been developed for the anthropogenic change information extraction. The temporal growths of anthropogenic changes on both test sites have been extracted for qualification and comparison. The extraction results indicate that the changed infrastructure landscapes of these two sites have different footprints linked with the oil sands production processes. Pixel- and object-based accuracy assessments have been also applied for validation of the change detection results. For the manmade disturbances except for those fine linear features such as the seismic lines, the accuracies at pixel level are about 80% for the anthropogenic disturbances and over 90% at object level, with overall accuracies about 95%.

Furthermore using the extracted information about oil sands disturbance footprints, a new landscape index, Re-growth Index, has been formulated at single object level and used for measuring the natural changes (re-growth of vegetation) in earlier disturbed lands in both test sites. It is found that the temporal behaviour of the Re-growth Index in an individual patch varies on the type of surrounding land covers. For both sites, the majority of the patches disturbed have been greener (re-growth). In addition, the Re-growth Index that measures the land capability for vegetation recovery in the disturbed (clean-cut) patches is also useful for understanding the accuracy of extracting the anthropogenic changes in the in-situ test site.

8893-2, Session 1

## Derivation of urban objects and their attributes for large-scale urban areas based on very high resolution UltraCam true orthophotos and nDSM: a case study Berlin, Germany

Anna Maria Poznanska, Deutsches Zentrum für Luft- und Raumfahrt e.V. (Germany); Steven Bayer, Freie Univ. Berlin (Germany); Tilman U. Bucher, Deutsches Zentrum für Luft- und Raumfahrt e.V. (Germany)

The availability of very high resolution airborne data with high geometric accuracy enables the derivation of detailed object features and their attributes, even in the regions of heterogenic cities with diverse building- and vegetation structures. Against the background of unavoidable expansion of many cities to agglomerations with high building density and the need for urban objects inventory, there is a high need for efficient extraction methods. The derivation of urban characteristics like building and vegetation structures plays a major role for many urban planning aspects, whereby one of the particular difficulties is the large data amount of large- or megacities.

For that reason not only development and optimization of automatic extraction methods for diverse urban objects but on the other hand a concept for large data handling covering the whole city are tasks to

be accomplished within the framework of the project 'Derivation of Building- and Vegetation Heights and Structures in Berlin'. This project is executed in cooperation with the Senate Department for Urban Development and Environment of the City of Berlin and consists of two phases: (1) object derivation in the inner city, input data 30 cm resolution and (2) object extraction in the hinterland, input data 50 cm resolution. The derived data are used as basis for the generation of a complex city climate model, which also takes the morphology of hinterlands into account. In this paper only the first phase is presented.

As input a photogrammetrically derived dataset of the digital airborne matrix camera UltraCamX is available. The true ortho mosaic consists of four spectral channels (R-G-B and IR). For the derivation of absolute object heights a normalized digital surface model (nDSM) was generated and for the delineation of roof tiles additional layers consisting of slope and aspect are created. The size of the whole area adds up to about 450 km<sup>2</sup> (phase 1) and up to 2,400 km<sup>2</sup> (phase 2). Phase 1 covers the Berlin city center and the inner suburb regions with diversified morphology. Within the scope of the project methods for accurate and robust extraction of buildings with roof tiles as well as vegetation with different structures were tested. To ensure that the resulting building layer is complete and includes no false objects also greened roofs, which are primarily classified as high vegetation, are automatically extracted and assigned to the class buildings. Elevated bridges and railway tracks are removed from the class buildings using intersection with the official cadastral data. To make the rule set transferable to the dataset of phase 2 as well as to the other datasets a multi-layered workflow consisting of automated data import and export, iterating segmentation methods (Multiresolution, Quad Tree, Contrast Split and Multi-threshold Segmentation), fuzzy classification and object reshaping methods was developed and applied to the whole data set. At the end the exported objects are intersected with the official cadastral building data to complement building tiles which are located under the trees. In this way complete building and elevated vegetation shapes with height attributes are derived. They are exported and integrated in a GIS and serve as input for climatic modeling. The accuracy assessment of the classification results has yet to be carried out, it is estimated to be very high (> 85 %).

In addition to urban-specific climate models, this detailed building and vegetation data can be used as a basis for modeling of noise pollution, the estimation of urban structure types or for town- or green space planning.

8893-3, Session 1

## Object-based change detection in rapid urbanization regions with remotely-sensed observations: a case study of Shenzhen, China

Lihuang He, Guihua Dong, China National Environmental Monitoring Ctr. (China); Wei-Min Wang, Lijun Yang, Hong Liang, Shenzhen Environmental Monitoring Ctr. (China)

China, the most populous country on Earth, has experienced rapid urbanization which is one of the main causes of many environmental and ecological problems. Therefore, the monitoring of rapid urbanization regions and the environment is of critical importance for their sustainable development. In this study, the object-based classification is employed to detect the change of land cover in Shenzhen, which is located in South China and has been urbanized rapidly in recent three decades. First, four Landsat TM images, which were acquired on Oct. 19, 1979, Dec. 10, 1988, Mar. 3, 2000 and Jan. 10, 2010, respectively, are masked based on Cloud and Shadow Assessment (CASA) algorithm. Atmospheric corrections are conducted on these images with improved dark-object subtraction technique and surface meteorological observations. Geometric correction is processed with ground control points derived from topographic maps. Second, a region growing multi-resolution segmentation and a soft nearest neighbor classifier are used to finish object-based classification.

After analyzing the fraction of difference classes over time series, we conclude that the comparison of derived land cover classes with



socioeconomic statistics demonstrates the strong positive correlation between built-up classes and urban population as well as gross GDP and GDPs in second and tertiary industries. Two different mechanisms of urbanization, namely new land development and redevelopment, are revealed. Consequently, we found that, the districts of Shenzhen were urbanized through different mechanisms.

#### 8893-4, Session 1

### Monitoring the effects of landuse/landcover changes on urban heat island

Ken Gee Ong, Universiti Teknologi Malaysia (Malaysia); Md Latifur Rahman Sarker, Univ. Teknologi Malaysia (Malaysia)

Urban heat island effects is very well known nowadays and is observed in cities throughout the World. The main reason behind the effects of urban heat island (UHI) is the transformation of landuse/landcover, and this transformation is associated with UHI through different actions: i) removal of vegetated areas, ii) land reclamation from sea/river, iii) construction of new building as well as other concrete structures, and iv) industrial and domestic activity. In a rapidly developing city, urban heat island effect increases very hastily with the transformation of vegetated/other areas into urban surface due to the increase of the population and economic activities.

In this research the effect of landuse/landcover change on urban heat island was investigated in two growing cities in South East Asia i.e. Singapore and Johor Bahru (Malaysia), using 10 years data (from 2002 to 2011) from Landsat TM/ETM+. Multispectral visible band along with indices, such as Normalized Difference Vegetation Index (NDVI), Normalized Difference Build Index (NDBI), and Normalized Difference Bareness Index (NDBal) were used for the classification of the major landuse/landcover types using Maximum Likelihood Classifier. On the other hand, land surface temperature (LST) was estimated from thermal image using Land Surface Temperature algorithm. Emissivity correction was applied to the LST map using the emissivity values from major landuse/landcover types, and validation of the UHI map was carried out using in situ data. Results of this research indicate that there is a strong relationship between landuse/landcover changes and UHI. Over this 10 years period, significant percentage of non-urban surface was decreased and at the same time urban heat surface increased because of the rapid urbanization. With this increase of UHI effect, it is expected that local urban climate has been modified and some heat related health problem has been exposed, so the appropriate measures should be taken in order to reduce UHI effect as soon as possible.

#### 8893-5, Session 2

### Generalized interpretation scheme for arbitrary HR InSAR image pairs

Markus Boldt, Antje Thiele, Karsten Schulz, Fraunhofer-Institut für Optronik, Systemtechnik und Bildauswertung (Germany)

Land cover classification of remote sensing imagery is an important topic of research. For example, different applications require precise and fast information about the land cover of the imaged scenery (e.g., disaster management and change detection).

Focusing on high resolution (HR) spaceborne remote sensing imagery, the user has the choice between passive and active sensor systems. Passive systems, for example multispectral sensors, have the disadvantage of being dependent from weather influences (fog, dust, clouds, etc.) and time of day, since they work in the visible part of the electromagnetic spectrum. Here, active systems like Synthetic Aperture Radar (SAR) provide support.

As an interactive method analyzing HR InSAR image pairs, the CovAmCoh method was introduced in former studies. CovAmCoh represents the jointly analysis of locality (coefficient of variation – Cov), backscatter (amplitude – Am) and temporal stability (coherence – Coh). It delivers information on physical backscatter characteristics of imaged scene objects or structures and provides the opportunity to detect easily different classes of land cover (e.g., urban, rural, infrastructure and activity areas). As example, railway tracks are easily distinguishable from other infrastructure due to their characteristic bluish coloring based on the gravel between the sleepers. In consequence, it can be stated that imaged objects or structures have

a characteristic appearance in CovAmCoh images which allows the development of classification rules.

In this paper, a generalized interpretation scheme for arbitrary InSAR image pairs using the CovAmCoh method is proposed. This scheme bases on analyzing the information content of typical CovAmCoh imagery using the semi-supervised k-means clustering. It is shown, that eight classes model the local information content of CovAmCoh images sufficiently. Furthermore, examples of classification rules are proposed.

#### 8893-6, Session 2

### Using high resolution lidar data for automated railroad infrastructure mapping

Reinhard Beger, Marco Neubert, Leibniz-Institut für ökologische Raumentwicklung (Germany); Marco Trommler, Technische Univ. Dresden (Germany); Hendrik Herold, Leibniz-Institut für ökologische Raumentwicklung (Germany)

The quality of remotely sensed data in regard to accuracy and resolution has considerably improved in recent years. Very small objects are detectable by means of imaging and laser scanning, yet there are only few studies to use such data for large scale mapping, e.g. corridor mapping of railroad infrastructure. This spatial information is of great importance for railway companies, such as Austrian Railways in this case study, for internal planning as well as for complying with international standards, e.g. regarding railroad safety.

In this study, an approach is presented that integrates both dense LiDAR point clouds and extremely high resolution ortho-imagery acquired by helicopter-borne sensors. These data sets are used to reconstruct railroad objects. A feature level data fusion is carried out in order to combine the advantages of both data sets and to achieve a maximum of accuracy and completeness for the extraction of railroad track centre lines. The workflow consists of three processing steps. First, object-based image analysis is used to derive a railroad track mask from ortho-imagery. This spatial location information is then combined with the height information in order to classify the laser points. Lastly, an adapted random sample consensus algorithm (RANSAC) is used to approximate the location of railroad track centre lines from the classified points. Based on the reconstructed track centre line, further railroad infrastructure objects such as masts, mounted catenary wires, railway signals, platform edges, and noise protection barriers are subsequently extracted from the LiDAR data using a knowledge-based point classification strategy. The methodology was found to deliver very accurate results (recall rates above 90% and a spatial accuracy of  $\pm 10$  cm) in a highly automated manner.

In order to achieve operational usability for large scale railroad mapping, the workflow is currently transferred to completely run within a spatial database (Oracle Spatial). Future work includes the adaptation of the algorithms to data from mobile sensor platforms, i.e. rail-borne laser scanners. The presented study demonstrates that it is possible to automatically extract even small-scale objects from 3D point clouds to gather precise spatial information.

#### 8893-7, Session 2

### Simulation of close range remote sensing of subsurface features using GPR for urban utility information system development

Almelu Mangamma V. Hebsur, Muniappan Nagarajan, Emmella P. Rao, Gopalakrishnan Venkatachalam, Indian Institute of Technology Bombay (India)

In rapidly urbanizing old cities underground utility maps or urban utility information systems seldom exist. Close range remote sensing using Ground penetrating radar (GPR) for detection of the utilities is quite common. GPR can also help in supplementing or updating the system, if present. GPRs are non-invasive subsurface mapping tools which give information about buried pipes, utilities, channels, subsurface geological and geotechnical features and buried building remains. GPRs transmit radar pulses into ground and gather the back scattered energy from dielectric discontinuities in the subsurface. GPRs are available over a range of center frequencies from 10MHz

to 4GHz. Frequency decides their capacity to penetrate, detect and resolve the buried objects or subsurface stratification and hence their appropriateness for a given application. For example, medium frequencies in the range of 200 to 600 MHz are recommended for shallow sub surface mapping and utility detection. The resulting response is presented in the form of a 2D section called radargram, which depicts the variation of amplitude of reflected signals with (traverse) distance and time of travel of pulse (or depth).

However, interpretation of GPR radargrams is a task demanding skill and knowledge of its principles and capabilities and also about the nature of response of subsurface features to GPR signals. Response of subsurface features depends on factors like, (a) antenna parameters such as center frequency, foot print and polarization, (b) host medium parameters like relative permittivity, conductivity and (c) object parameters like shape and size and relative permittivity.

It is an impractical task to generate the information about the responses directly in the field. Hence a numerical simulation of radar wave propagation is carried out using Finite difference time domain (FDTD) technique. The present work deals with the database generation of GPR responses through simulation using an exclusive software GprMaxV2.0. A buried utility pipe produces a hyperbolic pattern in the radargram. In general, utilities may be made of metal, concrete or PVC; many utilities lie within a shallow depth of about 1.0m and their diameters may vary over 0.2m to 1.0m; the relative permittivity of a dry soil could vary from about 4 to 12. Taking these aspects into consideration, the problem of a pipe buried in soil is formulated as shown in Fig. 1 (a) and radargrams are simulated (Fig. 1b). Variation of amplitudes and axes of hyperbolic patterns are studied. But, one important constraint is that, exhaustive simulation studies could be time-intensive. Therefore, Response surface method (RSM) is used to model amplitudes and hyperbolic patterns and express as functions of their influencing parameters. A complete set of GPR responses under a variety of conditions is thus produced. ANOVA indicates that, within the range of depth and diameters considered, object relative permittivity and medium relative permittivity significantly influence amplitudes and hyperbolic axes respectively. Studies demonstrate that through simulation and RSM, a broad insight can be gained into GPR responses and the effect of influencing parameters. A database covering a wider range generated through simulation can serve as a component of or complement to an urban utility information system.

### 8893-9, Session 3

#### GIS4schools: custom-made GIS-applications for educational use

Timo Demharter, Ulrich Michel, Pädagogische Hochschule Heidelberg (Germany)

The project "GIS4schools" is located at the University of Education in Heidelberg, Germany. The idea behind "GIS4schools" is to develop intuitive and well-designed web-applications for schools in the German federal state of Baden-Württemberg and beyond.

The use of curriculum relevant topics and the scientific exchange with the GIS-Station, an institution for training students, trainees and teachers, sets this project apart from any other. The GIS-Station supports the project with didactical concepts and with their experience as a competence and excellence center for geomedial education.

With the help of Team Education Germany of ESRI and the Baden-Württemberg Ministry for Science, Research and the Arts, the aspired goal is to make those applications platform-independent and usable at any time.

Aside from ESRI Technology (ArcGIS Server, ArcGIS Online for Organizations, ArcGIS Viewer for Flex) different development platforms like Java and Flex are used to create and modify several user interfaces. Each of these interfaces is tailor-made for the respective topics and tasks.

The first sample applications have already been developed. One deals with the exploration of a city district and its citizens, the other is about open-cast mining and infrastructural challenges. To solve these challenges, students have the possibility to use LANDSAT images of various dates and different channel combinations.

The first Java-based App addresses the subjects of large scale enterprises and working conditions. The goal of this application is to communicate the idea of global production chains, especially where

the students would have least expected them.

Along with teaching materials and a support forum, the applications will be published on an easy-to-navigate and self-explanatory website.

Several schools, primary and secondary, support the development of these applications by testing them in class. After the first stage of the project, teachers and students evaluate the applications and the corresponding teaching materials. Based on their feedback an adjustment of the apps and the teaching materials takes place.

### 8893-10, Session 4

#### Value-added humanitarian information delivery from Earth observation data: investigating synergies of data fusion and image segmentation in rapid mapping workflows

Chandi Witharana, Univ. of Connecticut (United States); Marco Neubert, Leibniz-Institut für ökologische Raumentwicklung (Germany); Daniel L. Civco, Univ. of Connecticut (United States)

In humanitarian emergencies the timeliness of data provision and the short time window available for dispatching value-added information pose major challenges to the mapping community. We have been engaged with a continuous research effort to explore novel ways to intensify EO-based humanitarian crisis information retrieval chain. This exploratory study aimed to unravel the synergies of data fusion and image segmentation in the context of EO-based rapid mapping workflows. Our approach pillared on the geographic object-based image analysis (GEOBIA) focusing on multiscale internally displaced persons' (IDP) camp information extraction from very high spatial resolution (VHSR) images. We applied twelve pansharpening algorithms to the two subsets of a GeoEye-1 image scene that has been taken over a former war-induced ephemeral settlement in Sri Lanka. A multidimensional assessment was employed to benchmark pansharpening algorithms with respect to their spectral and spatial fidelity. The multiresolution segmentation (MRS) algorithm of the eCognition developer software packages served as the key algorithm in the segmentation process. The first study site was used for comparing segmentation results produced from the twelve fused products at a series of scale, shape, and compactness settings of the MRS algorithm. The segmentation quality and optimum parameter setting of the MRS algorithm were estimated by using empirical discrepancy measures. Non-parametric statistical tests were used to compare the quality of image object candidates, which were derived from the twelve pansharpened products. A wall-to-wall classification was performed based on a support vector machine classifier to classify image objects candidates of the fused images. The second site simulated a more realistic crisis information extraction scenario where the domain expertise is highlighted in segmentation and classification. We compared segmentation and classification result of the original images (non-fused) and twelve fused images to understand the efficacy of data fusion. In light of GEOBIA framework, findings our exploratory study have challenged the well established view of data fusion community that is any error in the synthesis of the spectral signatures at the highest spatial resolution incurs an error in the decision. We have shown that the GEOBIA has the ability to create meaningful image objects during the segmentation process by compensating the fused image's spectral distortions with the high-frequency information content that has been injected during fusion. Our findings further questioned the necessity of the data fusion step in rapid mapping context. Bypassing time-intensive data fusion steps helps to intensify EO-based rapid mapping workflows. We; however, emphasize the fact that data fusion is not limited to VHSR image data but expands over many different combinations of multi-date, multi-sensor EO-data., thus, further research is needed to understand the synergies of data fusion and image segmentation with respect to multi-date, multi-sensor fusion scenarios and extrapolate our findings to other remote sensing application domains beyond EO-based crisis information retrieval.

8893-11, Session 4

## Radiometric processing of aerial thermography in the framework of the EnergyCity project: the case of Bologna (Italy)

Gabriele Bitelli, Paolo Conte, Francesca Franci, Emanuele Mandanici, Univ. degli Studi di Bologna (Italy)

The EnergyCity project is founded by the Central Europe programme and it aims to contribute to a better building energy management by providing data and models to depict the current practices and the status quo and to build an online Spatial Decision Support System (SDSS) to visualize and compare the cost-effectiveness and potential of different renewable energy solutions. Seven European cities are involved in the project, Budapest, Prague, Munich, Bologna, Treviso, Ludwigsburg and Velenje, and for each one a high resolution ortho-mosaic of thermal infrared images acquired by an aircraft platform has been produced and analysed.

The present paper provides a brief overview of the EnergyCity project, but it delves into some specific aspects of the data processing chain, through the case study of the city of Bologna. In particular the derivation of the surface temperature of the building roofs is discussed, as it is one of the main inputs of the SDSS. In fact this computation is a very critical task, because it involves an in-depth modelling of the effects of the atmospheric layer between the surfaces and the sensor, of the radiative behaviour of the different materials which constitute the observed surfaces and of the geometry of the acquisition. However, the lack of essential ancillary data over very large areas necessarily requires a simplified approach.

In the proposed processing, the computing of the radiometric quantities of the atmosphere (transmissivity, upwelling radiance, downwelling radiance) has been performed by the Modtran 5 radiative transfer code, using atmospheric profiles extracted from MODIS satellite data and from a radio sounding profile, together with meteorological ground data. To distinguish among the major roofing material types, an object-oriented supervised classification has been applied on a WorldView2 multispectral image, which provides 8 spectral bands at the resolution of 2 m. This step is required to model the effects of the emissivity of each material.

Some operation in the field was established in order to collect ground truth data. The surface temperature of the paving was measured at several selected locations at the same time as the aircraft acquired the thermal images. Furthermore the emissivity of some roofing materials was estimated by means of a thermal camera and a contact probe. All the surveys were georeferenced by GPS.

The validation of the surface temperature values derived from the processing of the aerial thermal images is still on-going, but the first results demonstrate the high sensitivity of the model to the variability of the surface emissivity and of the atmospheric parameters, especially transmissivity and upwelling radiance.

8893-12, Session 4

## Remote sensing of vegetation in a tropical mountain ecosystem

Brenner S. G. Silva, Jörg Bendix, Philipps-Univ. Marburg (Germany)

The hotspot of biodiversity in the tropical Andes of Southern Ecuador has been severely threatened by climate change and unsustainable land use. Due to a harsh tropical mountain environment, scientific investigations are hitherto restricted on those areas, which also hindered the application of earth monitoring systems with global coverage (e.g. MODIS, Landsat, Quickbird). In the Rio San Francisco basin, South Ecuador, a long-term research project has provided essential data and knowledge for investigations in biodiversity and ecosystem services of a tropical mountain. The present work aims to extend this knowledge using remote sensing techniques with applications in conservation of biodiversity, sustainable agriculture and forestry. In this approach we make use of a land model - the Southern Bracken Competition Model - to estimate primary productivity and evapotranspiration, which are important metrics in the context of forestry, agriculture, and climate regulation. The parameterization of the land model was first completely tested using field data (e.g.

spectroscopy, leaf area index, and porometry) of average individuals of bracken fern and of a pasture grass species, two representative plant functional types in the study area. Similarly, two woody-species were parameterized and initialized in a single point mode to calculate reference values of two representative functional types to the pristine forest and reforestation areas. To obtain area-wide estimates of the two variables of concern (primary productivity and evapotranspiration), high-resolution remote sensing data were first analysed in two steps and then used to initialize the model. First, the variability of calibrated high-resolution and broadband optical data (Quickbird) was calculated using an object-oriented approach, which considered tree-crowns and transects on land use and topography gradients. Second, vegetation metrics (e.g. cover and height) and narrow-band vegetation indices (e.g. PRI), respectively from recent airborne LiDAR and hyperspectral scanning surveys, were calculated for the same areas. A comparative analysis of the different data sources is done with the aim of calibration of the operational satellite (Quickbird). The normalized vegetation index and structural metrics were used to initialize the model based on correlation functions from the literature. Together with meteorological data estimates of potential primary productivity and evapotranspiration were calculated for the functional types of reference and for additional non-woody and woody species identified in the remote sensing data and by ground observations. This novel and descriptive investigation should serve as basis for the application of earth observation systems in tropical mountain ecosystems, for instance to monitor land response to climate and land use change in the future.

8893-13, Session 4

## Identification of urban tree crown in a tropical environment using WorldView-2 data: problems and perspectives

Marilia Gomes, Philippe Maillard, UFMG (Brazil)

With the availability of high-resolution satellite data, much research has been focused on the automatic detection and classification of individual tree crowns. Most of these studies were applied to temperate climates of the northern hemisphere, especially for forests of coniferous. Very few studies have been applied to the detection of trees in the tropical regions, least of all in the urban environment. Urban trees play a major role in maintaining or even improving the quality of life in cities by their contribution to the quality of the air, by absorbing rain water, by refreshing the air through transpiration and providing shadow. Furthermore, monitoring urban trees can serve as a gauge to urban environmental quality. In this study we explored the potential of high-resolution satellite data of the WorldView-2 for identification of urban individual tree crowns in the city of Belo Horizonte, Minas Gerais, Brazil, through an object-oriented approach. Irrelevant areas were masked (e.g. buildings, asphalt, shadows, exposed soil) using a threshold of NDVI. Three different approaches were tested to isolate and delineate individual tree crowns: region growing, watershed and template matching. The region growing algorithm segments the image using a seed pixel thereafter neighbouring pixels are examined and added to the growing region, if they are sufficiently similar to the seed pixel. Watershed algorithm recognizes an image as a topographic surface where the digital value of each pixel can be considered as an elevation point. The surface is inverted and flooded, from the minimum point, preventing the water in adjacent basins to mix with water from upper levels. The boundary of a relief corresponds to the boundaries of adjacent basins. Template matching algorithm is an approach to pattern recognition, which allows comparison of the image with a previously stored model, which is calculated by the measure of correlation between the image and the model. For the first two approaches several parameters were tested to find the best result for the isolation of the individual tree crowns. For the template matching approach has been developed a piece of software in Python language, which is based on the use of templates of different tree species. To evaluate the performance of three different approaches was performed visual interpretation of 300 individual tree crowns in the WorldView-2 image, chosen at random, and the conversion of these data to a raster file. Then, the comparison was performed between the raster visual interpretation and results of each approach by the difference between the areas as a ratio of the validated area. Our results show that the region growing approach provided the best results, with accuracy around 70%.

8893-14, Session 5

### Prospects and limitations of vegetation indices in archeological research: the Neolithic Thessaly case study

Athos Agapiou, Dimitrios D. Alexakis, Maria Stavrou, Cyprus Univ. of Technology (Cyprus); Apostolos Sarris, Foundation for Research and Technology-Hellas (Greece); Kyriakos Themistocleous, Diofantos G. Hadjimitsis, Cyprus Univ. of Technology (Cyprus)

Vegetation indices have been widely used for the detection of archaeological traces, based on crop marks, during different phenological stages. Such indices can be used in order to enhance interpretation performance of multispectral and hyperspectral satellite data, for identification of buried archeological remains. Although a variety of indices exists in the literature, research is still limited and only a small group of these indices have been explored. This paper aims to highlight the prospects as well the limitations of several broadband vegetation indices for the detection of Neolithic tells in the Thessalian plain (Greece). Several multispectral Landsat 5 TM and Landsat 7 ETM+ satellite images have been used for evaluating the effectiveness of such indices. In addition, new developed algorithms and hyperspectral narrowband indices, specially designed for archaeological research, have been also used and compared using hyperspectral satellite data (EO-Hyperion). Indeed, the Normalized Archaeological Vegetation Index (NAVI) as well as a linear transformation of the Landsat 5 TM were applied to satellite data. The above were also compared to other processing algorithms such as Tasseled – Cap algorithm and Principal Component Analysis. The results have shown that several indices and new algorithms may be used for the enhancement of crop marks, while some no-widely used indices can be successfully used for archaeological purposes.

8893-15, Session 5

### Fluorescence lidar measurements at the archaeological site House of Augustus at Palatino, Rome

Valentina Raimondi, Istituto di Fisica Applicata Nello Carrara (Italy); Chiara Alisi, ENEA (Italy); Kerstin Barup, Lund Univ. (Sweden); Alessandra Broggi, Univ. degli Studi di Roma La Sapienza (Italy); Cinzia Conti, Soprintendenza Speciale ai Beni Archeologici di Roma (Italy); Maria Paola Bracciale, Univ. degli Studi di Roma La Sapienza (Italy); Jenny Hällström, Lund Univ. (Sweden); David Lognoli, Lorenzo Palombi, Istituto di Fisica Applicata Nello Carrara (Italy); Maria Laura Santarelli, Univ. degli Studi di Roma La Sapienza (Italy); Anna Rosa Sprocati, ENEA (Italy)

Early diagnostics and documentation fulfil an essential role for an effective planning of conservation and restoration of cultural heritage assets. We present here part of the results of a joint Italian-Swedish project focussed on the assessment of the conservation status of the Casa di Augusto, an important Roman archaeological site. The site, that is only partially open to the public, is located in the south-west area of the Palatino hill in Rome, Italy, and was the private residence of the Emperor Augustus. The project was focussed on documenting and recording the status of some sections of the part closed to the public by using different non-invasive imaging techniques, from high-precision colour 3D Laser Scanner to fluorescence hyperspectral imaging lidar. The lidar used a tripled-frequency Nd:YAG laser emitting at 355 nm as excitation source and an intensified, gated 512x512-pixel CCD as detector. The lidar had imaging capabilities thanks to a computer-controlled scanning mirror. The studies included both the characterisation of historic materials and the detection and characterisation of biodeterioration processes occurring on the site walls. The diagnostic techniques were completely non-invasive.

The first stage of the project focussed on a spectroscopic study of several fragments, mainly made with the fresco technique, coming directly from the site. The samples were measured by means of a hyperspectral fluorescence lidar to investigate the potential for their characterisation on the basis of their fluorescence properties with a remote sensing technique. The samples were also characterised

using several spectroscopic techniques: micro-FTIR and FT-Raman spectroscopy for the identification of the pigments; ATR FTIR for the identification of binders and substrate. The second stage of the project focussed on remote sensing measurements at the site. Measurements were performed both with the 3D laser scanner and with the imaging fluorescence lidar. Portions of selected walls of the monument were measured by the lidar system to obtain a laser induced hyperspectral fluorescence image achieving a spatial resolution of the order of 1 cm. Selected walls comprehended both frescoed and non-frescoed surfaces. Frescoed surfaces were measured both to obtain a detailed map of the pigments and for the detection of the presence of phototrophic biodeteriogens. Non-frescoed surfaces were mainly analysed to better characterise the microbial communities present on the surface. Biological sampling, followed by cultivation in the laboratory and identification by molecular methods completed the information collected at the site.

8893-17, Session 5

### An analysis of the change of Aksu River in history and the relevant reasons based on remote sensing images

Jiantao Bi, Institute of Remote Sensing and Digital Earth (China); Guilin Luo, Central South Univ. (China); Xingxing Wang, Institute of Remote Sensing and Digital Earth (China); Zuoqia Zhu, Central South Univ. (China); Wenju Zhu, China Univ. of Geosciences (China)

The distribution of water system often plays a very important and even decisive role of the layout and development in an area. In this paper, we take Aksu River and its two major tributaries—Kumara River and Toxkan River which are located in Xinjiang province as the study object. Related to ancient history information and combined with comparative analysis of remote sensing image, we focus on the change process of the river systems in the former Han, Later Han Dynasty, Tang, Qing Dynasty and modern-times, five different historical periods, and analysis the factors which affects the change of water system. We conclude that: Before 1950s, the riverway changes of Aksu River in Xinjiang was mainly affected by natural factors, such as climate, river capture and so on; After the 1950s, because of the strengthen of intervention caused by human activities, such as building reservoirs, widely cultivating arable land, rapid population growth and other factors led to the sharp decrease of the flow of Aksu river, man-made diversion of riverway and several riverway disappeared, human activity gradually replaced natural factors and became the dominant factor which affected the water system changes of Aksu River basin.

8893-18, Session 6

### Spatially explicit modeling of agricultural land use dynamics for assessing the ecosystem regeneration potential on Tenerife (Canary Islands)

Sebastian Günthert, Simone Naumann, Alexander Siegmund, Pädagogische Hochschule Heidelberg (Germany)

Since the middle of the 1960s, the island Tenerife is subject to an economic change from an agrarian to a service based society, mainly focused on tourism. This development led not only to an increasing expansion of infrastructure near to the coasts but also to increasing fallow land in higher and backward areas. The formerly cultivated land can generally be seen as major factor influencing natural reforestation and renaturation. It provides potential space where adjacent ecosystems can spread and hence a natural regeneration can come into effect.

The main aim of the research is to address and valuate agricultural land use changes of the past decades, to simulate agricultural land use dynamics in future by an spatially explicit land use change model and to finally assess the regeneration potential for specific ecosystems in the investigation area. Therefore an object-based classification procedure for recent RapidEye data (2010), Spot 4 (1998) as well as SPOT 1 (1986-88) imagery was developed, followed by a multitemporal change detection analysis. In order to detect older

agricultural fallow land or agricultural set-aside with a higher level of natural succession, a second texture based technique for recent orthophotos (spatial resolution 40 cm) was generated. This method allows an exact identification of the total agriculturally affected area on Tenerife by extracting linear agricultural structures like plough furrows and field boundaries of arable land as well as utilised and non-utilised agricultural dry walls.

The modeling of spatially explicit agricultural land use dynamics in future has been realised with the hybrid modeling framework Dyna CLUE 2 (Dynamic Conversion of Land Use and its Effects model: Dyna-CLUE version 2). It consists of statistical modeling methods as well as process and expert knowledge in combination with neighborhood interactions similar to constrained cellular automata models and is supplied with information about: 1) the different socioeconomic and location-specific driving factors (location suitability), which are responsible for agricultural land use changes; 2) neighbourhood effects between the various land use classes (neighbourhood suitability); information about spatial policies and restrictions; 3) Conversion elasticities and restrictions as well as 4) specific land use demands, which are determined by e.g. trend analyses or economic models. After performing the parameterisation, calibration and validation of the land use change model, two different land use scenarios - on the one hand a "trend analysis scenario" and on the other hand an "EU-supported optimization of the Canarian agriculture scenario" - have been developed and used to assess the ecosystem regeneration potential in the research area until 2030.

In situ investigations and the abovementioned evaluations of the object-based and texture-based classification results showed that for instance 1/7 of the total laurel forest area is located at agricultural affected and thus former agriculturally used areas. By combining the model results of the land use scenarios with information about the potential natural vegetation, it can be stated out that the recent agricultural land use trend can have a very positive effect on the regeneration of the laurel forest, whereas especially the revival of local agriculture can seriously threaten the present positive development of ecosystem regeneration in specific mountainous regions of Tenerife.

8893-20, Session 6

### GMES AgrEnv core services for monitoring of agri-environmental measures extensification: case study, Guadalquivir River Basin, Spain

Hakki Emrah Erdogan, Palle Hastrup, European Commission Joint Research Ctr. (Italy)

The policies integration process between agriculture and environment in Europe fosters the development of agricultural practices that preserve the environment and safeguard the countryside. Various EU directives and programmes, such as the Rural Development Programme, the Water Framework Directive and others, set strategic guidelines for the Common Monitoring and Evaluation Framework by defining objectives and indicators to evaluate the progress and achievement in environmental protection measures. The AgriEnvironment Core Information Service (AgriEnv CIS) contribute to the improvement of the timely and accurate monitoring of agricultural land use state and its changes at European, national and regional levels by providing common methodologies and indicators to monitor the impact of the programmes and their measures. This study describes the background, the materials and the methods use as well as the definition, context, policy drivers, approaches and preliminary results for the elaboration of an agri-environmental indicator named "agri-environmental measures effectiveness" in the framework of the GMES-Geoland2 project.

8893-21, Session 6

### Determining suitable image resolutions for accurate supervised crop classification using remote sensing data

Fabian Loew, Julius-Maximilians-Univ. Würzburg (Germany); Grégory Duveiller, European Commission Joint Research Ctr. (Italy)

Crop mapping is a major component of monitoring agricultural resources using remote sensing. However, different aspects of crop mapping need to be addressed depending what specific application is considered. Some applications, such as creating crop masks, require delineating accurately where crops are located over the entire area of interest. Other applications, such as assessing regional crop status or yield, can rely on a subset of agricultural fields that can be representative of the entire region.

This study focuses on the latter aspect of crop mapping, and more specifically, on defining the adequate spatial resolution to identify the subset of crop specific fields. The multi-temporality that is often necessary to accurately identify crops via classification and to monitor crop growth generally comes at the expense of coarser observation supports. However, mixed pixels can lead to increasingly erroneous class allocations, thereby reducing the overall quality of crop identification. In terms of spatial resolution, the choice of imagery consequently should be conditioned by knowing the appropriate spatial frequency at which the landscape must be sampled with the imaging instrument in order to provide the required information from the targeted fields.

To do so, this study presents an extension of a previous work in which a conceptual framework was developed to quantitatively define the spatial resolution requirements based on simulating how agricultural landscapes, and more specifically the fields covered by a crop of interest, are seen by instruments with increasingly coarser resolving power. This was done by modelling a generic point spread function (PSF) that was convolved over high-resolution satellite images to simulate increasingly coarser pixel sizes. The convolution of the same PSF over crop masks result in crop specific purity maps at each scale. This allows controlling the degree at which the footprints of coarser pixels coincide with the target structures (e.g. fields belonging to certain crops).

In this case, this framework has been steered towards answering the question: "What is the coarsest acceptable pixel size (CAP) for crop identification via supervised classification?" The method is implemented over four distinct irrigated agricultural sites in Middle Asia. Inputs to the experiment were eight multi-temporal images from the RapidEye sensor, acquired over the growing season in 2011 in each site. The range of pixel sizes that has been explored goes from 6.5 m to 396.5 m. Constraining parameters for crop identification were defined by setting thresholds for classification accuracy metrics from the confusion matrix, and entropy based metrics based on the soft outputs from the classifiers. The results provide CAPs and pixel purities, respectively for crop identification using Random Forest (RF) and Support Vector Machine (SVM) as classification algorithms, and in addition give the finest acceptable pixel size for classification. The CAPs were found to vary from site to site, ranging from 260 – 396.5 m. The ranges of CAPs for the single crops differ, depending on the spatial structures and cropping pattern in the sites, and range from 78 m – 396.5 m, with corresponding pixel purities between 0.4 – 0.6. The proposed framework can be used to guide users in choosing adequate imagery for crop identification via image classification.

8893-22, Session 6

### Retrieval of fire radiative power and biomass combustion using the Korean geostationary meteorological satellite

Dae Sun Kim, Yang Won Lee, Pukyong National Univ. (Korea, Republic of)

Global climate warming induced by greenhouse gases is increasing wildfire frequencies and scale. Since wildfire again releases greenhouse gases into the air, the vicious cycle is repeated. Thus, many researchers have been interested in studies of observing wildfire. Most efficient way for detection of them is satellite-based fire detection because wildfires occur in any space and time. The location, size, and intensity of wildfire can be captured by analyzing the thermography of medium (4?m approx.) and thermal (11?m approx.) infrared bands of a meteorological satellite. The American MODIS (Moderate Resolution Imaging Spectroradiometer) and GOES-R (Geostationary Operational Environmental Satellite - R Series) and the European SEVIRI (Spinning Enhanced Visible and Infrared Imager) are now providing the satellite products for active wildfires.

Wildfires are estimated to be responsible for, on average, around 30% of global total CO emissions, 10% of methane emissions, 38% of tropospheric ozone, and over 86% of black carbon. As part

of aerosols, they affect the earth's energy balance by scattering or absorbing incident visible light energy from the sun. Also, they have indirect influences on climate by playing the role of cloud condensation nucleus and changing cloud properties. Therefore biomass combustion by wildfires should be measured for accurate estimation of aerosols. In addition, wildfires decrease carbon storage capacity of the ground, and increase carbon in the atmosphere by burning of vegetation. This situation brings a change in the global carbon cycle. So we need to quantify the emitted gases by biomass combustions, which can be also facilitated by satellite remote sensing.

In this paper, we developed the algorithm for retrieval of FRP (fire radiative power) and biomass combustion using COMS (Communication, Ocean and Meteorological Satellite), the Korean geostationary meteorological satellite. Our algorithm is applied in Indonesia, where wildfires occur frequently. We modified the GOES-R algorithm, for detecting actively burning wildfires and estimating their FRP/FRE (fire radiative energy) to measure biomass combustion. The FRP retrieval by MIR (Middle Infrared) radiance includes fire pixel area, Stefan-Boltzmann constant, fire broadband emissivity, and the spectral emissivity of MIR. Total FRE is derived from the time-integration of the FRP and the rate of biomass combustion. The FRE can potentially provide detailed information on the amount and rate of biomass consumption in wildfire pixels. We calculated the total of biomass combustion considering FRP/FRE, fuel types, wind speed and topography. Our biomass combustion products can be compared with aerosol products of COMS. The products of FRP and rate of biomass combustion are expected to be utilized as an important parameter for the studies of combustion engineering, aerosols, and global/regional carbon cycle. Our products can be also utilized as the baseline for retrieval of certified emission reductions.

#### 8893-23, Session 7

### Model-based assessment of land degradation trend and its relationship to land use change and climatic variability in semiarid zone by using remote sensed and situ data

Abdelnasir I. Ali Hano, Technische Univ. Dresden (Germany)

Adversely human activities (land use activities) and climatic factors are considered the main drivers of land degradation and desertification. And vegetation cover status is one of the important biophysical indicators of land degradation status particularly in semi-arid. Consequently, determination and model of land degradation trend and its linkage with the driven factors at spatiotemporal scale is critical step towards sustainably management of land and performing land degradation neutrality in arid region. Accordingly the research was carried out to build model based on assessment of geospatial-temporal scale of land degradation status (LD), based on vegetation cover status indicator and its linkage with LUC and climatic variability (CV) in 1973 – 2009, using remote sensing and situ data, in Elgeteina locality of White Nile State of the Sudan. MSS 1973, TM 1986, ASTER 2009 and TM 2010 were used; soil adjusted and atmospheric resistant vegetation index (SARVI), object-based image analysis (OBIA) and change detection - matrix were used for assessing LD trend and its relationship to LUC and CV, and then SPSS- Pearson coefficient correlation matrix (PCM) and multi-linear regression analysis (MRA) were used for building model of LD and its relation to LU and CV (climatic data collected from meteorological stations). The results revealed that there was partially geospatial mutual conversion occurred between the LD areas and the LU patterns change led to dynamic status of LD increasingly and decreasingly during 1973 – 1986 and 1986 – 2009 respectively. The important PCM results depicted that: LD correlation with the fallow land (FWL) was very strong and significantly (.995\*\*), and it was moderately with the residential area (RA) (.734\*\*). While LD correlation with the different climate elements was very weak, and the rainfall precipitation was little bit low (.477\*). The resultant model of LD relationship to LUC and CV was  $LD = 786.169 - .874 \text{ farm land} - 1.25 \text{ fallow land} - 1.065 \text{ residential} - .033 \text{ mean temperature}$ .

#### 8893-24, Session 7

### Remote sensing methods to monitor habitats potentially threatened by climate change

Michael Förster, Tobias Schmidt, Technische Univ. Berlin (Germany); Nadine Spindler, Kathrin Renner, EURAC research (Italy); Iris Wagner-Lücker, Univ. Wien (Austria); Marc Zebisch, EURAC research (Italy); Marco Neubert, Leibniz Institute of Ecological Urban and Regional Development (Germany)

The recognition and monitoring of vegetation and habitats for nature conservation is a vital point of research within the remote sensing community. It has been agreed on that there is no general solution on deriving information on habitats due to different data availability and spectral as well as textural behaviour of habitat main types (e.g. woodlands, grasslands, etc.). Therefore the monitoring should be rather multi-scale, versatile, user-friendly, and cost-efficient for predefined indicators.

In the presented study, five Central European test sites of natural vegetation communities in

- (1) an Alpine area: Rieserferner-Ahrn Nature Park, Italia,
- (2) a temperate forest: Vessertal - Thuringian Forest Biosphere Reserve, Germany,
- (3) a Pannonian grassland: Balaton Uplands National Park, Hungary,
- (4) a shallow steppic lake: Lake Neusiedl/Fertő - Hansag National Park, Austria/Hungary, and
- (5) a Carpathian grassland: Natural Park Bucegi, Romania,

have been investigated by multi-temporal remote sensing. For these studies, different time-series of RapidEye images from the years 2009 to 2011 were acquired. The amount of the images was depending on required acquisitions dates as well as weather conditions. The definition of the indicators was relying on the available ground truth data as well as the demands and judgement of the managing authorities in the nature conservation areas. The selected methods for deriving of the indicators depend on the time-series as well as the available calibration and validation data. The techniques vary between unsupervised classification, object-based approaches and supervised classification methods with algorithms such as support vector machines (e.g. SVM) or classification trees (e.g. See5). Often the named methods are utilized in combined approaches.

The resulting indicators for the monitoring are shrub encroachment (for 1), share of naturally occurring tree type (for 2), differentiation of grassland types (for 3 and 5) and the changing extent of a reed belt (for 4). All indicators seem to be valid and useful for the authorities within the conservation areas. However, a transferability of the methods or a general statement on good-practice remote sensing applications can hardly be derived from these specific case studies.

Thus, a future task would be a collection of valid remote sensing methods and indicators with their requirements regarding satellite data type and acquisition dates for more case studies.

#### 8893-25, Session 7

### Assessing error sources for Landsat time series analysis for tropical test sites in Viet Nam and Ethiopia

Michael Schultz, Alterra B.V. (Netherlands); Valerio Avitabile Pratihast, Martin Herold, Wageningen University (Netherlands)

In the future Sentinel 2 time series will be combined with existing Landsat time series. Researchers who use remotely sensed data can spend half of their total effort analysing prior data. If this data pre-processing does not match the application, this time spent on data analysis can increase considerably and can lead to inaccuracies. Despite the existence of a number of methods for pre-processing Landsat time series, each method has shortcomings, particularly for mapping forest changes under varying illumination and data availability conditions. Based on the requirements of mapping forest changes as defined by the United Nations (UN) Reducing Emissions from Forest Degradation and Deforestation (REDD) program, the accurate reporting of the spatio-temporal properties of these changes is necessary. We compared the impact of four fundamentally

different radiometric pre-processing techniques Moderate Resolution Atmospheric TRANsmission (MODTRAN), Second Simulation of a Satellite Signal in the Solar Spectrum (6S), Spectral Unmixing, and simple Dark Object Subtraction (DOS) on mapping forest changes using Landsat time series data. Breaks For Additive Season and Trend (BFAST) was used to jointly map the spatial and temporal agreement of forest changes at test sites in Ethiopia and Viet Nam.

The suitability of the pre-processing methods for the occurring forest change drivers was assessed using recently captured Ground Truth and high resolution data. Because the Vietnam test site has low data availability and an extremely intense topography, the time-consuming yet physically superior MODTRAN- based pre-processing method is expected to yield the best results. Spectral Unmixing is a suitable alternative, as it accounts for topographic effects as well. For the less topographically intense test site in Ethiopia and its higher data availability, the 6S technique is expected to be the most efficient in terms of processing complexity and accuracy. The combination of 6S (which accounts for atmospheric effects) and Spectral Unmixing (which accounts for topographic effects) is likely to be considered as the most robust and efficient pre-processing method for Landsat time series analysis tropical forest change mapping.

## 8893-26, Session 7

### The use of decision trees in the classification of beach forms/patterns on IKONOS-2 data

Ana Cláudia M. Teodoro, Dário Ferreira, Ctr. de Investigação em Ciências Geo-Espaciais (Portugal); Hernâni Gonçalves, Ctr. de Investigação em Ciências Geo-Espaciais (Portugal) and Univ. do Porto (Portugal)

Evaluation of beach hydromorphological behaviour and its classification is highly complex. Beach morphological classification was mainly established for Australian and American microtidal sandy environments. The available beach morphologic and classification models are mainly based on wave, tidal and sediment parameters. Since these parameters are usually unavailable for some regions – such as in the Portuguese coastal zone - a morphologic analysis using remotely sensed data seems to be a valid alternative. Based on this concept, Pais-Barbosa et al. (2009) presented a methodology to identify, measure and classify hydroforms and hydromorphologies, through visual analysis of vertical aerial photographs in a GIS environment. Later, further advances were achieved by Teodoro et al. (2009, 2011), who applied a pixel-based classification, an object-based method and a new approach based on principal components analysis.

Data mining for spatial pattern recognition is the process of discovering useful information, such as patterns, forms, changes and significant structures from large amounts of data. Data mining techniques, such as decision trees (DT) have been broadly applied in the field of remote sensing.

This study focuses on the application of data mining techniques, particularly DT, to an IKONOS-2 image in order to classify beach features/patterns, in a stretch of the northwest coast of Portugal. Based on the knowledge of the coastal features, six classes were defined: Sea, Suspended-Sediments, Breaking-Zone, Beachface, Beach and Null (mask for land). The dataset was randomly divided into training (70%) and validation subsets (30%).

Based on the testing of several DT algorithms, the CART algorithm was found to be the most adequate and was thus applied. CART is characterized by the fact it constructs binary trees, i.e., each internal node has exactly two outgoing edges. The CART growing method attempts to maximize within-node homogeneity. The extent to which a node does not represent an homogenous subset of cases is an indication of impurity. The Bhattacharyya distance was used as the separability measure between classes. The performance of the classification with the DT was evaluated through the error matrix, overall accuracy, kappa statistic, and producer and user accuracies.

The lower values for the separability measure were found between Beach-Face and Beach (1.61) and between Breaking-Zone and Beach-Face (1.81). The remaining values ranged between 1.96 and 2.00 indicating a good overall separability. The obtained DT considering the CART model had 7 nodes. The overall accuracy of the CART model was 97.8%, and the value of Kappa statistic was 0.97, indicating a very good agreement between the classification and the

reference data. The classified image presents a very good agreement with the beach forms/patterns identified by traditional algorithms (pixel-based and object-based classification).

The methodology presented in this paper provides promising results and should be considered in further applications of beach forms/patterns classification.

## 8893-27, Session 7

### Remote sensing and spatial analysis based study for detecting deforestation and the associated drivers

Mustafa M. El-Abbas, Elmar Csaplovics, Taisser H. Deafalla, Technische Univ. Dresden (Germany)

There are several challenges faces the forest sector worldwide which imposes the needs for well-designed information systems and management plans. One of these challenges is Land Use/Land Cover (LU/LC) changes, in particular deforestation and land degradation. Despite the importance of LU/LC changes as an environmental variable, the paucity of information about these changes is clear. Nowadays, remote-sensing technologies are becoming increasingly interlinked to the issue of deforestation. They offer a systematized and objective strategy to document, understand and simulate the deforestation process and its associated causes. In this context, the main goal of this study, conducted in Blue Nile region of Sudan, in which most of the natural habitats were dramatically destroyed, was to develop spatial methodologies to assess the deforestation dynamics and its associated factors. To achieve that, optical multispectral satellite scenes (i.e., ASTER and LANDSAT) integrated with field survey in addition to multiple data sources were used for the analyses. Spatiotemporal Object Based Image Analysis (STOBIA) was applied to assess the change dynamics within the period of study (1990 to 2010). Broadly, the above mentioned analyses include; Object Based (OB) classifications, post-classification change detection, data fusion, information extraction and spatial analysis. Hierarchical multi-scale segmentation thresholds were applied and each class was delimited with semantic meanings by set of rules associated with membership functions. Consequently, the fused multi-temporal data were introduced to create detailed objects of change classes from the input nine LU/LC classes, i.e. agriculture (Ag.), bare-land (Br.), crop-land (Cr.), dense-forest (DF), grassland (Gr.), orchard (Or.), scattered-forest (SF), settlements (St.) and water body (W). Subsequently, aggregated super level of change classes were identified representing hot spots deforested areas, successfully recovered and the remains unchanged areas. Furthermore, correlation analysis was also performed between objects of the introduced layers (i.e., anthropogenic and natural factors with hotspots areas) for better understanding of the change dynamics and its drivers. Various spatial and contextual information derived from the different object levels were investigated (e.g. areas, spatial relation features, distances and object indexes). The dynamic changes were quantified and spatially located as well as the spatial relations from adjacent areas were analyzed. The main finding of the present study is that, the forest areas were drastically decreased during the period of study (34.60%), while the gained areas were quite limited (6.14%). The spatial analyses indicate that the agrarian structure in the conversion of forest into agricultural fields and grassland was the main force which leads to deforestation. On the other hand, the capability of the area to recover was clearly observed, wherein more than one-half percent of the reforested areas were gained from abandoned agricultural fields. The study concludes with a brief assessment of an 'oriented' framework, focused at the alarming areas where serious dynamics are located and where urgent plans and interventions are most critical, guided with potential solutions based on the identified driving forces. Such methodological approaches could be applied to other neighbor regions of the degraded forests and contribute insights into conservation objectives and decision making.

## 8893-28, Session 8

### Remote sensing data and GIS for hydrological studies

Konstantinos G. Nikolakopoulos, Evi Kouzeli, Nikolaos Lambrakis, Univ. of Patras (Greece)

In this project a hydrogeological data base in GIS environment is presented. This database has been created in order to include the tables of meteorological data necessary for the water budget/balance of each region, the tables of hydrochemical data concerning the surface and underground water, all kinds of maps, topographical and geological, as well as the maps that were produced using the data from the base.

The design of the base was produced in combination of the realization of the hydrogeological study of the lakeside area located at the NW part of lake Trichonida so the experience and the details that will be required for this study according to data will be transferred with absolute accuracy at the construction of the base. Apart from the topographical and geological maps that were requested by the public services and were used after digitalization, for the hydrogeological study, the potentiometric map of the area, the precipitation map as well as hydrochemical distribution maps were necessary. These maps were created with the statistical tools that come with the ArcGIS 9.3. software after it was checked in order to find which one of the different methods for the spatial distribution data, Kriging, Coriging, Inverse Distance Weighting etc, gives better results.

### 8893-29, Session 8

## Landslide hazard assessment along a mountain highway in the Indian Himalayan Region (IHR) using remote sensing and computational models

Akhouri Pramod Krishna, Birla Institute of Technology and Science (India); Santosh Kumar, Birla Institute of Technology (India)

Indian Himalayan Region (IHR) suffers from landslide hazards of varying degrees accounting for considerable loss of lives and causing damages to the human settlements, civil structures, hydro projects, communication routes, agricultural and forest lands. Landslide hazard assessments using computational models, such as artificial neural network (ANN) and frequency ratio (FR), were carried out covering one of the important mountain highways in the Central Himalaya of IHR. Landslide influencing factors were either calculated or extracted from spatial databases including recent remote sensing data of LANDSAT TM, CARTOSAT digital elevation model (DEM) and Tropical Rainfall Measuring Mission (TRMM) satellite for rainfall data. Considered factors included slope, aspect, curvature, topography, lithology, distances from lineaments, drainage, land use/land cover and rainfall.

ANN was implemented using the multi-layered feed forward architecture with different input, output and hidden layers. This model based on back propagation algorithm derived weights for all possible parameters of landslides and causative factors considered. The training sites for landslide prone and non-prone areas were identified and verified through details gathered from remote sensing and other sources. Ability of learning is one of the most important characteristics of ANN and it helped perform multi-source classification in two stages viz. training and classification. Results of landslide hazard susceptibilities were cross validated using the known landslide locations of the study area.

Frequency Ratio (FR) models are based on observed relationships between the distribution of landslides and each landslide related factor. FR model implementation proved useful for assessing the spatial relationships between landslide occurrence location and factors contributing to landslide occurrence. Frequency was calculated from analysis of the relationship between landslides and the attribute factors. This revealed the correlation between the landslide locations and factors in the study area. Therefore, the frequency ratios of each type or range of factors were calculated from their relationship with landslide events. Usually in such FR based analysis, the ratio is that of the area where landslides occurred to the total area. This implies that a value of 1 is an average value and if the value is greater than 1, there is a higher correlation. Whereas, a value lower than 1 implies a lower correlation. Thus, greater the frequency ratio value, higher the hazard to landslide occurrence and vice-versa.

Above computational models generated respective susceptibility maps of landslide hazard for the study area. This further allowed the simulation of landslide hazard maps on a medium scale using GIS platform and remote sensing data. These two methods helped in the comparison and evaluation of their relative efficacy for the hazard susceptibility mapping. Upon validation and accuracy checks,

it was observed that both the models produced good results with FR having some edge over the ANN based mapping of this hazard. Such statistical and functional models led to better understanding of relationships between the landslides and preparatory factors as well as ensuring lower levels of subjectivity compared to the qualitative approaches.

### 8893-30, Session 8

## Mineralogical and geochemical studies on the clay deposits, North Sinai, Egypt: using remote sensing data

Safaa M. Sayed, Talaat M. Ramadan, National Authority for Remote Sensing and Space Sciences (Egypt)

Practical and economical constraints prompt the need of obtaining lithological and structural information with reduced field effort. In the present work, the clay deposits are recorded in several localities (e.g. east Gabal Libni, east Wadi El Hema and southwest Gabal Risan Eniza in north Sinai). Twenty samples from these deposits (Kafir El Sheik Fm) east Gabal Libni were analyzed using X-Ray Diffraction (XRD) analysis. These analyses revealed the samples are composed of the following minerals in a decreasing order of their abundance: quartz, montmorillonite, kaolinite and calcite. The chemical analyses for fifteen sample from these samples using XRF analysis indicate that SiO<sub>2</sub> ranging from 54.06 to 55.75 %, Al<sub>2</sub>O<sub>3</sub> ranging from 15.84 to 20.82% in samples T1, T2 and T3.

In this study, band ratioing, principal component analysis (PCA), false-color composition (FCC), and of ASTER (VINIR and SWIR bands) and ETM+ data have substantially improved visual interpretation for detailed mapping of the studied areas in North Sinai of Egypt. By compiling field, geochemical and spectral characteristic analysis data, controls on clay mineralization have been assessed in terms of association of clay deposits with particular lithological units and structure features. Spectral characteristic analysis (SCA) followed by both principal component analysis (PCA) and band ratio analysis of the nine ASTER bands enabled selection of appropriate band combination, principal components and band ratio for discriminating the exposed rock units associated with clay deposits throughout the study area. Comparing the resultant of both PC and band ratio color images with the available geological maps followed by field check as well as the chemical analyses indicates that ASTER data provides new information about the reflectance of the rocks that can be used for precise lithological mapping in unmapped areas and verify and update the existing geological maps.

### 8893-31, Session 8

## Groundwater exploration in northeastern desert, Egypt: using radar, aster and geophysical data

Safaa M. Sayed, National Authority for Remote Sensing and Space Sciences (Egypt)

The present study aims to investigate the structure: ground water and build up a geo-environmental database for the study area using radar and ASTER remote sensing data and geophysical data. The quantitative interpretation of the seventeen vertical electrical soundings is carried out to determine the thicknesses and true resistivity values. The final results used for construction four geoelectrical cross-sections which exhibits the six different geological units represented in the study area. The isopach maps are constructed to indicate the variation of the thicknesses of the first, second, third, fourth and fifth units through the studied area. The second layer represents the fresh water aquifer in the study area for upper Miocene age. The results of resistivity interpretation for depth, thickness and resistivity values for different layers indicated that the fresh water bearing aquifer has thickness from 5 to 85m and depth ranging from 5 to 25m.

Advanced Space borne Thermal Emission and Reflection Radiometer (ASTER) images have been used to study the lithological rock units. Robinson-3 level edge enhancement technique was applied on the RADARSAT2 fine beam image to emphasize the predominant fault and lineaments directions in the study area as well as detection of the buried structures and drainage systems. Depending on the qualitative



analysis of the spectral characteristic curves of the exposed rock units using nine ASTER bands in visible near infrared (VNIR) short wave infrared bands (SWIR), reflectance peaks occur at ASTER bands 1, 2, 4 and 6 while the spectral absorption values occur at bands 3, 5, 7, 8 and 9. The new proposed band ratio (1/5, 8/9 and 4/6) have been applied for more lithological discrimination of the exposed rock units of our study area.

From these results; six suggested new locations of boreholes for groundwater which can be used for construction, production and human uses.

8893-48, Session PS

### Use of ground penetrating radar for determination of water table depth and subsurface soil characteristics at Kennedy Space Center

Charles R. Bostater Jr., Gideon M. Hengari, Florida Institute of Technology (United States); Carlton R. Hall, Tim J. Kozusko, InoMedic Inc. (United States)

Climate change coupled with several human induced factors, such as unsustainable utilization of the natural resources and habitat degradation, resulted in endangerment and extinction of numerous species of fauna and flora. One way to ensure sustainable restoration of degraded habitats is to consider several factors such as vegetation distribution and abundance, surface and subsurface soil characteristics, and subsurface water depth. Several authors such as [2,3,4] emphasized the importance of water table dynamics on plant species composition and distribution in different temperate zones and wetlands. Conservation efforts to restore habitat of endangered flora and fauna utilize non-destructive tools to provide spatial and temporal data for decision making. Remote sensing has been the fundamental tool used in determining some of the biophysical and biochemical variables necessary for monitoring and research [5]. Use of airborne and satellite remote sensing works well in detecting bio-chemical, bio-physical attributes at the leaf and canopy level. Assessment of subsurface attributes necessary for vegetation monitoring are very limited using airborne and satellite remote sensing.

To fill this gap, ground penetrating radar (GPR), a technique that is applied to characterize the relatively shallow subsurface features at scales from centimeters to kilometers, has been widely used in past decades [6]. The GPR technique is similar in principle to seismic surveying. One antenna (the transmitter) radiates short pulses of high-frequency electromagnetic waves, while the other antenna (the receiver) measures the signal from the transmitter as a function of time [6]. GPR uses both active and passive remote sensing systems to transmit and record energy backscattered when the waves encounter an interface between materials with different dielectric permittivity.

The work presented here investigates the applicability of GPR in determination of water-table depth and associated subsurface soil characteristics at John F. Kennedy Space Center (KSC). GPR has been extensively used to map the shallow subsurface features due to its relatively high resolution [7]. Reflectance characteristics of leaves collected from myrtle oak (*Quercus myrtifolia*) and rust lyonia (*Lyonia ferruginea*), and leaf moisture content determination using the bands previously identified by [1] is also presented in this paper.

8893-49, Session PS

### Estimation and analysis of the movement of the Kuksay glacier in Muztag Ata from InSAR data

Jianmin Zhou, Zhen Li, Institute of Remote Sensing and Digital Earth (China)

The mountain glacier is an indicator of climate change and represents important archives of past climatic information. The effects of climate warming are for instance evident in the continuous retreat of glaciers in many mountainous regions, and even the most optimistic scenarios for future temperature change involve pronounced glacier retreat over many decades to come. Monitoring glacier flow rates is important in studies of glaciers responding to climate change; in particular, it helps in understanding their dynamic responses to climate change and their

potential impact on water resources, sea level, and glacier-related hazards.

The Muztag Ata is known as "the father of glacier" in the west of China. However, its glacier flow pattern has never been studied. We have mapped the glacier velocity of mountain glaciers in Muztag Ata using the combined methods (InSAR and offset-tracking) with satellite L-band SAR data. This map provide a detailed view of the Kuksay glacier flow patterns for the winter seasons of 2008, 2009 and 2010 using a 46 day-separation Advanced Land Observing Satellite (ALOS) SAR images acquired from ascending orbit. In this paper, we focus on analysis of the features of Kuksay glacier motion. Special effort was also made to assess the accuracy of estimation of glacier velocity. To assure the accuracy of the derived results, we have tested two methods (InSAR and offset-tracking) for estimating the motion of Kuksay glacier from ALOS SAR data. The validation of the two methods yield similar results and agree well with each other. The patterns of glacier velocity suggest a strong influence of mountain topography and monsoon. Occurrence of the flow local maxima and minima at consistent locations over different parts of glacier suggests that the subglacial topography, glacier size and glacier orientation affect the overall flow patterns. The velocities are very low in the glacier surface debris cover, which suggests debris covers have an impact on the glacier motion and the glacier is retreating during this period. The detailed mappings such as these, at regular intervals, provide an important observational capability for understanding the dynamics of glaciers in mountain regions like the Muztag Ata.

8893-50, Session PS

### Simulation, visualization and GIS analysis based on globe model for PL19-3 oil spill of Bohai Sea

Linchong Kang, Shi Suixiang, Zengan Deng, Jiye Jin, Feng Zhang, Haiyan Huang, National Marine Data and Information Service (China)

Multi-resolution remote sensing imagery and DEM of terrain is implemented with LOD based on Globe Model. A numerical simulation result of PL 19-3 oil spill based on General NOAA Operational Modeling Environment (GNOME) is visualized using particle trace and analysed on the globe model.

8893-51, Session PS

### Research and implementation of coalfield spontaneous combustion of carbon emissions WebGIS based on Silverlight and ArcGIS Server

Zuojia Zhu, Central South Univ. (China); Jiantao Bi, Xingxing Wang, Institute of Remote Sensing and Digital Earth (China); Guilin Luo, Central South Univ. (China)

As a considerable sub-topic of the natural process of carbon emissions data public information platform construction, the coalfield spontaneous combustion of carbon emissions WebGIS system has become an important study object of this article. In connection of data feature of coalfield spontaneous combustion of carbon emissions, a wide range of collection, rich and complex of data content, and the characteristics of geospatial, its data is divided into the attribute data and spatial data. Base on full analysis of the attribute data, completed the detailed design of the Oracle database and stored into the Oracle database. By the Silverlight rich client technology and the expansion of WCF services, achieved the attribute data of web dynamic query, retrieval, statistical, analysis and other function. For spatial data, take advantage of ArcGIS Server and Silverlight-based API to invoke GIS server background published map services, GP services, Image services and other services, implemented coalfield spontaneous combustion of remote sensing image data and web map data display, data analysis, thematic map production. The study found that the Silverlight technology base on rich client and object-oriented framework for WCF service can efficient constructed a WebGIS system, and then combined with ArcGIS Silverlight API to achieve interactive query attribute data and spatial data of coalfield spontaneous and can greatly improve the performance of WebGIS

system. At the same time, it provided a strong guarantee for the construction of public information of China's carbon emissions data.

#### 8893-52, Session PS

### Automatic reconstruction of building roof boundary from raw airborne lidar data

Luo Sheng, Zhengzhou Institute of Surveying and Mapping (China)

A novel method for automatic reconstruction of the multistorey building's roof boundary from irregularly spaced Light Detection and Ranging (LiDAR) data is presented. In the proposed method, the TIN model of the raw LiDAR data is built first using the Delaunay-triangle method, then according to the spacial characteristics of the building walls, roofs, and the non-building terrain feature such as vegetation, fence or ditch, the building roof LiDAR points are identified using the staged region growing algorithm. Usually if a point is on a roof boundary, the triangle which contains the point shall only has less than 3 connected triangles, so by calculating the number of each roof triangles' neighbors, the roof boundary points can be extracted. Searching the outmost roof boundary in a clockwise direction can obtain a raw and noisy boundary, so the next work is to regularize the raw roof boundaries. In order to promote the accuracy of the building roof boundary reconstruction, several constraints are introduced. Considering the direction of each roof during one multistorey building and the dominant direction of buildings which are adjacent to each other are almost consistent, the roughness of the building roof boundaries can be well improved. Three key procedures are needed to finish the regularization. The first step is to find the boundary key points which are the corners of the roof by analyzing the cross angle among five sequent raw boundary points. The second step is to find out the directions of each roof and the dominant direction of each building. The roof direction can be easily calculated by the direction of two connected key points which has the maximum distance between each other; the dominant direction of building is the direction of the roof that has the maximum area among the multistorey building roofs. If the direction is perpendicular or parallel to each other, then the two roofs or buildings can be further regularized in the third step. There are six situations to deal with the regularization of single roof boundary, after done the regularization of each roof, the last job is to parallelize the adjacent roofs or buildings according to the directions of roofs or the dominant directions of buildings. Two data sets from urbanized areas including large institutional, commercial buildings, fences, and small residential buildings, dense vegetation were employed to test the proposed method. A quantitative analysis showed that the total of omission and commission errors for extracted building roof points for both areas was about 5%, the accuracy and integrity for building roof boundary reconstruction were about 96.8% and 94.3%. The results demonstrated that the proposed method reconstructed building roof boundaries well.

#### 8893-53, Session PS

### Low frequency/high sensitivity triaxial monolithic inertial sensor

Fabrizio Barone, Fausto Acernese, Univ. degli Studi di Salerno (Italy); Rosario De Rosa, Univ. degli Studi di Napoli Federico II (Italy); Gerardo Giordano, Rocco Romano, Univ. degli Studi di Salerno (Italy)

This paper describes a new mechanical implementation of a triaxial sensor, configurable as seismometer and/or as accelerometer, consisting of three one-dimensional monolithic FP sensors, suitably geometrically positioned. The triaxial sensor is, therefore, compact, light, scalable, tunable instrument (frequency < 100 mHz), with large band ( $10^{-7}$  Hz - 10 Hz), high quality factor ( $Q > 1500$  in air) with good immunity to environmental noises, guaranteed by an integrated laser optical readout. The measured sensitivity curve is in very good agreement with the theoretical ones ( $10^{-12}$  m/sqrt(Hz) in the band (0.1 - 10 Hz). Typical applications are in the field of earthquake engineering, geophysics, civil engineering and in all applications requiring large band-low frequency performances coupled with high sensitivities.

#### 8893-54, Session PS

### Satellite and in-situ monitoring of urban air pollution in relation with children's asthma

Mariana R. Dida, Univ. of Medicine and Pharmacy of Craiova (Romania); Maria A. Zoran, National Institute of Research and Development for Optoelectronics (Romania)

Urban air pollution and especially aerosols have significant negative health effects on urban population, of which children are most exposed for the rapid increase of asthma disease. An allergic reaction to different allergens is a major contributor to asthma in urban children, but new research suggests that the allergies are just one part of a more complex story. Very early exposure to certain components of air pollution can increase the risk of developing of different allergies by age 7. The epidemiological research on the mutagenic effects of airborne particulate matter pointed their capability to reach deep lung regions, being vehicles of toxic substances. Toxicological studies, currently attempt to identify relation between particle characteristics responsible for adverse biological responses, and suggest that the chemical composition of PM (which reflects differences in source contributions) plays an important role in these responses. The current study presents a spatio-temporal analysis of the aerosol concentrations in relation with meteorological parameters in two size fractions (PM10 and PM2.5) and possible health effects in Bucharest metropolitan area. Both in-situ monitoring data as well as MODIS Terra/Aqua time-series satellite data of particle matter PM2.5 and PM10 concentrations have been used in an effort to qualitatively assess distribution of aerosols in the greater metropolitan area of Bucharest comparative with some other little towns in Romania during 2010-2011 period. It was found that PM2.5 and PM10 aerosols exhibit their highest concentration mostly in the central part of the towns, mainly due to road traffic as well as in the industrialized parts outside of city's centre. Many epidemiological studies examining the relationships between adverse health outcomes and exposure to air pollutants in urban agglomerations use ambient air pollution measurements like as PM10 and PM2.5 levels as a proxy for personal exposure levels. The measurements of environmental concentrations of particulate matter air pollutants have been correlated with some meteorological parameters (air temperature and pressure, relative humidity, wind intensity) in urban and periurban subtest areas. Accurate information of urban air pollution is required for environmental and health policy, but also to act as a basis for designing and stratifying future monitoring networks. Pediatric asthma can be managed through medications prescribed by a healthcare provider, but the most important aspect is to avoid urban locations with high air pollution concentrations of air particles and allergens. Epidemiological studies aim to detect the relative risks associated with particulate matter and gases present in the lower atmosphere. As asthma among children in urban populations in Romania continues to rise, identifying these complex associations with air particle pollution and climate change and acting upon them through better medical surveillance and more appropriate public policy may be very important in curtailing this alarming trend.

#### 8893-55, Session PS

### Satellite remote sensing image based-analysis of effects due to urbanization on climate and health

Maria A. Zoran, National Institute of Research and Development for Optoelectronics (Romania); Liviu-Florin V. I. Zoran, Univ. Politehnica of Bucharest (Romania); Adrian I. Dida, Transilvania Univ. of Brasov (Romania); Mariana R. Dida, Alexandra Theodora D. Zoran, Univ. of Medicine and Pharmacy of Craiova (Romania); Ovidiu M Ionescu, University Transilvania of Brasov (Romania)

Satellite remote sensing offers unique perspectives to study the relationship between urban systems and climate change because it provides spatially explicit and synoptic views of the landscape that are available at multiple spatial grains, spatial extents, and over time, able to provide detailed information of urbanization patterns. Due to significant anthropogenic changes that have occurred in the last several decades in Bucharest city's landscape, urbanization has become an important factor affecting urban surface parameters,

hence in the surface-atmosphere interaction processes, with a great potential to alter the local climate. Land use and land cover (LULC) influence a variety of processes important in characterizing urban / periurban biophysical parameters' quality, including aerosol deposition rates, biogenic emissions, albedo, surface temperatures, climatic parameters and other. Analysis of surface biophysical parameters changes in urban/periurban areas of Bucharest metropolitan area based on multi-spectral and multi-temporal satellite imagery (MODIS, Landsat TM/ETM and IKONOS) provides the most reliable technique of environmental monitoring regarding the net radiation and heat fluxes associated with urbanization at the regional scale. Investigation of radiation properties, energy balance and heat fluxes is based on information derived from various satellite sensors and in-situ monitoring data, linked to numerical models and quantitative biophysical information extracted from spatially distributed NDVI-data and net radiation. For detailed land cover classifications in a digital form is possible to analyze in a statistical way these properties. Have been derived surface biophysical parameters such as fractional vegetation cover (Fr), surface radiant temperature (Ts) and albedo over 1990 – 2012 period for Bucharest town and its periurban areas. These changes have been then, examined in association with climatic effects of land cover changes to illustrate how these parameters respond to rapid urban expansion in Bucharest and surrounding region. This study attempts to provide environmental awareness to urban planners suggesting that future changes in urban land cover could substantially affect climate and human health by altering biophysical land-atmosphere interactions. The local and regional climate response is of a similar magnitude to that projected for future greenhouse gas concentrations, climatic effects of land cover change should be carefully considered by urban decision makers for managing anthropogenic forcing of the climate system and human health protective measures through increasing urban green. Regional and urban local climate change is more rapid than global climate change and directly affects the activities and health of local people. The most impressive phenomenon is the urban thermo-effect, which refers to thermal environment changes within the area due to the alteration of energy balance. This is responsible of Urban Heat Island (UHI) phenomenon development during which the temperature of an urban area becomes higher than that of the surrounding rural area As results appear a high rate of heat-related health aspects, , high consumption of energy for air conditioning, and air pollution.

#### 8893-56, Session PS

### Measuring pasture degradation on the Qinghai-Tibet Plateau using hyperspectral dissimilarities and indices

Hanna Meyer, Lukas W. Lehnert, Philipps-Univ. Marburg (Germany); Yun Wang, Senckenberg Museum of Natural History (Germany); Christoph Reudenbach, Jörg Bendix, Philipps-Univ. Marburg (Germany)

Pasture degradation on the Qinghai-Tibet Plateau (QTP) is a global and local concern since the dynamics of the pastures affect climate and hydrology as well as livelihood of the Tibetan nomads. Despite its relevance, extent of pasture degradation is still unknown, however, in literature, livestock grazing is widely accepted as a major factor for pasture degradation.

This study investigated grazing induced spectral differences of vegetation patterns along gradients of grazing intensities for the most widespread vegetation types on the QTP using plot-based hyperspectral measurements. The spectral measurements were used to define spectral indicators for pasture degradation, which were applied to map asserted proxies for pasture degradation (vegetation cover, species numbers and grass percentage) on satellite images.

For this purpose, hyperspectral measurements using a HandySpec Field portable spectrometer (measuring range 305 to 1705 nm in 1nm steps) were taken at 11 sites on the north-eastern QTP. A transect design was chosen, since it was assumed that in a semi-nomadic pastoral system grazing intensity and therefore degradation are decreasing with increasing distance from settlements or camp-sites. Spectral measurements and vegetation records were taken at the heavily grazed begin of transects and the less grazed end of transects. A set of potential spectral indicators for degradation was derived from the spectra by calculating continuum removed absorption feature areas and NDVI-like narrow-band indices (NBI). The potential spectral indicators were compared between degraded and less degraded plots

by paired t-tests to assess spectral differences along the gradient. Additionally, linear regressions between the proxies for degradation and each of the potential spectral indicators were calculated to assess predictive performance of the indicators. The findings were exemplarily transferred to larger scales by applying these indicators on WorldView-2 (WV-2) scenes. The classifications were validated using the field records.

The results indicated that spectral differences between degraded and less degraded plots were obvious regarding a wide range of tested indicators. However, NBIs performed better than feature areas. The NBIs of the band combinations 750 - 1300 nm and 350 - 700 nm as well as 1400 - 1700 nm and 700 - 1300 nm showed closest correlations and can be considered as good spectral indicators for vegetation cover. Differences in vegetation cover were identified as major source explaining spectral differences between degraded and less degraded plots. Since species numbers were highly correlated to vegetation cover they could also be predicted by NBIs. WV-2 images were successfully classified into vegetation cover and species numbers using the identified indicators.

The results demonstrated the potential to classify proxies for pasture degradation on the QTP using spectrometer measurements and satellite data. Applying these techniques will contribute to a better estimation of degradation on the QTP on larger scales.

#### 8893-57, Session PS

### Execution of natural resources cadastral plan in Pasargadae city of Iran by using QuickBird images

Ghanimat Azhdari, Univ. of Tehran (Iran, Islamic Republic of); Kaveh Deilami, Univ. Teknologi Malaysia (Malaysia); Naser Mehrdadi, Mohammad Javad Amiri, Univ. of Tehran (Iran, Islamic Republic of)

Land information is crucial for planning and development in all countries. Iran is one of the countries that national lands, manage by governments, so there is a need for accurate land information. Consequently, executing of cadastral plan is an essential tool for authorities to deal with social, economic, technological and environmental problems.

In underdeveloped countries, cadastral surveying and cadastral mapping are time-consuming and expensive procedure. Also, it is mentioned as one of the major restrictions on economic development. Recently, employing remote sensing/ satellite and aerial images make new ways to resolve the problems of traditional approaches.

Thus, in this paper, the stages of preparing national cadastre maps in Iran by using satellite images are deliberated. In addition, the advantages and disadvantages of this technique are discussed. The case study is Pasargadae region which is located in north-east of Shiraz in Fars province with Latitude and longitude of 30° 15' 29" N and 53° 13' 29" E respectively. In order to generate the base maps of the project images from QuickBird satellite with 50-60 centimeters resolution were georeferenced by utilizing ground control points with accurate GPS coordinates.

Later, old paper maps with 1:10000 scale in local coordinate system from agriculture ministry in 1963 were digitized according to 1:25000 scale map from army geographical organization with AutoCad software. Beside all the above maps, paper maps with 1:50000 scale were used to find the changes during time. All the above maps were added to QuickBird images as new layers by using ArcMap software and required adjustments and corrections were applied to them.

In addition to above maps and information Google Earth Image also, were used to determine the changes.

By employing ArcMap software lands divide into 2 parts: firstly, lands with official document, and secondly national lands under different uses such as forestry, range management and desertification plans. In addition, some corrections were carried out to place the accurate locations of natural and man-made features such as roads, rivers, channels, water features and so on for reaching to international standard cadastre maps.

Consequently, final cadastral maps includes boundaries of each parcel, parcel identify, parcel dimension and area, various geographic features locations and names, forest, rangeland and pastureland borders etc.

The generation of natural resources cadastral plan leads to reliable

maps which increase the ability of authorities to monitor land-use and land-changes frequently.

Also, the current data base is updatable to the changes which occur during time as well as preventing of overlaying of information. In addition, producing cadastral maps prevent the destruction and illegal possession of natural lands by individuals.

8893-58, Session PS

### Design and construction of Information System of Ocean Satellite Monitoring for Air-sea CO<sub>2</sub> Flux (IssCO<sub>2</sub>)

Qiankun Zhu, The Second Institute of Oceanography, SOA (China); Fang Lei, Zhejiang Provincial Museum (China); Bai Yan, Xianqiang He, The Second Institute of Oceanography, SOA (China); Sun . Xiaoxiao M.D., Zhejiang Provincial Key Lab of GIS, Zhejiang University (China) and Zhejiang Provincial (China); Jianyu Chen, The Second Institute of Oceanography, SOA (China)

Climate change became top environmental issue in recent globalization and industrialization after COP15. The major view presented by IPCC recognized that the rise of global temperature is caused mainly by greenhouse gases, such as CO<sub>2</sub> generated by human activities. It also resulted in the high-frequent abnormal climate events. Satellite remote sensing is an efficient and economic measurement for CO<sub>2</sub> flux observation. This paper described the Information Systems of Ocean Satellite Monitoring for Ari-sea CO<sub>2</sub> Flux (IssCO<sub>2</sub>) which has been developed by the Second Institute of Oceanography, China. The reported system is designed for East China Sea specially. The main functions of IssCO<sub>2</sub> system include data acquisition, image process and map producing. It realizes the whole procedure from the satellite remote data obtaining to products distribution automatically. The final product of CO<sub>2</sub> flux is validated by in situ measurement. It can be obtained by using Web-GIS based service through Internet. The other accessible data includes SST, Chl-a, Wind, and so on. Our system offers the near real-time data query and download service in user-friendly way. It allows user to customize data analysis and data visualization.

8893-59, Session PS

### Impact of climate and anthropogenic changes on a periurban forest surface albedo derived from MODIS satellite data

Maria A. Zoran, Roxana S. Savastru, Dan M. Savastru, National Institute of Research and Development for Optoelectronics (Romania); Adrian I. Dida, Ovidiu M. Ionescu, Transilvania Univ. of Brasov (Romania)

Land surface albedo is a fundamental component in determining the earth's climate, being essential for assessment of both global and regional climatic models as well as for computing the surface energy balance. The seasonal and long-term forest vegetation dynamics that significantly impact the climate are reflected by the dramatic variations of albedo. The albedo of a forest surface is the extent to which it reflects light from the sun. Depending on its color and brightness, a change in forest land cover surface can have a positive (cooling) or negative (warming) effect on climate change. Forest land surface albedo is one of the most important biophysical parameter responsible for energy balance control and the land surface temperature and boundary-layer structure of the atmosphere. It has both diurnal as well as seasonal variations. In forest systems, albedo controls the microclimate conditions which affect ecosystem physical, physiological, and biogeochemical processes such as energy balance, evapotranspiration, photosynthesis. Due to anthropogenic and natural factors, forest land cover and land use changes result is the land surfaces albedo change. The main aim of this paper is to investigate the albedo patterns due to the impact of atmospheric pollution and climate variations on a periurban forest system placed to the North-Eastern part of Bucharest city, Romania based on satellite remote sensing Moderate Imaging Spectroradiometer (MODIS) data and climate station observations. The purpose of this paper is to describe spatio-temporal changes of a forest system and its

biophysical parameters derived from time series MODIS Terra/Aqua satellite data over 2003–2012 time period, each of which having specific influences on climatic regime. This study used MODIS land surface BRDF/albedo, NDVI/EVI (Normalized Difference Vegetation Index/ Enhanced Vegetation Index), ET (evapotranspiration), LST (Land Surface Temperature) products and in-situ monitoring ground data (as air temperature, aerosols distribution, relative humidity, etc.). Forest land cover change over the same investigated period was based on Landsat TM/ETM and IKONS imagery. Have been analyzed also other biogeophysical effects of forest land cover change in addition to surface albedo, particularly changes in the surface moisture budget leading to shifts in the ratio of latent and sensible heat fluxes and changes in rate of land surface temperature and precipitation. Due to deforestation albedo change appears to be the most significant biogeophysical effect in temperate forests. Satellite data and climate station observations show that surface albedo changes of a forested zone placed close to a large urban area highly respond to atmospheric pollution influence and climate variations. As the physical climate system is very sensitive to surface albedo, forest ecosystems could significantly feedback to the projected climate change modeling scenarios through albedo changes. In the frame of global climate warming, the results of this research may have a number of applications in weather forecasting, climate change, and forest ecosystem studies.

8893-60, Session PS

### Mine reclamation planning of Jharia area (Bastacola) through multi temporal remote sensing and GIS.

Sunny Soarabh, Mohammad S. Anwar, Indian School of Mines (India); Sunil Kumar, ISM Dhanbad (India)

Excavated overburden and ensuing from the surface mining activities pose a long term impact on the environment and the land safety measures. Lack of requisite reclamation of the stripped and the exploited coal in the BASTACOLA (Eastern Jharia, area) has resulted in the loss of substantially important agricultural and urban land. Accurate quantification of the extent of the area occupied by the overburden is important for the assessment and proper restoration of the waste land. Substantial quantity of non urban land monitored can be used to fill the excavated profiles of overburden, thus providing useful reclamation patterns. This research paper investigates the use of multi temporal remote sensing and satellite imagery for the location of the baseline of undulating overburden profiles to further their reclamation due to stripping activities. The process flow starts with the consideration of the imagery, LandSAT 5 TM multispectral ASTER DEM of the Jharia area, northing 23.756647N and easting 86.4214699 E, (year 2000 and 2010) for quantification of overburden, from national remote sensing center, India. The required AOI for the supervised classification, using maximum likelihood method, was obtained from the precise geo referencing and geosynchronisation of the area with the local coordinates. RASTIN of the AOI (obtained with ERDAS) via the ArcGIS gave the approximate legend in terms of the altitude of different pixel with total overburden area in lease and the volume above and below the reclamation plane. The area of interest extracted from the DEM was then processed to get the required level of reclamation through data mining and numerical analysis with the help of Newton's algorithm using DEV C++ compiler. However adjacent areas of thin or no forest land was taken into the AOI for subsistence and sustainable reclamation. The paper embeds the data acquisition through satellite imagery, data presentation via GIS and image registration and the final analysis and accuracy assessment. Besides the results obtained with the supervised classification of the AOI yields that overburden area have increased by 25.01% within the monitored timeframe, the reclamation surface calculated can then be shifted to the sustainable level at a later date. The markovian chain analysis with the cross tabulation of the land cover change with the supervised classification gives the quantities of conversion. Using the change matrices based on post transition comparison the data obtained can then be used for the prediction of the reclamation level for the area as the future part of the project. For this study transition matrices constructed from no reclamation to level plane (change matrices) obtained in the detection analysis and the modeling process implemented using the software supplied with the ENVI software. The interpolation of results and the statistics acquired can be used for the describing, analyzing and predicting the land use change over the considerable timeframe with the help of the Markov model and statistical and stochastic timeline analysis.

8893-61, Session PS

### Extraction of urban impervious surface information based on object-oriented technology

Aixia Liu, China Land Surveying and Planning Institute (China);  
Xiaojie Zhao, Jing Wang, Ting He, China Institute of Land  
Surveying and Planning (China)

Impervious surface is an important part of urban underlying surface, as well as an important monitoring index for city ecological system and environment changes. However, accurate impervious surface extraction is still a challenge. This paper uses the color, shape and overall heterogeneity features from the high spatial resolution remote sensing image to extract the impervious surface. An edge-based image segmentation algorithm is put forward to fuse heterogeneous objects which integrates edge features and multi-scale segmentation algorithm and uses the edge information to guide image objects generation. Results showed that this method can greatly improve the accuracy of image segmentation. Accuracy assessment indicated that the overall impervious surface classification accuracy and a Kappa coefficient yield 95.4% and 0.91, respectively.

8893-62, Session PS

### Attempt of identification of wet areas with ASTER images for archeological studies

Eleonora Bertacchini, Francesca Despini, Sergio Teggi,  
Alessandro Capra, Univ. degli Studi di Modena e Reggio Emilia  
(Italy); Marco Dubbini, Univ. degli Studi di Bologna (Italy)

Satellite images are a tool increasingly used in environmental monitoring and in recent years have become also strongly used in the field of archaeology. In this study it was conducted an experimental analysis on the identification of wetlands from satellite images in order to identify sites of interest from the archaeological point of view because probable sites of ancient settlements.

The studied area is the Plan de la Limagne which is located in North-East of the French city of Clermont-Ferrand. The terrain is flat and the area mainly consists of cultivated fields. In this area, archaeology attests an important sparse population, at least since the second Iron Age. For wet areas identification were used two ASTER satellite images and pre-existing cartography. Satellite sensor ASTER covers a large spectral region with 14 bands from visible to thermal infrared with high spatial, spectral and radiometric resolution. The spatial resolution changes with wavelength: 15 m in visible and near infrared (VNIR), 30 m for short wave infrared (SWIR), and 90 m in the thermal infrared (TIR). Each ASTER scene covers an area of 60 x 60 km. The two ASTER images were acquired in two different seasons (summer and winter). In this way it was possible to compare two different periods of the year with different climatic conditions in order to verify the permanence of wet areas with the change of seasons.

Different indexes have been used to identify wet areas. First of all, it was used the NDVI (Normalized Difference Vegetation Index) to discriminate bare soils. Secondly, through the Tasseled Cap transform, other indexes were obtained, such as the Greenness index, to identify better vegetation, the Brightness Index (SBI – Soil Brightness Index) and the Wetness Index. Then it has been used the ATI index (Apparent Thermal Inertia) that provides information on the thermal inertia of soils. Through these indexes, visual inspection and the study of spectral signatures, it has been tried not only to identify wetlands within the images, but also to find repeatable processes for the detection of these areas.

Some "anomalous" areas, that are probably wet areas, have been identified with this procedure. The identification of wet areas has been carried out in a raw way, this is surely a first approximation analysis. Certainly the in situ analysis would provide the possibility of a better evaluation, in fact field measurements could be used to calibrate the model and then find an effective and repeatable procedure for identifying wetlands.

To improve results in the future, images could be first pre-processed by applying the atmospheric correction required. Then could be used other stronger indexes such as SAVI (Soil Adjusted Vegetation Index), PVI (Perpendicular Vegetation Index) and TDVI (Temperature Vegetation Dryness Index).

8893-63, Session PS

### Wetland mapping and flood extent monitoring using optical and radar remotely sensed data and ancillary topographical data in the Zhalong National Natural Reserve, China

Xiaodong Na, Shuying Zang, Harbin Normal Univ. (China);  
Yuhong Zhang, Lei Liu, Harbin Normal University (China)

Information regarding the spatial extent and inundation state in the internationally important Wetlands as designated by Ramsar Convention is important to a series of research questions including wetland ecosystem functioning and services, water management and habitat suitability assessment. This study develops an expedient digital mapping technique using optical remotely sensed imagery of the Landsat Thematic Mapper (TM), Envisat ASAR active radar C-band imagery, and topographical indices derived from topographic maps. An ensemble classifier based on classification tree procedure (random forests) is applied to three different combinations of predictors: 1) TM imagery alone (TM-only model), 2) TM imagery plus ancillary topographical data (TM+DTM model), and 3) all predictors including TM imagery, ancillary topographical data and radar imagery, (TM + DTM + SAR model). Accuracy assessment results show that the radar and topographical variables reduced classification error rate of marsh obviously. The Kappa coefficients for the land cover classification increased significantly as radar imagery and ancillary topographical data were added. This study also provides a general approach to delineate the extent of flooding builds upon documented relationships between fields measured inundation state and SAR data response on each vegetation types. This analysis constitute a necessary step towards improved herbaceous wetland monitoring and provides ecologists and managers with vital information that is often missing or inferred using less direct means.

8893-64, Session PS

### An influence assessment of GSICS correction using sea surface temperature from geostationary satellite: COMS

Eun-Bin Park, Kyung-Soo Han, Jae-il Cho, Chang-Suk Lee,  
In-Hwan Kim, Kyoung-Jin Pi, Jae-Hyun Ryu, Jung-Mok Ha,  
Pukyong National Univ. (Korea, Republic of)

There is a strong need for accurate estimation of radiance from satellite regarding global climate circulation, change and Earth's atmosphere. Exact radiance measurements by the satellite are also important in numerical weather prediction models for climate change detection. In addition, the accurate measurements from the satellite rely critically on radiometric calibration of the sensors, which is a series of operation that applies the calibration coefficients. Related to improved calibration and inter-calibration of the sensors, the World Meteorological Organization (WMO) and the Coordination Group for Meteorological Satellite (CGMS) initiated the Global Space-based Inter-Calibration System (GSICS) in 2005, which provide coefficients to the user community to adjust satellite observations. The GSICS corrections were applied to Communication Ocean and Meteorological Satellite (COMS), which have Meteorological Imager (MI) sensor for meteorological missions. IR data from the COMS MI were calibrated by coefficients of the GSICS corrections comparison with IASI sensor that is reference sensor of the GSICS corrections. The data from the GSICS corrections were applied to level 2 products to assess the effects of the GSICS corrections. As the level 2 product, sea surface temperature (SST) products were chosen and calculated by IR channels, which were corrected by GSICS corrections.

8893-65, Session PS

## Lake Manyara catchment vegetation phenology response to climate variability over the past 30 years using RS, Northern Tanzania

Dorothea M. Deus, Richard Gloaguen, Technische Univ. Bergakademie Freiberg (Germany)

In this study we evaluate the response of lake Manyara catchment remotely sensed vegetation phenology to climate change. Changes in vegetation phenology affect the carbon and water cycles and energy fluxes through photosynthesis and evapotranspiration. Analysis of vegetation phenology changes can provide quantitative information on the influence of climate variability on the region. We relate phenology information derived from AVHRR and MODIS NDVI to the Indian Ocean Dipole (IOD), the Pacific Decadal Oscillation (PDO), and the Multivariate ENSO Index (MEI) and climate datasets. We observe that from 1982 to 2012 the trend of vegetation condition using NDVI exhibit almost similar fluctuation during both rain and dry season in a year. We also detect that the June–October season strongly correlates with PDO in March–April–May, while the PDO in December–February correlates with the start of the February– June season. The influence of IOD on the vegetation phenology is insignificant.

8893-66, Session PS

## Glacier stagnant in central Karakorum derived from DEOS mass transport model GRACE data and one monthly degree-day model

Xiaowen Zhang, Lanzhou Univ. of Finance and Economics (China); Shiqiang Zhang, Junli Xu, Cold and Arid Regions Environmental and Engineering Research Institute (China)

### 1. Introduction

Glaciers in the Greater Himalaya are reported to be diminishing rapidly due to climate warming in 1990s. However, there are some regional 'anomalies' in central Karakorum, where many glaciers expanded and numbers of glacier surged while many glaciers in the same basin retreated (Hewitt, 2005). 58% of 42 glaciers in the Karakoram were stable or slowly advancing with mean rate of about  $8 \pm 12$  m a<sup>-1</sup> during 2000 to 2008 (Scherler and others, 2011). Long-term glacier and climate records from high elevations in the Karakoram are virtually absent, it need to investigate from different sources.

### 2. Data and Method

The total monthly water storage variation in HRB was derived from the Delft Institute of earth observation and space system (DEOS) Mass Transport Model release 1 (DMT-1) Gravity and Climate Experiment (GRACE) data. The water storage variation of unglaciated area was simulated by using the Variable Infiltration Capacity (VIC) Micro hydrological model. The observed mass balances of glacier area were obtained from the mass variation difference between the GRACE data and the VIC model. The cumulative mass balance (CGM) also measured by the differences of glacier surface elevation between SRTM DEM and ASTER DEM.

### 3. Results

The comparison between simulated mass variations in glacier areas and unglacierized areas suggested that the basin mass variation is mainly controlled by the glacier mass balance. The simulated mass balance matches well with the observed one derived with the DMT-1 GRACE observations on the seasonal cycle. This indicates that the simulated ablation of glacier area seems to have a relatively high accuracy.

The GCM derived from GRACE data has no significant trend, indicates that the glacier in HRB didn't have significantly retreated during 2003 to 2008 on the regional scale. However, the simulated cumulative mass balance is -830.3 mm, indicates that the glacier accumulation probably underestimated.

The average glacier surface elevation difference between SRTM DEM and ASTER DEM is  $11.8 \pm 3.2$  m. The elevation differences along the main stream line of Batura glaciers and Mulungutti glacier are  $15.3 \pm 3.2$  m and  $3.3 \pm 3.2$  m, respectively, which indicates that ice volume

even increased since 1999.

Precipitation has a large spatial and altitudinal variability in the Karakoram mountain region, the underestimation of heavy snowfall at steep rockwalls areas is probably the main reason for underestimation of glacier accumulation and mass balance.

### Reference

Hewitt, K. 2005. The Karakoram Anomaly? Glacier Expansion and the 'Elevation Effect,' Karakoram Himalaya. Mountain Research and Development, 25(4): 332-340.

Scherler, D, Bookhagen B and Strecker MR. 2011. Spatially variable response of Himalayan glaciers to climate change affected by debris cover. Nature Geoscience, 4: 156-159.

8893-67, Session PS

## Comparison of different along the track high resolution satellite stereo-pair for DSM extraction

Konstantinos G. Nikolakopoulos, Univ. of Patras (Greece)

The possibility to create DEM from stereo pairs is based on the Pythagoras theorem and on the principles of photogrammetry that are applied to aerial photographs stereo pairs for the last seventy years. The application of these principles to digital satellite stereo data was inherent in the first satellite missions. During the last decades the satellite stereo-pairs were acquired across the track in different days (SPOT, ERS etc.). More recently the same-date along the track stereo-data acquisition seems to prevail (Terra ASTER, SPOT5 HRS, Cartosat, ALOS Prism) as it reduces the radiometric image variations (refractive effects, sun illumination, temporal changes) and thus increases the correlation success rate in any image matching.

Two of the newest satellite sensors with stereo collection capability is Cartosat and ALOS Prism. Both of them acquire stereopairs along the track with a 2,5m spatial resolution covering areas of 30X30km.

In this study we compare two different satellite stereo-pair collected along the track for DSM creation. The first one is created from a Cartosat stereopair and the second one from an ALOS PRISM triplet. The area of study is situated in Chalkidiki Peninsula, Greece. Both DEMs were created using the same ground control points collected with a Differential GPS.

After a first control for random or systematic errors a statistical analysis was done. Points of certified elevation have been used to estimate the accuracy of these two DSMs. The elevation difference between the different DEMs was calculated. 2D RMSE, correlation and the percentile value were also computed and the results are presented.

8893-68, Session PS

## Open quarry monitoring using gap-filled Landsat 7 ETM + SLC-off imagery

Konstantinos G. Nikolakopoulos, Univ. of Patras (Greece)

Active quarries are at the same time a necessity but also a source of pollution. Necessity as they supply to the construction companies the necessary aggregates and source of pollution as they affect biodiversity, vegetation cover and threaten water resources. The objective of this work is to indicate a monitoring methodology using Landsat ETM SLC off imagery.

On May 31, 2003, the Scan Line Corrector (SLC), which compensates for the forward motion of Landsat 7, failed. Without an operating SLC, the Enhanced Thematic Mapper Plus (ETM+) line of sight now traces a zig-zag pattern along the satellite ground track. As a result, imaged area is duplicated, with width that increases toward the scene edge. An estimated 22 percent of any given scene is lost because of the SLC failure. The maximum width of the data gaps along the edge of the image would be equivalent to one full scan line, or approximately 390 to 450 meters. The precise location of the missing scan lines will vary from scene to scene.

In this study a gap filling technique for Landsat ETM SLC off imagery is evaluated. Different Landsat 7 ETM+ images SLC off were restored and then compared to historical data and data from other sensors. The restored images have been used in order to monitor the expansion of an open quarry in western Peloponnese and the results are presented.

8893-69, Session PS

## Remote sensing and dynamic landscapes in region of Nâama, Algeria

Idriss Haddouche, Univ. Abou Bekr Belkaid Tlemcen (Algeria)

This study focuses on the characterization of desertization in the high plains steppe of southern West Algeria Oranaise by analyzing changes over time, reflecting better environmental response to climate change and anthropogenic pressures. It addresses voluntary all factors relating to dynamic landscapes issue.

To do this, we are based on a multiple approach and spatial analysis incorporating several indicators, which enabled us to assess the state of this phenomenon. The treatment applied to remotely sensed data on the Nâama region highlighted the changes that have affected the study area and characteristics of the ecological environment. The diachronic study by the satellite images has allowed us to make measurements of surface ground cover between two shots (for digitizing and thresholding). It notes that the recovery rate of vegetation, between medium and high, decreases from 39% to 7% of the area between 1987 and 2007. This decline is explained by the low recovery rate of vegetation (<30%) and bare soil that are increased from 61% to 93%.

The processing satellite imagery optical bi-dates and different sensors have highlighted widespread degradation of cover plant which accelerates the process of desertization whose socioeconomic impacts can be interpreted by the decrease of agricultural production and reduced grazing spaces, as fuelling factors for mass exodus from rural areas to cities already overcrowded as Mecheria, Nâama and Ain-Sefra.

8893-70, Session PS

## Integration of Standardized Precipitation Index (SPI) and remote sensing for drought monitoring in Sulaimani, the Kurdistan region of Iraq

Ayad M. Fadhil, Salahaddin Univ. (Iraq); Sarchil H. Qader, Univ. of Southampton (United Kingdom)

Drought has dramatically affected Kurdistan region and the other parts of Iraq throughout the last years which characterized by a large drop in the rainfall averages. Geo-information technology (Geographic Information Systems GIS, Remote Sensing RS, and Global Positioning System GPS) has played a key role in monitoring, mapping, and assesses different types of hazards either natural or man-made. Three Landsat images acquired in September of 1990, 2007, and 2008 which covered Sulaimaniya governorate were utilized for the purposes of this study. Six Landsat based indices; the Normalized Difference Vegetation Index NDVI, Transformed Soil Adjusted Vegetation Index TSAVI, Tassel Cap Greenness TCG, Tasseled Cap Wetness TCW, Land Surface Temperature LST, and Normalized Differential Water Index NDWI, as well as to the Standardized Precipitation Index SPI as a meteorological index have been used. The aim of this study was to investigate the role of an integration of remotely sensed based indices and the SPI index for drought monitoring in Sulaimaniya governorate, the Iraqi Kurdistan region during the years 1990, 2007, and 2008. The spectral and meteorological indices were employed to monitor the drought status and its impacts in the study area. Change detection was applied to the resultant thematic images to estimate the spatiotemporal changes that happened between the years 1990 and 2008, and for detection the drought severity as well. The study results revealed that a severe drought has occurred in Sulaimani governorate in 2008, whereas the lowest SPI value was -2.122 observed in Ahmad Awa site. Similarly, the drought of 2008 led to a significant decrease in the vegetative cover, water surface area, soil/vegetation moisture, and to an increase in the barren soil areas. The drought affected severely on the vegetation cover in the study area that was significantly declined by 28.4% in 2008 compared with 2007. Likewise there were significant shrinkage in the water surface bodies areas such as the lakes in the study area. A Lake Dukan surface area was significantly shrank by 16.5 and 32.5 % in 2007 and 2008, respectively compared with 1990. Moreover, Lake Darbandikhan was shrunk seriously to become a pond and a small stream in 2008. It is further confirmed that the NDVI was performing well for depicting the vegetation cover and was more realistic than the other vegetation indices that has been

used in the study. Significant correlations were found between the SPI index and the total Calcium Carbonate and the Cation Exchange Capacity CEC in the soil samples of the study area. The combined NDVI-SPI indices maps were produced and revealed that a worst and a severe drought was taking place in the Sulaimaniya district in 2008. The integrated indices can be employed as an efficient tool for drought monitoring, and in regional water resources management. Since Iraq is characterized by arid and semi-arid climatic conditions, it can be concluded that the use of combined indices of NDVI-SPI provides more reliable results for drought monitoring in the study area than any single index.

8893-71, Session PS

## Land use and land cover classification, changes and analysis in gum arabic belt in North Kordofan, Sudan (Invited Paper)

Hassan E. Adam, Univ. of Kordofan (Sudan); Elmar Csaplovics, Technische Univ. Dresden (Germany); Mohamed E. Elhaja, Univ. of Kordofan (Sudan); Mustafa M. El-Abbas, Technische Univ. Dresden (Germany)

The gum arabic belt in Sudan plays a significant role in environmental, social and economical aspects. The importance of forests and natural resources is indisputable, when considering the developing countries especially areas situated in the arid and semi-arid climatic zones. This research was conducted in North Kordofan State, which is affected by modifications in conditions and composition of vegetation cover trends in the gum arabic belt as in the rest of the Sahelian Sudan zone. This research studies the classification, changes and analysis of the land use and land cover in the gum arabic belt in North Kordofan State, Sudan. The study used imageries from different satellites (Landsat and ASTER) and multi-temporal dates (MSS 1972, TM 1985, ETM+ 1999 and ASTER 2007) acquired in dry season (November). The imageries were geo-referenced and radiometrically corrected by using ENVI-FLAASH software. Image classification (pixel-based), post-classification change detection and accuracy assessment were applied. Application of multi-temporal remote sensing data in gum arabic belt demonstrated successfully the identification and mapping of land use land cover into five main classes. Forest dominated by Acacia senegal class was separated covering an area of 21% in the year 2007. The land use and land cover structure in the gum arabic belt has obvious changes and reciprocal conversions between the classes indicating the trends and conditions caused by the human interventions as well as ecological impacts on Acacia senegal trees. Also the study revealed that A drastic loss of forest resources occur in the gum arabic belt in North Kordofan during 1972 to 2007 (25% for Acacia senegal trees). The study concluded that, using of traditional Acacia senegal-based agro-forestry as one of the most successful forms of natural forest management in the gum belt will give successful land cover recovery.

8893-72, Session PS

## Assessment of historical land use reconstruction and effect on the paleoflood

Pingping Luo, Bin He, Kaoru Takara, Kyoto Univ. (Japan); Weili Duan, Hunan Women's College (China); Daniel Nover, U.S. Environmental Protection Agency (United States)

Land use change has significant impacts on watershed processes that are often central to water related disasters. In this article, we chose the Kamo River basin (KRB) in Kyoto city, Japan as a study site because it experiences frequent heavy rainfall. The recent land use was converted from 100 meter remote sensing images in 1976 and the paleo-land use was reconstructed using the GIS-based paleo-landuse reconstruction (PLUR) methods. Moreover, land use change analysis was used to explore the effects of human activities on the hydrological response under the paleo and present environment conditions using a grid-based distributed hydrologic model. Based on the recent land use in 1976 and PLUR program, we reconstructed the historical land use of 1843, 1902, 1927. Peak river discharge under the recent land use was shown to have increased and arrived earlier due to the increasing development of buildings and decreasing areas of forests and rice fields. Finally, we discuss the impact of land use change on river

discharge and implications for land use planning in the future. This study connects remote sensing methods with watershed-hydrologic assessments and paleo-hydrology and offers guidance for flood risk management.

#### 8893-32, Session 9

### Evaluation of commercial available fusion algorithms for Geoeye data

Konstantinos G. Nikolakopoulos, Univ. of Patras (Greece);  
Aristides D. Vaiopoulos, Univ. of Athens (Greece)

GeoEye-1 is the first commercial satellite that collects images at nadir with 0.41m panchromatic and 1.65m multispectral resolution (panchromatic imagery sold to commercial customers is resampled to 0.5m resolution). In this study ten fusion techniques and more especially the Ehlers, Gram-Schmidt, High Pass Filter, Local Mean Matching (LMM), Local Mean and Variance Matching (LMVM), Modified IHS (ModIHS), Pansharpen, PCA, HCS (Hyperspherical Color Space) and Wavelet were used for the fusion of Geoeye panchromatic and multispectral data. The panchromatic data have a spatial resolution of 0.5m while the multispectral data have a spatial resolution of 2.0m. The optical result, the statistical parameters and different quality indexes such as ERGAS, Q, entropy and QNR were examined and the results are presented. The broader area of Pendeli mountain near to the city of Athens Greece was selected for this comparison. It has a complex geomorphology. The area combines at the same time the characteristics of an urban and a rural area thus it is suitable for a comparison of different fusion algorithms.

#### 8893-33, Session 9

### Forest structure estimates with GEOBIA and multiscale optical sensors

Mustafa M. El-Abbas, Elmar Csaplovics, Taisser H. Deafalla,  
Technische Univ. Dresden (Germany)

Sustainable forest management requires flexible, reliable and up-to-date information. Possible solution for updating forest attributes is GEOBIA (GEOgraphic Object-Based Image Analysis), which are presently being investigated and optical multispectral sensors are being considered as a data source to cover large areas rather than time consuming and costly at plot-level forest inventory method. The GEOBIA approach persists to reveal its effectiveness in remote sensing data analysis, which provides paradigms that integrate analyst's expert knowledge to generate semantically meaningful image-segments in way that emulate human perception. A hierarchical image objects have been generated, and the segments to predict forest attributes can be inferred at a higher level based on Land Use/Land Cover (LU/LC) segments. These segments might contribute for the reduction of problems associated with the analysis of discrete spectral value of pixel, such as illumination and shaded tree crowns. However, the challenge in this paper is to introduce a GEOBIA as a sophisticated framework toward the automation of forest structural attributes estimate. VNIR bands of ASTER scene were examined to develop models for the estimation of stand density, crown height, basal area, and volume. The integration of high-resolution satellite imagery offer exciting possibilities to enhance the measurement, mapping, and modeling of forest attributes. In this context, the higher resolution RapidEye scene was introduced to test the feasibility of increased quality of spectrum. Moreover, one of the addition values of this work was to predict a vertical attribute (i.e. crown height), which it has been rarely investigated based on optical sensors. Analyses were performed over a forested selected site in Blue Nile region of Sudan. The framework of the present research involved the following main pillars: (I) meaningful segment extraction, (II) field derived sample selection, (III) forest attribute generalization, (IV) model validation, and (V) mapping structural attributes based on the selected models. The rationale for incorporating these data is to offer a semi-automatic GEOBIA approach from which forest attribute is acquired through automated segmentation algorithms at the delineated tree crowns or clusters of crowns level (i.e., mean segment size of 0.04 to 0.09 ha). Correlation and regression analyses were applied to identify the relation between wide range of spectral, textural, contextual image metrics (e.g., Digital Number "DN", grey-level co-occurrence matrix "GLCM", Object Layer Value "OLV", etc.), and the field derived forest

attributes. Forest structural attribute estimation results acquired from our GEOBIA framework reveal strong relationships and precise estimates, based on the highest determination coefficient ( $R^2$ ) and the lowest Residual Mean Square Error (RMSE) criteria. Subsequently, the best fitted models were cross-validated with independent set of field derived samples, which revealed high degree of precision for the both set of imagery used. An important question is how the spatial resolution and spectrum used affect the quality of the developed model will be also answered based on the different sensors examined. Future work, addition testing is required to generalize the results in situations covering large areas, different weighting of the introduced data, and various forest stand conditions.

#### 8893-34, Session 9

### Ground-based multispectral measurements for airborne data verification in non-operating open pit mine 'Kremikovtsi'

Denitsa Borisova, Hristo N. Nikolov, Doyno Petkov, Space  
Research and Technology Institute (Bulgaria)

The impact of the mining-concentration industry on the environment is presented all over the world. Non-operating ferrous Kremikovtsi open pit mine and related waste dumps and tailings are the large pollutants for a densely populated region in Bulgaria. Correct estimation of the distribution of the iron oxides in open pit mines and the neighbouring regions is a key issue for the ecological state assessment of land cover. For this study airborne data combined with ground-based in-situ and laboratory acquired data were used for data verification and assessment of the environmental state from previous mining activities. As main indicator for presence of pollution the iron content was chosen since it could be reliably identified in the ranges used in this study and because of the wide-spread iron compounds in the most of the minerals, rocks and soils. The number of samples from every source was taken in the way to be statistically confident. Soil samples together with GPS measurements were collected during a field campaign in the study area for two types of laboratory measurements: the first one, chemical and mineralogical analysis and the second one, non-destructive spectroscopy. In this work satellite data from Landsat instrument TM/ETM+ and from ALI were used. Ground-based (laboratory and in-situ) spectrometric measurements were performed using designed and constructed in Remote Sensing Systems Department at Space Research and Technology Institute thematically oriented spectrometric system TOMS working in the 0.4-0.9 micrometers range. Spectral transformations such as normalized difference and relation using two wavelengths were applied for the proper comparison between the data obtained from the different sources. Dependence between the various spectral transformations and the quantitative content of the iron in the different type of compounds was established. The achieved results proved that this methodology could be extended for other regions of the country polluted by the mining activities and was also tested in the region of the copper and zinc extraction. In the next step of our research we intend to use the obtained results in the multitemporal analysis of the satellite and ground-based multispectral data for the same and the similar regions of interest.

#### 8893-35, Session 9

### Optimizing multiresolution segmentation algorithm using empirical methods: exploring the sensitivity of supervised discrepancy measures

Chandi Witharana, Univ. of Connecticut (United States);  
Dirk Tiede, Univ. Salzburg (Austria); Daniel L. Clvco, Univ. of  
Connecticut (United States)

Image segmentation serves as an important pre-requisite in the geographic object-based image analysis (GEOBIA) framework. The multiresolution segmentation (MRS) has proven to be one of the most successful segmentation algorithm in many remote sensing applications. It has been implemented originally in the eCognition software (Trimble Geospatial), lately the algorithm has been also implemented in similar form into other software packages, like for example BerkeleyImageSeg (BIS; <http://www.imageseg.com>) or



InterImage. This algorithm is relatively complex and user-dependent; scale, shape, and compactness are the main parameters available to users for controlling the algorithm. Plurality of segmentation results is common because each parameter may take a range of values within its parameter space or different combinations of values among parameters. Finding optimal parameter values through trial-and-error process is commonly practised at the expense of time and labour, thus, several alternative supervised and unsupervised methods have been proposed and tested. In case of supervised empirical assessments, discrepancy measures are employed for computing measures of dissimilarity between a reference polygon and an image object candidate. Evidently the reliability of the optimal-parameter prediction heavily relies on the sensitivity of the segmentation quality metric. The idea behind pursuing optimal parameter setting is that, for instance, a given scale setting provides image object candidates different than the other scale setting; thus, by design the supervised quality metric should capture this difference. In this exploratory study, we aimed to unravel the discriminative capacity of a recently proposed supervised quality metric (Euclidean Distance 2 (ED2)) for selecting optimal parameter values. We selected test image scenes from three different space-borne sensors with varying spatial resolutions and scene contents and systematically segmented them using the MRS algorithm at a series of parameter settings. The discriminative capacity of the ED2 metric across different scales groups was tested using non-parametric statistical methods. Our results showed that the ED2 metric significantly discriminates the quality of image object candidates at smaller scale values but it loses the sensitivity at larger scale values. This questions the meaningfulness of the ED2 metric in the MRS algorithm's parameter optimization. Our contention is that the ED2 metric provides some notion of the optimal scale parameter at the expense of time. In this respect, especially in operational-level image processing, it is worth to re-think the trade-off between execution time of the processor-intensive MRS algorithm at series of parameter settings targeting a less-sensitive quality metric and an expert-lead trial-and-error approach.

#### 8893-36, Session 10

### Development of a fire detection algorithm for the COMS (Communication Ocean and Meteorological Satellite)

Goo Kim, Dae Sun Kim, Yang Won Lee, Pukyong National Univ. (Korea, Republic of)

Forest fire causes much damages such as decrease in biodiversity and increase in flood hazard in ecological and economic aspects. Mountain area occupies more than half of land in Korea. When the forest fire occurs, they often suffered from extensive damages. Recently, big and small fires caused much ecological and economic damages in Korea. One of the reasons for the damages is because they couldn't rapidly deal with the fire in initial stages. Satellite remote sensing has an advantage of observing extensive area continuously so that we can cope with the forest fire using satellite remote sensing. Recently Korea launched a geostationary satellite COMS(Communication Ocean and Meteorological Satellite) that provides meteorological data every 15 minutes. In this study, we used the COMS data consisting of SWIR(short wave infrared:3.7 micrometer), IR1(infrared1:10.8 micrometer) and Visible(0.65 micrometer) channels. We aim to develop a near-real time fire detection algorithm using COMS data. Generally, fire pixels tend to have a significant increase in 4 micrometer brightness temperature but an insignificant increase in 11 micrometer brightness temperature. In order to detect fire, we first select potential fire pixels using threshold values for the brightness temperatures of 4 micrometer and 11 micrometer bands. We then select fire pixels more precisely by comparing the statistics between the selected potential fire pixel and its background window. We finally eliminate false alarms from the result.

False alarms occur mainly due to sun glint, desert, coastline and industrial complex. False alarm by sun glint occur when the angle between sun reflection and satellite location is almost the same. We eliminate such cases by using solar zenith angle, view zenith angle and relative azimuth angle. False alarms by coastline can occur because water pixels have low value in the 4 micrometer brightness temperature. So the pixels surrounded by water have relatively high brightness temperature in 4 micrometer, which makes the pixel classified as a fire pixel. Industrial complexes also can be misclassified as fire pixels, because they emit massive heats. We eliminated the false alarms by coastline and industrial complex using a land/sea

mask and GIS maps respectively.

We selected the 10 fire places with the damaged area over 0.5 ha on April 1, 2011.

We confirmed the result of our fire detection algorithm using statistical data of Korea Forest Service and ASTER(Advanced Spaceborne Thermal Emission and Reflection Radiometer) image. Eight of the ten places were correctly detected, but two of them were not. One of them was in the Quercus area and the energy emitted by the burning of "Quercus" is much less than other types of trees.

Another misdetection is because of too short burning time.

This result is a remarkable outcome when considering the limited channels of the COMS. To improve the accuracy and reliability of our algorithm, We should apply to dynamic threshold by the seasonal analyses of the brightness temperatures.

#### 8893-37, Session 10

### The impact of the day of observation of image composites on adequate time series generation

Rene R. Colditz, Rainer A Ressler, CONABIO (Mexico)

Many time series analysis techniques such as harmonic analysis require equidistant observations of a time series. In addition, ecological studies monitoring the phenological state of the vegetation (start, end, middle of the growing season) rely on highly accurate time series. Many remote sensing products useful for time series analysis and seasonal monitoring studies are offered in form of composites, because the view to the ground is often obscured by clouds or haze or the sensor may have failures such as missing lines. A composite combines a number of observations of a defined period and either selects the best value or computes a new value such as the mean. For vegetation indices (VI) common compositing rules use the maximum value or combine this rule with a selection of observations that are close to nadir; both are based on the assumption that VIs with high values were less likely obscured by atmospheric constituents or sensor issues. That, however, results in observations sampled at varying time intervals and rules out a large number of time series analysis techniques. If the day of observation is not known or not used in time series generation, it is common to define the starting day as the day of observation. On the one hand this assumption, from a practical point-of-view, overcomes the issue concerning potential time series analysis techniques but temporally shifts the series to earlier days. The issue may be mitigated by assuming the middle of the compositing period as the day of observation. However, it would be certainly preferable to use the actual day of observation and estimate from that time series any other day to sample a new time series at any desired interval.

This study investigates the impact of either using the day of observation to generate a time series or to assume the starting or middle day of the compositing period. For this study daily MODIS surface reflectance (reference set) and 16-day MODIS VI composites of 500m spatial resolution were employed. A 1000x500km region in central Mexico served as study site. Several statistical measures were used for time series analysis, including temporal cross-correlation, the root mean square error, and harmonic analysis. A temporal shift of approximately seven days with a high variability is introduced when using the starting day of the compositing period. The middle day mitigates the mean error close to zero but results in a high variation in error. Only time series that take into account the day of observation and estimate from that samples at equidistant intervals can be used for correct estimation of temporal characteristics and are also reliable for time series analysis techniques from a theoretical point-of-view. The latter will be exemplarily demonstrated for phenological states such as the start and end of the growing season.

#### 8893-38, Session 10

### Applying the Manning equation to determine the critical distance in non-point source pollution using remotely sensed data and cartographic modelling

Liliana M. Oliveira, UFMG (Brazil); Nádia A. P. Santos, Instituto

Mineiro de Gestão das Águas (Brazil); Philippe Maillard, UFMG (Brazil)

Non-point source pollution (NPSP) is perhaps the leading cause of water quality problems and one of the most challenging environmental issues given the difficulty of modelling and controlling it. In this article, we applied the Manning equation, a hydraulic concept, to improve models of non-point source pollution and determine its influence as a function of slope-roughness, that are parameters of the Manning equation. Quantifying and controlling NPSP often relies on mathematical models based on hydrological, hydraulic and water quality variables. While some relatively simple models often fail to capture the subtleties of NPSP problems, more complex models are frequently impractical to implement due to lack of data or data of inappropriate quality. With increasing capabilities of Geographic Information Systems (GIS), the most reliable models are now "distributed" meaning that they are spatially explicit. Since controlling whole watershed is often impossible, it is generally agreed that most attention must be given to the immediate surroundings of streams. This principle has made Brazil, among many other countries, implement specific laws to protect bands of fixed width from the river banks. However, it appears clear that the distance of greater influence is also a function of the relief (slope) and the land cover. The Manning equation is an empirical formula that governs open channel flow. In our study the equation is somewhat taken out of its usual context to be applied to the flow of an entire watershed. Here a digital elevation model (DEM) from the SRTM satellite was used to compute the slope and data from the RapidEye satellite constellation was used to produce a land cover map later transformed into a roughness surface. The combination of roughness and slope can then characterize the time for a raindrop, falling anywhere in the watershed to reach the stream. Given soil data, the time could then be transformed into infiltration and thus determine the minimum distance at which pollutants would not be able to reach the stream. We implemented our approach using region-based segmentation/classification software to produce the land cover map and an of-the-shelf GIS software for computing the remaining Manning variables. The methodology was applied to a watershed with 1433km<sup>2</sup> in Southeast Brazil mostly covered by forest, pasture, urban and wetlands. Buffers of varying width were generated inside of which the proportions of land cover were correlated through regression with four water quality parameters measured in situ: nitrate, phosphorous, faecal coliforms and turbidity. It was found that slope buffers outperformed fixed buffers with higher coefficients of determination up to 15%.

8893-39, Session 11

### Identification of bamboo patches in the lower Gangetic plains using very high resolution WorldView 2 imagery

Aniruddha Ghosh, Pawan K. Joshi, TERI Univ. (India)

Bamboo is a versatile group of plants which is capable of providing ecological, economic and livelihood security to the people in tropical countries. Realising the potential usage, India has identified National Bamboo mission for addressing the issues relating to the development of bamboo in the country. One of the major challenges is inventory of species through monitoring of existing coverage and assessment of potential sites for enhancing it. Hence, knowledge of spatial distribution of bamboo patches becomes necessary for the evaluation and monitoring of this resource.

A review of existing research suggests that bamboo mapping has mostly been performed using medium resolution satellite imagery. Such spatial resolution is ineffective for accurate classification when bamboo occurs in mosaic of small and mixed patches. The present study attempts to address this problem using Very High Resolution (VHR) (2 m multispectral/0.5 m panchromatic) WorldView 2 (WV 2) imagery. The study was conducted in South 24 Parganas, West Bengal which is a mosaic of rain fed croplands, plantations, forests and water bodies. West Bengal, a part of Bengal Bay ecological region is one of the areas where bamboo grows naturally.

Reference samples of bamboo patches were identified through ground survey. Spectral distances (Transformed Divergence, TD) of bamboo with croplands and other tree species suggest that only multi-spectral bands are not sufficient for differentiation of bamboo. Therefore the classification was carried out using additional features namely 2nd order texture measures of the first 3 principal components (PCs) of pan-sharpened 8 MS bands. Supervised kernel based (Support Vector

Machine, SVM) and ensemble based (Random Forest, RF) machine learning algorithms were applied on the dataset. Moreover, RF based variable importance was analyzed to find the most informative input predictors for classification of bamboo. Altogether seven land use land cover classes were mapped which include agricultural land, built-up, bamboo patches, large canopies (e.g. ficus), small canopy (e.g. mango, coconut), fallow land and water body.

The findings of this study indicate that bamboo mapping is possible with VHR WV 2 imagery. Variable importance analysis indicated that mean texture measure of principal component 1 and 2, and spectral information of MS band 8 (NIR 2) were the three most important predictor layers for bamboo mapping. Unlike, RF (accuracy 69%) higher overall accuracy of 73% was achieved using SVM classifier. The producer and user accuracy for bamboo was high. Using VHR pan-sharpened (0.5 m) image, bamboo could not be well differentiated in the areas surrounding residential units and intermixing of bamboo was seen with other canopies. The outcome of this study shows that the present framework is not only capable of identifying bamboo patches but also very promising for detecting other tree species which would support the development National Bamboo mission and related monitoring programs.

8893-40, Session 11

### Use of empirical land use dynamics models including climate and socio economic parameters: a case study in rain-fed agricultural area

Vidhya V. Rangasamy, Manonmani Raju, Anna Univ. Chennai (India)

Land use/ Land cover change encompass some of the most important human alteration affecting the surface of the earth. The changes in the agricultural patterns and the forest land are one important indicators of serious socio economic and environmental management implications. The main challenge for the agriculture sector from the rainfed areas is to sustain present livelihood conditions and to secure future demands and typically they are more fragile to the changing climates and demands. If the issues are not effectively addressed in a holistic manner, they can lead to major environmental problem. Remote Sensing and Geographical Information System coupled with empirical modeling is recognized as a powerful effective tool in detecting land use change and predict future changes. In this study, modeling and prediction of agricultural land use change across space and time using Logistic Regression and Geographically Weighted Regression in dry land region is attempted. The Pudukottai district that falls in the dry belt of southern India is taken as study area. Land use and land cover change is the function of interacting factors which are known as drivers, agents and determinants. The land use pertaining to 1985, 1995 and 2005 for the study area were generated to study and model the land use dynamics. The drivers for land use change based on the factors such as climatological data and socio economics data were identified and these are the triggers for particular change vector. The influence of these parameters was modeled using geographically weighted regression and binary logistic regression methods and applied to derive 2005 land use map. The models were validated with the help of land use map generated with 2005 remote sensing data. The validated ROC values are 0.64 and 0.72 respectively. The predicted land use based on the intrinsic driving parameters of the selected area using such models will be an important input for planners and administrators to understand the land use dynamics and to adapt suitable mitigation and preventative measures.

\*Institute of Remote Sensing, Anna University, Chennai 600 025, India  
Ph: 91 44 2235 8155; 09884113113 Fax: 91 44 2235 2166

mail: vidhya@annauniv.edu , vidhya.v.vanan@gmail.com , manonmani.mansa@gmail.com

8893-41, Session 11

### Assessment of vegetation change and its causes in the West Liaohe River Basin of China using SPOT-VGT image

Fang Huang, Huijie Zhang, Ping Wang, Northeast Normal Univ. (China)

Vegetation is sensitive to changes in the ecological environment in arid and semiarid regions, and the dynamics of vegetation cover changes may provide vital information for ecological environmental protection and early warning of ecosystem degradation. The West Liaohe River Basin is the east fringe of agro-pasture transitional zone in northern China and highly sensitive to global change. It is also one of the key regions in the West development strategies implemented by the Chinese Government. This region has been occupied by agricultural and nomadic culture alternatively in history and has been suffering high risk of sandy desertification during the past century. The main purposes of this study are to adequately investigate the interannual and seasonal variations in the coverage of vegetation in West Liaohe River Basin and to analyze the possible causes of vegetation changes for the period of 1999 to 2010.

In this study, 432 SPOT VEGETATION NDVI images between January 1-10, 1999 and December 21-31, 2010 were acquired for the West Liaohe River Basin. The yearly and seasonal average normalized difference vegetation index (YNDVI and SNDVI) were computed, which provide information about the inter-annual and seasonal variation of vegetation. Vegetation Anomaly Index (VAI) was utilized to evaluate the state of vegetation cover stress and the impact of drought on the vegetation cover. The correlation analysis (CA) method uses the Pearson correlation coefficient to explore the trend of vegetation change. The meteorological datasets consist of monthly averaged temperature and precipitation from 1999 to 2010. The yearly average temperature, yearly total precipitation, average temperature and total precipitation in spring, summer and autumn derived from these monthly data were computed for performing a correlation analysis with above NDVI data.

The results indicated that yearly NDVI slightly increased with an undulating trend. 30.24% of the study area had experienced a significant vegetation increase at the 0.05 level from 1999 to 2010. Positive Vegetation Anomaly Index (VAI) values depicted the absence of vegetation stress, while the negative values exhibited vegetation cover degradation impacted by the drought in 2000-2002 and 2009. The average NDVI values in autumn increased by 5.92%, whereas the spring NDVI decreased by -5.82%. 16.46% and 15.49% of the study area showed a significant vegetation increase in summer and autumn respectively. Changes in vegetation growth may be affected by spring precipitation, summer temperature and precipitation and autumn temperature. The NDVI increase trends in the south-east of the study area were related to the increased crop yield.

## 8893-42, Session 11

### Estimate ecological indicators of karst rocky desertification by spectral unmixing algorithm

Xia Zhang, Tong Shuai, Institute of Remote Sensing and Digital Earth (China); Banghui Yang, Institute of Remote Sensing and Digital Earth, Chinese Academy of Sciences (China); Zhi Zhuang, Institute of Remote Sensing and Digital Earth, Chinese Academy of Sciences (China) and University of Chinese Academy of Sciences (China)

Rocky desertification is the most severe ecological degradation in southeast Karst area in China. The high landscape heterogeneity increases the difficulty of monitoring rocky desertification by remote sensing technology. Hyperspectral remote sensing image, with hundreds of narrow bands, has the advantage of extracting land cover distribution by spectral unmixing algorithm. Coverage rates of vegetation and exposed bedrock are two key indicators of karst rocky desertification (KRD) environments. In this study, firstly, based on the field experiment data, the newly developed spectral indices of Karst rocky desertification (SIRD4-soil and SIRD4-rock), as well as modified chlorophyll absorption reflectance index(MCARI) were verified to have significant linear correlations with coverage rates of soil, rock and vegetation, with  $R^2$  of 0.76, 0.51 and 0.83 respectively. Then, based on spectral unmixing algorithm(extracting endmember by the sequential maximum angle convex cone, and calculating abundance by linear spectral unmixing), abundances of vegetation, soil and rock were retrieved from the hyperspectral Hyperion image. They were verified by the spectral indices of SIRDs and MCARI. It showed that the abundance had significant linear correlation with the spectral indices. The determinate coefficients ( $R^2$ ) were 0.93, 0.66, 0.84 for vegetation, soil and rock respectively, indicating that the abundances can characterize the corresponding coverage rates to a certain

extent. Finally, Referring to the specifications of State Environmental Protection Administration of China on sensitivity evaluation of rocky desertification, we chose the abundances of rock and vegetation to characterize their coverage rates. They were graded and integrated together to evaluate the rocky desertification in a typical Karst area: Qibainong town. The evaluation map indicated that The severe and extreme KRD mainly distributed in the south and south-west of the study area, which is quite coincident with our ground truthing data. This study implies that spectral unmixing algorithm based on hyperspectral remote sensing image will provide an promising way to monitor and evaluate KRD especially in improving the efficiency and objectivity.

## 8893-43, Session 11

### Snow cover and land surface temperature assessment of Gangotri basin in the Indian Himalayan Region (IHR) using MODIS satellite data for climate change inferences

Akhouri P. Krishna, Anurag Sharma, Birla Institute of Technology and Science (India)

There are wide ranging concerns regarding the climate change challenge in this century. Due to rise in the global temperature, our cryosphere may face the direct threat. Himalayan mountain ranges with high snow fields and numerous valley glaciers may bear the brunt of such changes as already being reported including the Intergovernmental Panel on Climate Change (IPCC) reports. Gangotri is one of the most prominent snowfed catchments of the Indian Himalayan Region (IHR) due to origin of the river Ganga situated within it. This snow and glacier fed river could become a seasonal river in the near future as a consequence of climate change. Therefore, spatio-temporal changes in the snow covered area of Gangotri basin were examined for the melting seasons (March to October) of the years 2006 to 2010. For this, standard snow data products (MOD10A2) of Moderate Resolution Imaging Spectroradiometer (MODIS)-Terra sensor with spatial resolution of 500 m were used. These 8-day composite of maximum snow cover allowed classification of the basin area into snow covered and snow free land covers as well as distinction of the cloud cover.

For all the years of reference, the snow covered area percentage was derived for their respective months of March to October representing the usual ablation or melting period within the Himalayas. However, to consider the maximum accumulation of snow before start of the melting periods, MODIS data of the last week of February months of all these years were also taken into consideration. Snow depletion curves were generated for the months beginning last week of February up to October of respective years. This was done for the years 2006 to 2010 and a latest reference year of 2012 as a special test case with respect to the reported hottest year of this century as of now. Cloud cover problem of MODIS snow data of some dates was rectified using suitable image processing techniques using ERDAS Imagine modeller considering adjacent snow pixel reflectance values to replace the cloud pixels. CARTOSAT digital elevation model (DEM) was used for topographic information of the terrain.

After obtaining the snow depletion curves for the periods as stated above, the relationship of the snow depletion curves with the land surface temperatures (LST) of the basin area was worked upon. For bare soil, LST is the soil surface temperature and for snow surface, it is the snow surface temperature. For this, Moderate Resolution Imaging Spectroradiometer (MODIS)-Terra LST (MOD11A2) product (version 5) with 1 km resolution at 8-day interval for the day time temperature was used. Land surface temperatures were extracted for the respective months of the above reference years. This was followed by the interpolation and simulation of snow cover areas on the basis of LST data. The study thus produced snow cover maps for the years of reference as well as their relationship with LST for climate change inferences.

8893-44, Session 12

### **Application of multidimensional geospatial data integration approach to study the geo-environmental and socio-economic vulnerability due to climate change: case study, cyclone Aila affected Dacop and Koyra Upazila**

Md. S. Rahman, BRAC Univ. (Bangladesh); Hafizur Rahman, Bangladesh Space Research and Remote Sensing Organization (Bangladesh); Nandan Mukherjee, Ainun Nishat, Roufa Khanum, Tahmid Huq Easher, BRAC Univ. (Bangladesh)

Climate is changing with its extremity and uncertainty. Though land use change is not the major anthropogenic driver that has been pushing the climate to change, however, the change in land use is aggravating the incremental loss and damage due climate change. Risk assessment is a prerequisite for adaptation and mitigation planning. Remotely sensed analytical support can effectively support the proxy indicators for assessing the current exposure. Social vulnerability is another driver of risk, which is more of determinant in nature, i.e., it can pose certain level of variability in the case of change in the exposure or land use change. Dynamism in social vulnerability level as a function of change in the exposure can be addressed combining multidimensional technology.

The principal objective of this study is to meet the contemporary challenges of integration of multidimensional information by applying a combination of space-based remote sensing, geospatial technology of GIS and geo-positional tools of GPS together with information like Census, Social and FGD in monitoring and assessing the state and evolution of a given geo-environment and socioeconomic vulnerability therein under climate change or disastrous condition. The study area includes the climatically vulnerable zone of the southwestern part of Bangladesh. The area is under continuous threats of climate change driven by both slow & rapid onset events. Analysis of time series satellite data demonstrates distinct differences between pre and post cyclone different surface features. Special focuses have been made on the water clusters occurring at different geographical positions on different dates appear to be associated with possible water logging mechanism. Seasonal growing pattern of vegetation has also been studied to verify whether the vegetation is consistent with observation in normal year prior to the cyclone Aila.

Spatial analysis of multi-date images depicts that the occupational pattern of the Aila affected region is dominated by the shrimp farming followed by small holding agriculture. Shrimp farming, was the principal occupation of the people that used to lead major economic activities in the area before the devastating cyclone Aila of 2009. Analysis of time series satellite of the area reveals that a major portion of the livelihood bases were devastated by Aila. The most affected segment of the livelihood is agriculture and as almost all the productive agriculture land went under saline water. Cyclone Aila caused extensive damages in this region, changed the landscape and uprooted many homes. Water logging and consequences of its spatiotemporal dynamics, such as no cropping and migration, are clearly being identified through the analysis of satellite images using the GIS platform. Eventually, the dynamics of landuse changes and losses of bio-diversity due to Cyclone Aila appear to have unambiguous impacts on livelihoods in this area. The whole operational processes develop a comprehensive understanding of the prevailing situation exposed by the cyclone Aila and provide an account of socio-economic and environmental scenario of the affected people and their present livelihood condition. Successful integration depicts the potentiality of this study for analysis of socioeconomic and geo-environmental vulnerability as a cost effective approach.

8893-45, Session 12

### **Analysis of principal parameters of forest fires and identification of desertification process in semi-arid land in Algeria**

Ahmed Zegrar, Ctr. National des Techniques Spatiales (Algeria)

The Forest in steppe present ecological diversity, and seen climatic unfavourable conditions in zone and impact of forest fires; we notes deterioration of physical environment particularly, deterioration of natural forest. This deterioration of forests provokes an unbalance of environment witch provokes a process of deterioration advanced in the ultimate stadium is desertification. By elsewhere, where climatic conditions are favourable, the fire is an ecological and acted agent like integral part of evolution of the ecosystems, the specific regeneration of plants are influenced greatly by the regime of fire (season of fire, intensity, interval), who leads to the recuperation of the vegetation of meadow- fire. In this survey we used the pictures ALSAT-1 for detection of zones with risk of forest fire and their impact on the natural's forests in region of Tlemcen. A thematic detailed analysis of forests well attended ecosystems some processing on the picture ALSAT-1, we allowed to identify and classifying the forests in their opinion components flowers. We identified amplexness of fire on this zone also. Some parameters as the slope, the proximity to the road and the forests formations were studied in the goal of determining the zones to risk of forest fire. A crossing of diaper of information in a SIG according to a very determined logic allowed classifying the zones in degree of risk of fire in middle arid in a forest zone not encouraging the regeneration on the other hand permitting the installation of cash of steppe which encourages the desertification.

8893-46, Session 12

### **Identification of impacts on the Egyptian Nile using remote sensing and GIS**

Alaa H. El Nahry, National Authority for Remote Sensing and Space Sciences (Egypt)

The current study aims at mapping soil and identifying the characteristics of the Nile course as well as its islands in order to provide the scientific bases, which help in planning the most suitable programs of land use, soil management, conservation and recognizing the intensive agriculture system of the Nile River islands The Nile River is the longest river in the world, 6,695 km long from its remotest headstream. Nile waters support practically all agriculture in the most densely populated parts of Egypt, furnish water for more than 20% of Sudan's total crop area, and are widely used throughout the basin for navigation and hydroelectric power.

The Nile River islands form an attractive agricultural area characterized with its nightly fertile soils, easy source, and its suitability to a wide range of land use. The present use of these Nile islands does not reach the maximum capability of these resources due to improper land use of these areas.. The obtained results showed that, changes in the Nile course from early seventieth to middle eighteenth were decreased by 51.34 Km<sup>2</sup>, from middle eighteenth to the present time were decreased by 40.30 Km<sup>2</sup>. The overall change in Nile course area decreased by 91.64 Km<sup>2</sup> in the investigation time. Belonging to the islands number and their areas in the investigation time, the changes in islands number from early seventieth to middle eighteenth were increased by 171 islands, from middle eighteenth to the millennium were decreased by 86 islands. Meanwhile, the islands areas from early seventieth to middle eighteenth were decreased by 4512.39 Fed. (4200 meter), from middle eighteenth to the millennium were decreased by 5446.97 Fed. The overall change in the investigation time for the total number of the islands was increased by 85 islands, meanwhile the islands areas were decreased by 9959.36 Fed.

# Conference 8894: Lidar Technologies, Techniques, and Measurements for Atmospheric Remote Sensing IX

Monday - Tuesday 23–24 September 2013

Part of Proceedings of SPIE Vol. 8894 Lidar Technologies, Techniques, and Measurements for Atmospheric Remote Sensing IX

8894-1, Session 1

## Fiber optic CW Doppler lidar using a synthetic broadband source (*Invited Paper*)

Ernst Brinkmeyer, Thomas Waterholter, Technische Univ. Hamburg-Harburg (Germany)

It is a common point of view from both range and noise considerations that laser sources in many Lidar applications should be narrowband. This alleged prerequisite applies in particular to wind sensing Doppler Lidars where the velocities of aerosol particles are determined from optical frequency shifts. By contrast, our Lidar system is based on laser sources with considerable bandwidths. It uses a Mach-Zehnder-like interferometric setup and basically yields quantum limited sensitivity, as other Lidars with heterodyne detection do. Since it is a CW system range resolution cannot arise from time of flight determination, and we are not content with the range resolution just arising from focusing the transmitted beam to a particular location. Instead, we use a source with finite spectral bandwidth for 'coherence gating': a detector signal of narrow electrical bandwidth is primarily generated if the path length from the source via a particular scattering object back to the receiver matches the (fiber optic) path length in the reference arm of the interferometer to within the coherence length. This reasoning also is the basic principle of white light interferometry, optical low-coherence reflectometry (OLCR) in waveguide optics, and optical low-coherence tomography where broadband sources like superluminescent diodes or ASE fiber sources are in use. In the case of atmospheric aerosol Lidar, however, we need spatial resolutions of the order of meters rather than micrometers because otherwise, despite quantum limited detection, the number of particles within the resolution element would be too low in general. Therefore, the optical bandwidth must be of the order of tens of MHz, a range which is readily accessible with single-transverse, single-longitudinal mode laser diodes. Nevertheless, natural laser sources are hardly suitable for our purposes because (i) they have a Lorentzian (rather than a Gaussian) power density spectrum, (ii) the bandwidth and, hence, the spatial resolution cannot be changed, and (iii) the optical phase noise as a function of time - which is the reason for the finite spectral width - is not known. For that reason we devised an off-line numerical algorithm for determining quasi-noise phase functions which yield optical spectra of given width and form - the latter preferably Gaussian because the corresponding coherence functions fall off rapidly and excellently define the spatial resolution zone. These predetermined numerical data are impressed on the optical wave from a narrowband laser diode by means of an optical phase modulator so that in total a well-controlled synthetic broadband source is formed. Moreover, it is important to note that the numerical values of the phase function are known. That knowledge allows for shifting the resolution zone to an arbitrary location by suitable numerical data processing without taking repeated measurements.

At the conference we will discuss further theoretical aspects, we will give numerical simulations for various applications as well as an analysis of detection limits and we will show how inevitable spurious reflections from the measurement setup can effectively be suppressed. In addition, current experimental results in the fields of range-resolved velocity measurements and differential absorption Lidar will be presented.

8894-2, Session 1

## Assessing the metrological capabilities of wind Doppler lidars

Ludovic Thobois, Leosphere France (France)

During the last 5 years, LEOSPHERE has developed and manufactured a full range of Windcube Doppler lidars for wind sensing. Applications include wind energy site assessment, wind turbine verification and control, operational meteorology and airport hazard monitoring. All lidars use the same fiber laser technology at 1550nm in pulsed operation but vary by their laser power, telescope aperture, scanning possibilities and signal processing. Range is

therefore between 200m for the smallest, and more than 10km for the most powerful.

So far, as more than 300 wind lidars have been manufactured and deployed all around the world, a full industrialization process of the Windcube technology has been setup in order to ensure the reliability of each unit but also its specifications. Among all the functional specifications, those related to the metrological performances are the most important for the customers.

To assess the metrological performance of the instruments, different methodologies have been developed. Principal parameters that need to be validated are velocity accuracy, spatial resolution, range, distance accuracy, scanner angular accuracy and data availability. The presentation will present the definition of the parameters, the theoretical estimation of mean value and possible biases, and the validation methods used for wind profilers and scanning lidars, during internal or external test campaigns.

8894-3, Session 1

## Direct detection lidar for wind measurement

Itai Afek, Gil Shamai, Pentalum Technologies (Israel)

### DIRECT DETECTION LIDAR FOR WIND MEASUREMENT

Wind sensing Lidars are considered a promising technology for high quality wind measurements required for different applications such as hub height wind resource assessment, power curve measurements and advanced, real time, forward looking turbine control. Until recently, the only available Lidar technology was based on coherent Doppler shift detection, whose market acceptance has been slow primarily due to its exuberant price. Direct detection Lidar technology provides an alternative to remote sensing of wind by incorporating high precision measurement, a robust design and an affordable price tag.

The use of elastic Lidars to measure wind velocity in the planetary boundary layer is well known. Generally, the methods to measuring wind are divided into two categories:

- a. Coherent detection
- b. Direct detection

Coherent detection is the method which underlies the Doppler Lidars. These Lidars actually measure the Doppler shift in the wavelength of the light reflected from the moving aerosols within an air probe volume. The Doppler shift is usually measured by a coherent optical system, whose light source phase is carefully controlled, by performing an interference of the reflected light with the local oscillator. Since the Doppler shift is proportional to the radial component of the velocity, it is necessary to perform such measurements in numerous locations in space in order to extract the full (average) wind velocity vector.

The direct detection method is based on sampling the atmosphere with laser pulses whose reflected intensity alone is received and sampled in time. The sampled time series represents the aerosol density in the line of sight of the transmitted pulse. By attaining aerosol map snapshots in different locations, at different times, and tracking the aerosol structures, one is able to extract the wind velocity.

8894-4, Session 2

## High-energy, double-pulsed 2-micron direct detection lidar for NASA's airborne CO<sub>2</sub> measurements (*Invited Paper*)

Upendra N. Singh, Jirong Yu, Mulugeta Petros, NASA Langley Research Ctr. (United States)

A 2-micron pulsed, Integrated Path Differential Absorption (IPDA) lidar instrument for ground and airborne atmospheric CO<sub>2</sub> concentration measurements via direct detection method is being developed at NASA Langley Research Center. This instrument will provide an alternate approach to measure atmospheric CO<sub>2</sub> concentrations

with significant advantages. The pulsed lidar approach inherently provides a means for determining range across the scattering targets. The reflected signals can be resolved between aerosols, clouds, and topographical surfaces. A high energy pulsed approach provides high-precision measurement capability by having high signal-to-noise level and unambiguously eliminates the contamination from aerosols and clouds that can bias the IPDA measurement. This paper describes the development of a 2-micron pulsed IPDA lidar instrument that will measure atmospheric CO<sub>2</sub> concentration from ground and airborne platform.

8894-5, Session 2

### **A direct detection 1.6 $\mu$ m DIAL with three wavelengths for high accuracy measurements of vertical CO<sub>2</sub> concentration and temperature profiles**

Yasukuni Shibata, Chikao Nagasawa, Makoto Abo, Tokyo Metropolitan Univ. (Japan)

No abstract available

8894-6, Session 2

### **Lidar sounding of volcanic plumes**

Luca Fiorani, ENEA (Italy); Alessandro Aiuppa, Univ. degli Studi di Palermo (Italy); Federico Angelini, Rodolfo Borelli, Mario Del Franco, Daniele Murra, Marco Pistilli, Adriana Puiu, ENEA (Italy); Simone Santoro, Univ. degli Studi di Palermo (Italy)

The composition of volcanic gases gives information on the processes inside volcanoes and on the transition from quiescence to eruption. Up to now, coupled gas-geophysical studies are sparse, due to the difference in their typical sampling frequency (>1 Hz for seismic signals and <10-5 Hz for gas data). This explains the interest of geophysicists in new techniques of gas detection, in particular for CO<sub>2</sub>, the second most abundant gas in volcanic fluids and the most directly linked to deep "pre-eruptive" volcanic degassing processes.

Lidars have been used in the past to determine aerosol load, SO<sub>2</sub> concentration and water vapor flux in volcanic plumes. One of the tasks of the recently begun FP7 ERC project BRIDGE (Bridging the gap between gas emissions and geophysical observations at active volcanoes) is the lidar measurement of CO<sub>2</sub> concentration in volcanic plumes.

CO<sub>2</sub> absorbs in the 15, 4.2, 2.1 and 1.6  $\mu$ m bands (in order of decreasing strength). Unfortunately, in the first two bands viable lasers are not available and atmospheric backscattering is rather low, so the 2.1 and 1.6  $\mu$ m bands have been suggested for its detection. Nevertheless, the DIAL measurement of CO<sub>2</sub> remains a difficult task because the absorption lines are narrow and weak.

In general, DIAL measurements of atmospheric CO<sub>2</sub> for climatic studies are carried out with Tm, Ho:YLF lasers (2.1  $\mu$ m) and fiber lasers (1.6  $\mu$ m). Unfortunately, these sources have a very limited tunability. Conversely, thanks to their wide range of tunability, from UV to near IR, and the occurrence of many absorption lines in these spectroscopic regions, dye lasers could sound not only CO<sub>2</sub>, but other species relevant to volcanic phenomena and atmospheric chemistry. Moreover, they allow freedom of choice on the CO<sub>2</sub> absorption line to be used, in order to minimize the water vapor cross sensitivity and to maximize the tradeoff between sensitivity and range of measurement.

Another advantage of dye lasers is that they are pumped by Nd:YAG lasers. A frequency tripled Nd:YAG laser has already been employed for Raman lidar measurement of CO<sub>2</sub> in the atmosphere, thus giving another string to our bow.

For all these reasons, the lidar under development for the BRIDGE project is based on a dye laser. The system will be positioned below the volcanic plume that will be probed with the laser beam. With such configuration, and scanning the plume in a vertical plane roughly perpendicular to the plume axis, the CO<sub>2</sub> concentration outside and inside the plume will be measured. In practice, the lidar will be aimed directing its optical axis by means of a plain mirror. These measurements, once integrated over the whole cross-sectional area of the plume, and upon scaling to the plume transport rate (as derived from the wind speed at the plume altitude), will allow the retrieval of

the CO<sub>2</sub> flux.

This paper reports on the mechanical, electronic and software architecture of the lidar under development, on spectroscopic studies for the identification of the best absorption lines and on simulations of lidar signal and CO<sub>2</sub> retrieval.

8894-7, Session 2

### **Scanning 1.6 $\mu$ m lidar measurements of atmospheric CO<sub>2</sub> concentration and wind profiles**

Yasukuni Shibata, Chikao Nagasawa, Makoto Abo, Tokyo Metropolitan Univ. (Japan)

Knowledge of present carbon sources and sinks including their spatial distribution and their variability in time is one of the essential information for predicting future carbon dioxide (CO<sub>2</sub>) atmospheric concentration levels. Moreover, wind information is an important parameter for transport simulations and inverse estimation of surface CO<sub>2</sub> flux. The differential absorption lidar (DIAL) and the Doppler lidar provide several advantages with respect to passive approaches toward high-precision and range-resolved CO<sub>2</sub> concentration and wind measurements.

We have developed a new mobile scanning lidar system to perform simultaneous measurements of CO<sub>2</sub> concentration and wind speed profiles in the atmosphere. The lidar system consists of combined 1.6 $\mu$ m CO<sub>2</sub>-DIAL and incoherent Doppler lidar, and installed in a trailer. The high power optical parametric generator (OPG) system developed for the CO<sub>2</sub>-DIAL is applied for the transmitter of the incoherent Doppler lidar. The receiving optics include the near-infrared photomultiplier tube with high quantum efficiency operating at the photon counting mode, a fiber Bragg grating (FBG) filter to detect Doppler shift, and a 25 cm telescope. Laser beam is directed to the sky via a steering mirror coaxially with the scanner. The motorized scanner provides coverage of 0 - 360 deg azimuth and 0 - 52 deg elevation.

The CO<sub>2</sub>-DIAL was operated with the range-height indicator (RHI) mode, and the 2-D measurement provided inhomogeneity in the boundary layer. Vertical CO<sub>2</sub> concentration profiles and wind profiles were also measured simultaneously. The elevation angle was fixed at 52 deg and CO<sub>2</sub> concentration profiles were obtained up to 1 km altitude with 200 m height resolution. Vertical wind vector profiles were obtained up to 5 km altitude with 1 km altitude resolution with two azimuth angles.

This work was financially supported by the System Development Program for Advanced Measurement and Analysis of the Japan Science and Technology Agency.

8894-8, Session 2

### **Investigating the effect of aerosol droplets in a volcanic plume for increasing sensitivity of a CO<sub>2</sub> DIAL measurement**

Manuel Queisser, Mike Burton, Istituto Nazionale di Geofisica e Vulcanologia (Italy); Luca Fiorani, Italian National Agency for New Technologies (Italy)

There is great interest in using Differential Absorption LIDAR (DIAL) techniques to remotely monitor volcanic CO<sub>2</sub> emissions, as these emissions contribute to the carbon cycle and variations in the magnitude of the emissions may help forecast future activity. CO<sub>2</sub> is typically the second most abundant volcanic gas, the first being H<sub>2</sub>O, which can condense upon emission, producing dense aerosol clouds. These aerosols will strongly affect absorption and backscattering of the probing DIAL light. It is therefore important to have a realistic quantitative estimation of the impact of these aerosols on the LIDAR signal. Given a droplet particle number density of 1e8 m<sup>-3</sup>, typical for atmospheric liquid water clouds, and a liquid water content of 0.4 g m<sup>-3</sup> we estimate the peak radius of the particles to be 10 microns with a log-normal particle size distribution. Since the particles are a similar size to the probing radiation (1.57 micron) we employ Mie's equations to calculate the scattering and extinction cross section of the aerosol particles. Then, we derive the corresponding volume backscattering and extinction coefficient. The total backscattering and

extinction coefficients are computed as the sum of the coefficients of the single atmospheric species, which are water vapor and CO<sub>2</sub> (for both species background and volcanic), as well as background aerosol and volcanic liquid water droplets. We find that both backscattering and extinction coefficient increase by ~4 orders of magnitude with respect to the case without any liquid water in the volcanic plume. Correspondingly, the fraction of light scattered back to the DIAL instrument in a single scattering event (ratio between the backscattering and extinction coefficient) increases from 12% without condensed water to 65% with condensed water.

Volcanic liquid water clouds are highly variable in space. So it is more reasonable to assume a spatially varying size distribution instead of a single distribution for the whole plume. For this purpose, we use a random field that is conditioned with the volcanic droplet number density mean and standard deviation. Since we model in 1D the random field is 1D. That means the total droplet number density per grid point within the plume is a normally distributed random number between  $1e7$  and  $1e8$  m<sup>-3</sup>. Thus, each grid point within the plume is associated with its own size distribution and hence a random backscattering and extinction coefficient. Spatial correlation is accounted for by convolving the random field with a Gaussian kernel of 5 times the grid length. For light scattered from within the cloud extension we see a maximum increase of signal between 4 orders of magnitude at the near edge of the plume and a minimum signal comparable to that without liquid water for signals from the far edge of the plume. This is expected since not only backscattering, but also the extinction increases significantly due to the water droplets. For locations in between the plume edges the signal scales with variation of droplet number density, ranging between the aforementioned minimum and maximum.

The results suggests that within the plume region high droplet number densities may act as strong reflectors, and greatly enhance the potential range of a DIAL system compared with backscattering in the clear atmosphere. This assessment helps us to design an optimal instrument for volcanic CO<sub>2</sub> DIAL measurements, minimizing optical power requirements.

### 8894-9, Session 2

#### Dual-wavelength resonant pumping of compact Er:YAG lasers providing high power output at 1645.55 nm for methane detection

Haro Fritsche, Oliver Lux, Casey Schuett, Technische Univ. Berlin (Germany); Stefan W. Heinemann, Wolfgang Gries, DirectPhotonics Industries GmbH (Germany); Hans Joachim Eichler, Technische Univ. Berlin (Germany)

Resonant pumping of Er:YAG is rapidly emerging as one of the most promising ways to generate high power lasers at room temperature with wavelengths around 1.6  $\mu$ m. This is particularly due to the high quantum efficiency of quasi-two-level laser operation which involves different Stark sub-levels of the laser transition  $4I_{13/2} \rightarrow 4I_{15/2}$  in the Er<sup>3+</sup>-ions. Here, population of the upper laser manifold can be achieved with pumping wavelengths in the range from 1455 nm to 1532 nm, while laser radiation occurs at 1645 nm. A common approach is to use fiber lasers as pump sources, however for multi wavelength pumping fiber lasers don't offer the desired wavelength range.

Our strategy is based on high brightness, wavelength stabilized diode laser modules which were employed to resonantly pump cw and pulsed Er:YAG lasers with an Er<sup>3+</sup>-doping concentration of 0.5 at%. Utilization of a first generation DirectPhotonics fiber-coupled Diode laser pump source at 1532 nm with a bandwidth of less than 0.18 nm (23 GHz) and a frequency stability of about 230 MHz resulting in an overall efficiency of the Er:YAG laser of about 23%

The system was also Q-switched by means of a Pockels cell generating single pulses with pulse energy of 6.6 mJ and pulse duration of 60 ns. The pulse energy was found to be independent of the pulse repetition frequency which was scaled up to 125 Hz.

Since the maximum pump power of diode laser modules is in the range of 40 W, the Er:YAG output power is limited to about 10 W. Power scaling of the Er:YAG laser could be demonstrated by dual-wavelength pumping of the gain material. For this purpose, an additional broadband diode laser module from LIMO operating at 1455 nm was used as second pump source. Although this laser only

provides a maximum optical efficiency of about 10% if it is utilized as the only pump source, the application of both lasers leads to an output power of 2.2 W. This is twice as much compared to the laser performance obtained under single-wavelength pumping using two equal pump laser modules at 1455 nm (P<sub>out</sub>=0.9W) or 1532 nm (P<sub>out</sub>=1.2W) in double-end-pumped configuration. Since a single end pump setup is already more efficient and stable and an absorption efficiency of 96% at 1532 nm were lately measured, we expect a much higher over all efficiency by combining two or more narrow bandwidth pump wavelengths in a single-end-pumped scheme.

The spectral characteristics of the Er:YAG laser were controlled by an intra-cavity etalon which not only provides narrowband and frequency-stable operation, but which also allows to switch the output wavelength between 1645.1nm and 1646.5 nm. This is especially interesting for methane DIAL applications where an online- and offline-wavelength in the spectral region around 1645 nm is required. We successfully demonstrated the potential of the Er:YAG laser in terms of methane detection. A multi-pass absorption cell was used to detect methane at low and high pressure values in the mbar regime.

### 8894-10, Session 3

#### Overview of Japan's Spaceborne Vegetation Lidar Mission (*Invited Paper*)

Jumpei Murooka, Takashi Kobayashi, Daisuke Sakaizawa, Tadashi Imai, Keiko Suzuki, Yohei Sato, Yoshikazu Chishiki, Shiro Yamakawa, Ryota Sato, Japan Aerospace Exploration Agency (Japan); Haruo Sawada, The Univ. of Tokyo (Japan); Kazuhiro Asai, Tohoku Institute of Technology (Japan)

Vegetation LiDAR, which measures an accurate canopy height, has been studied by JAXA. Canopy height is a very important parameter to estimate forest biomass, and global measurement of accurate canopy height leads to better understanding of the global carbon cycle.

The vegetation LiDAR is designed based on the assumption that it is to be mounted on the Exposed Facility (EF) of the Japanese Experiment Module (JEM, also known as "Kibo") on the International Space Station (ISS).

The vegetation LiDAR uses an array detector (2x2) for dividing the ground footprint, making it possible to detect the slope of the ground for improving the accuracy of canopy height measurement. However, dividing the footprint may cause a reduction in reflected lights and signal-to-noise ratio (SNR); hence, the vegetation LiDAR system needs high sensitivity and low-noise array detector module. We made a prototype of the array detector module and it satisfied the tentative target SNR which we set.

This presentation will introduce the mission objectives, the LiDAR system including experimental prototypes of array detector module, and some results of the study.

### 8894-11, Session 3

#### Waveform simulator and analytical procedure for JAXA's future spaceborne Lidar to measure canopy height

Takashi Kobayashi, Japan Aerospace Exploration Agency (Japan); Takahiro Endo, Remote Sensing Technology Ctr. of Japan (Japan); Yoshito Sawada, The Univ. of Tokyo (Japan); Shigeru Endo, Tokyo Univ. of Science (Japan); Masato Hayashi, National Institute for Environmental Studies (Japan); Yohei Satoh, Yoshikazu Chishiki, Shiro Yamakawa, Japan Aerospace Exploration Agency (Japan)

High-accuracy three-dimensional (3D) information of global area is very useful in various fields, such as global observations of canopy height, elevation, and ice sheet. Especially, there are pressing needs to advance understanding of how changes in the 3D structure of terrestrial vegetation are affecting the global carbon dynamics and their implications for climate change. Thus new space based observations are urgently needed to measure global maps of the 3D structure of vegetation.

Many studies were reported about the potential use of data obtained

with the Geoscience Laser Altimeter System (GLAS) aboard the Ice Cloud and land Elevation Satellite (ICESat) to map canopy height, above ground biomass, and other vegetation structure parameters, while ICESat/GLAS was designed with the primary objective which was monitoring ice sheets mass balance. There are various methods of analysis to estimate canopy height from the waveforms obtained by the ICESat/GLAS, and a large part of the canopy height error is likely to be caused by waveform analysis algorithm.

The Japan Aerospace Exploration Agency (JAXA) has started a conceptual study of a vegetation LiDAR mission which is designed to measure accurate canopy height with a space-borne LiDAR system. Considering the reports of canopy heights estimation from the ICESat/GLAS data, we consider studies of waveform analysis procedures to be important to obtain canopy height with high accuracy as well as the hardware design of the vegetation LiDAR.

To estimate waveforms of the vegetation LiDAR, a waveform-simulator was developed. Main variables of the simulator are laser power, incident angle of a laser pulse, diameter of a footprint, ground DEM data, tree species and phenology, wavelength, and reflectivities of objects. Some waveforms of the ICESat/GLAS were calculated by the simulator. Comparing with the actual waveform data, validity of the simulator has been studied.

Waveform analysis procedure of the vegetation LiDAR in which waveforms are fitted with a sum of Gaussian functions has been studied. Not only waveforms of the ICESat/GLAS but also waveforms obtained in field works whose footprints were comparable with canopy diameter (about 10 m) were analyzed with the procedure and availability of it has been discussed.

This paper aims at reporting the present status of our investigation for waveform analysis of the JAXA's future vegetation LiDAR mission.

### 8894-12, Session 3

## Design and development of a compact Dial system for aerial surveillance of urban areas

Pasquale Gaudio, Michela Gelfusa, Andrea Malizia, Maria Richetta, Arianna Antonucci, Univ. degli Studi di Roma Tor Vergata (Italy); Piergiorgio Ventura, Ctr. Tecnico Logistico Interforze NBC (Italy)

Recently surveying relative large areas in an automatic way, for early detection of harmful chemical agents, has become a strategic objective of both defence and public health organisations. The Lidar-Dial techniques are widely recognized as a cost-effective alternative to monitor large portions of the atmosphere but, up to now, they have been deployed almost exclusively as ground based stations. The design reported in this paper concerns the development of a Lidar-Dial system compact enough to be carried by a small airplane and capable of detecting sudden releases in air of harmful and/or polluting substances. The proposed approach consists of continuous monitoring of the area under surveillance with a Lidar type measurement. Once a significant increase in the density of backscattering substances is revealed, it is intended to switch to the Dial technique to identify the released chemicals and to determine its concentration. In this paper, the design of the proposed system is described and the simulations carried out to determine its performances are reported. For the Lidar measurements, commercially available Nd-YAG laser sources have already been tested and their performances, in combination with avalanche photodiodes, have been experimentally verified to meet the required specifications. With regard to the DIAL measurements, new compact CO<sub>2</sub> laser sources are being investigated. The most promising candidate presents an energy per pulse of about 50 mJ typical, sufficient for a range of at least 500m. The source is pulsed with a pulse duration equal to 50ns. The divergence of the output beam is equal to 1 mRad and the diameter of 6 mm. The maximum frequency of repetition (PRF) is 100Hz. The laser also provides the so called "agile tuning" option that allows you to quickly tune the wavelength. The optical design has been carried out with the help of the software package ZEMAX. The best solution identified consists of a Newtonian telescope, which unlike other configurations, presents a higher brightness at the expense of a lower image quality (more aberrations), and whose basic components are optical reflective easily available on the market. Since the detection of dangerous substances must be performed in an automatic way, the aerial system will be equipped with an adequate set of control and

communication devices for independent autonomous operation and for communication with ground base stations. Given the requirements of robustness and reliability of the foreseen applications, it has been decided to adopt focus industrial electronic components that can be mounted on a rugged system and that, in addition to being stable, allow data acquisition in real time and fast data storage. The standard PXI (PCI eXtensions for Instrumentation) is considered the most suited to provide the required performance. The results of the design, the simulations and some preliminary tests illustrate the potential of the chosen approach.

### 8894-13, Session 3

## Development and testing of a high-power Q-switched DPSS laser for lidar applications: ESA QOMA project case

Giorgos Avdikos, Raymetrics S.A. (Greece); Christos Evangelatos, Univ. of Athens (Greece); Dimitris Papadopoulos, Univ. of Ioannina (Greece); Paraskevas Bakopoulos, Giorgos Tsaknakis, Alexandros D. Papayannis, National Technical Univ. of Athens (Greece); Georgios D. Tzeremes, European Space Agency (Netherlands)

In this paper, we present experimental results of the development and testing of a diode-pumped solid-state laser (DPSSL) operating at 1064 nm under the frame of the QOMA project (QSwitched Master Oscillator based on Multidoping Nd:YAG Technology for Optoelectronics Space Applications) funded by the European Space Agency (ESA). This project is a collaboration between ESA, Raymetrics S.A., and the National Technical University of Athens (NTUA). The main goal of the project is the design, development and manufacture of a new low-weight, highpower diode-pumped laser source for application in future space-borne optoelectronic and lidar systems, dedicated to the study and monitoring of aerosols and the space environment. The laser is capable of transmitting at 1064 nm on a continuous wave (cw) or pulsed mode. The system's design is based on new laser engineering technologies combining high power pumping of a multisegmented crystal rod at 885 nm and novel crystal cooling configurations. As active material, a multi-segmented Nd:YAG crystal rod (0.1%, 0.23%, 0.6% at Nd) of 54 mm length and 2 mm diameter with 7 mm undoped end-caps on both ends and a uniform crystal (0.84 % at Nd, 2 mm diameter, 7 mm end-caps) is used for comparison showing the benefits of the multi-segmented Nd:YAG rod in terms of average power scaling capacity. Passive Q-switching operation based on Cr:YAG crystals is compared to active Q-switching based on an Acousto-optic Modulator (AOM) (Gooch and Housego S.A.). The AOM's crystal employs antireflection coatings covering both 946 and 1064 nm (dual AR coating), so it can be applied to laser configurations for the generation of 946 and 1064nm laser radiation. With the uniform crystal in a cavity of 450 mm length, with a Cr:YAG crystal used as the saturable absorber (50% initial transmission) and an output coupler of 10%, the energy per pulse goes up to 1.48 mJ, the repetition rate is 100 Hz and the pulse width is 45 ns. By further increasing the repetition rate, up to 500 Hz, (diode operation at Quasi-cw), the average power exceeds 530 mW. The beam profile remains excellent (M-square less than 1.2) for all cases. The energy per pulse increases to 2 mJ when the multi-segmented crystal is used in a laser cavity with an output coupler of 20% and the thermal lensing effect is improved by a factor over than 25%. Pulsed laser operation from 10 kHz down to 100 Hz with very good beam profile is achieved incorporating the AOM inside the laser cavity in conjunction with the multisegmented crystal. The average power value is more than 6 W, the energy per pulse values are between 1-2 mJ depending on the repetition rate, the pulse width is between 60-100 ns, and the measured M-square values are less than 1.3..



8894-14, Session 3

**Design and performance of a fiber array coupled multichannel photon-counting, 3D imaging, airborne lidar system**

Genghua Huang, Rong Shu, Libing Hou, Ming Li, Shanghai Institute of Technical Physics (China)

Single photon being sufficiently used with the Geiger-mode avalanche photodiode (APD) or other single photon detectors, photon counting laser radar is more sensitive than the direct-detection laser radar, less laser transmitted power required in the same altitude. With adding no more energy or weight, the laser ground sampling density could be advanced using multichannel detectors in the Geiger-mode. In this paper, a latest airborne photon counting 3D imaging LIDAR system is introduced. A passively Q-switched microchip output laser is divided into 1?8 laser spots, which correspond to eight Geiger-mode avalanche photodiodes coupled by a 1?8-pixel fiber array. Using the two-axle adjustable-speed scanning mirror, the mesh spacing could be adaptive for different altitude and velocity. This prototype version was installed in a helicopter with a set of GPS and IMU, which measured the position and the attitude of the LIDAR synchronizing with the laser PRF. Through several flights from 600 to 1,000 meters altitude, with the 40KHz equivalent sampling frequency and the 0.15m ranging precision, a large area with various targets were imaged with this photon counting LIDAR. The diameter of the telescope is only 30mm. With the low average power of less than 60W and the light weight of 25kg, this LIDAR could be widely used in the carrier of light or unmanned aircraft.

8894-15, Session 4

**Autonomous ozone and aerosol lidar measurements: a synergistic approach to air quality (Invited Paper)**

Kevin B. Strawbridge, Environment Canada (Canada)

Environment Canada is developing an autonomous tropospheric ozone and aerosol lidar system for deployment in support of short-term field studies. The basic design of the platform extends from the knowledge gained over the past six years through the development of several autonomous aerosol lidars designed and built by Environment Canada and operated as a network across the country. This particular instrument will employ two separate lidar transmitter and receiver assemblies. The tropospheric ozone lidar, based on the differential absorption lidar (DIAL) technique, uses the fourth harmonics of a Nd:YAG laser directed into a CO2 Raman cell to produce 276 nm, 287nm and 299 nm (first to third Stokes lines) output wavelengths. The aerosol lidar is based on the 3+2 design using a tripled Nd:YAG to output 355 nm, 532 nm and 1064nm wavelengths. Both lidars will be housed in a modified cargo trailer allowing for easy deployment to remote areas. The trailer modifications include a roof hatch assembly, basic meteorological tower, radar interlock system, climate control system and leveling stabilizers. The unit can be operated and monitored 24 hours a day via an internet link and requires an external power source. A precipitation sensor is used to operate the roof hatch and three pan/tilt webcams capture sky conditions and monitor the lidar system's health. Simultaneous ozone and aerosol lidar measurements will provide the vertical context necessary to understand the complex mixing and transformation of pollutants -particularly when deployed near other in-situ sensors. The design of the platform and preliminary results will be presented.

8894-16, Session 4

**Lidar measurements of atmospheric temperature profiles (2-15 km) by utilizing Rayleigh-Brillouin scattering**

Benjamin Witschas, Christian Lemmerz, Oliver Reitebuch, Deutsches Zentrum für Luft- und Raumfahrt e.V. (Germany)

Observational data on vertical distributions of atmospheric temperature are important as input to models predicting the atmospheric state, as well as input to retrievals of other atmospheric

properties such as wind, pressure, relative humidity or other trace gas concentrations. Currently, active devices such as lidar instruments enable the measurement of temperature with high accuracy (1 K), high vertical resolution (100 m) and long range (up to 105 km). For tropospheric temperature profiling it is common to make use of rotational Raman scattering on air-molecules (Behrendt and Reichardt). However, due to its low scattering cross section, high-power lasers and night-time operation are required to obtain reliable temperature profiles. Regarding this, it is beneficial to utilize high spectral resolution lidars (HSRL) and Rayleigh-Brillouin (RB) scattering with a scattering cross section of a factor of 53 larger than rotational Raman scattering. Furthermore, the narrow RB line width enables the application of narrow band filters to suppress solar radiation and thus enables daytime operation. Though the principle of this approach was already demonstrated in 1971 by Fiocco et al., it was shown that it is challenging to resolve the RB line shape accurately and to separate it from signals caused by scattering on aerosols (Mie scattering). Furthermore, it was pointed out that an appropriate RB line shape model for air is needed to avoid systematic errors within the temperature retrieval. Commonly, vapor filters are used to separate Mie-scattered light from the RB line shape. After that, temperature is derived by defining a response function calculated from an RB line shape model and assuming hydrostatic equilibrium. However, the  $\lambda^{-4}$  dependency of the Rayleigh scattering cross section favors the usage of ultraviolet (UV) wavelengths, a spectral region where vapor filters are complicated to implement. Thus, Hua et al. used an UV laser (355 nm) and three Fabry-Pérot interferometers (FPI) to derive temperature profiles from ground up to 4 km.

Here, we suggest a novel approach for lidar retrievals of tropospheric temperature profiles based on a single FPI, in which the entire RB line shape is sampled with high spectral resolution by scanning the laser frequency. Temperature is then obtained by relating the measured RB spectrum to an analytical line shape model which additionally considers the contribution of Mie scattering. Here, RB- and Mie scattering is not separated in different channels (as commonly done with HSRL), but information is gained from the different imprints in the measured spectrum. The temperature values derived at different range gates (altitudes) are independent of each other, as no response function has to be used for the retrieval.

The suggested approach is demonstrated with atmospheric daytime measurements which show temperature profiles from 2 km to 15.3 km in comparison to radiosonde temperature profiles. To our knowledge, this is the first time that temperature profiles up to this altitude are measured during daytime with an averaging time of 14 min. to 28 min. by utilizing RB scattering. The statistical error of the derived temperatures is calculated to be between 0.15 K and 1.5 K.

8894-17, Session 4

**PollyNET: a network of multiwavelength polarization Raman lidars (Invited Paper)**

Dietrich Althausen, Ronny Engelmann, Holger Baars, Birgit Heese, Thomas Kanitz, Leibniz Institut für Troposphärenforschung (Germany); Mika Komppula, Eleni Giannakaki, Anne Pfüller, Finnish Meteorological Institute (Finland); Ana Maria Silva, Jana Preissler, Univ. de Évora (Portugal); Frank Wagner, Juan Luis Rascado, Sérgio Pereira, University Évora, Centro de Geofísica de Évora (Portugal); Jae-Hyun Lim, Joon Young Ahn, National Institute of Environmental Research (Korea, Republic of); Matthias Tesche, Stockholm Univ. (Sweden); Iwona S. Stachlewska, Institute of Geophysics, Faculty of Physics, University of Warsaw (Poland)

PollyNET is a growing global network of automatized multiwavelength polarization Raman lidars of type Polly (Althausen, 2009). The goal of this network is to conduct advanced remote measurements of aerosol profiles and clouds by the same type of instrument.

Since 2006 this network assists the controlling and adjustment activities of Polly systems. A central facility receives the data from the Polly measurements. The observational data are displayed in terms of quicklooks at <http://polly.tropos.de> in near real time. In this way, the network serves as a central information platform for inquisitive scientists.

PollyNET comprises permanent stations at Leipzig (Germany), Kuopio (Finland), Evora (Portugal), Baengnyeong Island (South Korea), and

Stockholm (Sweden). Non-permanent stations have been used within several field experiments under both urban and very remote conditions - like the Amazon rain forest. These non-permanent were lasting from several weeks up to one year and have been located in Brazil, India, China, South Africa, Chile, and also aboard the German research vessel Polarstern across the Atlantic.

Within PollyNET the interaction and knowledge exchange is encouraged between the Polly operators. This includes support in international approved system calibration procedures, maintenance, and distribution of latest hardware and software improvements. The presentation will introduce the PollyNET. Main features of the Polly systems will be presented as well as recent instrumental developments. Some highlights of Polly measurements achieved within PollyNET will be shown.

#### 8894-18, Session 4

### Monitoring and characterization of atmospheric aerosols with Raman and dual-polarization lidars

Philippe ROYER, Laurent Sauvage, Anthony Bizard, Ludovic Thobois, Leosphere France (France)

Atmospheric aerosols play a key role on climate balance, on human health (breathing problems and lung cancer for pollution aerosols) and human activities (damage to aircraft engines by volcanic ashes). A continuous and long-term monitoring of aerosols is thus necessary in order to localize, characterize and quantify this threat. Active remote sensors by LiDARs are the only one capable of providing range-resolved measurements and thus determine the height of aerosol layers. A network of operational aerosol profilers is required to evaluate atmospheric dispersion of aerosols at regional scale. Furthermore, these profilers must be able to detect identify and possibly quantify the different structures/layers of aerosols and clouds in the troposphere from the lowest layers up to the tropopause.

R-Man510 has been specially designed in order to address these needs. This sensor combines the full performances of sophisticated LiDARs (high accuracy and low overlap function) with the low maintenance requirements of cloud ceilometers (use of diode-pump laser for a low maintenance). The two elastic channels at 355 nm (co- and cross-polarization) give information on base and top of aerosol layers and particle shape (measurement of depolarization ratio). Base and top of aerosol layers are detected using the vertical gradient on lidar profiles [1] (left panel on figure 1). The linear volume and particle depolarization ratios are retrieved from both co and cross-polarization channels using an on-site calibration procedure based on  $\pm 45^\circ$  method [2] (right panel on figure 1).

The nitrogen Raman detection at 387 nm is used for an accurate retrieval of extinction coefficient and lidar ratio or extinction-to-backscatter ratio [3]. The coupling of depolarization ratio with lidar ratio gives a classification of clouds and aerosol layers into 4 classes [4]: dust, volcanic, continental or marine aerosols. Figure 2 shows an example of cloud/aerosol classification during a dust event observed over Menorca Island in the framework of HyMex campaign. Dust aerosol layers are classified between 2 and 5 km when using Raman channel information.

Raman and dual-polarization LiDARs are a powerful tool for the detection, characterization and identification of aerosol layers in the atmosphere. The combining with ancillary measurements (size distribution, complex refractive index and density) enables to convert extinction coefficients from Raman lidar into mass concentration profiles with an overall uncertainty of ~30% for pollution aerosols and ~70% for volcanic aerosols.

[1] Morille Y. et al.: An Automated Algorithm to Retrieve the Vertical Structure of the Atmosphere from Single-Channel Lidar Data. *J. Atmos. Ocean. Technol.*, Vol. 24, No. 5, pages 761-775, 2007

[2] Freudenthaler, V. et al.: Depolarization ratio profiling at several wavelengths in pure Saharan dust during SAMUM 2006. *Tellus B*, Vol 61, No 1, DOI: 10.1111/j.1600-0889.2008.00396.x, 2009.

[3] Ansmann, A. et al.: Independent measurement of extinction and backscatter profiles in cirrus clouds by using a combined Raman elastic-backscatter lidar, *Appl. Opt.*, 31, 7113-7131, 1992.

[4] Burton et al.: Aerosol classification using airborne High Spectral Resolution Lidar measurements - methodology and examples, *Atmospheric Measurement Techniques*, doi:10.5194/amtd-4-5631-2011.

#### 8894-19, Session 4

### Assessment of long scale plume transport to the US East coast using coordinated CREST lidar network and synergistic AERONET and satellite measurements (Invited Paper)

Fred Moshary, Lina Cordero, Yonghua Wu, Barry M. Gross, The City College of New York (United States); Daniel Orozco, Patricia Sawamura, Raymond M. Hoff, Ruben Delgado, Univ. of Maryland, Baltimore County (United States); Jia Su, Kevin Leavor, Robert B. Lee III, Patrick McCormick, Hampton Univ. (United States)

The vertical stratification and optical characteristics of smoke and dust plumes during the transport are critical to evaluate their influences on the Earth's climate radiation and atmospheric environment and air quality. In this study, we present synergistic measurements of aloft aerosol plumes by the ground-based NOAA-CREST lidar network (CLN) of three lidars along the East Coast of United States from New York to Virginia, and AERONET-sun/sky radiometers and satellite observations. We focus on a typical plume episode that was simultaneously observed by the CLN sites on March 6 - 7, 2012, and show the variations of time-height distribution, optical characteristics, sources and long-range transport.

During the plume intrusion period, the CLN and AERONET measurements were consistent illustrating the onset of dust aerosol plumes. For example, we consistently observed two-layers of aerosol plumes located at 1.0 ~ 8.0 km in the free troposphere, resulting in a significant increase of aerosol optical depth (AOD=0.05-0.2 at 532-nm) and a decrease of the column Angstrom exponents from 1.7 to 1.0. The column-average volume size distributions show increasing concentration of both fine- and coarse-modes aerosols, but are dominated by the coarse-mode. Direct lidar inversions illustrate that the aerosol plume layers contribute up to 70% fraction of the total AOD and is consistent with AERONET volume size distributions.

The 3-day NOAA-HYSPLIT model trajectories indicate the transport from the mid-west US while the 10-day trajectories shows the trans-pacific transport of Asian-dust where the MODIS/Aqua verified a heavy dust storm event in the Gobi-deserts of north-west China. The space-borne lidar CALIPSO observations indicate the aloft dust layers at 4-8 km altitude in the eastern US on March 6, as well as a number of low-level dust layers in the mid-west US (Texas/New Mexico/Utah) during March 1- 6, 2012. The coarse-mode particles observed in the eastern US are also characterized by small Angstrom exponents (<1.2) from AQUA/MODIS retrievals. However, the NOAA-HMS satellite products illustrate the fire and smoke sources in the south-eastern US including Oklahoma/Kansas/Missouri and South Carolina/Georgia.

Accordingly, the upper layer of coarse mode aerosols is most likely transported from the East Asia, while the lower layer at 2-3 km altitudes consists of continental dust particles from the western US mixed with fine-mode smoke particles. In addition, the transport and sources of aerosol are further investigated with the NAAPS global aerosol transport model. The model illustrates that the total optical depth and mass concentration of aerosol are dominated by the dust particles at the CLN-sites; and the similar vertical structures of aerosol profiles between the lidar and NAAPS model are shown at 18:00UTC (daytime) on March 6, 2012; but much different in the night (00:00UTC) on March 7, 2012.

#### 8894-20, Session 4

### A versatile instrument with an optical parametric oscillator transmitter tunable from 1.5 to 3.1 $\mu\text{m}$ for aerosol Lidar and DIAL

Iain Robinson, Jim W. Jack, The Univ. of Edinburgh (United Kingdom); Cameron F. Rae, Univ. of St. Andrews (United Kingdom); John B. Moncrieff, The Univ. of Edinburgh (United Kingdom)

Lidar is a valuable tool for atmospheric monitoring, allowing range-resolved profile measurements of a variety of quantities including

aerosols, wind, pollutants and greenhouse gases. We report here the development of a versatile field-deployable instrument for monitoring the lower troposphere. This region includes the effects of surface-atmosphere interactions and is an area where the resolution of satellite data is generally poor.

Our instrument has been designed with the goal of making range-resolved measurements of greenhouse gases such as carbon dioxide, as well as probing the structure of the atmospheric boundary layer. The key component is a tunable laser source based on an optical parametric oscillator (OPO) covering the wavelength range 1.5–3.1  $\mu\text{m}$ . This range includes absorption lines of carbon dioxide and other greenhouse gases enabling the application of the differential absorption lidar (DIAL) technique, whilst also being suitable for eye-safe aerosol lidar. We also report the use of an avalanche photodiode detector with high sensitivity and low noise.

The OPO output was characterized to assess the beam quality and spectral properties. The M squared parameter and beam divergence were measured with a beam-profiling camera. To confirm the divergence of the transmitter, the beam diameter was also measured at an extended distance from the instrument. The wavelength, tuning curve, spectral width and stability of the free-running OPO were also determined.

Field tests of the instrument were performed, recording continuous lidar traces over periods of up to half an hour. The data were digitized at 8 traces per second and corrected for pulse-to-pulse fluctuations in the OPO output energy using the signal from a pyroelectric sensor mounted inside the laser transmitter. Scattering from aerosols and molecules was detected to a maximum range of 2 km, whilst scattering from cloud was recorded at up to 6 km. The data are plotted as time-versus-range images to show the dynamic state of the atmosphere evolving over time.

These results demonstrate that the lidar achieves key requirements for aerosol scatter and DIAL: tunability of the transmitter wavelength, sensitivity to molecular and aerosol scattering and alignment stability over extended periods. We also discuss further work to narrow the spectral width of the OPO by injection seeding and the use of active stabilization for locking the wavelength to a specific gas absorption line.

## 8894-21, Session 4

### Laser and microwave sensing of the stratosphere

Gennady G. Matvienko, Valerii N. Marichev, V.E. Zuev Institute of Atmospheric Optics (Russian Federation); Yury Y. Kulikov, Vitaly G. Ryskin, Institute of Applied Physics (Russian Federation)

The results of joint observations of ozone and temperature of the middle atmosphere over Tomsk in December 2012–January 2013 during the stratospheric warming are presented. The method of ground-based microwave radiometry and laser diagnostics have been used in the observations. The microwave radiometry and lidar technology allows the ozone and temperature variations to be studied during large-scale wave perturbations in the middle atmosphere, such as stratospheric warmings. In microwave observations of the ozone line, a spectrometer with a working frequency of 110.8 GHz has been used. This spectrometer allows the ozone emission spectrum to be measured for 20 min with an accuracy of ~ 2%. The measured ozone line has been used for the estimation of the vertical ozone distribution in a height range 20–60 km with an accuracy of about 10%. The vertical temperature distribution was measured by the lidar with a receiving mirror 1 m in diameter and a transmitter at an Nd:YAG laser with a wavelength of 532 nm, pulse energy of 200 mJ, pulse repetition frequency of 10 Hz, signal accumulation time of 2 h, spatial resolution of 192 m, and signal receiving in the single-electron photopulse counting mode. The backscattered radiation was received from heights of 15–60 km. The relative error was 2% at a height of 30–40 km. The stratospheric warming, during which the lidar and microwave observations were conducted, was of the major type. As a result, the air mass circulation in the upper stratosphere over the Western Siberia has changed from western transport to eastern transport. During winter anomalous events, marked variations of the ozone concentration and temperature in the stratosphere have been observed. The ozone concentration at height levels from 25 to 60 km varied from 1.5 to 2 times, and the amplitude of the variations has increased significantly. The peak of positive deviation of temperature

from its monthly average value achieved 70 K at a height of 30 km. In the mesosphere, the increased diurnal variations of the ozone concentration of, on average, 30% were observed at transitions from sunrise to sunset. Correlations between temperature and ozone variations were found at both the natural and perturbed states of the middle atmosphere. The observed results are compared with MLS/AURA data.

## 8894-5, Session PS

### A direct detection 1.6 $\mu\text{m}$ DIAL with three wavelengths for high accuracy measurements of vertical CO<sub>2</sub> concentration and temperature profiles

Yasukuni Shibata, Chikao Nagasawa, Makoto Abo, Tokyo Metropolitan Univ. (Japan)

The accurate vertical CO<sub>2</sub> profiles in the troposphere are highly desirable in the inverse techniques to improve quantification and understanding of the global budget of CO<sub>2</sub> and also global climate changes. Aircraft instruments can measure vertical profiles up to an altitude of 10 km but cannot perform continuous measurements. Therefore differential absorption lidar (DIAL) is an attractive method for obtaining vertical CO<sub>2</sub> profiles. Utilizing remote sensors to observe CO<sub>2</sub> in the lower and middle troposphere is helpful in reducing the uncertainties of the carbon sink and source estimation.

The 1.6  $\mu\text{m}$  DIAL measurement of the vertical CO<sub>2</sub> profile was already achieved successfully up to 7 km altitude with a random error less than 1.0 % by integration time of 30 minutes and range resolution of 300–600 m by our system. The absorption cross sections of gas vary with atmospheric temperature and pressure. Moreover, air density also depend on the temperature and pressure. Then precise temperature and pressure profiles are necessary for accurate CO<sub>2</sub> mixing ratio measurement by DIAL. But conventionally the radio sonde data near the lidar site have been used for DIAL analysis.

We report the new 1.6  $\mu\text{m}$  DIAL system that can measure the temperature profiles with the CO<sub>2</sub> concentration profiles simultaneously for improvement of measurement accuracy of the CO<sub>2</sub> density and mixing ratio (ppm). Laser beams of three wavelengths around a CO<sub>2</sub> absorption line is transmitted alternately to the atmosphere for simultaneous measurements of CO<sub>2</sub> concentration and temperature. We developed offset wavelength locking system for precise laser tuning. Moreover, a few processing algorithms of CO<sub>2</sub>-DIAL are also performed for improvement of measurement accuracy. Vertical CO<sub>2</sub> concentration and temperature profiles were simultaneously measured up to 7 km altitude with 1.8 km range resolution.

This work was financially supported by the System Development Program for Advanced Measurement and Analysis of the Japan Science and Technology Agency.

## 8894-22, Session PS

### Improving the accuracy of aerosol extinction coefficient inversion

Nianwen Cao, Cunxiong Zhu, Nanjing Univ. of Information Science & Technology (China)

This paper considers the relationship between the accuracy of aerosol extinction inversion and the boundary value, and derives a theoretical high-accuracy aerosol extinction coefficient inversion. Aerosol extinction coefficient profiles depend on the boundary value. The relationship function of the differential extinction coefficient and differential boundary value is expressed by a maximum value. The smaller the differential boundary value, the smaller the differential extinction coefficient. The clean atmosphere layer is easily found from the lidar range-corrected signal, and the extinction coefficient of the clean atmosphere layer can be obtained using the slope method. By relating the extinction coefficient of the clean atmosphere layer to the extinction coefficient profiles at different boundary values, an accurate aerosol extinction coefficient profile can be obtained.

Capsule abstract

By relating the extinction coefficient of the clean atmosphere layer

to the extinction coefficient profiles at different boundary values, an accurate aerosol extinction coefficient profile can be obtained.

#### Theory

Based on Lidar equation and extinction coefficient inversion theory, we do calculation as following:

where is the differential extinction coefficient and is the differential boundary value. Substituting and into equation (2), we obtain

For ease of calculation, the function is introduced to express the relationship between and . Equation (3) shows that the differential aerosol extinction coefficient depends on the relationship between the function and the differential boundary value.

#### Experimental data analysis

Aerosol measurement was carried out using a Rayleigh–Raman–Mie lidar in Nanjing, China, and Fig. 1 shows the results of the analysis of aerosol data. Figure 1(C) shows that the differential calculation of is a function of range, and it is zero at . Consequently, the maximum value of , occurs at , as shown in Fig. 1(D). Also, the maximum value of the range-corrected signal occurs at , as shown in Fig. 1(B). From Fig. 1(C) and equation (3), we can derive equation (5):

Figure 1. Analysis of the lidar signal. (A) Lidar return signal. (B) Lidar range-corrected signal. (C) Profile of the differential calculation relationship function of. (D) Relationship function of.

Equation (5) shows that the differential aerosol extinction coefficient is proportional to the differential boundary value : the smaller the boundary value , the smaller the differential aerosol extinction coefficient.

#### Simulation

To verify the assumptions on which equation (3) is based, we analyzed data from a simulated lidar signal (Fig. 2).

Figure 2 Analysis of data from the simulated lidar signal. (A) Simulated lidar return signal. (B) Simulated lidar range-corrected signal. (C) Profile of the differential calculation relationship function of . (D) Relationship function of based on the simulated lidar signal.

#### Aerosol extinction coefficient inversion

The results of the extinction coefficient inversion at different boundary values (Fig. 3) show that the extinction coefficient profiles vary with the boundary value.

Figure 3 Results of extinction coefficient inversion at various boundary values using experimental lidar data. Upper panel: extinction coefficient profiles at boundary values between  $1 \times 10^{-4}$  and  $1 \times 10^{-6}$  (increments of  $1 \times 10^{-5}$  and  $5 \times 10^{-6}$ ). Lower panel: enlarged view of extinction coefficient profiles at boundary values between  $1 \times 10^{-4}$  and  $9.2 \times 10^{-5}$ , but separated by a smaller increment of  $1 \times 10^{-6}$ , and over a narrower range.

To address this issue we attempted to identify a clean atmosphere layer within the lidar echo data (Fig. 4). The lower panel of Fig. 4 shows that the return signal approximates a straight line at a range between 2671.5 m and 3965.25 m, where the decay of the return signal increases with the range. The slope of the line is

Figure 4 Upper panel: lidar return signal. Lower panel: enlarged view of the lidar return signal at a range of 2000–4000 m.

Figure 5 shows the aerosol extinction coefficient profiles at different boundary values. In the upper panel of Fig. 5, the extinction coefficient values are around  $7.67 \times 10^{-6}$ ,  $4.10 \times 10^{-6}$ , and  $8.52 \times 10^{-7}$ , at ranges between 2670 m and 4000 m. The value of  $4.10 \times 10^{-6}$  is almost identical to the  $4.336 \times 10^{-6}$  obtained from Fig. 4. The aerosol extinction coefficient profile indicated by the cross within a circle, and corresponding to a value of  $4.10 \times 10^{-6}$ , is the most accurate. In the lower panel of Fig. 5, the extinction coefficient profiles relate to different boundary values, but with same division of  $1 \times 10^{-6}$ . The extinction coefficient values are around  $5.43 \times 10^{-6}$ ,  $4.64 \times 10^{-6}$ ,  $3.86 \times 10^{-6}$ ,  $3.08 \times 10^{-6}$ , and  $2.42 \times 10^{-6}$  when the range is between 2670 m and 4000 m. The value of  $4.64 \times 10^{-6}$  is close to the  $4.336 \times 10^{-6}$  obtained from Fig. 4. The extinction coefficient profile marked by the cross within a circle, and corresponding to  $4.64 \times 10^{-6}$  ( $\sim 4.336 \times 10^{-6}$ ), is the closest to the real aerosol extinction coefficient profile.

Figure 5 Upper panel: aerosol extinction coefficient profiles at different boundary values with a larger increment of  $5 \times 10^{-6}$  and smaller increments of  $5 \times 10^{-7}$  and  $5 \times 10^{-8}$ . Lower panel: aerosol extinction coefficient profiles at different boundary values with the same increment of  $1 \times 10^{-6}$ .

#### Conclusions

Aerosol extinction coefficient inversion is directly related to the extinction coefficient boundary value, and uncertainty regarding aerosol extinction is critically dependent upon changes to these

boundary values. Maximum values exist in the relationship function relative to the differential extinction coefficient and the differential boundary value. The difference between various extinction coefficient profiles is proportional to the difference in the boundary values. Comparisons between the extinction coefficient of the clean atmosphere layer, and extinction coefficients inversed at different boundary values, can be used to accurately determine the most realistic extinction coefficient profile.

### 8894-23, Session PS

#### Multiwave fine tuning laser source for simultaneous sounding atmosphere constituents and/or chemicals

Sergii M. Bashchenko, Ludmila Marchenko, Institute of Physics (Ukraine); Oksana Bashchenko, Kiev State Univ. (Ukraine)

Simultaneous multi-wave sounding may help to unveil fast (f.e. photochemical) processes in atmosphere. The scheme of multi-wave fine tuning laser source, suitable for simultaneous probing atmosphere constituents and/or chemicals by differential absorption with scattering method, is suggested..

Such a source may consist of excimer laser complex complemented with a converter implementing Stimulated Raman Scattering phenomena. Complex is and converter may be assembled and operate using “oscillator-amplifier” optical scheme, which provides simultaneous generation at a few wavelengths in a wide spectral range ( $\approx 200\text{--}900\text{ nm}$ ) due to discrete Raman conversion and with its both narrow bandwidth and fine tuning due to laser complex implementation. Use of various gases in both laser and converter provides wide set (tenths) of possible discrete line which may be generated. Narrow spectral bandwidth of lines in combination with its fine tuning provides the possibility to utilize fine (vibration) structure in absorption spectra of probing species for more precise obtained data interpreting.

Experimental pattern of many-waves laser source elaborated by this scheme is described. In our attempt laser source consists of XeCl<sup>+</sup>-excimer laser complex supplemented with Raman-converter with dense hydrogen. Possibilities of simultaneous generation at six lines – 273, 308, 353, 414, 500, 633 nm – with fine tuning of all lines within up to 1-2 nm are demonstrated. Beam divergence was  $\sim 10E\text{-}5$  radians, energy of lines was 1-10 mJ.

### 8894-24, Session PS

#### Stand-off mapping of the soot extinction coefficient in a refinery flare using a 3-wavelength elastic backscatter LIDAR

Renata F. Da Costa, Riad Bourayou, Eduardo Landulfo, Instituto de Pesquisas Energéticas e Nucleares (Brazil); Roberto Guardani, Escola Politécnica da Univ. de São Paulo (Brazil); Igor A. Veselovskii, A. M. Prokhorov General Physics Institute (Russian Federation); Juliana Steffens, URI (Brazil)

In this study, a mapping of the soot extinction coefficient in an oil refinery flare using a three wavelength elastic backscatter lidar system is presented. A log-normal aerosol size distribution was assumed for the flare, and a homogenous refractive index was assumed along the nearly horizontal beam path through the atmosphere, excluding the flare volume. The optical depth was estimated for each wavelength and from this the Angstrom exponent was calculated. The results were comparable with the literature, demonstrating that it is possible to distinguish small from large particles by this technique in low wind turbulence conditions.

### 8894-25, Session PS

#### 3D building model reconstruction using aerial lidar data: a case study in Hendijan, Iran

Laleh Moghtader, Mahsa Siavashi, Maryam Safari, Mehran Satri, Univ. of Isfahan (Iran, Islamic Republic of)

Airborne laser scanning data has a great potential for modelling man-made objects such as buildings, which form a substantial part of 3-D city models in urban management. In this paper for the determination of parameters of Iranian building types, invariant moments (as a model-driven method) applied to point clouds of LiDAR data has been discussed.

The proposed method works on the original, irregularly-distributed laser scanner data points, for avoiding effects caused by an interpolation to a regular grid. Using first and second order invariant moments, the seven parameters that describe a building (position, orientation, length, width, height, roof type and roof steepness) can be determined as a solution from ratios of binary and height-weighted moments of building point clouds.

Building model reconstruction is based on two methods: model-driven and data-driven methods.

Model-driven methods contain databases of fixed building models. This method depends on previous knowledge about variety of building models in the study area. Intrinsic resistance against the oscillation of the points from facets and the gap of data are the advantages of these methods. Although this reconstruction method is simple to understand and use, it's useful for simple building models such as flat roof buildings or gables; while there are a variety of complex building models. Thus this approach would not extract the model of all type of the buildings.

In data-driven methods, building model could be reconstructed after extracting the building facets and reconstructing the surface topology. These methods increase the flexibility in reconstruction of complex building model. Furthermore few assumptions about the structure are considered in these methods.

In Iranian architecture, buildings have flat roofs and roof entrances are built in difference level from roof. Moreover, roofs are covered with asphalt or bitumen and have skylight that are different from dormers of European buildings gables. Also some objects such as air conditioning or television antenna are located on the roof. The distances between adjacent buildings are very small (About 10 Cm) and in some cases the roofs of buildings have overlap and it is difficult (and sometimes impossible) to distinguish the borders of two buildings.

Due to mentioned specification of Iranian roofs and requirements of prior information about building models on both model-driven and data-driven methods, it is necessary to identify Iranian building models and develop a library of models for the reconstruction of building model. For this purpose, the technique was applied to a section of a Q560 laser scanner data set with an average point density of more than nine points per square meter, acquired over Hendijan, in Iran.

The evaluations show that all buildings complying with the assumed simple building types could be modeled successfully. The precision for the building parameters is in the order of 0.1-0.2 meter for the dimensions.

## 8894-26, Session PS

### Laser femtosecond sensing of the aerosol atmosphere

Gennady G. Matvienko, Victor G. Oshlakov II, Alexander Y. Sukhanov, V.E. Zuev Institute of Atmospheric Optics (Russian Federation); Andrey N. Stepanov, Institute of Applied Physics (Russian Federation)

First tentative results of application of white-light lidars (WLLs) based on the effect of filamentation have demonstrated their potential for sensing of the atmosphere up to heights of 12–15 km. The combination of WLLs with high-resolution Fourier spectroscopy opens a way for the more efficient solution of traditional problems of lidar sensing. WLLs provide a new insight into the multifrequency sensing of microphysical parameters of aerosol particles without, first of all, bulky and hard-to-control multilidar systems. It becomes possible to select optimal sensing wavelengths informative for a given class of meteorological objects. Our papers have demonstrated the principal possibility of remote detection of the size spectrum of aerosol particles through the recording of the backscattered supercontinuum signal at three or four visible wavelengths. Principles of selection of informative wavelengths for the optical sensing with the continuum radiation of broadband WLL are determined. Efficient algorithms for

reconstruction of vertical profiles of optical interaction coefficients and particle size spectrum within a stratified inhomogeneous cloud layer are proposed and developed. The algorithms are based on the application of the neural network approach and stochastic genetic search. The distributions of cloud droplets over lidar signals at wavelengths of 1.28, 1.56, 1.61, and 2.13  $\mu\text{m}$  have been obtained in a model experiment under boundary conditions corresponding to the actual lidar.

Then, within the framework of the study of possibilities of applying femtosecond sources to sensing of the aerosol atmosphere, in situ experiment of lidar sensing of an artificial aerosol cloud at a short (85 m) atmospheric path has been conducted. Signals backscattered from the artificial aerosol (ethylene glycol) with a particle diameter of 1  $\mu\text{m}$  exposed to the supercontinuum radiation from the laser beam filamentation zone have been received. The spectral distribution of backscattered signals was detected by Hr4000 spectrophotometer (Ocean Optics) in a range 0.2?1.1  $\mu\text{m}$ . This in situ experiment was copied in the closed numerical Monte Carlo simulation, and the inverse problem on reconstruction of modes of the particle size distribution was solved based on the genetic algorithm with the use of broadband spectral data. The particle distribution functions are obtained in the model case for particles with modal radii of 0.5, 1, 1.5, and 2  $\mu\text{m}$ . These functions appeared to be close to the initial data with deviations of only fractions of percent. For the experimental spectrum with a particle diameter of 1  $\mu\text{m}$ , the reconstruction yielded a mode with a radius of 0.498.

Further recommendations for the development of lidar sensing systems based on femtosecond radiation sources include the obtaining of the spatially resolved spectrum or the use of two receivers in the bistatic scheme, when one receiver is directed at an aerosol cloud, while another is directed into the space under the cloud.

## 8894-27, Session PS

### Mid-IR DIAL for high-resolution mapping of explosive precursors

Valentin Mitev, Ctr. Suisse d'Electronique et de Microtechnique SA (Switzerland); Sergey M. Babichenko, Laser Diagnostic Instruments AS (Estonia); Jonathan Bennes, Ctr. Suisse d'Electronique et de Microtechnique SA (Switzerland); Rodolfo Borelli, ENEA (Italy); Agnes Dolfi-Bouteyre, ONERA (France); Luca Fiorani, ENEA (Italy); Laurent Hespel, Thierry Huet, ONERA (France); Antonio Palucci, Marco Pistilli, Adriana Puiu, ENEA (Italy); Ott Rebane, Laser Diagnostic Instruments AS (Estonia); Innokenti Sobolev, Tallinn Univ. of Technology (Estonia)

A DIAL instrument on a moving platform is seen as a valuable remote sensing component in a sensor network for area monitoring targeting the identification of sites involved in authorized explosive manufacturing. Such instrument will perform the area mapping of the vapor concentration of key substances, known to be used as precursor in explosive fabrication, such as acetone and nitromethane. One of the targets in the FP7 project BONAS (BOmb factory detection by Networks of Advanced Sensors) is the design, development and the verification of such DIAL instrument. Such instrument is seen as a tool for the scanning of medium-sized areas for identification of such vapor sources.

The IR spectra of acetone and nitromethane in the gas phase have been measured in the laboratory, comparing our results with the best available databases and publications. After consideration of atmospheric transmittance and available laser sources, we conclude that the best spectral band for the DIAL operation is in the range between 3.0 $\mu\text{m}$  and 4.0 $\mu\text{m}$ .

The DIAL operation has been numerically simulated taking into account all noise sources. The code, based on a line by line approach, relies on the HITRAN database for the spectroscopic characteristics of molecules. As for the optical properties of the aerosol particles, they are issued from the usual models introduced in the radiative transfer codes or from the software package OPAC. The thermo-chemical properties of the atmosphere are taken from the U.S. Standard Atmosphere or from a climatological model.

Eventually, a combination of OPO (optical parametric oscillator) and OPA (optical parametric amplifier) has been chosen as a transmitter, where the idler wavelength, tunable in the range of 3.0 $\mu\text{m}$  and 4.0  $\mu\text{m}$ ,

is transmitted in the atmosphere after a beam expansion.

The pumping source for the OPO-OPA combination is a Nd:YAG laser. The optical receiver is an off-axis parabolic mirror. The scanner or targeting turret is mounted on top of the already co-axially aligned laser and FOV (field of view) of the detector. This enables the transmission and reception part of the DIAL to be aligned independently of the scanner angles. The scanner is able to scan almost 360 degrees horizontally and  $\pm 30$  degrees vertically. The scanner mirror is an elliptically-outlined first-surface aluminum mirror which covers the FOV of the telescope at all scanning angles.

The "on"- "off" probing is realized by tuning the OPO in a sequence. The detection is performed by a single photovoltaic photo-diode with 4-stage cooling and signal amplification. The signal digitization is done also by a single transient ADC (14bit amplitude resolution, 125 Ms/s digitization rate). The signal storage is synchronized with the wavelength "on"- "off", so the back-scatter signal resulting from laser pulses at "on" and "off" wavelengths are recorded as single files, one for each pulse.

At the conference we will present the details of the design and realization, the processing procedure with analysis of the precision limiting factors, as well as the first results in the DIAL functional and performance tests.

## 8894-28, Session PS

### Automatic methods to detect the top of ABL

Gregori A. Moreira, Riad Bourayou, Instituto de Pesquisas Energéticas e Nucleares (Brazil); Fabio J. da Silva Lopes, Univ. de São Paulo (Brazil) and Instituto de Pesquisas Energéticas e Nucleares (Brazil); Taciana A. Albuquerque, Neyval C. Reis Jr., UFES (Brazil); Gerhard Held, Univ. Estadual Paulista "Júlio de Mesquita Filho" (Brazil); Eduardo Landulfo, Instituto de Pesquisas Energéticas e Nucleares (Brazil)

A LIDAR system has been appointed by many authors as one of the best tools to obtain information that will allow to provide a good description and characterization of ABL (Atmospheric Boundary Layer), because the LIDAR's good spatial and time resolutions, besides this kind of system enables the realization of data capture without the influence in the study object.

The main objective of this work is to obtain methods that allow, automatically, qualitative detections of ABL height by LIDAR data. Case studies will be used to describe the more relevant days of a campaign carried on in July 2012, in Vitória – Espírito Santo state - Brazil. In this campaign a mobile LIDAR system for data capture was employed. The data analysis was made in order to make a comparison among three mathematical algorithms that provide automatically the ABL height: Gradient Method (GM), using the derivative of the Range Corrected Signal (RCS) logarithm, WCT (Wavelet Covariance Transform) and Richardson's Number, the latter although does not depend on the LIDAR data, rather it depends on radiosounding data, it was used to validate the methods above mentioned.

In stationary-condition days, all methods provided reasonable results, with little differences in the retrieved height values, as a sensitive factor being that the insertion of the threshold value, in WCT and GM methods, was very important to avoid confusions between the residual layer and the top of ABL. In days where there was an inner aerosol sublayer in the ABL, the GM method has shown great difficulty to detect the top of ABL, because of its large variability as the input was changed. The WCT method provided better results, but it needed a best refinement of the model function parameters, in order to give a better differentiation between the sublayers and consequently a correct value to maximum height of ABL. In turbulent days all methods have experienced great difficulty into looking for the correct value of the top of ABL, because the presence of clouds and aerosol sublayers within the ABL. To obtain better results it was needed to input a high threshold value in both methods, and specifically to WCT, the careful choose of function parameters was fundamental to obtain good results. The comparison between the methods have shown that as the presence of clouds and aerosol sublayer increased the more sensitive was the refinement needed to choose the "right" parameters, whereas even Richardson's method, used to validate the algorithms, had ambiguities in finding a good estimate of the ABL top.

This study gave us background for further improvements of the algorithms used in order to solve the difficulties encountered and a hint to implement a new method, based on the "curtain" plots images

obtained from LIDAR RCS data.

## 8894-29, Session PS

### A laser beam splitting and regulating technology of airborne laser radar: experiments and analysis

Ming Li, Weiming Xu, Rong Shu, Genghua Huang, Shanghai Institute of Technical Physics (China)

To promote the efficiency of getting 3-D imaging data of airborne laser, laser radar working in broom-sweep mode usually transmits a lot of laser beams simultaneously. The number and divergence of laser beams decides the sweep range and resolution of the system. For instance, airborne laser radar flying an altitude below 10 kilometers needs a divergence less than 100 micro-radian to get a resolution less than one meter. And hundreds of beams are acquired to cover a range of several hundred meters.

Based on fiber array technology, this paper realized a laser transmitting module, in which beam is split, regulated and compressed by an off-axis telescope. Over two hundred pieces of multi-mode fibers are arranged in an array and fixed in a base material. The end plane of the fiber array is polished to a certain shape. The laser beams are then sent to a set of off-axis telescope. The quality of the light spots, the separation angle, and the divergence are measured and analyzed. Factors influencing those parameters are discussed.

## 8894-31, Session PS

### Quality control of manual editing and checking for producing high resolution DEM from point cloud

Ming-Ko Chung, National Taipei Univ. of Technology (Taiwan); Che-Hao Chang, National Taiwan Univ. of Technology (Taiwan)

The use of airborne LIDAR get the point cloud has become one of the primary methods used for DEM generation. Point cloud classification correctness direct impact on the quality of the DEM, the improved classification correctness will be able to get a higher quality product. Domestic point cloud inspection in the past to take the usual standards, even if the classification results more closely true value, the final product, however, the DEM with a different level, that is, with different standards. How the two different standards, taking the balance is the main purpose of this study.

In this study, domestic 1/5000 DEM specification analysis of point cloud correct rate improve DEM quality. The experimental results showed that the increase, with the classification number the correctness rates also will increase, its corresponding point cloud interpolation after grid elevation difference specification allowable value, results show that not all changes in grid exceed the difference in elevation are standardize the allowable value, which this part of the grid point cloud classification results, does not affect the level of product quality, referred to as over-classification. This study each stage filtration complete point cloud classification results, whether there is still significantly influence of the grades, so the impact of the number is smaller than the statistical tolerance value, will be able to provide a job reference for the judge again classification necessity.

Airborne LIDAR can generate high resolution DEM from point cloud. In order to produce DEM from point cloud, filtering non-ground points is the major process. Filtering included automatic filtering and manual editing. Many automatic filtering methods have been developed and designed to keep correct ground points, but there is no perfect automatic filtering method. Therefore, manual editing is necessary for filtering work. After automatic filtering and manual editing, visual inspection insured filtering quality and found miss or error classification. Therefore, manual editing and visual inspection were repeated until correct classification.

## 8894-32, Session PS

### Ceilmeter, sun photometer and ozonometer measurements of the aerosol

## optical depth, angstrom coefficients, water vapor and total ozone content over Sofia (Bulgaria)

Nikolay Kolev, Tsvetina Evgenieva, Institute of Electronics (Bulgaria); Nikolay Miloshev, Plamen Muhtarov, National Institute of Geophysics, Geodesy and Geography (Bulgaria); Doyno Petkov, Space Research and Technology Institute (Bulgaria); Evgeni Donev, Danko Ivanov, Sofia Univ. "St. Kliment Ohridski" (Bulgaria); Ivan Kolev, Institute of Electronics (Bulgaria)

This contribution presents the results from three experimental campaigns carried out in June 2010, June 2011 and June 2012 at three sites in the city of Sofia (Institute of Electronics, Astronomical Observatory in the Borisova Gradina Park and National Institute of Geophysics, Geodesy and Geography (NIGGG)). A ceilometer CHM15k, two sun photometers Microtops II and an automatic meteorological station were used during the experiments.

The height of the mixing layer varied from 1500m to 2500 (3000)m during the measurements. The height of the residual layer ranged from 800m to 2000m. The stable boundary layer extended to 200-400m over the first campaign and reached 1200m during the second one.

The aerosol optical depth (AOD) at wavelength  $\lambda = 500\text{nm}$  ranged from 0.11 to 0.66 in the first campaign and from 0.24 to 0.55 in the second one and from 0.11 to 0.23 in the third one. Corresponding ranges for the water vapor content (WVC) were 1.26cm to 2.6cm. Different types of aerosol optical depth and water vapor content behavior were observed. The total ozone content (TOC) varied from 240 DU to 370 DU during the campaigns. The ground - based observation from ozonemeter Microtops II with satellite observation of Ozone Monitor Instruments (OMI) over Sofia (Bulgaria) are compared. Our results have implications for the further study of regional climate change.

## 8894-33, Session PS

### Studying Taklamakan aerosol properties with lidar (STAPL)

Paul W. Cottle, The Univ. of British Columbia (Canada); Detlef Mueller, Univ. of Hertfordshire (United Kingdom); Dong-Ho Shin, Gwangju Institute of Science and Technology (Korea, Republic of); XiaoXiao Zhang, Xinjiang Institute of Ecology and Geography (China); Kevin B. Strawbridge, Environment Canada (Canada); Ian McKendry, The Univ. of British Columbia (Canada); Guanglong Feng, Xinjiang Institute of Ecology and Geography (China)

The impact of dust on global energy cycles in the atmosphere is substantial, but global energy models that attempt to account for dust must rely on many assumptions about things like the optical properties and vertical distributions of these aerosols. It has been shown, however, that all of these physical, chemical and optical properties change during periods of extended global transport. The purpose of this study is to use a combination of lidar data and models to directly observe the changing properties of dust layers as they are transported from their origin in the Taklamakan Desert of western China.

With the co-operation of the Xinjiang Institute of Ecology and Geography, a portable micropulse lidar system was installed at Aksu National Field on the northern edge of the Tarim Basin in late April 2013, during the Spring dust storm season. Over six days, data were collected on the optical properties of dust emissions passing over this location. Model results show this dust was then transported across the region at least as far as Korea and Japan. Models from the Naval Aerosol Analysis and Prediction System (NAAPS) show that during transport the dust layers became intermixed with sulfate emissions from industrial sources in China as well as smoke from wildfires burning in south-east Asia. The 3+2 Raman lidar located in Gwangju South Korea was used to observe layer optical properties such as colour ratio, depolarization ratio and extinction coefficient after regional-scale transportation and mixing with other aerosols. By comparing the observations of the Gwangju lidar with those taken near the source at Aksu, we demonstrate the extent of the change in optical properties of the dust layers over time. There is some evidence that the layers were also observed by the CORALNet lidar in Vancouver,

BC and these observations are reported as well.

## 8894-34, Session PS

### Vertically resolved optical and microphysical particle properties over Portugal in February 2012

Jana Preissler, Sergio Pereira, Ana Maria Silva, Frank Wagner, Univ. de Évora (Portugal)

Unusual forest fire activities occurred in northern Portugal in the end of February 2012. This is generally the cold and wet season during which forest fires are very rare in this region. The smoke plumes were observed over Évora in southern Portugal by a multi-wavelength Raman lidar of the type PollyXT [1]. This type of instrumentation allows a detailed study of the vertical profiles of optical and microphysical aerosol properties.

For this work, several aerosol layers observed during February 2012 were studied considering optical and microphysical properties. The case discussed here was monitored during the night of 28 February 2012 between 3:00 and 4:00 UTC. Two aerosol plumes were detected above the shallow nocturnal boundary layer, one from 750 to 1500 m above sea level (asl) and one from 1650 to 1830 m asl. The mean particle lidar ratios were  $(23\pm 2)$  sr and  $(38\pm 7)$  sr at 355 and 532 nm, respectively, in the lower layer, and  $(22\pm 7)$  sr and  $(39\pm 4)$  sr at 355 and 532 nm, respectively, in the upper layer. Backscatter-related Ångström exponents were  $1.5\pm 0.1$  at the pair of wavelengths 355 and 532 nm and  $1.2\pm 0.0$  at the pair of wavelengths 532 and 1064 nm in the lower layer, and  $1.5\pm 0.2$  and  $1.3\pm 0.0$ , respectively, in the upper layer. The linear particle depolarisation ratio was about 7%.

Back-trajectories [2] were analysed in order to determine the source region of the aerosol plumes. For both layers, the air masses were transported from the north of Portugal and the northern Atlantic ocean. An increasing number of active fires were detected by the satellite-borne Moderate Resolution Imaging Spectroradiometer (MODIS)[3] over northern Portugal from 20 February 2012. However, the transport path over the Atlantic suggests a mixture of biomass burning smoke with marine aerosol.

Besides the optical properties, the vertical profiles of microphysical properties were analysed using an inversion algorithm [4]. The variation of the investigated quantities with altitude was small, as indicated by the standard deviations. Mean values and standard deviations of the effective radius were  $0.30\pm 0.05 \mu\text{m}$ , the surface area concentration was  $50\pm 9 \mu\text{m}^2/\text{cm}^3$ , the volume concentration was  $5\pm 1 \mu\text{m}^3/\text{cm}^3$ , the real part of the complex refractive index was  $1.61\pm 0.02$ , and the imaginary part was  $0.014\pm 0.003$ . The single scattering albedo (SSA) showed a very small wavelength dependence. Mean value and standard deviation of the SSA at 532 nm were  $0.93\pm 0.01$ .

[1] Althausen, D., et al. (2009), Portable Raman Lidar PollyXT for Automated Profiling of Aerosol Backscatter, Extinction, and Depolarization. *Journal of Atmospheric and Oceanic Technology*, 26, doi:10.1175/2009JTECHA1304.1.

[2] Draxler, R. R., and G. D. Rolph (2012), HYSPLIT (HYbrid Single-Particle Lagrangian Integrated Trajectory) Model access via NOAA ARL READY Website (<http://ready.arl.noaa.gov/HYSPLIT.php>), NOAA Air Resources Laboratory, Silver Spring, MD.

[3] Giglio, L., et al. (2003), An enhanced contextual fire detection algorithm for MODIS, *Remote Sensing of Environment*, 87, doi:10.1016/S0034-4257(03)00184-6.

[4] Kolgotin, A., and D. Müller (2008), Theory of inversion with two-dimensional regularization: profiles of microphysical particle properties derived from multiwavelength lidar measurements, *Applied Optics*, 47, 4472-4490.

## 8894-36, Session PS

### Historical site scanning and monitoring by terrestrial lidar: Taiwan Songshan cultural and creative park

Ming-Ko Chung, Che-Hao Chang, Yu-Wei Shih, National Taipei Univ. of Technology (Taiwan)

In this study, we scanning the historical site in the Taiwan Songshan Cultural and Creative Park regularly by LiDAR, inspect the damaged state of the chimney, reconstruct the entire building's 3D model for the subsequent monitoring, and provide the important data such as width, position of the cracks.

We went for pre-measurement field inspection in 2012.4.3, the boiler room is 24 meters long, 15 meters wide in dimension. The chimney is 35 meters in height with a diameter of 2.5 meters. To perform a complete scan of the entire chimney and boiler room area, 14 measuring points are needed, with 2 of them covering the rooftop of the boiler room. Certain zones were however shielded from the scanning point.

Our measuring instruments are as follows: TOPCON Image Station as the Total station; Riegl VZ-400 as the Terrestrial LiDAR; Hi-Target V30 as the e-GPS. We collected GPS data with the e-GPS, and measure 4 feature points with total station for the use of combining the LiDAR data. And then reconstruct the whole entire building's 3D model

We perform measurement accuracy examination, cracks examination, and tilt angle examination. the measurement accuracy is 4 millimeters, there are 6 cracks at the top of the chimney, the average length of the cracks is about 1.7 meters, and the width is about 0.1 meters. The tilt angle of the chimney is about 0.686 degrees.

8894-37, Session PS

## A temperature calibration method for CDOM fluorescence LIF Lidar

Peng Chen, Zhihua Mao, Jianyu Chen, The Second Institute of Oceanography, SOA (China)

The influence of temperature change on the determined concentrations of dissolved organic matter (DOM) in water was investigated by laser induced fluorescence (LIF) technique in laboratory. The effect of temperature on CDOM fluorescence was investigated in freshwaters of Xixi River and in aqueous standards. The total luminescence spectra (TLS) of CDOM in several types of water samples with laser-induced fluorescence (LIF) measurements using a 405 nm wavelength excitation source were measured in the laboratory, and the spectra of CDOM were pointed out and obtained with spectral fluorescence signature (SFS) technique. The spectrum of water Raman scattering and fluorescence of CDOM were separated from TLS with fitting Gaussian of the least squares method, and the curve of fluorescence peak intensity of CDOM against corresponding concentration of CDOM is showed. A temperature calibration equation was derived to standardize CDOM fluorescence measurements to a specific reference temperature. The form of the equation is:  $F_{CDOM} = FM / [1 + r(TM - TR)]$ , where T is temperature ( $^{\circ}C$ ), r is the temperature-specific coefficient of fluorescence ( $^{\circ}C^{-1}$ ), FM is the measured fluorescent intensity and the subscripts TR and TM stand for the reference and measured values. Laboratory experiments with a portable hyperspectral LIF LiDAR showed that CDOM fluorescence intensity decreased as ambient water temperature increased. High correlation ( $R^2=0.93$ ) was observed between concentration of CDOM and fluorescence normalized to water Raman scattering with the temperature calibration method. When applied to field data, temperature calibration removed the effect of multi-day trends in water temperature, and it also damped the diel CDOM cycle. We conclude that temperature calibration is a necessary and important aspect of CDOM monitoring using in situ fluorescence sensors.



# Conference 8895: High-Performance Computing in Remote Sensing III

Wednesday - Thursday 25–26 September 2013

Part of Proceedings of SPIE Vol. 8895 High-Performance Computing in Remote Sensing III

8895-1, Session 1

## Simulation of complex visibilities in synthetic aperture imaging radiometry with the aid of GPU

*(Invited Paper)*

Eric Anterrieu, Ctr. National de la Recherche Scientifique (France) and Univ. de Toulouse (France); François Cabot, Ctr. d'Etudes Spatiales de la Biosphère (France)

The idea of aperture synthesis is to obtain high-resolution images with the aid of the computer by combining passive interferometric measurements, known as complex visibilities, corresponding to spatial frequencies associated to pairs of receiving antennae. The concept of imaging interferometry by aperture synthesis has been initially developed for radio astronomy some decades ago and it has been recently used for remote sensing of the Earth surface in the microwaves range.

In conventional interferometry, the radio signals received by pairs of spatially separated antennae observing in the same direction are sampled and directly transmitted via coaxial cables, or fiber-optic links, to a correlator unit which produces the interference fringes in real time. In such arrays, the antennae are physically connected to the correlator and the complex visibilities are obtained in real time.

For unconnected arrays, the signals received by the antennae are sampled, recorded alongside with an accurate time base, and then stored on magnetic tape or on hard disk for deferred time analysis. At that later time, at the location of the correlator unit, the data are synchronized, played back together and combined just as if they were coming in real time from the antennae.

This contribution is concerned with the simulation of the signals emitted by a spatially incoherent source and collected by antennae, as well as with their numerical correlation.

According to the VAN-CITTERT ZERNIKE theorem, direct simulation of the complex visibilities provided by pairs of antennae observing the same scene is straightforward, whatever the correlation is performed in real time or in deferred time. However this approach rests on assumptions that do not allow studying the role and the impact of some important parameters like quantization and sampling rate of the signals collected by the antennae, integration time and clock errors at correlator level. Moreover, none of the effects that may alter the propagation from the source to the array can be taken into account.

The approach presented here aims at simulating the signal emitted by the source and captured by the antennae. Assuming that the atoms at any location of the extended source are responsible for the radiation by acting independently of one another, the resulting emission is modeled with short wave trains. The electromagnetic wave emanating from every point source is therefore a linear superposition of these random wave trains. Each wave is transported to the antennae where the voltage patterns are taken into account. The corresponding signals are then sent to the correlator unit for being cross-correlated.

Numerical comparisons conducted in the L-band around 1.415 GHz confirm that, in an ideal situation, both approaches lead to the same complex visibilities. However, only the second one can properly account for effects which may affect the propagation of the signal between emission at source level and capture at antenna level, as well as the cross-correlation at correlator level. Nevertheless, the drawback of this approach is the amount of calculations which makes necessary the use of a massive parallel architecture like that found in GPU.

8895-2, Session 1

## High-performance grid for spaceborne and ground-based facilities for remote sensing data processing in Bulgaria for environmental modeling

Hristo N. Nikolov, Doyno Petkov, Denitsa Borisova, Space Research and Technology Institute (Bulgaria)

In the last decade data from remote sensing observation of the Earth have become necessary in increasing number of businesses even in everyday life and it has become recognized at European level in Copernicus (former GMES) program. The technology behind this data turns out to be more complicated both in terms of data acquisition and its subsequent data storage and processing. For example the hyperspectral instruments onboard satellites and planes already provide data at no cost generating so-called hypercubes with more than 150 spectral channels in case of imaging camera. Expressed in terms of volumes of information for one single experiment one may obtain hundred of gigabytes per sole flight. In the proposed sample scenario those data must be transmitted from the flying platform to the ground receiving station, preprocessed there and then delivered to the end user expert for thematic processing. In this process of data transmission one could benefit from lossless data compression onboard the flying platform thus the data going to the ground is transmitted faster, but even in this case the data needs to be processed as fast as possible and here crucial is to have parallel hardware solution implemented on FPGA or DSP immediately after acquisition and transmission. Since one receiving station may service more than one experiment at the same time in order to preprocess data the different data layers could be processed separately by a local computing grid acting as cloud service. After that the pre-processed data is transferred for further processing via dedicated virtual private network using standard protocol for thematic processing. In common case the hyperspectral data undergo dimensionality reduction implementing linear spectral unmixing or other widely accepted technique. This next step might be realized on larger conventional computing grid being multiprocessor or heterogeneous or by specialized hardware where good candidate is a set of graphic boards having specialized processing units. The specifics of the problem solved is reflected by the single hardware solution selected from the before mentioned ones. In the discussed case of environmental modeling or disaster management a cloud implementation of open source GIS was used. The final results from the models in form of graphs and maps are part of a dedicated web service including also standard database engine such as Postgre.

In the framework of this study developed were an unmanned aircraft, control, stabilization and navigation systems, analysis and selection of UAV platform and determined were the concrete parameters of the system. Also developed was a radio interface for transmission of telemetry data and video stream with high resolution. Algorithms and models for thematic image processing techniques based on computer vision were created. Built up was a prototype for the ground station for storage and further processing of the data. Special attention was paid to the most important parameters vital for environmental monitoring and in disaster management response, which was essential for confirming the accuracy of the data obtained by developing algorithms and models to assess the current state of the region under study.

8895-3, Session 1

## Discrete cosine transform and hash functions toward implementing a (robust-fragile) watermarking scheme

Saeed H. Al-Mansoori, Emirates Institution for Advanced Science and Technology (United Arab Emirates); Alavi Kunhu, Khalifa Univ. of Science, Technology and Research (United Arab Emirates)

The purpose of this paper is to design and implement a Robust-Fragile watermarking scheme for color DubaiSat-1 satellite images. The proposed watermarking scheme aims to protect the copyright and authority of DubaiSat-1 satellite imagery. The robust watermark can be retrieved even if the watermarked image exposed to image processing manipulations (attacks). Such watermark is used in many applications with a view to protect the copyright of the image. On the other hand, the fragile watermark is designed to detect any change in pixel values and the location of its occurrence (tamper-proof). Thus, it is used to prove the authenticity of the image. Therefore, to design a Robust-Fragile watermarking approach two encoders are required. The first encoder is used to embed the watermark in the frequency domain using the Discrete Cosine Transform (DCT), while the second encoder

is used to embed the watermark in the time domain using Hash functions. The Peak Signal-to- Noise Ratio (PSNR) is used to assess the distortion caused by embedding the watermark. In addition, Strimark and other image processing manipulations have been used to evaluate the robustness of the proposed scheme. The experimental results show that the proposed scheme is robust against various attacks such as JPEG compression, additive noise and filtering. Moreover, any sensitive modification to the image can be detected.

#### 8895-4, Session 1

### CUDA implementation in the EM scattering of the large three-layer canopy

Wang-Qiang Jiang, Min Zhang, Xidian Univ. (China)

The electromagnetic (EM) scattering properties of the vegetation have been of significant interest in both military and civilian applications. However, the computational complexity of calculating EM scattering fields is large. The general serial method always takes lots of time to calculate the problems. Although the multi-core CPU in personal computer has the ability of running in parallel, its application is limited by the number of the cores which is just several at present. Nevertheless, with the development of the Graphics Processing Unit (GPU), the number of the processors on GPU is much more than that on CPU, and the Compute Unified Device Architecture (CUDA), created by NVIDIA, gives developers access to the virtual instruction set and memory of the parallel computational elements in CUDA GPU. We use the four-path method and the reciprocity theorem to predict the EM scattering properties from scatterers which are sampled by using Monte-Carlo method in a three-layer canopy model. With the help of CUDA, we let the program run on a GTX460 GPU and get a highest speedup of 294 times in comparison with the original serial algorithm on a Core(TM) i5 CPU. When calculating EM scattering properties of vegetation in large scale, the program consumes more memory than the existing memory. To solve this problem, we keep the data in the hard disk and let the program create a subsidiary thread to deal with the process of the data transmission between the memory and the hard disk. The GPU has a good parallel performance and it can accelerate the calculation obviously.

#### 8895-5, Session 2

### GPU-based parallel design of the WRF Yonsei University planetary boundary layer scheme (Invited Paper)

Melin Huang, Jarno Mielikainen, Bormin Huang, Univ. of Wisconsin-Madison (United States); Mitch Goldberg, Ajay Mehta, National Oceanic and Atmospheric Administration (United States); HungLung Allen Huang, Univ. of Wisconsin-Madison (United States)

The collected quantitative data about the current state of the atmosphere are used to foretell the future state. This requires numerical forecasting technology. The observational instruments sample the current state of the fluid at a given time and location, and further form an estimate for the future state of the fluid. Such weather estimate needs the aid of equations of fluid dynamics and thermodynamics that are based on laws of physics, chemistry, and fluid motion. The Weather Research and Forecasting (WRF) model is a collection of physics modules and dynamic solvers. It is designed to serve the needs of both operational forecasting and atmospheric research in a broad area of applications and has linked to our daily activity. The acquirement of accurate weather prediction in time is a challenge even with the fastest supercomputers. In particular for severe weather events, timely weather forecast is imperative. The WRF system supports the best possible models for accurate weather forecast. To expedite the WRF computation process, Graphics Processing Units (GPUs) appear to be an attractive alternative as opposed to traditional CPU architectures. In our study, an efficient GPU-based YSU PBL implementation was developed. Since this scheme is only one intermediate process of the entire WRF model, the involvement of the I/O transfer is not taken into account in the intermediate stage. Using one NVIDIA GTX 680 GPU in the case without I/O transfer, our optimization efforts on the GPU-based YSU PBL module can be achieved at a speedup of 110x with respect to

one CPU core, whereas the speedup for one CPU socket with respect to one CPU core is only 3.5x.

#### 8895-6, Session 2

### Creation of the BMA ensemble for SST using a parallel processing technique

Kim Kwangjin, Yang Won Lee, Pukyong National Univ. (Korea, Republic of)

Many countries provide various meteorological satellite products using remote sensing. To know the accuracy, each of the satellite products is verified by using the observations of the detected target. But despite the products of the same purpose, the values show differences among the satellites because they have different sensors and retrieval algorithms. Also, the channel values have inescapable, inherent uncertainties.

Efforts for reducing the uncertainties in the satellite products have been steadily progressed in terms of model averaging to synthesize several models. In ensemble forecasting, the arithmetic ensemble mean(AEM) has been widely used because it provides a better result than each ensemble member. However, this approach gives no information about the uncertainties contained in the predictions. Thus, the model averaging that considers the amount of uncertainty of each model is required. Bayesian model averaging(BMA) is one of the ensemble methods to solve such problem. A probability density function(PDF) of the BMA is obtained from the weighted average of PDFs of individual ensemble members. The weights are equal to the posterior probabilities of ensemble members. The posterior probabilities are a relative predictive technique that shows the degree of similarity between the satellite product and the observation. It can be calculated by the expectation-maximization(EM) algorithm, which is a method for finding the maximum likelihood estimator. The EM algorithm is iterative and alternates between two steps: the expectation step and the maximization step.

This study focuses on generating the ensemble of satellite products by considering the differences in the uncertainty in each product based on the BMA approach. Also, because the extensive and intensive computation is required, we employ Hadoop-based parallel processing for the BMA ensemble. Hadoop is the software framework that ensures the safe and fast calculation of big data using a parallel processing mechanism. For the computation of a BMA ensemble, we used sea surface temperature(SST) because SST is an important parameter for climate change.

We calculate the BMA ensemble for the SST of several satellites including MODIS and AVHRR by referencing the buoy observations. For the window of time synchronization, we set one-hour radius from the buoy data to each satellite product.

We compare each ensemble member, AEM and BMA ensemble with the buoy observations to verify the effects of BMA method. It is expected that the BMA ensemble reduces the root mean square error(RMSE) and the mean bias. The BMA method can be widely used as a more reliable approach to yield ensembles of satellite products.

#### 8895-7, Session 2

### An improved maximum simplex volume algorithm to unmixing hyperspectral data

Haicheng Qu, Harbin Institute of Technology (China); Bormin Huang, Univ. of Wisconsin-Madison (United States); Junping Zhang, Ye Zhang, Harbin Institute of Technology (China)

The maximum simplex volume algorithm (MSVA) is an automatic endmember extraction method based on geometrical properties of simplex in high-dimensional feature space. By utilizing the relation of volume between a simplex and its corresponding parallelepipedron in the high-dimensional space, the algorithm extracts endmembers directly from the initial hyperspectral image in a sequential manner without dimensionality reduction. It is thus considered to have overcome a major drawback of N-FINDER, which requires the data dimension reduced to one less than the number of the endmembers before extraction. However, the MSVA suffers from excessive computation resulting from massive determinant operations. In this paper an improved MSVA based on partitioned determinant operations

is proposed in this paper. Experimental results demonstrate that the proposed fast algorithm can greatly reduce computational time.

## 8895-8, Session 2

### Calculation of scattering characteristic of complex target on multicore platform

Xing Guo, Zhensen Wu, Xidian Univ. (China)

The scattering characteristic of complex target from terrestrial and celestial background radiance has been widely used in such engineering fields as remote sensing, feature extraction, tracking and recognition of target thus having been an attractive field for many scientists for decades. As the background radiance comes in all directions and in a wide spectrum and the complex target always consists of thousands of facets, in general it takes hours to complete the calculation. Consequently this limits its use in the real time applications. In this paper, the openMP, Intel CILK ++, Intel Threading Building Blocks (TBB) are used separately to leverage the processing power of multi-cores processors. Our experiments are conducted on a DELL desktop based on an Intel I7-2600K CPU running at 3.40 GHz with 8 cores and 16.0 GB RAM. The Intel Composer 2013 is employed to build the program. The results demonstrate that average speedups for three parallel models are 4.5X, 5X, 3.6X respectively.

## 8895-9, Session 2

### Acceleration of vertex component analysis for spectral unmixing with CUDA

Shih-Chieh Wei, Tamkang Univ. (Taiwan); Bormin Huang, Univ. of Wisconsin-Madison (United States); Antonio J. Plaza, Univ. de Extremadura (Spain)

Hyperspectral images can be used to identify the unique materials present in an area.

Due to the limited spatial resolution, each pixel of the image is considered as a mixture of several different pure substances or endmembers. Several spectral unmixing methods have been developed for endmember extraction in an image. Among them, the vertex component analysis (VCA) algorithm is a popular one for its superior performance. As there are a lot of matrix/vector operations involved in the algorithm, this work aims to apply the highly parallel computing power of recent GPUs which are reported to have success in acceleration of many compute intensive applications. In the experiment, the compute unified device architecture (CUDA) which provide more convenient programming model will be used. The speedup on a multi-core GPU will be measured with respect to a single core CPU for evaluation.

## 8895-10, Session 3

### Parallel method for sparse semisupervised hyperspectral unmixing (*Invited Paper*)

Jose M. Nascimento, Instituto Superior de Engenharia de Lisboa (Portugal); Jose R. Alves, Univ. Técnica de Lisboa (Portugal); Antonio J. Plaza, Univ. de Extremadura (Spain); Vitor M. Silva, Univ. de Coimbra (Portugal); José M. Bioucas-Dias, Univ. Técnica de Lisboa (Portugal)

Hyperspectral imagery is a continuously growing area in remote sensing applications. The spectral range extending from the visible region through the near-infrared and mid-infrared in hundreds of narrow contiguous bands, provides a very high spectral resolution, which allows the detection and the discrimination between different chemical elements of the observed image. The main problem of hyperspectral images is that the spatial resolution can vary from a few to tens of meters, thus each pixel is a mixture of several spectrally distinct materials (also called endmembers).

Hyperspectral unmixing is a source separation problem which amounts at estimating the number of endmembers, their spectral signatures and their abundance fractions (i. e., the percentage of each endmember). Over the last decade, several algorithms have been

developed to unmix hyperspectral data sets, from a geometrical and statistical point of view.

A semi-supervised alternative approach to unmix hyperspectral datasets consists of assuming that the observed image signatures can be expressed in the form of linear combinations of a number of pure spectral signatures known in advance (e.g., spectra collected on the ground by a field spectro-radiometer). Unmixing then amounts to finding the optimal subset of signatures in a spectral library that can best model each mixed pixel in the scene. In practice, this is a combinatorial problem which calls for efficient linear sparse regression techniques, since the number of endmembers participating in a mixed pixel is usually very small compared with the dimensionality of spectral libraries.

In recent years, high-performance computing systems have become more widespread in remote sensing applications, namely, graphics processing units (GPUs) have evolved from expensive application specific units into highly parallel and programmable systems. Several state-of-the-art hyperspectral imaging algorithms have been shown to be able to benefit from this hardware and take advantage of the extremely high floating-point processing performance, compact size, huge memory bandwidth, and relatively low cost of these units, which make them appealing for onboard data processing.

This paper proposes a parallel method designed for GPUs, to solve the constrained sparse regression problem. This method is based on the "spectral unmixing by splitting and augmented Lagrangian" (SUNSAL) that estimates the abundance fractions using the alternating direction method of multipliers (ADMM), which decomposes a difficult problem into a sequence of simpler ones, alleviating considerably the computational burden, and allowing a significant increase in processing speed. Additionally, this method is performed in a pixel-by-pixel fashion, thus, it is highly parallelizable, and can be effectively implemented by simply dividing large datasets onto smaller subsets without the need to establish an optimal size for them.

Experimental results, conducted using both simulated and real hyperspectral data sets and spectral libraries publicly available, indicate the potential of sparse regression techniques in the task of accurately characterizing mixed pixels using library spectra. This opens new perspectives for spectral unmixing, since the abundance estimation process no longer depends on the availability of pure spectral signatures in the input data nor on the capacity of a certain endmember extraction algorithm to identify such pure signatures.

## 8895-12, Session 3

### Massively parallel computation of soil surface roughness parameters on a Fermi GPU

Xiaojie Li, Northeast Institute of Geography and Agroecology (China); Changhe Song, Xidian Univ. (China); Bormin Huang, Univ. of Wisconsin-Madison (United States); Kai Zhao, Northeast Institute of Geography and Agroecology (China); Yunsong Li, Xidian Univ. (China)

Surface roughness is description of the surface micro topography of randomness or irregular. The standard deviation of surface height and the surface correlation length describe the statistical variation for the random component of a surface height relative to a reference surface. In the observation of the earth using microwave radiometers, surface roughness is an important factor to soil microwave radiation. When the number of data points is large, calculation of surface roughness parameters is time-consuming. With the advent of Graphics Processing Unit (GPU) architectures, inherently parallel problem can be effectively solved using GPUs. In this paper we propose a GPU-based massively parallel computing method for 2D bare soil surface roughness estimation. This method was applied to the data collected by the surface roughness tester based on the laser triangulation principle during the field experiment in April 2012. The total number of data points was 52,040. It took 47 seconds on a Fermi GTX 590 GPU whereas its serial CPU version took 5422 seconds, leading to a significant 115x speedup.

8895-13, Session 3

### Remote sensing image coding based on discrete wavelet transform using optimal adaptive direction prediction

Libao Zhang, Bingchang Qiu, Xianchuan Yu, Beijing Normal Univ. (China)

One efficient image coding paradigm is to provide a compact representation of signals that could make full use of statistical correlations and image characters. The discrete wavelet transform has been the most important new image coding approach and has been adopted by the JPEG2000 standard. The discrete wavelet transform can be implemented by the lifting structure. The lifting structure-based wavelet transform can decompose the FIR wavelet filter into several lifting steps, which are referred to as split, predict, update, and normalize. This type of lifting structure works well in presenting horizontal and vertical edges, but it fails to provide an efficient representation for directional areas, such as edges, and these edges may be neither horizontal nor vertical. In fact, remote sensing images often contain significant orientation information. We must consider the image orientation to avoid obtaining a large magnitude of these high frequency coefficients. In this paper, a new, efficient coding algorithm based on discrete wavelet transform and lifting scheme using optimal adaptive direction prediction so-called OADP is proposed for remote sensing image coding. The new algorithm first designs a fast directional prediction model based on two-dimensional gradient detection to obtain optimal adaptive direction prediction of lifting scheme. Then, the OADP executes the adaptive directional wavelet transform along the optimal transform direction. The edge and texture energy can be reduced on the non-horizontal and non-vertical direction of the high-frequency subbands of the remote sensing image. Finally, the new algorithm uses sampling function interpolation to predict the value of sub-pixels. During the image coding, the SPIHT algorithm is used to obtain the more efficient compression performance and the lower computational complexity. The experimental results for these remote sensing images show that, compared with traditional discrete wavelet transform, the non-horizontal and non-vertical high-frequency information can be reduced significantly, and the new algorithm improves the peak signal-to-noise ratio (PSNR) and the subjective quality of the reconstructed remote sensing images significantly. So the proposed algorithm has important value for the remote sensing image coding in the future.

8895-14, Session 4

### GPU accelerated FDTD method for investigation on the EM scattering from 1-D large scale rough surface under low grazing incidence

Chungang Jia, Li-xin Guo, Peng-ju Yang, Xidian Univ. (China)

Investigation on the statistical characteristics of electromagnetic scattering from random rough surface has attached considerable interest owing to its significant applications in the fields of remote sensing, target identification and radar detection. When the property of large scale rough surface with low grazing incident angles is investigated, the generated length of rough surface should be as long as possible, which leads to large numbers of unknowns. However, the parallel the finite-difference time domain (FDTD) method using the MPI library is too weak to deal with such large unknowns due to the limitation to cost of CPU. Fortunately, Compute Unified Device Architecture (CUDA) technology based on graphic processor unit (GPU) is extensively implemented for the large scale FDTD simulations successfully. Compared to the MPI technology, GPU can achieve huge speedup ratios at low cost for its powerful computing capability, which motives us into adopt the GPU-based FDTD technology for analyzing the scattering from large scale rough surface at large incident angles. In this paper, the graphic processor unit (GPU) implementation of FDTD is presented to investigate the electromagnetic (EM) scattering from one dimensional (1-D) large scale perfectly electrical conducting (PEC) Gaussian rough surface under low grazing incidence. The FDTD lattices are truncated by uniaxial perfectly matched layer (UPML), in which the finite-difference equations are carried out parallel for the total computation domain. Using Compute Unified Device Architecture (CUDA) technology, significant speedup ratios

are achieved for different incidence frequencies, which demonstrates the efficiency of GPUs accelerating FDTD method. To optimize the usage of device memory to obtain best performance on GPU, global, shared, and texture memory is utilized to achieve high parallelism. First, the theoretical formulas for calculating EM scattering from rough surface by FDTD are presented in detail. Furthermore, the programmable CUDA architecture for GPU is introduced, and more details about the implementations of GPU accelerated FDTD for rough surface are given. Finally, some numerical results are demonstrate. The accuracy of our method is verified by comparing the numerical results with these obtained by Central Processing Unit (CPU), which shows favorable agreements. Finally, the bistatic scattering from rough surface for the large incident angle is discussed in detail.

8895-15, Session 4

### GPU acceleration experience with RRTMG long wave radiation model

Erik Price, Jarno Mielikainen, Bormin Huang, HungLung A. Huang, Univ. of Wisconsin-Madison (United States); Tsengdar J. Lee, NASA Headquarters (United States)

An Atmospheric radiative transfer model calculates radiative transfer of electromagnetic radiation through a planetary atmosphere. One such model is the rapid radiative transfer model (RRTM), which calculates of longwave and shortwave atmospheric radiative fluxes and heating rates. Longwave broadband radiative transfer code for general circulation model (GCM) applications, RRTMG, is based on the single-column reference code, RRTM. The radiative effects of all significant atmospheric gases are included in RRTMG. It also treats the absorption and scattering from liquid and ice clouds and aerosols. A statistical technique for representing small scale cloud variability, such as cloud fraction and the vertical overlap of clouds, is included in RRTMG. Due to its accuracy, RRTMG has been implemented operationally in many weather forecast and climate models. GPUs can provide a substantial improvement in RRTMG speed by supporting the parallel computation of large numbers of independent radiative calculations. A GPU-compatible version of RRTMG was implemented and thorough testing was performed to ensure that the original level of accuracy is retained.

8895-17, Session 4

### Research on optimization of imaging parameters of optical remote sensing camera based on ground objects BRDF

Fangqi Li, Hongyan He, Yunfei Bao, Kun Xing, Zhi Zhang, Beijing Institute of Space Mechanics and Electricity (China)

With the development of high resolution remote sensing satellite in recent years, the research of typical objects is connecting more and more closely with remote sensing applications. In the TDI CCD camera on-orbit imaging process, great changes will happen on solar angles at different time, cause a certain change of BRDF of most objects of the earth's surface, and finally affect the remote sensing radiances of the sensors, even imaging quality. In order to solve this problem, optimization of on-orbit parameters based on the ground objects BRDF is necessary. A detailed investigation about the global imaging area of ground objects characteristics classification in four seasons is given in this paper. Inverse BRDF of different time based on Kernel-Driven BRDF model, establish database of ground objects BRDF of different times and seasons, simulate imaging effect with radiative transfer model and degradation model of remote sensor, and then optimize imaging parameters according to the imaging quality requirement. The simulation results show that the contrast, definition and dynamic range of image have improved, the proposed method in this paper can set imaging parameters reasonably according ground objects, improve the imaging quality of high resolution remote sensing satellites.

8895-18, Session 4

### GPU-based acceleration of the hyperspectral signal subspace identification by minimum error (HySime)

Xin Wu, Xidian Univ. (China); Bormin Huang, Univ. of Wisconsin-Madison (United States); Jianqi Zhang, Delian Liu, Xidian Univ. (China)

Signal subspace identification provides performance improvement in such hyperspectral applications as target detection, spectral unmixing and classification. HySime is a famous unsupervised algorithms to explore the signal subspace and determine its dimensionality without any prior knowledge. It first estimates the signal and noise correlation matrices and then selects the subset of eigenvalues by seeking the least squared error of signal estimation. The HySime applications to hyperspectral data involve various operations on large matrices which are computationally intensive. In this paper, we design a massively parallel algorithm to accelerate the HySime algorithm on graphics processing units (GPUs) using the compute device unified architecture (CUDA) language. Experimental results are conducted on simulated and real hyperspectral images to verify the performance improvement in estimating both the noise and signal subspaces on GPUs.

8895-20, Session 5

### GPU-accelerated performance of the WRF Goddard cumulus ensemble model

Melin Huang, Bormin Huang, HungLung Allen Huang, Univ. of Wisconsin-Madison (United States); Mitch Goldberg, Ajay Mehta, National Oceanic and Atmospheric Administration (United States)

The cloud system has a key influence to their surroundings in the chain of processes responsible for the weather forecast and other climate variations. The Goddard Cumulus Ensemble (GCE) model, a multi-dimensional non-hydrostatic dynamic/microphysical cloud resolving model, has been incorporated in the current Weather Research and Forecasting (WRF) and is adopted to simulate many different meso-scale convective systems that occurred in various geographic locations, where the Weather Research and Forecasting (WRF) model is a system of numerical weather prediction and atmospheric simulation with dual purposes for forecasting and research. The coding of the GCE model in the WRF model is suitable for massively parallel computation as there are no interactions among horizontal grid points. With the advent of the Graphics Processing Units (GPUs), more and more scientific applications have employed them to accelerate the computing performance. This report demonstrates our GPU-based massively parallel computation efforts on the GCE model in WRF. Using one NVIDIA GTX 680 GPU, the speedups of the GPU-based GCE programs can be achieved as high as 243x with respect to one CPU core in the case without I/O transfer and 203x for the case with I/O transfer, whereas the speedup for one CPU socket with respect to one CPU core is only 3.9x.

8895-21, Session 5

### A 64-bit orthorectification algorithm using fixed-point arithmetic

Joseph C. French, Eric Balster, Univ. of Dayton (United States); William F Turri, University of Dayton Research Institute (United States)

Imaging systems have increased in size and reliability while decreasing in noise and cost. As the cost has decreased, applications have become cost effective such as tracking, vegetation indexing, coast line monitoring, etc. Many of these applications require some aspect of geo-location and orthorectification to improve analysis. However, orthorectification is a computationally expensive process for remote systems as it has floating point operations and divisions in the algorithm. To reduce the computational cost of on-board processing two novel algorithm modifications are proposed. One modification is to compute the projection utilizing fixed point arithmetic. Fixed

point arithmetic removes the floating point operations and reduces the processing time by operating only on integers. The second modification is to remove the division inherent in projection with a multiplication of the inverse. With these modifications the processing time is reduced by a factor of 2.1483 with a maximum pixel position error of 0.35 of a pixel size.

8895-22, Session 5

### GPU-based ray tracing algorithm for fast coverage zone prediction under urban microcellular environment

Zhongyu Liu, Li-xin Guo, Chungang Jia, Xidian Univ. (China)

The rising demand for mobile communications, particularly in urban areas, has led to the adoption of microcellular systems to accommodate an influx of users despite limited frequency resources. The successful implementation of these systems requires a fast and accurate propagation prediction model for system deployment. In this study, an improved ray tracing propagation prediction model, which is based on creating a new virtual source tree in which the relationship between neighbor nodes is a left-son-and-right-brother one, is used because of their high efficiency and reliable prediction accuracy. In addition, the usage of threshold control of each ray path and the handling of visible grid points for reflection and diffraction sources are also adopted, resulting in an improved efficiency of coverage prediction over large areas. However, in the process of employing the ray tracing method for coverage zone prediction, runtime is linearly proportional to the total number of prediction points, leading to large and sometimes prohibitive computation time requirements under complex geographical environments. In order to overcome this bottleneck, the compute unified device architecture (CUDA), which provides fine-grained data parallelism and thread parallelism, is implemented to accelerate the calculation. Taking full advantage of tens of thousands of threads in CUDA program, the decomposition of the coverage prediction problem is firstly conducted by partitioning the image tree and the visible prediction points to different sources. Then, we make every thread calculate the electromagnetic field of one propagation path and then collect these results. Comparing this parallel algorithm with the traditional sequential algorithm, it can be found that computational efficiency has been improved dramatically.

8895-24, Session 6

### An efficient advanced research weather research and forecast dynamics subroutine in CUDA C

Jarno Mielikainen, Bormin Huang, HungLung A. Huang, Univ. of Wisconsin-Madison (United States); Mitch Goldberg, Ajay Mehta, National Oceanic and Atmospheric Administration (United States)

The Weather Research and Forecast (WRF) model is the most widely used community weather forecast and research model in the world. There are two distinct varieties of WRF. Advanced Research WRF (WRF-ARW) is an experimental, advanced research version featuring very high resolution. The WRF Nonhydrostatic Mesoscale Model (WRF-NMM) has been designed for forecasting operations. WRF consists of dynamics code and several physics modules. The WRF-ARW core is based on an Eulerian solver for the fully compressible nonhydrostatic equations. In the paper, we will use NVIDIA CUDA C programming language to substantially increase the performance of the most time consuming subroutine, rk\_tendency in the WRF-ARW dynamics core. We have taken version 3.4.1 of the WRF code and ported the subroutine to CUDA C. Thus, the computational performance of WRF will not plateau at or near current levels. Instead performance will scale with the future increase in the number of cores in GPUs. We will also describe the challenges we meet during the development of a high-speed dynamics code subroutine for a GPU. Furthermore, lessons learned from the GPU code optimization process will be discussed.

8895-25, Session 6

### Parallel Acceleration of Diffuse Scattering Model for Indoor Radio Prediction by CUDA

Xiao Meng, Li-xin Guo, Wei Tao, Xidian Univ. (China)

Abstract: Radio wave prediction is very important for the design of the mobile communication network. The ray-tracing algorithm does not consider the diffuse scattering of rough surface. A radio prediction model, which based on diffuse scattering theory, is described for the indoor radio coverage predictions. The diffuse scattering of indoor walls and ceiling and floor is calculated at a series of discrete time instance in this method.

And the sum of scattering power at each discrete time instance is calculated in the end. With the increasing frequency of the transmitting antenna, the surface of wall is no longer smooth, needing to consider the effect of diffuse scattering of rough surface. Therefore, this model is more suitable than the ray-tracing algorithm. In recent years, the compute unified device architecture (CUDA) of NVIDIA takes advantage of the GPU for parallel computing, and greatly improve the speed of computation. Because there is a large number of data to deal with, GPU-based diffuse scattering model for indoor radio prediction, which fully utilizes the parallel processing capabilities of CUDA, is introduced in order to further improve the computational efficiency. It can be found that good acceleration effect has been achieved.

Keyword—diffuse scattering, rough surface, ray-tracing, CUDA

8895-26, Session 6

### GPU acceleration of the N-FINDR algorithm

Xianyun Wu, Yunsong Li, Xidian Univ. (China); Bormin Huang, Univ. of Wisconsin-Madison (United States); Antonio J. Plaza, Univ. de Extremadura (Spain)

With the development of hyperspectral imaging technology, hyperspectral data analysis has become an active research field. The N-FINDR algorithm proposed by Winter is one of the most popular methods for automatic endmember detection and unmixing of hyperspectral images. The method finds the maximal volume of the simplex that can be formed using image pixels by sequentially evaluating each pixel of the image. Since every pixel must be evaluated at least  $N$  times in order to find  $N$  endmembers, the computational complexity of the N-FINDR algorithm is high. With the emergence of Graphics Processing Units (GPUs) architectures, we develop a new parallel N-Finder algorithm to run on these inexpensive hardware devices with the Computer Unified Device Architecture (CUDA) architecture developed by NVIDIA. A significant speedup is achieved after using CUDA and some optimization techniques.

8895-27, Session 6

### An improved two-scale model with volume and air bubble scattering for the dielectric sea surface

Longxiang Linghu, Zhensen Wu, Xidian Univ. (China)

The dielectric of the sea surface is calculated by the two-Debye theory depend on different temperatures and salinity of it, and the results is compared with the measured data to verify it. The effects of the surface slopes joint probability density, the shadowing function, the skewness of sea waves and the curvature of the surface on the backscattering from the ocean surface are discussed and an improved two-scale model modified by these four aspects is used to calculate the backscattering coefficient of the dynamic ocean surface. In order to deal with the surface skewness driven by wind, a new complementary term derived from the small perturbation method is included in the improved model, in which the Fourier transform of the third-order cumulant function, surface bispectrum, is employed. On this basis, with the oceanic whitecap coverage and air bubble behind taken into account, a composite model for predicting the ocean surface backscattering coefficient is constructed tentatively, which incorporates the volume scattering into the total one. Finally, with the vector radiative transfer (VRT) and Maxwell-Garnett mixing formula theory employed, numerical illustrations are carried out for the backscattering coefficients versus wind speed, incidence angle and azimuth angle, respectively. The predictions of the composite model are verified in and bands through the comparison of numerical results with many sets of measured data and the aircraft measurement experiment carried out in ZHOUSHAN sea area also supports this model.

# Conference 8896: Electro-Optical and Infrared Systems: Technology and Applications X

Monday - Tuesday 23-24 September 2013

Part of Proceedings of SPIE Vol. 8896 Electro-Optical and Infrared Systems: Technology and Applications X

## 8896-1, Session 1

### Investigation of index of refraction changes in chalcogenide glasses during molding processes

Ray J. Pini, Jacklyn Novak, LightPath Technologies, Inc. (United States); Erik F. Stover, M3 Measurement Solutions (United States); Alan Symmons, LightPath Technologies, Inc. (United States)

Precision glass molding has shown an effective decrease in the index of refraction of the glass during the molding process. This index drop can be of significant value where optical designs for molded lenses must take into account the index drop to accurately determine the optical performance of the final lens. Adoption of chalcogenide glasses for molded infrared optics has raised a series of questions as to the behavior of these glasses under molding conditions. This paper will investigate the index of refraction changes in different chalcogenide glasses during the molding process and establish working guidelines for optical designers using molded chalcogenide glasses in molding.

## 8896-2, Session 1

### Hyper-hemispheric and bifocal panoramic lenses

Claudio Pernechele, INAF - Osservatorio Astronomico di Padova (Italy) and CISAS - Ctr. for Studies and Activity for Space (Italy)

Panoramic objective are becoming, due to the availability of large digital sensors, a diffuse optical system to catch very wide field of view (FoV). A panoramic lens differs from the "cousin" fish-eye in having a much more viewing angle below the horizon, which is the plane orthogonal to the optical axis and passing through the center of the aperture stop. Many type of panoramic lenses have been realized, published and patented. Typical panoramic lens have a view angle of 360 deg in azimuth (the plane orthogonal to the optical axis), just like a fish-eye, and plus and minus tens of degrees in elevation angle, i. e. above and below the horizon. Most common panoramic lenses use a curved, usually aspheric, mirror placed in front of a commercial objective to capture a 360 deg area around the horizon. More recent design use a catadioptr instead of a mirror. Both of the solutions have the draw-back effect to obscure the frontal view of the objective, producing the classic panoramic "donut-shape" image in the focal plane. Panoramic lens found interest in robotics, surveillance and driver assistance automotive system. We present here a panoramic lens in which the frontal field is make available to be imaged in the focal plane (by means of a frontal optics), together with the panoramic field, producing a FoV of 360 deg in azimuth and 270 deg in elevation; it have then the capabilities of a fish eye plus those of a panoramic lens: we call it hyper-hemispheric lens. We design also a lens in which the frontal optics have a different focal length with respect to the equivalent panoramic; with this solution one can image, in the same sensor, the panoramic field plus an enlargement of a portion of it: that's the bifocal panoramic lens. Both the lenses has been designed and realized and we show here the optical scheme, the objective layout and results of the preliminary test.

## 8896-3, Session 1

### Two-lens designs for modern uncooled and cooled IR imaging devices

Norbert Schuster, John W. Franks, Umicore Electro-Optic Materials (Belgium)

In recent years, thermal detectors with a 17 micron pixel pitch have become well-established for use in various applications, such as thermal imaging in cars. This has allowed the civilian infrared market

to steadily mature. The main costs for these lens designs follows from the number of lenses used.

The development of thermal detectors, which have lower detectivities than quantum detectors, has compelled camera manufacturers to demand very fast F-numbers such as f/1.2 or faster, simultaneously minimizing the impact of diffraction in the 8-12 micron waveband.

The freedom afforded by the choice of the stop position in these designs has been used to create high-resolution lenses that operate near the diffraction limit. Based on GASIR@1, a chalcogenide glass, two-lens designs have been developed for all pixel counts and fields of view. Additionally, all these designs have been passively athermalized, either optically or mechanically.

Narrow field lenses cover also the XGA-resolution. Smaller pixel counts like VGA and QVGA restrict the horizontal field of view (HFOV) from 9.7o down to 3.1o. Medium field lenses are optimized up to the very fast f-number 1.0. Several wide field lenses up to 73deg (for VGA-detector) offer several opportunities for surveillance.

Lenses for cooled quantum detectors have a defined stop position called the cold stop (CS) near the FPA-plane. The solid angle defined by the CS fixes not only the F-number (which is less fast than for thermal detectors), but also the required resolution: a certain degree of diffraction limits the MTF both on-axis and off-axis.

The main cost driver of these designs is the lens diameter. Lenses must be sufficiently large to avoid any clipping of ray bundles intended to reach the cooled detector. In this paper, examples are shown of designs containing a minimal amount of lenses.

## 8896-4, Session 1

### Narcissus calculation from complicated mechanical structure of IR optical system using blackbody radiation

Jinsuk Hong, Samsung Thales Co., Ltd. (Korea, Republic of)

To visualizing the defect and its path with reasonable intensity level, forward tracing from the mechanical structure is more intuitive than backward tracing from the detector to the optical system. However, forward tracing tend to require much more time to trace rays than backward tracing method. To avoid the unnecessary computing time, the major narcissus contributor candidates were selected by backward ray tracing.

First, we traced the rays from the detector and sorted out the main critical objects seen from the detector by backward ray tracing method. To create the object's radiation source, each object's intensity level was calculated according to the given condition, such as temperature, extent and its orientation. Then, we performed the forward ray tracing. To compare the result with certain standard, we also performed 2nd forward tracing with actual target model with required temperature difference in the same manor.

We used ASAP software to calculate the blackbody radiation intensity of each object. So, naturally we have to confirm about the reliability of the simulation results. For the two ray tracing results mentioned previously contains the same methodology, we made an assumption that the simulation error can be nullified and ignored.

After comparing the results from one another, we came to the conclusion that the method we applied to the analysis is working fine and same methodology can be applied to the other optical systems.

## 8896-5, Session 2

### Comparison of flash and accumulation mode in range-gated active imaging (*Invited Paper*)

Frank Christnacher, Martin Laurenzis, Stéphane Schertzer, Institut Franco-Allemand de Recherches de Saint-Louis (France)

Range-gated active imaging has significantly been improved in the

recent past. Increasingly used for diverse applications, it has shown prominent capabilities for night vision, remote sensing or vision through diffuse medium (fog, smoke, camouflage netting ...). There are numerous applications for military purposes as well as for civilian uses. Due to the availability of high power laser diodes around 800-860 nm, it is possible to find off-the-shelf systems working with very sensitive light intensifier and laser diodes. Eye-safe systems working around 1.5  $\mu\text{m}$  suffer from a lack of intensified sensor in the SWIR range and only a few manufacturers as Intevac (electron-bombarded CMOS) or Selex (MCT avalanche photodiode) are able to propose intensified SWIR sensors. For eye-safe applications, due to the type of sensor, it is necessary to use a pulse power laser as an illumination source. Consequently, the type of source (diode or solid-state laser) gives fundamental differences between the two types of system.

The first technique which uses laser diodes,  $\mu\text{chip}$  or fiber lasers, is called "accumulation" imaging. These sources are characterised by a low-pulse power and high repetition rate, mostly around a few tens of kHz. Here, each image is the result of the accumulation of hundred of pulses during the frame time. The second technique which uses a solid-state laser illumination is called "flash" imaging. Here, each image is the result of a unique high power illumination of the scene at low repetition rate, mostly around the video rate.

In this paper, we will investigate the theoretical and practical differences between these two imaging modes and its influence on image quality, sensitivity to day light or stray light, fog penetration capacity, sensitivity to turbulences and laser safety (NOHD). For experimental purposes, we have built a range-gated active imaging system with an intensified camera and the two types of illumination. The camera can be triggered either on the first or on the second illuminator, and we are able to switch very fast from one to the other illuminator. Very precise comparative studies between the two types of illuminators have been carried out.

The result obtained in this study will be used to design an underwater system insensitive to day light. This system should be able to ameliorate the visibility in turbid water by a factor of three.

## 8896-6, Session 2

### Advanced range imaging with gated viewing: compressed sensing and coding of range gates

Martin Laurenzis, Emmanuel Bacher, Stéphane Schertzer, Frank Christnacher, Institut Franco-Allemand de Recherches de Saint-Louis (France)

Gated viewing is a prominent method for vision through obstacles, target identification and 3D imaging. The recorded images contain reflectivity as well as range information. Due to the time-of-flight of a pulsed laser illumination and a short sensor gate width, only information (i.e. light) that arrives within the right timing window at the imaging sensor contributes to the imaging process. Thus, a range-of-interest is recorded by the imaging sensor.

In the past years, different approaches were carried out to extract range information from gated viewing images. Typically a sliding gate was applied to sample range information from a scene. In a post processing, the range information was extracted for each pixel from delay-intensity transients. The resolution accuracy of these approaches was limited by the famous sampling criterion defined by Shannon and Nyquist which describes the limiting conditions for a minimal sampling resolution. To achieve higher ranging resolutions the number of sample points and therefore the number of images were increased by the application of shorter laser pulses and shorter sensor gate widths. In recent publications, different approaches were carried out to overcome this Shannon-Nyquist sampling limit by ranging based on compressed sensing and on coding of range gates. Both methods have been demonstrated to realize ranging from a small number of sampling points far beyond the Shannon-Nyquist criterion.

For the first time, we compare both methods and carry out characteristics, boundary conditions for their application and their advantages and drawbacks. Both methods are based on the assumption that the range information is of sparse nature. Thus, the number of return of range information is in the order of one. Using multiple exposure of the range gated images with certain sensor gate sequences, it is possible to sample the complete scene and record the full range information in a small number of images. In an advanced post-processing the range information and the reflectance

of the scene can be reconstructed using compressed sensing or decoding algorithms, respectively. While compressed sensing uses quasi-random gating sequences and a binary intensity pattern, the coding of range gates uses specific gate sequences and the dynamic range of the signal amplitude to estimate the range. It is shown that the coding of range gates is able to obtain high range accuracy from a very small number of images (two or three), but it is sensitive to the signal amplitude. Ranging based on compressed sensing needs more images (in the order of 20) to cover the same range with less good ranging accuracy, but it is less sensitive to the signal amplitude. Until now, multiple return signals can only be analyzed with compressed sensing.

## 8896-7, Session 2

### Comparison of three methods reducing the beam parameter product of a laser diode stack for long range laser illuminator applications

Yves Lutz, Jean-Michel Poyet, Nicolas Metzger, Institut Franco-Allemand de Recherches de Saint-Louis (France)

Laser diode stacks are interesting laser sources for active imaging illuminators. When used in quasi continuous mode, high power stacks allow the accumulation of large amounts of energy which is well suited for long-range image recording. However, even if they are equipped with fast-axis collimation (FAC) and slow-axis collimation (SAC) micro-lenses, broad-area lasers diodes have a beam parameter product (BPP) not compatible with a direct use in highly efficient and compact illuminators. This is particularly true when narrow divergences are required such as for long range applications. To overcome these difficulties, we conducted investigations in three different ways. A first near infrared illuminator based on the use of conductively cooled mini-bars was designed, realized and successfully tested during outdoor experimentations. The illuminator divergence is matched to the field of view of the receptor which is given by the active imaging scenario. Here, a divergence as narrow as  $3.5 \times 2.6$  mrad has been selected. To enable the recording of high quality images with the highest efficiency, the illumination profile must have firstly, the same geometry as the detector (which means in our case a rectangular shape with a width to height ratio of 4:3) and secondly, the intensity fluctuation must remain under a value of 5% over the complete surface. The realized mini-stack based laser diode illuminator exhibits an average power on the scene of 10W with a global efficiency of 67.5%.

This custom specified mini-stack was then replaced in a second step by an off-the-shelf FAC + SAC micro lensed laser diode stack where we conducted investigations on the brightness increasing by polarization overlapping.

The third method, still based on a commercial laser diode stack, uses a non imaging optical shaping principle resulting in a virtually restacked laser source with enhanced beam parameters. In order to reduce the gap between the BPP value along the fast axis and the BPP value along the slow axis, the method consists in dividing the emitter area in the slow axis direction and multiplying it by the same factor along the fast axis. The beam is then homogenized and projected on the scene in an easy way by using a multi reflection light guide and a projection lens. A comparison between ray tracing simulation and experimentation is also presented. This low cost, efficient and low alignment sensitivity beam shaping and homogenization method allows obtaining a compact and high performance laser diode illuminator for long range active imaging applications. In this last case, the total efficiency exceeds the value of 81% and the output lens clear aperture is limited to 62mm for the narrow divergence of  $3.5 \times 2.6$  mrad. The three brightness enhancement methods are presented and compared in this paper. As for active imaging, laser diode brightness improvement benefits to other applications such as fiber coupling or pumping of solid state or fiber laser.

## 8896-8, Session 2

### Surface enhanced vibrational spectroscopy for the detection of explosives

Hainer Hainer, Christoph Lenth, Sebastian Funke, Lars



Gundrum, Frank Rotter, Fritjof Büttner, Jan Hagemann, Mike Wellhausen, Laser-Lab. Göttingen e.V. (Germany)

The detection of trace amounts of explosive materials is an important task for national security and homeland defence, as witnessed by the bombings from Madrid and London. The challenge is that explosive materials involve different types of chemical substances such as organic nitro compounds (TNT, RDX), nitrates (ammonia nitrate, urea nitrate), organic peroxides (TATP) which necessitates different kind of detectors. Currently, we have detectors, which can detect trace amounts of special groups of explosives. Nitro containing compounds can be well detected by chemiluminescence, but fail to detect peroxides. Ion mobility spectrometry ionises the explosives, resulting sometimes in a degradation of the molecules. The detection limits are very low; however, some explosives cannot be identified unambiguously or at the same time. Another challenge is to decrease the false alarm rate. That means a detector which can identify the explosives and distinguish them from other molecules is needed.

Vibrational spectroscopy provides specific spectral information about molecules enabling the identification of analytes by their "fingerprint" spectrum. The sensitivity of the inherent weak Raman process can be increased by the Surface Enhanced Raman effect. Surface enhanced Raman scattering (SERS) is a sensitive spectroscopic tool with detection limits down to picogram and femtogram level. This is particularly attractive because it combines high sensitivity with high information content for establishing molecular identity.

Surface enhanced IR absorption spectroscopy (SEIRA) provides complementary information of the vibrational energy levels and thus can also be used for molecular identification.

Based on SER spectroscopy we have constructed a modular detection system (1, 2). Here, we want to show a combination of SERS spectroscopy and chemometrics to distinguish between chemically similar substances. Such an approach will finally reduce the false alarm rate. It is still a challenge to determine the limit of detection of the analyte on a SERS substrate or its enhancement factor. An approach for covalently bound molecules is shown by Christou et al. (3). For physisorbed molecules we have deposited volumes in the nanolitre range of analyte in solvent on the SERS substrate. After evaporation of the solvent, the area of the analyte fits in the laser spot. Thus, all molecules contribute to the SERS signal. By this approach the performance of plasmonic substrates and SERS enhancement of explosives can be evaluated.

Moreover, novel nanostructured substrates for SEIRA will be presented. A compound with a chemical similar structure to TNT is deposited on this substrate. The enhancement factor and a limit of detection are estimated.

1) Wackerbarth, H., Gundrum, L., Salb, C., Christou, K., Viöl, W., Applied Optics, 49 (23) 4367-4371, 2010.

2) Wackerbarth, H., Salb, C., Gundrum, L., Niederkrüger, M., Christou, K., Beushausen, V., Viöl, W., 49 (23) 4362-4366, 2010.

3) Christou, K., Knorr, I., Ihlemann, J., Wackerbarth, H., Beushausen, V., Langmuir, 26 (23), 18564-18569, 2010.

## 8896-9, Session 2

### A novel Sagnac fiber optic sensor employing time delay estimation for distributed detection and location

Yuan Wu, Pang Bian, Bo Jia, Qian Xiao, Fudan Univ. (China)

A novel Sagnac fiber optic sensor employing time delay estimation for distributed detection and location is proposed and demonstrated. The sensor employs Sagnac interferometer as interfering unit. A broadband, low-coherence source is spectrally sliced into two wavelength bands using wavelength division multiplexer. Therefore, the sensor consists of two Sagnac interferometers, multiplexed with a broadband light source, interfering unit and sensing fiber by wavelength division multiplexer, and hence four detected signals with two different wavelengths are obtained. After the demodulation scheme based on 3?3 coupler, two signals with fixed time delay are achieved and the location of the disturbance gained by time delay estimation enables the localization comparably accurate. Experimental results show that the sensor is especially advantageous for low location error to the application of intrusion detecting.

## 8896-10, Session 3

### Large format, small pixel pitch and hot detectors at SOFRADIR

Yann Reibel, Marie-Lise Bourqui, Michel Vuillermet, David Billon-Lanfrey, SOFRADIR (France); Gérard L. Destéfanis, Olivier Gravrand, CEA-LETI (France)

The exceptional physical properties of MCT and the maturity of the technology allows today the fabrication of more and more complex infrared FPAs with this material, keeping the highest performance.

We are pursuing further infrared developments on future MWIR detectors, such as the VGA format HOT detector that consumes 2W and the 10µm pitch IR detector which gives us a leading position in innovation. In the same time Scorpio LW expands Sofradir's line of small pixel pitch TV format IR detectors from the mid-wavelength to the long-wavelength, broadening the performance attributes of its long wave IR product line..

Large arrays with small pitches can be achieved in a large variety of cut of wavelengths such as SWIR, MWIR, LWIR, and VLWIR, including the visible. Pitch reduction has for first consequence an increase of the resolution but is also a major element for consumption reduction.

Thanks to fundamental considerations based on minority carrier lifetime, these FPA present, on suitable technologies, lower and lower dark currents. As a consequence they can operate at higher temperature reducing power consumption and making better reliability of cryogenic systems (SWAP).

This paper gives an overview of the most recent developments at Sofradir and Leti joint laboratory DEFIR on MCT detectors.

## 8896-11, Session 3

### InGaAs infrared detector development for SWIR imaging applications

Frank Rutz, Philipp Kleinow, Rolf Aidam, Wolfgang Bronner, Fraunhofer-Institut für Angewandte Festkörperphysik (Germany); Lutz Kirste, Fraunhofer-IAF (Germany); Martin Walther, Fraunhofer-Institut für Angewandte Festkörperphysik (Germany)

For surveillance and reconnaissance applications, high-performance infrared cameras with only moderate or even without any cooling are preferred. This can be achieved by short-wavelength infrared (SWIR, 1 – 2.5 µm) photodetectors which comprise wide-bandgap photoabsorber materials. For passive night vision, the lacking photon flux in the SWIR region according to Planck's law can be alleviated by the night glow as a natural light source in clear night skies, where emissions of hydroxyl radicals cause an intensity peak in the night glow spectrum at around 1.6 µm wavelength. Furthermore, active imaging systems can be realized with commercial telecommunication lasers. In pulsed operation, laser gated-viewing systems can be utilized to determine the distance to objects of interest or even generate a 3-dimensional model of the complete scene.

The InGaAs material system is very well suited for SWIR photodetectors. Grown lattice-matched on commercially available large-area InP substrates, InGaAs provides a bandgap corresponding to a cutoff wavelength of 1.7 µm. For both, passive and active imaging applications, SWIR camera systems are required to detect extremely low photon fluxes. An internal signal gain as provided by avalanche photodiodes (APDs) is beneficial for low-light-level detection. Such APDs usually comprise a photon-absorber layer and a multiplication layer that amplifies the current of the photo-generated carriers by consecutive impact ionization of further carriers in an external electric field.

Supported by the German MoD and the Bundeswehr Technical Center WTD 91, Fraunhofer IAF has started a new materials and technology development campaign for SWIR detectors based on InGaAs p-i-n diodes and APDs. Molecular beam epitaxy (MBE) is ideally suited for the growth of very thin layers with abrupt interfaces, which is required for optimized APD structures. Excellent crystalline quality has been achieved for detector structures grown on 3-inch InP substrates. The lattice constants of the MBE-grown epilayers match that of InP very well. High-resolution x-ray diffraction measurements yield a relative lattice mismatch far below 0.1 %. The commonly utilized planar

technology of APDs demands additional guard-ring structures, which inhibit focal plane arrays with a small pixel pitch such as 384x288 or 640x512 pixels with 24 or 15  $\mu\text{m}$  pitch, respectively. Hence, we decided to use our long-standing expertise in mesa technology for the SWIR detector development. Camera detector arrays as well as test structures with various sizes and geometries for materials and process characterization are processed using a dry-etch mesa technology. Within the process development the focus is set on a careful parameter choice for the dry-etching process and the consecutive dielectric passivation in order to minimize lattice damage, which acts as a major source for increased dark current. Aspects of the process development are presented along with measured dark-current and photo-current characteristics of the detector devices.

### 8896-12, Session 3

#### Semi-metal to semiconductor transition conductivity in infrared detector HgTe/CdTe nanostructure superlattice

Abdelhakim Nafidi, Aomar Idbaha, Hassan Chaib, Univ. Ibn Zohr (Morocco); Bernabé M. Soucase, Univ. Politècnica de València (Spain)

We report here magneto-transport properties and bands structure in HgTe ( $d_1=40\text{ nm}$ )/CdTe( $d_2=15\text{ nm}$ ) superlattice (SL) grown by MBE. The later is a stable alternative for application in infrared optoelectronic devices than the Hg<sub>1-x</sub>Cd<sub>x</sub>Te alloys. Especially in the region of second atmospheric window (around 10  $\mu\text{m}$ ) which is of great interest for communication.

Calculations of the spectres of energy  $E(d_2)$ ,  $E(k_z)$  and  $E(k_p)$ , respectively, in the direction of growth and in plane of the superlattice; were performed in the envelope function formalism. The energy  $E(d_2)$ ,  $?$ , 4.2 K), shown that when  $d_2$  increase the gap  $E_g$  decrease to zero at the transition semiconductor to semimetal conductivity behaviour (at  $d_2=10\text{ nm}$ ) and become negative accusing a semimetallic conduction. The angular dependence of the transverse magnetoresistance follows the two-dimensional with a residual resistance when the magnetic field is parallel to the plane of the SL. A reversal of the sign of the Hall coefficient occurs at about 3.2 T. It may be inferred to the existence of, at least, two types of carriers which suggests a semimetallic conduction. The weak-field Hall coefficient present a small maximum at about 30 K attributed to the presence of an acceptor resonant state. At 4.2 K, the sample exhibits n type conductivity with a Hall mobility of 1500  $\text{cm}^2/\text{Vs}$ . Whereas, the electrons mobility was  $\mu_n=6700$  and  $n=6.2 \cdot 10^{11}\text{ cm}^{-2}$  (with  $\mu_n/\mu_p=15$  and  $p/n=42$ ). In intrinsic regime, RH T<sup>3/2</sup> indicates a gap  $E_g = 5.3\text{ meV}$  in agreement with calculated  $E_g(?, 300\text{ K})=6\text{ meV}$ . The calculated bands gap  $E_g=E_1\text{-HH1}$  goes to zero at  $T=148\text{K}$  with a transition semimetal to semiconductor conductivity.

The formalism used here predicts that the system is semimetallic for our  $d_1/d_2 = 2.67$  and  $d_2 \supset 11\text{ nm}$ . Here,  $d_2=15\text{ nm}$  and  $E_g(?, 4.2\text{ K}) = -4.1\text{ meV}$  so this sample is a narrow gap semimetallic, two-dimensional and far-infrared detector (204  $\mu\text{m} < \lambda < 430\text{ microm}$ ).

References:

- [1] M. Braigue, A. Nafidi et al, AIP Conference Proceedings 1416, New York: American Institute of Physics, pp 68-71 (2011).
- [2] M. Braigue, A. Nafidi et al, Journal of Superconductivity and Novel Magnetism, Volume 25, Issue 8, (2012), pp 2611-2617, Springer,

### 8896-13, Session 3

#### Plasmonic absorption nanoantenna for frequency selective mid-Infrared detection

Yongqian Li, Yongjun Guo, Lei Su, Binbin Wang, Li Man, Northwestern Polytechnical Univ. (China); Zili Zhou, Science and Technology on Metrology and Calibration Laboratory (China)

The nanoantenna structures have some interesting properties to tailor electromagnetic wave, such as perfect absorption effect when the antenna structures are combined into metamaterials arrays, which provide strategies to inspire novel mid-infrared detection strategies.

The significant performances of antenna-based photodetectors arising from its intrinsic characteristics are the frequency selectivity and plasmon resonance enhanced photocurrent generation. The other functionality of nanoantenna structures could manifest itself as polarization sensitivity, or even phase modulation properties that could extract more information from a given scene. That promise photoreceptor cells enable the perception of color and polarization in mid-infrared.

In this paper, we discuss the mid-infrared detection which utilizes the nanoantenna structure to develop an increased functionality at the pixel level for next generation focal plane arrays. We investigated the plasmonic nanoantenna to achieve the frequency selectivity and polarization detection in mid-infrared wavelength. In one metal-insulator-semiconductor structures, the plasmon-enhanced photocurrent generation from the hot carriers is also analyzed. The devices cell consists of double dipole antenna and the metallic ground plane separated with dielectric layer. The dielectric layer plays a role of absorption and interference effect between the dipole antenna and the ground plane. The gathering ability of the electromagnetic wave is determined by the geometrical dimensional sizes such as the width and the antenna relative length. And the photoelectric energy conversion of hot carriers induced by the photo-conductivity effects is analyzed. The frequency selective characteristics at infrared frequency are analyzed through the physical model of the optical parameters. The electromagnetic permittivity and the permeability of optical antenna structure array are analyzed, which make the frequency selectivity understood.

### 8896-14, Session 3

#### Design and simulation of an X-ray detector for pulsar navigation

Liansheng Li, Jianwu Chen, Fuchang Zuo, Zhiwu Mei, Beijing Institute of Control Engineering (China)

Pulsar navigation is a technology that obtains the position, time and attitude information of the spacecraft through X-ray detectors, in which the measurement of time of pulse arrival, the construction of the pulse profile, and the signal processing are involved.

Detector plays an important role in the pulsar navigation system. The design requirements on X-ray detector become higher as more and more researches on pulsar navigation system are carried out. However, there are various defects in the existing conventional X-ray detectors, such as especially high voltage-supply, large bulk, low photon counting capability, low energy resolution, which cannot meet the practical requirements of pulsar navigation system.

Based on the analysis of the design requirements of the pulsar navigation system and the characteristics of both silicon drift detector (SDD) and avalanche photo diode (APD), a droplet-like avalanche drift diode detector (DADD) is proposed. The DADD integrates the advantages of SDD (smaller output capacitance, independent of its detecting area, high peak/background ratio) and APD (high gain), and adopts the method of irradiation entrance window on the front-side. Firstly, the overall structure of the DADD has been designed. Meanwhile, some structure parameters, such as the bow-shaped curves, density of substrate, distance of drifted ring, extra biased voltage, with N<sup>+</sup> protection between drifted ring and width of drifted ring have also been designed and analyzed. Secondly, the electrical field of the DADD has been simulated with commercial software, which shows that the differences of dark current of drifted ring can result in variety of voltage drops between different drifted rings. In addition, the influences rules of varied substrate resistance on the fully depleted voltage and electrical field of transverse drift, and the influences rules of the width of drifted rings and the distance between drifted rings on the leakage current and detector performance have been investigated. Finally, the detector structure with voltage on the drifted ring directly and N<sup>+</sup> type protection ring has been simulated. Both the leakage current of drifted ring and the density of electrons between drifted channels have been obtained. The simulation results show that, the proposed DADD has a good structure and features with high gain, smaller output capacitance, high photon counting capacity, and high detecting efficiency. As a result, the DADD is appropriate for the pulsar navigation system.

8896-15, Session 4

### Research on laser protection: an overview of 20 years of activities at Fraunhofer IOSB (Invited Paper)

Gunnar Ritt, Fraunhofer-Institut für Optronik, Systemtechnik und Bildauswertung (Germany); Dominik Walter, Fraunhofer IOSB (Germany); Bernd Eberle, Fraunhofer-Institut für Optronik, Systemtechnik und Bildauswertung (Germany)

Since the advent of the laser in 1960, the protection of human eyes and sensors against intended or unintended damage by laser radiation is still a hot research topic. As long as the parameters of a laser source such as the wavelength and the output power are known, adequate laser safety can be ensured simply by utilizing conventional laser protection filters which are based on absorption or interference effects. This is typically the case in cooperative environments like in a lab or in industrial facilities. A very different situation prevails in military defence or civil security. There, the parameters of encountering laser threats are usually not known. Protection measures, helping against all types of laser threats, are the long desired objective of countless research activities. The biggest challenge in finding an effective measure arises from single laser pulses of unknown wavelength. The problem demands for a passive protection concept and may be based for example on intensity dependent effects. Moreover, the solutions requested shall comprise add-on possibilities like thin films to be put on existing optics or windshields or glasses. Unfortunately, such an all-embracing solution concept is still far out of reach.

The Fraunhofer IOSB is working on the evaluation and development of non-conventional laser protection methods since 20 years. An overview of the past and present research activities shall be presented comprising measures against laser damaging and laser dazzling.

8896-16, Session 4

### Gun muzzle flash detection using a CMOS single photon avalanche diode

Tomer Merhav, Vitali Savuskan, Technion-Israel Institute of Technology (Israel); Yael Nemirovsky, Technion-Israel Institute of Technology (Israel) and Kinneret College on the Sea of Galilee (Israel)

Modern low intensity conflicts and acts of terrorism are stressing the need for military and law enforcement agencies to locate sporadic sources of hostile fire. The impact of gun detection systems on the battlefield depends not only on performance parameters of the single system but also on the abundance of the system among fighting forces. Si based sensors, in particular CMOS Image sensors, have revolutionized low cost imaging systems but to date have hardly been considered as possible candidates for gun muzzle flash detection, due to performance limitations, and low SNR in the visible spectrum.

In this study, a CMOS Single Photon Avalanche Diode (SPAD) module is used to record and sample muzzle flash events in the visible spectrum, from representative weapons, common on the modern battlefield. Weapons under study are the AK47, Dragunov, m16-A4, NATO G3 and Remington 700 Sniper Rifle. SPADs possess two crucial properties for muzzle flash imaging - Namely, very high photon detection sensitivity, coupled with a unique ability to convert the optical signal to a digital signal at the source pixel, thus practically eliminating readout noise. This enables high sampling frequencies in the Kilohertz range without SNR degradation, in contrast to regular CMOS image sensors. To date, the SPAD has not been utilized for flash detection in an uncontrolled environment, such as gun muzzle flash detection.

Gun propellant manufacturers use alkali salts to suppress secondary flashes ignited during the muzzle flash event. Common alkali salts are compounds based on Potassium or Sodium, with spectral emission lines around 769nm and 589nm, respectively. A narrow band filter around the Potassium emission doublet is used in this study to favor the muzzle flash signal over solar radiation. This research will demonstrate the SPAD's ability to accurately sample and reconstruct the temporal behavior of the muzzle flash in the visible wavelength under the specified imaging conditions. The reconstructed signal is clearly distinguishable from background clutter, through exploitation of flash intensity and temporal characteristics.

This novel detection approach will enable the development of gun detection systems in the visible wavelength, based on mature CMOS mass production technology. High sampling frequency will reduce the need for complex detection algorithms, enabling a cascade implementation involving on-pixel processing coupled with off-FPA processing in low-cost, low-power computational modules.

A demonstrator system was setup to simulate a conceptual detection system. The demonstrator was comprised of a component-off-the-shelf single diode CMOS SPAD module, a fish eye lens and a sampling board. Muzzle Flash detection was demonstrated both in a controlled indoor environment and a real world outdoor environment. Indoor firing experiments enabled the comparison of filtered muzzle flash signal to a non-filtered signal, without the need to attenuate solar background radiation. Outdoor testing verified the detection concept in a realistic scenario, where solar radiation demanded the use of an adequate spectral filter to keep signal to clutter ratio above one. Experiments showed that a repeatable muzzle flash response exists in the narrow Potassium band. The methodology may be extended to ammunition that utilizes other chemical compounds as flash suppressing agents.

8896-17, Session 4

### Multifunctional system for muzzle flash and sniper sight detection utilizing a laser and high frame rate SWIR-camera

Carl Brannlund, Jonas Tidstrom, Markus Henriksson, Lars J. Sjöqvist, Swedish Defence Research Agency (Sweden)

Snipers and other optically guided weapon systems are serious threats in military operations. We have studied a SWIR (Short Wave Infrared) camera-based system with capability to detect and locate snipers both before and after shot over a large field-of-view. The high frame rate SWIR-camera allows resolution of the temporal profile of muzzle flashes. This enables low false alarm rate shot detection. The capability to detect and discriminate sniper muzzle flashes with this system has been verified by FOI in earlier studies. In this work we have extended the system by adding a laser channel for optics detection.

A laser diode with slit-shaped beam profile is scanned over the camera field-of-view to detect retro reflection from optical sights. The optics detection system has been tested at various distances up to 1.3 km showing the feasibility to detect rifle scopes in full daylight. The high speed camera gives the possibility to discriminate false alarms by analyzing the temporal data. The intensity variation, caused by atmospheric turbulence, enables discrimination of small sights from larger reflectors due to aperture averaging, although the targets cover less than a single pixel.

It is shown that optics detection can be integrated in combination with muzzle flash detection by adding a scanning rectangular laser slit. The overall sniper detection capability by continuous surveillance of a relatively large field-of-view looks promising. This type of multifunctional system may become an important tool to detect snipers before and after shot.

8896-18, Session 4

### Analyzing the effectiveness of flare dispensing programs against pulse width modulation seekers using self-organizing maps

Mehmet C. Sahingil, Murat S. Aslan, TÜBİTAK BILGEM İLTAREN (Turkey)

Infrared guided missile (IRGM) seekers utilizing pulse width modulation (PWM) in target tracking is one of the most important threats against air platforms, as they are abundant and more resistive to countermeasures as compared to early generation reticle-based missile seekers. To be able to achieve a "soft-kill" protection of own platform against these type of threats, one needs to examine carefully the seeker operating principle with its special electronic counter-counter measure (ECCM) capability. One of the cost-effective ways of soft kill protection is to use flare decoys in accordance with an optimized dispensing program. Such an optimization, however, is not trivial. It requires a good understanding of the threat seeker, capabilities of the air platform and engagement scenario

information between them. Modeling and simulation is very powerful tool to achieve a valuable insight and understand the underlying phenomenology. In the simulation-based analysis, lots of Monte Carlo and batch runs in a predetermined parameter space should be performed. A careful interpretation of simulation results is crucial to infer valuable conclusions from the data. Such an interpretation is not easy to achieve, as one usually deals with a very high dimensional feature space, where several factors (features) affect the results. Therefore, powerful statistical tools and pattern recognition algorithms are of special interest in the analysis. In this paper, we show how self-organizing maps (SOMs), which is one of those powerful tools, can be used in analyzing the effectiveness of various flare dispensing programs against a PWM seeker. We perform several Monte Carlo runs for a typical engagement scenario between an IRGM with PWM seeker and an air platform utilizing a flare dispensing program in a MATLAB-based simulation environment which include air platform radiation and kinematics model, flare radiation and kinematics model and threat PWM seeker model. In each run, we randomly change the flare dispensing program and obtain corresponding class: "successful" or "unsuccessful", depending on whether the corresponding flare dispensing program deceives the seeker or not, respectively. Then, in the analysis phase, we use SOMs to interpret and visualize the results and obtain an effectiveness (successful class) boundary for the flare dispensing programs.

8896-19, Session 5

### Image quality testing of assembled IR camera modules

Daniel Winters, Patrik Erichsen, TRIOPTICS GmbH (Germany)

IR camera modules for the LWIR (8-12 $\mu$ m) that combine IR imaging optics with microbolometer focal plane array (FPA) sensors with readout electronics are becoming more and more a mass market product. At the same time, steady improvements in sensor resolution in the higher priced markets raise the requirement for imaging performance of objectives and the proper alignment between objective and FPA. This puts pressure on camera manufacturers and system integrators to assess the image quality of finished camera modules in a cost-efficient and automated way for quality control or during end-of-line testing.

In this paper we present recent development work done at Trioptics in the field of image quality testing of IR camera modules. This technology provides a wealth of additional information in contrast to the more traditional test methods like minimum resolvable temperature difference (MRTD) which give only a subjective overall test result. Parameters that can be measured are image quality via the modulation transfer function (MTF) for broadband or with various bandpass filters on- and off-axis and optical parameters like e.g. effective focal length (EFL) and distortion. If the camera module allows for refocusing the optics, additional parameters like best focus plane, image plane tilt, autofocus quality, chief ray angle etc. can be characterized. Additionally, the homogeneity and response of the sensor with the optics can be characterized in order to calculate the appropriate tables for non-uniformity correction (NUC). The technology can also be used to control active alignment methods during mechanical assembly of optics to high resolution sensors.

Other important points that are discussed are the flexibility of the technology to test IR modules with different form factors, electrical interfaces and last but not least the suitability for fully automated measurements in mass production.

8896-20, Session 5

### Blackbody reference sources with high speed temperature stabilization time

Catherine Barrat, HGH Systèmes Infrarouges (France)

It is really a new way of working that HGH Infrared Systems is offering to engineers using high temperature cavity blackbody as reference sources to characterize and calibrate near-IR and IR sensors. Until now, the particularly long thermal inertia of this kind of devices, key elements in characterization benches, has had to be taken into account in test strategy. It could contribute to major shift in projects schedules, in case of unexpected results during test campaigns. HGH Infrared Systems has developed an innovative internal structure

on its best-selling RCN blackbody to highly reduce its temperature stabilization time.

The RCN1200N1 is a high temperature cavity blackbody used for the calibration of infrared radiometric instruments, for applications in research and development (nuclear or spatial sector, spectral calibration of special infrared detectors). It is a unique combination of high-end features: broad temperature range up to 1200 $^{\circ}$ C, emissivity higher than 0.99 on whole infrared spectral bands (SWIR, MWIR, LWIR), high angular and spatial uniformity, regulation stability better than 0.1 $^{\circ}$ C, over the whole range, including 1200 $^{\circ}$ C. It is a reliable reference source for researchers and engineers.

To achieve such performance, it has been designed to confine the energy at the heart of the device (the cavity) and to limit at maximum heat exchange with the environment. This structure, as on conventional cavity blackbodies, leads to a cooling time, from high temperature to low temperature of about 5 hours. Users of cavity blackbody, thus, have to calibrate their system exclusively by increasing temperatures (the warm up time from ambient to 1200 $^{\circ}$ C is far shorter, of less of a hour). This constraint is particularly damaging in the context of Research and development projects.

HGH innovates by incorporating a device to accelerate the cooling time of the cavity. It will take half the time now to stabilize the source at a lower temperature, while maintaining the high radiometric performance. It is no longer necessary to wait until tomorrow to test again at an intermediate temperature point.

8896-21, Session 5

### Performance simulation model for a MWIR airborne camera for missile plume detection

Jeeyeon Yoon, LIG Nex1 Co., Ltd. (Korea, Republic of); Dongok Ryu, Sangmin Kim, Sehyun Seong, Yonsei Univ. (Korea, Republic of); Jieun Kim, Agency for Defense Development (Korea, Republic of); Hyunki Lee, LIG Nex1 Co., Ltd. (Korea, Republic of); Woongsup Yoon, Sug-Whan Kim, Yonsei Univ. (Korea, Republic of)

We report a new airborne camera designed for surveillance of ballistic missile plumes with improved optical performance in MWIR wavelength ranges. The camera design uses refractive optical elements and its InSb detector. Both imaging and radiometric performance of the camera are studied by using ray tracing, and targets and background scene models. Ballistic missile plume radiance in computation model is calculated from CFD type radiative transfer algorithms and used as the light source. The atmospheric background is computed using MODTRAN with forms of path thermal radiance, single/multiple scattered radiance and transmittance. The ray tracing simulation results demonstrate successfully that the camera design satisfies the imaging and radiometric performance requirements in MWIR band.

8896-22, Session 5

### Research on simulation credibility of space-based optical imaging system

Yi Han, Huayan Sun, Huichao Guo, Yinchun Li, Lin Du, The Academy of Equipment Command & Technology (China)

Because of the restriction of actual conditions, we have to demonstrate and validate the space-based optical imaging system performance by using computer simulation technology. Therefore we utilize the theories of linear systems mathematics and Fourier transforms to build and model the key elements of the end-to-end imaging chain for optical imaging system mathematically, and use VC++ and OpenGL as the develop tool to realize the space-based imaging system simulation software, which is consisted of the space scene visualization, target optical scattering properties analysis, imaging simulation and system performance analysis modules. But whether the simulation model can replace the actual model and whether the simulation accuracy can meet corresponding requirements, the simulation credibility must be researched and evaluated, which is the degree that users believe in simulation results under certain conditions.

Simulation credibility is related to all stages of simulation, and at the same time is related to the input and output of simulation system. Therefore, when evaluating the credibility, on the one hand we should evaluate the process of building the models of imaging chain; on the other hand we should evaluate initial input parameters and output results. At last, these two aspects should be synthesized and given different weights.

In this paper we construct the credibility evaluation scales, evaluation index system and evaluation framework respectively. Then build the mathematic comprehensive evaluation model by using the fuzzy analytic hierarchy process method (fuzzy AHP), which is synthesized by the analytic hierarchy process method and the fuzzy comprehensive evaluation method. The credibility values of each index are given by expert group and the credibility of entire simulation system is calculated at last.

After the establishment of the evaluation hierarchical framework of imaging simulation system, we process the weights assignment by fuzzy AHP. And in this method, the pair-wise comparison scales are fuzzy numbers instead of crisp numbers which are used in classical AHP. The fundamental process of fuzzy AHP used in this paper is summarized as follows: Step 1, According to the criteria in the hierarchical framework, a series of comparison consultation sheets are made. Step 2, to construct the k-th expert's fuzzy judgment matrix. Step 3, to compute the k-th expert's fuzzy normalized weight vector. Step 4, to summarize all the expert's opinions. Step 5, hierarchy general sorting. By the processes listed above, we get the weights of criteria with respect to their superior criterion. In order to assure the precision of ranking in AHP, it is necessary to check the consistency of judgment matrix.

Since the fuzzy AHP method has considered fuzzy characteristic existing in people's judgment, it can increase the subjective effects and is more reasonable. The application results in this paper show that this method is suitable, easy and feasible.

These researches on simulation credibility can increase the correctness of the simulation results and reduce the risk of applying the optical imaging simulation system; it can promote the in-depth research on software engineering, system testing and evaluation, simulation accuracy and other issues. It can test the errors early and minimize the total investment. It can also help to analyze issues better, solve problems and produce more predictable results.

## 8896-23, Session 6

### Results from the electro-optic sensors domain of the materials and components for missiles innovation and technology partnership (phase 1) (*Invited Paper*)

Mark Bray, Robert Shears, SELEX ES Ltd. (United Kingdom)

The Materials and Components for Missiles (MCM), Innovation and Technology Partnership (ITP) is a research programme supporting research for guided weapons at Technology Readiness Levels 1 to 4. The Anglo-French initiative is supported by the DGA and the MoD, with matched funding from industry. A major objective is to foster projects which partner UK and French universities, SMEs and larger companies. The first projects started in January 2008 and the current phase is due to complete in spring 2013. Providing funding is secured the next phase of the programme is due to start later in 2013.

The programme is split into eight domains, with MBDA as the overall leader:

- Systems
- RF Sensors
- EO Seekers
- Rocket Propulsion
- Turbojet Propulsion
- Warheads
- SAUs and Fuses
- Electronics and Materials

Selex ES leads Domain 3 of the MCM-ITP which develops Electro-Optic sensor technology. In collaboration with DGA, MoD and MBDA, the prime contractor, we identified 2 key objectives for the first ITP phase and focussed resources on achieving these:

- Better imagery – this is required as counter measures become more

difficult to overcome and as the targets become more difficult to distinguish from bystanders

- Low overall through life cost – clearly financial pressure will remain over the foreseeable future and value for money will be key for any new technologies

To date nine normal projects and one innovation fund project have been supported within the domain. The technology providers have included 3 SMEs and 7 research centres from both the United Kingdom and France.

The projects have covered all aspects of the sensors ranging from optical elements through detectors to post capture processing. Projects have covered all the major optical atmospheric transmission windows from UV (<400nm) to long wave infrared (>10,000nm).

Highlights will be presented both of the domain's technical results and the opportunity for exploiting the achievements. An outline of the priorities for the domain for the new phase will be provided and we encourage organisations with suitable technology to contact us to get involved.

## 8896-24, Session 6

### Feature-based automatic configuration of semi-stationary multi-camera components

Ann-Kristin Grosselfinger, David Muench, Wolfgang Hübner, Michael Arens, Fraunhofer-Institut für Optronik, Systemtechnik und Bildauswertung (Germany)

Semi-stationary multi-camera components which are able to operate autonomously are the core modules of ad-hoc multi-view methods. A rough overview of an entire scene with a wide angle camera is not enough: On the one hand a situation recognition system needs enough visual input to detect fine grained situations, and on the other hand when recognizing the occurrence of a car or the presence of a person a close-up view of that interesting agent is required to further refine the information or identify that interesting agent. This part can be done by an additional active pan-tilt-zoom camera to capture high-resolution close-up views of an agent.

The problem arising in a multi-camera system is the configuration of one camera to the other. In this paper we address of what can be seen in an overview-camera to the motor configuration of a PTZ camera. As the proposed system is semi-stationary on the one hand the hardware architecture is designed to be independent of any wired connection and on the other hand the methods work online and reliable.

Images are captured from a uniformly moving PTZ camera until the entire scene captured by the master camera is covered. Along the way a lookup table (LUT) is generated by corresponding motor coordinates of the PTZ camera and the image coordinates in the master camera. To match each pair of images, features are detected in both images, selected by nearest neighbor distance ratio (NNDR) and matched. A homography is adapted to these matches and applied to transform the image of the PTZ camera to the master image. After having collected enough data in the LUT one function for each motor coordinate as function of master image coordinates is determined using linear regression and RANSAC. With these functions two comprehensive LUT, one for pan, one for tilt, for every pixel in the master image are calculated and stored.

In this paper we evaluated different features according to the robustness, accuracy and runtime of the configuration. The robustness and accuracy are quantitatively evaluated. Features evaluated are SURF, SIFT. When the cameras have a similar field of view the mean angular accuracy is below two degrees in an outdoor scenario. An initial full calibration run with over 36 markers takes about 300 seconds.

Further work includes the online refinement of the registration with detected objects in low-textured environments and integration in a holistic scene understanding framework.

8896-25, Session 6

### **A new long wave IR spectral imager based on uncooled camera and Circular Variable Filter (CVF) for spectral separation**

Dario Cabib, CI Systems (Israel) Ltd. (Israel)

LWIR spectral imagers for industrial, airborne and research applications that have been described in the literature use interferometers in their basic optical design to provide the spectral information of the pixel radiance.

In this work I show the optical design, calibration challenges and procedure, preliminary test measurements and results of a new LWIR spectral imager using an uncooled camera and Circular Variable Filter (CVF) combination instead of an interferometer to provide the spectral content information of the pixel radiance. This type of design has advantages of its own: compactness and low cost combined with signal to noise ratio, spectral resolution and Noise Equivalent Temperature (NET), which are acceptable for many applications. CVF's are a very convenient optical monochromator device: I will also show the latest development on this subject, including a high resolution version.

8896-26, Session 6

### **A Long Wave Infrared (LWIR) spectral imager (7.7 to 13 microns) based on cooled detector array and high resolution Circular Variable Filter (CVF)**

Dario Cabib, Moshe Lavi, Amir Gil, Eran Ohel, Uri Milman, CI Systems (Israel) Ltd. (Israel)

Spectral imagers in the Long Wave IR spectral range suffer from the problem of high production costs because the existing cooled array detectors are expensive, and in fact they are prohibitively expensive for many applications.

As a result, the drive to lower the cost of IR spectral imagers is strong, and CI has found a way to achieve this feat by significantly lowering the cost of the monochromating method used to provide the spectral information. In fact, CI Systems has developed a long wave IR (7.7 to 13 micron) spectral imager using a Circular Variable Filter (CVF) instead of the common interferometric Fourier Transform method used in this spectral range. The CVF method is an environmentally stable, easy-to-align optical set-up, which may be suitable for many applications in which a spectral resolution in the range of 0.5% of the wavelength or 50 nm at 10  $\mu$ m (best case) to 2% of the wavelength or 200 nm at 10  $\mu$ m (worst case) is acceptable. System design, calibration procedure and examples of preliminary measurements, applications and specifications will be given in this paper.

8896-27, Session 6

### **A novel sampling method for the sparse recovery of infrared sea surveillance images**

Serdar Cakir, Hande Uzeler, Tayfun Aytaç, TÜBITAK BILGEM ILTAREN (Turkey)

Compressive sensing framework states that a signal which has sparse representation in a known basis may be reconstructed from samples obtained from a sub-Nyquist sampling rate. Due to its inherent properties, the Fourier domain is widely used in compressive sensing applications. Sparse signal recovery applications making use of a small number of Fourier Transform coefficients have made solutions to large scale data recovery problems, i.e. images, applicable and more practical. The sparse reconstruction of two dimensional images is performed by making use of sampling patterns generated by taking into consideration the general frequency characteristics of natural images. In this work, instead of forming a general sampling pattern for infrared images of sea-surveillance scenarios, a special sampling pattern has been obtained by making use of a new iterative algorithm that uses a database containing images recorded under similar conditions. It has been shown by experimental results that, the proposed sampling pattern provides better sparse recovery results in

terms of PSNR (peak signal-to-noise ratio) compared to the baseline sampling methods proposed in the literature.

8896-28, Session 6

### **Image generation for single detector infrared seekers via compressive sensing**

Hande Uzeler, Serdar Cakir, Tayfun Aytaç, TÜBITAK BILGEM ILTAREN (Turkey)

In this paper, we investigate the application of compressive sensing theory to single detector IR seekers. Compressive sensing is a novel signal processing technique which enables a compressible signal to be constructed using fewer measurements obtained in a specific way below the Nyquist rate. Single detector image reconstruction applications using compressive sensing have been shown to be successful. Infrared seekers utilizing single detectors suffer from low performance compared to costly focal plane array detectors. The single detector, pseudo-imaging rosette scanning seekers scan the scene with a specific pattern and process the resultant signal with signal processing methods to estimate the target location without forming an image. In this context, this type of old generation seekers can be converted to imaging systems by utilizing the samples obtained by the scanning pattern in conjunction with the compressive sensing theory framework. In this study, infrared images have been reconstructed from samples obtained by the rosette scanning pattern for different sample numbers and it has been shown that the results obtained are comparable to other sampling methods proposed in the literature.

8896-29, Session PS

### **A simulation model of vegetation temperature based on physiological characteristics**

Wei Lin, Beijing Institute of Technology (China); Ji-Yuan Wang, Yu-hua Chen, Rong-hua Su, Beijing Canbao Architecture Design Institute (China); Song-lin YU, Beijing Canbao architecture design institution (China)

To acquire and predict the infrared radiation characteristics of natural background is a foundation of modeling and simulation for the infrared imaging system, particularly it requires to master the variation regulation of infrared characteristics for the ground-object at different times, which determines the factuality of the simulation scenarios and the credibility of the quantitative results, it is an important approach to study the characteristic differences between background and target?and it is also an important measure to evaluate the effectiveness for the surveillance and monitoring system and the performance for the camouflage and interference measures. At present, a radiation model and an empirical model are usually used to simulate the infrared characteristics of vegetation. But the empirical model seems so difficult to apply it in more complex environmental conditions, and its accuracy is too low. In the radiation model, in which the latent heat component is only used to characterize the transpiration of vegetation, but this model has so many parameters which is so complex and it is so difficult to acquire.

Experimental validation shows that the radiation model is still difficult to meet the high-precision requirements for the thermal infrared simulation. To this purpose, start from the ambient temperature, the solar radiation and the vegetation physiological characteristics, we deeply analyze the relationship between vegetation physiological characteristics and environment, and put forward a temperature simulation method based on vegetation physiological characteristics, which is called physiological model.

In this physiological model, we firstly comprehensive considered the respiration and transpiration of the vegetation life, then according to the relationship between transpiration rate, breathing rate and environmental temperature, we combined the biodegradable heat with the evaporation latent heat, and derived the quantitative relationship of breathing rate and transpiration rate to leaf temperature, respectively. Secondly, according to the existing biometric experimental results, we analyzed the diurnal variation regulation and monthly variation regulation of vegetation physiological activities, in which the complex radiation heat transfer process and the convective heat transfer

process have been ignored; the relationship between the vegetation temperature and air temperature, as well as the transpiration and respiration has been established. Then we realized simulation of the temperature variation regulation of vegetation through the variation regulation of vegetation physiological characteristics.

In order to compare the radiation model with the physiological model, we carried out a measurement experiment on field vegetation for two consecutive days, by using the thermal imager and the wild weather station, as well as the vegetation photosynthesis meter. The data of respiration rate, transpiration rate, thermal infrared images, temperature, wind speed, humidity, etc., have been recorded every 30 minutes.

The experimental results have been simulated by the radiation model and the physiological model, respectively. Results shows that in the average error of the vegetation temperature simulated by the radiation model is about 4k, but the average error of the physiological model is about 1k. Obviously, the physiological model has higher accuracy of simulation, simpler arithmetic, lesser parameters, more effectively, and it greatly improves the efficiency and accuracy of the thermal infrared simulation system.

### 8896-30, Session PS

#### A Calibration Method of the Multi-channel Imaging LiDAR

Weiming Xu, Shanghai Institute of Technical Physics (China); Jun Liu, Information Engineering Univ. (China); Rong Shu, Shanghai Institute of Technical Physics (China)

We designed a kind of imaging lidar with sixteen channels, which consists of a fiber laser, two scan motors, distance measurement circuits and information processing circuits etc. The image lidar provides sixteen distance measurements for one laser shot and the distance accuracy of each channel is about 4cm. This paper provides a method to calibrate the point cloud images of this multi-channel lidar. This method needs to construct different inclined planes to cover a scanning strip, and establish the precise plane formula in the known ground coordinates, then fit the plane from the laser point clouds of planes and calculate the correction parameters of all channels through the error model. The image accuracy is better than 5cm processed by this calibration method.

### 8896-31, Session PS

#### Deformation measurement for satellite antennas by close-range photogrammetry

Shanping Jiang, Yang Linhua, China Academy of Space Technology (China)

The photogrammetric system in vacuum cryogenic environment is designed to measure the sharp deformation of the satellite antenna due to the thermal deformation. The method of the measurement is based on the close-range photogrammetric techniques. This system includes CCD photography assembly, scale bars, support structures and the software. A test was performed by using this system, and the sharp deformation of a reflecting antenna was measured. In the test, a plenty of data was acquired, then the measurement method was proved feasible. According to analysis, we can acquire that the relatively measurement precision by this system can reach to 1:20000.

### 8896-32, Session PS

#### Optical design of a large-scale in-door illumination simulating system

Jie Xu Sr., Shanping Jiang, Qingsheng Xiao, Pengsong Zhang, Linhua Yang, Hongsong Li, Yanhong Xiang, Beijing Institute of Spacecraft Environment Engineering (China)

A large-scale in-door illumination simulating system was developed by Beijing Institute of Spacecraft Environment Engineering (BISEE) for image test requirements of a deep-space sensor, the optical design of the system was present in this paper. Metallic halide lamps and tungsten halogen lamps which had high-power, good accuracy and

small collimating angle collectors and matched the sunlight spectrum very well, distributed beside the wall of the laboratory vertically. Incident angle of the system was between 15° and 45°. The uniformity with 15°, 30° and 45° were  $\pm 12.4\%$ ,  $\pm 8.1\%$  and  $\pm 14.9\%$  respectively. In the 30° condition, the uniform illumination area was 20m<sup>2</sup>20m, total average radiation intensity was 400.4W/m<sup>2</sup>, spectrum intensity was 48.5W/m<sup>2</sup> in 600nm-700nm and 5.1W/m<sup>2</sup> in 965nm-995nm. The shadow profile of the obstacle in the area was as clearly as illuminated by sunlight in all incident angles. Acceptance data matched the calculation results very well and met the specifications totally. The system had been used successfully in the test of the sensor many times.

### 8896-33, Session PS

#### Determination of the microbolometric FPA's responsivity with imaging system's radiometric considerations

Slawomir Gogler, Grzegorz Bieszczad, Michal Krupinski, Military Univ. of Technology (Poland)

In areas like military systems, surveillance systems, or industrial process control, more and more often there is a need to operate in limited visibility conditions or even in complete darkness. In such conditions vision systems can benefit by using thermal vision cameras. Thermal imagers and used therein infrared array sensors are subject to calibration procedure and evaluation of their voltage sensitivity on incident radiation during manufacturing process. During typical calibration procedure, detectors used in calibration set-up are illuminated by infrared radiation transmitted through an optical system. To account for manufacturing differences in each single detector, all detectors are assumed to be linear in response and their voltage response is corrected, so that each detector yields the same voltage output when subject to the same temperature. In order to assure, that the scene is faithfully imaged on the sensor (in terms of temperature variations), numerous physical phenomena have to be taken into account. One such phenomenon is the decrease of the radiant flux reaching off-axis image points, what might be perceived as a false decrease in temperature and makes interpretation of the image difficult. The said effect, is often referred to as "cosine to the fourth" law in classical textbooks. Derivation of the law assumes small aperture angles approximations which cannot be valid in thermal cameras that work with optical systems with low F-number (usually close to 1). Presented method makes use of radiative heat transfer equations for evaluation of irradiance distribution on the FPA and so makes no assumptions with regard to the angles or source and detector sizes. It does however assume uniform optical absorption, which, in real life, would cause further decrease in irradiance distribution that would vary from optical system to optical system. Moreover it assumes Lambertian nature of the radiator (i.e. angular independence of luminance). For validation purposes, a set of configurations comprising different aperture sizes and aperture-to-detector distances have been measured on specially designed measurement stand and compared with the model.

### 8896-34, Session PS

#### System for critical infrastructure security based on multispectral observation-detection module

Piotr Trzaskawka, Mieczyslaw Szustakowski, Mariusz Kastek, Rafal Dulski, Marek Zyczkowski, Wieslaw Ciurapinski, Jaroslaw Barela, Military Univ. of Technology (Poland)

Recent terrorist attacks and possibilities of such actions in future have forced the development of security systems for critical infrastructures that embrace sensors technologies and technical organization of systems. The used till now perimeter protection of stationary objects, based on construction of a ring with two-zone fencing, visual cameras with illumination are efficiently displaced by the systems of the multisensor technology that consists of: visible technology – day/night cameras registering optical contrast of a scene, thermal technology – cheap bolometric cameras recording thermal contrast of a scene and active ground radars – microwave and millimetre wavelengths that record and detect reflected radiation. Connection of these three

different technologies into one system requires methodology for selection of technical conditions of installation and parameters of sensors.

This procedure enables us to construct a system with correlated range, resolution, field of view and object identification. The second technical problem connected with the multispectral system is its software, which helps couple the radar with the cameras. This software can be used for automatic focusing of cameras, automatic guiding cameras to an object detected by the radar, tracking of the object and localization of the object on the digital map as well as identification and alarming. Based on unique "plug and play" architecture, system provides unmatched flexibility and simplistic integration of sensors and devices in TCP/IP networks. Using a graphical user interface it is possible to control sensors and monitor streaming video and other data flow over the network, visualize the results of data fusion process and obtain detailed information about detected intruders over a digital map. System provide high-level applications and operator workload reduction with features such as sensor to sensor cueing from detection devices, automatic e-mail notification and alarm triggering.

In this paper two essential issues connected with multispectral system are described. Efficient range of detection, recognition and identification of persons and vehicles depends on the field of view of a scene and types of the used devices. There is also a variety of applications and control of cameras set for a target detected by radar. The paper presents a structure of critical infrastructure protection that bases on a module multisensor security system and its elements. We focus on methodology of selection of sensors parameters. The results of the tests in real condition will be also presented.

#### 8896-35, Session PS

### Determining the range parameters of observation thermal cameras on the basis of laboratory measurements

Jaroslaw Barela, Krzysztof Firmanty, Mariusz Kastek, Piotr Trzaskawka, Military Univ. of Technology (Poland)

Range parameters are main factors in assessing the performance of observation devices. They can be determined on the basis of computer simulations, field or laboratory measurements, with the latter method being the most reliable and practical. The paper presents the methods used for the determination of detection, recognition and identification ranges based on well-known Johnson criteria and recently emerged TTP model. Theoretical background for both approaches are given, and the laboratory test stand is described together with brief methodology adopted for the measurements of selected, necessary characteristics of a tested observation system. Measurements of all required parameters were conducted in the IOE, MUT on a MST test stand by CI SYSTEM. This test stand consists of IR collimator, IR standard source, rotating wheel with test patterns, a computer with a video grabber card and specialized software. Parameter measurements were conducted for three observation-class thermal cameras. Two of them were uncooled, microbolometer devices without temperature stabilization, where the last one was MWIR cooled camera. The measurement results are presented and the calculated ranges for a selected set of IR cameras are given, obtained on the basis of both Johnson criteria and TTP model. Finally the results are discussed and the final thoughts on the TTP model application are presented.

#### 8896-36, Session PS

### Test stand for non-uniformity correction of microbolometer focal plane arrays used in thermal cameras

Michal Krupinski, Jaroslaw Barela, Krzysztof Firmanty, Mariusz Kastek, Military Univ. of Technology (Poland)

Uneven response of particular detectors (pixels) to the same incident power of infrared radiation is an inherent feature of microbolometer focal plane arrays. As a result an image degradation occurs, known as Fixed Pattern Noise (FPN), which distorts the thermal representation of an observed scene and impairs the parameters of a thermal camera. In order to compensate such non-uniformity several NUC correction

methods are applied in digital data processing modules implemented in thermal cameras. Coefficients required to perform the non-uniformity correction procedure (NUC coefficients) are determined by calibrating the camera against uniform radiation sources (blackbodies).

Non-uniformity correction is performed in a digital processing module in order to remove FPN pattern in the registered thermal images. Relevant correction coefficients are calculated on the basis of recorded detector responses to several values of radiant flux emitted from reference IR radiation sources (blackbodies).

The measurement of correction coefficients requires specialized setup, in which uniform, extended radiation sources with high temperature stability are one of key elements. Measurement stand for NUC correction developed in Institute of Optoelectronics, MUT, comprises two integrated extended blackbodies with the following specifications: area 200x200 mm, stabilized absolute temperature range  $\pm 15^{\circ}\text{C} \div 100$  [°C], uniformity of temperature distribution across entire surface  $\pm 0.014$  [°C]. Test stand, method used for the measurement of NUC coefficients and the results obtained during the measurements conducted on a prototype thermal camera will be presented in the paper.

#### 8896-37, Session PS

### Analysis and design of infrared swing scanning control system

Xinling Tian, Xuli Liu, Mintao Tan, Weihua Wang, Danfeng Li, Beijing Institute of Control Engineering (China)

Swing scanning control system is the core unit of infrared scanning system, which determined the performance of the system. This paper put forward to a kind of method to design infrared swing scanning control system aiming at the system's requirement. The method can realize the system control in low speed of rotation?small angle?high precision (swing frequency 1-2 Hz, swing amplitude  $\pm 0.125^{\circ}$ , precision over than  $\pm 0.0125^{\circ}$ )?

This paper makes the modeling of the system and simulates the controller, which adopts double closed loop PID controller based on current feedback and position feedback. The mechanical scanning device of swing scanning control system is realized by brushless dc motor and flexibility pivot, which can satisfy that swing times is more than  $4.5\text{E}+9$ . The angel signal detection of the system is realized by grating encoder with resolution of  $0.01^{\circ}$ . It takes subdividing of the resistance chain and direct physical to realize high resolution of  $0.0005^{\circ}$ . The control system takes digital controlling method based on FPGA to realize high precision.

The infrared swing scanning system has passed PID parameter's adjusting and testing to make the system's error be less than  $0.01^{\circ}$ . The method can work out the difficult problem that the system control in low speed of rotation?small angle and high precision?

#### 8896-38, Session PS

### Charge control of electrostatically actuated micromechanical infrared Fabry-Pérot filters

Sebastian Lehmann, Martin Ebermann, Norbert Neumann, InfraTec GmbH (Germany)

It is well known that many gases, fluids and solids yield material specific absorption spectra within the infrared range. Tunable MEMS Fabry-Pérot filters ( $\mu\text{FPF}$ ) can be applied in miniature sensors, which identify certain substances that are optically active in mid-wavelength infrared. Researchers focus not only on improving accuracy, sensitivity and robustness of such sensors but also on reducing chip area, costs and supply voltage of the  $\mu\text{FPF}$ .

We use bulk micro-machined  $\mu\text{FPF}$  with Bragg-reflectors deposited on thick carriers, one fixed and the other suspended by springs. It is actuated electrostatically to tune the reflector distance and hence the filter wavelength. Therefore, acceleration sensitivity to external forces and reduced tuning range due to stability problems are central issues when using these kinds of actuators.

Applying a constant voltage to the filter limits the maximum tuning range to one third of the initial electrode distance. Furthermore, the effective stiffness of the system decreases with increasing voltage,



causing displacement dependent acceleration sensitivity. Hence voltage controlled electrostatic actuators result in tough tradeoffs between initial electrode distance, spring stiffness, supply voltage and chip area.

In order to overcome the limitation of the tuning range and to relax these tradeoffs one can directly control the effective charge on the electrodes. By using switched capacitor amplifiers, we investigated the applicability of charge control circuits in combination with our  $\mu$ FPF. In contrast to typical electrostatic actuators the electrode area of our  $\mu$ FPF is arranged around a field-free optical area making it difficult to center the electrostatic force and to control rotary motions for large electrode displacements.

First experiments have shown that it is possible to obtain a stable relative displacement of 45% limited by reflector tipping. Measurements of the acceleration sensitivity also confirmed the expected displacement-independent behavior. Thus, it is possible to downsize the initial electrode distance by 25% and the spring stiffness by 50% in order to achieve the same optical tuning range and acceleration sensitivity as in voltage mode. Together, both can reduce the supply voltage to 50% or electrode area by 80%.

Increased electrode displacements of about 60% and a reduced supply voltage of about 33% can be achieved by further improvements of the spring design and electrode layout.

### 8896-39, Session PS

#### Ultra-narrow mid-infrared bandpass interference filters for use in stabilized external-cavity QCLs and imaging

Jan F. Kischkat, Mykhaylo P. Semtsiv, W. Ted Masselink, Humboldt-Univ. zu Berlin (Germany)

Ultra-narrow mid-infrared bandpass interference filters for use in stabilized external-cavity QCLs and imaging

We present progress on transmissive Bandpass Optical Interference Filters with freely designable central wavelengths in the 3-12 micrometer range based on single-cavity and coupled-cavity designs with passband widths of less than 0.2% of the central wavelength and over 60% peak transmission. Some filters can be tuned by tilting with respect to the incident beam and offer orders of magnitude larger angular dispersion than diffraction gratings.

The filters employ a first-order Fabry-Perot cavity with high finesse of approximately 400, made of Distributed Bragg Reflectors (DBRs) deposited on the front side of two-side polished silicon substrates. We compare the case where the back side of the substrate is coated with an anti-reflection coating with one where the back side is coated with a highly reflective coating. For a 4.4 micrometer filter, the former case produces a single, tunable transmission peak of less than 6  $\text{cm}^{-1}$  width, inside a wide stop band of 1900  $\text{cm}^{-1}$  width. In the latter case, the substrate itself forms an additional high-order Fabry-Perot cavity, whose transmission lines are superimposed on the transmission peak of the first-order Fabry-Perot cavity. This creates very narrow transmission peaks spaced by few reciprocal centimeters. When the modes of the two cavities coincide, they produce a dominant transmission with greatly reduced side-modes. This effect can produce transmission lines that are a fraction of a reciprocal centimeter wide at central wavelengths of thousands of reciprocal centimeters.

The material system in use is YF3-Ge on silicon. Yttrium Fluoride is a known low refractive index material with very low absorption in the infrared and is well suited to complement Germanium. The great challenge is due to its poor mechanical properties. Yttrium fluoride normally produces highly stressed layers that crack and flake off when deposited at the thicknesses necessary for mid-infrared applications, also, it does not adhere well to Germanium. Through careful optimization of the deposition parameters using electron beam evaporation, we are able to produce filters with the aforementioned optical properties that have good environmental and mechanical durability and pass the tests for adhesion and abrasion as stated in MIL-C-48497.

Use of such filters is highly desirable for Tunable External-Cavity Quantum-Cascade Lasers (ECQCLs) for the detection of trace gases. The usual setups using diffraction gratings to provide wavelength-dependent feedback into the QCL's active region are mechanically very unstable, since vibration around the tuning axis introduces

spectral fluctuations and very slight misalignment in the perpendicular plane immediately renders the laser non-functional because feedback is lost. ECQCLs using transmission filters to select the wavelength have two crucial advantages. One, a self-aligning "cat's-eye" type retroreflector can be employed for feedback eliminating the problem of lost feedback. Two, the large angular dispersions of interference filters inherently decrease the spectral fluctuations due to angular vibrations. This application gets discussed in more detail.

Other applications include mid-infrared imaging with extremely narrow spectral response. This includes long stand-off imaging and detection of explosives and other gases with sufficient spectral resolution to discriminate between isotopologues.

### 8896-40, Session PS

#### Trends in Infrared Imaging Detecting Technology

Jinxiang Fan, Shanghai Research Institute of mechanical and electrical engineering (China); Jianyu Yang, University of Electronics Science and Technology of China (China)

Infrared imaging detecting technology plays a significantly role in modern wars. In this paper, the current status of infrared imaging detecting technology is introduced briefly. The fundamental law of the development of infrared imaging detecting technology is summarized according to the changes of external causes and the internal causes. The developing trends and main characteristics of future infrared imaging detecting technology are deduced. Furthermore, technology directions that should be concerned are introduced according to the development of new concept and technologies for infrared imaging detecting.

### 8896-41, Session PS

#### Reliability-based structural design for infrared cryostat

Songlin Yu, Chunsheng Wang, North China Research Institute of Electro-Optics (China)

Cryostat is an essential package structure of the long linear IRFPA, which can provide hermetic vacuum environment, cold operating temperature, and interfaces of optics, electronics, and mechanics. To ensure reliability of the whole long linear IRFPA, cryostat is required to have high inherent reliability.

There is considerable uncertainty about design variables of cryostat structure such as external load, geometric feature, and material property, which tends to reduce the reliability level. The traditional design approach has adopted safety factors to minimize the effects of the uncertainties. However, the design results may turn out to be lack of quantitative reliability index and excessively conservative.

In this paper, a reliability-based structural design method is put forward to obtain a cryostat design with a quantitative reliability index. In this method, the reliability analysis is performed by integrating the finite element software ANSYS (functioning as the deterministic analyzer) with the probabilistic engineering analysis software NESSUS (functioning as the probabilistic calculator), in which design variables are treated as random parameters. The probability of failure and probabilistic sensitivity level of design variables are calculated, which would provide a quantitative judgment about whether there should be a redesign and which parameters should be modified in the redesign.

An example is illustrated in the paper. It is known that, under a given random vibration, there would be a displacement of the IR focal plane. The displacement is a key parameter of the IR detector assembly because large displacement is likely to impair the quality of thermal images. In this paper, the probability of the focal plane displacement exceeding a limited value is analyzed in order to improve the structural reliability level of cryostat.

A three-dimensional ANSYS finite element model of the cryostat is used to calculate the structural response under a given random vibration. The key model parameters, including the outer radius of the cold finger ( $D_o$ ), inner radius of the cold finger ( $D_i$ ), the length of the cold finger ( $L$ ), the modulus of elasticity ( $E_x$ ), and the poisson ratio ( $P_r$ ) of the titanium alloy, are parameterized in the ANSYS model. These parameters are also treated as random variables in NESSUS. The

random variables are directly mapped to the finite element model parameter.

The analysis result reveals that the probability of failure (focal plane displacement exceeding the limited value) in the original design is unacceptably high (18%), and thus, a redesign is necessary. Sensitivity analysis results indicate that the failure probability is highly sensitive to the standard deviation of the modulus of elasticity ( $E_x$ ). A single modification in this parameter is sufficient to reduce the probability of failure to an acceptably low level. The reliability of random vibration induced focal plane displacement would increase from 82% to 99.9999%. It is safe to draw a conclusion that the focal plane in redesigned cryostat is perfectly stable.

In summary, the reliability-based structural design method reveals more valuable information that would not have been available in traditional design method. It can simulate the uncertainties in design variables and quantitatively predict the structural reliability. In addition, it can provide

probabilistic sensitivity index to indicate which input parameters can influence reliability the most. The method can be widely applicable in the fields where uncertainty is assumed to have a significant impact on the structural response.

## 8896-42, Session PS

### Application of infrared uncooled cameras in surveillance systems

Rafal Dulski, Jaroslaw Barela, Piotr Trzaskawka, Tadeusz Piatkowski, Military Univ. of Technology (Poland)

The recent necessity to protect military bases, convoys and patrols gave serious impact to the development of multi-sensor security systems for perimeter protection. One of the most important devices used in such systems are IR cameras. IR camera plays an important role in multi-sensor security systems, because of their unique features and effectiveness, that cannot be matched by conventional daylight cameras. The detection efficiency of IR camera is caused mainly by its principle of operation. It detects thermal contrast, which is difficult to mask. As a result it is difficult to hide from thermal camera and, additionally, the passive operation mode of a camera does not reveal its presence. The thermal cameras are a very good and cost effective solution for protecting a perimeter. Although at present a thermal camera is more expensive than VIS camera, smaller number of such devices needs to be deployed to cover the same area. Furthermore, since thermal camera produces a clear image in the darkest of nights, no complimentary technologies like light or infrared illuminators need to be used. It is also known that thermal cameras generate fewer false alarms which is a common problem with VIS cameras with video motion detection or video content analysis software. Effective ranges of detection depend on the class of the sensor used and the observed scene itself. Application of IR camera increases the probability of intruder detection regardless of the time of day or weather conditions. It also increases the probability of intruder detection and simultaneously decreased the false alarm rate produced by the system. The paper discusses technical possibilities and limitations to use uncooled IR camera in a multi-sensor surveillance system for perimeter protection. The role of IR cameras in the system was discussed as well as technical possibilities to detect human being. Comparison of commercially available IR cameras, capable to achieve desired ranges was done. The required spatial resolution for detection, recognition and identification was calculated. The simulation of detection ranges was done using a new model for predicting target acquisition performance which uses the Targeting Task Performance (TTP) metric. Like its predecessor, the Johnson criteria, the new model bounds the range performance with image quality. The scope of presented analysis is limited to the estimation of detection, recognition and identification ranges for typical thermal cameras with uncooled microbolometer focal plane arrays. This type of cameras is most widely used in security systems because of competitive price to performance ratio. Detection, recognition and identification range calculations were made, and the appropriate results for the devices with selected technical specifications were compared. The results of analysis were finally discusses.

## 8896-43, Session PS

### A new method for discriminating the Moon interference based on CES software

Zhijun Tu, Zhiwu Mei, Jun Yuan, Loulou Deng, Beijing Institute of Control Engineering (China)

Abstract?Unusual measurement of the conical scanning infrared earth sensor device (CES) caused the abnormal attitude of the China-Brazil Earth Resource satellite (CBERS) 01 and 02 flying in orbit?Through the comparative analysis of the radiation intensity of the moon and the earth in 14 ~ 16.25 $\mu$ m wavelength range, we found when the moon and the sun light enter into the field of view (FOV) of the CES, the attitude of the spacecraft will be affected due to the wrong CES measurements?To solve this problem?we propose a new method based on the CES software without more hardware, which can identify the lunar interference and also the solar interference?Normally, the CES circuit outputs a front edge pulse (S/E P) when the CES FOV move from the sky into the earth, then after a while the circuit outputs a trailing edge pulse (E/S P) when the CES FOV move from the earth into the sky?The chord width, the angle between the S/E P and the E/S P are usually in the range of 30 $^\circ$  - 260 $^\circ$ ?Through analyzing the optical system and the circuit system, we found that the CES circuit just outputs one S/E P when moon light entering the CES FOV, but that caused by the sun are one S/E P and E/S P with the chord width less than 5 $^\circ$ ?Therefore, we set it as a criteria in the CES software to eliminate the lunar interference when multiple S/E P appears in one earth scanning cycle, and eliminate the solar interference by a small chord width like 8.5 $^\circ$ ?A series of ground experiments and simulations are designed to verify the effectiveness of this method, and the result exactly coincide with the telemetry data from the in orbit flight?At present, the software has been successfully applied to the satellites in low earth orbit such as CBERS 02B and 02C?

# Conference 8897A: Electro-Optical Remote Sensing VII

Wednesday - Thursday 25–26 September 2013

Part of Proceedings of SPIE Vol. 8897 Electro-Optical Remote Sensing, Photonic Technologies, and Applications VII; and Military Applications in Hyperspectral Imaging and High Spatial Resolution Sensing

8897-28, Session PS

## Polarization state imaging in long-wave infrared for object detection

Grzegorz Bieszczad, Sławomir Gogler, Michał Krupinski, Military Univ. of Technology (Poland)

In modern thermal imaging systems the the distribution of intensity of electromagnetic radiation with a wavelength range from 3  $\mu$ m to 5  $\mu$ m or 8  $\mu$ m to 12  $\mu$ m is registered and displayed in the form of the image. In the image the brightness or color corresponding to the intensity of radiation. Often the distribution of electromagnetic radiation in this range is converted to the temperature of the observed object by the fact that the dominant contribution to radiation other objects according to Planck's law. Currently used thermal imaging systems typically respond to only one physical quantity: radiance. There are more complex systems performing different measurements of radiance in narrow sub-bands of the radiation, and by means of Fourier analysis allows the detection of materials that have a known emissivity variation as a function of wavelength. Such systems are called multispectral or hyperspectral and are used for example for the detection of gases. However, in these systems, electromagnetic radiation is treated as a scalar field and hence the degree and the state of polarization of the radiation reaching is ignored. The electromagnetic radiation coming from the object, however, can also be characterized by a specific state of polarization. Analysis of radiation in terms of the manner and degree of polarization, and in particular the spatial distribution can provide a lot of additional information about the objects in the scene.

The article discusses the use of modern imaging polarimetry from the visible range of the spectrum to the far infrared. The paper presents the analyzes and examining the potential for imaging polarimetry in the far infrared for remote sensing applications. In article a description of measurement stand is presented for examination of polarization state in LWIR. Stand consists of: infrared detector array with electronic circuitry, polarizer plate and software realizing detection method. The article also describes first results of measurements in presented test bed. Based on these measurements, it was possible to calculate some of the Stokes parameters of radiation from the scene. The analysis of the measurement results show that the measurement of polarization state can be used to detect certain types of objects. Measuring the degree of polarization may allow for the detection of objects on an infrared image, which are not available by other techniques, and in other spectral ranges. Due to the method for measuring the state of polarization is required by the measurement of radiation intensity of the different configurations of the optical detector and the polarizing filter elements at least partially characterize the polarization state of the stage. Due to additional filtering elements in optical path of the camera, the NETD parameter of the camera with polarizer in proposed measurement stand was equal to about 240mK. In order to enhance the polarization characteristics of objects in the infrared image, a method of imaging measurement results imposing them on the thermal image. Imaging of measurement results of polarization of radiation is to add color and saturation of color to black and white thermal image where brightness corresponds to the intensity of infrared radiation.

8897-1, Session 1

## Future electro-optical sensors and processing in urban operations (*Invited Paper*)

Piet B. Schwering, TNO Defence, Security and Safety (Netherlands); Christina Grönwall, Swedish Defence Research Agency (Sweden)

In the ESUO study we pave the way for the European Defence Agency (EDA) group of Electro-Optics experts (IAP03) for a common understanding of the optimal distribution of processing functions between the different platforms. Combinations of local, distributed and centralised processing are proposed. In this way one can match processing functionality to the required power, and available data transfer, to obtain the right reaction times.

In the study three priority scenarios were defined. For these scenarios, present-day and future sensors and signal processing were studied. The priority scenarios were camp protection, patrol and house search.

A method for analyzing information quality in single and multi-sensor systems has been applied. A method for estimating reaction times for transmission of data through the chain of command has been proposed and used. These methods are documented and can be used to modify scenarios, or be applied to other scenarios.

Present day data processing is organized mainly locally. Very limited exchange of information is present to other platforms; mainly at high information level only. Main issues that arose from the analysis of present-day systems and methodology is the slow reaction time due to the limited field of view of present-day sensors and the lack of robust automated processing. Efficient handover schemes between wide and narrow field of view sensors may however reduce the delay times.

The main effort was in forecasting the signal processing of EO-sensors in the next ten years. Distributed processing is proposed between hand-held and vehicle based sensors. This can be accompanied by cloud processing on board several vehicles. Additionally, for sensor fusion between different platforms, and making full use of UAV imagery, distributed and centralised processing is essential. There is a central role for sensor fusion of non-heterogeneous sensors in future processing.

Automated detection requires robust detection and sufficient post processing so that the operator can be confident with results from the processing. Especially in urban environment, it will take efforts to reject urban clutter in a robust manner, and to be able to classify intent.

Operations will depend on local processing in many cases. Robust local processing can be limited under conditions where the amount of data and complexity of threat information is large. In those cases, distributed processing can be addressed in nearby vehicles, as in cloud processing, to support the operations, providing robustness, and also to provide backup processing. Local processing will form a graceful degradation of the distributed case.

While distributed processing is requested, imaging sensors require a high data rate transmission system. To keep fine details in the imagery, sufficient data rates are needed in order to be able to detect and recognise threats with automated processing.

For identification purposes, image enhancement tools providing sharper imagery are supported by research into motion de-blurring and turbulence compensation. Combination of various sources of information will improve quality of information in different scenarios.

The use of additional sensors also requires that a human machine interface will be sufficient in order to avoid operator overload. Although automated processing supports this point, additional sensors may give an additional load to the operator. The battle management system should support the operator to select the right sensors and processing for the task.

The changes that occur in the urban operations of the future due to the application of these new technologies will be the improved quality of information, with shorter reaction time, and with lower operator load.

8897-2, Session 1

## Experiments and models of active and thermal imaging under bad weather conditions

Erwan Bernard, Sagem SA (France) and ONERA (France); Nicolas Riviere, ONERA (France); Mathieu Renaudat, Sagem SA (France); Pierrick Guiset, Michel Pealat, Sagem (France); Emmanuel Zenou, Institut Supérieur de l'Aéronautique et de l'Espace (France)

Active imaging involves a high powered laser source to illuminate and image a small volume of a scene.

This gated viewing technique applies a pulsed laser and a fast gated camera. One of the key advantages of active imaging is the ability

to perform target recognition and to retrieve reflectances of objects. There are ongoing research programs to image a scene at several kilometres with high resolution. Thermal imaging involves cameras detecting radiation in the infrared range. It makes possible to see one's environment with or without visible illumination as emissivities may change as a function of temperature in materials. Thermal and active imagers are often used to enhance night vision. Both technologies are well experienced under clear meteorological conditions. Models including atmospheric effects such as turbulence predict accurately their performances. In this paper, we carry out experiments in a rain-tunnel under bad weather conditions (rain and haze). We point out their effects on controlled physical parameters (extinction, transmission, spatial resolution, thermal background, speckle, turbulence). Rain and haze impact the image quality and consequently the range of active and thermal systems. We also model these bad weather conditions and then compare with experimental data. Simulated images of the field results will be presented to validate our model including effects experimentally observed.

### 8897-3, Session 1

#### Surveillance in long-distance turbulence-degraded videos

Yitzhak Yitzhaky, Eli Chen, Oren Haik, Ben-Gurion Univ. of the Negev (Israel)

This paper presents an efficient algorithm that detects and tracks moving objects in long-distance video sequences degraded by atmospheric turbulence. Automatic detection and tracking of moving objects such as people and vehicles through relatively long horizontal distances (about two kilometers and above) is important but yet a very challenging task. The challenge in long-range imaging stems from the effects of atmospheric turbulence that cause time-varying image shifts and blur. The blur damages the shape and contrast of the real moving objects and thus may increase the miss detection (false negative) rate, while the shifts induce additional movements in the scene (spatio-temporal clutter), which may increase the false detection (false positive) rate. These effects become more and more significant as the imaging distance increases and as the sizes of the objects of interest in the image are smaller.

Numerous methods exist for detecting and/or tracking moving objects in both static and non-static environments, but only few dealt explicitly with background movements caused by atmospheric turbulence which may have unique characteristics. The paper presents in its first part an overview of previous approaches for detecting and tracking moving objects in both static and non-static environments including atmospheric turbulence.

The approach proposed in this paper is based on novel criteria for discriminating true from false detections. The proposed method we also leveraged elements from the moving target tracking algorithm of [G. Baldini, P. Campadelli D. Cozzi, and R. Lanzarotti, "A simple and robust method for moving target tracking," in Proc. of the IASTED International Conf. on Signal Processing, Pattern Recognition and Applications, 108-112, 2002] and adapted them to the special case of non-static background motion caused by turbulence. In particular, we perform background subtraction with an adaptive new thresholding procedure, based on each pixel's temporal (intensity) behavior. Next, we generate an activity based false-alarm masking, that represents, for each detected object, the likelihood that it belongs to a background movement caused by turbulence. Objects with higher probability of being turbulence movements should satisfy stiffer conditions in order not to be filtered during the next phase of object tracking. The criteria for distinguishing between true and false moving object detections take into account the temporal consistency of both shape and motion properties of the detected objects. We have experimented the proposed method with many challenging real video sequences taken at different atmospheric conditions, which included different levels of turbulence induced motion, atmospheric blur and noise. The videos also included a variety of moving objects. The proposed method was compared to two state of the art methods for detecting moving objects in long-distance turbulence-degraded videos ([O. Oreifej, X. Li, and M. Shah, "Simultaneous video stabilization and moving object detection in turbulence", IEEE Transactions on Pattern Analysis and Machine Intelligence, 35(2), 450-462, Feb. 2013] and [B. Fishbain, L. P. Yaroslavsky and I. A. Ideses, "Real-time stabilization of long range observation system turbulent video", J Real-Time Image Proc. 2, 11-22, 2007]). Better results, mainly lower false alarm rate and lower computational cost, were obtained compared to previous approaches.

### 8897-4, Session 1

#### Measurements and analysis of active and passive multispectral imaging

Christina Grönwall, Swedish Defence Research Agency (Sweden) and Linköping Univ. (Sweden); Ove K. Steinvall, Håkan Larsson, Swedish Defence Research Agency (Sweden); Dominique Hamoir, ONERA (France); Peter Lutzmann, Endre Repasi, Fraunhofer-Institut für Optronik, Systemtechnik und Bildauswertung (Germany); Laurent Hespel, Olivier Vaudelin, Michel Fracès, Bernard Tanguy, ONERA (France); Benjamin Göhler, Fraunhofer-Institut für Optronik, Systemtechnik und Bildauswertung (Germany)

This paper describes on-going work on active and passive imaging for target ID using different wavelength bands. We focus on data collection at NIR-SWIR wavelengths but we also include the thermal region. Active imaging in NIR-SWIR will support the passive imaging by eliminating shadows during day-time and allow night operation.

Among the applications that are most likely for active multispectral imaging, we focus on long range person identification. We also study the combination of active and passive sensing. A typical scene includes persons holding different objects and associated activities. We investigated laser imaging for target detection and classification up to 1 km assuming that another cueing sensor – passive EO and/or radar – is available for target acquisition and detection. Broadband or multi-spectral operation will reduce the effects of target speckle and atmospheric turbulence. Longer wavelengths will improve performance in low visibility conditions due to haze, clouds and fog.

We are currently performing indoor and outdoor tests to further investigate the target/background phenomena that are emphasized in these wavelengths. We also investigate how these effects can be used for target identification and image fusion. Performed field tests and the results of preliminary data analysis are reported.

### 8897-5, Session 2

#### Non-line of sight active imaging of scattered photons (*Invited Paper*)

Martin Laurenzis, Institut Franco-Allemand de Recherches de Saint-Louis (France); Andreas Velten, Univ. of Wisconsin-Madison (United States)

Active imaging is a prominent sensing technology for optical imaging in hash environments. Therefore, this technique can be applied for the vision through fog, smoke and other degraded environmental conditions as well as for the vision through sea water in submarine operation. Typically, a direct imaging of non-scattered photons (or ballistic photons) in the sense of geometrical optics is preferred to obtain a direct image of the scenario. With range gated viewing it is possible to reduce the impact of scattered photons on the imaging process by means of temporal filtering. This imaging of non-scattered photons is linked to a certain line of sight or field of view. Unfortunately, range and performance of ballistic photon imaging is limited by attenuation or the free optical path length i.e. the length in which a photon can propagate without interaction with scattering particles or object surfaces.

Alternatively, the imaging and analysis of scattered photons can overcome these classical limitations and it is possible to realize a non line of sight imaging. The spatial and temporal distribution of scattered photons can be analyzed by means of computational optics and their information of the scenario can be restored. In the case of Lambertian scattering sources (e.g. particle in sea water) the scattered photons carry information of the complete environment. In contrast to medical imaging scattering media like sea water or fog are more homogeneous and less scattering than tissue. Especially the information outside the line of sight or outside the visibility range is of high interest. Thus, imaging in a wide synthetic field of view and in wider range is possible as well as non line of sight vision (e.g. vision around a corner or vision behind objects).

In this presentation we will discuss some approaches for non line of sight active imaging with different indirect and direct illumination concepts with scattered photons like point and surface scattering sources as needed for imaging around the corner and volume

scattering sources such as on fog and under water. Further we will present approaches for the analysis of data from scattered photon imaging and their application in different fields (vision around a corner, vision behind objects or vision through fog).

## 8897-6, Session 2

### Lidar/DIAL detection of bomb factories

Luca Fiorani, Adriana Puiu, Olga Rosa, Antonio Palucci, ENEA (Italy)

Terrorist bombings of last years led to an increased demand for the development of new technologies able to prevent such events. Prevention means rapid identification of illegal bomb factories, employed to produce improvised explosive devices (IEDs), often based on triacetone triperoxide (TATP). TATP (C<sub>9</sub>H<sub>18</sub>O<sub>6</sub>) is a powerful explosive, easy to make using commonly available chemicals such as acetone (C<sub>3</sub>H<sub>6</sub>O) and hydrogen peroxide (H<sub>2</sub>O<sub>2</sub>). Being not difficult to synthesize, TATP is often the explosive of choice for terrorists. TATP is one of the most dangerous explosives known, being extremely sensitive to impact, temperature change and friction. Just a few hundred grams of the material produce hundreds of liters of gas in a fraction of a second. Thus, the development of sensing systems able to identify illegal factories where IED are produced turns out of critical importance for security of people and territory.

Nowadays, IED detection is possible thanks to the emerging remote sensing technologies based on recently developed laser sources. In particular, the stand-off detection of acetone is feasible, thanks to the identification of its vapor outside the building where TATP is prepared.

The FP7 project BONAS (BOmb factory detection by Networks of Advanced Sensors) aims to develop an innovative sensor wireless network, in order to increase citizen protection from terrorist attacks and especially from IED threats. In the frame of BONAS, a stand-off detector of IED precursors is under development. It is based on the lidar/DIAL (differential absorption lidar) measurement of precursor vapors that will escape the building where IEDs are made. In this paper we report, for the first time to our knowledge, on lidar/DIAL detection of acetone by means of an optical parametric oscillator (OPO) laser system. We used the "IR Opolette HE 3034" model by Oportek that has the benefit of being a portable compact laser source, tunable in the range 3 – 3.45  $\mu\text{m}$ , where both TATP and its precursor acetone have quite strong absorption peaks.

At first, a spectroscopic study has been carried out: the IR (infrared) spectrum of acetone in the gas phase has been procured from available databases and checked with cell measurements. Then, the feasibility of a lidar/DIAL for the detection of acetone vapors has been shown in laboratory, simulating the experimental conditions of a field campaign. The results of this test indicate that the measured signal coincide with the calculated one within about 10%, paving the way for the application of the lidar/DIAL system to the remote sensing of acetone and TATP vapors. Eventually, having in mind measurements in a real scenario, an interferent study has been performed, looking for all known compounds that share with acetone IR absorption in the spectral band selected for its detection. Possible interfering species were investigated, simulating both urban and industrial atmospheres, and limits of acetone detection in both such environments were identified. This study confirmed that a lidar/DIAL can detect low concentration of acetone at considerable distances.

## 8897-7, Session 2

### Range accuracy of a gated-viewing system as a function of the gate shift step size

Benjamin Göhler, Peter Lutzmann, Fraunhofer-Institut für Optronik, Systemtechnik und Bildauswertung (Germany)

Primarily, a Gated-Viewing system provides range gated imagery. By increasing the camera delay time from frame to frame, a so-called sliding gates sequence is obtained by which 3-D reconstruction is possible. An important parameter of a sliding gates sequence is the step size by which the gate is shifted. In order to reduce the total number of required images, this step size should be as large as possible without significantly degrading the range accuracy.

In this paper we have studied the influence of the gate shift step size on the resulting range accuracy. Therefore, we have combined

the Intevac Gated-Viewing detector M506 with a pulsed 1.57  $\mu\text{m}$  laser source. The maximal laser pulse energy was 65 mJ. The target was a one-square-meter-plate at a distance of 500 m. The plate was laminated with a Spectralon layer having Lambertian reflection behavior with a homogeneous reflectance of 93%. It was orientated diagonally to the line of sight of the sensor in order to provide a depth scenario. We have considered different combinations of the two parameters "gate length" (13.5 m, 23.25 m, 33 m) and "signal-to-noise ratio" (SNR) (1 dB, 2 dB, ..., 9 dB). For each considered set of parameters, a sliding gates sequence of the target was recorded. Per range, 20 frames were collected. The gate shift step size was set to the minimal possible value, 75 cm. By skipping certain ranges, a sliding gates sequence with a larger gate shift step size is obtained. For example, skipping the ranges 2, 3, 5, 6, 8, 9, ... (equivalent: taking the ranges 1, 4, 7, ...) results in a gate shift step size of 2.25 m. Finally, the range accuracies were derived as a function of the gate shift step size. Additionally, the influence of the number of averaged images per range was studied.

## 8897-8, Session 2

### Investigation of synthetic aperture lidar for land surveillance applications

Simon Turbide, Linda Marchese, Marc Terroux, Alain Bergeron, INO (Canada)

Long range surveillance of land is a critical need in numerous military and civilian security applications, such as threat detection, terrain mapping and disaster prevention. A key technology for land surveillance has been synthetic aperture radar (SAR) that for over 50 years continues to provide high resolution radar images in all weather conditions from remote distances. In more recent years, Interferometric SAR (InSAR) and Differential Interferometric SAR (D-InSAR) have become powerful tools adding high resolution elevation and change detection measurements. State of the art SAR systems based on dual-use satellites are capable of providing ground resolutions of one meter; while their airborne counterparts obtain resolutions of 10 cm. D-InSAR products based on these systems can produce cm-scale vertical resolution image products.

Certain land surveillance applications such as land subsidence monitoring, landslide hazard prediction and tactical target tracking could benefit from improved resolution, both in the ground plane and vertical direction. The ultimate limitation to the achievable resolution of any imaging system is its wavelength. SAR systems typically operate in the wavelength range of about 30 cm to 3 cm. Thus, the state-of-the-art systems are approaching the limits of SAR theoretical potential. The natural extension to improve resolution is to thus decrease the wavelength, i.e. design a synthetic aperture system in a different wavelength regime. One such system offering the potential for vastly improved resolutions in three dimensions is Synthetic Aperture Ladar (SAL). This system operates at infrared wavelengths, from about 1.5  $\mu\text{m}$  to 9  $\mu\text{m}$  which is about ten thousand times smaller than for SAR.

This paper discusses an initial investigation into a concept for an airborne SAL specifically aiming at land surveillance. The system would operate at 1.55  $\mu\text{m}$  and would integrate an optronic processor on-board to allow for immediate transmission of the high resolution images to the end-user on the ground. Estimates of the size and weight, as well as the resolution and processing time are given. Lastly, results from laboratory set-ups of scaled-down target detection and land subsidence scenarios are presented.

## 8897-10, Session 3

### Image processing in aerial surveillance and reconnaissance: from pixels to understanding (*Invited Paper*)

Judith Dijk, Adam W. van Eekeren, Olga Rajadell Rojas, Gertjan J. Burghouts, Klamer Schutte, TNO Defence, Security and Safety (Netherlands)

Surveillance and reconnaissance tasks are currently often performed using an airborne platform such as a UAV. The airborne platform can carry sensors such as EO/IR camera's which can be used to view a certain area from above.

To support the task from the sensor analyst, different image

processing techniques can be applied on the data, both in real-time or for forensic applications. These algorithms aim at improving the data acquired to be able to detect objects or events and make an interpretation of those detections. There is a wide range of techniques that tackle each of these three challenges and we group them in classes according to the goal they pursue (enhancement, detection, interpretation). An overview of these different techniques and different concepts of operations for these techniques are presented in this paper.

The first class of techniques is image enhancement, where an improved image or series of images is produced based on the raw imagery. Typical image enhancement techniques are contrast enhancement, super-resolution reconstruction and stabilization. The camera images can also be used to make a 2D mosaic or a 3D model of the scene. The challenge for airborne here is to determine and correct for the camera movement, which has many degrees of freedom and may have high frequency movements as well.

A second type of techniques is object detection, tracking and classification. This must provide answers such as "there is a moving object in the scene, this object is moving from point A to point B and it is a person". This gives the operator an idea what kind of actors are present in the scene. For airborne systems the challenge is to have techniques which are able to perform on small objects as well.

The third type of techniques also classifies actions of these actors, thereby not only answering the question who/what is present in the scene but also what these actors are doing. Typical actions that can be distinguished are "two persons meeting" and "one person following another".

For airborne systems the challenge is, as for the object detection class, that there should be enough pixels on the target to observe the action.

This means that subtle actions may not be observed.

All these data can be used for event detection and providing situational awareness. Here all detections and actions are used to see a certain event, and to assess what is going on. Also the detection of pattern-of-life patterns and anomalies to this patterns can be determined. The challenge for airborne systems is that the time they observe a certain area is limited, but should be long enough to make these assessments.

In this paper examples are provided for these algorithms and possible concepts of operations, both for real-time task as for forensic applications.

### 8897-11, Session 3

## Segmentation and wake removal of seafaring vessels in optical satellite images

Henri Bouma, Rob J. Dekker, Robin M. Schoemaker, Ali A. Mohamoud, TNO Defence, Security and Safety (Netherlands)

Maritime situation awareness is of vital importance in monitoring and control of for instance irregular migration, piracy, traffic safety, and fisheries. Monitoring systems that an operator generally has command over are divided in cooperative (e.g. transponder systems such as AIS, VMS and LRIT) and non-cooperative systems (e.g. satellite and airborne observation systems). Cooperative systems are not required for small and non-fishing vessels, can be spoofed, erroneous, or just switched off. In that case an operator falls back on non-cooperative systems, and the vessel length is an important parameter for an operator to classify a vessel. Vessel length is also an important parameter in automatic recognition systems.

This paper focusses on the segmentation of seafaring vessels in optical satellite images, which allows more accurate length estimation. The system consists of robust foreground-background separation, wake detection and ship-wake separation, simultaneous position and profile clustering and a special module for small vessel segmentation. We compared our system with a baseline implementation on 54 vessels that were observed with GeoEye-1. The results show that the relative L1 error in the length estimates is reduced by 88%.

### 8897-12, Session 3

## Geometric calibration of thermal cameras

Philip Engström, Joakim Rydell, Håkan Larsson, Swedish Defence Research Agency (Sweden)

There exist several tools and methods for camera resectioning, i.e. geometric calibration for the purpose of estimating intrinsic and extrinsic parameters. The intrinsic parameters represent the internal properties of the camera such as focal length, principal point and distortion coefficients. The extrinsic parameters relate the cameras position to the world, i.e. how is the camera positioned and oriented in the scene. With both sets of parameters known it is possible to relate a pixel in one camera to the world or to another camera. This is important in many applications, for example in stereo vision.

The existing methods work well for standard visual cameras in most situations. Intrinsic parameters are usually estimated by imaging a well-defined pattern from different angles and distances. Checkerboard patterns are the most widely used. The intersections between the black and white squares form high contrast points that can be positioned very accurately. Knowing the precise dimension and structure of the pattern enables calculation of the intrinsic parameters. Extrinsic calibration can be performed in a similar manner if the exact position and orientation of the pattern is known. A common method is to distribute markers in the scene and to measure their exact locations. The key to good calibration is well-defined points and accurate measurements.

Thermal cameras are a subset of infrared cameras that work with long wavelengths, usually between 8 and 14 microns. At these wavelengths all objects above absolute zero temperature emit radiation making, it ideal for passive imaging in complete darkness. Therefore, thermal cameras are widely used in military applications. The issue that arises when trying to perform a geometric calibration of a thermal camera is that a typical calibration checkerboard for cameras in the visual spectrum emits more or less the same amount of radiation in the black squares as in the white. In other words, the calibration board that is optimal for calibration of visual cameras might be completely useless for thermal cameras.

A calibration board for the thermal range should ideally be a checkerboard with high contrast in thermal infrared. It is of course possible to use other sorts of objects or patterns but since most tools and software expect a checkerboard pattern this is by far the most straightforward solution. Depending on the application it should also be more or less portable and work both in indoor and outdoor scenarios.

In this paper we present several years of experience with calibration of thermal cameras in various scenarios. Checkerboards with high contrast both for indoor and outdoor scenarios are presented as well as different markers suitable for extrinsic calibration.

### 8897-13, Session 3

## Multispectral and hyperspectral advanced characterization of soldier's camouflage equipment

Mariusz Kastek, Tadeusz Piatkowski, Rafal Dulski, Piotr Trzaskawka, Military Univ. of Technology (Poland); Philippe Lagueux, Martin Chamberland, Vincent Farley, Telops (Canada)

The requirements for soldier camouflage in the context of modern warfare are becoming more complex and challenging given the emergence of novel infrared sensors. There is a pressing need for the development of adapted fabrics and soldier camouflage devices to provide efficient camouflage in both the visible and infrared spectral ranges. The Military University of Technology has conducted an intensive project to develop new materials and fabrics to further improve the camouflage efficiency of soldiers. The developed materials shall feature visible and infrared properties that make these unique and adapted to various military context needs. This paper presents the details of an advanced measurement campaign of those unique materials where the correlation between multispectral and hyperspectral infrared measurements is performed.

Field tests (in a close-to-real environment) were carried out at MUT facility, where different ground coverage can be found (grass, gravel, and sand). The tests involved thermal imaging, carried out in 0.2-2.5

$\mu\text{m}$ , 3-5  $\mu\text{m}$  and 7.5-11.5  $\mu\text{m}$  spectral bands (performed with high performance thermal cameras) and hyperspectral measurements in 1.5-5.5  $\mu\text{m}$  and 7.5-11.5  $\mu\text{m}$  spectral bands performed with imaging Fourier transform spectrometers (IFTS). The analysis of signatures recorded during the tests will be presented. The analysis of results from multispectral and hyperspectral registration will also be shown. Analysis of the recorded data consisting of background temperature distributions for different seasons and weather conditions resulted in determining the measures of camouflage effectiveness.

8897-14, Session 3

## Characterization of aircraft and flares used in the infrared scene simulation system

Azwitamisi E. Mudau, Johannes J. Calitz, Cornelius Willers, Alta de Waal, Council for Scientific and Industrial Research (South Africa)

Infrared (IR) scene simulation systems such as the Optronic Scene Simulator (OSSIM), SHIPS, DIRSIG and DISC are widely used for the development and evaluation of aerospace products and their applications. The Optronic Scene Simulator is used in the development of optronic systems, missile and countermeasure systems, mission preparation, signature prediction, flight test preparations, aircraft vulnerability analysis and real time synthesis of infrared and visible scenes. Two of the key tasks in preparing such simulations are signature measurement and model construction; typically of aircraft, infrared countermeasure (IRCM) systems and missiles models. These models are required and used in a variety of simulation tasks within the IR scene simulation system. The primary objective of the modelling process is to capture the geometric and radiometric properties of the physical object and its behaviours under dynamic conditions. Researchers at the Optronic Sensor Systems (OSS) Competency Area at the Council for Scientific and Industrial Research (CSIR) unit for Defence, Peace, Safety and Security (DPSS) use calibrated IR thermal imagers as well as a Fourier transform infrared (FTIR) spectroradiometer to obtain the essential information required to build accurate model used in the IR scene simulation systems.

In this paper we review the procedures followed from the planning to the point where the results are ready for the construction of the model and implementation in the simulation system as well as the challenges encountered when capturing the data to construct aircraft model and flare models. This paper will first address the IR thermal imagers and FTIR spectroradiometer and the factors that influence the results obtained with these instruments. The second part focuses on the data required (spatial fuselage temperature and plume radiance) to construct an aircraft model and validation of the measured fuselage temperature using aerodynamic heating. The spatial fuselage temperatures presented are measured in the LWIR spectral band and the plume radiance measured in the MWIR spectral band. The paper closes with a summary of a countermeasure flare measurement and modelling process.

8897-15, Session 4

## Image structural analysis in the tasks of automatic navigation of unmanned vehicles and inspection of Earth surface

Vadim R. Lutsiv, Igor Malyshev, S.I. Vavilov State Optical Institute (Russian Federation)

The problems of automatic analysis and matching of images of terrain are urgent for several decades, the analysis of aerospace photographs is especially important. On the one hand, such analysis is a base of solving the tasks of automatic navigation of unmanned vehicles (the ground vehicles among them). On the other hand, the amount of information formed and transferred to the Earth by modern video-sensors increases every year, thus a preliminary classification of such data by onboard computer becomes urgent. Especially, it concerns the huge amounts of hyper-spectral data. The information of interest should be automatically chosen for closer specifying and transmitting through communication channel for detailed analysis by human experts at the earth-based control centers.

The automatic matching of images of real scenes is a difficult task,

and it can be especially complicated for aerospace photographs. The changes in aspect angles of observation, the day-time and season changes of terrain, the results of human activity (including the military activity), the natural and technogeneous catastrophes, the differing properties of video-sensors applied, – this is a short list of factors influencing the automatic analysis and matching of aerospace pictures.

We developed an object-independent approach to structural matching of images. While choosing the alphabet of structural elements and creating the methods of image structural description based on such elements, we did our best to abstract away from the partial peculiarities of scenes to be analyzed. Only the most general limitations were taken into account that were derived from the laws of organization of observable environment and from the properties of video-sensors and image formation systems most often applied.

Practical application of this theoretic approach enables reliable matching the aerospace photographs acquired from differing aspect angles, in different day-time and seasons by sensors of differing types – the optical pictures taken in visible and IR ranges and images formed by radars with synthesized aperture. The airspace photographs can be matched even with the geographic maps of raster and vector formats. The partial or full-scale application of developed approach enabled efficient solving of difficult tasks of automatic navigation of unmanned flying vehicles and ground-based mobile robots. The signs of changes and catastrophes also could be automatically detected by means of matching and comparison of aerospace photographs acquired at different time.

In the paper, we present the theoretical proofs of synthesis of alphabet of object-independent structural elements, a substantiation of chosen strategy of hierarchical structural description and matching of images is also presented. Several examples of successful structural matching of acquired images with template pictures and maps of terrain are finally shown within the frameworks of navigation of different kinds of unmanned vehicles or detection of signs of disasters.

8897-16, Session 4

## A signal-processing system of digital pixel binning based on bi-cubic filtering algorithm

Bin Bao, Ning Lei, Beijing Institute of Space Mechanics and Electricity (China); Nina Peng, Institute of spacecraft system engineering CAST (China); Zhixue Han, Beijing Institute of Space Mechanics and Electric (China)

As the development of semiconductor technology, the manufacture process of CCD sensors has been improved continuously. In recent years some new technologies appear on CCD sensors. Analog pixel Binning technology is one of them. In this paper, a new signal-processing system of digital pixel binning based on bi-cubic filtering algorithm is designed. The system overcomes the shortcomings of losing some image details, caused by analog pixel binning which does simply summation of pixel signals. The signal-processing system of digital pixel binning can keep high frequency information through bi-cubic filtering algorithm, which can improve the contrast and MTF of the remote sensing images. This system can achieve pixel binning with lower computational complexity and also it has the good real-time capability for large-scale remote sensing images.

8897-17, Session 4

## Optic flow aided navigation and 3D scene reconstruction

Malcolm P. Rollason, QinetiQ Ltd. (United Kingdom)

An important enabler for low cost airborne systems is the ability to exploit low cost inertial instruments. An Inertial Navigation System (INS) can provide a navigation solution, when the Global Position System signal is denied, by integrating measurements from inertial sensors. However, the gyrometer and accelerometer biases of low cost inertial sensors cause compound errors in the integrated navigation solution.

In this paper we describe our experiments to establish whether fusion of measurements from an on-board video camera, with measurements

from the inertial sensors, can aid the inertial navigation.

We sought to establish whether optic flow can provide a useful aid to navigation when the 3D structure within the observed scene is unknown. We also investigated whether the INS output can be used to help infer 3D scene content from video.

Experiments with both real and synthetic data have been designed to answer the questions posed. We collected real data, using an AR Parrot "Drone 2" – a low cost system costing a few hundred pounds.

To support the empirical results, and to quantify the potential benefit of optic flow to navigation performance, a Monte Carlo assessment was conducted using simulated data for a simulated trajectory. The simulated trajectory is of approximately 1 minute in duration and covers 16 km, with an apogee of ~2 km.

A navigation estimator was developed to fuse the measurements from the inertial sensors with measurements of optic flow. The estimator is common to the experiments with both real and synthetic data, and provides corrections to the INS. It estimates the error in the INS calculated position, velocity, and platform attitude, as well as the biases in the inertial instruments, hence comprising a total of 15 states.

Empirical results compare the navigation performance achieved with, and without, the use of optic flow measurements to aid the INS. With optic flow aiding, the INS computed trajectory is consistent with the true camera motion. Without optic flow aiding of the INS, a rapidly increasing position error results (the data represents ~40 seconds, after which the INS is ~50 metres in error and has passed through the ground).

This empirical result illustrates that optic flow provides a useful aid to navigation, even when the 3D structure of the observed scene is not available to the estimator.

We carried out Monte Carlo simulations to quantify the benefit to navigation that could be expected from optic flow. The SiIMU02@ Inertial Measurement Unit (IMU) was assumed, and the performance of unaided navigation also quantified. Position errors, which grow as a quadratic function of time when unaided, are substantially checked by the availability of good optic flow. (The noise level of optic flow was commensurate with 5 cameras, each with 15 degree Field Of View).

The QinetiQ scheme for Structure From Motion (SFM) infers both camera motion and 3D scene content from video imagery. We provided the (optic flow aided) INS derived camera motion, as an additional input, to the SFM scheme. The resulting estimate of the 3D scene content represents an improvement over the counterpart result obtained without information from an INS.

## 8897-18, Session 4

### Robust motion filtering as an enabler to video stabilization for a tele-operated mobile robot

Romain Chereau, Toby P. Breckon, Cranfield Univ. (United Kingdom)

An increasing number of inspection and hazardous environment tasks use mobile robotic vehicles manually tele-operated from a live video feed from an on-board camera. Resulting video imagery frequently suffers from vibration effects compromising the accuracy and security of operation and the viable duration for human tele-operation. Physical camera stabilization is often a trade-off between platform weight, portability and cost.

Here we aim to automatically remove these visual vibration effects using a novel real-time video stabilization approach. Prior work for hand-held and vehicle mounted cameras are ill-suited to the high-frequency, large magnitude (10-15% of image size) vibration encountered on the short wheelbase, non-suspension robotic platforms typically deployed in such tasks.

Without prior knowledge of the robot ego-motion (or platform vibration characteristics) we develop a novel approach to identify the both Local Motion Vectors (LMV) and the Global Motion Vector (GMV) in successive video frames whilst preserving the required real-time responsiveness of the video for tele-operation. A multi-scale image pyramid approach initially identifies edge feature information in successive images as a method of rapid image simplification. Traditional blocks-matching then determines a set of a set of LMV over which a novel extended set of down-selection filters are applied to arrive at a final integral sub-set from which a GMV can be robustly

determined. This is achieved in real-time over poor-quality transmitted video from an example platform.

Experimental results over a range of tele-operation scenarios show that the method provides both significant qualitative visual improvement and a quantitative reduction in measurable video image displacement (due to vibration).

## 8897-19, Session 4

### An automatic geo-spatial object recognition algorithm for high resolution satellite images

Mustafa Ergül, Aydın A. Alatan, Middle East Technical Univ. (Turkey)

The recent developments in satellite technology cause the formation of the huge amount of data in electronic formats, which cannot be interpreted effortlessly by a human analyst. Therefore, a remarkable number of algorithms have been proposed for automatically recognizing geo-spatial objects from satellite images. Although a majority of these approaches generally run fast and have performances with high recall rates, they also have several drawbacks. The first one is that they produce results with innumerable false positives during their detection process, since these approaches do not have enough discriminative capabilities between target and non-target classes. Another disadvantage is due to the sliding window mechanism utilized during detection process that only states whether there exists an object in the current window. Hence, such algorithms cannot return exact location information for the detected objects. Furthermore, the same target can be identified multiple times due to the overlapping sliding windows and such multiple detections might cause dramatic decline in the precision rate. Therefore, a novel geo-spatial object recognition method combining a local feature based method and a shape based method is proposed to minimize the aforementioned imperfections. There are two main steps in the improved approach: a hypothesis generation step and a verification step. In the hypothesis generation step, a set of hypothesis for possible object locations is generated after aiming low-missed detections and high false-positives. For this purpose, a version of Bag of Visual Words (BoVW) object detection algorithm is employed and the most discriminative visual word locations are considered as hypothesis points representing the existence of objects. During the verification step, the feasible foreground is first extracted via semi-supervised GrabCut foreground extraction algorithm, after utilizing these hypothesis points, as if they are user inputs. Next, the extracted binary object masks are described by means of the integrated version of two shape description techniques, Angular Radial Transform (ART) and Fourier Descriptors. Afterwards, SVM classifier is utilized to identify the target objects. Based on experimental results, the proposed algorithm achieves both high precision and high recall rates by taking advantage of two types of object detection approaches. Moreover, after the object mask is extracted from the image, the target position can be precisely obtained with together the object mask itself which can be used for determination of the target properties such as size, orientation, model and type etc. Extensive experimental results verify that the proposed algorithm has promising results in terms of accuracy during identification of geo-spatial objects, such as airplanes and ships.

## 8897-20, Session 5

### Real-time imaging DUSPEN lidar for helicopter situational awareness in DVE (Invited Paper)

James T. Murray, Jason Seely, Jeffrey J. Plath, Gregory J. Fetzer, William L. Ryder, Neil R. Van Lieu, Ron Goodwin, Eric Gottfredson, Tyler J. Wagner, Nick Kridler, John R. Engel, Ken Panici, Anthony Mitchell, Arete Associates (United States)

One of the major technical challenges of military rotary wing aviation is the ability to effectively and safely operate in brownout, whiteout, sea-spray, fog, and rainy conditions. Landing or maneuvering in a Degraded Vision Environments (DVE) is a common problem for pilots. Blinding plumes of dust, snow, sea-spray, fog, and rain can envelop helicopters as they land or take-off, increasing the likelihood that pilots



will lose their bearings and drift into unseen obstacles, including other rotary wing aircraft in multi-ship operations. These conditions can escalate into crashing descents, lateral drift rollovers, and collisions with ground features or obstacles.

Imaging laser radar (ladar or lidar) is a particularly promising DVE sensor technology because it can provide wide field-of-regard, high-resolution, 3-dimensional real-time imagery of the region surrounding a helicopter in severe DVE conditions. Areté Associates has developed and flight tested next-generation real-time dust-penetrating (DUSPEN) lidar system under Office of Naval Research, Future Naval Capability program Helicopter Low-Level Operations (HELO) Product 2.

Areté's DUSPEN system captures full lidar waveforms and uses sophisticated real-time detection and filtering algorithms to discriminate hard target returns from dust and other obscurants. Down-stream 3D image processing methods are used to enhance visualization of threat objects (e.g. wires, cables, poles, posts, foliage, obstacles, etc.) and ground features (e.g. ditches, berms, rocks, boulders, sloping terrain, etc.). Areté is maturing the DUSPEN packaging under separate DoD funding for integration into an existing FLIR turret.

This paper will show results from recent flight tests at Yuma Proving Grounds from a CH-53 platform.

## 8897-21, Session 5

### Image change detection using a SWIR active imaging system

Armin L. Schneider, Institut Franco-Allemand de Recherches de Saint-Louis (Germany); Martin Laurenzis, David Monnin, Frank Christnacher, Institut Franco-Allemand de Recherches de Saint-Louis (France)

Improvised explosive devices (IED) are a major menace worldwide. From January 2004 until December 2009, Afghanistan suffered from more than 7500 attacks by means of IEDs. At least 11600 people have been wounded (4700 civilians); more than 5400 people have been killed (2100 civilians). Unfortunately, the construction of an IED is quite easy: the required materials are easily available (e.g. fertilizer, but also unexploded ordnance devices like mines or artillery shells). In addition, an IED can be disguised as a harmless object like a backpack, hidden in a car – it can even be a suicide bomber. It is therefore impossible to apply automatic target recognition algorithms for their detection. We are currently developing a low-cost system which consists of a GPS receiver, a three-axis magnetic compass as well as a video camera. The system doesn't detect explosives at all but rather indicates any changes occurring along a frequently used itinerary to an observer. This is done by comparing actual images with images from the same scene, which have been acquired during a previous measurement.

The luminosity of images from two different passages is usually different (due to different meteorological conditions). Whereas the global luminosity can be adjusted using non-linear luminosity correction, the treatment of shadows is more difficult.

Since meteorological conditions cannot be controlled, we are investigating the possibility of using an active imaging system in the SWIR domain to illuminate the scene. Using appropriate filters for the camera, we are completely independent of natural illumination and in addition, the system can also be used at night.

## 8897-23, Session 5

### Questions about using of atmospheric attenuation calculating the nominal ocular hazard distance

Ove K. S. Gustafsson, Swedish Defence Research Agency (Sweden)

The Maximum Permissible Exposure, MPE, define the irradiance level, for instance from a laser or other strong light source, which an eye safely might be exposed for. The distance where risk for injuries or damage of a unprotected eye or eyes behind some kind of telescope or binoculars, when laser irradiance level exceeded the MPE, is the Nominal Ocular Hazard Distance (NOHD) or the Extended Nominal Ocular Hazard Distance (ENOHd).

The Laser safety requirements can be set, as an example, for a common Nd:YAG laser with defined repetition rate, pulse width and wavelength out of the requirements on; i/ max energy per pulse, ii/ minimal divergence, where the intensity has fallen to the  $1/e$ - value in far field of the laser beam, iii/ minimum aperture of the laser output (the laser beam width is defined by  $1/e$  value).

The common way calculating the NOHD abandons the use of atmospheric attenuation as a lowering the irradiance level. The NOHD for a typical Nd:YAG laser with small divergence can be several tens of kilometers. One way handling those risk distances, which might be too long for ordinary firing ranges or embargoed areas, are probabilistic calculations of danger. But at the same time for such long laser beam path the atmospheric transmission will be more than insignificant. The suppression of the risk distance can be substantial even for moderate extinctions coefficient. Simple simulations shows that the NOHD might be reduced by than 60% -70% at a visibility of 50 km.

The question is what kind of extinction coefficient model should one accept or use with those calculations. The contribution discuss the question about the limiting the NOHD out of atmospheric attenuation and the choice of extinction coefficient versus visibility.

## 8897-24, Session 5

### On-the-fly adaptable spatial resolution real-time imaging lidar system

Jordi Riu Gras, Santiago Royo Royo, Univ. Politècnica de Catalunya (Spain)

The proposed work deals with the design and construction of a new type of lidar device capable of measuring adaptable spatial resolution 3D images through an on-the-fly configuration approach. The patented scanning system enables to dynamically change the image resolution depending on external information provided by other sensors like grey scale or hyper spectral 2D images.

Advanced security and defence applications like object detection, tracking and identification require a concrete balance between image acquisition time and spatial resolution especially when the target is in movement. Sometimes this balance could be significantly different according to the target shape, movement speed, distance or behaviour. In scanning systems, the image frame rate is inversely proportional to the number of measured points due to the sequential measuring process. We propose a lidar imaging system that can modify the scanning conditions from one image to the next according to the target nature and state. For slow moving objects a higher level of detail can be obtained by setting a high image spatial resolution (up to the hundreds of Kpx). And vice versa, fast frame rates (up to 40Hz) can be configured when the object moves fast at expense of image point density. In addition, for distant objects a higher spatial resolution can be configured to minimize the loss of detail and inversely when the objects are closer. The detection range is maintained high up to several hundreds of meters and the field-of-view can be adapted to application needs.

A highly versatile 3D imaging lidar system is presented offering unknown and outstanding performance for advanced applications like object detection, tracking and identification through a real-time adaptable scanning system for each situation and target behaviour.

## 8897-25, Session 6

### Investigation of LTR analysis for detection of multiple concealed objects

Simon J. Hutchinson, Michael J. Fernando, David A. Andrews, Nicholas J. Bowring, Stuart Harmer, Manchester Metropolitan Univ. (United Kingdom)

This paper investigates the use of Late Time Response (LTR) analysis for identifying the presence of multiple targets in Concealed Object Detection. When a conductive object is illuminated by an Ultra-Wide band (UWB) frequency signal, the surface currents developed across the object give rise to LTR signals which are re-radiated to the transceiver. The results for the LTR signal from targets including a 6.5 cm needle, a kitchen knife, a replica revolver and composite targets such as two 6.5 cm needles and a kitchen knife with a replica revolver are presented. The distance between the objects that make up the composite targets is increased in increments of 5 cm to determine the

point at which the two objects can be discerned from one another. The single needle, kitchen knife and replica revolver objects are included for comparison with the composite targets made up of multiple objects.

The frequency range used in this experiment is 300 MHz to 18 GHz, double ridged horn antennas in a pseudo-monostatic arrangement are used as transmitter and receiver for the experimental set up. The distance between the antennas and the target object was 60 cm for all experiments performed. The experiments were performed with the targets suspended in isolation in a non-anechoic lab environment requiring that background signals be accounted for in processing.

The Fast Fourier Transform (FFT) and the Continuous Wavelet Transform (CWT) are used to process the return signals and extract the LTR from the background clutter. A Generalised Pencil-of-Function (GPOF) is then used to determine the poles of the signal. All data was processed in matLAB which was used to de-convolve the signal and remove the background clutter.

Results are presented which demonstrate the ability to determine the presence of multiple objects within the radar beam using the poles of the targets and their reliance on physical separation from each other.

### 8897-26, Session 6

#### High-power multi-beam diode laser transmitter for a flash imaging lidar

Christer Holmlund, Petteri Aitta, Sini Kivi, VTT Technical Research Ctr. of Finland (Finland); Risto Mitikka, VTT Elektronikka (Finland); Lauri Tyni, Veli Heikkinen, VTT Technical Research Ctr. of Finland (Finland)

The future medium-term robotic and long-term human space exploration missions need new guidance, navigation and control (GNC) technologies to fulfil the requirements. The light detection and ranging (LIDAR) technology is considered as one key enabling technology for mission phases involving assistance for the descent and soft-landing of exploration spacecraft, rover autonomous planetary navigation, and in-orbit docking/rendezvous between the orbiting spacecraft and canisters transporting samples collected on celestial objects. This paper presents the design, realisation and testing of the multi-beam laser transmitter to be used in a 256x256 pixel flash imaging lidar. Depending on the target distance, the lidar has three operation modes: ranging (RAN), slopes imaging (SLI), and hazard imaging (HZI). In the long-range RAN mode the transmitted optical power is concentrated in the central beam whose divergence is set to the minimum to achieve reliable single-point distance measurements. In the medium-range the SLI mode is used to get slope measurements, which helps in the selection of suitable landing area. Here the optical power is split into 5 beams pointing at different angles. In the short-range the system operates in the HZI mode where the central optical beam is widened up to 12 degrees and cloud of distance points is generated by the sensor to discriminate objects with a resolution of few centimetres. The transmitter can be configured for different object distances by modifying the number of beams and their divergence, efficiently using the limited optical power available, still fulfilling the functionalities needed by the GNC system. This paper describes the transmitter part of the flash imaging lidar with focus on the electronics and especially the laser diode drivers. The transmitter contains eight fibre coupled commercial diode laser modules with a total peak optical power of 40 W at 808 nm. The modules contain the laser diode, a monitoring photodiode, a thermo-electric cooler, and a thermistor. The modules, designed for CW and low-frequency operation, made challenging demands on the driver design. The main requirement for the laser diode drivers was linear modulation up to a frequency of 20 MHz allowing, for example, low distortion chirps. Measurement results are presented on frequency response, eye diagrams for pseudo-random binary sequences, and time skew between the eight outputs.

### 8897-29, Session 6

#### Digital colour management system for colour parameters reconstruction

Karol Grudzinski, Piotr Lasmanowicz, Military Institute of Engineer Technology (Poland); Agnieszka Pawlicka, University of São Paulo, São Carlos Institute of Chemistry (IQSC) (Brazil); Adam Januszko, Military Institute of Engineer Technology (Poland)

The paper is dedicated to a digital colour rendering method which would allow for transformation of a real image into a set of colour pixels displayed on a computer monitor. The Digital Colour Management System (DCMS) can analyse pixels' colour which comprise images of the environment (such as desert, semi-desert, jungle, farmland or rocky mountains) in order to prepare a camouflage pattern most suited for the terrain (an adaptive camouflage).

Based on digital photography, the innovative technology of the XX century, the method for color parameters reconstruction has been developed. Using the digital system for color management (DSCM) the color parameters and camouflage pattern is now being synthesized. All today's known camouflage application are using passive, non-changeable patterns and colors. However, an idea to exchange passive camouflage pattern into active – real time color changing – pixels, in the same way as in the nature e.g. chameleon or octopus, is to use electrochromic materials. The field of electrochromism is rapidly expanding both in terms of the range of electrochromic systems that has been reported and the novel of commercial applications that are being proposed.

There are several inorganic and organic materials possessing colors which can be useful for military and other camouflage purpose e.g. cobalt oxide (green - brown), manganese oxide (yellow - brown), N-ethyl carbazole (green), polyaniline PANI (yellow, green, blue, black). Tailoring the color of electrochromic materials remains a particularly active research area.

We propose to use the subtractive colors mixing method to construct the real time color changing electrochromic window/pixel for camouflage purpose.

# Conference 8897B: Military Applications in Hyperspectral Imaging and High Spatial Resolution Sensing

Tuesday 24–24 September 2013

Part of Proceedings of SPIE Vol. 8897 Electro-Optical Remote Sensing, Photonic Technologies, and Applications VII; and Military Applications in Hyperspectral Imaging and High Spatial Resolution Sensing

8897-30, Session 7

## Snapshot imaging Mueller Matrix instrument

Michael W. Kudenov, Michael J. Escuti, North Carolina State Univ. (United States); Eustace L. Dereniak, Nathan Hagan, College of Optical Sciences, The Univ. of Arizona (United States); Kazuhiko Oka, Hokkaido Univ. (Japan)

A novel way to measure the Mueller matrix image enables a sample's diattenuation, retardance, and depolarization to be measured within a single camera integration period. Since the Mueller matrix components are modulated onto coincident carrier frequencies, the described technique provides unique solutions to image registration problems for moving objects. In this paper, a snapshot imaging Mueller matrix polarimeter is theoretically described, and preliminary results shows it to be a viable approach for use in surface characterization of moving objects.

8897-31, Session 7

## Efficient implementations of hyperspectral chemical-detection algorithms

Cory J. C. Brett, Northeastern Univ. (United States); Robert S. DiPietro, Dimitris G. Manolakis, MIT Lincoln Lab. (United States); Vinay K. Ingle, Northeastern Univ. (United States)

Many military and civilian applications depend on the ability to remotely sense chemical clouds using hyperspectral imagers, from detecting small but lethal concentrations of chemical warfare agents to mapping plumes in the aftermath of Hurricane Katrina. Real-time operation is critical in these applications but becomes more and more difficult to achieve as the number of chemicals we search for increases. In this paper, we present efficient implementations of matched-filter based algorithms so that real-time operation can be maintained with higher chemical-signature counts. We start by describing the computational complexity of the various components of the algorithms, both from a simple flop-count perspective and from a more realistic time-to-completion perspective. We focus on CPU implementations, and we show that memory-hierarchy based optimizations are crucial to fast processing. We provide both naïve and optimized C implementations, along with naïve and optimized performance comparisons for each component of the algorithms, including background-mean estimation, background-mean subtraction, and background-covariance estimation. Overall, order-of-magnitude speed-ups are realized even when flop counts remain fixed. Finally, we discuss some of the pros and cons of moving to a highly-parallel GPU architecture, and we conclude with open problems that may lead to significant advances in real-time hyperspectral processing.

8897-32, Session 7

## Combined airborne sensors in urban environment

Alwin Dimmeler, Hendrik Schilling, Fraunhofer-Institut für Optronik, Systemtechnik und Bildauswertung (Germany); Michal Shimoni, Royal Belgian Military Academy (Belgium); Dimitri Bulatov, Wolfgang Middelmann, Fraunhofer-Institut für Optronik, Systemtechnik und Bildauswertung (Germany)

Military operations in urban areas became more relevant in the past decades. Detailed situation awareness in these complex environments is crucial for successful operations. Within the EDA (European Defence Agency) project on "Detection in Urban scenario using Combined Airborne imaging Sensors" (DUCAS) an extensive data set of hyperspectral and high spatial resolution data as well as three

dimensional (3D) laser data was generated in a common field trial in the year 2011 in the city of Zeebrugge, Belgium.

In the frame of DUCAS, methods were developed at two levels of processing. In the first, single sensor data were used for land cover mapping and the detection of targets of interest (i.e. personnel, vehicles and objects). In the second level, data fusion was applied at pixel level as well as information level to investigate the benefits of combining sensor systems in an operational context.

Providing data for mission planning and mapping is an important task for aerial reconnaissance and it includes the creation or the update of high quality 2D and 3D maps. In DUCAS, we used (semi-) automatic methods and a wide range of sensor data (hyperspectral, LiDAR, high resolution orthophotos and video data) to create highly detailed land cover maps as well as urban terrain models. Combining the diverse information gained by different sensors increases the information content and the quality of the extracted information.

In this paper we will present advanced methods for the creation of 2D/3D maps, show results and the benefit of fusing multi-sensor data.

8897-33, Session 7

## Concept and integration of an on-line quasi-operational airborne hyperspectral remote sensing system

Hendrik Schilling, Andreas Lenz, Fraunhofer-Institut für Optronik, Systemtechnik und Bildauswertung (Germany); Dominik Perpeet, Sebastian Wuttke, Wolfgang Gross, Fraunhofer IOSB (Germany); Wolfgang Middelmann, Fraunhofer-Institut für Optronik, Systemtechnik und Bildauswertung (Germany)

Modern mission characteristics require the use of advanced imaging sensors in reconnaissance. In particular, high spatial and high spectral resolution imaging provides promising data for many tasks such as classification and object recognition of military relevance, such as camouflaged units or IEDs. Especially in asymmetric warfare with highly mobile forces, ISR needs to be available close to real-time. This demands the use of UASs in combination with downlink capability.

This contribution describes an integrated system, designed for the real-time acquisition and analysis of hyperspectral data. German space and aerial technology company OHB System AG provides the flight platform with the data downlink, a Stemme Condor S10, which is a remotely controllable MALE motor glider with a payload of two 60 kg wing-pods. One wing-pod contains technology for broadband radio transmission (Aerial Reconnaissance Data System) to a ground control station. The multi-sensor system is integrated in the second pod. The main component is a Specim AISA Eagle II hyperspectral sensor, covering the VNIR spectral range with a spectral resolution up to 1.2 nm and 1024 pixel across track, leading to a ground sampling distance below 1 m on a typical flying height. The pushbroom characteristic of the hyperspectral sensor demands an inertial navigation system for rectification and georeferencing of the image data. Additional sensors are a high resolution RGB frame camera and a thermal imaging camera.

A rugged and embedded high-performance data acquisition computer provides the required interfaces like a camera link frame grabber card. It simultaneously collects and saves all imaging and navigation data. For on-line application, the data is preselected, compressed and transferred to the downlink-pod as well as completely stored for post processing purposes.

The ground control station consists of the downlink antenna pedestal, together with a mobile data processing system and storage servers. The hyperspectral data is transferred in chunks containing 1 s of data acquisition. Each chunk runs through an on-line radiometric and geocorrection routine, including a direct georeferencing procedure under consideration of synchronized navigation data and IMU misalignment information (boresight), which is calibrated pre-mission. Final result is a hyperspectral orthorectified GeoTIFF, which is filed in the ERDAS APOLLO geographical information system. APOLLO

allows remote access to the data and web-based analysis tools.

A screening-operator monitors the incoming RGB image data and reports possible points of interest, which could be investigated using the hyperspectral data. The data analysis consists of spectral matching, anomaly detection and image classification. Further analysis towards fusion of heterogeneous sensor data, such as airborne LIDAR, is to be considered.

The scope of this paper is the implementation of the real-time hyperspectral processing chain as well as the assembly of the integrated multi-sensor platform.

8897-35, Session 7

## Effects of radiometric accuracy and extended spectral range on hyperspectral imaging applications

Florent M. Prel, Louis Moreau, Nicolas Ho, Robert Bouchard, Christian A. Vallieres, Claude B. Roy, ABB Analytical Measurement (Canada)

Hyperspectral Infrared signature measurements are performed in both military and civilian domains. Military applications include aircrafts and ships stealth characterization, detection/lock-on ranges, flares efficiency characterization, and Chemical Warfare Agents detection and identification. The same technologies are also used for environment monitoring, Toxic Industrial Chemicals detection, and for material chemical characterization and monitoring.

The MR-i is a versatile dual-band Hyperspectral Imaging Spectroradiometer designed for defense, security and environment monitoring. It is configurable and easily adaptable to a specific application.

Its controlled internal temperature, embedded calibration blackbodies and advanced radiometric calibration algorithms combined with the advantage of imagery high fill factor makes the MR-i radiometric measurements very accurate. A radiometric model of the instrument showing the spectral radiometric accuracy as a function of target and calibration temperatures under several measurement scenarios will be presented in this paper as well as external contributors affecting the radiometric accuracy.

The MR-i four ports architecture enables users to populate the instrument with two sensors at the same time. Different sensors combinations are available and depend on measurement scenarios. In this paper, results from the MWIR and LWIR 256 x 256 pixels operating from 14 – 8  $\mu\text{m}$  and 5.5 – 1.5  $\mu\text{m}$  spectral range will be presented. A demonstration of gases measurements application with the extended range MR-i LWIR camera will demonstrate the additional chemical species detection capability when compared to a classical 8 – 12  $\mu\text{m}$  camera.

8897-36, Session 7

## Real time intelligent image dissemination using hyperspectral information

Gary J. Bishop, Ainsley Killey, BAE Systems (United Kingdom)

No Abstract Available

# Conference 8898A: Technologies for Optical Countermeasures X

Wednesday - Thursday 25-26 September 2013

Part of Proceedings of SPIE Vol. 8898 Technologies for Optical Countermeasures X; and High-Power Lasers 2013: Technology and Systems

8898-1, Session 1

## Quantum cascade lasers and their advanced capabilities for defense and security (*Keynote Presentation*)

Timothy O. Day, Daylight Solutions Inc. (United States)

Quantum cascade laser (QCL) systems are mature and at the vanguard of a new generation of products that support military applications such as Infrared Countermeasures (IRCM) and targeting. The demanding product requirements for aircraft platforms that include reduced size, weight, power consumption and cost (SWaP-C) extends to portable, battery powered handheld products. QCL technology operates throughout the mid-wave (MWIR) and long-wave (LWIR) infrared to provide new capabilities that leverage existing thermal imaging cameras. In addition to their suitability for aircraft platforms, QCL products are a natural fit to meet operator demands for small, lightweight pointer and beacon capabilities. Field-testing of high power, lightweight, battery operated devices has demonstrated their utility across a range of air and ground applications. This talk will present an overview of QCL technology and the Defense and Security products and capabilities that are enabled by it. This talk will also provide an overview of the extensive environmental and performance testing associated with products based on QCL technology.

8898-2, Session 1

## Thulium fiber lasers: increasing 2 micron power for defense and industry (*Invited Paper*)

Eric Park, Q-Peak (United States)

Thulium fiber lasers with emission around 2 microns (1.94-2.05 micron) have been maturing rapidly. Componentry necessary for laser system architectures has been under development as well allowing all fiber implementations with output powers in excess of 500 Watts CW and record reported values in excess of 1kW. Designs for 5 kW have been developed and modeling shows common fiber laser difficulties such as SBS don't arise until power levels reach ~80kW. Practical thermal limitations based on the silica host fiber for the Thulium ion dopant may well be the functional constraint. Q-Peak has been involved in this development holding the published output power record at 1050 W CW. This paper will report on our ongoing development efforts toward defense and commercial applications of Thulium fiber lasers including modeling, pumps, architectures, SBS measurements, and components for specific applications.

8898-3, Session 1

## Fiber laser-based, mid-IR and novel wavelength lasers (*Keynote Presentation*)

Robert Afzal, Angus J. Henderson, Lockheed Martin Aculight (United States)

Fiber lasers have demonstrated performance at very high power and beam quality and can serve as ideal sources for nonlinear optics. Either operating with at fixed wavelengths or combined with nonlinear optics, fiber laser based systems have demonstrated the full span of the optical spectrum from Mid-IR to the visible.

8898-4, Session 2

## Design issues and physics for high-performance quantum-cascade lasers (*Invited Paper*)

W. Ted Masselink, Mykhaylo P. Semtsiv, Mikaela Elagin, Yuri V.

Flores, Grygorii Monastyrskiy, Sergii Kurlov, Jan F. Kischkat, Humboldt-Univ. zu Berlin (Germany)

Quantum-cascade lasers (QCLs), first conceived of 40 years ago [1] and first demonstrated almost 20 years ago [2], are lasers whose optical transitions are between different subbands of the conduction band of a semiconductor heterostructure. Because the laser transition takes place between different spatially quantized subbands of the conduction band, the emission wavelength is determined by the structure and is not by the band gap of the materials used. Today QCLs emit with a wide range of wavelengths, from 2.6 to 250  $\mu\text{m}$  (1.2 THz) [3,4] and have found application in a number of areas including gas sensing for security, environmental and medical uses, as well as for communication and defense-related IR countermeasures. Power of several watts with very good optical mode quality has been realized and corresponding efficiency approaching 30% at room temperature [5].

Driving these advances and successes is an increasing understanding of the critical design issues and physics of the QCL. An important recent advance is the use of mixed-height barriers to engineer the interface scattering of the different levels involved in the lasing process [6]. This design strategy appears to be universally applicable, across the entire range of QCL emission wavelengths. By using low barriers where the upper laser state has its maximum probability and high barriers where the lower laser state has its maximal probability in strain-compensated designs for short wavelength emission, the lifetime of the upper laser state can be increased, while decreasing the lifetime of the lower laser state. First realizations of this design result in  $J_{th}=1.7 \text{ kA/cm}^2$  at 300 K, slope efficiency  $\eta = 1.4 \text{ W/A}$ ,  $T_0 = 175 \text{ K}$ , and  $T_1 = 550 \text{ K}$ . Further increases in efficiency can be achieved through designs in which parasitic states near the upper laser level are separated from it, either energetically or oscillator strength. These states may be associated with other  $k$  values, or with higher-lying subbands [7].

[1] R. F. Kazarinov and R. A. Suris, *Fiz. Tekh. Poluprovodn.* 5, 797 (1971) [*Sov. Phys. Semicond.* 5, 707 (1971)].

[2] J. Faist, F. Capasso, D. L. Sivco, C. Sirtori, A. L. Hutchinson, and A. Y. Cho, *Science* 264, 553 (1994).

[3] O. Cathabard, R. Teissier, J. Devenson, J. C. Moreno, and A. N. Baranov, *Appl. Phys. Lett.* 96, 141110 (2010).

[4] C. Walther, M. Fischer, G. Scalari, R. Terazzi, N. Hoyler, and J. Faist, *Appl. Phys. Lett.* 91, 131122 (2007).

[5] Y. Bai, S. Slivken, S. Kugoya, S. R. Darvish, and M. Razeghi, *Nat. Photonics* 4, 99 (2010).

[6] M. P. Semtsiv, Y. Flores, M. Chashnikova, G. Monastyrskiy, and W. T. Masselink, *Appl. Phys. Lett.* 100, 163502 (2012).

[7] Y. V. Flores, M. P. Semtsiv, M. Elagin, G. Monastyrskiy, S. Kurlov, A. Aleksandrova, J. Kischkat, and W. T. Masselink, *J. Appl. Physics* (to be published).

8898-5, Session 2

## Advances in quantum cascade laser technology to meet the needs of defense applications (*Invited Paper*)

C. Kumar N. Patel, Pranalytica, Inc. (United States)

Quantum cascade lasers operating in the mid wave infrared (MWIR) and long wave infrared (LWIR) spectral regions are the only directly electrically pumped semiconductor lasers available that produce multiwatt continuous wave (CW) power output at room temperature (RT). These spectral regions are important because of the two low atmospheric transmission loss windows, the first atmospheric window from  $\sim 3.5 \mu\text{m}$  to  $\sim 5.0 \mu\text{m}$  and the second atmospheric window from  $\sim 8.0 \mu\text{m}$  to  $12 \mu\text{m}$ . High power laser sources in these two windows are of great importance for a variety of defense applications including infrared countermeasures, IFF beacons, target illuminators and designators and local as well as standoff detection of explosives and chemical warfare agents. There are equally important civilian and commercial applications of QCLs, which are beginning to materialize,

but which will not be discussed here.

Over the past three years, performance of MWIR and LWIR QCLs has continued to improve. These advances fall into three categories:

**Improvement in QCL structure designs:** With the invention of the nonresonant extraction design principle for the QCL structures, it is now possible to obtain multiwatt CW/RT power with double digit wallplug efficiency at all wavelengths from about 3.8  $\mu\text{m}$  to about 10  $\mu\text{m}$ . In particular, we are able to obtain, from fully packaged single emitter QCLs in a hermetically sealed butterfly packages with beam collimating optics, >4 W CW/RT power at ~4.6  $\mu\text{m}$ , >2.5 W CW/RT power at ~4.0  $\mu\text{m}$ , and > 2 W CW/RT power at ~9.5  $\mu\text{m}$ , all with excellent beam quality.

**Improvement in thermal management:** A part of the performance improvement has come from the invention of higher thermal conductivity submount material that still provides perfect coefficient of thermal expansion match to InP.

**Improvement in QCL packaging:** The high wallplug efficiency of MWIR and LWIR QCLs also make them ideal for handheld, battery operated applications. With QCLs operating in quasi-CW (high duty cycle pulsed operation) mode, which do not require TEC's for QCL operation, advances in QCL packaging have resulted in ultra miniature fully packaged QCLs, which weigh less than 50 g and deliver >3 W of average power output at ~4.6  $\mu\text{m}$  and > 2.0 W average power at ~9.5  $\mu\text{m}$ , from a package volume <10 cm<sup>3</sup>. These packaged QCLs are extremely rugged and meet the MIL-STD vibration, shock and thermal requirements.

I will discuss the above performance advances and applications and provide insight into what future holds for even higher performance QCLs, both at single emitter level as well as at system level with various beam combining techniques.

### 8898-6, Session 2

#### **Progress in efficiency-optimized high power diode lasers (*Invited Paper*)**

Agnieszka Pietrzak, Ralf Hülsewede, Martin Zorn, Olaf Hirsekorn, JENOPTIK Diode Lab GmbH (Germany); Jens Meusel, JENOPTIK Optical Systems GmbH (Germany); Petra Hennig, JENOPTIK Laser GmbH (Germany); Jürgen Sebastian, JENOPTIK Diode Lab GmbH (Germany); Paul Crump, Hans Wenzel, Steffen Knigge, Andre Maassdorf, Frank Bugge, Götz Erbert, Ferdinand-Braun-Institut (Germany)

High-power diode lasers are used as highly efficient sources of optical energy for many industrial and defense applications, either directly or as pump sources for solid state or fiber lasers. The diode lasers are fabricated in single emitter or bar format, and packaged as needed for the specific application. Advances in diode laser design and device technology enable the performance to be continuously improved, with results that were previously only as lab demonstrators now available commercially. Specifically, in recent years both the reliable optical output power and conversion efficiency at the operation point of diode lasers have been substantially increased. Simultaneously, the far field emission angle has been reduced, enabling low loss, alignment tolerant coupling into an optical system, and maximum "on target" power density. First, an overview is presented of recent progress at Jenoptik in the development of commercial diode lasers optimized for peak performance, robust high-yield manufacture and long lifetimes. These diode lasers are tailored to simultaneously operate with reduced vertical carrier leakage, low thermal and electrical resistance and low optical losses. In this way, the highest electro-optical efficiencies are sustained to high currents. For example, 940 nm bars with high fill factor are shown to deliver continuous wave (CW) output powers of 280 W with conversion efficiency of > 60%. These bars have a vertical far field angle with 95% power content of just 40°. In addition, 955 nm single emitters with 90  $\mu\text{m}$  stripe width deliver 12 W CW output with a power conversion efficiency at the operating point of 69%. In parallel, complementary research and development at the Ferdinand-Braun-Institut is working to enable the next generation of high power diode lasers, by determining the key limitations to performance and by pioneering new technologies to address these limits. An overview of recent studies at the FBH will therefore also be presented, illustrating some of the remaining performance challenges, and reviewing progress in novel device designs. Examples will include structures with further reduced far field angles, higher lateral beam quality and increased peak power. Prospects for further performance improvement will be discussed.

### 8898-7, Session 3

#### **Mid-IR (1-5 $\mu\text{m}$ ) supercontinuum generation in ultra-low loss, dispersion-zero shifted tellurite glass fiber (*Invited Paper*)**

Rajesh Thapa, NP Photonics Inc (United States); Dan L. Rhonehouse, Dan Trung Nguyen, Jie Zong, Arturo Chavez-Pirson, NP Photonics, Inc. (United States)

Mid-infrared sources are a key enabling technology for various applications such as remote chemical sensing, defense communications and countermeasures, and bio-photonic diagnostics and therapeutics. Conventional mid-IR sources include optical parametric amplifiers, quantum cascade lasers, synchrotron and free electron lasers. An all-fiber approach to generate a high power, single mode beam with extremely wide (1  $\mu\text{m}$ -5  $\mu\text{m}$ ) and simultaneous wavelength coverage has significant advantages in terms of reliability (no moving parts or alignment), room temperature operation, size, weight, and power efficiency. Here, we report single mode, high power extended wavelength coverage (1  $\mu\text{m}$  to 5  $\mu\text{m}$ ) supercontinuum generation using a tellurite-based dispersion managed nonlinear fiber and an all-fiber based short pulse (20 ps), single mode pump source. We have developed this mid IR supercontinuum source based on highly purified solid-core tellurite glass fibers that are waveguide engineered for dispersion-zero matching with Tm-doped pulsed fiber laser pumps. The conversion efficiency from 1917nm pump to mid IR (2  $\mu\text{m}$ -5  $\mu\text{m}$ ) supercontinuum is greater than 30%, and approaching 60% for the full spectrum. We have achieved > 1.2W covering from 1  $\mu\text{m}$  to 5  $\mu\text{m}$  with 2W of pump. In particular, the wavelength region above 4  $\mu\text{m}$  has been difficult to cover with supercontinuum sources based on ZBLAN or chalcogenide fibers. In contrast to that, our nonlinear tellurite fibers have a wider transparency window free of unwanted absorption, and are highly suited for extending the long wavelength emission above 4  $\mu\text{m}$ . We achieve spectral power density at 4.1  $\mu\text{m}$  already exceeding 0.2mW/nm and with potential for higher by scaling of pump power.

### 8898-8, Session 3

#### **Compact high-power/high-energy 2 $\mu\text{m}$ and mid-infrared laser sources for OCM (*Invited Paper*)**

Christelle Kieleck, Anne Hildenbrand, Martin Schellhorn, Georg Stoepler, Marc Eichhorn, Institut Franco-Allemand de Recherches de Saint-Louis (France)

The paper describes two laser prototypes devoted to the jamming or the damaging of heat-seeking missiles for use in field-trials.

The semi-ruggedized compact jamming prototype is based either on an OP-GaAs or a ZnGeP2 OPO directly pumped by a 2.09  $\mu\text{m}$  Q-switched Ho<sup>3+</sup>:YAG laser pump source. The 2.09  $\mu\text{m}$  Ho<sup>3+</sup>:YAG beam can directly be modulated for jamming. It can also pump the OPO to generate beams in the 3  $\mu\text{m}$  - 5  $\mu\text{m}$  range which can also be modulated separately.

Up to 20 W of average power are achievable around 2.1  $\mu\text{m}$  and the repetition rate varied from 20 kHz to 100 kHz. For example at 66 kHz, the pulse duration was around 54 ns at the maximum output power. The M<sup>2</sup> was estimated to be less than 1.2.

In band II, up to 3.5 W of averaged power were obtained. Repetition rate in band II varied also from 20 to 100 kHz. For example at 66 kHz, the pulse duration was around 36 ns at the maximum output power. For 3.5 W of averaged output power, the M<sup>2</sup> of the signal beam was estimated to be less than 1.4 and less than 1.2 for the idler beam.

For destruction, a Ho:LLF MOPA laser system with is used to pump a ZGP OPO. The maximum pulse energy of the Ho:LLF MOPA pump system was 82 mJ at a repetition rate of 100 Hz. To prevent damage on the ZGP crystal during pumping the OPO, the pump system was limited to 50 mJ at a pulse width of 30 ns. The pump beam quality was measured to M<sup>2</sup><sub>x</sub> = 1.01 and M<sup>2</sup><sub>y</sub> = 1.03 at a wavelength of 2053 nm

The threshold of the OPO was measured to 7 mJ and it was pumped up to 6.5x above threshold without role-over. At an incident pump energy of 45.6 mJ a maximum output energy of 13.4 mJ and 10 mJ was observed at signal and idler wavelengths, respectively, with slope efficiencies for the signal and idler of 39 % and 28 %. The total 3-5  $\mu\text{m}$  energy was 23.4 mJ, corresponding to an optical-to-optical

conversion efficiency of 51 %. The  $M^2$  of the signal was  $M^2_x = 1.81$  and  $M^2_y = 1.98$ . The  $M^2$  values of the corresponding idler beam were  $M^2_x = 1.91$  and  $M^2_y = 1.94$ .

ISL is also currently working on new laser sources and non linear conversion setups that will allow proposing new versions that should be more compact, more efficient and more integrable.

### 8898-10, Session 3

#### **Average power and pulse energy scaling of 1.6 $\mu\text{m}$ resonantly-diode-pumped erbium lasers**

Lukasz Galecki, Marc Eichhorn, Institut Franco-Allemand de Recherches de Saint-Louis (France); Waldemar Zendzian, Military Univ. of Technology (Poland)

The paper is devoted to a pulsed erbium lasers operating in the eye-safe spectral band around 1.6  $\mu\text{m}$  at the repetition rate of minimum 100 Hz. Even though resonant pumping shifts a significant part of thermal load from gain medium to pumping diodes, at such repetition rate thermally-induced effects become significant. It is noticeable especially in case of lasers which are based on a low-diameter, TIR (total-internal-reflection) end-pumped laser rods of 'fiber-like' geometry. Gain media of this kind are somehow flexible and additionally exhibit uniquely strong thermal-lensing, which renders mounting, uniform cooling and cavity designing challenging tasks. In the paper it will be shown that by using simple means like e.g. utilization of undoped end caps and overall system optimization (including proper control of pumping diodes) it is possible to reduce significantly undesired, thermo-induced effects in gain medium. The results of thermal lens simulations for the composite rods of different diameters (1.2 mm, 1.5 mm, 2.0 mm) will be presented in case of pumping conditions reflecting the experimental ones. It will be discussed what is maximum, acceptable diameter of the cavity mode inside these rods in order to obtain diffraction-limited beam quality and which cavity design assures proper thermal lens compensation and the mentioned optimum mode size. As a summary we will present setups and output characteristics of Q-switched Er<sup>3+</sup>:YAG lasers based on rods of diameter 1.2 mm and 2.0 mm capable to deliver pulse energy of, respectively, 12 mJ and 24 mJ with diffraction limited beam quality.

### 8898-11, Session 4

#### **Advancing the applications of chalcogenide glass for infrared power transmission (Invited Paper)**

Daniel W. Hewak, Chris Craig, Khouler Khan, Edwin Weatherby, Paul Bastcock, Univ. of Southampton (United Kingdom)

Both passive and active infrared transmitting materials have played an important role in aerospace and defence applications for decades. While there are often a range of materials that provide the properties needed for an individual application, there is no panacea amongst IR materials. The suitable semiconductors, crystals, hot press ceramics or CVD sulphides and selenides that are available have their problems. They can be extremely hygroscopic, toxic, expensive, fragile and increasingly difficult to source.

Chalcogenide glasses provide a powerful material base for mid-IR photonic and electro-optical applications especially optical fibre. While high quality fiber drawn from alloys containing a variety of chalcogen elements have been realized, their delicate nature, complicated fabrication methodology and expense has restricted widespread application and commercial acceptance. In this paper we describe our current work on the fabrication and application of chalcogenide fiber and our vision for their practical implementation in the future.

At the University of Southampton's Optoelectronic Research Centre, chalcogenide materials in the form of optical fibres, bulk glass components, thin films, microsphere and most recently as plasmonic and metamaterials, have been studied since 1991. We describe our work with gallium and germanium sulphide based glasses and describe our efforts to achieve improved low loss IR fibre for the 3-10 micron transmission window.

### 8898-12, Session 4

#### **Maximizing the bandwidth while minimizing the spectral fluctuations using supercontinuum generation in photonic crystal chalcogenide fibers (Invited Paper)**

Curtis R. Menyuk, R. Joseph Weiblen, Univ. of Maryland, Baltimore County (United States); Jonathan Hu, Baylor Univ. (United States); Ishwar D. Aggarwal, Sotera Defense Solutions, Inc. (United States); Brandon Shaw, Jasbinder S. Sanghera, U.S. Naval Research Lab. (United States)

Supercontinuum generation in the mid-infrared (mid-IR) spectrum has a broad array of potential applications in medicine, environmental sensing, and defense. Mid-IR sources play a crucial role in defending aircraft against missile attacks. It is desirable to have a source that acts like a mid-IR "light bulb" to produce a broadband, flat, and incoherent spectrum. In work to date, we have demonstrated that it is possible to obtain a bandwidth of 4 microns in As<sub>2</sub>Se<sub>3</sub> chalcogenide hexagonal photonic crystal fibers that are pumped at 2.5 microns with pulse durations that are 500 fs or longer and pump peak powers of 1 kW or more with careful design of the fiber parameters. We have also shown that it is possible to put more than 25% of the power in the range of 3-5 microns in As<sub>2</sub>S<sub>3</sub> chalcogenide fibers with a pump at 2 microns.

A difficulty with this early work is that the bandwidth is highly sensitive to changes in both the pump power and the pulse duration. Changes of less than 1% of either of these parameters lead to changes in the bandwidth that can be greater than 20% in some parameter ranges]. Moreover, the spectral power with a single set of parameters fluctuates rapidly as a function of wave-length and can change by more than 20 dB within 0.1 microns, leading to the prospect of undesirable open windows in the power spectral density. However, in real systems both the pulse energy and the pulse duration will fluctuate by a large amount — about 10% in experiments that have been carried out at the Naval Research Laboratory. As a consequence, we expect that the actual spectrum that is produced by supercontinuum generation is far smoother and the bandwidth more stable than single-simulation results would indicate, and more recent results bear out this expectation.

In recent work, we have carried out extensive simulations to determine the spectrum that would appear in a real system and to find computationally efficient methods for calculating that spectrum. Using simulations with up to one million individual simulation runs, we have shown that the spectrum can be reasonably estimated with as few as 100 simulation runs and that the spectral fluctuations with a 0.1 nm range are just a few dB. In this presentation, we will both review our older results and present our new results.

### 8898-13, Session 4

#### **Low loss, wide transparency, robust tellurite glass fibers for mid-IR (2-5 $\mu\text{m}$ ) applications**

Dan L. Rhonehouse, Jie Zong, Arturo Chavez-Pirson, NP Photonics, Inc. (United States)

Mid-infrared sources are a key enabling technology for various applications such as remote chemical sensing, defense communications and countermeasures, and bio-photonic diagnostics and therapeutics. Low loss and robust optical fibers capable of transporting, multiplexing, and distributing mid-IR laser light from, for example, optical parametric amplifiers, quantum cascade lasers, and supercontinuum fiber lasers is needed for these applications. However, conventional mid IR optical fibers based on ZBLAN or chalcogenide glass have not met all the application requirements due to their fragility, low melting temperature, sensitivity to moisture, and undesirable impurity absorption. Here, we report on our work with tellurium oxide based glasses and fibers. These glasses are attractive, because of their stability, strength, high temperature, and chemical durability as well as their high optical nonlinearity ( $n_2 = 1 \times 10^{-20} \text{cm}^2/\text{W}$ ). However, up to now, it has been difficult to remove deleterious hydroxide (OH) from the glass and fiber that leads to high absorption at 3.37 $\mu\text{m}$ . We have undertaken a fundamental study of the tellurium oxide glass system, selected glass compositions which have no absorption in the mid-IR band and have successfully produced

glass and fiber with substantially no OH. We have engineered this glass to be compatible with a rod-in-tube fiber preform method, and a fiber drawing process – such that we achieve low propagation losses (< 0.2 dB/m) over the transparency window. Different types of fiber structures have been successfully fabricated, including high power handling large core (100µm) multi-mode, small core (down to 3µm) single mode, and dispersion-managed fibers.

**8898-14, Session 5**

**Simulation of laser propagation through jet plumes using computational fluid dynamics**

Markus Henriksson, Henrik Edefur, Oskar Parmhed, Shia-Hui Peng, Lars J. Sjöqvist, Jonas Tidström, Stefan Wallin, Swedish Defence Research Agency (Sweden)

We have investigated the possibilities of using computational fluid dynamics (CFD) simulations to characterize the impact of refractive index fluctuations in a jet engine plume on DIRCM system performance. The jet plume was modelled using both Reynolds-averaged Navier-Stokes (RANS) and large eddy simulation (LES) formulations of Navier-Stokes equations. The RANS calculations provided a time-averaged description of the refractive index and the turbulence strength. The more computationally intense LES model provided time resolved data on large scale turbulent eddies within the engine plume. The smaller structures are assumed to be isotropic and are modelled implicitly to reduce the computational demands to levels that are feasible with our cluster. The refractive index data from the CFD calculations was integrated along the optical propagation path to produce phase screens. For RANS data this approach provided time averaged aberrations, whereas for LES data the temporal variation of low spatial frequency aberrations were available for a short time sequence. Modal descriptions of the phase screens were investigated to allow study of temporal variation at longer time scales. Alternatively the structure parameter (Cn2) was estimated and used to generate snap-shot phase screens. The generated phase screens were used to calculate laser beam system level quality parameters including beam wander, Strehl ratio and power in bucket. The point spread function of the fine-track sensor was also studied. The paper focuses on method development, but examples of a jet plume simulation showing that the engine plume turbulence has a significant impact on DIRCM system functionality are presented.

**8898-15, Session 5**

**Comparison of MODTRAN5 to measured data in the UV band**

Leon Smith, Mark Richardson, Cranfield Univ. (United Kingdom); Roy Walmsley, Chemring Countermeasures Ltd. (United Kingdom)

The UV band of the electromagnetic spectrum has potential as a host medium for the operation of guided weapons. Unlike in the IR, a target which is propelled by an air breathing jet engine generates no detectable radiation in the UV band, and is opaque to the background UV produced by the Sun. In theory the blocking of UV radiation from the sun causes a detectable 'negative contrast' between the target and the background. In order to determine the outcome of engagement scenarios between airborne platforms and guided weapon systems that utilise a guard channel operating in the UV, it is necessary to accurately model background UV levels.

This paper presents a comparison between the atmospheric modelling code MODTRAN@5 (MODERate resolution atmospheric TRANsmission) and measured data. The Spectral Irradiance levels generated by the MODTRAN@5 code are compared to those of the WOUDC (World Ozone and Ultraviolet Data Centre) database, for various global positions and times of year. Radiance data collected at the Defence Academy of the United Kingdom (Shrivenham, England) for various observer geometries is also compared to that generated by the MODTRAN@5 code.

**8898-16, Session 6**

**Non-lethal laser dazzling as a personnel countermeasure (Invited Paper)**

David C Shannon, Consultant (United States)

Laser dazzling is likely one of the original and simpler optical countermeasure concepts with a technology history dating back to the 1800's. The objective is to distract or suppress either equipment or personnel with optical radiation from a safe distance. This paper is intended to review and expand on the concepts presented at the 2012 meeting; "Non-Lethal Optical Interruption (Dazzling): Technology, Devices, and Scenarios".

This presentation will focus primarily on the technology and techniques associated with the safe laser dazzling of personnel. Key product design guidelines will be highlighted and reviewed. Recent advances in laser technology and their associated impact on hand-held devices will also be discussed.

**8898-17, Session 6**

**Laser dazzling impacts on car driver performance**

Ove K. Steinvall, Stig Sandberg, Ulf Hörberg, Rolf Persson, Folke Berglund, Kjell Karlsson, Johan Öhgren, Swedish Defence Research Agency (Sweden); Per G. Söderberg, Uppsala Univ. (Sweden); Zhaohua Yu, Uppsala University (Sweden)

Eye safe laser dazzling has been accepted as a tool for temporarily blinding and to disorient a potentially hostile person preventing him to complete dangerous actions. Lasers designed to cause permanent blindness are banned by the 1995 United Nations Protocol on Blinding Laser Weapons

Initially developed for military use, laser dazzlers are now also becoming available for use in law enforcement and security. Powerful handheld lasers are however also accessible by people who are using them in a provocative and dangerous manner, for example against car drivers and aircraft pilots. These incidents are not only causing problems for the traffic safety, but may also scare and cause considerable problems for individuals being hit by lasers, and are associated with a burden on the health care system. It is therefore of interest to investigate the impact of laser dazzling on driving performance and to use such information to describe the consequences on laser dazzling to drivers, as well as to describe simple protective means such as the use of a sun shields.

This paper will describe experiments of laser dazzling on car driver performance under varying daylight conditions. The influence of laser radiation levels varying from 0.1 to 0.8MTE (MTE=maximum permissible exposure=10 W/m2 for a continuous wave 532 nm laser) on driving performance is rather limited in full daylight but can be severe in low light conditions.

**8898-18, Session 6**

**Effects of high power illuminators on vision through windscreens and driving behavior**

Alexander Toet, Johan W. A. M. Alferdinck, TNO Defence, Security and Safety (Netherlands)

We developed a test protocol for the qualification of high power illuminators that are intended to be used as warning devices or non-lethal weapons to deny car drivers their view on the outside world through windscreens. The test is based on a measurement of the amount of veiling glare resulting when a high intensity light source hits a windscreen. We measured the veiling glare for new, used and colored windscreens that were either clean or dirty. We found no significant difference between the scatter function for new, used and colored windows. The scatter function for dirty windscreens is a factor 14 larger than for clean windscreens. We also derived a method to assess the impact of the illumination of a windscreen by a high intensity light source on driving behavior. The method is based on the assumption that drivers reduce their speed when veiling glare



**Conference 8898A:  
Technologies for Optical Countermeasures X**

reduces the detection distance of objects on the road. Estimates of respectively the detection distance for objects on the road and the maximum safe driving speed are directly related to operational requirements, and can therefore be used to assess the operational effectiveness of high intensity light sources as powerful warning devices or non lethal weapons.

8898-19, Session 7

**Detection of dim targets in multiple environments** (*Invited Paper*)

Grace Mirsky, Northrop Grumman Corp. (United States);  
Matthew Woods, Northrop Grumman Corp. (United States)

The proliferation of a wide variety of weapons including Anti-Aircraft Artillery (AAA), rockets, and small arms presents a substantial threat to both military and civilian aircraft. To address this ever-present threat, Northrop Grumman has assessed unguided threat phenomenology to understand the underlying physical principles for threat detection. These principles, based upon threat transit through the atmosphere, exploit a simple phenomenon universal to all objects moving through an atmosphere comprised of gaseous media and rely upon a simple phenomenon to detect and track the threat in the presence of background and clutter.

Threat detection has rapidly become a crucial component of aircraft survivability systems that can provide situational awareness to the crew. As a result, it is particularly important to platforms which may spend a majority of their time at low altitudes and within the effective range of a large variety of weapons. Detection of these threats presents a unique challenge as this class of threat typically has a dim signature coupled with a short duration. Correct identification of each of the threat components is important to determine trajectory and intent while minimizing false alarms and maintaining a high detection probability in all environments.

8898-20, Session 7

**Target discrimination strategies in optics detection** (*Invited Paper*)

Lars J. Sjöqvist, Lars Allard, Markus Henriksson, Per Jonsson, Magnus Pettersson, Swedish Defence Research Agency (Sweden)

Detection and localisation of optical assemblies used for weapon guidance or sniper rifle scopes has attracted interest for security and military applications. Typically a laser system is used to interrogate a scene of interest and the retro-reflected radiation is detected. Different system approaches for area coverage can be realised ranging from flood illumination to step-and-stare or continuous scanning schemes. Depending on the application the system can be controlled by an operator or work autonomously. The latter increase the requirements on target discrimination. However, independently of the chosen approach target discrimination is a crucial issue, particularly if a complex scene such as in an urban environment is considered. False targets include e.g. road signs, different kind of reflectors, optical reflexes and glints from specular surfaces or windows.

In this work target discrimination strategies in optics detection are discussed. Typical parameters affecting the reflected laser radiation from the target are the wavelength, polarisation properties, temporal effects and the range resolution. Knowledge about the target characteristics is important to predict the target discrimination capability. By analysing the polarisation properties of the reflected radiation information can be retrieved from the target when using a known polarisation state for interrogation. The wavelength dependence of the reflected power, caused by chromatic effects within the optical assembly, can be analysed using a multispectral system. Another approach is to use range information from the target if the system is capable of high resolution range-profiling.

Polarisation properties and range resolution information from studied targets including e.g. traffic signs, optical reflexes, rifle sights and optical references will be discussed using experimental results. Here a system with a rectangular laser beam using a dual channel approach; with one channel providing position and the other range information to the target, respectively, was used. In addition a high resolution range-profiling system provided information used to classify different

target types. Examples from experimental results using the two approaches are presented. If autonomous operation is required target discrimination becomes critical in order to reduce the number of false alarms.

8898-21, Session 7

**Optical countermeasures against CLOS weapon systems**

Alexander Toet, TNO Defence, Security and Safety (Netherlands); Koen W. Benoist, TNO (Netherlands); Joost N. J. van Lingen, Ric H. Schleijsen, TNO Defence, Security and Safety (Netherlands)

There are many weapon systems in which a human operator acquires a target, tracks it and designates it. Optical countermeasures against this type of systems deny the operator the possibility to fulfill this visual task. We describe the different effects that result from stimulation of the human visual system with high intensity (visible) light, and the associated potential operational impact. Of practical use are flash blindness, where an intense flash of light produces a temporary "blind-spot" in (part of) the visual field, flicker distraction, where strong intensity and/or color changes at a discomfortable frequency are produced, and disability glare where a source of light leads to contrast reduction. Hence there are three possibilities to disrupt the visual task of an operator with optical countermeasures such as flares or lasers or a combination of these; namely, by an intense flash of light, by an annoying light flicker or by a glare source. A variety of flares for this purpose is now available or under development: high intensity flash flares, continuous burning flares or strobe flares which have an oscillating intensity. The use of flare arrays seems particularly promising as an optical countermeasure. Lasers are particularly suited to interfere with human vision, because they can easily be varied in intensity, color and size, but they have to be directed at the (human) target, and issues like pointing and eye-safety have to be taken into account. Here we discuss the design issues and the operational impact of optical countermeasures against human operators.

8898-22, Session 7

**Laser irradiation delayed nonlinear response of IR matrix detectors**

Yuri A. Rezunkov, Research Institute for Complex Testing of Optoelectronic Devices and Systems (Russian Federation)

The modern progress in lasers is also directed into a wide application of laser technologies for space exploration. In particular, the ground-based lasers are used to monitor the satellites and space debris orbits in a space surrounding the Earth. For that the International Laser Ranging Service (ILRS) is set up for the example. But, uncontrolled illumination of the satellites can derange its opto-electronic devices. In that mean, a special interest concerns a nonlinear response of matrix photo detectors upon the laser radiation, including such effect as persistence".

In the paper, the results of experimental investigations of the delayed nonlinear response of the InSb matrix photo detectors upon IR laser radiation are discussed. Two types of the matrix nonlinear after-images are observed when the laser radiation exposure is unloaded after illumination. Low detector signal as against the detector dark current and sensed like "a dark spot" is registered if the laser irradiance changes from 10-3 W/cm<sup>2</sup> through 10-1 W/cm<sup>2</sup>. The dark spot relaxes during a few tens of minutes after that. At increasing the matrix irradiance greater than 1 W/cm<sup>2</sup>, the nonlinear after-image signal is higher than the dark current and it is sensed like "a light spot" in the image. The light spot relaxes during a few tens of seconds after the matrix illumination. The delayed nonlinear response of the detector matrix occurs both at the pulsed and CW irradiance of the detectors.

The concept description of the delayed nonlinear response of IR matrix detectors is considered basing on the experimental results obtained as well as similar investigations made by other researchers.

# Conference 8898B: High-Power Lasers 2013: Technology and Systems

Monday 23–23 September 2013

Part of Proceedings of SPIE Vol. 8898 Technologies for Optical Countermeasures X; and High-Power Lasers 2013: Technology and Systems

8898-25, Session 8

## 50 kW Laser Weapon Demonstrator of Rheinmetall Waffe Munition (*Invited Paper*)

Markus Jung, Klaus Ludewigt, Thomas Riesbeck, Alexander Graf, Rheinmetall Waffe Munition GmbH (Germany)

We will present the setup of a 50 kW Laser Weapon Demonstrator (LWD) and results achieved with this system.

The LWD is a ground based Air Defence system consisting of a Skyguard sensor unit for target acquisition and two laser equipped weapon turrets. The weapon turrets used are standard air defend turrets of Rheinmetall Air Defence which were equipped with several 10 kW Laser Weapon Modules (LWM).

Each LWM consists of one 10 kW fiber laser and a beam forming unit (BFU). Commercial of the shelf fiber laser were modified for our defence application, The BFU providing diffraction limited beam focusing, target imaging and fine tracking of the target was developed.

The LWD was tested in a firing campaign at a Rheinmetall test ground in Switzerland. All laser beams of both weapon turrets were superimposed on stationary and dynamic targets. Test results of the LWD for the scenarios Air Defence and C-RAMM (counter rockets, artillery, mortar and missiles) will be presented.

An outlook for the next development stage towards a 100kW class laser weapon on RWM will be given.

8898-26, Session 8

## Latest developments on the Er<sup>3+</sup>:YAG solid state heat-capacity laser (*Invited Paper*)

Stefano Bigotta, Thierry Ibach, Marc Eichhorn, Institut Franco-Allemand de Recherches de Saint-Louis (France)

In this paper, we illustrate the latest advancement on the eye-safe Solid State Heat-Capacity Laser (SSHCL) investigated for the development of medium and high energy laser sources at ISL. Nearly all the solid-state lasers investigated or considered up to now for defence applications in Europe and overseas in the range of 10 kW up to over 100 kW emit at a wavelength of 1.03  $\mu\text{m}$  - 1.06  $\mu\text{m}$ . Therefore, we perform research on an alternative emitting around 1.6  $\mu\text{m}$ , which as much as possible unites also many advantages in use (robustness, a simple technology, flexibility in volume and weight). This is based on a very promising and simple concept: the erbium heat-capacity laser, characterized by a compact design, and a scaling law which in principle allows the generation of laser powers far beyond megawatts at small volumes. The heat-capacity principle, in which the laser material is cooled only after the laser action has ended, results in low temperature gradients in the laser medium during the laser operation, leading to a good beam quality together with high performance.

Previous investigations demonstrated the scalability of the heat-capacity laser principle and up to 4.65 kW and 440 J in less than 800 ms have been achieved using optimized doping levels for up-conversion reduction in this resonantly-diode-pumped Er<sup>3+</sup>:YAG SSHCL, representing the current world record in eye-safe diode-pumped solid-state laser technology. Optical-to-optical efficiencies of over 41% and slope efficiencies of over 51% are obtained with respect to the incident pump power.

In this report we will further investigate the possibility of compensating any parasitic residual heating that may impede the scalability of the heat-capacity laser to higher energies. Indeed, it has been shown that the optimal laser operation in the sense of highest efficiency, highest output energy and the longest operating duration (in the range of some seconds), is directly coupled with the intensity distribution of the laser mode inside the laser medium. The ideal resonator configurations are those which allow an extraction of the laser energy as homogeneous as possible. Using an intra-cavity adaptive optics system beams with phase wavefronts as flat as possible, on the order of less than 1/10 of the wavelength for each of the considered Zernike polynomials have been generated, and the shot duration has been lengthened

by ~50%. Additionally, the influence of the crystal geometry on the pump distribution homogeneity and possible ways for maximizing the extraction efficiency are investigated.

8898-27, Session 8

## Recent developments in high power thin disk lasers at TRUMPF Laser

Tina Gottwald, Vincent Kuhn, Christian Stolzenburg, Sven-Silvius Schad, Alexander Killi, TRUMPF Laser GmbH & Co. KG (Germany)

In this contribution recent advances of thin disk laser technology will be discussed. The disk laser benefits from a unique combination of properties. It combines low thermal lensing effects by the axial heat flux in the gain medium, cost-effective operation through low brightness constraints on the pump diodes, the possibility of power scaling by increasing the beam diameter, insensitivity to back reflections through strong gain saturation and low output coupling and - even at very high peak powers - negligible nonlinearities based on the short path in the gain medium. These properties allow the combination of high optical-to-optical efficiencies, excellent beam quality and high average and peak output powers. At the same time the insensitivity to back-reflections and lowest pump brilliance requirements of any high power laser platform allow for highly reliable and at the same time cost-effective operation with high wall-plug efficiencies.

The versatile thin disk-laser concept can be utilized both for cw and pulsed laser systems, the latter including high average power systems with  $\mu\text{s}$  to ns pulse lengths, regenerative amplifiers, and mode-locked oscillators in the ps regime. Disk lasers are widely used in industrial material processing. CW lasers perform welding and cutting tasks especially in the automotive industry, the pulsed lasers are used for example in the consumer and electronics industry and for micromachining.

This contribution highlights the latest advances of disk laser technology at TRUMPF Laser. In the new generation of CW disk lasers, 6 kW are extracted from one disk in an industrial product at beam qualities suitable for welding. Output powers of up to 4 kW are available at beam qualities suitable for cutting applications. Laboratory results with up to 8 kW of laser power with a beam quality of 4 mm mrad (suitable for a laser light cable with 100  $\mu\text{m}$  diameter and NA 0.1) from a single disk and even higher output power levels with lower beam quality will be presented. These advances are enabled by a combination of system optimizations with regard to pump source and pump light distribution as well as resonator technology. The continuous improvements allow for increasingly higher output power levels and beam qualities with reduced costs per Watt of high reliability laser power.

In addition, applications of the disk laser principle to pulsed operation with ns duration at infrared and green wavelengths are discussed. Also for this regime new power scaling results are presented.

8898-29, Session 9

## New fiber developments for amplifiers operating at 1 $\mu\text{m}$ and 2 $\mu\text{m}$ (*Invited Paper*)

Bryce N. Samson, Adrian L. Carter, Kanishka Tankala, Imtiaz Majid, Liang Dong, Nufern (United States); Alexander V. Hemming, Defence Science and Technology Organisation (Australia)

Recently the progress in fiber amplifiers operating at high power levels has shifted to the fiber itself rather than the many other supporting components such as high brightness diodes and couplers, which have traditionally been the limiting factor. In the case of Yb-doped fibers operating at 1 $\mu\text{m}$ , the problems of stimulated Brillouin Scattering (SBS) when amplifying narrow linewidth sources and multimode instabilities in large mode area (LMA) fibers have received

much attention in the last few years. In the case of 790nm pumped Tm-doped fibers operating around 2?m, the problems of thermal management have limited power scaling to the 1kW power level with little progress in the last few years. In both of these cases, new fiber developments may offer progress towards solving the problems and Nufern is involved in exploring novel waveguide designs as a valuable tool to help overcome these problems. One such tool, is designing the fiber with intrinsic high loss for higher order modes in the LMA fiber and Nufern together with Clemson University have been developing a new all-glass leakage channel fiber which shows some promise for scaling mode field whilst preserving single mode beam quality. In the case of 2?m fibers, Nufern is working with Defence Science and Technology Organisation (DSTO) in Australia to demonstrate resonant pumping of Ho-doped fibers as a promising method for power scaling fiber amplifiers at 2.1?m and in this paper the recent fiber designs and results will be reviewed.

#### 8898-30, Session 9

### Recent advances in passive phase locking of fiber lasers thanks to intracavity phase contrast filtering

David Sabourdy, Jean-Eucher Montagne, CILAS (France); François Jeux, EADS Astrium (France); Agnès Desfarges-Berthelemot, XLIM Institut de Recherche (France); Vincent Kermène, Alain Barthelemy, Univ. de Limoges (France)

Passive techniques for coherent coupling of lasers offer an appealing way for the generation of high brightness laser beam because of their simplicity and their all-optical operation. Many configurations have been investigated which yield coherent summation of the optical power available from separate fiber amplifiers. An array of fiber amplifiers inserted in a common laser cavity and delivering an array of phase-locked beams appears most of time as the best suited to high power operation. It was quickly evidenced however that passive coherent coupling became less efficient as the size of the laser array increased. This is the reason why research in that field focused on some way to overcome the threshold size of about 10 lasers for an efficient coherent coupling. All the different published approaches (phase conjugation, coupled cavity) involved an optical nonlinearity. In that context we proposed and investigated a new cavity design featuring unidirectional ring geometry combined with a specific spatial filter. The nonlinearity considered here is due to the contribution of the population inversion (the gain) to the optical phase in the amplifiers. The gain-dependent refractive index change is significantly larger than the non resonant Kerr non linearity of silica in fiber amplifiers. It is usually assumed that the nonlinear phase shift evolves linearly with the gain (Kramers-Krönig relationships). We have carried out experiments using an Ytterbium doped fiber amplifier which confirm an almost linear relationship whatever the pump level. Then the basic idea behind our new cavity design is the following. Self-organization of the laser in standard design only relies on the selection of the lowest loss mode after iterative linear filtering. With a great number of lasers assumed to be of different length (with uncontrolled variations induced by the environment) longitudinal modes actually common to all the cavity arms no longer exist. The laser beams are no more perfectly in phase and phase deviations are observed in the array outputs. We suggested transforming the phase deviations into power deviations so that the gain can vary from one channel to another. Therefore a gain-dependent phase introduced during amplification can compensate for the linear phase delay between the different laser fields. In one implementation of that principle we proposed to use the set-up of phase-contrast microscopy due to Zernike. A simple phase plate inserted in the far field performs the phase to amplitude conversion. To assess the potential of the new scheme we made numerical simulations of the laser operation. Our model takes into account the linear properties of the cavity as well as the gain bandwidth, saturation, and added phase in each amplifier. Starting from noise it reproduces the laser modes build-up until steady state giving the final laser frequencies and spatial pattern. Numerical results that will be reported at the conference show a gain in efficiency offered by the investigated configuration by comparison with previous schemes. After some preliminary experimental demonstration with 9 laser beams we will present new results with 15 and then 20 laser beams.

#### 8898-31, Session 9

### Single-element beam shaper for conversion of a fiber laser beam into a near-diffraction-limited dark hollow beam

Haotong Ma, Haojun Hu, Wenke Xie, Guangwen Jiang, Xiaojun Xu, National Univ. of Defense Technology (China)

In recent years, fiber lasers have attracted more and more attentions due to their compactness, high efficiency, and beam quality. However, the intensity distribution of the output beam from a single-mode fiber laser is quasi-Gaussian distribution, which limits capability for many applications. Beams with dark hollow intensity distributions have attracted more and more attentions in practical applications. Dark Hollow beams with flat wavefront show great prospect for the applications of laser launching system, such as laser communications, laser tracking, directed energy systems, etc. In laser projection systems, obstructed Cassegrain telescopes are often used as transmitters. Because of the central obscuration of the second mirror, the dark hollow beams are usually chosen to improve the power efficiency. Investigation results show that dark hollow beams have advantages over Gaussian beams for overcoming the destructive effect of atmospheric turbulence. Many techniques which include amplitude filtering, phase filtering by refractive or diffractive optics, and resonator mode control have been proposed to generate dark hollow beam. Amplitude filtering suffers from huge transmission losses. The phase filtering by refractive or diffractive optics should contain two or more optical elements for generating dark hollow beam with flat wavefront.

In this paper, we propose and demonstrate a single-element beam shaper for transforming a fiber laser beam into a near-diffraction-limited dark hollow beam. The single-element beam shaper contains two aspheric surfaces. One aspheric surface redistributes the intensity distribution of the incident beam and the other re-collimates the output beam. The distributions of these surfaces are derived by the energy conservation condition and constant optical path length condition. The comparisons between the single-element beam shapers based on different working principles are analyzed in detail. Based on the Fourier optics and Geometrical optics, the influences of deviations of the beam waist and beam shape from the assumed value are studied in detail. The near field and far field intensity distribution of the output beam are also studied in detail. Results show that the wavefront distribution of the output beam is maintained and the conversion efficiency of the shaping system is nearly lossless. The dark hollow intensity distribution of the output beam can be maintained for a certain distance in the near field and the far field intensity distribution exhibits airy disk pattern.

Up to now, the generation of near-diffraction-limited dark hollow beam with a single-element beam shaper has never been reported. Compared with other beam shaping techniques, this technique has high conversion efficiency and compact structure and does not need complex phase retrieval algorithm. This technique can be used in optical communication, deep space optical communication and directed energy systems.

#### 8898-32, Session 9

### High power fiber isolator for 1 micron fiber lasers

Shibin Jiang, AdValue Photonics, Inc. (United States)

Current free-space fiber pigtailed isolators limit the maximum throughput power of fiber lasers, which means high power fiber isolator is needed for power scaling and beam combining. We developed an all-fiber isolator using our proprietary highly Tb-doped optical fiber with high Verdet constant as Faraday rotator, which is fusion spliced together with fiber based polarizer. All-fiber isolator using Tb-doped Faraday rotating fiber was demonstrated, and a prototype was developed and tested. This presentation will describe the Tb-doped Faraday rotating fiber, fusion splicing, and test results of this all-fiber isolator.

8898-33, Session 9

**High-power diode lasers between 1.8 $\mu$ m and 3.0 $\mu$ m for military applications**

Sascha A. Hilzensauer, Marc Kelemen, m2k-laser GmbH (Germany)

Over the last years high-power diode lasers in the wavelength window between 1.8 $\mu$ m and 3.0 $\mu$ m have demonstrated impressive characteristics in terms of output power, beam quality and efficiency. GaSb based diode lasers are naturally predestined for this wavelength range and offer clear advantages in comparison to InP based diode lasers in terms of output power and wall-plug efficiency. This facilitates the realization of compact and efficient light sources for use in the field of infrared countermeasures (IRCM), optically pumped semiconductor lasers emitting in the 2-4 $\mu$ m regime, low probability of intercept communication links, and trace gas analysis. Civilian applications exist in the fields of laser surgery, medical diagnostics and dermatological treatments as well as direct materials processing such as plastics or aqueous varnish processing. The small size of a diode laser chip of typically less than a square millimeter allows for the fabrication of compact scaleable laser modules with output powers of up to 140W:

We will present results on MBE grown (AlGaIn)(AsSb) quantum-well diode laser single emitters and bars emitting between 1.8 $\mu$ m and 3.0 $\mu$ m. Different epitaxial and resonator designs have been investigated in cw and pulsed mode in order to meet industrial needs of high wallplug and fiber-coupling efficiencies. Also AuSn soldering of GaSb based lasers has been established instead of traditional Indium soldering. More than 30% maximum wall-plug efficiency in cw operation for single emitters and laser bars has been reached together with output powers for single emitters of 2W (cw) and 9W (pulsed).

The single emitters and bars are all suitable for fiber coupling. For a 1-bar module typical coupling efficiencies between 70% and 80% have been established for 400 $\mu$ m core fibers. In terms of output power, an AuSn soldered laser stack built of 10x 20% fill factor bars emitting at 1908nm, results in a record value of 140W at 58A in cw condition.

8898-34, Session 10

**DPAL: historical perspective and summary of achievements (Invited Paper)**

Boris V. Zhdanov, Randall Knize, U.S. Air Force Academy (United States)

Alkali vapor lasers are under extensive research and development during the last decade because of their potential for scaling to high powers while keeping a good beam quality. Also, a possibility of using efficient diode lasers for pumping of alkali vapors promises high total wall plug efficiency for Diode Pumped Alkali Laser (DPAL). Since the first DPAL demonstration with output power of 130mW in 2005 [1], a significant progress in this field was achieved. The output power of about 1 kW in continuous wave (CW) operation with optical efficiency close to 50% was recently demonstrated for Cs DPAL [2]. Also, the DPALs based on other alkali metals (Rubidium and Potassium) were also demonstrated [3, 4].

In spite of these significant achievements, there are still several problems in DPAL power scaling exist that must be addressed. Among them are the thermal [5] and photoionization [6] issues that become important even at several tens of watts CW power level.

In this talk we will present a short historical review of the alkali laser research and development, discuss the most important achievements and future perspectives in this field of research.

**Acknowledgements:** The research projects performed by U.S. Air Force Academy and described in this talk were supported by the High Energy Laser Joint Technology Office (HEL JTO), Air Force Office of Scientific Research (AFOSR), and the Air Force Research Laboratory (AFRL)

**References:**

1. T. Ehrenreich, B. Zhdanov, T. Takekoshi, S. P. Phipps, and R. J. Knize, "Diode Pumped Cesium Laser", Electronics Letters, 41(7), 47-48 (2005)
2. A.V. Bogachev, S.G. Garanin, A.M. Dudov, V.A. Yeroshenko, S.M. Kulikov, G.T. Mikaelian, V.A. Panarin, V.O. Pautov, A.V. Rus, S.A. Sukharev, "Diode-pumped caesium vapour laser with closed-cycle laser-active medium circulation" Quantum Electronics, 42 (2) 95 – 98

(2012)

3. J. Zweiback, W. Krupke, "28W average power hydrocarbon-free rubidium diode pumped alkali laser", Optics Express 18 (2), 1444-1449 (2010)
4. B.V. Zhdanov, M.K. Shaffer, R.J. Knize, "Demonstration of a diode pumped continuous wave potassium laser", Proc. SPIE Vol. 7915, 791506-1 – 791506-6 (2011)
5. Zhdanov, B.V., Sell, J. and Knize, R.J., "Multiple Laser Diode Array Pumped Cs laser with 48 W Output Power", Electronics Lett., 44 (9), 582-583 (2008)
6. R.J. Knize, B.V. Zhdanov and M.K. Shaffer, "Photoionization in Alkali Lasers", Optics Express, 19 (8), 7894-7902 (2011)

8898-35, Session 10

**What can we gain from supersonic operation of diode pumped alkali lasers: model calculations**

Salman Rosenwaks, Boris D. Barmashenko, Karol Waichman, Ben-Gurion Univ. of the Negev (Israel)

In recent years, extensive studies of diode pumped alkali lasers (DPALs) have been carried out [1,2]. In these studies, static and flowing-gas DPALs have been investigated. Modeling of these devices has been conducted as well [1,3-8] and fluid dynamics and kinetic processes have been taken into account, but for flowing-gas DPALs only subsonic velocity of the gas was considered. In this presentation we explore the feasibility of operating DPALs with supersonic expansion of the gaseous laser mixture, consisting of alkali atoms, He and (frequently) hydrocarbon molecules. The motivation for this exploration stems from the possibility of fast and efficient cooling of the mixture by the supersonic expansion.

We concentrate on Cs and K atoms DPALs because they represent quite different characteristics with respect to the energy gap between the 2P<sub>3/2</sub> and 2P<sub>1/2</sub> pumped and lasing states, respectively, and therefore of the preferred buffer gas.

In gas mixtures consisting of Cs atoms and hydrocarbon molecules, the pumped 2P<sub>3/2</sub> state relaxes efficiently by the hydrocarbon to the 2P<sub>1/2</sub> state [1,5]. He gas will not do this job but can be added to improve heat transfer. Cs/He/CH<sub>4</sub> mixture was used in a 1-kW flowing-gas subsonic DPAL with ~ 48% efficiency [4]. The main advantages of supersonic expansion in this case would be efficient cooling and high flow velocity and we estimate the extent of this advantage compared to subsonic flow. A drawback of this mixture is the reaction between highly excited Cs atoms or ions with the hydrocarbons [1].

A big advantage of K over Cs is that it can be mixed only with He, which efficiently relaxes 2P<sub>3/2</sub> to 2P<sub>1/2</sub>. The use of He also eliminates the problem of reaction of highly excited K atoms. Another advantage of using pure He is its very small refraction index. Although the fine-structure splitting of the 2P states of K is only ~58 cm<sup>-1</sup>, efficient lasing in K optically pumped laser was obtained at 470 °K [9]. It is thus expected that at lower temperatures the efficiency will be higher.

For a supersonic Cs DPAL with parameters similar to those of the 1-kW flowing-gas subsonic Cs DPAL [4], the maximum value of lasing power,  $P_{lase}$ , for the former is larger than that for the latter by 25%. Optimization of He/CH<sub>4</sub> buffer gas composition and flow parameters shows that for the resonator parameters of Ref. 4, extremely high power and optical-to-optical efficiency, 21 kW and 82%, can be achieved in the supersonic device. For the supersonic K DPAL  $P_{lase} = 43$  kW (twice as that for Cs) is 70% larger than for subsonic with the same resonator and K density at the inlet, the maximum optical-to-optical efficiency being 82%. We checked, using classic nucleation theory, that the nucleation and clustering during expansion in a supersonic nozzle of 2-3 cm length amounts to only 0.001% of the atoms and therefore is insignificant.

The results of the model calculations indicate that for scaling-up the power and optical-to-optical efficiencies of DPALs, supersonic expansion should be investigated.

1. W.F. Krupke, J. Prog. Quantum Electron. 36, 4 (2012).
2. B.V. Zhdanov and R.J. Knize, Optical Engineering 52(2), 021010 (February 2013).
3. G.D. Hager and G.P. Perram, Applied Phys. B 101, 45 (2010).
4. A.V. Bogachev, S.G. Garanin, A.M. Dudov, V.A. Yeroshenko, S.M.

Kulikov, G.T. Mikaelian, V.A. Panarin, V.O. Pautov, A.V. Rus, and S.A. Sukharev, *Quantum Electron.* 42, 95 (2012).

5. G.A. Pitz, C.D. Fox, and G. P. Perram, *Phys. Rev. A* 84, 032708 (2011).

6. B.D. Barmashenko and S. Rosenwaks, *Opt. Lett.* 37, 3615 (2012).

7. B.D. Barmashenko, S. Rosenwaks, and M.C. Heaven, *Opt. Commun.* 292, 123 (2013).

8. B. D. Barmashenko and S. Rosenwaks, *J. Opt. Soc. Am B.* in press (2013).

9. J. Zweiback, G. Hager, and W. F. Krupke, *Opt. Commun.* 282, 1871 (2009).

## 8898-36, Session 10

### Model calculations of kinetic and fluid dynamic processes in diode pumped alkali lasers

Boris D. Barmashenko, Salman Rosenwaks, Karol Waichman, Ben-Gurion Univ. of the Negev (Israel)

Diode pumped alkali lasers (DPALs) [1] operate on the  $D1(n2P1/2 \rightarrow n2S1/2)$  transition of alkali atoms (where  $n = 4, 5, 6$  for K, Rb and Cs, respectively) pumped via the  $D2(n2S1/2 \rightarrow n2P3/2)$  transition, followed by rapid relaxation of the upper to the lower fine-structure level,  $n2P3/2$  to  $n2P1/2$ . At higher power ( $> 50$  W) the heat release due to relaxation between the fine-structure levels of the alkali atoms and quenching of these levels results in a considerable increase of the temperature  $T$  in the pumped region [2], causing an increase of the thermal population of  $n2P3/2$  and hence a decrease of the pump absorption. In addition, the atoms are excited to the higher levels  $n2D3/2, 5/2$  and  $(n+2)2S1/2$  by pump and laser radiation, and by energy pooling collisions. Photo- and Penning- ionization of these levels result in reduction of the density of neutral atoms participating in lasing and hence decrease of pump absorption and gain. The loss of alkali atoms can also be caused by their chemical reaction with methane or ethane, usually present in the laser medium [1]. Both the temperature rise and the loss of atoms decrease the slope and of the overall optical-to-optical efficiency. Another phenomenon, that can affect the operation of static DPAL, is the natural convection in the laser cell [2].

To avoid the temperature rise and replenish the lost alkali atoms, flowing-gas DPALs are used [3]. We report on a semi-analytical model of flowing-gas and static DPALs which includes the natural convection in the static case and takes into account the influence of the losses of alkali atoms due to ionization and chemical reactions on the output power of the static and flowing-gas DPAL. The model [4-6] is applied to both low power (10-50 W) static DPAL [2] and to the recently reported 1 kW flowing-gas DPAL [3]. It considers a typical configuration of a DPAL with end-pump geometry. Longitudinal gas flow in the optical axis direction with velocity  $u$  is primarily studied but transverse flow is also considered.

We first applied the model to Cs DPAL with static gas reported in [2]. Calculated values of  $P_{lase}$  are in good agreement with the measured values. To further test the model, we applied it to the 1 kW flowing-gas Cs DPAL [3]. At pump power  $P_p < 3$  kW applied in [3] the calculated values of lasing power  $P_{lase}$  are in a good agreement with the measured values. At higher  $P_p$  for which measurements are not available, the calculated  $P_{lase}$  values for the transverse flow are larger than for the longitudinal flow with the same  $u$ . The maximum calculated  $P_{lase}$  is  $\sim 3$  and 4 kW for the longitudinal and transverse flows, respectively. Increase of  $T$  from 393 to 403 K results in substantial rise of the maximum  $P_{lase}$  to  $\sim 6$  kW. Very recently the model was applied to study the feasibility of supersonic DPALs [7]. Three-dimensional computational fluid dynamics modeling of flowing gas DPALs is in progress.

1. W.F. Krupke, *J. Prog. Quantum Electron.* 36, 4 (2012).

2. B.V. Zhdanov, J. Sell, and R.J. Knize, 44, 582 (2008).

3. A.V. Bogachev, S.G. Garanin, A.M. Dudov, V.A. Yeroshenko, S.M. Kulikov, G.T. Mikaelian, V.A. Panarin, V.O. Pautov, A.V. Rus, and S.A. Sukharev, *Quantum Electron.* 42, 95 (2012).

4. B. D. Barmashenko and S. Rosenwaks, *Opt. Lett.* 37, 3615-3617 (2012).

5. B. D. Barmashenko, S. Rosenwaks, and M. C. Heaven, *Opt. Commun.* 292, 123 (2013).

6. B. D. Barmashenko and S. Rosenwaks, *J. Opt. Soc. Am B.* in press (2013).

7. B. D. Barmashenko and S. Rosenwaks, abstract submitted to the present meeting.

## 8898-37, Session 11

### Laser-induced thermal breakdown of optical coatings (Invited Paper)

Joseph J. Talghader, Univ. of Minnesota, Twin Cities (United States)

Laser-induced breakdown has been studied for decades by researchers working with ultra-short pulse lasers. The intense fields of these lasers excite carriers, for example by multiphoton absorption, from the valence states of atoms of an optical coating to higher states or bands. These carriers are accelerated by the very high fields of the laser pulses, and impact ionization creates further carriers, beginning a runaway process that thermally destroys the local area of the coating. However, continuous wave lasing conditions are far more typical of laser weapons systems, and here the breakdown process is very different, depending much more on absorption, direct heat transfer, and the thermal properties of a coating and substrate, rather than bandgap, carrier excitation, and mean free path. In this talk, the thermal properties of optical coatings, their measurement, and implications are discussed with respect to high power lasers. It has been found that many films that typically deposit as partially polycrystalline films can be induced to become amorphous if atomically thin layers of an alternative material are introduced periodically during deposition. Laser damage testing under continuous-wave or long-pulse conditions shows that these films breakdown at lower damage thresholds than pure partially polycrystalline films. This is the opposite behavior that would be expected for ultra-short pulses on amorphous versus polycrystalline materials. Possible explanations may involve the thermal conductivities of the films. The use of atomic layer deposition (ALD) to tailor film structure will be discussed, and ALD coatings will be compared to traditional ion-beam assisted sputtered (IBS) coatings. We also discuss the effects of nano-patterning and surface particulates on laser breakdown.

## 8898-38, Session 11

### Controlling plasma channels through ultrashort laser pulse filamentation

Andrey A. Ionin, P.N. Lebedev Physical Institute (Russian Federation)

A review of studies fulfilled at the Lebedev Institute in collaboration with the Moscow State University and Institute of Atmospheric Optics in Tomsk on influence of various characteristics of ultrashort laser pulse on plasma channels formed under its filamentation is presented. Filamentation of high-power laser pulses with wavefront controlled by a deformable mirror, with cross-sections spatially formed by various diaphragms and with different wavelengths was experimentally and numerically studied. An application of plasma channels formed due to filamentation of ultrashort laser pulse including a train of such pulses for triggering and guiding long electric discharges is discussed

8898-28, Session PS

## Advanced cooling system for space high-power solid-state laser

Yue Zhang, Zheng Wang, Beijing Institute of Space Mechanics and Electricity (China)

Abstract Cooling system for space high power solid-state laser is vital to output wavelength stability and life-span of chips. With the rapid development of laser and photoelectron technologies, the output power of space laser is higher, and temperature control accuracy is higher. Cooling system becomes one of the problems for space application of high power laser.

Cooling systems and their key technologies of advanced space high power space lasers were researched. And this paper summarized the cooling advantages of some cooling systems, such as full conductive cooling system, cryogenic loop heat pipe, heat pump, spray cooling system, micro-channel cooling system, and so on. According to the results above and design requirements of space high power laser with output power  $>1000\text{W}/\text{cm}^2$ , a cooling system was designed. Simulation result showed that the cooling system can meet design requirements well.

Our results can offer reference for conceptual design for cooling system of space high power laser, and can offer reference for its detail design.

# Conference 8899A: Emerging Technologies

Monday 23–23 September 2013

Part of Proceedings of SPIE Vol. 8899 Emerging Technologies in Security and Defence; and Quantum Security II; and Unmanned Sensor Systems X

8899-1, Session 1

## 3D computational ghost imaging (*Invited Paper*)

Matthew P Edgar, Baoqing Sun, Univ. of Glasgow (United Kingdom); Richard Bowman, Univ. of Cambridge (United Kingdom); Stephen S Welsh, Miles J. Padgett, Univ. of Glasgow (United Kingdom)

Computational ghost imaging is an alternative technique to conventional imaging that removes the need for a camera. Instead, ghost imaging illuminates the scene with a series of known patterns and infers the image from the backscattered intensities, measured with a single point detector. Using four detectors gives four different images, their apparent shading depending on the location of the detector. This shade information has previously been used to deduce the 3D surface profile in a technique called “shape from shade”. We adopt the same technique to give 3D images of head-sized objects using a single data projector and four photodiodes. We use a desk-top computer to generate a series of random checker-board patterns which are projected using a Texas Instruments Light Commander. The object is positioned approximately 500mm from the projector. The light backscattered from the object is detected using four 10mm diameter photo diodes separated from each other by approximately 300mm. The output signals from these detectors are recorded and registered to each pattern. The inherently high display rate of the projector, 1440Hz, is utilized to display both the positive and negative of the pattern in alternate frames, and the detector output demodulated at this bit plane rate to give the signal, hence discriminating against fluctuations in background light. A few seconds of data is sufficient to obtain both 2D and 3D image reconstructions. This approach is of particular relevance for imaging outwith the visible spectrum where the availability of cameras is limited.

8899-2, Session 1

## MultiBiometrics Encryption and Its Management Architecture

Obaidul Malek, Anastasios Venetsanopoulos, Ryerson Univ. (Canada); javad Alirezaie, Ryerson Univ (Canada)

Vulnerability of biometric template increases with the increase of its demands in the field of information technology. Currently, various methods are using to secure a secret key along with biometric features. For example, one of such methods in which captured biometric image or feature is compared and authenticated at secure location before releasing the secret key. Unfortunately, biometric features can be retrieved from this cryptographic system, if the secret key or the location of the secret key is obtained by the imposter. Another most recent encryption method, where proposed an algorithm to bind a digital key with the fingerprint biometric images to create a secure block of data known as Bioscrypt. However, there are two problems with this method. First, the method is designed based on the cooperative target where single biometric trait is used. Secondly, author is assumed that all fingerprints are completely aligned. Furthermore, the resulting false acceptance rate (FAR) and false rejection rate (FRR) are not stated by the author.

Therefore, objective of this paper is to propose a novel multimodal biometric encryption algorithm and its management architecture in order to protect the biometric features from security, privacy and unlinkability attacks. In this proposed encryption model, system generates a random private key which is monotonically bonded with the extracted face and fingerprint features at the fundamental level in order to create cryptographic bond, BioCryptoBond. More importantly, to further enhance the security protection, a new orthogonal tensor projection method and its detail algorithmic structure as a function of user fingerprint orientation angle is developed. Moreover, biometric data management architecture is also developed using secret BioCryptoBond in conjunction with hash function, composite foreign key and data segmentation technique, to improve the authentication accuracy. In this case, target is considered to be non-cooperative, and neither biometric features nor the secret key can retrieve without

a successful biometric authentication process. On the other hand, proposed model, not only protects dynamic biometric features, but also provides a secure data protection architecture for stored information into database system. Importantly, biometric features can only be retrieved using the target biometric features in presence of the legitimate user during target authentication process.

Finally, performance of the proposed solution are evaluated by the false acceptance and the false rejection rates. Simulation results presented here are illustrated the effectiveness of the proposed biometric model.

8899-3, Session 1

## Multidimensional compressive imaging (*Keynote Presentation*)

Bahram Javidi, Univ. of Connecticut (United States); Abhijit Mahalanobis, Lockheed Martin Missiles and Fire Control (United States); Xiao Xiao, Univ. of Connecticut (United States); Yair Rivenson, Ben-Gurion Univ. of the Negev (Israel); Ryoichi Horisaki, Osaka Univ. (Japan); Adrian Stern, Ben-Gurion Univ. of the Negev (Israel); Pedro Latorre Carmona, Jaume I Univ. (Spain); Manuel Martinez, Univ. de València (Spain); Filiberto Pla, Univ. Jaume I (Spain); Jun Tanida, Osaka Univ. (Japan)

In this keynote address paper, we present an overview of our previously published work on using compressive sensing in multi-dimensional imaging. We shall examine a variety of multi dimensional imaging approaches and applications, including 3D multi modal imaging integrated with polarimetric and multi spectral imaging, integral imaging, digital holography, 3D scene reconstruction, and 3D object recognition.

8899-4, Session 2

## Infrared imaging: ready for prime time? (*Invited Paper*)

Sanjay Krishna, The Univ. of New Mexico (United States)

Infrared imaging (3-12  $\mu\text{m}$ ) has been a valuable tool for detecting small temperature changes in a scene and has been around for the past 50 years. However, it has made dramatic strides in the past decade with the advent of new technologies that has pushed up the operating temperature of the imagers and dramatically driven the cost down. The third generation of infrared detectors has laid emphasis on higher operating temperature (HOT), multicolor and large format arrays. In this talk, I will provide two perspectives. I will provide a possible road map for the fourth generation of infrared detectors using bio-inspired sensors, in which there is an increased emphasis on obtaining detectors with enhanced functionality at the pixel level. Meta-infrared detectors in which meta materials are combined with metamaterial structures are a promising way to realize this. The infrared region is appealing due to the low metallic loss, large penetration depth of the localized field and the larger feature sizes compared to the visible region. In the second part of the talk, I will highlight some of the advances in infrared imaging and make a case for the use of infrared imaging in medicine. As with many inventions, such as the Internet and the GPS, the defense applications fostered initial research and development, while the commercial sector brought the technology to the masses. The open question for discussion is “Is infrared imaging ready for prime time

## 8899-5, Session 2

### Uncooled MWIR InAs/GaSb type-II superlattice grown on a GaAs substrate

Matthew J. Hobbs, Faebian Bastiman, Chee Hing Tan, John J. P. David, The Univ. of Sheffield (United Kingdom); Sanjay Krishna, Elena Plis, The Univ. of New Mexico (United States)

Photon detectors for use as low cost uncooled focal plane array (FPA) detectors are currently unavailable in the mid-wave infrared (MWIR) wavelength range (3-5  $\mu\text{m}$ ). Current MWIR FPAs which exist currently exist require cryogenic cooling, leading to issues with both cost and size, making them unsuitable for applications such as seekers. The InAs/GaSb type-II superlattice (T2SL) is seen as an affordable compact uncooled MWIR FPA detector for such applications.

InAs/GaSb T2SLs are attractive due to their potentially low dark currents and high responsivity. These low dark currents arise due to reduced Auger recombination caused by the spatial separation between the electrons and holes. Coupling these two aspects together leads to the potential of high operating temperature and high  $D^*$ . An additional attraction of T2SLs is their wavelength tunability; the wavelength can be tuned between 3 to 12  $\mu\text{m}$ , making them attractive for the militarily important MWIR and long-wave infrared (LWIR) bands. Varying the  $N \times N$  monolayer (ML) period of the InAs and GaSb material leads to this tuning of wavelength.

InAs/GaSb T2SLs are traditionally grown upon GaSb substrates due to lattice matching of the type-II material on GaSb. However, GaSb substrates are relatively small and expensive compared with GaAs, leading to increased cost. Additionally, the high absorption coefficient of GaSb requires the substrate to be removed prior to use in FPAs.

We present an InAs/GaSb T2SL grown upon a GaAs substrate which operates at room temperature. A room temperature spectral response could be measured for the layer, with responsivity and shot-noise limited specific detectivity ( $D^*$ ) of 0.45 A/W and  $8.0 \times 10^8 \text{ cm}^2/\text{Hz}^{1/2}/\text{W}$ , respectively, at a bias voltage of -0.3V. This uncooled operation  $D^*$  is the best to date compared with the literature for a p-i-n or n-i-p MWIR structure grown upon a GaAs substrate. However, the layer showed a large surface leakage component at room temperature, which did not reduce with temperature. This shows that there is still work to be done on the etching process to make further improvement.

At room temperature, it was found that both the dark current and photocurrent were symmetrical about 0V. This suggests that the photocurrent has very weak dependence upon depletion, implying that photocurrent increases due to another mechanism. We believe that the layer is exhibiting photoconductive behaviour, which is caused by the large background doping, and that increased background doping leads to reduced depletion and therefore photoconductive behaviour. Additionally, cooling of the layer resulted in improvement in responsivity and  $D^*$ . With the weak room temperature dependence on depletion, we believe that this improvement in photocurrent with cooling is from a mechanism other than depletion, and therefore requires further investigation.

## 8899-6, Session 2

### Compact camera technologies for real-time false-color imaging in the SWIR band (Invited Paper)

John Dougherty, Pixelteq, Inc. (United States)

No Abstract Available

## 8899-7, Session 2

### Performance modeling of mid-infrared Cr<sup>2+</sup>:ZnSe thin disk laser

Vishal Saxena, The Univ. of Southern California (United States)

Solid state tunable mid-infrared lasers operating at room temperature have attracted an intensive interest in a variety of spectroscopic and industrial applications like; laser radar; target designation, obstacle avoidance and counter measures, remote sensing; atmospheric constituents and gas trace analysis, and medicine; eye-safe laser

sources for noninvasive medical diagnosis [1, 2, 3]. However, the production of mid infrared laser beams is limited due to availability of laser materials in the 2- 5  $\mu\text{m}$  range. Though, hetero-structures junction diodes, quantum cascade lasers and Cr, Tm, Fe and Ho doped lasers and nonlinear frequency conversion and optical parametric oscillator techniques have been developed in past, there remains an urgent necessity for widely tunable mid infrared sources [3, 4, 5].

Since the early spectroscopic studies by DeLoach and Page, of several II-IV chalcogenides with different transition metal doped ions as potential mid-infrared laser materials, the option, of Cr<sup>2+</sup> ions doped into ZnSe material in becoming most noticeable in the spectral range of 2-3 $\mu\text{m}$  [3]. These lasers can be run at cw mode, and, achieve high peak power via Q-switching or mode locking [3, 4]. However, one of the most important factors that hinders further improvement is the sensitivity of Cr<sup>2+</sup>: ZnSe to the thermal distortion, and temperature dependent nonradiative relaxation [4].

Among various designs proposed to minimize thermal effects, the face cooled thin disk design and a pump spot larger in diameter than the disk thickness has been proposed to reduce the radial thermal gradient responsible for thermal lensing in the active medium. However, reducing the disk thickness beyond certain limit causes the problem of insufficient pump absorption. Cr<sup>2+</sup>: ZnSe material exhibits strong nonradiative relaxation at temperatures greater than 50° C, which in turn significantly reduce upper laser level lifetime and thus laser gain [3, 5].

In this paper, a 'performance modeling' is presented that accounts the factors like bleaching, and temperature dependent nonradiative relaxation responsible for defining the actual temperature profile in thin disk lasers. Model incorporates the compensation for absorption loss for various concentrations of Cr<sup>2+</sup> doping ions in ZnSe, pump powers and beam shapes and the subsequent nonradiative loss due to thermal effects.

## References

- [1] G. J. Wagner and T. J. Carrig, "Power scaling of Cr<sup>2+</sup>: ZnSe lasers" in OSA Trends in Optics and Photonics, Adv. Solid State Lasers, vol. 50, Washington, DC, 2001, pp. 506-510.
- [2] L. D. DeLoach, R. H. Page, G. D. Wilke, S. A. Payne, and W. F. Krupke, "Transition metal doped zinc chalcogenides: Spectroscopy and laser demonstration of a new class of gain media," IEEE J. Quantum Electron., vol. 32, no. 6, pp. 885-895, Jun 1996.
- [3] J. B. McKay, W. B. Roh, and K. L. Schepler, in Conference on Lasers and Electro Optics, (Optical Society of America, 2002), Vol. 73, pp. 119-120.
- [4] A. S. Egorov, O. N. Eremykin, K. Yu. Pavlenko, A. P. Savikin and V. V. Sharakov, "Tunable repetitively pulsed Cr<sup>2+</sup>: ZnSe laser," Quantum Electronics, vol. 42, no. 12, pp. 1106-1110, 2012.
- [5] A. Gallian, V. V. Fedorov, J. Kernal, S. B. Mirov, V. V. Badikov, "Laser Oscillation at 2.4  $\mu\text{m}$  from Cr<sup>2+</sup> in ZnSe Optically Pumped over Cr Ionization Transitions," in Advanced Solid State Photonics 2005 Technical Digest on CD-ROM (Optical Society of America, Washington DC, 2005), MB 12.

## 8899-8, Session 3

### Future directions in photonic integrated circuits for wireless communication and sensing (Invited Paper)

Andreas Stöhr, Univ. Duisburg-Essen (Germany)

The famous statement: "The future is wireless, but with lots of strings attached to it" refers to the fact that an ever increasing number of mobile devices will be used. Naive persons may ask then, why fixed access lines are necessary, as everything is connected wirelessly. But that question omits the fact that an increasing wireless data rate has to be delivered from radio base stations whose reach scales inversely with the data rate. As the data rate per base station increases, copper is no longer suitable for the backhauling of the base station data and fiber optical links have to be installed. This leads to a multitude of users being connected to the optical core network either directly by a fiber connection or via a wireless connection fed by a fiber connection. This scenario of truly converged optical and wireless networks for communications but also for sensing applications is driving the development of a new generation of functional and integrated photonic circuits for enabling seamless signal transmission between the optical and the wireless worlds. The presentation will focus on the



future directions for such integrated photonic circuits. Advanced lasers serving as local oscillators in wireless communications supporting dense WDM will be discussed together with integrated optical modulators and ultra-fast photodiodes providing spectral efficient modulation and direct optical up/down-conversion. Novel photonic integration concepts and approaches enabling photonic-electrical integration will be presented.

### 8899-9, Session 3

#### Arbitrary waveform generation using optical direct digital synthesis (*Invited Paper*)

John E Chester-Parsons, EW Simulation Technology (United Kingdom)

The objective of this paper is to describe the progress of a project designed to build on recent photonic capabilities in order to develop an ultra-wide band, true Arbitrary Waveform Generator (AWG) capable of providing radar quality signals in the 500MHz to 20GHz spectrum using photonic integration. Within this scope, it is planned to create a single channel radar environment simulator based on a photonic waveform generator, which will demonstrate the dynamic range, stability, and high signal fidelity required to simulate the modern complex radar environment. The paper will present recent measurements of critical parameters that are vital for the practical realisation of this system on a chip. A true AWG is an advanced signal generator that can generate a waveform of any shape. The generated waveform can then be used in many applications, from radar signal generation, secure communication systems and reconfigurable software defined radio transmitters. By using photonic advances in ultra-low noise laser generation the AWG will find many applications so far unobtainable by conventional methods. Based on recent work on wide band Radio over Fibre (ROF) photonic links and previous work in the field of integrated Photonic structures, a fully photonic AWG is proposed and its design and trade-offs are discussed in this paper. Photonic integration technologies are of vital importance for creating such a low-cost and high-performance system and the recent advances in photonic architectures, modular laser systems and electronic integration now make this System on a Photonic Chip (SOPoC) a real possibility

### 8899-10, Session 3

#### Advances in AlGaInN laser diode technology for defence applications

Stephen P. Najda, Piotr Perlin, Tadek Suski, Lucia Marona, Michal Bozkowski, Mike Leszczynski, P. Wisniewski, Robert Czernecki, TopGaN Ltd. (Poland); Robert Kucharski, Ammono Sp. z o.o. (Poland); George Targowski, TopGaN Ltd. (Poland); Scott Watson, Anthony E. Kelly, Univ. of Glasgow (United Kingdom)

The latest developments in AlGaInN laser diode technology are reviewed for defence applications such as underwater telecommunications, sensor systems etc. The AlGaInN material system allows for laser diodes to be fabricated over a very wide range of wavelengths from u.v., i.e. 380nm, to the visible, i.e., 530nm, by tuning the indium content of the laser GaInN quantum well. Advantages of using Plasma assisted MBE (PAMBE) compared to more conventional MOCVD epitaxy to grow AlGaInN laser structures are highlighted. Ridge waveguide laser diode structures are fabricated to achieve single mode operation with optical powers of >100mW in the 400-420nm wavelength range with high reliability. Visible light communications at high frequency (up to 2.5 Gbit/s) using a directly modulated 422nm Gallium-nitride (GaN) blue laser diode is reported. High power operation of AlGaInN laser diodes is also reviewed. We demonstrate the operation of a single chip, high power AlGaInN laser diode 'mini-array' consisting of a 3 stripe common p-contact configuration at powers up to 2.5W cw in the 408-412 nm wavelength range. Low defectivity and highly uniform GaN substrates allow arrays and bars of nitride lasers to be fabricated. Packaging of nitride laser diodes is substantially different compared to GaAs laser technology and new processes & techniques are required to optimize the optical power from a nitride laser bar. Laser bars of up to 5mm with 20 emitters have shown optical powers up to 4W cw at

~410nm with a common contact configuration. An alternative package configuration for AlGaInN laser arrays allows for each individual laser to be individually addressable allowing complex free-space and/or fibre optic system integration within a very small form-factor. TopGaN are developing a new range of high power laser array technology over the u.v.- visible spectrum together with new packaging solutions for optical integration.

### 8899-11, Session 3

#### Patterned resistive sheet for infrared microbolometers

Dean P. Neikirk, Hoo Kim, Jong Yeon Park, The Univ. of Texas at Austin (United States); Joo-Yun Jung, Korea Institute of Machinery and Materials (Korea, Republic of)

We present a wide range of absorbers applying patterned resistive sheet for use in mid-wave and long-wave infrared microbolometers. These structures range from wavelength selective dielectric coated Salisbury screen to patterned resistive sheets to stacked multi-spectral devices. For basic three color devices in the LWIR band we have designed and fabricated wavelength selective dielectric coated Salisbury screen (DSS) absorbers suitable for use in microbolometers. In order to produce wavelength selective narrowband absorption, the general design rules for DSS microbolometers show that the thickness of the air gap should be a half wavelength and the optical thickness of the dielectric support layer should be a quarter wavelength. This structure is also air gap tunable; i.e., by varying only air gap thickness, the center wavelength of the absorption curve is shifted. FTIR microscope measurements have been made on a number of the different devices demonstrating three color capability in the LWIR while maintain very high efficiency absorption. We have also shown that the use of a patterned resistive sheet consisting of a properly sized array of cross-shaped holes acts as a polarization independent frequency-selective absorber allowing a three-color system spanning the 7-14 micron band. For realistic metal layers the skin effect produces a complex surface impedance that can be quite large in the LWIR band. We have shown that metal layers of thickness between one and three skin depths can act as the absorber layer, and have shown that thick metal layers can still produce excellent absorption in the LWIR. Holes in the dielectric support layer also reduce the thermal mass in the system without compromising spectral selectivity. Broadband designs using rectangular holes that produce substantially reduced thermal mass (over 50%) while maintaining efficient spectral absorption have also been found. Finally, we have considered multispectral stacked structures, including Jaumann absorbers and stacked dipole/slot patterned resistive sheets. These structures promise either two band (MWIR/LWIR) or two to three color LWIR in a multi-layer stacked pixel.

### 8899-12, Session 3

#### MiSPiA: Microelectronic single-photon 3D imaging arrays for low-light high-speed safety and security applications (*Invited Paper*)

Alberto Tosi, Franco Zappa, Politecnico di Milano (Italy)

We designed and developed fully CMOS compatible SPAD detectors and arrays for 2D imaging and 3D depth-resolved ranging with single photon sensitivity. The SPAD detectors developed show the best-in-class state-of-the-art performance among CMOS SPAD ever reported in literature, with just 100 cps dark-count rate for 30  $\mu$ m diameter SPADs and only 200 kcps for 500  $\mu$ m diameter ones, with extended photon detection probability of 60% at 400nm and still 5% at 850 nm. The two 3D cameras are based on direct and indirect Time-of-Flight, for long- (in the range 200 m – 1 km) and short- (up to 40 m) depth ranges respectively. The former imager is based on 32x32 smart pixels with SPAD and 300ps in-pixel TDC, capable of 5 cm single-shot depth resolution, further improved after repetitive high-rate acquisitions. The latter imager is a 64x32 array of pixels with 30 $\mu$ m SPADs, able to reconstruct the distances through phase-resolved photon counting of either pulsed-light or continuous-wave modulated illumination of the scene, with 9 bit dynamics and centimeter resolution. The CMOS SPAD imagers are able to process at pixel-level both intensity-data

(for 2D imaging) and depth-information (for 3D ranging) of rapidly changing scenes in light-starved environments. In fact we present the results obtained in two different applications: high frame-rate (above 200 imager per second) short-range 3D ranging cameras for prompt intervention in front- and back- pre-crash Safety systems in Automotive field; long-range 3D ranging systems for Security surveillance. These CMOS SPAD cameras can be further disseminated and exploited to wider communities and markets, in Safety (e.g. environmental surveillance, traffic and workplace safety monitoring, product safety analysis, food and agriculture quality and safety assessment) and Security (access control, biometrics, surveillance systems, dangerous agents monitoring, homeland security, fire hazards) applications, but also in microscopy, biology, adaptive optics.

8899-13, Session 4

### Emerging active electro-optics (*Invited Paper*)

Gary W. Kamerman, FastMetrix, Inc. (United States)

Laser Remote Sensing has been an emerging military technology for the last 30 years. Although active electro-optics technology has revolutionized the battlefield, its full impact is not widely understood and its significance is largely undervalued. Emerging active electro-optical technologies are nearing the point where they may revolutionize the battlefield and homeland defense again. Failure to anticipate these technologies could result in technological surprise with severe consequences. A recent study undertaken by the United States National Academy of Sciences has concluded that the defense and homeland security of many countries are vulnerable to these advances. The Academy has also attempted to evaluate the magnitude of the effects of these new technologies on homeland security and defense. This paper will review those conclusions and provide an outlook for future developments.

8899-14, Session 4

### Technologies for blue-green underwater optical communications (*Invited Paper*)

Richard C. Hollins, Defence Science and Technology Lab. (United Kingdom)

The paper will examine the potential of emerging technologies for a simpler, cheaper approach to underwater optical communications. A blue-green diode laser has been demonstrated at the wavelength of a Fraunhofer line, within which the daylight background is reduced. Fibre laser and other architectures offer the potential of scalability to higher power levels. Sensitive detection based on wide-gap semiconductor photodiodes and photon counting offers the prospect of reducing laser power requirements. The spectral widths of the Fraunhofer lines and the candidate lasers and spectral filters influence the selection of an optimum operating scheme, particularly in the presence of scattered light which affects the duration of optical pulses and the effective bandwidth of some filters

8899-15, Session 4

### Design of high sensitivity detector for underwater communication system

Jeng Shiuh Cheong, The Univ. of Sheffield (United Kingdom); Jennifer S. Ong, Univ. Malaysia Perlis (Malaysia); Jo Shien Ng, Andrey B. Krysa, Faebian Bastiman, John J. P. David, The Univ. of Sheffield (United Kingdom)

Underwater communication systems that rely on light transmission should operate in the range of 470-500 nm due to their good transmittance in seawater at these wavelengths. While silicon photodiodes can comfortably cover this wavelength range, their wide spectral response makes them susceptible to light from extraneous sources such as the sunlight. We report on a high sensitivity detector that has an intrinsic narrow spectral response around 486.1 nm which corresponds to the Fraunhofer H-Beta line, where there is a very low solar background.

III-V compound semiconductors can be chosen to naturally cover the 470-500 nm wavelength range with a good responsivity but also with a narrow spectral response. Without using any filters, an Al<sub>0.8</sub>Ga<sub>0.2</sub>As homo-junction p<sup>+</sup>-i-n<sup>+</sup> has a narrow full width half maximum (FWHM) of 47 nm with a peak response at 487 nm. A combination of GaInP-AllnP p<sup>+</sup>-i-n<sup>+</sup> photodiode can provide a peak response of 480 nm and a FWHM of 45 nm at room temperature. More recently, we showed an AllnP homo-junction p<sup>+</sup>-i-n<sup>+</sup> could provide a much narrower FWHM of 22 nm with similar peak response.

A spectral response model showed that a narrow FWHM could be obtained from a homo-junction p<sup>+</sup>-i-n<sup>+</sup> with a thick p<sup>+</sup> cladding, however at the expense of a reduced quantum efficiency.

The poor sensitivity due to the thick p<sup>+</sup> cladding can however be improved through an avalanche process. High gains up to 100 can be obtained in a simple AllnP homo-junction p<sup>+</sup>-i-n<sup>+</sup>. In this work, we report on an AllnP homo-junction Separate-Absorption-Multiplication Avalanche Photodiode (SAM-APD). The SAM-APD utilises a thick absorption region of 1.0 μm to improve the peak quantum efficiency without compromising the narrowness of the spectral response FWHM. Such a structure offers a very low dark current, high sensitivity photodiode at around 486.1 nm with a narrow spectral response FWHM.

8899-16, Session 4

### Stretchable optics

Luca Ravagnan, WISE S.r.l. (Italy); Cristian Ghisleri, WISE S.r.l. (Italy) and Univ. degli Studi di Milano (Italy); Marco A. C. Potenza, Mirko Siano, Univ. degli Studi di Milano (Italy); Paolo Milani, WISE S.r.l. (Italy) and Univ. degli Studi di Milano (Italy)

The integration of diffractive optical elements on stretchable substrates opens the way to the realization of a completely novel class of stretchable photonics systems, characterized by the ability of changing their optical properties upon modification of their shape due to tensile or compressive strain and to be highly conformable to complex surfaces [1]. The interest in such devices is tremendously increasing driven by the need of bio-mimicking adaptive optical devices. Several attempts have been already made to fabricate stretchable diffracting optical elements by depositing reflective metallic films on gratings embossed on PDMS [2]. The bad adhesion of the metallic layer degraded the optical quality of the diffraction grating even upon a very small deformation [2].

Here we present an effective approach to the fabrication of diffractive stretchable optical components, based on Supersonic Cluster Beam Implantation (SCBI) [3]. A stretchable diffraction grating is obtained by replicating the structured surface of a rigid grating on PDMS. The optically active side is then implanted with silver nanoparticles by means of SCBI, in order to create a nanocomposite reflective layer with a thickness of tenths of nanometers. The extremely good resilience upon deformation of the silver-PDMS nanocomposite allows maintaining extremely good optical performance upon substantial deformation of the grating and a large number of deformation cycles.

Optical characterization at a single wavelength shows a good linear proportionality between the stretching of the implanted device (25% stretching) and the decrease of the diffraction angle at the first diffraction order, as expected, due to the increase of the grating pitch. The optical quality of the diffracted beams is good after hundredths of cycles of stretching. As a comparison, a PDMS grating obtained by thermal evaporation of silver atoms shows a poor optical quality prior to stretching because of the observed cracking of the rigid reflecting coating and an increase in intensity of two transversal diffracted spots with a worsening of the diffracted beams quality after few stretching cycles. AFM analysis demonstrates that the implanted grating maintains the diffractive structure of the PDMS replica, while the evaporated one presents many cracks in the reflective layer, mainly in the transversal direction respect to the grooves direction, and a deterioration of the grooves profile.

These results indicate that SCBI is an enabling tool for the fabrication of diffracting optical components on soft, stretchable and highly conformable substrates, preserving their optical properties and qualities after extensive cycles of stretching.

[1] Simonov A.N., et al., Optics Expr. 2007, 15, 9784-9792

[2] Wilbur J.L. et al., Chem. Mater. 1996, 8, 1380-1385.

[3] Corbelli et al., Adv. Mater. 2011, 23, 4504-4508.

# Conference 8899B: Quantum-Physics-Based Information Security II

Monday - Tuesday 23–24 September 2013

Part of Proceedings of SPIE Vol. 8899 Emerging Technologies in Security and Defence; and Quantum Security II; and Unmanned Sensor Systems X

8899-20, Session 5

## How secure is quantum cryptography? (Invited Paper)

Renato Renner, ETH Zurich (Switzerland)

No abstract available

8899-21, Session 5

## Essential elements lacking in security proofs for quantum key distribution (Invited Paper)

Horace P. Yuen, Northwestern Univ. (United States)

All the currently available (unconditional) security proofs on quantum key distribution, in particular for the BB84 protocol and its variants including continuous-variable ones, are invalid or incomplete at many points. In this paper we indicate most of the known problems and discuss some of them. Most fundamentally, the generated key is not uniform with probability one, contrary to the prevalent claim in the literature that it is uniform with a high probability. What requirements are then needed for operational security guarantee when the key is not uniform? This basic issue is addressed systematically here for the first time. Other serious issues of a mathematical or physical nature in the security proofs will be brought out. Comments will be made on the principal security claims of current experimental cryptosystems. The major problem of model completeness brought into focus by detector blinding attacks will be discussed. It appears that a provably secure system is not in sight just theoretically. Some implications will be drawn.

8899-22, Session 5

## Hacking attacks on quantum cryptography (Invited Paper)

Vadim Makarov, Inst. for Quantum Computing, Univ. of Waterloo (Canada)

Quantum key distribution, although absolutely secure in theory, is currently under assault from hackers. They break its security via practical attacks that exploit imperfections in components and implementations of opto-electronic hardware. The issue of implementation security is well-known in classical cryptography, however it proved to be somewhat of a surprise to the quantum cryptography community when it became apparent several years ago. I will give a brief overview of the current situation, give examples of recent attacks and countermeasures, and explain how quantum cryptography research and manufacturing community handles this issue.

8899-23, Session 5

## Quantum key distribution: vulnerable if imperfectly implemented (Invited Paper)

Gerd Leuchs, Friedrich-Alexander-Universität Erlangen-Nürnberg (Germany)

In quantum cryptography (QC), if an adversary, Eve, attempts to eavesdrop on the secret key exchange between two legitimate parties, Alice and Bob, then she inevitably introduces errors that may reveal her presence. This inevitability, based on the principles of quantum mechanics, is at the heart of all QC protocols. The protocol itself is encompassed by a theoretical model which ultimately defines and describes a quantum key distribution (QKD) system and upon which any security proof is based. Therefore, if this theoretical model is not

correctly implemented in practice, or if it fails to provide a complete description of the physical implementation, loopholes may arise that allow Eve to successfully breach the security of the QKD system. All well-known loopholes that have been exploited in proof-of-principle 'quantum hacking' experiments were either the result of technological deficiencies or operational vulnerabilities. Here, we shall discuss some of these recent experiments pursued at MPL Erlangen (in collaboration with Vadim Makarov's Quantum Hacking group). While all the attacks were done on the commercial QKD system 'Clavis2' from ID Quantique, the latest attack has also been applied to a home-built continuous variable (CV) QKD system. We shall discuss the hacking of a vulnerability in the calibration sequence run by Clavis2 to synchronize the Alice and Bob devices before performing the secret key exchange. This hack induces a temporal detection efficiency mismatch in Bob that can allow Eve to break the security of the cryptosystem using faked states. We also experimentally investigated the superlinear behaviour in two types of single-photon detectors (SPDs): avalanche photodiodes and superconducting detectors. Due to this superlinearity, the SPDs feature an actual multi-photon detection probability which is generally higher than the theoretically-modelled value. We show how this increases the risk of detector control attacks on QKD systems employing such SPDs. Finally, we review the experimental feasibility of Trojan-horse attacks. On Clavis2-Bob, the objective is to read Bob's phase modulator to acquire knowledge of his basis choice as this information suffices for constructing the raw key in the Scarani-Acin-Ribordy-Gisin 2004 (SARG04) protocol. We are also implementing this attack on a home-built CVQKD system to read Alice's random modulation. We routinely notified ID Quantique in advance about all these loopholes. Also, wherever possible, we proposed patches, so that suitable countermeasures could be implemented.

8899-24, Session 5

## Polarity inversion attack prevention by physical properties of Y-00 quantum stream cipher

Takehisa Iwakoshi, Osamu Hirota, Tamagawa Univ. (Japan)

Y-00 protocol was proposed by H. P. Yuen [1] in 2000 to hide even ciphertexts from eavesdroppers under quantum noise of coherent light. Then prototype systems were developed using Phase-Shift-Keying (PSK) [2] and Intensity-Shift-Keying (ISK) [3]. Theoretical security analyses and proposals of security enhancements have been made. However, a polarity inversion attack has not studied enough. The definition of the attack is as follows:

Definition: A polarity inversion attack is an attack where the attacker in the middle of the communication line intercepts known messages from the legitimate sender and resends false messages to the legitimate receiver by inverting signal polarities.

In the field of mathematical ciphers, message falsification is recognized as a major issue. Therefore, it is useful to study if it can be prevented physically by the Y-00 systems.

Recent studies showed that ISK Y-00 systems can prevent the attack probabilistically [4, 5]. Here is a brief explanation. By a basic ISK Y-00 system, the legitimate sender Alice and the legitimate receiver Bob share a secret M-ary running key. Alice chooses a pair of signals based on the running key. This pair corresponds to the pair of plaintext  $x = 0$  or  $1$ . Then Alice sends a signal based on plaintext  $x$ . Bob discriminates 0 and 1 by a threshold based on the running key  $k$ .

Suppose that the attacker Eve can intercept the signals without any losses. In most cases, Eve can falsify the plaintext  $x$  by resending the opposite polarity of the signal. However, if the signal intensity Alice sent is nearly the average intensity, Eve fails in polarity inversions [4, 5]. The average probability where Eve fails in the attack is about 5.6%.

To enhance the probability to about 66.7%, the quadruple-signal-based Y-00 is proposed, where the Alice and Bob communicate based on sets of 4 signal intensities. These signal intensities corresponds to quad-ary plaintext by referring a look-up table [6].

Numerical analysis has not made yet. Thus our manuscript will show numerical prevention property against the attack.

References

- [1] H. P. Yuen, arXiv:quant-ph/0311061 Nov. 2003
- [2] G. A. Borbosa, E. Corndorf, G. S. Kanter, P. Kumar, and H. P. Yuen, Phys. Rev. Lett., vol. 90, num. 22, 2003, Art. ID 227901
- [3] O.Hirota, M.Sohma, M.Fuse, and K.Kato, Phys. Rev. A, 72, 022335, 2005
- [4] T. Iwakoshi, O. Hirota, IEICE Tech. Rep., vol. 110, no. 281, ISEC2010-57, pp. 51-55, Nov., 2010 (in Japanese)
- [5] T. Iwakoshi, Tamagawa University Quantum ICT Research Institute Bulletin Vol.1 No.1, 2011
- [6] T. Iwakoshi, Tamagawa University Quantum ICT Research Institute Bulletin vol.2 no.1, 2012

**8899-25, Session 5**

**Saturation attack on continuous-variable quantum key distribution system**

Hao Qin, Rupesh Kumarps, Romain Alléaume, Telecom ParisTech (France)

Continuous-variable (CV) quantum key distribution (QKD) is proven secure against collective attacks and recent works have shown progress in proving security against arbitrary attacks [1]. Nevertheless the validity of security proofs relies on assumptions that may be violated in practical setup, opening loopholes that may be exploited to mount attacks. For example direct [3] or indirect [4] manipulation of Local oscillator (LO) intensity can fully compromise the security. This imposes to monitor LO intensity and to use filters to forbid wavelength-dependent LO intensity manipulations.

We study here the consequences of detection saturation in a practical CV QKD setup, and more precisely prove that it can lead to an attack on the Gaussian-modulated coherent state protocol [2] with homodyne detection. A fundamental assumption in the security model is that Bob's quadrature measurement is supposed to vary linearly with the quadrature value sent by Alice. This assumption does not hold if Bob's homodyne detection saturates.

Saturation typically occurs when the input field quadrature overpasses a threshold that depends on parameters of detector's electronics, such as the amplifiers linearity domains or the data acquisition card range. The important point is that saturation can always be induced by displacing the field quadratures strongly enough. We have experimentally confirmed this prediction by observing saturation of our homodyne detection for high local oscillator intensity.

We have moreover constructed an attack that combines the intercept-resend (IR) attack with saturation of Bob's detector. The key idea in this attack is that saturation can be induced by strongly displacing the mean value of the field quadratures received by Bob. Indeed, we have shown that by controlling the displacement value, Eve could bias the evaluation of the excess noise to arbitrarily small values.

Our saturation attack strategy is then simple: Eve implements a full IR attack and gets knowledge of both quadratures from Alice. She then resends a state whose quadratures consist in her measurement results combined with a strong displacement. A full IR attack normally introduces two shot noise units of excess noise, which would reveal the presence of Eve. However, due to saturation of detector, the excess noise evaluation can be biased to an arbitrary low value by Eve. Under such attack, Alice and Bob may be led to believe they share some positive "secret key" rate and accept keys that are however totally insecure.

Our saturation attack is achievable with current technology and impacts the security of a practical CV QKD system. It highlights the importance of exploring the assumptions in security proofs when implementing QKD protocol on practical setups. We have proposed a counter measure that consists in monitoring quadratures mean value and are working on its integration to the security model, so that practical implementations could effectively protect themselves against saturation-based attacks.

- [1] A. Leverrier, et al. , Phys. Rev. Lett. 110, 030502 (2013).
- [2] F. Grosshans, et al. , Nature. 421, 238 (2003).
- [3] H. Häselser, et al. , Phy. Rev. A. 77, 032303 (2008).
- [4] J.-Z. Huang, et al. , arXiv:1302.0090v1 (2013).

**8899-26, Session 6**

**Practical QKD (Invited Paper)**

Andreas Poppe, AIT Austrian Institute of Technology GmbH (Austria)

No Abstract Available

**8899-27, Session 6**

**Continuous QKD and high speed data encryption (Invited Paper)**

Hugo Zbinden, Univ. of Geneva (Switzerland)

We present the results of the project QCRYPT, a collaborate effort of eight research teams in Switzerland with the ambition to produce a complete and practical fiber based QKD and high speed encryption system. For the QKD part, we put the emphasis on continuous operation with a wavelength multiplexed service channel for synchronization and distillation, efficient hardware real-time distillation, finite key security analysis and frugal authentication. For the secure high-speed encryption of large data volumes, we developed a system able to multiplex up to ten 10 Gbit/s Ethernet inputs, pass the 100 Gbit/s data stream through authenticated encryption before transmitting it over an optical fiber to the decryptor. The cipher cores apply and frequently refresh the quantum keys delivered by the QKD system.

**8899-28, Session 6**

**Notes on Evanescent Wave Bragg-Reflection Waveguides (Invited Paper)**

Benedikt Pressl, Univ Innsbruck (Austria); Gregor Weihs, Univ. Innsbruck (Austria)

For fundamental tests of quantum physics as well as for quantum communications non-classical states of light are an important tool. We will present two approaches towards semiconductor-based and integrated sources of single photons and entangled photon pairs.

In the first approach we demonstrate efficient photon pair generation in an AlGaAs Bragg-reflection waveguide. Spontaneous parametric down-conversion creates photon pairs at telecommunication wavelengths. The various phase-matching solutions present in our device can be used to create time-bin or polarization entanglement. This approach can lead to a fully integrated photon pair source with the pump laser, active and passive optical devices all on a single semiconductor chip.

In our second approach we use resonant two-photon excitation of a single InAs/GaAs quantum dot to deterministically trigger a biexciton-exciton cascade. We demonstrate Rabi oscillations, Ramsey interference and all-optical coherent control of the quantum dot resulting in single and paired photons with a high degree of indistinguishability. This indistinguishability results in time-bin entanglement, which is a useful variant for long distance communication.

**8899-29, Session 6**

**Towards a high-speed quantum random number generator**

Damien Stucki, id Quantique SA (Switzerland); Samuel Burri, Edoardo Charbon, Ecole Polytechnique Fédérale de Lausanne (Switzerland); Christopher J. Chunnillall, National Physical Lab. (United Kingdom); Alessio Meneghetti, Univ. degli Studi di Trento (Italy); Francesco Regazzoni, Technische Univ. Delft (Netherlands)

Random numbers play an important role in a number of applications such as cryptography, numerical simulations or the gaming industry. There are two types of random number generator: software- and physical random number generators. The first type is implemented on

**Conference 8899B:  
Quantum-Physics-Based Information Security II**

computers which are deterministic. So for a given input, the output will always be the same. The second type relies on classical or quantum physical processes. Random number generators based on classical physics are fundamentally deterministic – as is classical physics – even if the complexity of the system can hide the determinism. Random number generators based on quantum physics are true random number generators as quantum physical phenomena are intrinsically random.

In cryptographic applications, random numbers are vital in applications which ensure confidentiality and authentication. To ensure the confidentiality of a message, a clear-text message is encrypted using a key. The quality of random numbers is vital to guarantee the strength of the key, and thus the security of the cipher. As always in the field of cryptography, random numbers are also necessary to ensure the authenticity of communications by providing material for secret authentication keys. One other application of random numbers is for numerical simulations. For instance, Monte Carlo simulations require high bit rates of high-quality random numbers. The gaming and lottery industry also requires high quality random numbers to guarantee a uniform winning probability for all players. For all these applications, high-speed and high quality random number generators are required.

The presented quantum random number generator is based on a matrix of single photon detectors (Swiss NCCR FastQ project). The detector matrix is illuminated by a low intensity source of photons. During the propagation between source and detectors, the photon behaves as a wave and is described by a wave-function. Then the photon will collapse randomly in the plane of the detectors. Thus the detectors in the array will randomly click and generate a raw bit sequence. The generation of the random bit sequence can be obtained by pairing neighbouring detectors and keeping only the case in which exactly one detector among the two detectors clicks. The bit value '1' ('0') is associated to a detection in the 'first' ('second') detector of the pair. Another possibility to extract a random bit sequence from the detection sequence is to evaluate the entropy of the sequence and then apply an extractor algorithm to generate the random sequence.

To well understand the behaviour of the quantum random number generator, a model has been developed. In the model, various parameters were included: the dark count of the detector, the afterpulsing probability, the detection efficiency, the cross-talk probability and the light distribution. Finally the model assumes that the quantum random number generator is a Markov chain of order 1. The entropy and the collision entropy rate are computed from the model, which can be compared with the entropy computed from the raw sequence. To precisely estimate the values of the input parameters, measurements have been made in collaboration with European National Metrology Institutes through the European Metrology Research Programme (EMRP) project IND06-MIQC.

**8899-30, Session 6**

**Truly Random Number Generation: An Example**

Daniela Frauchiger, Renato Renner, ETH Zurich (Switzerland)

The generation of good random numbers is not only of academic interest but also of practical importance: For example it is well known that the use of strong Random Number Generators (RNGs) is essential to guarantee the security of RSA encryption systems. True randomness is also needed in quantum cryptography, numerical simulations and in statistics.

How can we prove that the output of a RNG is indeed random? First, we need to agree on a definition of randomness. For an infinite string one possibility is to directly define the corresponding randomness by its Kolmogorov complexity, which is given by the length of the shortest possible description of the string in some fixed universal description language. However, we are dealing with finite strings, for which the Kolmogorov complexity is no longer uniquely defined. Moreover, it is not computable.

Here we use a different approach where, instead of the concrete sequences generated by a RNG, we consider the process that generates them. A natural definition for a process to be truly random is that its outcome is not predictable from any information available before the process has been started. The advantage of using quantum systems for random number generation compared to classical

approaches lies in the fact that the unpredictability of the randomness can be proven based on physical principles. Moreover, a recent result implies that the unpredictability is not only guaranteed within quantum mechanics but also within any extension. In practice however, due to imperfections of the devices, the resulting raw randomness also depends on classical noise and therefore does not fulfil this definition either.

We provide a framework for generating almost perfect true randomness using noisy devices by appropriate post-processing (hashing) of the raw randomness. Compared to previous work on random number generators (RNGs), we take this noise into account as side information, which is necessary to meet the above definition of true randomness.

The idea is to model the device by separating it into two parts: One part corresponds to the quantum measurement and is described by a random variable  $Q$ . The second part includes all the processes contributing to the noise that we want to eliminate and is associated with a random variable  $R$ . The raw randomness  $X(Q,R)$  is a function of both  $Q$  and  $R$ . The Leftover Hash Lemma with Side Information asserts that the output  $f(X)$  of a suitable function  $f$  of  $X$  is arbitrarily close to random. This function is chosen randomly from a set of two-universal hash functions that map  $l$ -bit strings to  $m$ -bit strings. The compression rate (more precisely, the parameter  $m$ ) is determined by the conditional min-entropy  $H_{\min}(X|R)$  of  $X$  given  $R$ .

Our approach assumes that the process generating the raw randomness is correctly described by a quantum model. Compared to device-independent randomness expansion, this has the advantage of being practical (it is applicable to commercially available devices) and does not require pre-existing randomness. We stress, however, that our results do not rely on any completeness assumption regarding the model or quantum theory.

We illustrate our proposal for a Quantum Random Number Generator (QRNG) based on a beam splitter and show how the post-processing procedure used in some of the current devices can be improved.

**8899-31, Session 7**

**QKD over long distances with trusted and untrusted repeater nodes (Invited Paper)**

Norbert Lütkenhaus, Will Stacey, Razieh Annabestani, Univ of Waterloo (Canada); Xiongfeng Ma, Center for Quantum Information, Institute for Interdisciplinary Information Sciences, Tsinghua Unive (China)

Traditional point-to-point QKD technology has a distance limitation when implemented over optical fibers or free-space links. There are two approaches to overcome this challenge: one can build quantum repeater networks, for which we currently develop the technology, or one can build trusted repeater stations to extend the distance.

We will concentrate here on approach of trusted repeater networks. We will discuss how Simplified Trusted Nodes [1] can reduce the workload on intermediate nodes. In a usual implementation, intermediate nodes need to do significant data processing for the purpose of error correction and privacy amplification to arrive at two secret keys which are shared with their respective nearest neighbors. This step is then followed by an announcement that joins these two keys to a key shared by the neighbors directly, thus ultimately generating secret keys between the end nodes. In our variation of the protocol, we connect the neighbors on the level of raw data, and only the end users need to do data processing to obtain a final key.

We perform a complete security analysis of the system based on the framework developed by R. Renner, using the symmetry of the underlying point-to-point systems to find analytic secret key rates of our systems.

We will discuss the implications of this new work for satellite QKD and fiber based networks. We will contrast this approach with recent developments in the domain of quantum repeater technology.

[1] WIPO patent application WO 2013/037062 A1 (March 21, 2013) "System and Method for Quantum Key Distribution"

8899-32, Session 7

### Protocols and prospects for building a quantum repeater (*Invited Paper*)

Peter van Loock, Johannes Gutenberg Univ. Mainz (Germany)

An overview will be given of various approaches to implementing a quantum repeater for quantum communication over large distances. This includes a discussion of systems and protocols that are experimentally feasible and thus realizable in the midterm in order to go beyond the current limit of a few hundred km given by direct quantum-state transmissions. At the same time, these schemes should be, in principle, scalable to arbitrary distances.

In this context, the influence of various elements and strategies in a quantum repeater protocol on the final fidelities and rates shall be addressed: initial entanglement distribution, Bell measurements, multiplexing, postselection, quantum memories, and quantum error detection/correction. Solely on the hardware side, the differences in using just single quanta or instead employing many quanta for the flying (photons) and the stationary (atoms) qubits will be pointed out.

8899-33, Session 7

### Quantum access networks (*Invited Paper*)

Zhiliang L. Yuan, Bernd Froehlich, James F. Dynes, Marco Lucamarini, Andrew W. Sharpe, Andrew J. Shields, Toshiba Research Europe Ltd. (United Kingdom)

Quantum access networks will in the future allow access to quantum key distribution (QKD) services – verifiable secure transmission of cryptographic keys<sup>1,2</sup> – to a multitude of users. However, so far no convincing answer has been given to the question of how to realise these quantum networks in practice. Dedicated point-to-point links between the service node and each user would make access to the QKD infrastructure prohibitively expensive for most applications. Other proposals, such as sharing a common transmitter between multiple receivers,<sup>3</sup> still require adding a single-photon detector per user and therefore do not overcome one of the main obstacles restricting the widespread use of QKD.

Here we propose and demonstrate a novel network architecture which allows to overcome this restriction. Using an upstream approach, in which a common receiver at the local exchange is shared between multiple transmitters positioned at the users' premises, we are able to show that we can share a high speed single-photon detector between up to 64 users and therefore significantly reduce the hardware requirements for each added user. We develop independently operating quantum transmitters which pre-compensate phase and polarisation fluctuations for stable and high rate key exchange with the quantum receiver and demonstrate operation of the network using both passive optical splitters and wavelength-division multiplexing components. Furthermore, a detailed study of the cross-talk between the transmitters allows us to show that networks with a capacity of up to 64 users are feasible. Our results for the first time present a viable method for realising multi-user QKD networks and therefore greatly broaden the appeal of this technology.

[1] N. Lütkenhaus & A. J. Shields, *New Journal of Physics* 11, 045005 (2009).

[2] V. Scarani et al., *Reviews of Modern Physics* 81, 1301 (2009).

[3] P. D. Townsend, *Nature* 385, 47 (1997).

8899-34, Session 7

### Towards continuous-variable quantum key distribution in atmospheric channels

Vladyslav C. Usenko, Palacký Univ. Olomouc (Czech Republic)

Quantum key distribution (QKD) is aimed at providing two trusted parties with the methods (protocols) to share a secure key, which can be lately used for one-time pad classical cryptosystem. While the first ideas and implementations in the field of QKD were based on the discrete-variable coding using qubits (two level quantum systems), implemented as single photons or weak coherent pulses, the recent developments in QKD are concerned with the continuous-variable (CV) coding using quantum systems with infinite-dimensional

state spaces (practically implemented as multi-photon pulses of coherent, squeezed or entangled light modes). The main family of CV QKD protocols is based on Gaussian encoding using quadrature observables of a light mode so that the extremality of Gaussian states can be used to show the optimality of Gaussian collective attacks and to assess the security of the protocols in the conditions of a particular quantum channel (inclined to loss and untrusted noise, which limits the security), and devices. CV QKD protocols are well studied in case of the fixed channels, which correspond to the fiber-type links. In such channels attenuation and noise can be considered stable during the transmission and security bounds on the channel parameters can be estimated. Alternatively, CV QKD can potentially be implemented using free-space channels, in which atmospheric effects such as turbulence result in the fluctuations of transmittance. Such implementation is especially important because it waives the necessity in the existing fiber-optical infrastructure and also potentially allows truly-long distance extraterrestrial quantum communication through a satellite. Thus, in our work we study the possibility to perform CV QKD over atmospheric channels, taking into account the channel fluctuations caused by the turbulence. We show that effect of fading can be expressed as modulation-dependent channel noise and derive the bounds on Gaussian security and entanglement of the states in such fading channels in the general case. We also consider the particular type of mid-range channels, where transmittance fluctuations are mostly caused by beam wandering around the receiver aperture. We show the trade-off between the spot size and strength of wandering fluctuations such that spatial filtering can be potentially helpful for quantum communication. Further, we propose the method of post-selection of fixed sub-channels and show that it is able to restore the security and entanglement properties of Gaussian states after the fading channels. We check our results in conditions of the real atmospheric channel, which was experimentally characterized by the relative intensity measurements. We confirm the possibility to restore the security of the protocol by post-selection after such real atmospheric channel. In particular, we show that optimal post-selection combined with optimal state modulation allows significant improvement of the robustness to noise of the coherent-state based CV QKD over the fading channel. We also discuss the role of nonclassicality of the signal states in the case of fluctuating channels. Finally, we address the finite-size effects and imperfect channel estimation upon sub-channel post-selection and show the stability of our results against the reduction of the data ensemble size caused by the optimal post-selection.

8899-35, Session 7

### Unambiguous state discrimination approach to experimental photonic quantum digital signatures in fiber

Ross J. Donaldson, Robert J. Collins, Heriot-Watt Univ. (United Kingdom); Vedran Dunjko, Edinburgh Univ. (United Kingdom); Partick J. Clarke, Erika Andersson, Heriot-Watt Univ. (United Kingdom); John Jeffers, Univ. of Strathclyde (United Kingdom); Gerald S. Buller, Heriot-Watt Univ. (United Kingdom)

As society becomes more reliant on electronic communication and transactions, ensuring the security of these becomes more important. Digital signatures are a form of cryptography which allows parties to certify and authenticate the origins of their communications, meaning that one party, Alice, can send information to other parties in such a way that the other parties can authenticate Alice's communication. Classical digital signatures may be based on the Rivest, Shamir and Adleman (RSA) algorithm, with security depending on the difficulty of determining the prime factors of a large number. The security of RSA depends on how quickly large numbers can be factorized. Ways of factorizing include the use of brute force attacks (trying every different combination of numbers) and improved algorithms. With increasing computing power, the use of more efficient algorithms and the possibility of quantum computers, RSA is at risk of becoming too insecure to use.

Quantum digital signatures (QDS) are the quantum analogue of digital signatures and offer the potential for increased information security. Our system uses an in-fiber network of interferometers (multiport) to perform non-demolition comparison between signature states sent from Alice to two parties, Bob and Charlie. These signatures are encoded at a clock rate of 100 MHz in the phase of coherent states and the choice of photon number, signature length affects the level of

security possible by this approach.

We have previously presented what is, to the best of our knowledge, the first experimental implementation of QDS. In that system, Alice phase-encodes coherent states to be detected by Bob and Charlie who used an active method of demodulation. The asymmetric interferometers used at Bob and Charlie employed a phase modulator which allowed them to actively select a demodulation phase-shift for a particular phase state sent by Alice. In our revised experiment Bob and Charlie use a passive method of demodulation called unambiguous state discrimination, meaning they employ a fixed asymmetric Mach-Zehnder interferometer for each phase state in Alice's encoding, thus allowing them to avoid using quantum memory. This is the first time unambiguous state discrimination has been applied to QDS. In addition, the revised set up also features polarization routing in the Alice's, Bob's and Charlie's interferometers, which prevents photons from taking non-interfering paths, thereby significantly reducing the losses of our system.

We will present results from the QDS system employing passive demodulation using unambiguous state discrimination, in which Alice is sending a sequence of phase states, each of them chosen from four different states, through the multipoint to Bob. Because Alice may choose between four different phase states, Bob uses four asymmetric Mach-Zehnder interferometers, each one is locked to measuring one phase state. Bob also monitors his multipoint in order to track any cheating by Alice. The signature state pulse rates at Bob and the errors in his measurements will be presented. The mean photon number per coherent state has been controlled and varied to show how security is affected and these results will also be presented.

8899-36, Session PS

### **The simple theoretical analysis of quantum well wires superlattice (QWSL) of communication technology**

Subhamoy Singha Roy, JIS College of Engineering (India)

The thickness and the doping dependences of the field emission from all the aforementioned cases have been studied for the purpose of relative comparison, taking GaAsP<sub>1-y</sub> and AlAs lattice matched to InP quantum wire superlattice (QWSL) as an example.

8899-38, Session PS

### **The accurate measurement of photon orbital angular momentum carried by helical beams through amplitude computer-generated hologram**

Zheng Wang, Beijing Institute of Space Mechanics and Electricity (China); Jingtao Xin, Beijing Institute of Technology (China); Yue Zhang, Beijing Institute of Space Mechanics and Electricity (China)

The photon orbital angular momentum (OAM) carried by helical beams can be used as an information carrier of the quantum cryptographic communication which is fast developing as an absolutely safe key distribution technology in recent years. A new method is proposed to accurately measure the photon OAM carried by helical beams through the amplitude computer-generated hologram (CGH) loaded on a liquid crystal display spatial light modulator (LCD-SLM). In order to study the diffraction process of different beams passing through the variety of diffractive optics generated by CGH, an interface was designed and developed using the GUI module of the MATLAB software. With the help of plane wave angular spectrum diffraction formula and Collins formula, this interface could simulate the diffraction processes of Hermite-Gaussian beams, Laguerre-Gaussian beams and Bessel beams with different orders passing through the parameters adjustable diffractive optics such as circular aperture, triangular aperture, Young's double-slit, phase gratings, helical phase plate and etc. Then the propagation property of helical beams passing through Young's double-slit and triangular aperture is studied by theoretical simulation and experiment, and the measurement of photon OAM carried by helical beams is also achieved with those two amplitude diffractive optical elements. Due to the fact that changing and controlling the CGH loaded into the SLM is able to flexibly and accurately change the

configuration, dimension and location of diffractive optical elements, the accurate measurement can be conveniently achieved.

8899-39, Session PS

### **Determination of conduction band tails in heavily doped semiconductor by quantum modeling**

Subhamoy Singha Roy, JIS College of Engineering (India)

The band tail diffusion energy decreases with increasing film thickness in an oscillatory manner under (quantum wells, quantum well wires) size quantization. Now the present theory exhibits better conformity with experimental result than that of the conventional come up to of influential the band tail diffusion energy for optical and optoelectronic compounds having arbitrary band structure [1-7].

8899-40, Session PS

### **Demonstrating feasibility of a Trojan-horse attack on a commercial quantum cryptosystem**

Nitin Jain, Imran Khan, Christoffer Wittmann, Max Planck Institute for the Science of Light (Germany); Elena Anisimova, Vadim Makarov, Insitute for Quantum Computing, University of Waterloo (Canada); Christoph Marquardt, Gerd Leuchs, Max Planck Institute for the Science of Light (Germany)

An optical pulse launched into a network of optic and optoelectronic components, e.g., a quantum key distribution (QKD) system, encounters several sites of Fresnel reflection (and specular reflection, in case mirror-like surfaces are present) and Rayleigh scattering. Some light therefore travels opposite to the propagation direction of the input pulse. The properties and functionality of some component inside a QKD system may thus be probed from the quantum channel by sending in sufficiently-intense light and analyzing the back-reflected light. This forms the basis of a Trojan-horse attack. We propose and experimentally demonstrate the necessary tools for implementing such a Trojan-horse attack to break the security of the commercial quantum cryptographic system (Clavis2) from ID Quantique while it is operating the Scarani-Acin-Ribordy-Gisin (SARG04) protocol.

Using optical time domain reflectometry measurements, we first find a suitable back-reflection and the time that it would come out of Bob (on the quantum channel). By homodyning the weak coherent state in this pulse with an appropriately delayed local oscillator, we show that Eve can get information about Bob's basis choice (applied phase shift = 0 or  $\pi/2$ ) with a high accuracy. Since the basis choice is essentially the raw secret key in SARG04 protocol, Eve could in principle know the whole key. However, a problem that Eve needs to circumvent is that of afterpulsing caused by the bright pulses impinging on the avalanche photodiode based single-photon detectors in Clavis2-Bob. This increases the dark counts or false clicks, thus directly translating into a higher quantum bit error rate (QBER) that could expose Eve. Nonetheless, we devise an attack strategy that shows, by means of a simulation, that for long channel lengths (more precisely, channel transmission  $T \sim 0.2$  or lesser), Eve may successfully eavesdrop on a non-negligible percentage of the final secret key. Furthermore, if Bob does not monitor the overall detection rate, then Eve can breach the security of the QKD system at almost any channel transmission.

# Conference 8899C: Unmanned/Unattended Sensors and Sensor Networks X

Monday 23–23 September 2013

Part of Proceedings of SPIE Vol. 8899 Emerging Technologies in Security and Defence; and Quantum Security II; and Unmanned Sensor Systems X

8899-41, Session 8

## Meeting performance and sensing-cost requirements for detection and recognition systems

Christopher J. Willis, BAE Systems (United Kingdom)

Systems designed for surveillance and reconnaissance applications are frequently comprised of multiple sensors and often multiple platforms. However, the effects of individual sensor performance, operational approaches and sensor interaction can lead to some surprising results for the system as a whole. To examine these effects the modelling of multiple sensor systems is important, but can also be challenging. It is possible that the sensing system may be comprised of sensors of several different types, including active and passive approaches in radio frequency and optical portions of the spectrum. Some may have well-understood performance, whereas others may be only poorly characterised. Application of a modelling approach can be useful in the selection of sensors or sensor combinations of sufficient performance to achieve operational requirements, or for understanding how the system might be best exploited in the fulfillment of mission objectives.

A simulation framework has been developed examining sensor options across different sensor types, parameterisations, search strategies, and applications. The framework is based around Bayesian Decision Theoretic principles along with simple sensor models and search environment. It uses Monte-Carlo simulation to derive statistical measures of performance for systems comprised of single sensors or sensor combinations. The framework has been designed to encompass detection, recognition and identification problems and also to treat cases in which sensors have only a weak characterisation.

The performance of each sensor is represented by a collection of simple statistics. For a detection sensor these may be the probabilities of correct detection and of false alarm or, for a recognition sensor, they may be related to the expected confusion matrix. All types may additionally have a cost associated with making a measurement, with this cost representing, for example, the impact on on-board processing or communications bandwidth.

The sensor system modelling framework has been applied to a number of illustrative problems. These range from simple target detection scenarios using sensors of differing performance or of different regional search schemes, through to examinations of: the number of measurements required to reach threshold performance; the effects of sensor measurement cost; issues relating to the poor characterisation of sensors within the system, and; the performance of elaborate combined detection and recognition sensor systems. Generally these results show that the method is able to quantify qualitative expectations of performance, and is sufficiently powerful to highlight some unexpected aspects of operation.

Experiments are presented which consider the number of measurements that must be made to achieve a given system performance and how this might vary with uncertain sensor characteristics. The results reveal limitations due to having only small sets of data with which to characterise sensor behaviour. The simulations demonstrate that, where only a few ground-truthed examples are available to assess the sensor, strong system performance might be expected, but only mediocre levels achieved. Further results illustrate the effects of the cost of making each sensor measurement. It is shown that, where systems are resource-limited, measurement cost may have an influence on sensor preference.

8899-42, Session 8

## Multi-modal target detection for autonomous wide area search and surveillance

Toby P. Breckon, Anna Gaszczak, Ji W. Han, Marcin L. Eichner, Stuart E. Barnes, Cranfield Univ. (United Kingdom)

We present a real-time approach for the detection of people and vehicle targets using combined visible-band (EO), thermal-band (IR) and radar sensing from a deployed network of multiple autonomous platforms with results proven over extended wide-area trials.

Autonomous target detection is an important aspect of autonomous platform deployment for wide-area search and surveillance. Despite a range of prior work on both target detection and automated sensor understanding, wide-scale multi-sensor platform deployment raises a number of empirical and theoretical challenges largely unaddressed in prior studies. Here, we present the autonomous detection of {people|vehicles} using an autonomous sensing network of aerial (UAV) platforms and ground (UGV) platforms. This is used as an empirical test case to explore the optimization of an observation model for the environment when distributed over multiple sensors, platforms and resulting target detection signatures. Furthermore we challenge prior evaluation approaches based on per-sample or per-signature performance to consider the concept of episodic evaluation (i.e. target detection over the entire task/mission).

Essentially we address the following key issue with relation to such multi-platform deployment:- given a search path and sampling strategy for the platform within the environment (including multi-passes/samples per target), the characteristics of the sensors (constrained by weight/power/bandwidth) and a priori precision/recall characteristics of multiple classifiers how can episodic performance be maximized.

Targets are automatically detected using a multi-stage classification approach combining information from on-board {visible, thermal} (UAV) and {visible, thermal, radar} sensing using an ensemble of variable signature classifiers. These detections are combined temporally and spatially to facilitate consistent wide-area target detection and real-time situational awareness. Each target detection is reported with a varying detection confidence, derived directly from multi-modal signature classification, further facilitating target prioritization and platform re-tasking where further localized sampling for target confirmation may be required.

Extended results are presented from three wide-area system trials carried out in the UK, including the MoD Grand Challenge finale and subsequent large scale trials events. Our approaches are shown to be robust to highly variable imagery and variable conditions resulting in high accuracy target detection and localization within the environment.

Related Work & Example Videos:

MoD Grand Challenge / SATURN: Sensing & Autonomous Tactical Urban Reconnaissance Network - <http://www.cranfield.ac.uk/~toby.breckon/demos/modgrandchallenge/>

Automated Vehicle Detection in UAV Imagery: <http://www.cranfield.ac.uk/~toby.breckon/demos/uavvehicles/>

Automated People Detection in UAV Imagery: <http://www.cranfield.ac.uk/~toby.breckon/demos/uavpeople/>

Pathway Detection for Autonomous Navigation <http://www.cranfield.ac.uk/~toby.breckon/demos/pathwaydetection/>

8899-43, Session 8

## FMCW radar for the sense function of sense and avoid systems onboard UAVs

Eric Itcia, Jean-Philippe Wasselin, Sébastien Mazuel, Rockwell Collins France (France); Matern Otten, Albert G. Huizing, TNO Defence, Security and Safety (Netherlands)

Civilian and government-operated Unmanned Air Vehicles (UAVs) are nowadays only authorized to operate in segregated airspace. The main challenge of the next coming years is to allow them operate alongside other manned aircraft in civil integrated airspace. This challenge requires innovative technology development and system demonstrations for UAVs to be considered fully airworthy and for the right regulatory framework to be in place for this integration. Above all, robotic aircraft and their operators will need to demonstrate a high level of operational robustness and the ability to “sense and avoid” other air traffic.



In this challenging context, Rockwell Collins France (RCF) radar department, in close collaboration with TNO in The Hague, The Netherlands, is developing a FMCW radar system candidate for the Sense Function of Sense & Avoid Systems onboard UAVs.

Due to its operational context, the system has to operate whatever the weather conditions, and has to conciliate two apparently mutually exclusive constraints:

- Cover a wide field of view with a high refresh rate, the field of view required is in the order of magnitude of 100° horizontal x 40° vertical
- Detect small traffic targets, typically a Cessna, at long range.

This second constraint imposes a high coherent observation time on target, which seems contradictory with the first constraint of high refresh rate, using a scanning antenna.

Long range detection is also a challenge for FMCW sensors which are known to be limited in term of sensitivity by their transmit leakage into the receiver.

The radar system that has been developed by RCF and TNO at X/Ku band combines state of the art FMCW technology and Digital Beam Forming (DBF) for complying to the two above mentioned constraints. This radar system architecture is protected by several TNO/RCF Patents.

#### A. FMCW Transmit / Receive

The transmitter transmits a continuous wave modulated in frequency (FMCW Frequency Modulated Continuous Wave). For minimizing the transmit leakage into the receiver, the spectral purity of the transmitter has been enhanced by an “offset-frequency” phase-locked loop principle. In addition, the transmit antenna is separated from the receive antenna for ensuring sufficient isolation between transmit and receive. The receiver is of homodyne type, while a single Side Band Receiver has been realized in order to achieve 3 dB lower noise than a simpler Double Side Band receiver. The receiver design is small enough in size to allow a half-wavelength spaced horizontal array of receivers. Vertically spaced arrays allow elevation angle estimation.

The transmitter employs a flexible waveform generator that allows adaptation of waveform parameters (sweep length, repetition frequency, bandwidth) to the application. This FMCW radar technology allows achieving remarkable performances in terms of range and radial speed resolutions.

Moreover, for a given range, it requires a transmitted peak power much lower than the power required by classical pulse radar technology for achieving the same Signal to Noise Ratio (SNR).

#### B. Flood illumination / Digital Beam Forming

The radar system transmitter “illuminates” the whole required field of view with a global transmit antenna.

The receiving antenna is an antenna array, where each element of the receive array is individually digitized. The mapping of targets in receive is then obtained through processing of the data that are received by this array antenna. The digital beam forming allows creating simultaneously all the narrow receive beams covering the complete required coverage.

This process ensures at the same time:

- a long observation time on targets over the whole required coverage, which provides a high radial velocity resolution and increases the probability of small target detection,
- a high refresh rate for the surveillance of the whole field of view required.

## II. THE FLIGHT TEST CAMPAIGN

### A. Overview

Rockwell Collins has conducted a flight test campaign to evaluate the potential and performance of one of its FMCW radar system for UAS “Sense & Avoid” applications. The main objective was to demonstrate the detection capability of FMCW radar in terms of maximum detection range.

### B. Test scenarios

Specific flight phases relative to traffic detection have been performed: chase from behind, head-on approach, 45° approach, 90° approach, at speed around 90kts for each platform.

- Carrier platform = Eurocopter AS350
- Target = Cessna 172 (considered as a representative object of interest for an air traffic detection application)

### C. Radar processing

Raw radar data were recorded during the flight scenarios and processed off-line.

In order to maximize the SNR of the target and thus the detection range, the following processing steps are applied:

- Digital beam forming in azimuth and elevation in order to survey the whole field of view simultaneously with multiple receive beams,
- Coherent integration over a high integration time,
- the optimum observation time for coherent integration is determined
- Range migration compensation on the AC/HC relative speed
- CFAR detection
- Target tracking
- On target confirmation, multiple beams are digitally formed around the target bearing in order to further enhance its SNR and angular designation accuracy

Although the maximum detection ranges are obtained when detecting in thermal noise, strategies for detection in the clutter have also been explored.

#### D. Test results – Operational ranges

## III. CONCLUSION

Test flight results have confirmed the expected range performance and have validated the digital beam concept in which wide angle coverage, high velocity resolution, and high refresh rate can be combined, offering a distinct advantage over conventional scanning radar solutions.

## 8899-44, Session 8

### Utilizing wide area maritime domain awareness (MDA) data to cue a remote surveillance system

Anthony W. Isenor, Richard Cross, Sean Webb, Anna-Liesa S. Lapinski, Defence Research and Development Canada, Atlantic (Canada)

Maritime Domain Awareness (MDA) is the effective understanding of all things in the maritime domain. For MDA to occur, data sources and human awareness must combine to construct an understanding of the maritime environment. Since MDA is broad in scope, the diverse data sources supporting MDA can also support a multitude of activities related to search and rescue, defence, and security. For example, vessel-based data from the Automatic Identification System (AIS) was designed to help ensure safe navigation but is also a significant contributor to MDA. The AIS contribution to MDA is especially important in remote locations (e.g., open ocean or areas with minimal infrastructure), where space-based collection of AIS has proven to be a valuable data source for constructing an awareness of vessel traffic. Land-based surveillance systems also represent significant data contributors to MDA, where the infrastructure exists.

Defence Research and Development Canada (DRDC) Atlantic is currently involved in research on the topic of northern MDA. One project, entitled Situational Information for Enabling Development of Northern Awareness (SEDNA), includes research on the exploitation of MDA data in northern areas. One aspect of this research is to utilize wide area MDA data to provide awareness to an unattended, land-based system. In this paper, we describe how the linkage of such a system to space-based AIS (SAIS) could be achieved. By linking the two systems, the land-based surveillance system can be reactive to the information acquired from the wide area MDA system. Such a link effectively expands the situational awareness zone of the land system using the MDA data source.

This paper will describe the research and development (R&D) that could be utilized to achieve the linkage between the unattended systems. The SAIS system being used is a Department of National Defence data feed received directly from the commercial provider exactEarth Ltd. The land-based surveillance system used is the remote northern system constructed within the DRDC Technology Demonstration Project known as Northern Watch. Northern Watch is a multi-year project intended to show state-of-the-art, unattended, surveillance capabilities in the Canadian north. The component that would link the SAIS data to the Northern Watch information management system is the Maritime Situational Awareness Research Infrastructure (MSARI). MSARI is an assembly of data sources, users, applications, and product management techniques that collectively support research in areas such as information management and MDA data exploitation. One component of MSARI is a PostgreSQL database that provides management of the incoming data. MSARI

includes Geographic Information System (GIS) extensions as supported by PostGIS.

As part of the R&D description, this paper will include high-level descriptions of the systems along with elaboration on the AIS vessel recognition function managed by MSARI, the notifications that would be sent to the Northern Watch southern command site, and the resulting actions that could be taken by the Northern Watch surveillance system. Applicability of the technique to other data sources will also be discussed.

8899-45, Session 9

## Automated generation of high-quality training data for appearance-based object models

Stefan Becker, Arno Voelker, Hilke Kieritz, Wolfgang Hübner, Michael Arens, Fraunhofer-Institut für Optronik, Systemtechnik und Bildauswertung (Germany)

Methods for automated person detection and person tracking are an essential core component in modern security and surveillance systems. They are a prerequisite for most subsequent analysis or interpretation approaches. Most state-of-the-art person detectors follow a statistical approach, where prototypical appearances of persons are learned from training samples with known class labels. Selecting appropriate learning samples has a significant impact on the quality of the generated person detectors. For example, training a classifier on a rigid body model using training samples with strong pose variations is in general not effective, irrespective of the classifiers capabilities.

Generation of high-quality training data is, apart from performance issues, a very time consuming process, comprising a significant amount of manual work. Furthermore, due to inevitable limitations of freely available training data, corresponding classifiers are not always transferable to a given sensor and are only applicable in a well-defined narrow variety of scenes and camera setups.

Semi-supervised learning methods are a commonly used alternative to supervised training, in general requiring only few labeled samples. However, as a drawback semi-supervised methods always include a generative component, which is known to be difficult to learn. Therefore, automated processes for generating training data sets for supervised methods are needed. Such approaches could either help to better adjust classifiers to respective hardware, or as a complement to existing data sets.

Towards this end, this paper describes a processing chain that is able to automatically generate labeled training data, including positive and negative samples from video sequences.

The proposed method assumes that the camera is static. Moving objects are first roughly categorized with respect to the aspect ratio of the enclosing bounding boxes, using simple blob detection methods built on a background subtraction algorithm. Since this naïve method is not very robust, we propose a subsequent processing step that applies a multi frame registration process to the initially selected regions of interest. Therefore, the method is able to compensate the position and scale of the region of interests. Aligning multiple regions in parallel is done with a robust estimator, using the differential evolution algorithm in order to deal with local minima. In order to be scalable to large datasets a bootstrapping method is introduced, which is further able to integrate training data from different video sequences or video sources. The effectiveness of the method is illustrated by adapting a pedestrian detector to the cameras of a sensor network.

8899-46, Session 9

## Image super-resolution applied to moving targets in high dynamics scenes

Olegs Mise, GE Intelligent Platforms (United States); Toby P. Breckon, Cranfield Univ. (United Kingdom)

In modern Intelligence, Surveillance, and Recognition (ISR) systems the ability to obtain high resolution images is highly desirable. However, in real-life front-end video systems, such as video trackers, the ISR systems suffer from the limitations that cannot always

guarantee good quality images. These limitations can be caused by low quality video sensors, internal noise of the front-end system, high target dynamics or other surrounding factors such as poor weather conditions, dust, smoke etc.

A development effort has been directed to improve visual appearance of the moving targets in high dynamics video scenes. This is accomplished by incorporating an adaptive representation of the target using a mixture of the Gaussians model in conjunction with a gradient descent algorithm which produces accurate sub-pixel motion estimation for the subsequent super-resolution stage of the system. The novelty of this approach lies in the use of the combination of motion estimation algorithms. The combination effectively improves the registration result that is crucial for the super-resolution stage of the algorithm.

The proposed solution combines modified Sum of the Absolute Differences (SAD) and gradient descent algorithms that subsequently allow to reliably estimate target motion with sub-pixel accuracy under large degrees of freedom of the target transformation. Here the modified Sum of the Absolute Differences algorithm acts as a pre-calculation stage in order to provide an initial position and to constrain a degree of freedom of the gradient descent algorithm that is highly prone to errors. Further, the implementation of the adaptive target representation through the mixture of the Gaussians model provides a reliable target/reference update. The final stage of the algorithm re-maps the target pixels into a high resolution domain where the super-resolution stage has occurred.

This paper discusses the issues involved in improving the visual target representation in high dynamic scenes. It also demonstrates robust integration of the developed algorithm with the modern tracking and/or Surveillance and Recognition systems.

8899-47, Session 9

## Microradar sensor technology

Pavlo A. Molchanov, Naval Air Warfare Ctr. Aircraft Div. (United States)

New micro-radar sensor technology is proposed for detecting and tracking ground and airborne low profile low altitude targets. Distributed along border or around protected object (military facility and buildings, camp, stadium) small size low power radar sensors allow not only detecting and tracking of low profile targets, but can recognize and classify targets by using diversity signals and intelligent processing. Application of array of directional antennas is allows to exclude mechanical antenna scanning or antenna phase processor and radically decrease size of micro-radar sensor. Proposed micro-radar better protected because of transmitting a few order smaller power than regular scanning radars. Micro-radars are inexpensive (approx a few hundred dollars) and can be expendable.

Proposed micro-radar sensors network can be applied for treaty verification, cooperative monitoring or border protection. Sensors network may be easy connected to one or few operators by point-to-point invisible from outside communication. The array of directional antennas with point-to-point communication provide jam, spoof protection capability by verification of spatial position. Communications are "invisible" to guided missiles because of 20 dB smaller irradiation outside the beam and spatial separation. This solution can be implemented with current technology. Directional antennas have higher gain and can be multi-frequency or have wide frequency band in contrast to phase antenna arrays. The multi-directional antenna array provides a multi-functional communication network and simultaneously can be used for command control, data link and GPS.

8899-48, Session 9

## Management of unmanned moving sensors through human decision layers: a bi-level optimization process with call to costly sub-processes

Frederic Dambreville, Ecole Nationale Supérieure de Techniques Avancées (France)

While there is a variety of approaches and algorithms for optimizing the mission of an unmanned moving sensor, there are much less works which deal with the implementation of several sensors within a human organization. Some organizations, typically military organizations, are characterized by a hierarchical structure, where decisions are made through multiple human-driven levels. Only the humans at first level will handle a sensor and the environmental information directly, thus applying specific and efficient algorithms for an optimal management of the sensor of his responsibility. Higher levels will work on coordinating sensors through their human handlers, given a global observation mission.

As a consequence, the management of the sensors is done through at least one human decision layer, and the sensors management as a whole arises as a bi-level optimization process. In this work, the following hypotheses are considered as realistic:

- a- Sensor handlers of first level plans their sensors by means of elaborated algorithmic tools based on accurate modeling of the environment,
- b- Higher level plans the handled sensors according to a global observation mission and on the basis of an approximated model of the environment and of the first level sub-processes.
- c- In order to enhance the accuracy of the model and of the global planning, higher level may request the first level for evaluating (possibly partially) global plans,
- d- Each request to the first level is costly: it implies communication procedures, as well as the parameterization and execution of the algorithmic tools by the sensors handlers.

This paper investigates approaches for solving a dual criterion: enhance the accuracy of the high level modeling by means of optimal requests of the first level; optimize the global observation mission.

This problem is formalized very generally as the maximization of an unknown function, defined a priori by sampling a known random function (law of model error). In such case, each actual evaluation of the function increases the knowledge about the function, and subsequently the efficiency of the maximization. The issue is to optimize the sequence of value to be evaluated, in regards to the evaluation costs. There is here a fundamental link with the domain of experiment design.

Jones, Schonlau and Welch proposed a general method, the Efficient Global Optimization (EGO), for solving this problem in the case of additive functional Gaussian law. This approach is based on iterative maximization of the expected improvement of the best actual evaluations. In this work, a generalization of the EGO is proposed, based on a rare event simulation approach applied to the expected improvement maximization. This simulated approach makes possible the implementation of non Gaussian functional law, and even of simulated functional law. It is applied to the aforementioned bi-level sensor planning.

At last, our approach will also be compared on a simple example to an exact approach: this exact approach is solved as a Partially Observable Markov Decision Process.

8899-49, Session 10

## High precision object geo-localization and visualization in sensor networks

Simon Lemaire, Christoph Bodensteiner, Michael Arens, Fraunhofer-Institut für Optronik, Systemtechnik und Bildauswertung (Germany)

The availability of previously acquired, geo-referenced imagery enables automatic video based solutions for high precision object geo-localization and visualization. This enables a low bandwidth transfer of object information within sensor networks. In this paper we

outline a generic method which geo-references objects seen in UAV video streams and visualizes them on modern smartphones using augmented reality.

Methods

First we geo-localize the UAV video stream. Usually UAV onboard inertial sensors only provide a rough initialization for geo-localization. Therefore we assume intrinsically calibrated cameras and exactly determine the 6 DoF camera pose of the UAV camera data with respect to a geo-referenced background model (e.g. aerial imagery from Google Maps). We perform an initial keyframe registration with the background model based on a standard features (SURF) and an intensity based camera pose refinement approach. Then we perform camera tracking based on visual features (FAST). In this work we combine a standard recursive Bayesian filter framework for short term tracking and a keyframe based bundle adjustment back-end for superior dynamical consistency. However, to achieve real-time performance we only optimize over a window of recently recorded keyframes with sufficient camera translation. The automatically determined geo-coordinates of the manually picked objects in the UAV video-stream are then transferred to our mobile device network using standard IP protocols. We use a customized server client system to provide a fast and safe data transfer between the UAV station and the smartphone. We use augmented reality techniques in combination with the integrated inertial sensors of our smartphones to visualize the object location. The internal smartphone measurements are then used to determine the 6 DoF orientation of the smartphone camera. To achieve a higher accuracy of the internal sensor readings we additionally employ a windowed smoothing of recent sensor measurements. Our implementation is based on an android system environment in combination with OpenCV (Smartphone) and standard open-source C++ libraries (VTK, Toon, VXL, Bundler) on the UAV side.

Results

The feasibility of the approach was experimentally validated using Mini-UAV ("MD-400") and high altitude UAV video footage in combination with modern off-the-shelf smartphones (Samsung Galaxy Note 2). The proposed video registration pipeline operates at video frame rate (>35FPS) and achieves a highly accurate registration performance in case of high altitude video footage.

In order to display the picked object from the UAV video stream an augmented reality object is shown on the smartphone camera display and additionally Google Maps is used to verify the object position.

Conclusion and outlook

Applications of this approach are widespread and include for instance crisis and disaster management or military applications. To this end we only used an image based geo-localization refinement on the acquisition side. However, we plan to use 3D-LiDAR data to enable the proposed registration pipeline on the receiver (Smartphone) side as well. Considering the performance and memory size of modern smartphones we are confident to achieve a highly precise geo-localization and visualization of objects seen in smartphone cameras as well.

8899-50, Session 10

## Optical system components for navigation grade fiber optic gyroscopes

Marcus Heimann, Technische Univ. Berlin (Germany); Maximilian Liesegang, Fraunhofer-Institut für Zuverlässigkeit und Mikrointegration (Germany); Norbert Arndt-Staufenbiel, Technische Univ. Berlin (Germany); Henning Schroeder, Fraunhofer-Institut für Zuverlässigkeit und Mikrointegration (Germany); Klaus-Dieter Lang, Technische Univ. Berlin (Germany)

Interferometric fiber optic gyroscopes belong to the class of inertial sensors. Due to their high accuracy they are used for absolute position and rotation measurement in manned/unmanned vehicles, e.g. submarines, ground vehicles, plains or satellites. The important system components are the light source, the electro optical phase modulator, the optical fiber coil and the photodetector. This paper is focused on approaches to realize a stable light source and fiber coil. Superluminescent diode and erbium doped fiber laser were studied to realize an accurate and stable light source. Therefore the influence of the polarization grade of the source and the effects due to backreflections to the source were studied by using optical isolators

and Lyot depolarizers. If superluminiszenz diodes that are monitored by photodiode and mounted on a thermoelectric cooler are used together with optical isolator and Lyot depolarisator, accurate and stable optical sources can be realized. Erbium doped fiber lasers shown also good results, but is limited in their application fields due to their radiation sensitivity. During operation thermal working conditions severely affect accuracy and stability of the optical fiber coil, which is the sensor element. To use the relativistic Sagnac effect the optical signal is split and coupled in clock wise and counter clock wise direction into the optical fiber coil. After the split signals have propagated through the fiber coil they are recombined and the resulting interferometric signal is analyzed. Thermal gradients that are applied to the fiber coil have high negative effects on the achievable system accuracy of the optic gyroscope. Therefore a way of calculating and compensating the rotation rate error of a fiber coil due to thermal change is introduced. A simplified 3 dimensional FEM of a quadruple winded fiber coil is used to determine the build-up of thermal fields in the polarization maintaining fiber due to outside heating sources. The rotation rate error due to these sources is then calculated and compared to measurement data. A simple regression model is used to compensate the rotation rate error with temperature measurement at the outside of the fiber coil. Based on the approach, predictions about an ideal fiber coil housing design and the effect of different coil winding schemes, e.g. cylindrical, differential and quadruple, are made. To realize a compact and robust optical package for some of the relevant optical system components an approach based on ion exchanged waveguides in thin glass was developed. The single mode waveguide structures are manufactured in borosilicate glass and offer a gradient refractive index profile. This waveguides are used to realize 1x2 and 1x4 splitter with fiber coupling interface or direct photodiode coupling.

8899-51, Session 10

### **An object-oriented modeling and simulation framework for bearings-only multitarget tracking using an unattended acoustic sensor network**

Murat S. Aslan, TÜBITAK BILGEM ILTAREN (Turkey)

Ground target tracking is a challenging field because of the limited capabilities of most low cost sensors. In this context microphone arrays have a potential of being useful: They can provide a direction to the sound source, they can have a range that is better than many other ground sensors, and the sound characteristics can provide a basis for target classification. However, there are also many problems. One of them is the difficulty to resolve multiple sound sources, another is that they do not provide distance, a third is the presence of background noise from wind, sea, rain, distant air and land traffic, people, etc., and a fourth is that the same target can sound very differently depending on factors like terrain type, topography, speed, gear, distance, etc. For a critical performance assessment of various sensor data fusion algorithms for tracking multiple targets in an acoustic sensor network, a high fidelity simulation and modeling environment that accounts for the mentioned problems is necessary.

In this paper, we propose an object-oriented modeling and simulation framework for tracking multiple road targets in an unattended acoustic sensor network where each sensor is a microphone array providing bearing-only measurements to targets. We present a model for road network, targets (motion and acoustic power) and acoustic sensors in an object oriented fashion where different and possibly time-varying sampling periods for each sensor node is possible. Moreover, the sensor detection is modeled using a constant false alarm rate (CFAR) type of detection and we put a model for receiver operating characteristics (ROC) curve for each sensor which results in false alarms as well as missed detections. The proposed simulation framework can be used for ground-truth generation for road-constraint multiple target tracking using an unattended acoustic sensor network by avoiding expensive field trials.

Sample views from the simulator outputs namely, road network with sensor locations, target movements, sensor bearing measurements, and probability of detection values are shown below.

8899-52, Session 10

### **Position determination of disturbance along a modified saganac interferometer**

Pang Bian, Yuan Wu, Qian Xiao, Bo Jia, Fudan Univ. (China)

Distributed sensing is one of the most attractive features of optical fiber sensors. The disturbance on the fiber can cause the change of the length and index of the fiber which can leads to a phase shift of the light wave traveling in the fiber. In this case, interferometer offers a economical and a effective measurement.

However, all the interferometers based on the sagnac loop or M-Z interferometer is sensitive to the noise caused by the polarization change or the sensing element of the system must be annular, which limits the use of the distributed sensor.

We present another type of interferometer sensor for the detection and location of the disturbances on different sensing fibers. This system is based on the sagnac interferometer and modified by a faraday rotator mirror, changing the traditional sagnac loop into a linear structure.

The interferometer has two different sensing fibers, which can detect and locate disturbance along them at the same time. With a piezoelectric ring with optical fiber wound around it placed at the end of one of the two sensing fibers to perform as the phase-modulator, disturbance signal along this sensing fiber is modulated to a higher frequency. With the technique of the frequency-division-multiplexing, the disturbances from the two different areas can be detected at the same time. and then be separated by a multiplier and low-pass filters. And the cross-talk of the interferometer can be minimized by adjusting the amplitude of the signal which excites the piezoelectric ring.

With the signals from the different areas and the position determination theory, the location of the disturbances along the fiber can be figured out.

To verify the concept and result of the interferometer, a set of ten disturbances was applied at ten equally spaced locations on the two sensing fibers sequentially.

The result of the experiment shows that the disturbances on the two sensing fibers can be detected independently without cross-talk. The system is insensitive to slowly varying disturbance such as the change of the temperature and by using the faraday mirror, the noise caused by polarization change can be reduced. The error of the location is less than 500m

8899-53, Session 10

### **Lower bound on number and sizes of telescopes in an optical array receiver for deep space optical communication**

Ali J. Hashmi, National Univ. of Sciences and Technology (Pakistan); Ali A. Eftekhar, Ali Adibi, Georgia Institute of Technology (United States); Farid Amoozegar, Jet Propulsion Lab. (United States)

Optical communications technology has the characteristics to provide a broadband communication support for the future missions launched for exploration of solar system in deep-space. Traditionally, telescopes are employed in astronomical applications for observations of celestial objects. However, in extremely long-distance free-space optical communication, such as interplanetary deep space optical communication, telescopes are employed as antennas both at the transmitter and receiver end. Keeping in view the constraints of telescope size at the transmitter of a spacecraft, a large aperture size telescope (i.e.,  $\approx 10$  m) is needed at an earth-based receiver to support the acceptable data rates for free-space optical communication. However, it is a formidable task to fabricate and maintain a high-quality and extremely large diffraction-limited telescope. Comparatively, an array of smaller telescopes, electrically connected to form a bigger photon-collecting aperture is an attractive alternative to a large telescope for an optical receiver operating in a deep-space optical communication link.

In this paper, performance of an optical array receiver is evaluated for a free-space optical communication link between Earth and Mars, with an objective to find the lower bound on the number of telescopes that can be employed in an earth-based optical array receiver. Theoretically, an optical array receiver consisting of any number of

telescopes would perform equivalent to single large telescope, as long as the total photon-collecting aperture is same as that of the single telescope. The objective in this paper is to verify this premise in an actual operational scenario of a free-space optical communication link between Mars and Earth.

In the analysis, specifications of the transmitter, receiver, and other link budget parameters are chosen based upon the state-of-the-art, space-qualified technology. A 5W laser operating at 1.06 and a 30 cm telescope is selected at the transmitter of a spacecraft in Mars orbit. Photon-counting detectors with the capability of detection of single photon arrivals are assumed at the receiver end. Pulse-position modulation is employed for the communication link. The performances of different array architectures are evaluated using analytical techniques and Monte-Carlo simulations.

The analysis and results are presented for a wide range of operational conditions including the Mars-Earth opposition and Mars-Earth conjunction phase. Various limiting factors such as, background noise and atmospheric turbulence are also included in the simulations and analysis. The results are evaluated for different array architectures ranging from one telescope with 10 m aperture diameter to thousands of smaller telescopes in the array, with the equivalent total aperture diameter. The results show that during an actual operational scenario between Earth and Mars, performance of an array consisting of 100 telescopes with 1 m diameter is almost equivalent to a single telescope with 10 m aperture diameter. The performance loss of an array consisting 135 telescopes with 0.86 m is also minimal. However, if the telescopes diameters are reduced below 0.86 m, the performance degradation is substantial. Hence, it can be concluded that an optical array receiver can replace a monolithic 10 m telescope as long as the individual telescope diameter exceeds that of the 0.86 m. Additionally, it is further shown that compared to the current RF technology, a telescope array receiver can support the data rates of about 120 M bit/s during the Earth-Mars opposition phase and 13 M bits/s during the Earth-Mars conjunction phase.

## 8899-55, Session 10

### Space security and defense of GEO satellites

Enyu Gao, China Academy of Space Technology (China)

GEO satellites are very important and highly valuable properties to both civil and military users. Failure and lost GEO satellites may cause serious damage to communication, broadcast and many other space applications. GEO orbit positions and communication frequency are very rare space resources. This article mainly focuses on security and defense of GEO satellites which are suffering damage or about to be confronted with. Damage sources will be categorized and deeply analyzed. For example, micro falling stars are the most common attacking natural stuffs which come from deeper space probably give heavy impact on satellite structure and antennae. When this situation happens, satellites may suddenly interrupt working or even lost control. Because micro falling stars are hardly observe and predict, suggestion of negative defense is given to enhance satellite structure intensity. Space debris is the most common man made attacking sources which threaten the security of satellites. Suggestion of positive defense is given to prevent satellite from attacking of space debris. From the space debris observing system, debris which may cause satellite damage is tightly monitored and able to predict its orbit parameters. Accordingly, orbit maneuver of satellite is executed to positively avoid the knock of the space debris.

## 8899-54, Session PS

### Analysis of rain effects on free space optical communication based on data measured in the Libyan climate

Mahmud M. Badi, Adam F. Adam, Al-Fateh Univ. (Libyan Arab Jamahiriya); Mohammed Twati, Tripoli University (Libyan Arab Jamahiriya)

In this paper, the effect of rain on Free Space Optical link (FSO) performance based on data measured and recorded in the Libyan National Meteorological Center (LNMC) is investigated. A modified FSO link equation based on CARBONNEAU empirical model is used to provide a direct relation between the rain fall rate and the maximum allowable FSO link length. The effect of the heaviest case of rainfall occurred in Libya for the FSO is simulated, and the maximum allowable link length is obtained.

# Conference 8900: Millimetre Wave and Terahertz Sensors and Technology VI

Tuesday - Wednesday 24-25 September 2013

Part of Proceedings of SPIE Vol. 8900 Millimetre Wave and Terahertz Sensors and Technology VI

8900-1, Session 1

## Reflect-array based mm-wave people screening system (*Invited Paper*)

Brendan N. Lyons, Emil Entchev, Michael K. Crowley, Smiths Detection Ireland Ltd. (Ireland)

For the past number of years manufacturers have been developing people screening technology to the point where it will shortly be in widespread use in a significant number of countries. This paper reports on a reflect-array based system that has shown excellent real time image performance during trials and is currently in the final stages of certification for automated threat recognition in check-point applications.

The system consists of two 1m x 1m reflect-array panels mounted one on top of the other to achieve a 2m high by 1m wide aperture. Each panel is configured as an elliptical mirror with a fixed focus at a transceiver and a programmable focus which scans a 3D volume in front of the panel. The panels consist of an array of patch antennas with each patch terminated in a FET. The FET is a conventional low noise HEMT commonly used in LNBS for satellite TV. Using only the on and off states of the FET it is possible using appropriate matching to terminate the patch in equal but opposite phase reflection coefficients. Thus an efficient binary phase approximation to the ideal programming of the elliptical mirror can be achieved.

The transceiver is fixed frequency, continuous wave and currently operates at 24GHz. The power delivered to the focus is approximately -20dBm. This equates to a time averaged power density many orders of magnitude below acceptable exposure levels. The panels are coherent allowing the transmission from one panel to be received coherently by the second panel. This enables the system to use reflections which emanate from one panel and return to the second thus allowing the system to benefit from the combined aperture area. The lateral resolutions in width and height are 8mm and 6mm respectively. The depth resolution is approximately 7mm in the centre of the scan volume increasing to 10mm at the outer edge.

24GHz has been found to be very effective for imaging. The resolution is adequate for the likely threat objects yet clothing is transparent. At higher frequencies clothing becomes more obvious, introducing clutter into an already complicated automatic threat detection scenario.

The focusing process of the system consists of setting the phase of each patch such that the path length from the transceiver to the focal point is a whole number of wavelengths. This ensures constructive interference at the focus. The patterns themselves are calculated on demand, facilitating zooming during operation and electronic corrections for system imperfections.

The system has a data rate of 10 mega samples per second. This rate is inadequate for real time imaging of a 2m x 1m x 1m scan volume at a fine resolution. To compress the data requirement the volume is sampled using a crude grid to determine occupied areas within the scan volume. A fine scan with the optimum resolution is then applied to the desired regions of the scan volume in order to build the final image. This approach when applied to a person in the scan volume reduces the data requirement to 10% of that if the whole volume was scanned allowing real time video imaging of the person.

Details of the design implementation, associated trade-offs and practical constraints will be discussed in the paper.

8900-2, Session 1

## A fast imaging MMW radiometer system for security and safety applications

Stephan Dill, Markus Peichl, Deutsches Zentrum für Luft- und Raumfahrt e.V. (Germany)

The SUMIRAD system (SUM Imaging Radiometer) is a fast fully-mechanical scanning radiometer system which can provide close to real-time quasi-optical millimeter-wave (MMW) images. Its original purpose is reconnaissance in a multi-sensor vehicle based forward looking surveillance system. Hence SUMIRAD observes the road area in front of the vehicle in order to enhance the knowledge of the actual

threat situation and detect automatically suspicious objects. As a MMW system it offers the advantage to detect and localize objects and persons under all atmospheric obstacles and also extends the surveillance capabilities behind non-metallic materials like clothing or thin walls, covers and thin vegetation.

SUMIRAD was developed as a cost-effective fully-mechanical scanner using only two MMW radiometer receivers. The innovative and light-weight design satisfies the demand for a very large field-of-view (FOV: 30° in elevation x 80° in azimuth) in combination with a high frame rate (up to 1 image per second) and a spatial resolution well below 1 degree.

The broadband receivers operate in W band (82 -102 GHz) providing sufficient radiometric sensitivity of better than 2 K at the minimum image acquisition time of 1 second. Longer times, up to 90 seconds per image, could be selected for higher radiometric sensitivity ( $\ll 2$  K). The compact integration of the complete receiver electronics allow to change easily the polarization of each receiver between horizontal (H) and vertical (V). Both radiometer receivers cover nearly the identical FOV. Hence two different imaging modes are possible depending on the selected polarization mode. In the first mode (identical polarization) the superposition of both nearly identical images improves the radiometric sensitivity by about a factor of 1.4. This mode is useful for short image acquisition times. In the second mode (different polarization), the two independent images provide different polarimetric information simultaneously from the same scene.

The previously mentioned imaging capabilities allow operating SUMIRAD for a multitude of applications. Beside the originally intended vehicle based operation under driving conditions, the static operation of the system from a fixed position can monitor fast or slow changes of a scene. For example, such applications are the volume estimation of actual truckload through non-metallic containers, through-wall imaging for the detection of objects or persons and the long term observation of weather phenomena in a maritime environment. In general the system can be used for many ground-based observations where close to real-time radiometric imaging at large FOV in combination with a long observation period is useful.

The paper addresses the operational principle of SUMIRAD and discusses the requirements of key imaging parameters. Imaging results from several measurement campaigns are presented.

8900-3, Session 1

## A large (1.6 m) 35 GHz security screening portal imager is re-commissioned with upgraded software for reduced fixed pattern noise and higher sensitivities

Neil A. Salmon, MMW Sensors Ltd. (United Kingdom) and Manchester Metropolitan Univ. (United Kingdom); Nicholas J. Bowring, Manchester Metropolitan Univ. (United Kingdom)

A 1.6 m aperture 35 GHz security screening portal imaging system is being re-commissioned at the Manchester Metropolitan University to quantify its enhanced performance with new image processing software. The new software enables a more accurate calibration of fixed pattern noise and enables longer integration times to offer better signal to noise ratios in the recognition of non-metallic anomalies carried on persons and in their bags. The portal uses a quasi-optical imaging system developed by QinetiQ to image subjects at a range of 1.6 m from the imager aperture, doing this with a spatial resolution of 2-3 cm and a depth of field of around 5 cm. The system is designed for indoor use and image contrast is enhanced by spatially incoherent illuminating panels. However, this illumination generates fixed pattern noise in the image. These patterns will be calibrated to enable their removal from the image. The system will then be used to image non-metallic threats concealed under clothing and in various types of hand luggage such as rucksacks, briefcases and handbags.

8900-4, Session 1

**A feasibility study into the screening and imaging of hand luggage for threat items at 35 GHz using an active large aperture (1.6 m) security screening imager**

Nicholas J. Bowring, Neil A. Salmon, David A. Andrews, Nacer D. Rezgui, Stuart W. Harmer, Manchester Metropolitan Univ. (United Kingdom)

No abstract available

8900-30, Session 1

**History and challenges of passive millimeter wave imaging**

Albert N. Pergande, Lockheed Martin Missiles and Fire Control (United States)

The history of Passive Millimeter wave imaging extends back farther than many people realize. This paper begins with a historical perspective on high frequency technology, discusses the major milestones that enabled Passive Imaging, and wraps up with a discussion of formerly promising technologies that have failed to improve imager performance.

8900-5, Session 2

**Motion effects in multistatic millimeter-wave imaging systems (Invited Paper)**

Andreas Schiessl, Sherif S. Ahmed, Rohde & Schwarz GmbH & Co. KG (Germany); Lorenz-Peter Schmidt, Friedrich-Alexander-Univ. Erlangen-Nürnberg (Germany)

Personnel screening systems are increasingly deployed at checkpoints at airports and critical infrastructure buildings in order to screen passengers and personnel for potentially dangerous objects. Reliable detection of hidden objects requires mm-wave images featuring high resolution and dynamic range. Those requirements drive the development of next-generation mm-wave imaging systems. Usually, mm-wave imaging systems assume static scenarios during data recording for a mm-wave image, but personnel screening systems have to tolerate movement of persons to be screened to some extent as motion of living people cannot be predicted. Movement causes phase errors, and these errors propagate through the image formation algorithm. Short measurement time is crucial to avoid image quality degradation by movement of persons to be screened. Fully electronic systems feature higher measurement speeds compared to mechanically scanning systems, and multistatic imaging arrays greatly reduce the measurement acquisition time to be performed as measurements can be performed in parallel. These improvements allow the use of higher frequencies which provide finer resolution but also increase sensitivity of image quality with regard to motion during measurement. The measurement flow of such a modern multistatic imaging system for personnel screening, which has been optimized for quick data recording to reduce motion effects, will be presented. Design parameters which affect measurement time are explained. Test objects which enable measuring the effect of motion on image quality are shown. The test objects are rotationally symmetric and include periodic structures. They are rotated in front of the system so that the lateral speed of the structures increases with distance from the test object's rotation center. Mm-wave images of the moving test objects are used to demonstrate the effects of motion in multistatic digital-beamforming mm-wave imaging systems. Loss of resolution and dynamic range vs movement speed is demonstrated. Millimeter-wave images of standing and moving persons are shown to illustrate the motion effects.

8900-6, Session 2

**A W-band passive imaging system implemented with rotating diffraction antenna technology**

Sergiy Shylo, Yuriy Sydorenko, Usikov Institute of Radiophysics and Electronics (Ukraine); Dana Wheeler, Radio Physics Solutions, Inc. (United States); Douglas Dundonald, Radio Physics Solutions, Ltd. (United Kingdom)

The concept and operational results are presented for a working prototype of a W-band passive imaging system based on the planar diffraction type antenna, rotating around the viewing axis by means of a low power electromechanical drive. A multi-beam rotating antenna pattern is generated by a 40x40 cm diffraction grating which forms the receiving aperture. The dispersive properties of the antenna are derived from a diffraction grating: millimetre wave radiation incident upon the diffraction grating is transformed to a surface wave, which couples to a planar dielectric waveguide positioned in the near-field of the grating. Different regions of space can be 'viewed' as the antenna beams' angular positions with respect to the rotation axis are dependent on frequency. The total frequency band of 16 GHz (84-100 GHz) is split into 64 equal width sub-bands, each constituting a 'beam.' The resulting 64-beam pattern is formed symmetrically about the antenna rotation axis and the action of antenna rotation allows complete image capture within a prescribed field of view. Image formation rate can be as high as 16 frames per second with a conical field of view of 19 degrees. Imaging at short distances of several meters is possible due to the placement of a stationary lens in front of rotating antenna unit; imaging at long distance is also possible without any additional lens. Technical parameters and imaging results from the prototype unit are discussed.

8900-7, Session 2

**Review of the characteristics of 384x288 pixel THz camera for see-through imaging**

Linda Marchese, Marc Terroux, Francis Genereux, Bruno Tremblay, Martin Bolduc, Alain Bergeron, INO (Canada)

THz is a field in constant expansion. Multiple applications are foreseen including see-through imaging. To develop deployable systems, real-time two-dimensional cameras are needed rather than monapixel detectors or linear arrays that require mechanical scanning systems.

INO has recently developed a real-time (video rate) uncooled 384x288 THz camera exhibiting excellent sensitivity and low noise levels. This camera is based on a 35 um pixel pitch bolometers.

The core of the THz camera is the detector that is based on INO's uncooled VOx microbolometer technology. The THz detectors are fabricated, packaged and sealed on-site. The package is a standard ceramic type, and the final sealing is performed using a high resistivity float zone silicon (HRFZ-Si) window having an anti-reflective coating consisting of Parylene. By changing the thickness of the Parylene coating the transmission can be optimized for a specific center wavelength. The packaged and sealed FPA is then mounted on an INO IRXCAM electronic core giving a passive THz camera assembly. The additional THz objective consists of a refractive 44 mm focal length F/1 THz lens assembly. The two lenses of the assembly are also made from HRFZ-Si and have a Parylene coating matching that of the window.

Despite its small pixel size, respectively two and three times smaller than the wavelength at 70.51 um and 118.83 um, the camera resolution is beneficial to the imaging quality. Furthermore, these small pixels provide a key element in the development of a compact system, the focal length and consequently the size of the optics being proportional to the size of the pixel.

It is well known that the absorption in the THz waveband of a specific material varies according to its composition. Thus, depending on the given application, a different THz wavelength is desired. The INO THz detector is inherently broadband and as mentioned depending on the window and lens coatings, the FPA can be optimized for a specific wavelength. On the other hand, although THz source are available at various wavelengths, depending on the technology and the wavelength sought after, the power available and the size of the system may vary by orders of magnitude. Furthermore,

the transmission of the atmosphere varies according to the THz wavelength and will influence the choice of the source. While for short distances the atmosphere attenuation is of less importance, for standoff imaging it may play an important role. The development of a complete imaging system has thus to consider the foreseen application as well as each of the various components.

In this paper, a review of the characteristics of the THz camera is performed. The sensitivity of the camera at various THz wavelengths is presented along with examples of the resolution obtained with the IRXCAM-384-THz camera core. Lastly, an overview of different see-through imaging system configurations is given, where parameters including imaging distance, atmospheric and barrier material absorption, source wavelength and power as well as camera resolution and sensitivity are all considered.

## 8900-8, Session 2

### Development of an ultra-wide band microwave radar-based footwear scanning system

Nacer D. Rezgui, Nicholas J. Bowring, David A. Andrews, Stuart W. Harmer, Matthew J. Southgate, Dean R. O'Reilly, Manchester Metropolitan Univ. (United Kingdom)

At airports security screening can cause long delays. In order to facilitate and speed up screening, a need for a solution to avoid passengers removing their shoes to have them x-ray scanned is required. To detect threats or contraband items hidden within the shoe, a method of screening using frequency swept signals between 15 to 40 GHz has been developed, where the scan is carried out whilst the shoes are being worn and the subject is stationary. Most footwear is transparent to microwaves to some extent in this band. The scans, data processing and interpretation of the 2D image of the cross section of the shoe are completed in a few seconds.

Using safe low power UWB radar, scattered signals from the shoe can be observed which are caused by changes in material properties such as cavities, dielectric or metal objects concealed within the shoe. The resolution of the return signals is bandwidth dependent and for the frequency scan used is 6 mm. By moving the transmission horn along the length of or across the shoe, a 2D image corresponding to a cross section or 3D reconstruction through the footwear is built up, which can be interpreted by the user, or automatically, to reveal the presence of a concealed threat within the shoe. Procedures for enhancing the image by background subtraction, windowing, antenna deconvolution and combining successive measurements at different spatial positions through synthetic aperture techniques have been investigated and shown to give improved contrast and spatial resolution. Methods used to enhance the image through techniques used image processing will also be discussed. The optimization of operating frequency has also been investigated and takes into account the attenuation and dielectric properties of different shoe materials. This has been compared with the results of finite element model simulations.

A prototype system intended to be integrated with current portal security scanning systems has been developed. It has been evaluated for a wide range of commonly worn footwear, some of which has been modified by the inclusion of concealed foreign material. Clear differences between the measured images of modified and unmodified shoes are seen.

## 8900-31, Session 2

### Passive video imaging at 350 GHz with 251 transition edge sensor bolometers

Daniel T. Becker, National Institute of Standards and Technology (United States); Cale M. Gentry, The Univ. of Colorado (United States); James A. Beall, Hsiao-Mei Cho, William D. Duncan, Dale Li, Gene C. Hilton, Kent D. Irwin, Nicholas G. Paulter Jr., Carl D. Reintsema, Robert E. Schwall, National Institute of Standards and Technology (United States); Peter A. Ade, Carole E. Tucker, Cardiff Univ. (United Kingdom); Simon R. Dicker, Univ. of Pennsylvania (United States); Mark Halpern, The Univ. of British Columbia (Canada)

Millimeter wavelength radiation holds promise for detection of security threats at a distance, including suicide bomb belts and maritime threats in poor weather. The high sensitivity of superconducting Transition-Edge-Sensors (TESs) makes them ideal for passive imaging of thermal signals at these wavelengths. We have built a 350 GHz video-rate imaging system using large-format arrays of feedhorn-coupled TES bolometers. The system operates at a standoff distance of 16-28 m with a spatial resolution of 1 cm (at 16 m). It currently contains one 251-detector subarray, and will be expanded to contain four subarrays for a total of 1004 detectors. The system has been used to take video images which reveal the presence of weapons concealed beneath a shirt in an indoor setting. We will present analysis of these videos as well as the results of beam mapping and optical efficiency measurements.

## 8900-9, Session 3

### Automated detection and identification of illegal drugs and explosives using terahertz time domain spectroscopy (*Invited Paper*)

Rene Beigang, Fraunhofer-Institut für Physikalische Messtechnik (Germany) and Univ. of Kaiserslautern (Germany); Frank Ellrich, Daniel Molter, Joachim Jonuscheit, Fraunhofer-Institut für Physikalische Messtechnik (Germany); Frank Platte, Kostantinos Nalpantidis, IANUS Simulation GmbH (Germany); Thorsten Sprenger, Daniel Hübsch, Tobias Würschmidt, Hübner GmbH (Germany)

Terahertz time domain spectroscopy (TDS) is used to identify hidden explosives and drugs. A reliable method for the automatic identification of substances from reflection and transmission spectra has been developed based on chemometric methods. In principle, terahertz spectra can provide a "fingerprint" of substances to be detected. In most cases, however, the substance-specific information is masked by various environmental contributions to the terahertz spectra. It is essential to apply appropriate mathematical algorithms to pre-process the raw data in the time or frequency domain before a classifier can be derived. Using raw data only would lead to unacceptably large values of „false positive“ and „false negative“ results. We demonstrate that the data pre-processing (pipeline of filters) is essential for the discrimination of the measurements within the so-called "feature space". Based on a reliable and robust mathematical model, methods of pattern recognition can then be used for automatic identification of substances. We also demonstrate that data derived from measurements in the reflection mode demand a much higher effort than for those recorded in transmission mode. The identification performance is demonstrated using a spectrometer which is used to inspect mail. The substances to be identified were hidden in various postal envelopes and covered by a variety of materials. The spectrometer is based on a terahertz time domain spectroscopy system using state of the art laser technology. Fiber coupling inside the spectrometer allows for stable and reliable operation even in rough environments. The spectral bandwidth of more than 3 THz is within the spectral region of interest for most commonly used drugs and explosives.

## 8900-10, Session 3

### Target decomposition and polarimetric radar applied to concealed threat detection

Dean R. O'Reilly, Nicholas J. Bowring, Nacer D Rezgui, David Andrews, Manchester Metropolitan Univ. (United Kingdom)

Target decomposition is of interest to the security and defence community as it enables data sets to be reduced to their principle identifying components as a pre-processor to running machine recognition algorithms. An investigation into the application of target decomposition theory for concealed threat detection is presented. Polarimetric radar has been used in the measurement of scattering matrices for various target scenarios. The radar comprises of a Vector Network Analyser (VNA), an Orthomode Transducer (OMT) and a single conical feed horn antenna in a monostatic configuration. A radar calibration technique is described to ensure accurate measurement of the scattering matrices. Validation of the target decomposition algorithm is achieved by analysing targets with well-known scattering



mechanisms. The decompositions of more complex targets such as those encountered in Concealed Threat Detection (CTD) scenarios are analysed. The decomposition is performed as prescribed by Cloude and the scattering of the illuminating wave due to the target is mapped onto a 3D space detailing polarimetric entropy (H), anisotropy (A) and alpha-angle (?). The decomposition of these complex scattering mechanisms is then used to classify the data. Both simulation and measurements are used to validate this technique. A statistical analysis of this approach is performed which provides useful information such as detection rates and false alarm rates.

### 8900-11, Session 3

#### **A calibration concept for passive MW imaging using beam steering by frequency shift and aperture synthesis**

Eric Schreiber, Markus Peichl, Matthias Jirousek, Deutsches Zentrum für Luft- und Raumfahrt e.V. (Germany)

Passive microwave (MW) remote sensing is used in Earth observation missions for example to estimate the salinity of oceans or the soil moisture of landscapes. In these cases the absolute brightness temperature numbers are important for sufficient accuracy of the estimated geo-physical parameters. Consequently a suitable system calibration network is required. At DLR a radiometric demonstrator for fully-electronic MW imaging was set up at Ka band, which is based on a combination of beam steering by frequency shift using a broadband slotted-waveguide antenna for one scanning direction, and the application of aperture synthesis for the other direction. Aperture synthesis is well known from radio astronomy, but it is still a new imaging principle for Earth observation or security applications. Hence as well new calibration techniques have to be developed for this kind of scanning mechanism. In this paper a novel approach for a noise-source based calibration method taking into account the antenna losses will be introduced. When using aperture synthesis techniques to determine the absolute brightness temperature values, it is very important, among other things, to know the exact phase transfer function of the system in order to achieve the desired radiometric resolution. Consequently our approach enables phase calibration as well. The paper outlines a proof of concept for this calibration method using a two-element interferometer called VESAS (Voll Elektronischer Scanner mit AperturSynthese) as a demonstrator. Various calibrated measurement results will be presented and discussed.

### 8900-12, Session 3

#### **Multispectral THz-VIS passive imaging system for hidden threats visualization**

Marcin Kowalski, Norbert Palka, Mieczyslaw Szustakowski, Military Univ. of Technology (Poland)

Terahertz imaging, is the latest entry into the crowded field of imaging technologies. Many applications are emerging for the relatively new technology. THz radiation penetrates deep into nonpolar and nonmetallic materials such as paper, plastic, clothes, wood, and ceramics that are usually opaque at optical wavelengths. The T-rays have large potential in the field of hidden objects detection because it is not harmful to humans. The main difficulty in the THz imaging systems is low image quality thus it is justified to combine THz images with the high-resolution images from a visible camera. Image fusion can be used in a wide range of security applications for example detection and identification of hidden objects. Security applications very often require a person to operate a system, thus the fused image is intended for presentation to a human observer for easier and enhanced interpretation. THz images are more difficult to assimilate for a human eye than visible images because they present a reality invisible for humans. Visible images are natural for human vision. Our studies show that the fused image should contain information mostly from the visible image with superimposed elements from the THz image showing a detected object.

An imaging system is usually composed of various subsystems. Many of the imaging systems use imaging devices working in various spectral ranges. The aim of our studies is to detect and visualize objects hidden under clothing. Detection of potentially dangerous objects is important, but without proper visualization, can be difficult

to utilize. Our goal is to build a system harmless to humans for screening and detection of hidden objects using a THz and VIS cameras.

The presented system draws attention not only on the properties offered by a single camera but also on the potential of synergetic effects of the system by using the fusion of data registered by different sensor units. In this paper we present the multispectral passive imaging system for hidden threats visualization based on THz and VIS cameras.

### 8900-13, Session 3

#### **Expanded opportunities of THz passive camera for the detection of concealed objects**

Vyacheslav A. Trofimov, Vladislav V. Trofimov, Igor E. Kuchik, Lomonosov Moscow State Univ. (Russian Federation)

Using the original filters we demonstrate new opportunities for the detection of concealed objects captured by passive THz cameras manufactured by different companies. We focus our attention on the opportunity of seeing the trace on the skin of human body from the water or other food eaten by person. To see this, it is necessary to use the passive THz camera which produces sufficient good quality of the image.

In this report, the modern problem of the image quality improvement discusses also. Due to using computer processing of the THz image of objects concealed on the human body, one may improve it many times. As a consequence, the instrumental resolution of such device may be increased without any additional engineering efforts.

### 8900-14, Session 3

#### **Terahertz time-domain spectroscopy for distinguishing different kinds of gunpowder**

Tomas Gavenda, Tomas Bata Univ. Zlin (Czech Republic); Vojtech Kresalek, Tomas Bata Univ. of Zlin (Czech Republic)

Terahertz time-domain spectroscopy is one of the new and most useful applications of terahertz radiation in security industry. The need for new and reliable methods of distinguishing dangerous material such as drugs, explosives or toxics from common material is leading to development of terahertz security systems. This study is focused on distinguishing different kinds of gunpowder as possible explosive material.

Three samples of gunpowder were measured during preliminary measurement. The first sample was common shotgun gunpowder, the second was gunpowder commercially known as MDN-9 and the third was gunpowder commercially known as S35-01. Terahertz time-domain spectroscopy setup was used to measure absorbance spectra of each sample in the range from 0.5 THz to 2 THz (using device TPS Spectra 3000 by TeraView Ltd.). The vacuum was used to purge the measurement chamber from water vapors. The preliminary results are shown in Figure 1.

Three lines in the Figure 1 represent gunpowder absorbance frequency dependency and the differences between them are clearly noticeable. None of the measured samples has any characteristic sharp peak in frequency range from 0.5 THz to 2 THz, but the shape of absorbance spectra can be established as characteristic. The absorbance spectrum of shotgun undefined gunpowder has local maximum at 0.7 THz followed by slight decrease of absorbance which rises again after reaching frequency of 1.2 THz. The absorbance spectrum of MDN-9 has upward trend through the whole frequency range without any characteristic behavior; there are just two small peaks around 1.7 THz caused by remaining water vapors. The absorbance spectrum of S35-01 is increasing up to the local maximum at 1.3 THz, then the absorbance decreases. Described differences can be used to distinguish all three kinds of gunpowder from each other. Thus the terahertz time-domain spectroscopy can be used for distinguishing different kinds of gunpowder.

The next research of gunpowder absorbance is still needed to strengthen the preliminary results and to increase the accuracy of the measurement. In the first measurement the different sizes of granules of gunpowder were used without measuring their size and dispersion

on sample holder; this fact could affect the preliminary results. The database of gunpowder absorbance (or explosive material absorbance in general) is needed for development of terahertz security check system and this study will provide some of the necessary data to store in this database.

## 8900-26, Session PS

### The evaluation of THz-VIS fused images

Marcin Kowalski, Norbert Palka, Mieczyslaw Szustkowski,  
Military Univ. of Technology (Poland)

A growing interest in terahertz technology finds support in a large number of applications. One of the most interesting applications of terahertz waves is imaging. The terahertz range of electromagnetic radiation has large potential in the field of hidden objects detection because it is not harmful to humans. However, the main difficulty in the THz imaging systems is low image quality due to low sensitivity and a small number of pixels in detecting modules of cameras. Considering the fact that even THz images with low pixel resolution still provide valuable information, it is justified to combine them with the high-resolution images from a visible camera. Image fusion can be used in a wide range of security applications for example detection and identification of hidden objects. Our goal is to build a system harmless to humans for screening and detection of hidden objects using a THz camera. Detection of potentially dangerous objects is important, but without proper visualization, can be difficult to utilize. Security applications very often require a person to operate a system, thus the fused image is intended for presentation to a human observer for easier and enhanced interpretation. THz images are more difficult to assimilate for a human eye than visual images because they present a reality invisible for humans. Visible images are natural for human vision. Our studies show that the fused image should contain information mostly from the visible image with superimposed elements from the THz image showing a detected object.

A very important aspect of applying various processing techniques to images is proper assessment of image quality. Image quality assessment (IQA) is essential to determine the possible benefits of fusion as well as to compare results obtained with different algorithms. Furthermore, IQA methods are necessary in order to obtain an optimal setting of parameters for a specific fusion algorithm. We propose a combination of two image quality assessment methods (IQA) as a methodology of assessing quality of the fused images and a method to compare image fusion algorithms.

In this paper we present the results of various image fusion methods and propose a method of assessing quality of the fused image by calculating values of two image quality methods.

## 8900-27, Session PS

### Detection of the THz waves from the 5m distance

Norbert Palka, Michal Walczakowski, Mieczyslaw Szustakowski, Military Univ. of Technology (Poland); Adam Czerwinski, Maciej Sypek, Warsaw Univ. of Technology (Poland)

We report on technical aspects connected with detection of the THz waves reflected from a small target which is situated at the distance of 5 meters. The THz radiation is generated by a commercially available optical parametric oscillator (OPO) working in the range 0.7-2.5 THz with repetition rate 53 Hz, duration of the impulse of about 20 ns and energy 10 nJ. The OPO slightly divergent beam with a diameter of about 20 mm (1/e<sup>2</sup>) is collimated by two 2" concavo-plane polyethylene lenses with the 15-mm focal length. Afterwards, the beam is directed by a 4" flat mirror to the target – the flat 30-mm steel disc. Since the diameter of the THz beam is wider than the diameter of the disc, the disc is situated in a holder that scatters all unwanted radiation. Only radiation from the disc is reflected back, transmits 5m through the atmosphere and is directed to a detector through a flat 4" mirror and a 4" off axis parabolic mirror. The incident angle is about 30°. The beam is detected by the fast and sensitive hot electron bolometer operating at 8K thanks to the pulse tube cryocooler. The signal losses (about 30-40dB) are mainly associated with attenuation of the atmosphere and mismatch between the beam and the disc diameters. Although such heavy losses, the detection in this setup

was possible with S/N ratio even up to 100 what reveals the potential for stand-off detection of materials.

## 8900-28, Session PS

### THz devices evaluation in a time domain spectroscopy system at 1.55 μm pulse excitation

Ioannis Kostakis, The Univ. of Manchester (United Kingdom); Alireza Zandieh, Daniel Hailu, Daryoosh Saeedkia, TeTechS Inc. (Canada); Mohamed Missous, The Univ. of Manchester (United Kingdom)

Recently, great efforts have been dedicated to developing small and compact sources and detectors capable of emitting and detecting radiation in the terahertz (THz) frequency range of the electromagnetic spectrum. The interest in this frequency range stems from the nature of THz waves, which allow scientific problems to be solved in ways that cannot be addressed by any other existing approach. The unique properties, such as absorbance by water, transparency to many optically opaque materials (i.e. clothes, plastics and papers) and ability to penetrate deep into many organic materials without causing any damage, unlike X-rays, make the THz radiation a vital tool for biological and medical applications as well as for security applications. Since the THz region ranges from frequencies of about 100 GHz to 10 THz, it lies between electronics and photonics. Therefore, efforts are devoted in the extension of microwave electronics towards higher frequencies (up-conversion) or in the development of photonic devices towards lower frequencies (down-conversion). To date the latter have proved to be most suitable for room temperature applications.

The operation of such sources relies on the irradiation of semiconductor based photoconductive antennas excited by pulsed or continuous-wave (CW) lasers. At present the most efficient and widely used semiconductor material for THz photoconductive antennas is the low temperature grown GaAs (LT-GaAs) due to its unique properties, which are high dark resistivity, high mobility and ultra-short carrier lifetime. Although spectroscopy systems based on this material are already available commercially, its relatively large energy band gap imposes certain limits on lasers that can be used which on the whole tend to be bulky and requires expensive components hindering the wider commercial use. Therefore, the key challenge is the development of THz systems based on materials with smaller energy band gap, which will allow the use of low cost and smaller in size lasers. The most desirable system comprises photoconductive antennas combined with optically fibre coupled communication laser operating at 1.55 μm wavelength. The operation at this wavelength opens the way to compact, portable and all fiber coupled systems with ease of use and deployment. In this work we present photoconductive antennas fabricated on low temperature Beryllium (Be) doped InGaAs-InAlAs multi quantum well structures in which material properties such as resistivity and mobilities are precisely controlled through structural design. We show that the fabricated devices can generate and detect strong THz pulses in a Time Domain Spectroscopy (TDS) system at 1.55 μm excitation wavelength with 60 dB signal to noise ratio and spectral range up to 3 THz. Finally, the possibility of building a low cost, compact and portable THz spectrometer based on this material is discussed.

## 8900-29, Session PS

### Polarization contrast techniques for THz imaging applications

Piotr Garbat, Warsaw Univ. of Technology (Poland); Norbert Palka, Janusz Parka, Military Univ. of Technology (Poland)

In this paper, we investigate the liquid crystal filters for polarization difference imaging system in THz range. We describe the adaptive polarization difference imaging algorithm and its modification for THz imaging applications. The algorithms presented in this paper have been evolved from adaptive polarization difference imaging (APDI) technique originally developed for optical imaging. In the optical imaging domain APDI algorithm provided significant image contrast enhancement. The APDI algorithm developed for optical imaging of polarization information is modified. to serve for target detection purposes in a scattering media for THz imaging. The input data was

gathered in THz imaging setup with tunable liquid crystal filters. The filter was constructed by two directly adjacent quartz plates and liquid crystal mixture 1852 layer between them. This LC mixture has high birefringence 0.32 and low dispersion in very large spectral range. The quartz plates were separated by copper wires which were also used as electrodes. The average distance between wires was 13mm. In order to align the LC molecules, a electric field was applied. In this work the influence of scattering media on THz imaging and methods for contrast enhancement was examined. The Time Domain Spectroscopy was used to investigate the influence of the amount of scattering media on transmission in the (0.1÷2.5)THz range. Experimental results confirmed the efficiency of proposed techniques, but its strongly depended on scattering media type. The efficiency of scattering depends on the diameter of particles and used radiation. The imaging of object through scattering media using THz signals offers various applications in civilian and defense scenarios.

**8900-15, Session 4**

**Biomedical applications of Terahertz technology (Invited Paper)**

Vincent P. Wallace, The Univ. of Western Australia (Australia)

Early experiments by pioneers of THz imaging demonstrated that the technique could have a variety of applications, including medicine and dentistry - terahertz images of bacon showed contrast between lean meat and fat; changes in refractive index of teeth at THz frequencies allow for the detection of early decay.

Since then there have been many studies of tissues, from wax embedded tissue block, histopathological samples, excised tissues and even some in vivo imaging. Some of this most significant work revealed contrast between regions of healthy skin and basal cell carcinoma, the most common form of skin cancer, in vitro and in vivo. Further, other work on excised breast carcinoma has shown good contrast between tumours and normal tissues. This has led to the development of a prototype handheld (intra-operative THz) imaging probe for use during breast surgery.

The high absorption of THz by water in this range (23 mm<sup>2</sup> at 1 THz) makes transmission imaging through a body impossible, but it is the difference in absorption due to water content which explains the contrast seen between muscle and adipose tissue and between tumour and normal tissue. Terahertz spectroscopic measurements of carcinoma show significant differences in the frequency dependent refractive index and absorption coefficient. Such contrast on the surface is often obvious at optical frequencies but it is the ability of THz to penetrate below the surface that provides the potential for medical imaging, in particular, of epithelial tissues (cancer with origins in tissue surfaces both external and internal), which includes skin, breast and colon cancer, accounts for 85% of all cancers.

More recently, it has been shown that THz can detect dysplastic changes (pre-cancer) in excised colon tissue and the THz data have been correlated to histopathological images using stains that show angiogenesis related changes. New blood vessels (angiogenesis) are known to be "leaky" and thus more interstitial fluid is present leading to increased absorption of the THz signal. It is the ability of THz to penetrate just below the surface that provides the, as yet not fully realised, potential for tissue imaging, visualisation of the subsurface spread of tumours and other applications. Full understanding of the contrast mechanisms in tissues and their physiological significance will enable THz to fulfil its potential for medical applications.

To date in vivo measurements have been limited due to the restricted nature of imaging systems. Compact, mobile THz imaging systems are now being developed which allows for TPI measurements in a clinical setting.

**8900-16, Session 4**

**Terahertz technology for medical applications**

Joo-Hiuk Son, The Univ. of Seoul (Korea, Republic of)

Terahertz (THz) imaging is a promising modality for medical diagnosis because it is non-ionizing, sensitive to water molecules, and capable of spectroscopic analysis. In this presentation, various examples of medical imaging using THz radiation will be reviewed.

First, the feasibility of THz dynamic imaging for visualizing serial changes in the distribution and penetration of a topical transdermal drug is demonstrated and compared with the Franz cell diffusion test. Secondly, some cases of cancer imaging using THz radiation are shown, which include brain tumor and oral melanoma. The THz imaging results are also compared with magnetic resonance (MR) imaging and conventional histology. Thirdly, the principle of terahertz molecular imaging (TMI) technique using nanoparticles is explained and the factors related to molecular imaging, such as sensitivity, resolution, and quantification property are characterized. The technique is applied to the diagnosis of cancerous tumors targeted with phase-conjugated nanoparticles and the distribution measurement of nanoparticle drug delivery to organs in vivo and ex vivo. Lastly, THz imaging is also utilized to analyze blood non-invasively. The THz complex optical constants of blood and its constituents such as water, plasma, and red blood cells (RBCs) are measured and used to extract the concentrations of RBCs. In conclusion, the author believes that there are some points where terahertz imaging can contribute to the real-world medicine.

**REFERENCES**

[1] Son, J.-H., "Terahertz electromagnetic interactions with biological matter and their applications," J. Appl. Phys. 105(10), 102033 1-10 (2009).  
 [2] Oh, S. J., Kang, J., Maeng, I., Suh, J.-S., Huh, Y.-M., Haam, S. and Son, J.-H., "Nanoparticle-enabled terahertz imaging for cancer diagnosis," Opt. Express 17(5), 3469-3475 (2009).  
 [3] Oh, S. J., Choi, J., Maeng, I., Park, J. Y., Lee, K., Huh, Y.-M., Suh, J.-S., Haam, S. and Son, J.-H., "Molecular imaging with terahertz waves," Opt. Express 19(5), 4009-4016 (2011).

**8900-17, Session 4**

**Ultra-compact THz spectrometer for biomolecule detection**

Martin Muthee, Sigfrid K. Yngvesson, Univ. of Massachusetts Amherst (United States)

Terahertz spectroscopy of biomolecules is traditionally performed in a free-space propagation mode, employing either Fourier Transform Spectrometers (FTS), Time-Domain Spectroscopy (TDS) or Photo-mixer systems. We have developed an alternative technique that employs a coplanar waveguide (CPW) THz Integrated Circuit (TIC) and a Single Carbon Nanotube THz Source (CNTS), positioned at one end of the CPW, all on a single silicon substrate. The THz power is radiated from the opposite end of the CPW by an integrated circuit slot bow tie antenna, through a silicon lens, and is then captured by a compact custom-built FTS system. The CNTS source has a broadband incoherent output power of about 100 nW, and can be designed to have output up to 10 THz, but the actual useful frequency range is primarily determined by the matching of the CNTS, CPW and the antenna. The samples are placed on top of the CPW. Employing transmission line methods, the required amount of sample can be much less than in free-space transmission measurements. The CPW is well suited for this application due to the field distribution which has a considerable fraction of the fields in the air, as was made clear from HFSS simulations. The TIC also includes a low-pass filter for introduction of bias to the source. As a demonstration of this system we have measured the THz spectrum of the polymer Polyhydroxybutyrate (PHB) in powder form. The spectrum displays two characteristic absorption lines at ~2.4THz and ~2.9THz typical of PHB. Spectra of additional materials will be presented at the conference. Although in this scheme the PHB was deposited globally on the chip, future iterations aim for a design where the sample is localized only on the transmission line, specifically in the area with high E-fields. Later versions will include nano-fluidic channels fabricated in the silicon substrate before the THz Integrated Circuit is defined on top of the substrate. This version will allow measurements of biomolecules such as DNA suspended in buffer solutions, flowing in the nano channels. Our early results demonstrate a new type of THz spectroscopy system, fully integrated on a silicon chip, with the exception of the detector and the FTS. Furthermore, future integration with conventional CMOS electronics is feasible, given the monolithic nature of the system.

8900-18, Session 4

## Imaging with a single frequency Terahertz system for breast cancer margin detection

Benjamin St. Peter, Kan Fu, Paul R. Siqueira, Patrick A. Kelly, Sigfrid K. Yngvesson, Univ. of Massachusetts Amherst (United States); Ashraf Khan, Stephen J. Glick, Andrew Karellas, Univ. of Massachusetts Medical School (United States)

In breast conservation surgery, the surgeon attempts to remove malignant tissue with a surrounding margin of healthy tissue. Subsequent pathological analysis must determine if the margins are clear of malignant tissue, a process that typically requires at least one day. Only then can a determination about possible follow-up surgery be made, with undesirable consequences in terms of healthcare cost and undue emotional stress.

In a joint UMass/Amherst – UMass Medical School/Worcester (UMMS) project we have developed a new technique, “Single Frequency Terahertz Imaging (SFTI)”. SFTI Imaging systems could potentially contribute toward a solution of the above problem. We image 2 mm thick specimens cut from breast lumpectomies in reflection by employing a 1.89 THz terahertz (THz) gas laser system (wavelength 158 micrometers) as a source and mechanically scanning the samples over a 2 cm x 2 cm area. The images are correlated with optical histological micrographs of the same specimens, and a mean discrimination (i.e., area under the ROC curve) of 73% was found for five out of six samples using Receiver Operating Characteristic (ROC) analysis. The system design and characterization will be discussed briefly. The initial results are encouraging but further development of the technology is ongoing. We are in particular studying our calibration methods in order to improve the accuracy of the absolute reflectivity that we measure on actual samples. We are also performing measurements in two polarizations that may yield further information that distinguishes cancerous from regular tissue. We will report recent results at the conference.

Finally, we will describe how we envision that FDTI can be transitioned into a very compact, inexpensive CMOS THz camera for use in the operating room.

8900-19, Session 5

## T-Sense a millimeter wave scanner for letters (*Invited Paper*)

Dirk Nuessler, Sven Heinen, Fraunhofer FHR (Germany); Thorsten Sprenger, Daniel Hübsch, Hübner GmbH (Germany)

Letter bombs are an increasing problem for companies and public persons. Nowadays every big company uses in his headquarters inspection system to control the incoming correspondence. Generally x-ray systems are used to inspect complete baskets or bags of letters. This concept which works very fine in big company with a large postal centre is not usable for small companies or private persons. For an office environment with a small number of letters x-ray systems are too expensive and oversized. X-ray systems visualize the wires and electric circuits inside the envelope. If a letter contains no metallic components but hazard materials or drugs, the dangerous content is invisible for the most low-cost x-ray systems. Millimeter wave imaging systems offer the potential to close this gap.

The biggest disadvantage of millimeter systems is that they cannot transmit metallic structures like x-ray systems, but they offer many advantages in the detection and differentiation of non conducting. The first question is how to develop a cheap imaging system in the millimeter wave region. Line arrays are too expensive and normal linear xy-scanner concepts too slow. The simplest and fastest scanning system consist of two rotary discs with a conveyor band. One antenna is mounted on the transmitter disc and the other one resides on the receiver disk so that during the rotating scanning process both antennas face each other. The letters move on a conveyor band linearly between the two antennas.

The system works fully coherent and it is possible to analyze in addition to the attenuation also the phase values shifted by the dielectric properties of the letter content. The measurement configuration of T-Sense is a common transmission mode. To decrease the cost of such a scanner system the transmitter and the receiver are based upon commercial millimeter wave components

under 100 GHz. For a first design 78 GHz was selected. On the one hand many high frequency components are very cheap for this frequency range on the other hand through the longer wavelength the resolution of an imaging systems decreases. Antenna geometries using a focusing approach realizes a resolution of several millimeters. This resolution is too poor to detect small amounts of drugs or even small metallic wires. To increase the resolution dielectric tips were used. Though the near field characteristic of the probe heads the resolution can be increased. Depending on the dielectric properties of the device under test (DUT) and the distance between probe head and DUT resolutions under 1 mm for 78 GHz were realized.

The paper describes the development of an autonomous and compact millimeter wave scanning measurement system for security applications which works in the W-Band (CW@78GHz). T-sense was developed to demonstrate the high potential and usability of the millimeter wave region for material classification. With realistic samples the advantages and problems of mmW imaging systems will be demonstrated.

8900-20, Session 5

## Performance simulations of near-field aperture synthesis imaging systems

Neil A. Salmon, MMW Sensors Ltd. (United Kingdom)

The performance of a new generation of near-field aperture synthesis imagers with hundreds of receiver channels systems for portal security screening of personnel will be examined using validated simulation software. The software was validated on a range of aperture synthesis imaging systems developed in previous phases of this research programme. In particular the software is used to examine the spatial resolution of the near-field aperture synthesis approach when the array is non-coplanar, for which refinements to the standard radio astronomy algorithms are required. A variety of imaging array configurations will be used, including a walk through portal and a spherical imaging chamber. It should be noted that these configurations are unique to electronic imaging and have no quasi-optical imaging counterpart, as no optical components exist which could image these configuration without aberrations. As such the resolution limits of Abbe and Fraunhofer diffraction may not apply. These configurations may offer unique new imaging capabilities that could be used not just for security screening and all-weather capabilities, but also for medical imaging when operated at lower frequencies where human tissue is semi-transparent.

8900-21, Session 5

## Impulse radar imaging system for concealed object detection

Frank J. W. Podd, Marcus David, Gohar Iqbal, F. Hussain, David Morris, Efosa Osakue, Yit Yeow, Saquib Zahir, David W. Armitage, Anthony J. Peyton, The Univ. of Manchester (United Kingdom)

Electromagnetic systems for imaging concealed objects at checkpoints typically employ radiation at millimetre and terahertz frequencies. These systems have been shown to be effective and provide a sufficiently high resolution. However there are difficulties and current electromagnetic systems have limitations particularly in accurately differentiating between threat and innocuous objects based on shape, surface emissivity or reflectivity, which are indicative parameters. In addition, water has a high absorption coefficient at millimetre wavelength and terahertz frequencies, which makes it more difficult for these frequencies to image through thick damp clothing.

This paper considers the potential of using ultra wideband (UWB) in the low gigahertz range. The application of this frequency band to security screening appears to be a relatively new field. The business case for implementing the UWB system has been made financially viable by the recent availability of low-cost integrated circuits operating at these frequencies. Although designed for the communication sector, these devices can perform the required UWB radar measurements as well.

This paper reports the implementation of a 2 to 5 GHz bandwidth linear array scanner. The paper describes the design and fabrication of transmitter and receiver antenna arrays whose individual elements

are a type of antipodal Vivaldi antenna. The antenna's frequency and angular response were simulated in CST Microwave Studio and compared with laboratory measurements.

Different types of measurement systems are compared for cost and performance. These systems comprise: a bench top vector network analyser which is a frequency domain method, and two impulse excitation methods: a bench-top pulser plus oscilloscope, and a commercial radar module. The measurement systems are connected to the antenna array through a switching matrix.

The data pre-processing methods of background subtraction and deconvolution are implemented to improve the image quality. The background subtraction method uses a reference data set to remove antenna crosstalk and room reflections from the data set. The deconvolution method uses a Wiener filter to "sharpen" the returned echoes which will improve the resolution of the reconstructed image. The filter uses an impulse response reference data set and a signal-to-noise parameter to determine how the frequencies contained in the echo data set are normalised. The chosen image reconstruction algorithm is based on the back-projection type. The algorithm was implemented in MATLAB and uses a pre-calculated sensitivity matrix to increase the computation speed.

The results include both 2D and 3D image data sets. The 3D data sets were obtained by scanning the dual sixteen element linear antenna array over the test object. The system has been tested on both humans and mannequin test objects. The front surface of an object placed on the human/mannequin chest is clearly visible, but its presence is also seen from a tell-tale imaging characteristic. This characteristic is caused by a reduction in the wave velocity as the electromagnetic radiation passes through the object, which manifests as an indentation in the reconstructed image that is readily identifiable. The prototype system has been shown to easily detect a 12x30x70 mm plastic object concealed under clothing.

## 8900-22, Session 5

### THz remote sensing with $\mu\text{m}$ resolution

Janez Trontelj, Aleksander Sešek, Andrej Vigelj, Univ. of Ljubljana (Slovenia)

Several industrial processes require accurate remote and contactless monitoring of width or thickness dimensions of materials. These materials are usually not optically transparent, so the measurements require either x-rays or radioactive radiation for accurate measurements.

Many of these materials are transparent or semi-transparent to THz radiation. The mm wave length reduces the ability to perform measurements much below the radiation wave length, so the use of THz has been reduced to less accurate requirements.

In the paper a system with much higher accuracy is presented. The system consists of a solid state THz source capable to be frequency modulated in about 10% frequency range at central frequencies from 0.2THz to 1THz. A novel THz detector array with a square law characteristic with a very large dynamic range is used as a mixer of transmitted THz signal and received signals from the target.

The detector itself has very low noise when operating at room temperature and NEP is typically less than  $3\text{pW}/\sqrt{\text{Hz}}$ , with a high sensitivity in the range up to  $1000\text{V/W}$ .

The signal-to-noise ratio is further improved using the heterodyne receiver approach using the portion of illuminating signal for local oscillator. The resulting mixed frequencies represent the information of the target distance from the source and detector.

The object under investigation is placed between the source and the reflective surface, normally a simple metal plate, which acts as a good mirror and requires no special polishing as the operating wave lengths are in mm range. The resulting mixed frequencies represent several reflections from the target, mirror, and also the secondary mirrored signals.

As described before, four different signal components are present on the sensor array. The first is part of primary THz beam which is used for local oscillator for mixing, the second component which presents a reflection from objects front plane, the third component is a reference plate reflection, and the fourth component presents a secondary reflection from objects' rear plane. There are many other components, which were ignored due to small amplitudes and easier presentation. On the receiving sensor all signals are mixed and processed. As a result the information of amplitude and phase of each component is

calculated.

The analysis of the received reflected signals provides robust information regarding the distances and dimensions of the investigated object, and also includes some material properties of the target.

The measurement results of the phase of the selected reflected beams are shown. The phase values versus calculated distance from source are presented, where the phase is shifted by 72 degrees for a  $100\mu\text{m}$  range. From measurement results it is seen that the phase is linear and the precision of position in the  $\mu\text{m}$  range can be easily determined, therefore precise location of observed object can be obtained. The position equivalent noise in the measurement is less than  $1\mu\text{m}$ .

In the paper the details of the measurement system are shown, the algorithms and procedures for extraction of object signal reflection data are presented, and measurement results are discussed.

## 8900-23, Session 5

### Design and operation of ACTPol, a millimeter wavelength, polarization sensitive receiver for the Atacama Cosmology Telescope

Benjamin L. Schmitt, Univ. of Pennsylvania (United States); ACTPol Collaboration, Princeton University (United States)

We highlight considerations for the design and operation of ACTPol, a new receiver for the Atacama Cosmology Telescope (ACT), capable of making polarization-sensitive, millimeter-wavelength observations of the Cosmic Microwave Background (CMB) at arcminute angular scales. ACT is a six-meter telescope located in northern Chile, dedicated to enhancing our understanding of the structure and evolution of the early Universe by direct measurement of the CMB. We describe the design of the ACTPol focal plane at full-deployment, consisting of dual 150 GHz array package modules and a multichroic array package with simultaneous 90 GHz and 150 GHz sensitivity. Each of these detector array packages resides behind a set of custom-designed, high-purity silicon reimaging optics with a novel anti-reflective coating geometry, the characteristics of which will be detailed. Each array package module consists of  $\sim 1000$  transition-edge sensor (TES) bolometers used to measure the response of  $\sim 500$  feedhorn-coupled polarimeters, enabling characterization of the linear orthogonal polarization of incident CMB radiation. The polarimeters are arranged in three hexagonal and three semi-hexagonal silicon wafer stacks, mechanically coupled to an octakaidecagonal, monolithic corrugated silicon feedhorn array ( $\sim 140$  mm diameter). Readout of the TES polarimeters is achieved using time-division SQUID multiplexing. Each array package is cooled using a custom-designed dilution refrigerator providing a 100 mK bath temperature to the detectors, which have a target  $T_c$  of 150 mK. Given the unique cryomechanical constraints associated with this large-scale monolithic superconducting focal plane, we address the design considerations necessary for integration with the optical and cryogenic elements of the ACTPol receiver. With first light projected for Spring 2013, details of the ACTPol receiver deployment and early results will be highlighted. Finally, specific consideration will be given to the context of these associated technologies and their synergistic application supporting allied field applications, including interests in national security, counterterrorism, and nuclear nonproliferation.

## 8900-24, Session 6

### Broadband THz detection and homodyne mixing using GaAs high-electron-mobility transistor rectifiers (Invited Paper)

Sascha Preu, Stefan Regensburger, Friedrich-Alexander- Univ. Erlangen-Nürnberg (Germany); Sangwoo Kim, Tanner Research, Inc. (United States); M. Mittendorff, Helmholtz-Zentrum Dresden-Rossendorf e. V. (Germany); Stephan F. Winnerl, Helmholtz-Zentrum Dresden (Germany); Stefan Malzer, Friedrich-Alexander- Univ. Erlangen-Nürnberg (Germany); Hong Lu, Peter G Burke, Arthur C. Gossard, Univ. of California, Santa Barbara (United States); Heiko B. Weber,

Friedrich-Alexander-Univ. Erlangen-Nürnberg (Germany); Mark S. Sherwin, Univ. of California, Santa Barbara (United States)

We report on a THz detector based on rectification in field effect transistors at frequencies high above the cut-off frequency for amplification. The rectification is due to simultaneous modulation of the carrier velocity and the carrier concentration by an incident THz wave [1]. The device generates a DC bias at the source-drain port that is proportional to the THz power. The device can be coupled to a broadband antenna and mounted on a hyperhemispherical, high-resistive silicon lens in order to improve the coupling efficiency. The rectification effect remains highly efficient even high above the cut-off frequency for amplification, allowing for implementation as THz detector. GaAs-based high electron mobility transistors offer an excellent platform for this detection principle since they offer excellent material properties at room temperature. However, they can also be operated at cryogenic temperatures. They further allow for high speed operation, in contrast to thermal detectors. We designed and characterized several rectifier layouts for room temperature operation. We will present measurements on the responsivity and noise equivalent power of ultra-broadband devices attached to a logarithmic-periodic antenna that have been characterized from 70 GHz to 0.5 THz using the lock-in detection technique. The broadband antenna was either coupled to source and drain or to source and gate. The fast response of the device was examined up to a maximum frequency of 100 kHz, limited by the lock-in amplifier. With antenna-less devices, where the THz field couples directly to an array of FETs that are connected in series, time constants in the 30 ps range can even be reached however, at the cost of responsivity.

We further show a layout of a homodyne mixer for frequencies between 200 GHz and 450 GHz, with optimum performance at 370 GHz [2]: Two orthogonal dipole antennas are implemented, one coupled to source and drain (SD port) the other to source and gate (SG port). Since there is very little cross talk, the two ports can be excited independently by the choice of polarization of the THz wave. This allows for a multiplicative mixer architecture where the DC read out bias at the SD port is proportional to the product of the THz field coupled to the respective antennas. We show simulations on the cross talk, and measurements on the noise equivalent power, and the sensitivity on the THz phase between SD and SG port. Furthermore, we show that the very same detector can be switched to a direct power detector by altering the excitation and read out conditions. Optimized versions of this detector may represent an alternative to state-of-the art Schottky diode mixers.

[1] S. Preu et al., J. Appl. Phys. 111, 024502 (2012)

[2] S. Preu et al., IEEE Trans. on THz Sci. Technol 2, 278-283 (2012)

8900-25, Session 6

## Preliminary Fabrication and Characterization of Low-Leakage Hybrid Coaxial Cable

Arkady Rudnitsky, David Elbaz, Zeev Zalevsky, Bar-Ilan Univ. (Israel)

In this paper we present the fabrication and the initial characterization of a new type of coaxial cable having reduced leakage characteristics and the capability of transmitting optical signals, in addition to the RF signal, through the glass medium between the metallic conductors. The suggested decreased leakage and material loss is obtained by using different metallic shield geometry. The suggested model is composed of a central conductor surrounded by plurality of metallic wires circularly disposed (the central metallic core is shielded by plurality of metallic wires circularly disposed). Those wires help to electromagnetic interference and compatibility as they reduce the electromagnetic leakage of the cable. A glass medium between the metallic cores can be used for transmission of optical information in addition to the transmission of the electromagnetic currents through the metallic core itself.

In the paper we present the numerical design, a new type of simple fabrication technique that was used to realize the proposed cable and then preliminary experimental characterization of this new type of coaxial cable done with 4-ports vector network analyzer.

# Conference 8901A: Optics and Photonics for Counterterrorism, Crime Fighting and Defence IX

Monday - Tuesday 23-24 September 2013

Part of Proceedings of SPIE Vol. 8901 Optics and Photonics for Counterterrorism, Crime Fighting and Defence IX; and Optical Materials and Biomaterials in Security and Defence Systems Technology X

8901-1, Session 1

## Raman spectroscopy for the detection of explosives and their precursors on clothing in fingerprint concentration: a reliable technique for security and counterterrorism issues

Salvatore Almaviva, Sabina Botti, Luciano Cantarini, Antonio Palucci, Adriana Puiu, ENEA (Italy); Frank Schnürer, Wenka Schweikert, Fraunhofer-Institut für Chemische Technologie (Germany); Francesco S. Romolo, Univ. de Lausanne (Switzerland)

The development of new methods for the detection of explosives, fast and direct is increasingly important for applications related to security and, more generally, related to the fight against terrorism and crime and as support of scientific investigation work. In these tasks the sensitivity and specificity in the detection of explosives is a crucial objective.

Among the modern techniques of major interest Raman Spectroscopy (RS) plays an important role due to its molecular specificity and the ability to examine the unknown samples without the need to be manipulated, in a non-destructive way. RS has gained increasing interest because the Raman band frequencies relate to chemical bondings in the compound to be identified, so detection by RS offers the distinct advantages of chemical specificity and benefits from the ability to generate valid reference Raman spectra under laboratory conditions, comparable with spectra obtained in the field.

In this work we report the results of RS measurements on some common military explosives, (Pentaerythritol tetranitrate, PETN, trinitrotoluene, TNT, urea nitrate, UN) and some of the most common explosives precursors (Ammonium nitrate, AN, ammonium perchlorate, AP) deposited on clothing fabrics, both synthetic and natural such as polyester, polyamide, leather and denim cotton.

RS Spectra were obtained using an integrated table-top Raman system (i-Raman from BWTEK inc.), exciting the samples with a solid state GaAlAs laser emitting at 785 nm (linewidth < 0.3 nm), with adjustable power in the range 3 - 300 mW. The detector is a CCD equipped with a built-in thermoelectric cooler working at 10° C, with 2048 pixel (14 um x 200 um), while the spectrometer covers the spectral range up to 3200 cm<sup>-1</sup> with a resolution of 4.5 cm<sup>-1</sup> @ 912 nm. A maximum exposure time of 10 s was used, focusing the laser light through the lenses of an optical microscope (10X, 20X and 40X magnification lenses to focus the laser light in spots of 45, 90, 180 um diameter), while the substances were deposited starting from commercial solutions in concentration of few hundreds of ug/cm<sup>2</sup> with a GeSiM Micropipetting Nano-Plotter, ideal for generating high-quality spots by non-contact dispensing of sub-nanolitre volumes of solutions in order to simulate an homogeneous stain on the fabric surface with a concentration comparable to that of a single fingerprint.

The spectral features of each explosives substance were clearly identified and discriminated from those belonging to the substrate fabrics or from the surrounding fluorescence. Particles of micrometric dimensions trapped between fabric fibers were optically and spectrally identified. Our results show that the application of RS using a microscope-based apparatus can provide interpretable Raman spectra directly from explosive particles of few um<sup>3</sup> for a fast analysis. In addition, this approach leaves the sample completely unaltered. Thus, a clear application of the microscope-based RS is proposed here as a reliable tool for identification of suspicious microparticles during inspections of clothings. The same approach can be thought for the detection of other illicit substances like drugs.

8901-2, Session 1

## Detection of bottled liquid explosives by near infrared

Hideo Itozaki, Hideo Sato-Akaba, Osaka Univ. (Japan)

NIR spectra of beverages and threat liquids were investigated. The absorption peaks related to water, ethanol and sugar were observed in the spectra of the beverages. However, the variation of the spectra for the beverages was very limited so we concluded that complete collection of the spectra from all beverages is not necessary. The distinction of flammable liquids and threat liquids from the beverages was possible with the aid of principal component analysis.

This technique can be applied to the inspection of bottles at airport security and at similar locations. We hope that NIR bottle checkers like this will soon be installed in airports, and the restrictions on carrying bottles will be removed for the convenience of passengers.

8901-3, Session 1

## Spatially offset Raman spectroscopy for explosives detection through difficult (opaque) containers

Guy T. Maskall, Cobalt Light Systems Ltd. (United Kingdom)

With the continuing threat to aviation security from homemade explosive devices, the ban on taking a volume of liquid greater than 100 ml onto an aircraft remains in place. This ban is, however, soon to be lifted, placing an urgent requirement on airports to implement rapid, and effective, screening of liquids that are to be taken on board, in passengers' bags. Raman spectroscopy offers a highly sensitive, and specific, technique for the detection and identification of chemicals. Spatially Offset Raman Spectroscopy (SORS), in particular, offers huge advantages over conventional Raman spectroscopy for detecting and recognizing contents within optically challenging (high opacity) containers; by offsetting the stimulating laser beam from the imaged area, a greater proportion of (Raman) photons from the contents can be recorded with a reduced contribution from the container. Some contribution from the container will inevitably, generally, still be present and this component must be removed, or otherwise dealt with, in order to obtain the best possible measurement of the Raman spectrum of the contents. One of the most challenging aspects for a SORS-based detection system is performing this step in a fashion that generalizes well across the variety of containers presented to it. Containers vary enormously in their composition; glass type, plastic type, thickness, reflectance, and pigmentation will all be variable and cause an infinite range of absorbances, fluorescence background, Rayleigh backscattered laser light, and container Raman bands. In this paper we describe how the data processing chain for Cobalt Light Systems' INSIGHT100 bottlescanner has been developed to cope with, and be robust to, just such variability. By making a set of two measurements, one at the 'zero' position (coincident with the area being imaged), and one at an 'offset' position, the system then automatically removes spectral baselines whilst retaining key spectral (Raman) features and subsequently automatically performs a scaled subtraction of the zero from the offset measurement to leave a residual 'SORS' spectrum that, essentially, comprises the Raman spectrum of the contents. The detection stage is a piecewise-linear discriminant and we also discuss issues of model selection for the detection stage, and how multivariate regression can greatly aid the process. Finally, we demonstrate the high sensitivity of the system on a range of contents and containers, along with its outstandingly low false alarm rate across a large benign set (the Ventress set).

## 8901-4, Session 1

### Characterization of optically compressing diode array for spectroscopic applications

Steven T. Griffin, Univ. of Memphis (United States)

Spectroscopic detection and classification techniques suffer from the collection of excessive data and utilize only a fraction of the information collected for classification. Both human and automated systems utilize an approach where some type of wide band pattern recognition technique is used to establish an understanding of the spectroscopic situation or universe model. This is followed by an examination of a very narrow band spectral region for specific lines verifying the spectral overview. Many automated systems implement this by utilizing traditional optical signal processing via Czerny-Turner (CZ) or related spectrograph, Linear Detector arrays (LDA), and general purpose computers. Ultimately these utilize Principle Components Analysis (PCA) or Partial Least-Squares Discriminant Analysis (PLS-DA) for classification. The flexibility obtained from generating a set of eigen-functions from the wide-spectrum-generated universe model, followed by a sort by significance in classification, results in frequent application in fielded instruments. However, some difficulty has been encountered with implementation due to large physical size, power consumption, mass, and difficulties with low cost implementations. This is particularly the case for small mobile platforms.

Compressed Sensing (CS) techniques have increasingly been utilized in optical, photonic, electronic, and controls applications. This limits data collection to the essentials and reduces the hardware, software, and computational requirements. Limiting the application of CS to just the general computational system prevents the realization of the benefits across the entire system. Thus, vast amounts of data are collected which are ultimately discarded. This results in excessive power consumption, mass, sizes, and complexity. Compressive Sensing requires, at a minimum, a non-uniform encoding system with a non-linear decompression system for total reconstruction. Pseudo-random encoding is frequently preferred because of its close relationship to the  $p \ln(p)$  style information theory limit for signal content. Total reconstruction of a compressed signal has been shown to be very computationally intensive and other optical-based techniques have been demonstrated - accelerating the result. Prior work has demonstrated that total reconstruction is not necessary for PCA and other spectroscopic relevant techniques. In addition, prior work revised the system design and modified the signal processing, both electronic and computational, to reduce system requirements. To propagate this savings back into the photonics and outsized optical chain, it is necessary to further develop alternative techniques. In particular, a modification to the traditional LDA allows the contraction of primary optics - the principle size and mass offender.

In this presentation an optical detector scheme is detailed. A number of configurations are considered with the most savings achieved by a spatial integrating version that allows the maintenance of optical and photonic SNR by collecting a number of photons greater than or equal to the traditional LDA. Since primary optical diameter is largely specified by the need to subtend an angle sufficient to overcome system noise, optical diameters can be reduced by up to an order of magnitude. This also mitigates the optical diameter driven resolution at the detector plane. Some third order and higher issues exist and are addressed. Theoretical development with limited empirical support is to be presented. Treatment is by combination of geometrical optics and electro-optics.

## 8901-5, Session 1

### Effective criteria for the identification of substance using the spectral lines dynamics of reflected THz signal

Vyacheslav A. Trofimov, Nikolay V. Peskov, Svetlana A. Varentsova, Lomonosov Moscow State Univ. (Russian Federation)

We propose new effective criteria for the detection and identification of substances, including explosives. These criteria are integral criteria on time and they are based on the SDA method. We apply these criteria for the detection of explosive in the most difficult cases of the explosive identification. In the first case, we consider the complicated shape of the PWM C4 explosive. In second case we

consider the compound explosive. In all cases we detect and identify the substance. We developed first version of code for real-time identification of substance.

## 8901-6, Session 2

### Spectroscopic studies of the several isomers of UO<sub>3</sub>

Lucas E. Sweet, Dallas D. Reilly, Thomas A. Blake, James E. Szecsody, David E. Meier, Yin-Fong Su, Carolyn S. Brauer, Edgar Buck, Timothy J. Johnson, Pacific Northwest National Lab. (United States)

Uranium trioxide is known to adopt seven different structural forms. While these structural forms have been well characterized using x-ray or neutron diffraction techniques, less work has been done on understanding their optical spectroscopic properties. The structural isomers of UO<sub>3</sub> all have very similar thermodynamic stabilities and they also tend to hydrolyze under open atmospheric conditions. As a result, mixtures of the UO<sub>3</sub> phases and its several hydrolysis products are common. Much effort went into isolating pure phases of UO<sub>3</sub>. Utilizing x-ray diffraction as a sample identification check, infrared, UV/Vis and Raman spectroscopic signatures of amorphous-UO<sub>3</sub>, ?-UO<sub>3</sub>, ?-UO<sub>3</sub>, and two hydrolysis products have been obtained. The spectroscopic signatures of the pure phases can now be used to characterize typical samples of UO<sub>3</sub>, which are often mixtures of isomers and the hydration products.

## 8901-7, Session 2

### Evaluation of adaptive algorithms for detection and classification of fluorescent aerosols in the atmosphere

Pierre Lahaie, Jean-Robert Simard, Sylvie Buteau, Defence Research and Development Canada, Valcartier (Canada)

Laser induced fluorescence (LIF) can be used to detect fluorescing aerosols in the atmosphere. At DRDC Valcartier, an effort is made to use the spectral information contained in the LIF return signal to identify or classify the particles at the origin of the signal. The signal level being very low, photon counting spectral information is envisioned as a way to provide the highest possible signal to noise ratio. With the development of photon counting technology, detection and classification methods are required to evaluate the potential of the technology. The average of the signal in this case can be modeled by the addition of an unknown concentration of particles to a slowly varying background. The measured signal will be discrete and will present an equal mean and variance according to a photon shot noise model. The objectives of the developed algorithms are to estimate the concentration and to classify the contaminant with the use of a database.

Many algorithms have been developed for elliptically symmetric distribution such as the Gaussian or the Multivariate T-distribution. Examples of these algorithms are the Adaptive Matched Filter (AMF) [1] and the Adaptive Correlation Estimator (ACE) [2]. These algorithms are obtained through the Generalized Likelihood Ratio Test (GLRT) [3]. Gaussian distribution can be used to approximate a large Poisson distributed random variable. The AMF and ACE algorithms described in the literature have been developed in a context where only the background contributes to the noise. In photon shot noise conditions, this is not the case because when a contaminant is added to the background aerosols, the number of photons increases and even if the signal to noise ratio increases, it does not increase linearly with the signal level. However, while the algorithms are not optimal for our specific application, they are good candidates.

In [4], a number of measurements of aerosolized biological simulants produced in various conditions are presented. These measurements are used in this study to perform signal simulations and to build a database for classification. The required covariance matrices are built with simulated background data only. The contaminated signals are processed with the algorithms cited above and their performances are evaluated in terms of detection and classification efficiencies. ROC curves are produced for detection and confusion matrices are given for classification.



## Conference 8901A: Optics and Photonics for Counterterrorism, Crime Fighting and Defence IX

[1] Robey F.C., Kelly E.J., Nitzberg R., "A CFAR Adaptive matched filter detector", IEEE Transactions on aerospace and electronic systems, Vol. 28, no 1, January 1992, PP. 208-216

[2] Scharf L., McWhorter L.T., "Adaptive matched subspace detectors and adaptive coherence estimators", Prof Asilomar Conf. on signals, systems and computer, Novvember 1996.

[3] E.J. Kelly, "An adaptive detection algorithm", IEEE Transactions on aerospace and electronic system, vol. AES 22, no1, March 1986,PP. 115-127

[4] Laflamme C., Simard J.R., Buteau, S., Lahaie P., Nadeau D., Houle O., MathieuP., Dery B., Roy G., Ho J., Duchaine C., "Effect of growth media and washing on the spectral signatures of aerosolized biological simulants", Applied Optics, Vol. 50, Issue 6, PP. 788-796, 2011

### 8901-8, Session 2

#### Experimental realization of SDA-method for the detection of substance at long distance

Vyacheslav A. Trofimov, Lomonosov Moscow State Univ. (Russian Federation)

In this report the experimental realization of set-up for the detection and identification of substance at long distance (1-4 meters) is discussed. The feasibility of the detection is demonstrated using the SDA (Spectral Dynamics Analysis) method. Some neutral substances are considered as examples.

### 8901-9, Session 2

#### Standoff detection of bioaerosols over wide area using a newly developed sensor combining a cloud mapper and a spectrometric LIF lidar

Sylvie Buteau, Jean-Robert Simard, Gilles Roy, Pierre Lahaie, Defence Research and Development Canada, Valcartier (Canada); Denis Nadeau, Pierre Mathieu, Defence Research and Development Canada (Canada)

A consequence of the increase in the availability of biological warfare agents combined with the unstable geo-politic world climate and proliferation of asymmetric threats is an increasing biological menace. An efficient stand-off biological warfare detection system providing a detect-to-warn capability would be an important asset for both defence and security communities. Defence R&D Canada (DRDC) had developed, by the end of the 90s, a stand-off bioaerosol sensor prototype based on intensified range-gated spectrometric detection of laser-induced fluorescence (LIF). This sensor called SINBAHD demonstrated the capability to detect and characterize bioaerosols from a stand-off position. Strengthen by these results; DRDC initiated in 2005 the BioSense project, combining the SINBAHD technology with a geo-referenced infrared (IR) lidar cloud mapper. The scope of this technology demonstration project was to demonstrate the capacity of a spectrometric LIF lidar scanning device to detect, map, track and classify bioaerosol from multi-kilometre distances and over wide area.

The concept of the system is based on a two steps dynamic surveillance: 1) cloud detection using an infrared (IR) scanning cloud mapper and 2) cloud classification based on a staring UV Laser Induced Fluorescence (LIF) interrogation. The system can be operated either in an automatic surveillance mode or using manual intervention. The automatic surveillance operation includes several steps: mission planning, sensor deployment, LIF background monitoring, automatic surveillance, cloud detection, LIF anomaly detection, classification and finally alarm generation based on the classification result. Each of these steps has their own challenges, which must all be adequately addressed in order to obtain, at the end, an operational system. As an example, the classification results can greatly suffer of an insufficiently well characterized background. One of the main challenges is the classification step which relies on a spectrally resolved UV LIF signature library. The construction of this library relies currently on in-chamber releases of various materials that are simultaneously characterized with the standoff sensor and referenced with point sensors such as Aerodynamic Particle Sizer® (APS). The system was tested at three different locations in order to evaluate its capacity to

operate in diverse types of surroundings and various environmental conditions. Additionally, the test followed an incremental difficulty scheme in order to evaluate the system performances but also to identify its limits. The system was challenged with various types of biological materials including several interferents both from natural and anthropological origin. The system showed generally good performances even though the troubleshooting of the system was not completed before initiating the Test and Evaluation (T&E) process. The cloud mapping functionality showed very good results and the identified limits were mostly all related to the choices made for the cloud detection algorithms, which can relatively easily be improved. The standoff system performances appeared to be highly dependent on the type of challenges, on the climatic conditions and on the period of day. The real-time results combined with the experience acquired during the 2012 T&E allowed to identify potential future ameliorations and investigation avenues.

### 8901-10, Session 3

#### Radon transform based automatic metal artefacts generation for 3D threat image projection

Najla Megherbi, Toby P. Breckon, Greg Flitton, Andre Mouton, Cranfield Univ. (United Kingdom)

Threat Image Projection (TIP) plays an important role in aviation security. In order to evaluate human security screeners in determining threats, TIP systems project images of realistic threat items into the images of the passenger baggage being scanned. In this proof of concept paper, we propose a 3D TIP method which can be integrated within new 3D Computed Tomography (CT) screening systems. In order to make the threat items appear as if they were genuinely located in the scanned bag, appropriate CT metal artefacts are generated in the resulting TIP images according to the scan orientation, the passenger bag content and the material of the inserted threat items. This process is performed in the projection domain using a novel methodology based on Radon Transform. The obtained results using challenging 3D CT baggage images are very promising in terms of plausibility and realism.

It is well known that detecting threat items using human screeners is important for aviation security. To enhance and monitor screeners' detection performance, TIP technology is used. This is incorporated in the X-ray screening machines to assess aviation security screeners in detecting threats during routine baggage screening operations. In cabin baggage screening, X-ray images of realistic threat items are projected by the TIP system into the X-ray images of the passenger bags being scanned. The use of TIP technology is currently limited to the conventional 2D X-ray baggage screening systems in which the screener looks at the 2D X-ray image of the bag being scanned.

CT technology initially developed for 3D medical imaging applications is in increased use in airports for luggage inspection. Clearly, extending the use of TIP technology in the 3D volumetric CT scanning systems would be of great importance for enhancing screener threat detection performance. Instead of superimposing 2D images of threat items into the 2D X-ray images of passenger bags, 3D TIP requires the 3D insertion of threat item images into the 3D CT image of the passenger bag. This paper addresses these challenges.

Related Work & Example Videos:

Threat Image Projection (TIP) in 3D CT Baggage Imagery

<http://www.cranfield.ac.uk/~toby.breckon/demos/3dtip/>

Automated 3D CT Baggage Screening

<http://www.cranfield.ac.uk/~toby.breckon/demos/baggagevolumes/>

### 8901-11, Session 3

#### Defining human contrast sensitivity and contrast discrimination from complex imagery

Sophie Triantaphillidou, John Jarvis, Gaurav Gupta, Univ. of Westminster (United Kingdom); Harbinder Rana, Defence Science and Technology Lab. (United Kingdom)

Shape, form and detail delineate image structure in our visual

world. These attributes are defined primarily by local variations in luminance contrast within scenes in our visual field. Defining human contrast sensitivity (our threshold of contrast perception) and contrast discrimination (our ability to differentiate between variations in contrast) directly from real complex scenes is of outermost relevance to our understanding of the human visual response to various complex visual scenarios related to field operations, as well as in the design and evaluation of imaging equipment used both in field operations and in security applications.

The overall aim of the first phase of this project presented in this paper is to specify experimentally and further model spatial frequency response functions, which quantify human sensitivity to spatial information in real complex scenes, with and without the presence of noise. In all experimental phases, visual performance is examined for a range of scenes, luminance levels and types of spatial and spatiotemporal noise. We measure four visual response functions:

- i) Isolated Contrast Sensitivity Function (iCSF), describes the ability of the visual system to detect any spatial signal in a given spatial frequency band (visual octave) in isolation and is the closest equivalent to a conventional sinewave CSF.
- ii) Contextual Contrast Sensitivity Function (cCSF), describes the ability of the visual system to detect a spatial signal in a given octave contained within an image. A comparison between isolated and contextual band conditions indicates the extent that spatial information outside of the band of interest acts as a source of signal masking.
- iii) Isolated Visual Perception Function (iVPF), describes visual sensitivity to changes in suprathreshold contrast of any spatial signal in a given spatial frequency octave in isolation.

iv) Contextual Visual Perception Function (cVPF), describes visual sensitivity to changes in suprathreshold contrast in an image.

For the purpose the measurements above, three different relevant complex image contrast metrics, will be discussed: rms luminance contrast, Peli's local band limited contrast and our modified version of the latter. In the paper we will present their implementation in measuring the contrast of a database of complex stimuli and discuss their suitability for measuring perceived image contrast.

Progress will be also given in the paper in the following areas:

- i) stimulus acquisition and characterization, ii) imaging system characterization and set-up, iii) spatial decomposition of the image stimuli to a number of spatial frequency bands, iv) experimental methodology for subjective tests.

VPF and CSF measurements will be presented and compared with 'classical' findings measured using simple visual stimuli, such as sine wave gratings, as well as with more recent relevant work in the literature that employed complex stimuli. Finally, a survey of models of human sensitivity to spatial information, using results from similar investigations that employ complex stimuli, suggests that the contrast sensitivity and discrimination mathematical frameworks developed by Barten can provide a sound starting position for our own modeling studies. We explain our choice of model and its relevance to our work and its use in various image quality metrics.

## 8901-12, Session 3

### Particle swarm optimization on low dimensional pose manifolds for monocular human pose estimation

Jürgen Brauer, Wolfgang Hübner, Michael Arens, Fraunhofer-Institut für Optronik, Systemtechnik und Bildauswertung (Germany)

Automatic assessment of situations with modern security and surveillance systems requires sophisticated discrimination capabilities. Therefore, action recognition, e.g. in terms of person-person or person-object interactions, is an essential core component of any surveillance system. A subclass of recent action recognition approaches are based on space time volumes, which are generated from trajectories of multiple anatomical landmarks (e.g. hands, shoulders, etc.). A general prerequisite of these methods is the robust estimation of the body pose, i.e. a simplified body model consisting of several anatomical landmarks.

In this paper we address the problem of robustly estimating 3D poses from monocular person image sequences.

The first stage of our algorithm is the localization of body parts in the

2D image.

For this, a part based object detection method is used, which in previous work has been shown to provide a sufficient basis for person detection and landmark estimation in a single step.

More exactly, we use the Implicit Shape Model (ISM) not only to detect and track persons, but also to learn the spatial relationship between visual words of a codebook and the locations of 15 anatomical landmarks on the human body.

The output of the ISM processing step is a probability distribution for each landmark and image indicating possible locations of this landmark in image coordinates.

These probability distributions typically show multiple local maxima, especially due to left/right ambiguities -- i.e. left and right body parts are hard to distinguish on a single frame basis.

The second stage of our algorithm searches for 3D pose estimates that best fit to the 15 landmark probability distributions. For resolving the ambiguities introduced by uncertainty in the landmark locations, we perform an optimization within a Particle Swarm Optimization framework.

The population of particles allows to represent a multi-modal probability distribution over all 3D pose hypotheses. Each hypothesis is represented by an individual particle and updated such that it runs into directions of poses that are supported by the image evidence which is represented by the vote densities.

Nevertheless, the search in the high-dimensional 3D pose search space needs further guidance to deal with the inherently restricted 2D input information. Towards this end we propose to compress large motion capture databases into a compact probability distribution.

The probability distribution can be considered as a regulator in a maximum likelihood estimation process which is mainly driven by the maximization of the vote densities.

From the prior we can extract low dimensional manifolds and place the particles directly onto these manifolds in order to limit the search space. Further, the size of the population and its variance is dynamically adapted over time: in cases of high uncertainty about the landmark locations we automatically increase the population size and the variance to search in a broader area of the search space.

Results of the proposed method are shown on the UMPM benchmark and show state-of-the-art performance.

## 8901-13, Session 3

### Human pose classification within the context of near-IR imagery tracking

Ji W. Han, Anna Gaszczak, Ryszard Maciol, Stuart E. Barnes, Toby P. Breckon, Cranfield Univ. (United Kingdom)

Human behaviour analysis remains a major challenge within automated image understanding. To date a wide range of prior work concentrates on the challenges of human pose recovery and understanding within visible-band (EO) imagery with an eventual aim of reliable behaviour understanding. Here, by contrast we target basic human pose classification in thermal-band (IR) imagery with a view to the prioritization and assessment of activity within a tracking context.

Unlike prior work in the field, we leverage the key advantages of thermal imagery in the localization of limb positions. Combined with robust initial detection based the prior prior work of [1, 2] we target two varying pose classification problems:- a) the identification of passive or active individuals within the scene and b) the identification of individuals carrying weapons (or similar large objects).

Active or passive classification is targeted using Histogram of Oriented Gradient (HOG) features descriptors extracted over a set of image sub-regions identified earlier detections [1]. Support Vector Machine classification is used achieving approximately 70% success on this highly challenging problem.

By contrast a range of classification approaches are compared for automatic weapon detection based on a rich geometrical feature descriptor extracted from prior localization of the limbs within the thermal image instance. A successful detection rate of approximately 85% is achieved.

Results are presented using a combined visible-band (EO) and thermal-band (IR) sensor arrangement where individuals are tracked over a range of evaluation scenarios.

Example Videos: <http://www.cranfield.ac.uk/~toby.breckon/demos/>

humantrackingpose/

Prior Related Work (human detection in IR imagery):

[1] MoD Grand Challenge / SATURN: Sensing & Autonomous Tactical Urban Reconnaissance Network - <http://www.cranfield.ac.uk/~toby.breckon/demos/modgrandchallenge/>

[2] Consistency in Multi-modal Automated Target Detection using Temporally Filtered Reporting <http://www.cranfield.ac.uk/~toby.breckon/demos/multimodaldetection/>

## 8901-14, Session 3

### Learning transmodal person detectors from single spectral training sets

Hilke Kieritz, Wolfgang Hübner, Michael Arens, Fraunhofer-Institut für Optronik, Systemtechnik und Bildauswertung (Germany)

Automatic person detection in video sequences is a core problem in many vision based surveillance systems. It provides the basis for action recognition, detection of trespassing, or anomaly detection. The wide range of appearances of people due to pose variations, lighting changes, and differing clothing makes person detection a challenging task.

While person detection in the visible spectrum is quite sensitive to changes in lighting conditions, infrared sensors are able to capture a person's appearance during night times, usually at good contrasts. As opposed to the visible spectrum, infrared images strongly dependent on the temperature of the environment. Therefore the information from both spectra are complementary and the combination can be used to make person detection more robust. In related work infrared and visible spectra are fused at pixel level using a registration between both images. To obtain a flexible system, which can work under a wide range of conditions, a detector which can detect persons in both spectra independently is worthwhile.

Until now person detection using only infrared images or visible images has been investigated separately. Nevertheless, the approach to detect persons is similar in both cases, since the overall shape of a person is the same. For appearance based methods large training data is necessary in order to capture most variations of person's appearance. While high quality training data is available in visible spectrum, only few infrared data sets have been released so far.

In this work we analyze the potential of a transmodal classifier. While being trained on data from the visual spectrum, the transmodal classifier is able to detect persons in the visible spectrum as well as in infrared images. The analyzed classifier is based on integral channel features (e.g. gradient, intensity) which has been shown to give superior performance on standard pedestrian benchmark tests. It utilizes the sum of a channel region as features. Each feature builds the basis for a weak classifier, which are greedily selected and combined by a boosting method in order to generate the final classifier.

In the detection phase the image channels are computed over the whole image, and a sliding window is used to search the image. By using integral images the calculation of single features can be efficiently done. A fast detection is achieved by arranging the weak classifiers in a soft cascade, where false hypothesis are rejected already after evaluating only a few features.

We show initial results on how different integral channel features influence the detection rate in the visible and infrared spectrum, which is the essential prerequisite for achieving transmodality. The convergence properties of the boosting method are analyzed, in order to give further insights into how information is transferred from the visible spectrum to the infrared images.

## 8901-15, Session 4

### Gait patterns for crime fighting: statistical evaluation

Katerina Sulovská, Silvie Belasková, Milan Adámek, Tomas Bata University in Zlín (Czech Republic)

The aim of this paper is to introduce results of our research from the field of gait pattern analysis for safety issues. The paper introduces

recent results of a fundamental study focused on various gait patterns during different conditions. The measurement in proposed range was not done before as the main focus is mainly on the biomedical research of influence of aids and health conditions on gait patterns. Our research is targeted on one-to-one and one-to-many statistical evaluation of patterns' similarity. Such research is capable of deep insight into biometric systems, which may be also used in cooperation with surveillance systems to ensure safety in endangered areas (e.g. stadiums, casinos, hotel, and banks).

The VICON Mocap System was used to obtain 3D data, which were consequently divided into 2D data to get data similar from those from commercial surveillance systems in ideal positions. The VICON system consisted of eight cameras (220 f.p.s.) with the infra-red backlight of 780 nm AlGaAs LED diodes. Each person from the group of 21 subjects (6 women, 15 men) was covered with 31 retro-reflexive marks on selected body parts. Participants were asked to walk in different conditions – normal gait with their natural walking pace, walking on music (2 different rhythms) with no specification, walking on set rhythm (4 different rhythms – M.M. 66, 92, 120, 144), and walking after 5 minute workout on self pace. Each participant walked through the corridor 10 times to obtain at least 10 single steps (or 3 double-steps). Acquired data were exported to the \*.xls format for further work in statistical software. Data were statistically evaluated in the Origin and STATISTICA software.

The results of various statistical tests (t-test, Sheffe post-hoc test, Mann-Whitney U test, one-way ANOVA, cluster test) showed slight differences in results of individual patterns' groups in most cases. The intra-group (e.g. female vs. female) and inter-group (e.g. female vs. man) results depicted better contradistinction and different behavior of each curve. However, some of the results suggests that some body parts are not suitable for recognition as their dissimilarity is minimal.

Preliminary results suggest that gait patterns may be used as biometric characteristics for smaller biometric systems. However, to support their utilization in bigger system is uncertain as we do not have bigger amount of data from different people to compare. In the light of these facts emerging opportunity for employment of gait recognition in greater areas with big databases of thousands of people cannot be confirmed by our research.

## 8901-16, Session 4

### WPSS: watching people security services

Henri Bouma, TNO Defence, Security and Safety (Netherlands); Jan Baan, Technisch Fysische Dienst-TNO (Netherlands); Sander Borsboom, Cameramanager.com B.V. (Netherlands); Kasper van Zon, Xinghan Luo, VicarVision (Netherlands); Ben Loke, Noldus Information Technology BV (Netherlands); Bram Stoeller, Eagle Vision Systems B.V. (Netherlands); Hans van Kuilenburg, VicarVision (Netherlands); Judith Dijk, TNO Defence, Security and Safety (Netherlands)

To improve security, the number of surveillance cameras is rapidly increasing. However, the number of human operators remains limited and only a selection of the video streams is observed. Intelligent software services can help to evaluate people's behavior and show the most relevant and deviant patterns. In this paper, we present a software platform that contributes to the observation and analysis of human behavior. This platform was developed by a consortium of multiple companies in the WPSS-project. The platform consists of several components. It uses real-time tracking in multiple mono-cameras for overview, tracking in stereo-cameras for high location accuracy, and person re-identification to couple information between cameras. To enrich the person description, we used face analysis, body-part detection and 3D pose estimation. Finally, information is combined, tracks are analyzed, behavior is interpreted by a reasoning engine and directly visualized. The security services fuse all information and the results are made available in an online platform. This system has been tested and demonstrated in a crowded shopping mall with multiple cameras and different lighting conditions.

8901-18, Session 4

## Usage of cornea and sclera back reflected images captured in security cameras for forensic and card games applications

Zeev Zalevsky, Asaf Ilovitsh, Bar-Ilan Univ. (Israel); Yevgeny Beiderman, Bar-Ilan Univ (Israel)

In this paper we present an approach allowing seeing objects that are hidden and that are not positioned in direct line of sight with security inspection cameras. The trick we are using is based on inspecting the back reflections obtained from the cornea and the sclera of the eyes of people attending the inspected scene and which are positioned in front of the hidden objects we aim to image. The scene can be a forensic scene or for instance a casino in which the application is to see the cards of poker players seating in front of you. As the sclera is not a perfect optical surface (in opposed to the cornea) and it has roughness much larger than the one of the cornea, we first map the space variant point spread function (PSF) that is generated when a point light source is being reflected from the sclera. The mapping is done by turning on a point light source positioned next to the inspecting camera and seeing the obtained back reflected point image. As the eyes of the person facing the camera and whose eyes are used for the back reflection are constantly moving, the spatial mapping of the PSF is obtained in a short time. After mapping of the space variant PSF, the obtained result is used to construct a space variant filter that is applied to the spatial sharpening of the back reflected images obtained from the sclera and the cornea of the eyes of the people positioned in front of the security imaging camera. Image super resolving algorithms that take into account the constant movement of the eyes of the people positioned in front of the security camera are proposed to further enhance the constructed back reflected image. Experimental results that validate the proposed concept are presented.

8901-19, Session 4

## Recent developments in automatic lip-reading

Richard Bowden, Univ. of Surrey (United Kingdom); Stephen Cox, Richard Harvey, Yuxuan Lan, Univ. of East Anglia (United Kingdom); Jon Ong, Univ. of Surrey (United Kingdom); Barry-John Theobald, Univ. of East Anglia (United Kingdom); Gari Owen, Annwyn Solutions (United Kingdom)

Human lip-readers are increasing being presented as useful in the gathering of forensic evidence but, like all humans, suffer from unreliability. Here we report the results of a long-term study in automatic lip-reading with the objective of converting to video-to-text (V2T). The V2T problem is surprising in that some aspects that look tricky, such as real-time tracking of the lips on poor-quality interlaced video from hand-held cameras, prove to be relatively tractable. Whereas the problem of speaker independent lip-reading is very demanding due to unpredictable variations between people. Here we systematically review the problem of automatic lip-reading for crime fighting and identify the critical parts of the problem.

8901-20, Session PS

## Ammonia detection using optical reflectance from porous silicon formed by metal-assisted chemical etching

Igor Iatsunskyi, Valentyn Smyntyna, Nickolay Pavlenko, Yuliia Kirik, Olga Kanevska, Valeryi Myndrul, Odessa I.I. Mechnikov National Univ. (Ukraine)

Ammonia detection draws a considerable interest with regard to military, environmental, industrial and medical perspectives. Different sensor technologies are available for ammonia detection in various application areas. Optical and mass spectroscopic techniques exist for ammonia detection. Those techniques provide more reliable and selective measurements. However, the high complexity and large size of spectroscopic sensors obstruct their miniaturization, portability and

manufacturing at low cost. While optical spectroscopic sensors are mature and widely used, emerging alternative optical technologies are significantly contributing to advancements in the current sensing techniques. Silicon photonic sensors are examples of such emerging technologies. Porous silicon exhibits a great potential in optical sensor applications due to the possibility to change its reflectance index and luminescence properties after adsorption of molecules. The sensitivity of an optical sensor depends on the adsorption properties of the measured substances and the interaction of the specific analyte with the porous silicon, which can be adjusted and improved by proper fabrication parameters. Porous silicon, obtained conventionally by anodisation of crystalline p-type silicon (electrochemical method), is a potential platform for high efficiency gas sensors mainly due to its very large surface to volume ratio, which enhances adsorption of the sensing gas, a primary step for gas sensor. Recently, a new method, termed metal-assisted chemical etching, has been developed, which is relatively simple compared to the electrochemical method. The method does not need an external bias and enables a formation of uniform PS layers more rapidly than the conventional methods.

Results of ammonia detection using optical reflectance from porous silicon formed by metal-assisted chemical etching are discussed. Reflected light of various wavelengths scattered from the rough surface of porous silicon with different morphology is compared before and after exposure to ammonia gas. After exposure to gas the optical reflectance for all wavelengths is increased indicating the presence of ammonia molecules. The porous silicon is most sensitive for short optical wavelengths (435 nm). It is found that using a macroporous silicon is more efficiently than microporous silicon. The ammonia detection limit is estimated at about 20 ppm.

8901-21, Session PS

## Investigating existing medical CT segmentation techniques within automated baggage and package inspection

Najia Megherbi, Toby P. Breckon, Greg Flitton, Cranfield Univ. (United Kingdom)

3D Computed Tomography (CT) Image segmentation is already well established tool in medical research and in routine daily clinical practice. However, such techniques have not been used in the context of 3D CT image segmentation of novel Unaccompanied Baggage and Package Screening (UBPS) systems using CT imagery. UBPS CT systems are increasingly used in airports for security luggage examination. We propose in this contribution an investigation of the current 3D CT medical image segmentation methods for use in this new domain. Experimental results of 3D segmentation on real UPBS CT imagery using a range of techniques are presented and discussed.

In recent times, aviation security has received significant attention worldwide. Security screening technologies such as CT systems are becoming increasingly used for luggage examination to detect potential threats. Currently screening is a manual inspection process based on human interpretation of 2D X-ray (or 3D CT density) images. This process is tedious and subject to operator's skill and training. Also the image interpretation process itself is difficult task in the case of cluttered luggage with overlapping objects. It is therefore desirable to provide a functionality that allows the operator to specify objects of interest for examination and to separate them out to view them individually. Displaying and manipulating the object in 3D allows the operator to access information which is not available in a 2D X-ray image and provides better viewing and interpretation than traditional 2D inspection techniques.

Such functionality can be achieved by integrating 3D object segmentation techniques into this visual inspection process. This functionality has the advantage that it reduces the amount of visual data that needs to be analyzed and focuses analysis on suspicious objects found in the luggage. Also it allows consistency, minimizes subjectivity and most importantly improves reliability and efficiency of the overall process. From the literature, no previous work has been done on the integration of 3D object segmentation into the UBPS inspection process. By contrast the use of such techniques in the domain of medical imaging is well established both in the field of exploratory medical research and in routine daily clinical practice. In this paper we present a novel work which aims to investigate the effective use of 3D CT medical image segmentation techniques and how they can be applied to the task of automating the existing manual CT baggage inspection processes.

8901-22, Session PS

### Ultra-long range surveillance camera for critical infrastructure protection research range

Marek Zyczkowski, Mieczyslaw Szustakowski, Mateusz Karol, Rafal Dulski, Jaroslaw Barela, Mariusz Kastek, Military Univ. of Technology (Poland); Piotr Markowski, Marcin Kowalski, Military Univ of Technology (Poland)

Visible, LLTV and Anty-Fog cameras have different abilities to capture external information, and combining these abilities of the three can greatly improve the environment perception ability of intruders or emergency situations. Designed specifically for professional surveillance use, multi active pixel sensor camera of this type allows targets to be monitored at long distance and tracked using the proportional pan, tilt and zoom system. The article describes the research carried out for the camera to determine realistic and standardized parameters, especially the range of detection, recognition and identification of humans. The paper presents measuring equipment, procedures and results.

8901-23, Session PS

### The use of fiber optic sensors for the direct, physical protection of museums and cultural heritages

Marek Zyczkowski, Military Univ. of Technology (Poland)

The fibre optic sensors are used in intrusion detection where the natural benefits of the material are matched by parallel developments in support technologies and applications experience. This paper describes some developments and applications by sensors and systems. In particular, for the immediate protection of museum collections and the protection of large area monuments and memorials.

8901-24, Session PS

### Passive automatic anti-piracy defense system of ships

Marek Zyczkowski, Mieczyslaw Szustakowski, Mateusz Karol, Wieslaw Ciurapinski, Mariusz Kastek, Military Univ. of Technology (Poland); Ryszard Stachowiak, Internet Sp. z o. o. (Poland); Piotr Markowski, Military Univ of Technology (Poland)

The article describes the technological solution for ship self-defence against pirate attacks. The paper presents the design solutions in the field of direct physical protection. They are connected with the latest optoelectronic and microwave systems and sensors to detect, recognize and the threat posed by pirates. In particular, were carried out tests of effectiveness and the detection-range of technology demonstrator developed by a team of authors.

8901-25, Session PS

### Detection of explosive liquid mixtures by spatially offset raman spectroscopy

Qiaoyun Wang, Northeastern Univ. at Qinhuangdao (China)

Spatially Offset Raman Spectroscopy (SORS) was used to detect the explosive liquid mixtures through diffusely scattering containers. SORS method relies on the collection of Raman Spectra from spatial regions offset from the point of illumination on the sample surface. Compared with conventional Raman, the SORS sensitivity is enhanced by suppressing fluorescence and the Raman spectra of sample from the diffusely scattering package overwhelming the subsurface Raman signal. In this paper, the measurements focus on the mixtures of hydrogen peroxide solution, a critical component of liquid explosives, with highly absorbing or fluorescing beverages and

creams. This method enabled the detection of concealed hydrogen peroxide solution in all the studied cases.

8901-26, Session PS

### Photoacoustic detection by means of a differential double resonator cell applied to security and defence

Arturo S. Vallespi, Instituto de Investigaciones Científicas y Técnicas para la Defensa (Argentina); Veronica Slezak, Alejandro L. Peuriot, Francisco Gonzalez, Andrea Pereyra, CEILAP-CITEDEF (Argentina); Guillermo D. Santiago, Univ. de Buenos Aires (Argentina)

The purpose of this article is to present a sensitive optical system for immediate detection of trace substances associated with security in public spaces (TNT, RDX, nitroglycerine, ammonium nitrate, NH<sub>3</sub>, etc.) and storage or explosive detection. Since these substances present a strong absorption band between 9 and 11 μm, we propose its detection by means of photoacoustic spectroscopy (PAS) and study some properties with both a pulsed CO<sub>2</sub> laser (TEA) and a CW CO<sub>2</sub> laser. The laser beam is aimed to an innovative dual resonator differential cell (Fig. 1) designed by means of finite elements method, which lowest resonant frequency is the first longitudinal mode at 1204 Hz. The beam is modulated at the cell's resonance by means of a chopper with a special blade which allows both reflection and transmission of the laser beam. A differential microphone (Knowles NR 23160) is coupled to both resonators [1] [2] at the midpoint of the cell. The characteristics of the differential microphones would minimize noise from distant sources, such as ambient noise and local heating of the cell windows. With the aim of characterizing the system we started the studies with ammonia. The chosen cell's material is polypropylene, suitable for reducing the effects of adsorption due to the polarity of the ammonia molecule [3]. In order to take into account error sources during the measurements of low concentrations, physical adsorption-desorption at the cell's walls is studied by means of the record of the PA signal decay using the TEA CO<sub>2</sub> laser. A theoretical model, based on Langmuir's isotherms, fits well the experimental results. As a result, a 5 % PA signal decay from an enclosed sample of 248 ppmV of NH<sub>3</sub> in N<sub>2</sub> was registered within 1 hour. Based on this result, minimum errors of the concentrations values are expected from measurements carried out on flowing gas mixtures passing through both resonators. The setup for CW CO<sub>2</sub> laser excitation takes advantage of the differential microphone by picking up out of phase signals. For this purpose, a polished chopper wheel was prepared to allow generating the direct and the reflected beam, alternatively aimed to one resonator and the other (Fig. 2). The measurements show that for the double resonator configuration a signal increase is achieved as expected from the study of the sensitivity of both resonators separately, which had been previously characterized. The first measurements with this system indicate a limit of detection of around 90 ppbV at 1W, deduced from one standard deviation of the PA signal from pure N<sub>2</sub>.

References:

- [1] R. Bernhardt, G. Santiago, V. Slezak, A. Peuriot, M. González. Sensors and Actuators B 150; (2010) 513–516.
- [2] A. Schmohl, A. Miklós, and P. Hess. Appl Opt. 41; (2002) 1815-1823.
- [3] N. Melander and J. Henningsen. AIP Conf. Proc. 463; Proceedings of the 10th international conference on photoacoustic and photothermal phenomena, (23-27 Aug 1998) 78-80.

# Conference 8901B: Optical Materials and Biomaterials in Security and Defence Systems Technology X

Wednesday 25–25 September 2013

Part of Proceedings of SPIE Vol. 8901 Optics and Photonics for Counterterrorism, Crime Fighting and Defence IX; and Optical Materials and Biomaterials in Security and Defence Systems Technology X

8901-30, Session 5

## Lasing and random lasing based on organic molecules (*Invited Paper*)

Jaroslaw Mysliwiec, Lech Sznitko, Adam Szukalski, Konrad Cyprych, Andrzej Miniewicz, Wrocław Univ. of Technology (Poland)

Here we present experimental results of studies on the amplified spontaneous emission (ASE) phenomenon, lasing and random lasing with the use of different luminescent organic molecules and polymeric matrices. As active molecules we have used well know Rhodamine 6G, derivative of spiropyranes and selected derivatives of pyrazoline. As polymeric matrices we have used biopolymeric based materials with different surfactants, poly(methyl methacrylate), poly(N-vinyl carbazole) and poly carbonate. We report on ASE, lasing and random lasing characteristics in function of different excitation pulse energy densities evaluating thresholds, exponential gain coefficients and reporting the influence of the specific matrix-dye interactions on the photo-degradation process of the dye.

8901-31, Session 5

## Matrix influence on photoluminescence of organic dyes in solid medium (*Invited Paper*)

Ileana Rau, Univ. Politehnica of Bucharest (Romania); Aurelia Meghea, Univ Politehnica of Bucharest (Romania); Alexandrina Tane, François Kajzar, Roxana Zgarian, Gratiela Tihan, Univ. Politehnica of Bucharest (Romania)

For development of organic light emitting diodes important is an easy fabrication of solid films containing fluorescent molecules with highest possible quantum efficiencies. One of the important problems encountered with efficient photoluminescent molecules is the fluorescence quenching which is principally due to the molecules aggregation. It limits the quantum efficiency of organic light emitting diodes made with them. Therefore having an adequate matrix limiting these effects is highly desirable. One of a possible solution is offered by biopolymers like DNA and DNA-surfactant complexes. Due to their specific double strand helical structure a larger free volume is available determining weaker interaction between molecules. In this presentation we will review results of our recent studies of fluorescence of several organic dyes in DNA and DNA-CTMA matrices as function of their concentration and we will compare them with that measured when some synthetic polymers, like PMMA are used as host medium.

8901-32, Session 5

## Preparation, linear and NLO properties of DNA-CTMA-SBE complexes

Ana-Maria Manea, Ileana Rau, François Kajzar, Aurelia Meghea, Univ. Politehnica of Bucharest (Romania)

The deoxyribonucleic acid (DNA) was first functionalized with the surfactant cetyltrimethylammonium (CTMA) and after with sea buckthorn extract (SBE) at different concentrations. The complexes were processed into good optical quality thin films by spin coating on different substrates such as: glass, silica and ITO covered glass substrates. SBE contains many bioactive substances that can be used in the treatment of several diseases, such as cardiovascular disease, cancer, and acute mountain sickness [1]. The obtained thin films were characterized for their spectroscopic, fluorescent, linear and nonlinear optical properties as function of SBE concentration. The third-order nonlinear optical (NLO) properties of thin films were determined by the optical third-harmonic generation technique at 1 064.2 nm fundamental wavelength. The thin film refractive indices were determined by the Fabry-Perot (FP) interferences.

Acknowledgements

The work of Ana-Maria Manea was funded by the Sectoral Operational Programme Human Resources Development 2007-2013 of the Romanian Ministry of Labour, Family and Social Protection through the Financial Agreements POSDRU/107/1.5/S/76903. The authors acknowledge also the financial support of Romanian Ministry of Education, Research, Youth and Sports, through the UEFISCDI organism, under Contract Number 3/2012, Code Project PN-II-PT-PCCA-2011-3.1-0316.

[1] Zu Y, Li C, Fu Y, Zhao C, Simultaneous determination of catechin, rutin, quercetin kaempferol and isorhamnetin in the extract of sea buckthorn(Hippophae rhamnoides L.) leaves by RP-HPLC with DAD, J Pharm Biomed Anal 41 (2006) 714–719.

8901-33, Session 5

## Speed and direction sensing with a patterned bacteriorhodopsin film (*Invited Paper*)

Yoshiko Okada-Shudo, The Univ. of Electro-Communications (Japan)

Patterned photosensors using a light-sensitive protein can detect the speed and direction of a moving light spot allowing for improvements in robotic sensors. We designed photosensors based on the bacteriorhodopsin pigment found in the cell membrane of Halobacterium salinarum and showed that motion detection is possible using only one sensing element. These sensors have been successfully demonstrated on an autonomous maze-navigating robot. Biophotosensors also offer many advantages: pre-processing functions at the material level, environmental friendliness in terms of material production and disposal, and lower costs. They therefore can provide efficient devices for robot vision applications. The bR-based sensors also respond strongly to rapidly moving objects, though not at all to slow ones.

8901-34, Session 6

## Polymer laser vapour sensors for explosives (*Invited Paper*)

Graham A. Turnbull, Yue Wang, Ying Yang, P. Morawska, Ifor D. W. Samuel, Univ. of St. Andrews (United Kingdom)

A major post-conflict challenge in war affected countries is the detection and removal of landmines and other explosive remnants of war. Conventional approaches for detection of landmines include the use of metal detectors and ground-penetrating radar. Within the FP7 security project TIRAMISU (Toolbox Implementation for the Removal of Anti-personnel Mines, Submunitions and UXO) we are developing compact polymer-based sensors for detecting vapours of explosives to complement these other detection techniques in humanitarian demining.

In this talk we will introduce organic semiconductors- unusual plastic materials that can emit light and conduct electricity. We will show how these can be used to make miniature plastic lasers powered by LEDs, and how the photophysics of the materials can be exploited to make very sensitive sensors for vapours of explosives. We present nitroaromatic explosive vapour detection using polymer lasers, and show how the speed of detection and sensitivity can be controlled by molecular design.

8901-35, Session 6

### Detection of explosive vapours with Diketopyrrolopyrrole thin films: exploring the role of structural order and morphology on thin film properties and fluorescence quenching efficiency

Callum J. McHugh, Andrew McLean, Monika M. Warzecha, Jesus Calvo, Univ. of the West of Scotland (United Kingdom); Alan R. Kennedy, Univ. of Strathclyde (United Kingdom)

The synthesis, spectroscopy and fluorescence quenching behaviour of several Diketopyrrolopyrrole (DPP) small molecules are reported. DPP platforms are promising candidates in solid state optical and optoelectronic molecular sensing applications owing to the high degree of diversity in the parent molecular scaffold, which enables optimisation of solid state structure and morphology and control of important electronic properties such as fluorescence quantum yield and charge transport. We report the preparation of amorphous and ordered DPP thin films with strong solid state luminescence, which was confirmed using powder x ray diffraction, electron microscopy and absorption and emission spectroscopy techniques. Underpinned by molecular modelling studies and single crystal x-ray diffraction studies we will demonstrate that electronic coupling in the films is strongly influenced by interactions of the DPP core via intermolecular  $\pi$ -overlap of the phenyl rings and can be subtly altered in a predictable manner via judicious variation of phenyl ring substituents. Thus, a high level of control of optical properties in these materials is possible through the careful control of their periodical order. The effects of thin film properties on modulation of fluorescence in response to nitroaromatic explosives are reported. Solid state fluorescence is efficiently reduced in amorphous and ordered films upon exposure to 2,4-DNT (80 % overall) and nitrobenzene (100 % overall), with fluorescence quenching generally occurring more rapidly in the amorphous materials. In addition to important physical properties such as explosive reduction potential and vapour pressure we will demonstrate that the quenching efficiency is strongly influenced by the thickness, morphology and crystalline order and stability in the DPP films. The rapid and efficient quenching of DPP thin films toward nitroaromatic derivatives qualifies their application as optical sensors in the vapour detection of these explosives.

8901-36, Session 6

### Nanovectors as a complex solution for optical securing

Artur Bednarkiewicz, Dariusz Hreniak, Wieslaw Strek, Nanovectors Ltd. (Poland)

Nanovectors technology is a comprehensive solution, which includes unique luminescent nanolabels (nanovectors), dedicated equipment for reading of the same and verification algorithms – all devoted for anti-forgery protection of valuable objects. Nanovectors themselves have a complex and unique luminescence spectrum fingerprint resulting from the selection of their composition, type and substrates, which make any attempt to fake the spectral information practically impossible. Nanovectors constitute a special code enabling correct identification only for specified measurement conditions. Moreover, Nanovectors may be used for marking of a wide range of products such as documents, ID cards, access cards and employee cards, spare parts, elements of packaging, liquids, greases etc. Either entire volume of objects during their production process, pressing in a specified location of an object after production or unique printing on the object's surface may be conveniently employed. Nanovectors are most often manufactured as invisible security features and, therefore, special tools are necessary to detect their presence.

The conducted research was focused on experimental verification of reproducibility of Nanovectors reading and theoretical estimation of maximal number of distinguishable optical codes, which confirmed the ability to unequivocally detect thousands of such spectral fingerprints.

8901-37, Session 7

### High- and low-index superhybrid materials for photonic device applications (*Invited Paper*)

Okihiro Sugihara, Tohoku Univ. (Japan)

Organic polymers containing inorganic nanoparticles are promising candidate to realize ultralow and ultrahigh refractive indices. Superhybrid materials with low and high indices below 1.4 and over 1.9, respectively were synthesized by using various kinds of nanoparticles, polymers and coupling agents. High resolution waveguide core ridge was fabricated by nanoimprint process, and multi-layered optical devices were fabricated using hybrid materials.

8901-38, Session 7

### Nanosopic actuators in light-induced deformation of glassy azo-polymers

Marina Saphiannikova Grenzer, Vladimir P. Toshchevikov, Leibniz-Institut für Polymerforschung Dresden e.V. (Germany); Jaroslav Ilnytskyi, Institute for Condensed Matter Physics (Ukraine)

Further progress of human civilization is unthinkable without technologies based on smart materials, which are able to execute specific functions in response to external stimuli. Light is a clean energy and can be controlled rapidly and remotely, with a submicron-precision. Therefore, light-controllable polymers have a fascinating potential for green nanotechnologies, serving as templates, sensors, artificial muscles and actuators. Undoubtedly, the most perspective class of these compounds are polymers containing azobenzene (azo) chromophores. The photoisomerization between trans and cis azo-states is a primary source of photo-mechanical deformation in azo-polymers, the driving mechanism being well-understood in the case of specially-designed liquid crystalline azo-networks.

Sufficiently large deformations can be also induced in amorphous glassy azo-polymers by polarized light: both uniaxial deformations [1] and bending were observed [2]. However, the nature of the underlying driving mechanism stays nearly two decades a controversial and unsolved issue. None of the numerous theories proposed so far is able to predict the sign of the deformation, i.e. expansion/contraction or concave/conclave bending, for a sample with a particular molecular structure. This shows a great need for an advanced theoretical approach, which would open a way for correct and accurate prediction of photomechanical properties of glassy azo-compounds from the molecular architecture. Here we present such approach.

It is based on the reorientation mechanism of azos perpendicular to the polarization of light. The analytical part of our approach is a generalization of the recent microscopic theory [3] to predict photo-deformation behavior of glassy azo-molecules. The theory is complemented by appropriate molecular architecture data evaluated from molecular dynamics (MD) simulations [4]. In particular, we model a side-chain azo-polyester which is observed to expand along the light polarization under uniform illumination [1]. MD simulations revealed that azos belonging to the same molecule build propeller-like structures, consorted reorientation of which transfers the light energy into a uniaxial stress. This is the first direct observation of nanoscopic light actuators, responsible for photoinduced deformations in glassy azo-polymers. Moreover, the tensile stress, induced by reorientation of azos, is found to be large enough to expand the glassy sample. This is in a perfect accord with the experimental observations [1] and thus demonstrates a great predictive strength of our combined approach.

This work was supported by the DFG grant GR 3725/2-2.

References

1. D. Bublitz et al. Appl. Phys. B 2000, 70, 863.
2. D. H. Wang et al. Macromolecules 2011, 44, 3840.
3. V. Toshchevikov et al. J. Phys. Chem. B 2009, 113, 5032.
4. J. Ilnytskyi et al. J. Chem. Phys. 2011, 135, 044901.

## 8901-39, Session 7

### Surface roughness induced random lasing in organic media

Lech Sznitko, Adam Szukalski, Konrad Cyprych, Andrzej Miniewicz, Jaroslaw Mysliwiec, Wroclaw Univ. of Technology (Poland)

Here we report on the surface roughness induced random lasing phenomenon observed in biophotonic matrix: an modified deoxyribonucleic acid with cationic surfactant cetyltrimethylammonium chloride (DNA-CTMA), doped with Rhodamine 6G (Rh6G) laser dye. The potential for photonic application of DNA-CTMA has been shown in many recent fields of research like: bio-organic light emitting diodes construction (bioLEDs), optical switching, luminescence and amplified spontaneous emission enhancement and distributed feedback laser fabrication [1-4]. All mentioned above features together with easy fabrication using casting technique prompt us to study this media as a materials for random lasing.

The random lasing was achieved using doubled in frequency Nd:YAG nanosecond pulse laser as a source of photo-excitation. The threshold for laser emission varied from  $r_{th} = 16.6 \text{ mJ/cm}^2$  to  $r_{th} = 33 \text{ microJ/cm}^2$  for different excitation conditions. The average resonator length was estimated to amount 37 microns using Fast Fourier Transformation of obtained emission spectrums.

We believe that further investigations of polymeric materials for which surface roughness can be easily induced may contribute to commercialization of polymeric random lasers.

This work was financially supported by Polish National Science Centre, (Dec-2011/01/B/ST5/00773) and Wroclaw University of Technology.

#### References

- [1] A. J. Steckl, Nature Photonics 1 3-5 (2007)
- [2] A. Miniewicz, A. Kochalska, J. Mysliwiec, A. Samoc, M. Samoc, JG. Grote, App. Phys. Lett. 91 041118 (2007)
- [3] Z. Yu, W. Li, JA. Hagen, Y. Zhou, D. Klotzkin, J. G. Grote, A. J. Steckl, Appl. Opt. 46 1507-1513 (2007)
- [4] L. Sznitko, J. Mysliwiec, P. Karpinski, K. Palewska, K. Parafiniuk, S. Bartkiewicz, I. Rau, F. Kajzar, A. Miniewicz, Appl. Phys. Lett. 99 031107 (2011)

## 8901-40, Session 7

### electro-optic properties of novel azobenzene polymers

Oksana Krupka, Vitaly Smokal, Sergei Studzinsky, Nikolay A. Davidenko, National Taras Shevchenko Univ. of Kyiv (Ukraine); François Kajzar, Univ. Politehnica of Bucharest (Romania); Beata Derkowska, Institute of Physics, N. Copernicus University (Poland)

Polymers containing azobenzene dyes or azobenzene lateral groups are of special interest for their application as optically active media, particularly, as polarization sensitive media for applications such as: optical data storage, surface relief gratings, photoswitching, alignment of liquid crystals, optical elements etc. Intensive research has been carried out the previous years to synthesize and investigate the second order nonlinear optical response of azobenzene/polymer systems. The desirable properties of these materials are attributed to the high efficient photoinduced trans-cis and vice versa isomerization of azobenzene moieties. This transformation is connected with the volume change of molecules, followed by the change of their rotational mobility. The trans-cis isomerization process is exploited also in all optical poling of polymers and play also an important role in optical depoling. Generally this phenomena are induced by light with frequencies higher than half of the main resonance of material and its efficiency is resonantly enhanced via one-photon absorption. They are possible also by multiphoton absorptions. In this presentation we will report the synthesis of methacrylic polymers with azobenzene side chains. The electro-optic effects in these polymers will be also presented and discussed.

## 8901-41, Session 8

### Switching between negative and positive refraction in nanosphere dispersed liquid crystal driven by electric field (*Invited Paper*)

Grzegorz Pawlik, Wroclaw Univ. of Technology (Poland); Wiktor Walasik, Institut Fresnel (France); Antoni C. Mitus, Wroclaw Univ. of Technology (Poland); lam Choon Khoo, The Pennsylvania State Univ. (United States)

We discuss the concept of reversible electrical switching between positive and negative refraction in nanosphere dispersed liquid crystal (NDLC) metamaterial for TM polarization. The proposed design offers an interesting possibilities of real-time control using external electric field of positive-negative refraction and reflection for the Poynting vector at infrared frequencies. Exemplary switching parameters and physical composition of the material are theoretically demonstrated. Finite Element (FE) simulations (Comsol) confirm this effect.

## 8901-42, Session 8

### Semiconductor alloys for optoelectronic applications: ab initio modeling

Pawel P. Scharoch, Wroclaw Univ. of Technology (Poland); Maciej Winiarski, Institute of Low Temperature and Structure Research (Poland); Maciej Polak, Wroclaw Univ. of Technology (Poland)

Semiconductor alloys, in particular group III metal nitride and phosphide, such as  $\text{In}_x\text{Ga}_{1-x}\text{N}$  or  $\text{Al}_x\text{N}_{1-x}\text{P}_x$  are materials of interest for optoelectronic applications (light emitting diodes, lasers, detectors). The potential possibility of tuning (via variation of the composition) of the band-gap and the lattice constant make them particularly attractive. The idea of tuning the band-gap (from infrared to ultraviolet), although simple in principle, requires solving a variety of practical problems, like lattice constants misfit of parent compounds, associated with atom sizes, thermodynamically determined phase segregation, system stability, band-gap bowing, efficiency of radiative transitions etc. The density functional theory (DFT) based 'ab initio' modeling is of particular importance in the field, since it allows to predict theoretically the physical limits for various properties. It also provides a hint in which direction, technologically and experimentally, to proceed. We present the basic ideas behind the 'ab initio' modeling and, as an example, the calculation results of structural, elastic and the electronic properties of  $\text{In}_x\text{Ga}_{1-x}\text{N}$  and  $\text{Al}_x\text{N}_{1-x}\text{P}_x$ .

In the case of  $\text{In}_x\text{Ga}_{1-x}\text{N}$  the alchemical mixing approximation which is the 'ab initio' pseudopotential specific implementation of the virtual crystal approximation (VCA) has been employed to study from first principles the wurtzite (WZ) and zinc blende (ZB) alloy. The investigations were focused on structural properties (the equilibrium geometries), elastic properties (elastic constants and their pressure derivatives), and on the band-gap. The elastic constants have been evaluated directly from the strain-stress relation. The band-gap has been calculated within MBJLDA approximation. The evaluated composition dependent quantities have been found to be in a very satisfactory agreement with the available literature data. Some results have been obtained which, to authors knowledge, have not been reported previously in the literature (e.g. composition dependent elastic constants in ZB structures or composition dependent pressure derivatives of elastic constants). The applied method is supposed to simulate a random alloy and when combined with the supercell approach may serve as supplementary tool for 'ab initio' studies of alloy systems.

In the case of  $\text{Al}_x\text{N}_{1-x}\text{P}_x$  the electronic structure has been calculated from first principles. Structural optimization has been performed within the framework of LDA (local density approximation) and the band-gaps calculated with the modified Becke-Jonson (MBJLDA) method. Two approaches have been examined: the virtual crystal approximation (VCA) and the supercell-based calculations (SC). The composition dependence of the lattice parameter obtained from the SC obeys Vegard's law whereas the volume optimisation in the VCA leads to an anomalous bowing of the lattice constant. A strong correlation between the band-gaps and the structural parameter in the VCA method has been observed. On the other hand, in the SC method the supercell size and atoms arrangement (clustered vs. uniform)



appear to have a great influence on the computed band-gaps. In particular, an anomalously big band-gap bowing has been found in the case of clustered configuration with relaxed geometry. Basing on the performed tests and obtained results some general features of MBJLDA are discussed and its performance for similar systems predicted.

#### 8901-43, Session 8

### Gold nanoparticles as optical limiting materials against cw lasers (*Invited Paper*)

Maria Chiara Frare, Raffaella Signorini, Verena Weber, Renato Bozio, Univ. degli Studi di Padova (Italy)

Improvements in laser technology have made available and easy to use a large variety of continuous wave (CW) lasers: from laser pointers to medical applications, and also in military optical pointing systems. The diffusion of lasers, together with the wide range of wavelengths available, has driven the need of agile sensor protection devices from accidental or intentional damage, especially for the human eye. Interference filters are of limited use because they operate in a very narrow range around a definite wavelength. Therefore, we need smarter devices, the so-called optical limiters, that are able to control light by light through various nonlinear optical (NLO) phenomena exhibited by suitably designed materials.

These "smart materials" should be able to activate the protection at high input light energy, with a large dynamic range and to work in a wide wavelength interval.

Optical nonlinearity exhibited by materials under CW illumination is predominantly refractive and generates a focusing or defocusing effect of the incident laser beam, usually associated with nonlinearity of thermo-optic origin. These materials are able to modify the propagating beam with a well defined distribution: generally a ring pattern can be observed at far field when a Gaussian distribution illuminates a thin sample of the nonlinear material.

In the last years, several nanostructures, like gold nanoparticles (AuNPs) in solution and in a solid matrix, have been studied for applications as active materials for the realization of optical limiters for CW lasers.

Our choice is to realize a solid state protection device, embedding gold nanoparticles in a polymer matrix. In particular we use polycarbonate, widely employed to produce high quality optical components with superior mechanical properties.

The gold NPs are synthesized by the Turkevich method, analyzed by absorption measurements and TEM analysis, and then transferred into an organic solvent to blend them with the polymer matrix. Thin films of optical quality are obtained by drop casting.

We have investigated the optical limiting behavior under CW illumination at three different wavelengths: 488, 514 and 647 nm. The nonlinear transmission measurements are comparable with literature for CW studies.

The optical limiting threshold, as a function of the AuNPs concentration, has been studied. Closed aperture Z-scan measurements show that the behavior of the samples is due to the non-local thermal nonlinear refraction process with a negative nonlinear index in the order of  $\sim 10^{-6} \text{ cm}^2/\text{W}$ , comparable with liquid samples in the literature. Therefore, the use of a polymer matrix does not impair the thermo-optical properties compared to solutions. In the range of AuNPs concentration investigated the nonlinear effect increases linearly with the increasing particle concentration.

A critical parameter in assessing the effectiveness of the optical limiting action is the time response of the material at varying input powers. It gives us information on the transmitted irradiance in a 300 milliseconds time interval, corresponding to the blinking of the human eye, therefore on the total fluence reaching the retina. There is still some work needed to attain the safety limit estimated around  $1 \text{ mJ/cm}^2$  but exploitation of the strong localized plasmon of AuNPs appears to be a promising approach.

#### 8901-44, Session 8

### Fuel cell based on hydrogenized nanocrystalline film for MEMS applications

Dmitry E. Milovzorov, Fluens Technology Group Ltd. (Russian Federation)

Fuel cell based on nanocrystalline silicon films deposited on cerium dioxide layer was proposed as microscopic power supplier of micromechanical electronic devices. The electric field assisted diffusion causes the drift of oxygen atoms from cerium dioxide to the hydrogenized silicon film. Atomic oxygen reacts with hydrogen inside the film due to the significant electron negativity. The water molecules are desorbed from the surface of silicon film. The anomalous behaviour of conductivity was detected by determined temperatures of film. The electron spin resonance spectrum shows the EX defects in structure. Raman spectroscopy measurements shows the spectral changes by applying the electric field. It is suggested that there is a proton migration as a oxygen electro-diffusion to the interface area.

# Plenaries

## Remote Sensing

### Very High Resolution Imaging Systems

Andreas Eckardt, Institute of Robotics and Mechatronics of the German Aerospace Center DLR, Germany

Starting at the end of the 90th with IKONOS (1 m GSD) and the Hubble Space Telescope a fast development for high spatial resolution systems for civil applications have become available. Today with GeoEye-2 and Worldview 3 the 35 cm range will be reached. Key Drivers for such developments are different governmental requirements for their own capabilities, which are related to dual use aspects. But there is also a need for mapping applications with lower resolution. Other aspects are the investigations of gases (CO<sub>2</sub>, etc. ) which can be based on laser systems or high resolution spectrographs.

**Very High Resolution can be related to the following dimensions**

- Spatial (20 cm or less)
- Spectral (hyperspectral systems from UV up to thermal infrared)
- Time (real time implementations in CMOS, real time calculation on FPGA)

**Major challenges at various system levels can be related with payload and platform:**

#### *Payload*

- Telescope Optics,
- Active Optics,
- Focal Plane Technology,
- Active high speed focus control.

#### *Platform*

- High Torque Wheels,
- AOCS,
- On Board high speed data link.

Auxiliary instruments for atmospheric parameter measurements and laser distance measurements for TDI synchronisation are important for the reproducibility of the image quality. The presentation focuses on new trends, which are also related to developments in our institute.

### Novel Imaging Spectrometers and Polarimeters

Eustace L. Dereniak, Univ. of Arizona, College of Optical Sciences, United States

The use of two dimensional arrays has enabled the development of novel imaging spectrometers and polarimeters. This presentation will discuss the development of imagers that use new optical designs based on old ideas. The presentation contains an overview of the various types of imaging sensors that have been developed at the Optical Detection Lab of the University of Arizona. The goal of our research is to develop instruments capable of discriminating objects in a remote sensing environment. These instruments are capable of spectrally monitoring simultaneously chemical or biological processes in real time in four dimensions (x,y,z,t).

## Security + Defence

### The Force of Light

Roland Sauerbrey, Scientific Director of the Helmholtz-Zentrum Dresden-Rossendorf (HZDR), Germany

Lasers today reach intensities of about 10<sup>22</sup> W/cm<sup>2</sup>. At such laser intensities the interaction of light and matter is dominated by relativistic effects. These new effects include laser particle acceleration with potential applications in radiation oncology as well as polarization of the vacuum.

### High Power Fiber Lasers for Defence Applications

Markus Jung, Rheinmetall Defence, Germany

Lasers are widely used for defence and sensor applications ranging from laser range finders, LIDAR, obstacle avoidance systems for helicopters, explosive detection. High power lasers are developed for use in Air Defence, UXO, DIRCM applications deployed to operate on stationary sites, ships, vehicles, airborne platforms against various threats from missiles, UAV's, mortars to speed boats.

Laser technology has shifted from gas lasers to diode pumped solid state laser DPSSL in the last decade, in order to fulfil the demanding requirements of these applications regarding optical output power, beam quality, power efficiency, wavelength selection and ruggedness.

An attractive and power scalable DPSSL concept for these applications is based on rare-earth-doped optical fibers. By using large mode area fibers continuous laser power in the 10kW range combined with beam qualities close to fundamental mode operation have been demonstrated. Compact, reliable fiber laser systems with wall plug efficiencies above 25% are commercially available and have been used in laser weapon demonstrations world wide.

The contribution will discuss in particular the requirements for defence applications and give a compressed review on science and technology of fiber lasers and amplifiers. The prospects for future developments in power scaling of fiber lasers and beam combining technologies will be discussed.



# 2014

## Security+ Defence

Europe's leading defence and security event.

[www.spie.org/sd14](http://www.spie.org/sd14)

## Remote Sensing

Europe's largest remote sensing event.

[www.spie.org/rs14](http://www.spie.org/rs14)

See the latest advances at these co-located European meetings

**Mark your calendar**

**Conferences & Courses**  
22–25 September 2014

**Exhibition**  
23–24 September 2014

**Location**  
Amsterdam, Netherlands





SPIE®

# 2014 Photonics Europe

Advances in applications of photonics, optics, lasers,  
and micro/nanotechnologies

---

## Call for Papers

Submit your abstract by 4 November 2013

[www.spie.org/pe2014](http://www.spie.org/pe2014)

### Conferences & Courses

14–17 April 2014

### Exhibition

15–16 April 2014

### Location

Square Brussels Meeting Centre  
Brussels, Belgium